CSCE'21

3rd Conference on Sustainability in Civil Engineering

PROCEEDINGS BOOK

August 11, 2021

ISBN: 978-969-23344-2-6

Published By
Department of Civil Engineering
Capital University of Science and Technology, Islamabad-Pakistan
www.csce.cust.edu.pk | www.cust.edu.pk

Proceedings of

3rd Conference on Sustainability in Civil Engineering

(CSCE'21)

Publication Note

August 11. 2021

Published By
Department of Civil Engineering
Capital University of Science and Technology, Islamabad – Pakistan
ISBN: 978-969-23344-2-6

www.csce.cust.edu.pk
www.cust.edu.pk

Foreword

Welcome to the CSCE 2021, 3rd Conference on Sustainability in Civil Engineering (CSCE'21) is going to be held by Department of Civil Engineering, Capital University of Science and Technology, Islamabad, Pakistan. The main focus of CSCE'21 is to highlight sustainability related to the field of civil engineering. It aims to provide a platform for civil engineers from academia as well as industry to share their practical experiences and different research findings in their relevant specializations. We hope all the participants experience a remarkable opportunity for the academic and industrial communities to address new challenges, share solutions and discuss future research directions. The conference accommodates several parallel sessions of different specialties, where the researchers and engineers interact and enhance their understanding of sustainability in the civil engineering dynamics.

This year, we have wonderful and renowned keynote speakers for this edition of CSCE. We have received 188 manuscripts from different countries around the world including UK, USA, KSA, Hongkong, Turkey, China and Pakistan. All papers have undergone a comprehensive and critical double-blind review process. The review committee comprised of 54 PhDs serving in industry and academia of UK, Hungry, Australia, New Zealand, Chile, Poland, Germany, China, Malaysia, Hongkong, KSA, Oman, Sri Lanka, and Pakistan. After the screening and review process, 62 papers are to be presented in Conference.

We are grateful to all the reviewers and keynote speakers who have dedicated their precious time to share their expertise and experience. With this opportunity, we would also like to express our gratitude to everyone, especially all the faculty and staff at the Capital University of Science and Technology for their great support and participation.

In this regard, the participation and cooperation of all the authors, presenters and participants is also acknowledged, without whom this conference would not have been possible. Last but not the least, an appreciation to our advising and organizing committees whose hard work and dedication has made this day possible.

Conference Chair of CSCE'21

Dr. Majid Ali

Professor, Civil Engineering Department

Capital University of Science & Technology,
Islamabad, Pakistan

Technical Committee CSCE'21

1	Dr. Rabee Shamass	London South Bank University, UK
2	Dr. Shunde Qin	WSP, UK
3	Dr. Hamid Mehmood	Transport Dept. Victoria, Australia
4	Dr. Mizan Ahmed	Monash University, Australia
5	Dr. Mohsin Shehzad	Mott MacDonald, New Zealand
6	Dr. Wajiha Mohsin Shehzad	Massey University, New Zealand
7	Dr. Anas Bin Ibrahim	UiTM Cawangan Pulau Pinang, Malaysia
8	Dr. Waris Ali Khan	Universiti Putra Malaysia
9	Dr. Khairunisa Binti Muthusamy	Universiti Malaysia Pahang, Malaysia
10	Dr. Wesam Salah Alaloul	Universiti Teknologi PETRONAS (UTP), Malaysia
11	Dr. Teh Hee Min	Universiti Teknologi PETRONAS (UTP), Malaysia
12	Dr. Noor Aina	Universiti Pertahanan Nasional Malaysia
13	Dr. Cao Mingli	Dalian University of Technology (DUT), China
14	Dr. Li Li	Northwest A&F University, China
15	Dr. Fenyvesi Oliver	University in Budapest, Hungary
16	Dr. Libo Yan	Technische Universität Braunschweig, Germany
17	Dr. Piotr Smarzewski	Lublin University of Technology, Poland
18	Dr. You Dong	The Hong Kong Polytechnic University, Hong Kong
19	Dr. Mehran Khan	The Hong Kong Polytechnic University, Hong Kong
20	Dr. Claudio Oyarzo Vera	Universidad Católica de la Santísima Concepción (UCSC), Chile
21	Dr. Munir Ahmed	DAR Engineering, Kingdom of Saudi Arabia
22	Dr. Umar Farooq	Islamic University of Madinah, Kingdom of Saudi Arabia
23	Dr. Mohsin Usman Qureshi	University in Sohar, Oman
24	Dr. Buddhika Gunawardana	University of Moratuwa, Sri Lanka
25	Dr. M Zia ur Rehman Hashmi	Global Change Impact Studies Centre, Pakistan
26	Dr. Irfan Yousuf	National Electric Power Regulatory Authority, Pakistan
27	Dr. Hassan Nasir	Water & Sanitation Services Peshawar, Pakistan
28	Dr. Shahid Nasir	Finite Element Pvt. Ltd.
29	Dr. Ayub Elahi	University of Engineering and Technology, Taxila, Pakistan
30	Dr. Naeem Ejaz	University of Engineering and Technology, Taxila, Pakistan
31	Dr. Faisal Shabbir	University of Engineering and Technology, Taxila, Pakistan
32	Dr. Usman Ali Naeem	University of Engineering and Technology, Taxila, Pakistan
33	Dr. Naveed Ahmad (Transportation)	University of Engineering and Technology, Taxila, Pakistan
34	Dr. Afaq Ahmad	University of Engineering and Technology, Taxila, Pakistan
35	Dr. Naveed Ahmad (Geotech)	University of Engineering and Technology, Taxila, Pakistan
36	Dr. Naveed Ahmed (Structures)	University of Engineering and Technology Peshawar, Pakistan
37	Dr. Sher Jamal Khan	National University of Science & Technology, Islamabad, Pakistan
38	Dr. Rao Arslan	National University of Science & Technology, Islamabad, Pakistan
39	Dr. Khuram Iqbal Ahmed Khan	National University of Science & Technology, Islamabad, Pakistan
40	Dr. Hammad Anis Khan	National University of Science & Technology, Islamabad, Pakistan
41	Dr. Sabahat Hassan	HITEC University Taxila, Pakistan
42	Dr. Tahir Mehmood	COMSATS University Wah, Pakistan
43	Dr. Ahsan Maqsoom	COMSATS University Wah, Pakistan
44	Dr. Adnan Nawaz	COMSATS University Wah, Pakistan
45	Dr. Faisal Javed	COMSATS University, Abbottabad, Pakistan
46	Dr. Khan Zaib Jadoon	International Islamic University, Islamabad, Pakistan
47	Dr. Zeeshan Alam	International Islamic University, Islamabad, Pakistan
48	Dr. Affaq Khattaq	International Islamic University, Islamabad, Pakistan
49	Dr. Mudassir Muneer Khan	Bahauddin Zakariya University, Pakistan
50	Dr. Saqib Ehsan	NFC Institute of Engineering and Fertilizer Research, Faisalabad, Pakistan
51	Dr. Malik Muneeb Abid	University of Sargodha, Pakistan
52	Dr. Shaukat Ali Khan	Abasyn University Peshawar Campus, Pakistan
53	Dr. Salamat Ullah	Abasyn University Islamabad Campus, Pakistan
54	Dr. Shaukat Ali Khan	MYU, Islamabad Campus, Pakistan

Advisory Committee

Dr. M. Mansoor Ahmed
(Vice-Chancellor CUST Islamabad)
Patron

Dr. Imtiaz Ahmed Taj
(Dean Faculty of Engineering)
General Advisor

Dr. Ishtiaq Hassan
(Head of Civil Engineering Department)
Principle Advisor

Organizing Committee

Dr. Majid Ali
Chair

Dr. Syed Shujaa Safdar Gardezi
Co – Chair

Engr. Mehran Sudheer
Conference Secretary – I

Engr. Umair Ahmed
Conference Secretary –II

Keynote Speakers

Dr. Salman Azhar *William A. Hunt Endowed Professor* *Auburn University, Alabama, USA*	***Towards Construction 4.0: Emerging Technologies in The Modern AEC Industry***
Dr. Muhammad Jamaluddin Thaheem *Postgraduate Course Director* *Deakin University, Australia*	***Green and Sustainable Housing: Sociocultural and Architectural Perspectives and Challenges***
Dr. Nasir Shafiq *Professor* *Universiti Teknologi PETRONAS, Malaysia*	***Towards Sustainable Development in Infrastructure Management: Challenges and Issues***
Dr. Noor Muhammad Khan *Director Center of Excellence in Water Resources* *UET, Lahore, Pakistan*	***Inflow Variability for Improved Water Resources Management***
Dr. Furqan Qamar *WSP UK*	***Assessment Process for Various Bridges as Per BS Standards***
Dr. Shaukat Ali Khan *Associate Dean, FoE&C* *Abasyn University Peshawar, Pakistan*	***A Monte-Carlo Simulation-Based Earthquake Risk Assessment Framework for Developing Countries***
Dr. Hassan Nasir *Chief Executive Officer* *WSSP, Peshawar, Pakistan*	***Water And Sanitation Services Delivery In KP: Challenges and Opportunities***

TABLE OF CONTENTS

STRUCTURAL ANALYSIS

CONSTRUCTION MANAGEMENT

WATER ENGINEERING

TRANSPORTATION ENGINEERING

GEOTECHNICAL ENGINEERING

ENVIRONMENTAL ENGINEERING

STRUCTURAL MATERIALS

3rd Conference on Sustainability in Civil Engineering (CSCE'21)
Department of Civil Engineering
Capital University of Science and Technology, Islamabad Pakistan

A REVIEW ON FRP REPAIRING OF FIRE DAMAGED RC MEMBERS

[a] Blawal Hasan, [b] Sami Ullah

a: Civil Engineering Department, University of South Asia, Lahore. blawalhasan@gmail.com
b: Civil Engineering Department, University of Engineering and Technology, Peshawar. samiullahktk426@gmail.com

Abstract- The mechanical properties of concrete are highly affected by the fire event. Load bearing-capacity of reinforced concrete (RC) structural members reduced due to reduction in concrete strength caused by the elevated temperature. This study presents a review on repairing techniques of fire damaged RC structural members. The investigations covered physical dimensions, loading-effect method and bonding behavior and residual-strength assessment. The advantages of fiber reinforced polymers (FRP) recall of RC members' performance/strength over the steel coating, enlargement of the section, steel-plate bolting (SPB) and fiber reinforced polymers (FRP) are discussed. The fiber reinforced polymers (FRP) post-fire repairing technique reviewed to achieve the design or more strength, as compared to pre-heated, of damaged RC member. It was observed that FRP coating, around the RC members, enhanced the strength up to or more than the pre-heated design strength of concrete.

Keywords- Fire damaged RC members, fire exposure, post-fire assessment, post-fire repairing methods.

1 Introduction

In the construction industry, concrete is the most widely used building material since it is easily available, very cheap material. More importantly, it can be molded into any shape with less skilled labor as compared with the steel structures. As concrete is quasi-brittle material, it has very high strength in compression but weak in tension. Reinforced concrete (RC) structure consists of several structural members, such as slab, beams, columns and footing. The collapse of the building occurs due to the failure of these structural members. Failure of the structural members can occur due to degradation, which can be caused by earthquakes, overloading, blast, high temperature exposure, deformation caused by seismic loading, variation in structural design and lack of maintenance. The ultimate strength of RC structural members decreases due to the fire exposure causing the reduction in strength and stiffness of the material. In the case of fire, the mechanical decay of concrete and even significant effects at the structural level may occur due to spalling and reinforcement exposure [1].

The elevated temperature and cooling affect the load bearing capacity by reducing the strength of concrete [6]. After fire, it becomes necessary to assess the mechanical properties of the RC members and adopt some repairing methods if required. There are a lot of methods for the treatment of RC structural members. The main methods which are being used are the bolt plating method, section enlargement method, fiber reinforced polymers (FRP) coating/jacketing method [2]. Steel coating for the retrofitting can be used for improving the seismic shear strength but the rectangular column's coating can be buckled at the hinged area when subjected to lateral loading [7]. Steel-plate-bolting (SPB) method is usually adopted for the RC flexural members by fixing steel plates, both opposite sides, with the help of bolts [8]. The replacement method is, only used when the cost factor is not important, mostly adopted for the slab repairing [3]. FRP unidirectional repair of the RC column can enhance the load bearing capacity of the post-heated column up to or greater than the original level of pre-heated column [4]. FRP coated RC structural members can be capable of achieve satisfactory resistance during fire [5].

After the fire event, proper repairing and retrofitting are required for further use of the structure. This is because the high-temperature leaves adverse effects on concrete. This can be in form of spalling of concrete debonding between steel and concrete. There are many studies on the repairing techniques of concrete but this study focuses on the significance of the FRP repairing of the RC members after the fire. Steel jacketing and increasing the dimensions of the structural members are costly methods of repairing techniques. The use of the FRP repairing technique is economical compared with other techniques and no extra load is applied over the member as it is light in weight. Also, this technique doesn't reduce the workspace and free area between the repaired members. Post-fire repairing of RC members with FRP can even help in enhancing, more than pre-fire, the strength of the member.

2 Properties of Fire Subjected RC Members

Reinforced concrete gets a permanent decrease in strength due to high temperatures. Elevated temperature leaves adverse effects on reinforced concrete (RC) members. Initial morphology varied after the event which results in a decrease in mechanical properties of concrete after fire [9]. Microstructural properties of concrete are exposed at elevated temperatures [10]. Spalling of concrete depends upon two factors, pour-vapor pressure and thermal stress caused by the elevated temperature as described in Figure 1. Pore-vapor pressure cannot form spalling but only contribute to micro-cracks along with heat surface. Under thermal stress, these micro-cracks likely to buckle and spall near the heating surface [15]. Different RC members behave differently which are described below.

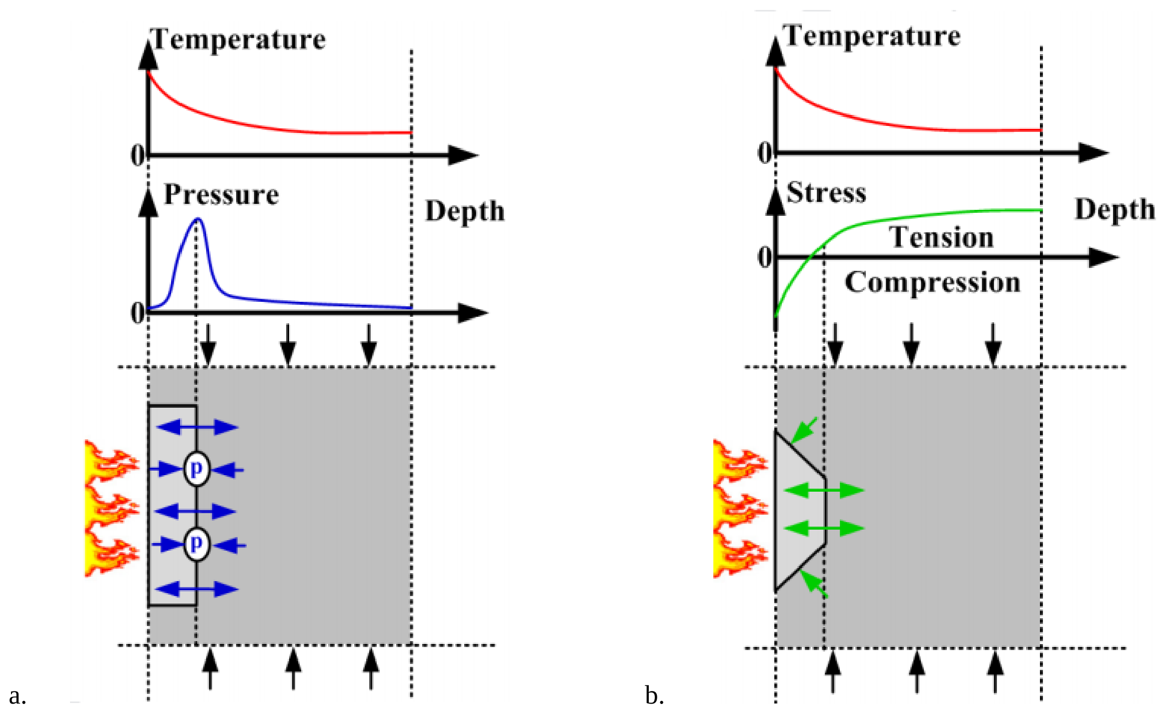

Figure 1: Spalling Factors of concrete due to Fire, a. pore-vapor pressure, b. thermal stress [15]

2.1 Compression Members (Columns)

The column can suffer fire up to four dimensions. Bending type depends upon the number of faces exposed to fire. One- and three-sided exposed column may be considered subject to uniaxial bending and if two or four faces exposed to fire will be considered subject to biaxial bending. Tan et al. [11, 12] developed a method, for one-, two-, three- and four-sided exposed column, to examine the fire resistance of column while spalling of concrete was not considered. The decrease was observed in residual strength of corner column two-sided exposed to asymmetric fire and subjected to uniaxial and biaxial bending [13]. Enlargement of dimensions of columns enhances the fire resistance [14].

2.2 Flexural Members

2.2.1 Beams

Many research studies have been conducted on the performance of flexural members exposed to elevated temperatures. In an analysis of experimental study considering beam type, beam load ration and concrete cover thickness, it was concluded that primary beams are shown better fire resistance in comparison with secondary beams because the tensile strength wasn't degraded [16]. Variations in shear failure modes were observed mandatory in frame-restrained beams and cantilever beams after exposure to elevated temperature. So, for evaluation of after-fire shear capacity, the design of RC beams is not acceptable under room temperature [17].

2.2.2 Slabs

Several studies have been conducted to evaluate the performance of slabs under fire. Three main factors that influence the fire resistance are load level, the thickness of concrete cover and temperature. Spalling in concrete produced by fire seriously reduces the structural and thermal response of the slab which makes it less resistant to fire [18]. It is obvious, in high temperatures, that the degradation of stiffness and strength of the material is the main factor affecting the behavior of structure [19]. During the fire, the complications in the behavior of structure are cracking, degradation and thermal expansion. The stress-strain graph at different elevated temperatures has been presented in Figure 2.

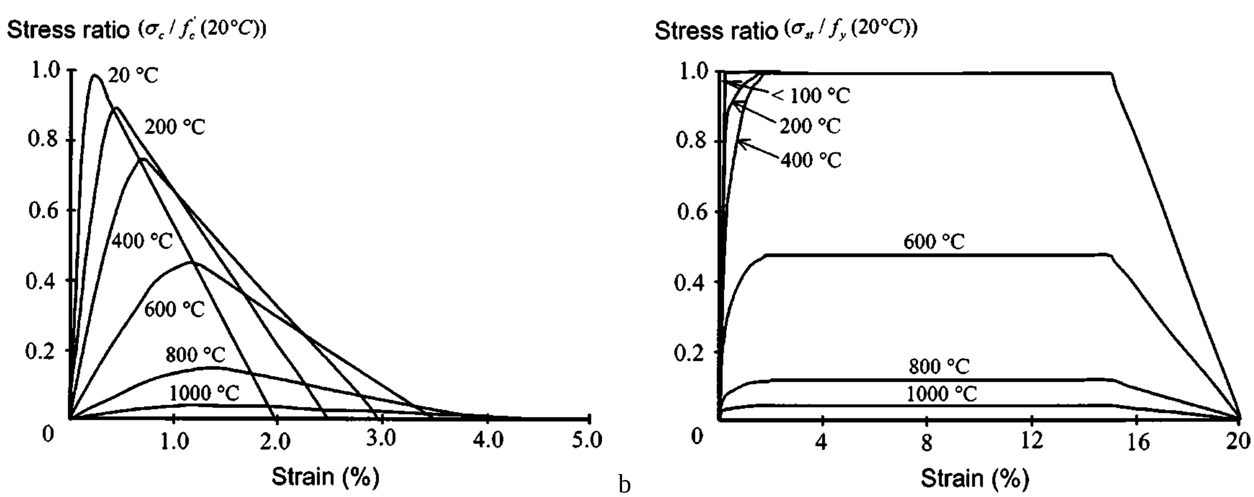

a b

Figure 2: Stress-strain relationship for concrete at elevated temperature, b. Stress-strain relationship for steel at elevated temperature [19]

3 Types of Repairing Techniques of RC Members

Several techniques are being used for repairing fire damaged RC members. The most commonly adopted techniques are steel jacketing/coating, section enlargement and FRP repairing technique. The technique is adopted based on the damaged condition of the member. Table 1 provides the detailed damaged condition so that the repairing method is adopted accordingly. It is proposed that the level two damaged segment can be fixed by the section enlargement technique, and the third level damaged is appropriate for the steel jacketing or with FRP repairing technique. Level four is more severe damage case it should be replaced. The member falling in the damage category of dangerous cannot be repaired. There is only way to use it is to reconstruct it instead of repairing. The serious level can be repaired by the section enlargement technique after removing the most damaged [20]. FRP and steel plate bolting (steel jacketing) techniques can be used for the moderate and mild level of damaged RC members.

Table 1- Description of Damages and Repairing Technique Proposed According to Damaged Type [20]

Degree of damage	Dangerous	Serious	Moderate	Mild
Level of damage	Level four	Level three	Level two	Level one
Temperature of concrete	≥700	600-700	400-500	<400
Temperature of reinforcement	400-500	350-400	100-300	<100
Damaged condition	Out of plane deformation	Deflection exceeding one to three times	Deflection meeting the limit	No changes

The advantage of the techniques used for repairing fire-damaged RC members improve the structure bearing capacity, stiffness, stability, and give economical solutions to exceed the life of the structures. The techniques are used also to improve the ultimate load capacity of the structure members and provide anti-corrosion to the member as well. The disadvantage of the techniques using is that they will never achieve the original strength of the structural members.

3.1 Steel Jacketing Technique.

In this technique, the steel is wrapped around the fire damaged RC structural member. The steel plates and sheets are attached to the surface of the RC member with the epoxy resins or cement paste. Install the angle on the corners of RC members (beam and column) and connect them with a splicing plate. The size of the angle and plate is determined by the designated bearing capacity. The ends are interconnected with another transverse member. The upper end of the column's steel jacketing extended up to the upper floor while the lower end anchored to the foundation. The steel has more density which adds additional weight to the structure as well. The bolting and cutting of steel plates according to section, needed to be repaired, size and shape make it uneconomical. This technique is suggested for severe fire damaged RC members.

3.2 Section enlargement Technique

The section enlargement technique is the strengthening technique used to achieve the ultimate load bearing capacity of stability and stiffness. In this technique, the residual strength is investigated first and the section is enlarged so that the ultimate bearing capacity and strength should be achieved to support the desired loading. The section enlargement technique was adopted for repairing the bridge columns, after two hours of fire exposure, after determining the residual strengths [21]. The section enlargement reduces the free area between the RC columns and the headroom between the beam and the floor. This technique can be used for recall of strength of moderate and mild type of fire damaged members.

3.3 FRP Repairing Technique

Fire badly affects the RC members and due to which it cannot be used for the desired purpose because of a reduction in its mechanical properties. Without any retrofitting of the structural members, it is very risky to utilize the building after the fire event. For this one of the repairing methods is FRP. In this technique, the sheet of FRP attached with the structural members to rehabilitate the ultimate strength of RC members reduced due to fire.

3.4 Superiority of FRP repairing over other techniques

FRP repairing technique is more economical than any other repairing technique. Fibers present inside the polymers enhance the strength of the RC members. As the FRP is lightweight than steel jacketing and section enlargement, there is no need to tackle additional loading of repairing materials. Easy to handle, place and cut as it is lightweight than the steel. Compared with section enlargement repairing technique, reduction in free area and headroom is very little that it is negligible. Above discussed advantages make FRP repairing better than others.

4 FRP Repairing Method Adopted Fire Damaged RC Members

Fire event leaves adverse effects on reinforced concrete members. The degradation and spalling of concrete are the major defects caused by the fire event. The increase in corrosion damage reduction is a factor reducing the flexural strength of damaged RC beams. Reinforced concrete coating and steel coating are traditionally used for the rehabilitation of the reinforced concrete members. Past few years, the use of fiber reinforced polymers has been increased as a strengthening method as it is lightweight and less complex of anchorage. The characteristics of FRP like lightweight, high strength, high impact resistance, durability, and corrosion resistance have made it a better material for the rehabilitation of RC [22, 23]. FRP coating is more effective in rehabilitating the flexural member with damage location on top of the member than the bottom. FRP with the provision of the epoxy coating and coarse aggregates inside the coating surface shown in better distribution of stress and cracks propagation [24]. There are two ways of applying the FRP repairing on RC members, one is externally bonded FRP strengthening and the second is near surface mounted FRP strengthening.

4.1 Externally bonded FRP strengthening

For externally bonded FRP strengthening, the FRP sheets are attached to the surface to restore the ultimate capacity of RC members [25]. The test was conducted on fire damaged beams strengthened by FRP sheets with novel coating. From the test, it was concluded that the novel coating improved the fire resistance of FRP sheets [26]. Figure 3 illustrates the externally bonded FRP strengthening technique to restore and rehabilitate the ultimate strength of a T-beam. The bonding behavior of the RC T-beam and the carbon fiber reinforced polymer was observed. The FPR restores the ultimate strength and there is no need to enlarge the dimensions of the reinforced concrete structural member.

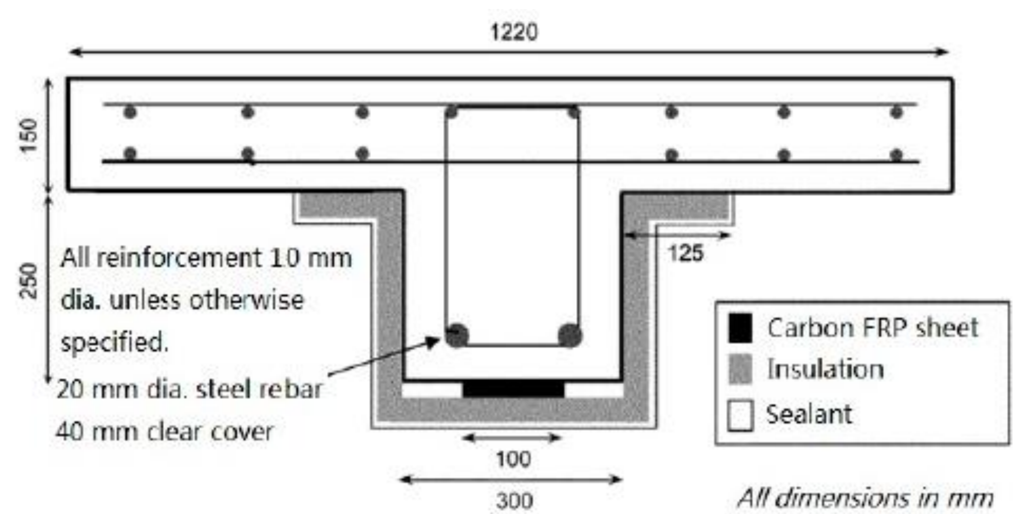

Figure 3: Externally bonded FRP strengthening [26]

4.2 Near surface mounted FRP strengthening

Near surface mounted (NSM) FRP strengthening is an advanced technique that was developed last decade. Mahmoud et al. conducted research on NSM's enhanced performance [27]. In comparison with the externally bonded method, NSM gives better safety from external damage. Figure 4 elaborates the arrangements for the NSM of the RC beam. The epoxy resin is used for inter-surface bonding. The adhesive property of epoxy resin improved the bonding between FRP sheets and concrete at elevated temperatures. The RC members repaired with NSM technique give fire endurance of two hours.

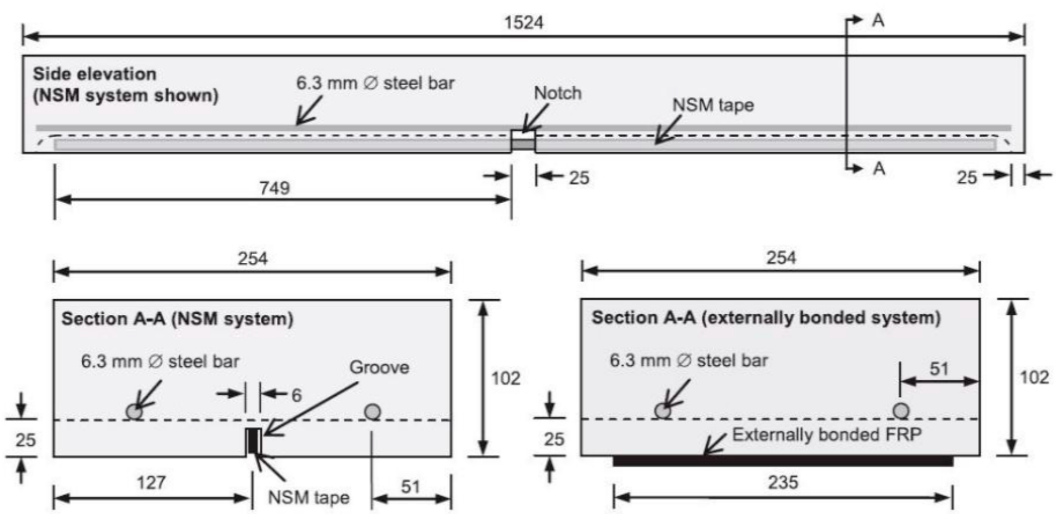

Figure 4: Near surface mounted and Externally bonded FRP strengthening [28]

5 Conclusions

This paper provides a review of the FRP repairing technique of RC structural members damaged by a fire event. Other repairing techniques like section enlargement and steel coating were also discussed. The techniques using for repairing fire-damaged review are done to achieve the desired or required properties of the structure to make it usable instead of reconstructing the whole structure. The techniques using are very effective for improving the structural members' properties as well as to increase the lifespan of the structure.

The outputs of the study summarized as follows:

- The FRP, steel coating and section enlargement method were used for the repairing of RC members damaged by fire. The FRP, concrete reinforcement and section enlargement repairing techniques are applicable for the RC slabs after exposure to elevated temperature. Since the section enlargement is an effective and economic solution for the slab repairing.
- FRP rehabilitation method is the most widely used in the world. Externally bonded FRP and near surface mounted FRP strengthening techniques were compared. NSM has shown better results such as more ductile performance and the anchoring of FRP is better in NSM than the externally bonded FRP technique.
- FRP repairing is far good for the rehabilitation of the RC beams
- The section enlargement technique can more effectively enhance the stiffness and ultimate load of compression members. Also, the construction is simple but the building clearance decreases.
- The properties of FRP are deeply studied. FRP coating, compared with steel coating and section enlargement, is easy to handle, lightweight, high strength to weight ratio and corrosion resisting.

It is concluded in this study that the FRP repairing technique is an easy method of repairing and does not apply any additional load on members caused by the weights of other repairing materials.

Acknowledgment

The author would like to thank all the organizations and persons who helped throughout this study, especially Engr. Prof. Dr. Majid Ali for his kind support and guidance in framing and improving the manuscript. The careful review and constructive suggestions by the anonymous reviewers are gratefully acknowledged.

References

[1] Q. Ma, R. Guo, Z. Zhao, Z. Lin, K. He (2015). "Mechanical properties of concrete at high temperature—A review", *Construction and Building Materials*, Volume 93, 15 September 2015, Pages 371-383..

[2] C.J. Jiang, Z. D. Lu, L. Z. Li, (2017) "Shear Performance of Fire-Damaged RC Beams Repaired by a Bolted Side-Plating Technique," *Journal of Structural Engineering.* 2017, 143.

[3] P. Knyziaka, R. Kowalskia, J. R. Krentowskib (2019), "Fire damage of RC slab structure of a shopping center," *Engineering Failure Analysis*, Volume 97, March 2019, Pages 53-60.

[4] M. Yaqub, C.G. Bailey (2011) "Repair of fire damaged circular reinforced concrete columns with FRP composites," *Construction and Building Materials,* Volume 25, Issue 1, January 2011, Pages 359-370.

[5] Fereshtehnejad E, Banazadeh M, Shafieezadeh A (2016), "System reliability-based seismic collapse assessment of steel moment frames using incremental dynamic analysis and Bayesian probability network" *Journal of Engineering Structrures,* 118:274–286.

[6] J. Wróblewska & R. Kowalski (2020), "Assessing concrete strength in fire-damaged structures", *Construction and Building Materials*, Volume 254, 10 September 2020, 119122.

[7] M.J.N. Priestley, F. Seible, Y. Xiao, R. Verma (1994), "Steel jacket retrofitting of reinforced concrete bridge columns for enhanced shear strength-part 1: Theoretical considerations and test design", *ACI Structural Journal*, 1994, 91, 394–405.

[8] L.Z. Li, S.H. Lo, R.K.L. Su (2013), "Experimental Study of Moderately Reinforced Concrete Beams Strengthened with Bolted-Side Steel Plates", *Advances in Structural Engineering*, . 2013, 16, 499–516.

[9] A.H. Akca and N. Özyurt (2018). "Effects of re-curing on microstructure of concrete after high temperature exposure", *Construction and Building Materials,* 168 (2018) 431–441.

[10] J.D.A. Oliveir , J.C.L. Ribeiroa , L. Pedroti, C.S.D. Faria, G.H. Nalon, A.L.D.O. Júniora, "Durability of Concrete After Fire Through Accelerated Carbonation Tests, " *Materials Research*,vol.22,2019.

[11] K.H. Tan, Y. Yao (2003), "Fire Resistance of Four-Face Heated Reinforced Concrete Columns", *Journal of Structural Engineering ASCE*, 2003, 129, 1220–1229.

[12] K.H. Tan, Y. Yao (2004), "Fire Resistance of Reinforced Concrete Columns Subjected to 1-, 2-, and 3-Face Heating", *Journal of Structural Engineering ASCE,* 2004, 130, 1820–1828.

[13] W.C. Jau and K.L. Huang (2008), "A study of reinforced concrete corner columns after fire", *Cement Concrete Composites,* 2008, 30, 622–638.

[14] B. Wu, Z. Hong, G.H. Tang, C. Wang, (2009), "Fire Resistance of Reinforced Concrete Columns with Square Cross Section", *Fire Safety Journal*, 2009, 44, 869–880.

[15] L. Shena, W. Lib, X. Zhouc, J. Feng, G.D. Luzioe,Q. Rena, G. Cusatisb, (2020), "Multiphysics Lattice Discrete Particle Model for the Simulation of Concrete Thermal Spalling", *Cement and Concrete Composites*, Volume 106, February 2020, 103457

[16] F.X., Ding, Z. Li, S.S. Cheng, Z.W. Yu, (2018) "Stress redistribution of simply supported RC beams under fire conditions", *Journal of Centera South University,* 2018, 25, 2093–2106.

[17] C.J. Jiang, J.T. Yu, L.Z. Li, X. Wang, L. Wang, J.H. Liao, (2018) "Experimental study on the residual shear capacity of fire-damaged RC frame beams and cantilevers", *Fire Safety Journal,* 2018, 100, 140–156.

[18] X. Hou, W. Zheng, V.K.R. Kodur, (2013), " Response of unbonded prestressed concrete continuous slabs under fire exposure", *Engineering Structures,* Volume 56, November 2013, Pages 2139-2148

[19] Z. Huang, I.W. Burgess, R.J. Plank, (2003) "Modeling Membrane Action of Concrete Slabs in Composite Buildings in Fire. I: Theoretical Development", *Journal of Structural Engineering*, 2003.129:1093-1102.

[20] J. Zhou and L. Wang, (2019), " Repair of Fire-Damaged Reinforced Concrete Members with Axial Load: A Review", *Sustainability*, 2019, 11, 963.

[21] X.D. Deng, L. Wang, (2016) "Application of section enlargement method in fire-damaged bridge reinforcement" J. Mt. 2016, 13, 66–71.

[22] A.U. Al-saadi, T. Aravinthan, W. Lokuge, (2018), "Structural applications of fibre reinforced polymer (FRP) composite tubes: A review of columns members", *Composite Structures* 204 (2018) 513-524

[23] E. Oller, M. Pujol, A. Marí, (2018) "Contribution of externally bonded FRP shear reinforcement to the shear strength of RC beams", *Composites Part B: Engineering* (2018).

[24] A.A. Mohammed, A.C. Manalo, G.B. Maranan, M. Muttashar, Y. Zhuge, P.V. Vijay, J. Pettigrew, (2020) " Effectiveness of a novel composite jacket in repairing damaged reinforced concrete structures subject to flexural loads", *Composite Structures,* Volume 233, 1 February 2020, 111634

[25] G.F. Ji, G.Q. Li, W. Alaywan, (2013) "A new fire resistant FRP for externally bonded concrete repair", *Construction and Building Materials* 2013, 42, 87–96.

[26] B. Williams, V.K.R. Kodur, M.F. Green, L.A. Bisby, (2008) "Fire endurance of fiber-Reinforced polymer strengthened concrete T-beams", *ACI Structural Journal,* 2008, 105, 60–67.

[27] F. Al-Mahmoud, A. Castel, R. Francois, C. Tourneur, (2010), "RC beams strengthened with NSM CFRP rods and modeling of peeling-O failure", *Composite Structures,* 2010, 92, 1920–1930.

[28] P.J. Burke, L.A. Bisby, M.F. Green, (2013) "Effects of elevated temperature on near surface mounted and externally bonded FRP strengthening systems for concrete", *Cem. Concr. Compos.* 2013, 35, 190–199.

3rd Conference on Sustainability in Civil Engineering (CSCE'21)
Department of Civil Engineering
Capital University of Science and Technology, Islamabad Pakistan

COMPRESSIVE TOUGHNESS AND EMPIRICAL MODELLING OF NATURAL FIBER REINFORCED SILICA FUME BASED CONCRETE

[a] Mehran Khan*, [b] Waqas Ahmad, [c] Ali Rehman, [d] Ayaz Ahmad

a: Department of Civil Engineering, Dalian University of Technology, Dalian, Liaoning, China,
b: Department of Civil Engineering, Comsats University Islamabad, Abbottabad, Pakistan
c: Department of Civil Engineering, Comsats University Islamabad, Abbottabad, Pakistan
d: Department of Civil Engineering, Comsats University Islamabad, Abbottabad, Pakistan
* Corresponding author Email ID: drmehrankhan@outlook.com

Abstract- The use of natural fiber is increasing day by day because it is an economical and waste material as well as has advantages from the environmental aspects. Among the natural fibers, coconut fibers (CF) have the maximum toughness. The addition of supplementary cementitious materials like silica fume together with coconut fiber will lead to complementary benefits in terms of mechanical performance and environmental aspects. Additionally, the establishment of an empirical equation will be helpful for the researchers to predict the experimental stress-strain response. Therefore, in this study, the control mix, silica fume concrete, coconut fiber reinforced concrete, and coconut fiber reinforced silica fume based concrete are investigated for compressive toughness and empirical modeling. Furthermore, scanning electron microscopy (SEM) is also performed to study the microstructure of the matrix. It was found that the addition of coconut fiber and silica fume in the matrix improved the compressive toughness and microstructure of concrete. In addition, the stress-strain curves obtained from the empirical equation showed the goodness of fit with the experimental data.

Keywords- Coconut fiber, silica fume, concrete, compressive toughness, empirical modeling.

1 Introduction

In agriculturally progressive countries, natural fibers and plant fibers are available abundantly. These fibers can produce environmentally friendly materials when added to the concrete as reinforcement. Fibers added to the concrete tend to enhance the concrete performance such as energy absorption capacity, post cracking response, strength, etc [1-4]. As a plant residual waste, natural fibers have a significant economic value because of their use in construction materials all over the world. Natural fibers have the potential to reduce the quantity of basic ingredients in various composite materials that leads to environmentally friendly material. As compared to synthetic fibers, natural fibers contribute with the same properties when added to composites in terms of strength against shear, tension, temperature, and impact. The disadvantages of concrete that can be improved include the brittle behavior, low tensile strength, less resistance to cracks occurrence and propagation. The uniformly distributed fibers in the matrix play an important role in the improvement of concrete properties. Additionally, the incorporation of fibers in composites helps in controlling cracks [5]. The use of natural/plant fibers in building materials is from the Biblical times (approximately 3500 years ago) e.g. in clay sun-baked bricks [6]. Natural fiber is an economical and waste material, so it has also advantages from the ecological aspects. Among the natural fibers, coconut fibers (CF) have the maximum toughness [7], [8, 9]. The mechanical properties of CF reinforced concrete were investigated by Ali et al. [10]. The best performance was observed with 2% fiber content having 50 mm length. Currently, composites having fibers and mineral admixtures are introduced by the researchers for civil engineering applications [11], [12]. Luther [13] used different contents of silica fume (SF) i.e. from 5-15% in concrete and the best overall results were obtained with 11.5% content of SF by mass of cement. Thus, the combined use of natural fiber together with supplementary cementitious material will be helpful form improve performance of concrete in term of mechanical properties as well as sustainability.

The basic mechanical characteristic for fiber reinforced composites (FRC) is the stress-strain curve that is obtained from the uniaxial compressive load test. For example, an analytical model was developed by Ou et al. [14] for the stress-strain curve from compression test for the concrete reinforced with different sizes of steel fibers. The model was established to characterize the stress-strain behavior of composite with a high reinforcing index. It was reported from the results that the developed analytical model showed good agreement with the experimental results. Li et al. [15] studied the experimental characterization of polyvinyl alcohol engineered cementitious composite (PVA-ECC) established in the form of stress-strain curves. It was reported that PVA-ECCs showed that the established model presented good results with that of experimental results. Wang et al. [16] developed a rational fraction expression that both segments (i.e. ascending and descending) can be expressed by the rational formula. Saber et al. [17] examined the compressive stress-strain performance of high strength concrete (HSC) reinforced with synthetic fibers. The two simple models for the compressive stress-strain curve of the composite were used. It was suggested from the results that, the proposed models are able to predict the experimental results with better precision. Bencardino et al. [18] performed a comparative study on the experimental data of steel fiber reinforced concrete and proposed empirical models for stress-strain relationships. It was found that empirical models showed good agreement with test results. Furthermore, other researchers such as Li et al. [19] and Cao et al. [20] also conducted a comparative study on compressive modeling and reported a good correlation between experimental results and empirical models. Thus, it will be of great interest to develop a model for the composites reinforced with natural fiber for better prediction of experimental data.

The motivation for the current research is to deliver an economical and environmental friendly material to the construction industry using natural fibers. It is a major issue all over the world for sustainable development to manage agricultural waste. If instead of synthetic fibers, natural fibers are used in the construction industry it will result in greener and sustainable development. Lately, the use of natural fibers got special attention in many structural components [10], [21], [22], [7]. The main focus of the current study is the establishment of empirical modeling instead of evaluating material behavior. That is why other properties from the compressive test i.e., peak stress, peak strain, elastic modulus, etc. were not studied. Also, the studies on such material properties of CF reinforced concrete have been reported in the literature [9], [23]. The significance of the present research is to develop a model that can be helpful to predict the experimental results of natural fibers reinforced concrete for a structural design application in civil engineering. In this study, the coconut fiber together with silica fume is studied for the compressive toughness and empirical modelling. In addition, the microstructure of the matrix is also studied by scanning electron microscopy (SEM).

2 Experimental Procedures

2.1 Raw ingredients.

The ingredients used in the present experimental work include CF, SF, cement, coarse aggregate, fine aggregate, and water. The SF was bought from Sika Pakistan Pvt. Ltd. The SF used was as per requirements of ASTM C-1240 [24] and contains a minimum of 85% silicon dioxide (SiO_2) and its specific gravity was 2.26. The maximum size was 12.5 mm for coarse aggregate and the fineness modulus of fine aggregate was 2.7. The length and average diameter of CF used in the current work was 50 mm and 0.3 mm, respectively. The CF of 2% content by mass of cement was used. The reason for selecting the length and content for CF is that most of the literature reported the best performance of CF with 50 cm length and 2% content by mass of cement [10], [7], [25], [26], [27]. The mix design for all the mixes is shown in Table 1. The w/c for CF reinforced concrete was kept relatively higher to achieve proper compaction of the mix along with good workability. At lower w/c of the mix containing CF, proper compaction of the fresh mix was not possible which may result in reduced strength. Since, compaction has more influence on concrete properties, as compared to w/c. A similar approach for the addition of CF in concrete is also reported in the previous studies [10, 23].

Table 1- Mix proportions

Mix Type	Symbols	Cement	Sand	Aggregate	W/C ratio	Silica fume	Coconut fiber
		(Kg/m^3)	(Kg/m^3)	(Kg/m^3)	(-)	(%)	(%)
Control mix	CM-SF0	400	810	810	0.45	0	0
Silica fume concrete	CM-SF10	400	810	810	0.45	10	0
Coconut fiber reinforced concrete	CFRC-SF0	400	810	810	0.50	0	2
Coconut fiber reinforced silica fume based concrete	CFRC-SF10	400	810	810	0.50	10	2

Note: All percentages are by mass of cement.

The mixing of all the mixes was done by the layer's method reported by Ali et al. [10]. Cylinders of 100 mm diameter and 200 mm height were cast for compressive properties. A set of two specimens were cast from each mix type and the average of their result was considered in the analysis. A similar practice of using an average of two specimens is also reported in the previous study [28]. The casting and curing of specimens were done following ASTM standard C192M-16a [29]. The compressive strength test of the cylinders was performed following ASTM C39/C39M-17b standard [30]. For the SEM analysis, the samples were taken from the crushed cylinders after performing the compressive strength test.

3 Results

3.1 Compressive toughness.

The toughness and specific toughness (ST) are used to determine the compressive energy absorption capability of concrete. The area under the stress-strain curve is used to calculate the toughness and the ST is calculated as the ratio of compressive toughness to the compressive strength of the same specimen [31]. The best overall performance was obtained when both SF and CF were used in the same mix as shown in Figure 1. The addition of SF in concrete has shown a significant effect on the enhancement of toughness as well as ST. This enhancement is because of filling the pores in the concrete and the pozzolanic reaction caused by SF. Furthermore, the addition of CF also shown a considerable increase in toughness and ST of coconut fiber reinforced composites. This increase in toughness and ST is due to the bridging effect provide by CF under loading.

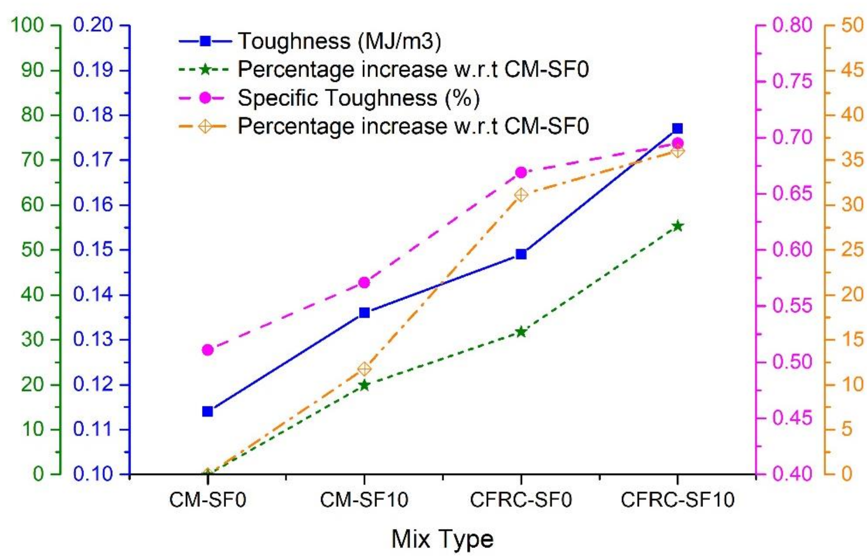

Figure 1: Compressive toughness

3.2 Empirical modeling.

The empirical model is shown in Equation (1) consists of a simple rational power function having parameter A. Figure 2 demonstrates the comparison between normalized stress-strain curves and empirical model curves. The parameter "A" is obtained from fitting the experimental normalized stress-strain curves. The acquired stress-strain curves based on the empirical model are well fitted in accordance with the experimental normalized stress-strain curve. This indicates that the empirical model can obtain a better stress-strain response from the experimental stress-strain curves. The highest correlation coefficients are achieved, i.e. greater than 0.95. This shows that the present model can be applied to predict the response of the compressive stress-strain curve from experimental data.

$$Y = \frac{AX}{A-1+X^{A}} \qquad (1)$$

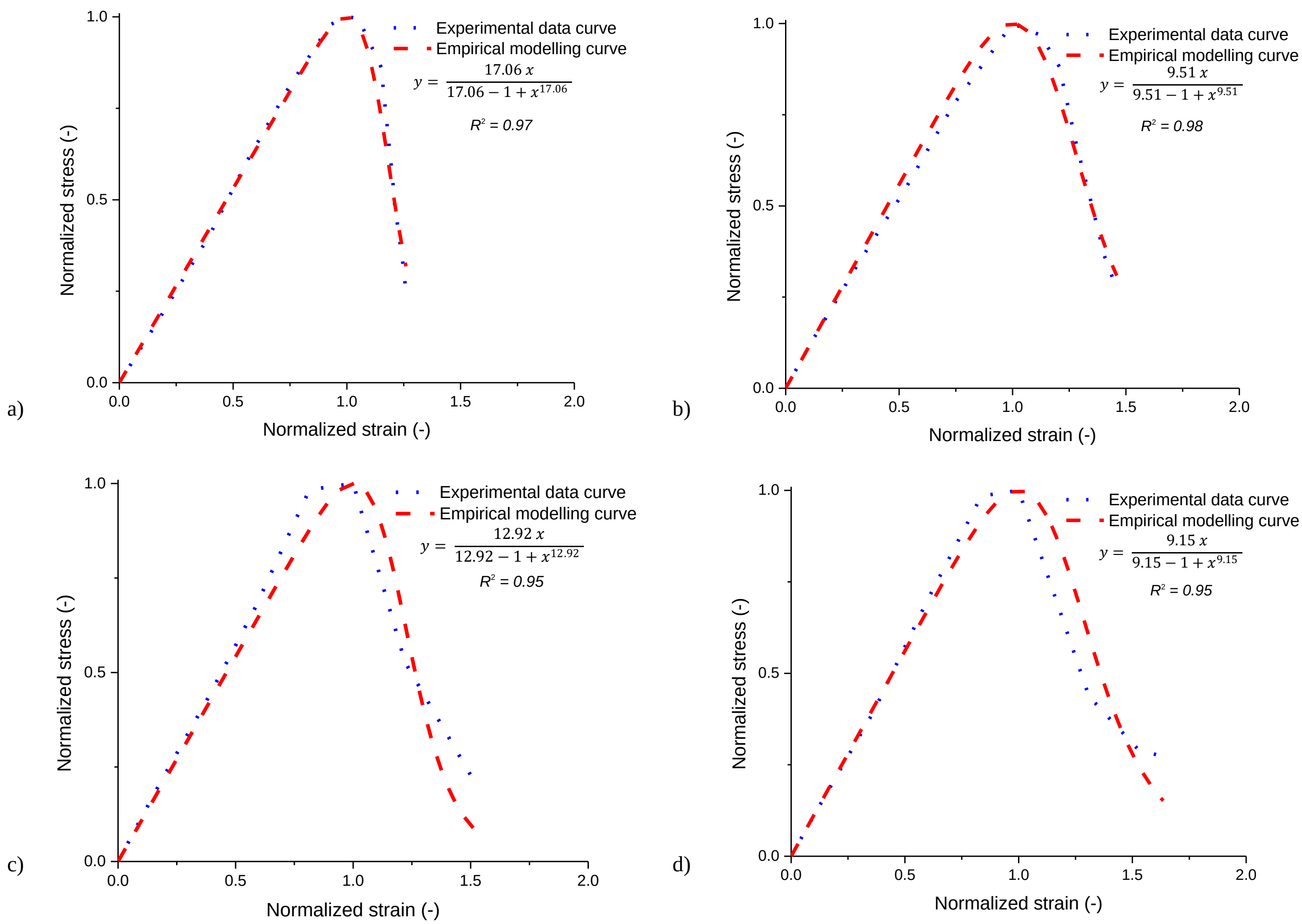

Figure 2: Empirical modelling, a) CM-SF0, b) CM-SF10, c) CFRC-SF0, and d) CFRC-SF10

3.3 Scanning electron microscopy analysis.

SEM analysis was performed to investigate the micro-cracks in the matrix, fiber-cement bonding, cracks in the matrix, and fiber condition before and after pullout from the matrix. The fiber bridging effect due to the incorporation of CF in concrete showed resistance against crack propagation as shown in Figure 3 (a). Also, a proper bond between the CF and matrix can be observed in Figure 3 (b). The SEM images of CF surface before mixing and after pull-out are also presented in Figures 4 (c) and 4 (d), respectively. The surface of CF after pull-out was observed to be damaged. Also, the crack was observed on the surface after fibers pull-out as compared to that of the fiber surface before mixing. The observations of enhanced toughness properties due to CF addition from experimental results were also supported by SEM analysis. Hence, the CF addition in concrete favors its utility to be used in civil engineering applications due to improved performance. The cementitious composites are brittle and there are micro-cracks and voids in the matrix formed during the hydration process. These micro-cracks propagates during loading, become macro-cracks, and ultimately results in the destruction of the structure. So, the failure process starts from the micro-cracks present in the matrix which leads towards material failure. As fibers can provide resistance to the crack propagation by bridging effect. Therefore, fiber addition in the cementitious composites enhanced the mechanical properties of composites by preventing crack expansion. Regarding the damaged surface of coconut fiber, it is recommended for future to develop some treatment methods for the improved surface of coconut fiber that will be beneficial to enhance the bond performance after pull out.

a)

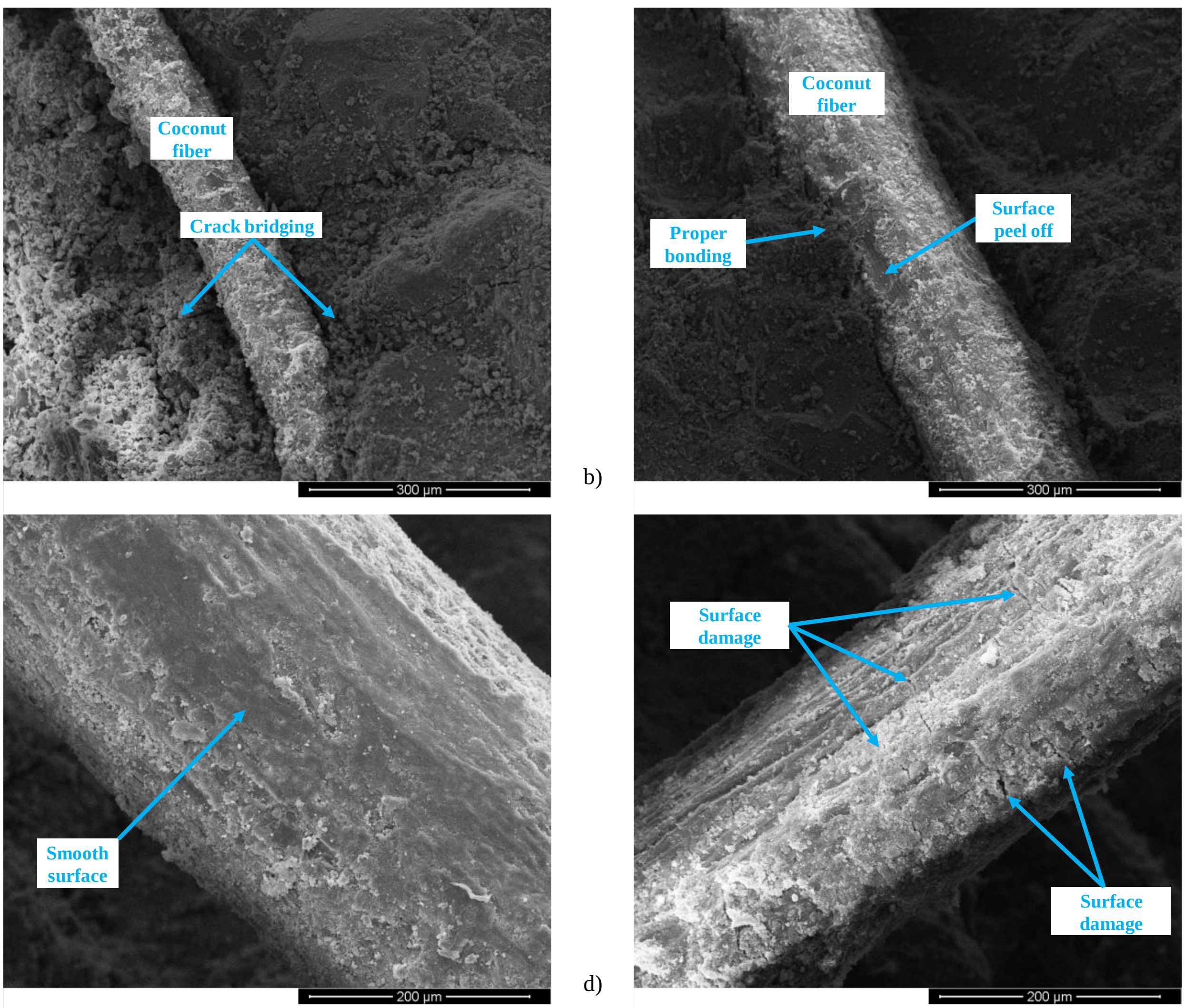

Figure 3: Scanning electron microscopy analysis, a) fiber bridging, b) fiber bonding and surface peel off, c) fiber surface before mixing, and d) fiber surface damage after the pullout

4 Conclusion

In this study, the coconut fiber reinforced silica fume based composites are explored for compressive toughness, empirical modeling, and microstructural analysis. The following conclusion can be drawn:

- The addition of silica fume as well as coconut fiber increased the toughness and specific toughness of concrete.
- The stress-strain curves results obtained from the presented empirical model showed good agreement with the experimental data.
- The SEM analysis showed the fiber bridging, proper bonding, and fiber surface damage and also supported the results of improvement in compressive properties due to the addition of CF in concrete.
- The overall best performance was observed with the addition of both coconut fiber and silica fume in the same mix as compared to that of fiber reinforced concrete reinforced individually with silica fume and coconut fiber.

It is recommended that further studies should be carried out by using more content of CF in concrete for empirical modeling. In addition, it is suggested to investigate the durability of coconut fiber as a concrete fiber reinforcement. Furthermore, the study on the overall pore shape and pore continuity of the coconut fiber material for the concrete application needs to be explored in the future.

Acknowledgment

The authors would like to thank all the people/organizations who helped throughout the research. The careful review and constructive suggestions by the anonymous reviewers are gratefully acknowledged.

References

[1] W. Ahmad, M. Khan, and P. Smarzewski, "Effect of Short Fiber Reinforcements on Fracture Performance of Cement-Based Materials: A Systematic Review Approach," *Materials,* vol. 14, no. 7, p. 1745, 2021.
[2] B.-T. Huang, K.-F. Weng, J.-X. Zhu, Y. Xiang, J.-G. Dai, and V. C. Li, "Engineered/strain-hardening cementitious composites (ECC/SHCC) with a compressive strength over 210 MPa," *Composites Communications,* p. 100775, 2021.
[3] M. Khan, M. Cao, C. Xie, and M. Ali, "Efficiency of basalt fiber length and content on mechanical and microstructural properties of hybrid fiber concrete," *Fatigue & Fracture of Engineering Materials & Structures,* 2021.
[4] L. Li, M. Khan, C. Bai, and K. Shi, "Uniaxial Tensile Behavior, Flexural Properties, Empirical Calculation and Microstructure of Multi-Scale Fiber Reinforced Cement-Based Material at Elevated Temperature," *Materials,* vol. 14, no. 8, p. 1827, 2021.
[5] A. M. Brandt, "Fibre reinforced cement-based (FRC) composites after over 40 years of development in building and civil engineering," *Composite structures,* vol. 86, no. 1-3, pp. 3-9, 2008.
[6] J. Daniel, V. Gopalaratnam, and M. Galinat, "State-of-the-art report on fiber reinforced concrete, ACI Committee 544, Report 544, 1R-96," *American Concrete Institute, Detroit, USA,* 2002.
[7] P. Baruah and S. Talukdar, "A comparative study of compressive, flexural, tensile and shear strength of concrete with fibres of different origins," *Indian concrete journal,* vol. 81, no. 7, pp. 17-24, 2007.
[8] D.-Y. Yoo, N. Banthia, and Y.-S. Yoon, "Ultra-high-performance fiber-reinforced concrete: shrinkage strain development at early ages and potential for cracking," *Journal of Testing and Evaluation,* vol. 45, no. 6, pp. 2061-2070, 2017.
[9] W. Ahmad *et al.*, "Effect of coconut fiber length and content on properties of high strength concrete," *Materials,* vol. 13, no. 5, p. 1075, 2020.
[10] M. Ali, A. Liu, H. Sou, and N. Chouw, "Mechanical and dynamic properties of coconut fibre reinforced concrete," *Construction and Building Materials,* vol. 30, pp. 814-825, 2012.
[11] A. Comite, "544, 2002. State of the Art Report on Fiber Reinforced Concrete Reported (ACI 544.1 R-96 Reapproved 2002)," *ACI Structural Journal,* vol. 96, p. 66.
[12] K. S. Kene, V. S. Vairagade, and S. Sathawane, "Experimental study on behavior of steel and glass fiber reinforced concrete composites," *Bonfring international journal of industrial engineering and management science,* vol. 2, no. 4, pp. 125-130, 2012.

[13] M. Luther, "Silica fume (microsilica) concrete in bridges," *Concrete International*, vol. 15, no. 4, pp. 29-33, 1993.
[14] Y.-C. Ou, M.-S. Tsai, K.-Y. Liu, and K.-C. Chang, "Compressive behavior of steel-fiber-reinforced concrete with a high reinforcing index," *Journal of Materials in Civil Engineering*, vol. 24, no. 2, pp. 207-215, 2012.
[15] V. C. Li, S. Wang, and C. Wu, "Tensile strain-hardening behavior of polyvinyl alcohol engineered cementitious composite (PVA-ECC)," *ACI Materials Journal-American Concrete Institute*, vol. 98, no. 6, pp. 483-492, 2001.
[16] P. Wang, S. Shah, and A. Naaman, "Stress-strain curves of normal and lightweight concrete in compression," in *Journal Proceedings*, 1978, vol. 75, no. 11, pp. 603-611.
[17] S. Fallah-Valukolaee and M. Nematzadeh, "Experimental study for determining applicable models of compressive stress–strain behavior of hybrid synthetic fiber-reinforced high-strength concrete," *European Journal of Environmental and Civil Engineering*, vol. 24, no. 1, pp. 34-59, 2020.
[18] F. Bencardino, L. Rizzuti, G. Spadea, and R. N. Swamy, "Stress-strain behavior of steel fiber-reinforced concrete in compression," *Journal of Materials in Civil Engineering*, vol. 20, no. 3, pp. 255-263, 2008.
[19] L. Li, M. Cao, C. Xie, and H. Yin, "Effects of CaCO3 whisker, hybrid fiber content and size on uniaxial compressive behavior of cementitious composites," *Structural Concrete*, vol. 20, no. 1, pp. 506-518, 2019.
[20] M. Cao and L. Li, "New models for predicting workability and toughness of hybrid fiber reinforced cement-based composites," *Construction and Building Materials*, vol. 176, pp. 618-628, 2018.
[21] S. S. Munawar, K. Umemura, and S. Kawai, "Characterization of the morphological, physical, and mechanical properties of seven nonwood plant fiber bundles," *Journal of Wood Science*, vol. 53, no. 2, pp. 108-113, 2007.
[22] M. Ali, X. Li, and N. Chouw, "Experimental investigations on bond strength between coconut fibre and concrete," *Materials & Design*, vol. 44, pp. 596-605, 2013.
[23] M. Khan, A. Rehman, and M. Ali, "Efficiency of silica-fume content in plain and natural fiber reinforced concrete for concrete road," *Construction and Building Materials*, vol. 244, p. 118382, 2020.
[24] ASTM, "ASTM C1240: Standard specification for silica fume used in cementitious mixtures," ed: ASTM International West Conshohoken, PA, USA, 2014.
[25] M. Khan and M. Ali, "Effectiveness of hair and wave polypropylene fibers for concrete roads," *Construction and Building Materials*, vol. 166, pp. 581-591, 2018.
[26] M. Khan and M. Ali, "Improvement in concrete behavior with fly ash, silica-fume and coconut fibres," *Construction and Building Materials*, vol. 203, pp. 174-187, 2019.
[27] U. A. Khan, H. M. Jahanzaib, M. Khan, and M. Ali, "Improving the Tensile Energy Absorption of High Strength Natural Fiber Reinforced Concrete with Fly-Ash for Bridge Girders," in *Key Engineering Materials*, 2018, vol. 765: Trans Tech Publ, pp. 335-342.
[28] A. Zia and M. Ali, "Behavior of fiber reinforced concrete for controlling the rate of cracking in canal-lining," *Construction and Building Materials*, vol. 155, pp. 726-739, 2017.
[29] A. C192, "ASTM C192/C192M—16a standard practice for making and curing concrete test specimens in the laboratory," *ASTM Standard Book*, pp. 4-9, 2016.
[30] C. ASTM, "Standard test method for compressive strength of cylindrical concrete specimens," *Chủ biên*, 2012.
[31] G. M. Chen, Y. H. He, H. Yang, J. Chen, and Y. Guo, "Compressive behavior of steel fiber reinforced recycled aggregate concrete after exposure to elevated temperatures," *Construction and Building Materials*, vol. 71, pp. 1-15, 2014.

s

3[rd] Conference on Sustainability in Civil Engineering (CSCE'21)
Department of Civil Engineering
Capital University of Science and Technology, Islamabad Pakistan

IMPACT OF CHOPPED BASALT FIBRES ON THE MECHANICAL PROPERTIES OF CONCRETE

[a] Rabee Shamass*, [b] Aziz Urahman Hakimi, [c] Vireen Limbachiya

a: Civil and Building Services Engineering, London South Bank University, shamassr@lsbu.ac.uk
b: School of Civil, Environmental & Geomatic Engineering, University College London, aziz.hakimi.20@ucl.ac.uk
c: Civil and Building Services Engineering, London South Bank University, limbachv@lsbu.ac.uk
* Corresponding author: Email ID: shamassr@lsbu.ac.uk

Abstract- Basalt fibre is a novel inorganic fibre which is produced from basalt rock. In this study the impact of chopped basalt fibres on the concrete workability, compressive and tensile strength, and concrete's modulus of rupture at 7 and 28-days was investigated. The concrete used in this research was normal strength concrete with a target compressive strength of 30/37 MPa. In this research, fibre reinforced concrete samples were produced using basalt chopped fibres of two quantities (4 kg/m^3 and 8 kg/m^3) and three different fibre lengths, namely 25.4-mm, 12.7-mm, and 6.4-mm. The test findings revealed that slump decreased as the quantity of fibres increased and shorter fibres were used. The mechanical properties of concrete were affected by the fibre dosage and length. Overall, the results indicated that adding chopped basalt fibres improved the compressive, tensile, and flexural strength of concrete, particularly at early age, while slightly reducing the compressive strength at 28-days by an average of 3.9%. The results indicated that adding 4 kg/m^3 of 25.4-mm long chopped basalt fibre into concrete provided the best performance of concrete in compressive and tensile strength, and modulus of rupture.

Keywords- Basalt fibres; Fibre reinforced concrete; Mechanical properties; workability

1. Introduction

Civil engineers are keen on using construction materials that are cost effective, environmentally friendly, and robust. Concrete is known as one of the most highly consumed construction materials and plays a vital role in many aspects of everyday life. Although the plain concrete is strong in compression, it is weak in tension. Microcracks are formed in concrete during hardening stage [1] and they grow and extend in the concrete matrix when concrete is exposed to external loads. In order to sustain the developed tensile stresses, an addition of reinforcing elements in plain concrete is needed. Mixing relatively short and closely spaced fibres can constrain the development and formation of the cracking, hence, enhancing the mechanical and dynamic characteristics of plain concrete [2]. The reduction of crack width and numbers in the concrete matrix and the strength gaining are due to the bridging effect in which the fibres inside the cracks form a kind of bridges between the separated crack's edges [3], as seen in the Figure 1.

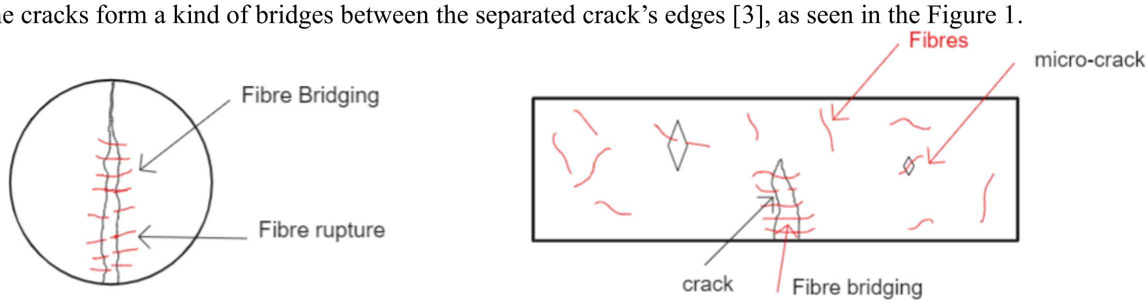

(a) (b)

Figure 1: Fibre bridging effect (a) concrete spitting, (b) concrete rupture.

The most commonly used fibres in concrete are steel and polyethylene fibres but they have a great amount of embodied energy. Among the disadvantages of using steel fibres is high susceptibility to corrosion, high specific gravity, high cost of raw material and non-uniform distribution within the concrete mixture [4]. Basalt fibres are considered a unique product made from basalt rock, a natural material that is found in volcanic rocks. They are a relatively new composite material characterized by their high corrosion and thermal resistance, their light weight (one-third of the steel weight) and high strength [5]. Basalt fibres have no toxic reaction with air or water and have no chemical reactions when they encounter other chemicals which may damage health or the environment. Basalt fibres have an excellent alkali resistance, and excellent acoustic and thermal properties [6]. Basalt fibres do not need any chemical additives or hazardous materials in the melting process; hence they are easier and safer to produce [7]. Their recyclability is also easier, unlike glass and carbon fibres which require high temperature or chemicals to recycle [8], hence basalt fibres are more environmentally friendly.

Research studies have investigated the influence of chopped basalt fibres on the mechanical properties of basalt fibre reinforced concrete (BFRC). Ayub et al. [9] investigated the effect of various dosages of chopped basalt fibres on the mechanical properties of high-performance fibre reinforced concrete. Results showed that adding chopped basalt fibres slightly improved the compressive strength of concrete while there was significant improvement in the tensile and flexural strength after 28-days. Similarly, Kizilkanat el at. [10] found that adding 0.25% of chopped basalt fibres in concrete slightly increased the compressive strength while adding 1% of fibres increased the tensile strength by 40%. In another research study, Iyer et al. [11] investigated the effect of different dosages and fibre lengths on the compressive strength and modulus of rupture of concrete at 28-days. The study found that 36-mm-long fibre and a fibre amount of 8 kg/m^3 were optimum to achieve enhancement in compressive and tensile strength of concrete. The study also found that workability decreased as the fibre length and dosage were increased. Similar research was conducted by Tumadhir and Borhan [12] using slightly shorter chopped basalt fibres (25.4 mm) with different dosage, the results indicated that the concrete's compressive strength increased with increasing chopped basalt fibres dosage up to 0.3% volume fraction. Nevertheless, when the dosage of fibres was increased to very high levels such as 0.5%, the compressive strength decreased. Ramakrishnan et al. [13] conducted an experimental study using 13-mm long chopped basalt fibres with contents varying between 0.1 to 0.5% volume fraction. The study concluded that when large dosage of fibre was added to concrete, the impact and toughness strength of the concrete were increased. However, the addition of chopped basalt fibres did not improve the compressive and flexural strengths of concrete at 28-days. Xinzhong et al. [14] concluded that the optimal basalt fibre content and length were 0.15% and 12 mm, respectively, at which the compressive strength of concrete at 7- and 28-days increased by 62.5% and 25.2%, respectively, while the tensile strength at 28-days increased by 13.26%. Jiang et al. [15] found that using 12 mm long fibre increased the compressive strength, splitting tensile and flexural strength of concrete at 28-days. They concluded that the suitable amount of the fibres was about 0.3% by volume. In contrast, Dias and Thaumaturgo [16] reported that the addition of 0.5% of chopped basalt fibres reduced the compressive strength of concrete at 28-days by 3.9%. Similarly, Jalasutram et al. [17] found that adding basalt fibres marginally reduced the compressive strength of concrete while it enhanced the tensile strength and flexural toughness.

It can be noted that the impact of length and dosage of basalt fibres on the physical and mechanical properties of concrete at 7- and 28-days is inconsistent, and further experimental investigations are required to better understand their influence on plain concrete. Therefore, the main aim of this study is to investigate the impact of chopped basalt fibres' length and dosage on the mechanical properties of concrete at early age and 28-days. The fundamental properties of BFRC such as slump, compressive strength, splitting tensile strength, and modulus of rupture are tested and analysed in this study. Two chopped basalt fibres dosages were used, namely 4 kg/m^3 and 8 kg/m^3 and three fibres lengths were used, 6.4, 12.7 and 25.4-mm, as shown in Figure 2. This study suggests optimum fibre length and dosage to achieve the best concrete performance.

2. Experimental Program

A C30/37 concrete mix was designed using BRE Concrete Mix Design [18]. The details of the mix proportions are summarised in Table 1. The maximum aggregates size used was 10 mm. The moisture content of the aggregates could change due to unpredicted weather. To avoid the discrepancies in the moisture content and their effect on the properties of the concrete, the coarse aggregates and sand were air dried inside the laboratory. A number of concrete mix trails were conducted in which the basalt chopped fibres were added either in a dried mix (i.e., after mixing the sand, aggregates and cement) or a wet mix (i.e., after mixing water with dried aggregates) to achieve satisfactory results. It was decided to mix the sand, coarse aggregates, and cement for 2-3 minutes, then add water and mix for 2-3 minutes, thereafter, the chopped basalt fibres were added and mixed for 5 minutes.

Seven mixes were prepared to test the compressive, tensile and rupture strength of BFRC at 7- and 28-days. There were two concrete mixes with 25.4-mm length fibres (4F-25.4, 8F-25.4), two concrete mixes with 12.7 -mm length fibres (4F-12.7, 8F-12.7), two mixes with 6.4 -mm length fibres (4F-6.4, 8F-6.4) and one concrete mix without fibres acting as a control mix (Plain). Each concrete mix is named based on the dosage of the basalt chopped fibres added into the concrete mix per m^3 (4 kg/m^3 and 8 kg/m^3) and the length of the basalt chopped fibres (25.4-mm, 12.7-mm and 6.4-mm). For example, 4F-25.4 denotes for a mix with 4 kg/m^3 chopped fibres with 25.4-mm length. Six standard 100×100×100 mm cubes were produced for the compressive strength test, three Ø150×300 mm cylinders for the splitting tensile strength test and three 100×100×500 mm prismatic beams for the modulus of rupture test, according to BS EN12390: Testing hardened concrete. The moulds were removed on the following day and the concrete samples were stored in a curing tank at 20°c.

Table 1: Concrete mix design.

Target concrete grade	**w/c ratio**	**Cement (kg/m^3)**	**Sand (kg/m^3)**	**Coarse aggregate (kg/m^3)**	**Max Aggregate size (mm)**	**Chopped basalt fibre (kg/m^3)**
C30/37	0.54	463	700	927	10	4 and 8

25.4-mm chopped fibres

12.7-mm chopped fibres

6.7-mm chopped fibres

Figure 2: The chopped basalt fibre used in this study.

3. Results and Discussions

3.1 Concrete Workability

The workability of fresh concrete can be affected by many factors including aggregate properties such as shape, size and grading, water-to-cement ratio and the added fibres. In this study, the slump test was conducted according to BS EN 12350: Testing fresh concrete to determine the fresh concrete workability. Table 1 illustrates the influence of the fibres' length and dosage on the concrete workability. The workability in general decreases with increasing the quantity of basalt fibres for all fibre lengths used in this study. It can be noted that adding fibres dramatically reduces the concrete workability. For plain concrete, the slump was 245 mm. When adding 4 kg/m^3 of 25.4 -mm, 12.7 -mm and 6.4 -mm length basalt fibres, the slump reduced by 59%, 55% and 37%, respectively. Due to the high fibres surface area and content, the friction between fibres and cement paste increases, resulting in reduction of slump. Results obtained from the tests showed that workability decreased when shorter fibres were being used and as the fibres contents increases. For instance, adding 8 kg/m^3 of 25.4 -mm and 6.4 -mm fibres reduced the slump by 65%, 74% respectively. For low fibres content (i.e., 4 kg/m^3) the slump for concrete mix with 25.4-mm fibres was lower than the slump for the mix with 6.4-mm fibres. The assumption is that for shorter fibres being used with large fibres dosage in the mix, there are larger fibre distribution density and more fibres per unit volume. Therefore, the fibres are harder to distribute consistently in the concrete matrix, resulting in reduction in concrete workability [15]. Although the workability of concrete was reduced with the addition of fibres, no difficulties was found in placing and consolidating the fresh concrete using the table vibrator. It was observed that the fibres were uniformly distributed throughout the concrete without balling, bleeding, or segregation.

3.2 Compressive Strength

Table 2 shows the compressive strength results and the strength-effectiveness (%) for each BFRC concrete mix at 7- and 28-days. The strength-effectiveness of BFRC is more evident at concrete early age than at 28-days. In comparison to plain concrete, adding fibres improved the compressive strength of concrete at 7-days by an average of 28.6%. The highest strength-effectiveness was achieved when 8 kg/m^3 of 6.4 -mm basalt chopped fibres was added (38.7%), while the lowest strength improvement was achieved when 4kg/m^3 of 25.4 -mm fibres was added (20.8%). In the presence of basalt chopped fibres, the concrete compressive strength at 28-days tended to decrease by an average of 3.9%. There is a negligible reduction of the compressive strength at 28-days for 8F-6.4 (0.5%). The compressive strength reduction of BFRC at 28-days with 4 kg/m^3 and 8 kg/m^3 dosage fibres ranges from -3.5% to -7.0% and from -0.5% to -3.8%, respectively. The Scanning Electron Microscope images conducted by Jiang et al. [15] indicated that there was a good bonding between the fibres and cement matrix at early age while there was bond degradation at 28-days. This confirmed that the aging of the interface between the cementitious matrix and the fibres reduced the compressive strength of concrete at 28-days. Similar results were reported by Dias and Thaumaturgo [16] in which the inclusion of basalt chopped fibres slightly reduced the concrete compressive strength by 3.9%. The results also showed that fibre length had an effect on the strength-effectiveness of BFRC. For instance, for BFRC with 8 kg/m^3, as the fibre length reduces, the concrete compressive strength at 7-days enhances and the change in compressive strength at 28-days becomes negligible, as for 8F-6.4.

Table 2: Concrete slump test and compressive strength for different mixes

Mix	Slump (mm)	Compressive strength (MPa) 7-days		Compressive strength (MPa) 28-days	
		Measured	strength-effectiveness (%)	Measured	strength-effectiveness (%)
Plain	245	21.2	-	37.2	-
4F-25.4	100	28.1	32.5	35.8	-3.8
8F-25.4	85	25.6	20.8	35.1	-5.6
4F-12.7	110	25.9	22.2	34.6	-7.0
8F-12.7	75	27.6	30.2	36.1	-3.0
4F-6.4	155	26.9	26.9	35.9	-3.5
8F-6.4	65	29.4	38.7	37	-0.5

3.3. Splitting Tensile strength

Table 3 shows the tensile strength of concrete and the strength-effectiveness of BFRC at 7- and 28-days. The results show that the concrete tensile strength at 7- and 28-days increases with addition of basalt chopped fibres, except for the mix 4F-12.7 for which the tensile strength at 28-days slightly reduces by 4.2%. The increase in the tensile strength is assumed to be due to the bridging effect of the fibres which delays the development of macro cracks. In comparison to the plain concrete, the tensile strength for BFRC with 4 kg/m^3 dosage of 25.4-mm basalt fibres at 7-days and 28-days increased by 26.4% and 14.4 %, respectively. In general, the concrete tensile strength at 7-days increased as the amount of chopped basalt fibres increased, except for the BFRC with 25.4-mm length fibres. For instance, as the amount of fibres increases from the 4 kg/m^3 to 8 kg/m^3 the tensile strength at 7-days for BFRC with 12.7 -mm fibres increases from 7.7% to 24.7%, respectively, and from 15.4% to 21.4%, respectively, for BFRC with 6.4 -mm fibres, in comparisons to plain concrete. A similar trend is observed at 28-days as the quantity of fibres increases from 4 kg/m^3 to 8 kg/m^3 the tensile strength at 28-days increases from 14.4% to 4.2%, respectively, for BFRC with 25.4.7 -mm fibres and from 1.9% to 3.4% for BFRC with 6.4 -mm fibres, in comparisons to plain concrete. Furthermore, the results showed in general an increase in tensile strength for an increasing in fibres length, although the trend is not obvious. In comparison to the plain concrete, as the length of fibres increases from 6.4 -mm to 25.4 -mm the tensile strength of BFRC increases from 15.4% to 26.4% at 7-days, respectively, and from 1.9% to 14.4% at 28-days, respectively, for 4 kg/m^3 fibre dosage. The reason could be that the longer of the fibres being used, the higher of the pulling-out resistance of the fibres from the cement matrix and the stronger of the bridging effect of the fibres, which contributes to the tensile strength improvement.

Table 3: Concrete tensile strength for different mixes

Mix	Tensile strength (MPa) 7-days		Tensile strength (MPa) 28-days	
	Measured	strength-effectiveness (%)	Measured	strength-effectiveness (%)
Plain	1.82	-	2.64	-
4F-25.4	2.3	26.4	3.02	14.4
8F-25.4	2.06	13.1	2.75	4.2
4F-12.7	1.96	7.7	2.53	-4.2
8F-12.7	2.27	24.7	2.66	0.8
4F-6.4	2.10	15.4	2.69	1.9
8F-6.4	2.21	21.4	2.73	3.4

3.4 Modulus of Rupture (Flexural Strength)

Table 4 shows the results of the modulus of rupture and strength-effectiveness of BFRC at 7- and 28-days. Previous research indicated that adding fibres into concrete enhanced the modulus of rupture of BFRC. Kizilkanat et al. [10] stated that addition of basalt or glass fibre had beneficial effects on the flexural strength of concrete when compared with plain concrete. As expected, all BFRC specimens tested in this study showed an increase in the modulus of rupture, in comparison to plain concrete specimens. As for the tensile strength, the strength-effectiveness of BFRC is more noticeable at an early age of concrete with an average strength enhancement of 12.7%. The highest strength improvement at 7-days is achieved for BFRC with 8 kg/m^3 of 12.7 -mm basalt fibres (28.2%). When compared with plain concrete, the modulus of rupture at 7-days for BFRC with 12.7 and 6.4 -mm basalt fibres increased from 8.7% to 28.2% with increasing the dosage of basalt fibre from 4 kg/m^3 to 8 kg/m^3. The length of fibres has a significant effect on the modulus of rupture. For BFRC mixes with 4 kg/m^3 fibres, as the length of fibres increases from 6.4 -mm to 25.4 -mm, the strength at 7-days increases from 8.7% to 14.6% respectively while the strength at 28-days increases from 8.8% to 17.1%, respectively, in comparisons to plain concrete. On the other hand, for higher amount of basalt fibres, the modulus of rupture for BFRC with 24.5-mm fibres is lower than for BFRC with 12.7-mm fibres. As explained before that longer fibres provide more noticeable bridging effect. However, for high content of fibres, it is more difficult for longer fibres to distribute uniformly in cementitious composites, hence the bridging effect of fibres may be affected in some regions of the concrete mix.

Table 4: concrete tensile strength for different mixes

Mix	Modulus of rupture (MPa) 7-days		Modulus of rupture (MPa) 28-days	
	Measured	strength-effectiveness (%)	Measured	strength-effectiveness (%)
Plain	3.55	-	4.2	-
4F-25.4	4.07	14.6	4.92	17.1
8F-25.4	3.63	2.3	4.49	6.9
4F-12.7	3.88	9.3	4.59	9.3
8F-12.7	4.55	28.2	4.76	13.3
4F-6.4	3.86	8.7	4.57	8.8
8F-6.4	4.00	12.7	4.32	2.9

4. Conclusion

This study is an experimental investigation on the effect of chopped basalt fibres on the compressive, tensile, and flexural strength of BFRC at 7- and 28-days. Two dosages of fibres were used, 4 kg/m^3 and 8 kg/m^3 and three lengths of fibres were investigated, 25.4 -mm, 12.7 -mm and 6.4 -mm. Based on results obtained, it can be concluded that:

- The workability of fresh concrete decreased as the amount of fibres increased and when using shorter fibres. The slump is lower for mix with longer fibre length and lower content.
- Experiment results showed that inclusion of basalt fibres enhanced the compressive strength of concrete at 7-

days by 20% to 38.7%, depending on the fibre dosage and length. However, slight reduction in compressive strength of BFRC at 28-days was observed, with an average of 3.9%. BFRC with 8 kg/m^3 of 6.4 -mm basalt fibres performed the best in compression for which negligible reduction of concrete strength at 28-days and 38.7% strength enhancement at 7-days were observed.

- Generally, the tensile strength of BFRC was increased at 7- and 28-days. The average strength-effectiveness of tensile strength of BFRC at 7-days was 18.1% while it was 3.2% at 28-days. BFRC with 4 kg/m^3 of 25.4-mm basalt fibres performed the best in tension for which the strength at 7- and 28 days was increased by 26.4% and 14.4%, respectively, in comparison to plain concrete.
- Experiment results showed that inclusion of basalt fibres enhanced the modulus of rupture of concrete at 7-days by 2.3% to 28.2%, and at 28-days by 2.9% to 17.1%, depending on the fibre dosage and length. The average strength-effectiveness of modulus of rupture of BFRC at 7- and 28-days was 12.6% and 9.7%, respectively. BFRC with 8 kg/m^3 of 12.7 -mm basalt fibres performed the best for which the flexural strength at 7- and 28 days was increased by 28.2% and 13.3%, respectively, in comparison to plain concrete.

Acknowledgements

The authors would like to thank Access to Innovation A2I, a match funded project between London South Bank University and ERDF, for funding the tests. Furthermore, they would also like to thank the technicians Graham Bird and Paul Elsdon for their continuous support in the Laboratory. Basalt Technologies UK Limited is acknowledged for supplying the chopped basalt fibres.

References

[1] M.V. Mohod, "Performance of steel fiber reinforced concrete". *Int. J. of Eng. Sci.*, *vol. 1 no. 12*, p.1-4., 2012

[2] Y.-R. Zhao, L. Wang, Z.-K. Lei, X.-F. Han, and J.-N. Shi, "Study on bending damage and failure of basalt fiber reinforced concrete under freeze-thaw cycles," *Constr. Build. Mater.*, vol. 163, pp. 460–470, 2018.

[3] M. Wydra, P. Dolny, G. Sadowski, and J. Fangrat, "Flexural behaviour of cementitious mortars with the addition of basalt fibres," *Materials (Basel)*, vol. 14, no. 6, p. 1334, 2021.

[4] C. Ipbüker, H. Nulk, V. Gulik, A. Biland, and A. H. Tkaczyk, "Radiation shielding properties of a novel cement–basalt mixture for nuclear energy applications," *Nucl. Eng. Des.*, vol. 284, pp. 27–37, 2015.

[5] R. Shamass and K. A. Cashell, "Experimental investigation into the flexural behaviour of basalt FRP reinforced concrete members," *Eng. Struct.*, vol. 220, no. 110950, p. 110950, 2020.

[6] V. J. John and B. Dharmar, "Influence of basalt fibers on the mechanical behavior of concrete—A review," *Struct. Concr.*, vol. 22, no. 1, pp. 491–502, 2021.

[7] Q. Fu *et al.*, "Dynamic compressive mechanical behaviour and modelling of basalt–polypropylene fibre-reinforced concrete," *Arch. Civ. Mech. Eng.*, vol. 18, no. 3, pp. 914–927, 2018.

[8] J. Sim, C. Park, and D. Y. Moon, "Characteristics of basalt fiber as a strengthening material for concrete structures," *Compos. B Eng.*, vol. 36, no. 6–7, pp. 504–512, 2005.

[9] T. Ayub, N. Shafiq, and M. F. Nuruddin, "Effect of chopped Basalt fibers on the mechanical properties and microstructure of high performance fiber reinforced concrete," *Adv. Mater. Sci. Eng.*, vol. 2014, pp. 1–14, 2014.

[10] A. B. Kizilkanat, N. Kabay, V. Akyüncü, S. Chowdhury, and A. H. Akça, "Mechanical properties and fracture behavior of basalt and glass fiber reinforced concrete: An experimental study," *Constr. Build. Mater.*, vol. 100, pp. 218–224, 2015.

[11] Iyer, S. Y. Kenno, and S. Das, "Performance of fiber-reinforced concrete made with basalt-bundled fibers," *Adv. Civ. Eng. Mater.*, vol. 5, no. 1, p. 20150027, 2016.

[12] M. Tumadhir and Borhan, "Thermal and Mechanical Properties of basalt fibre reinforced concrete," *International Journal of Civil and Environmental Engineering*, vol. 7, no. 4, pp. 334–337, 2013.

[13] V. Ramakrishnan, N. S. Tolmare, and V. B. Brik, "Performance evaluation of 3-D basalt fiber reinforced concrete & basalt rod reinforced concrete." 1998.

[14] W. Xinzhong *et al.*, "Experimental study on the axial compression of short basalt fiber reinforced concrete columns with spiral stirrups," *J. Eng. Sci. Technol. Rev.*, vol. 10, no. 1, pp. 55–60, 2017.

[15] C. Jiang, K. Fan, F. Wu, and D. Chen, "Experimental study on the mechanical properties and microstructure of chopped basalt fibre reinforced concrete," *Mater. Eng.*, vol. 58, pp. 187–193, 2014.

[16] D. P. Dias and C. Thaumaturgo, "Fracture toughness of geopolymeric concretes reinforced with basalt fibers," *Cem. Concr. Compos.*, vol. 27, no. 1, pp. 49–54, 2005.

[17] S. Jalasutram, D. R. Sahoo, and V. Matsagar, "Experimental investigation of the mechanical properties of basalt fiber-reinforced concrete: JALASUTRAMet al," *Struct. Concr.*, vol. 18, no. 2, pp. 292–302, 2017.

[18] D. C. Teychenne, *Design of normal concrete mixes: (BR 331)*, 2nd ed. Bracknell, England: IHS BRE Press, 1997.

3rd Conference on Sustainability in Civil Engineering (CSCE'21)
Department of Civil Engineering
Capital University of Science and Technology, Islamabad Pakistan

EVALUATING THE FLEXURAL PERFORMANCE OF FUNCTIONALLY GRADED CONCRETE USING STEEL FIBRES AND RECYCLED AGGREGATES

[a] Sabireen*, [b] Faheem Butt,

a: Department of Civil Engineering, University of Engineering and Technology Taxila, Pakistan
sabireen@students.uettaxila.edu.pk
b: Department of Civil Engineering, University of Engineering and Technology Taxila, Pakistan
faheem.butt@uettaxila.edu.pk
* Corresponding author: Email ID: sabireen@students.uettaxila.edu.pk

Abstract- The objective of this research is to compare the flexural performance of functionally graded concrete (FGC) to that of conventional Steel fibres reinforced concrete (SFRC). In this study, four concrete mixes were prepared, containing one SFRC mix, and three combinations of FGC mixes. The hooked end steel fibres were used in 0.75 % of the total mix volume in the SFRC and FGC mixes. In FGC mixes, recycled plastic aggregates (RPA) and recycled concrete aggregates (RCA) have been substituted for natural aggregates by 15% by weight. Under third-point loading, the flexural performance of beam-shaped specimens with the dimensions of 100x100x500mm was assessed. In addition, an Ultrasonic pulse velocity test was conducted on cubic specimens having dimensions of 100x100x 100mm to find the quality of concrete under the influence of steel fibres and recycled aggregates. According to the findings, FGC has a lower post-cracking flexural efficiency than ordinary SFRC. Furthermore, UPV values of FGC are higher than conventional SFRC. This research reveals the economic advantages of using the functionally graded materials (FGMs) concept to minimize the use of fibres.

Keywords- Recycled concrete aggregate, Recycled plastic aggregate, functionally graded concrete, Steel fibres reinforced concrete, Sustainability.

1 Introduction

Nowadays concrete is globally used for construction purposes. The high compressive strength, workability, and durability of ordinary Portland cement concrete (PCC) are some of the recognition factors. The PCC contributes satisfactory performance in the compression zone and no requirement of giving fibres as reinforced in this zone. It is, however, a brittle material with poor tension efficiency (about 10% of compressive strength) [1].To avoid the brittleness of PCC, various types of fibres are frequently utilized as reinforcement. Fibre-reinforced concretes (FRC) can boost the concrete's toughness, flexural strength, and failure mode [1]. Multi-scale fibres with macro fibre and calcium carbonate (CaCO3) whisker (CW) will increase the mechanical properties and peak strain energy of cementitious composites substantially [2], [3]. Besides, numerous studies have revealed that fibres might somewhat or entirely replace conventional reinforcement [4]. According to researchers, the dispersion of fibres over the entire volume of the concrete portion makes it uneconomical material [5]. In order to minimize the use of fibres, functionally graded concrete (FGC) was introduced. Functionally graded materials (FGMs) were first suggested by materials scientists in 1984 [6]. Functionally Graded concrete (FGC) is a layer-by-layer fabrication technique that produced with a gradation in mechanical properties to achieve an intended function. On the other hand, large volumes of waste are dumbed such as plastics and demolition wastes which badly affect the natural environment. Electronic waste in developing countries has the potential to damage people's health and cause pollution [7]. The idea of reusing demolition waste and plastics to generate RCA and RPA is strongly recommended to solve these issues.

The addition of fibres to ordinary PCC will increase its flexural strength. Substituting natural aggregates for recycled aggregates (RCA and RPA) in concrete can help to limit environmental harm. Due to its ecological and economic benefits, Almeshal et al.presented a study of 103 articles and concluded that reusing plastic waste in the manufacture of concrete or mortar appears to be an environmentally sustainable alternative for getting rid of plastic waste [8]. Recycled concrete aggregates make up a large portion of building and demolition waste, and their recycling is important for long-term construction sustainability [9]. A functionally graded concrete (FGC) concept was developed to combine the benefits of fibres and recycled aggregates. FGMs have the ability to combine different materials to form a continuous monolithic structure [10].In comparison to a standard single-layered lining, the outcomes show that functionally graded lining has a higher elastic ultimate bearing potential [11]. Further study shows that under cyclic loading FGC performs better than ordinary FRC [12].

The aim of this study is to compare the flexural performance of functionally graded concrete (FGC) by using Steel fibres and recycled aggregates (RPA, RCA) to that of conventional SFRC. There is a lack of research on the effects of combining recycled aggregates and fibres [13]. Therefore in this research three types of aggregates were used: natural coarse aggregate (NCA), recycled concrete aggregate (RCA), and recycled plastic aggregate (RPA).In this study, steel was used as fibre-reinforced material. This study presents the models of steel fibre reinforced concrete (SFRC) (A) and FGC concrete mixes (B, C, D). FGC mixes consists of Portland cement concrete (PCC) +SFRC (B), recycled concrete aggregate (RCA) +SFRC (C) and recycled plastic aggregate concrete (RPAC) +SFRC (D). As a reference mix, the SFRC mix was used. The basic third-point loading test was executed to compare the flexural performance of FRC and FGC. Whereas, the Ultrasonic pulse velocity test was performed to determine concrete's quality under the influence of fibres and recycled aggregates. The results of each mix are discussed, and conclusions are presented.

2 Experimental Procedures

2.1 Materials

Ordinary Portland Cement (OPC) according to ASTM C-150 was utilized in this study. And ordinary drinkable water was chosen. As a fine aggregate, Natural sand of the Lawrencepur brand was used. Three types of coarse aggregates were used: natural coarse aggregate (NCA), recycled concrete aggregate (RCA), and recycled plastic aggregate (RPA). The NCA of the Margalla brand was used. Recycled concrete aggregate (RCA) was obtained through the manual crushing of tested specimens of concrete. As a plastic aggregate, recycled electronic waste (E-waste) was used. Fig 2(a) depicts the E-waste aggregate. The particle size distributions (PSDs) are shown in Fig 1.

In this study Steel fibre (MasterFibre S 65) was used as reinforcement. The MasterFibre S 65 is a hooked end that complies with ASTM A820, Type 1. The length (L) of this fibre is 35 mm, the aspect ratio (L/D) is 64 and the tensile strength is 1345 MPa. Bonding agent 'ULTRA SBR latex' complying with ASTM C1059-86 was utilized. It was produced in the ratio of SBR: water: cement 1:1:3. Fig 2(b) depicts the steel fibres utilized in this study.

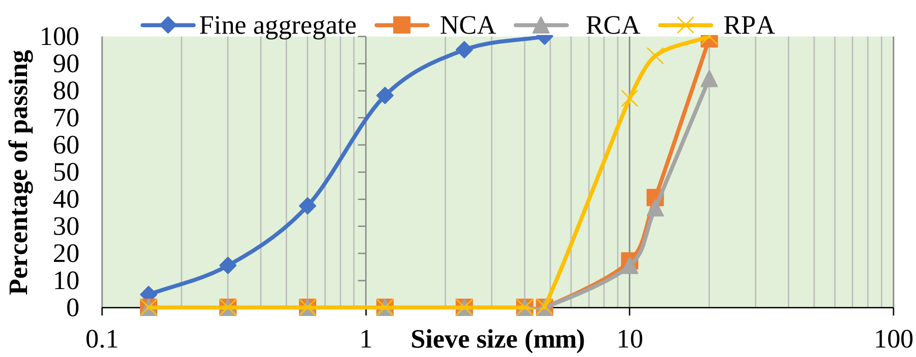

Figure 1: Particle size distributions (PSDs) of fine aggregates, NCA, RCA and RPA

2.2 Concrete mixes and testing procedures

Figure 3 depicts the models of four concrete mixes used in this research. These models consist of steel fibre reinforced concrete (SFRC) (A) and functionally graded concrete (FGC) mixes (B, C, D). FGC is made up of two layers of equal thickness. FGC group embraces Portland cement concrete (PCC) +SFRC (B), recycled concrete aggregate (RCA) +SFRC (C) and recycled plastic aggregate concrete (RPAC) +SFRC (D). Steel fibres were used to strengthen the bottom layer of all FGC mixes. Because concrete pavements are often bent, and thus the upper and lower layers are subjected to compression and tension, respectively [14]. Subsequently, PCC carries comparatively little tension loads; therefore, the reinforcement is only needed in the lower layer. All FGC mixes were compared to the SFRC mix, which was used as a reference mix.

To make the concrete mixes mentioned above, a total of four mix designs are required as shown in table 1. A 0.5 ratio of water to cement was selected. Steel fibres accounted for 59 kg/m3 of the total (0.75 percent in volume). Previous research has shown that when the fibres are between 0.5 and 1 percent of the concrete volume, there is a greater increase in residual flexure strength [15]. Furthermore, Debieb et al. reported an increase in compressive and flexural strength, especially at the 10% and 20% replacement levels [16]. As a result, the substitution percentage by weight of the natural coarse aggregates with recycled aggregates (RCA, RPA) was set at 15% in this study, and steel fibres accounting for 0.75 percent of concrete volume.

(a) (b)

Figure 2: (a) The prepared E-waste aggregates and (b) the used Steel fibres

A mechanical mixer was used to mix the concrete. The mixing process consists of two stages: the first stage involved the mixing of fine and coarse aggregates with half percent water for 4 minutes; the second stage involved the mixing of cement with the remaining half percent water for another 4 minutes. During the second level, steel fibres were added. The FGC mixtures were mixed for 8 minutes, while the SFRC mixtures were mixed for 12 minutes.

2.3 Production of concrete samples

Prismatic (100x100x500mm) samples were cast to test the flexural performance of the concrete mixes. Besides, an Ultrasonic pulse velocity test was also performed on cubic specimens having dimensions of 100x100x100mm to estimate the quality of concrete under the influence of recycled aggregates and steel fibres. The upper and bottom layers were defined using moulds (Fig 4. a-b). The bottom layer of concrete was mixed and cast according to the defined mark, then vibrated for 25 seconds. After that, a bonding agent (ULTRA SBR latex) was produced in the ratio of SBR: water: cement (1:1:3) and applied to the surface (Fig. 4. c-d). When a bonding agent becomes effective second layer (upper layer) of concrete was cast about 25 minutes later, up to the mould height (Fig. 4. e-f). The vibration of the top layer was decreased by 50 percent to prevent a mixture of the layers. A total of 12 prismatic and 12 cubic samples were made. After casting, all specimens were demoulded for 24 hours and cured for 28 days in water at room temperature (approximately 20 °C). A flexural strength test was used to assess the mechanical performance of steel fibres reinforced concrete (SFRC) and functionally graded concrete (FGC). Whereas, to ensure the quality and uniformity of concrete the Ultrasonic pulse velocity test was carried out.

Table 1- Mix designs (kg/m3)

Mixes ID	Cement	Water	Fine Aggregate	Coarse Aggregates			Fibres
				NCA	RCA	RPA	
Portland cement concrete(PCC)	422	211	672	1344	-	-	-
recycled plastic aggregate concrete(RPA)	422	211	672	1142	-	78	-
recycled concrete aggregate(RCA)	422	211	672	1142	202	-	-
steel fibre reinforced concrete (SFRC)	422	211	672	1344	-	-	59

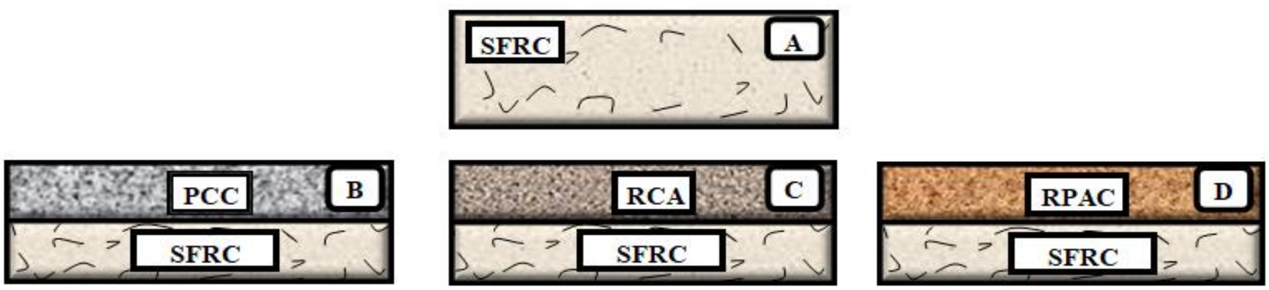

Figure 3: concrete mixes considered in this study

2.4 Flexural strength test

Modulus of rupture (MR) is another name for this examination. Under third-point loading at a rate of 0.5mm/minute, the flexural strength test was executed on beam-shaped specimens with dimensions of 100x100x500mm, as per ASTM C78 [17]. During the testing, flexural behavior and the crack pattern was being observed. Three samples were cast for each blend. Figure 5(a) depicts the prismatic sample being tested. Since fractures begin in the tension zone in the middle third of the span length, the formula for calculating the modulus of rupture (MR) is as follows:

$$f_r = \frac{P_u l}{bd^2} \tag{1}$$

2.5 Ultrasonic pulse velocity (UPV) test

Non-destructive ultrasonic pulse velocity measurements are used to interpret concrete insufficiencies, such as non-uniformity and crack presence. This test was carried out on three cubic specimens, each measuring 100x100x100mm. Figure 5(b) depicts the cubic sample testing. This test is performed by sending an ultrasonic pulse through the concrete to be tested and measuring the time it takes for the pulse to pass through the structure. The values of ultrasonic pulse velocity were taken from the Ultrasonic Non-destructive Tester in accordance with ASTM C597-09 [18].

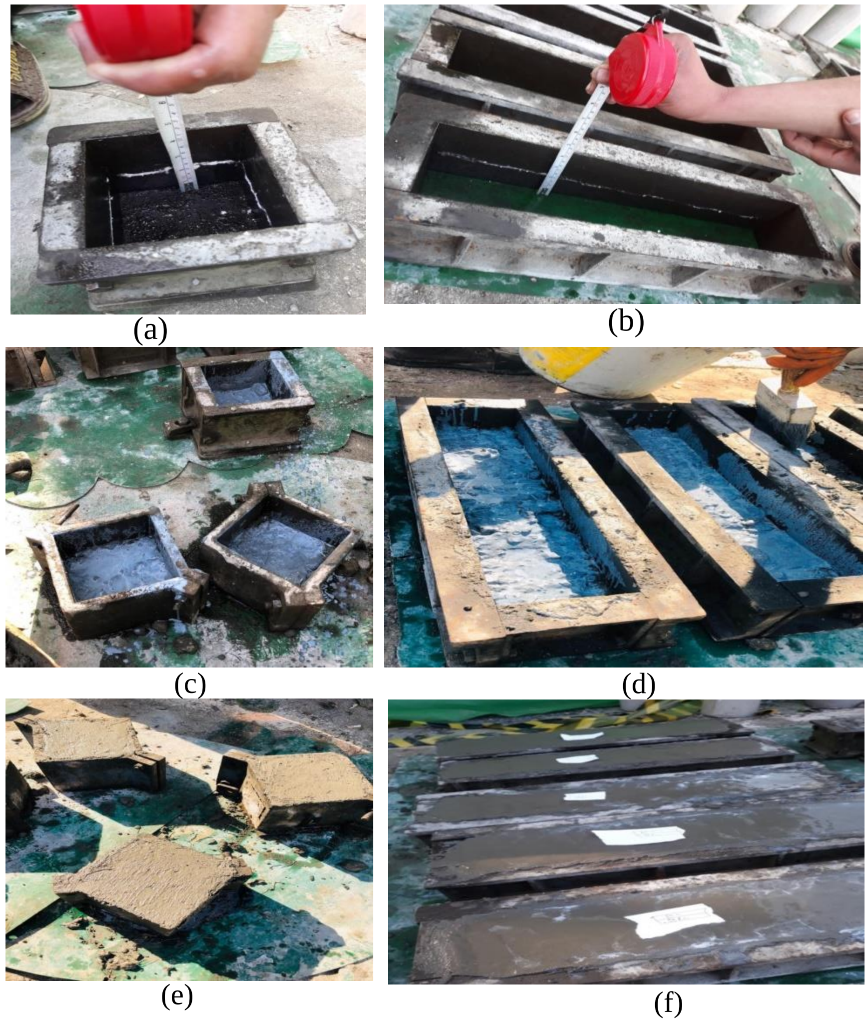

Figure 4: Moulds are marked to define the upper and bottom layers: (a) cubic sample (b) Prismatic sample. The casting of the bottom layer along with an application of ULTRA SBR latex: (c) cubic sample, (d) Prismatic sample; and after casting of the upper layer (e) cubic sample, (f) Prismatic sample.

Figure 5: (a) flexural strength testing and (b) UPV testing

3 Results and discussion

3.1 Flexural strength

Flexure strength results (mean value) of all concrete mixes (SFRC and FGC) are presented in fig.6. All of the FGC mixes were compared to the conventional SFRC mix. Eq. (2) can be used to calculate relative strength, from which the difference in strength can be calculated. The differences in flexural strength between FGC mixes and SFRC are thoroughly explained.

$$(f_{FGC} / f_{SFRC}) \times 100 \quad (2)$$

Figure 6 shows a comparison of steel fibres reinforced concrete (SFRC) and functionally graded concrete (FGC). PCC + SFRC mix has 5.5 % more flexural strength than traditional SFRC, RCA +SFRC mix has 1.8 % more flexure strength, and RPAC + SFRC mix has 13.3 % lower flexure strength. The best FGC mix was PCC + SFRC, which provided 5.5 % more flexural strength than conventional SFRC. Using recycled concrete aggregate (RCA) in concrete, on the other hand, helps to save the world by reducing the capacity of construction waste that closes up in landfills [19]. Therefore, FGC compositions of replaced recycled aggregates (RCA, RPAC) cast in the upper layer, combined with a bottom layer of fibres reinforced concrete, will eliminate environmental waste, thus leading to sustainable growth.

Cement optimization, serviceability performance, and an FGC member having the same deflection strength as a homogeneous component are just a few of the benefits of the FGC [20]. Concrete's functional gradation can be linked to a reduction in the element's mass and the formation of multifunctional properties [21]. As a result, using FGC in new construction can increase PCC's post-cracking behavior. Furthermore, the FGC concept in new construction is much more effective in bending members, enabling us to reduce the use of fibres that precede society's economic growth.

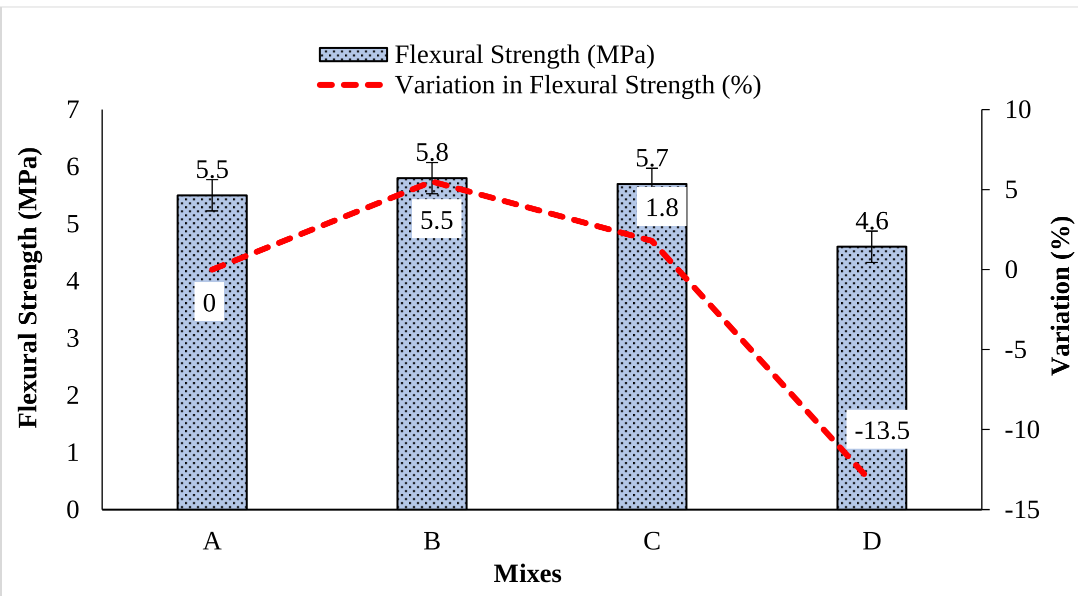

Figure 6: Flexure strength comparison of SFRC and FGC mixes

3.2 Ultrasonic pulse velocity (UPV) test

The UPV test was used to measure concrete's consistency under the influence of steel fibres and recycled aggregates. The UPV test results are presented in Figure 7. As suggested that Concrete has good durability when its pulse velocity value varies between 3660–4575 m/s [22]. Higher velocities indicate good material quality and consistency, while slower velocities can reveal concrete with numerous cracks or voids [23]. From the results, it can be observed that all calculated values are within the range indicated, which confirms the quality of both SFRC and FGC. Furthermore, the SFRC mix exhibits a lower UPV value than all FGC mixes. All FGC mixes have higher velocities than the SFRC mix because if we use FGC instead of SFRC, it will use fewer fibres. If the amount of fibres is reduced, then there will be fewer pores in the concrete and its UPV value will be greater. The results are in good agreement with the findings of L. Li.[24], who reported that the addition of fibres and calcium carbonate whisker (CW) decrease the ultrasonic pulse velocity (UPV) value. Finally, it has been concluded that FGC increases the quality and durability of concrete as compared to SFRC.

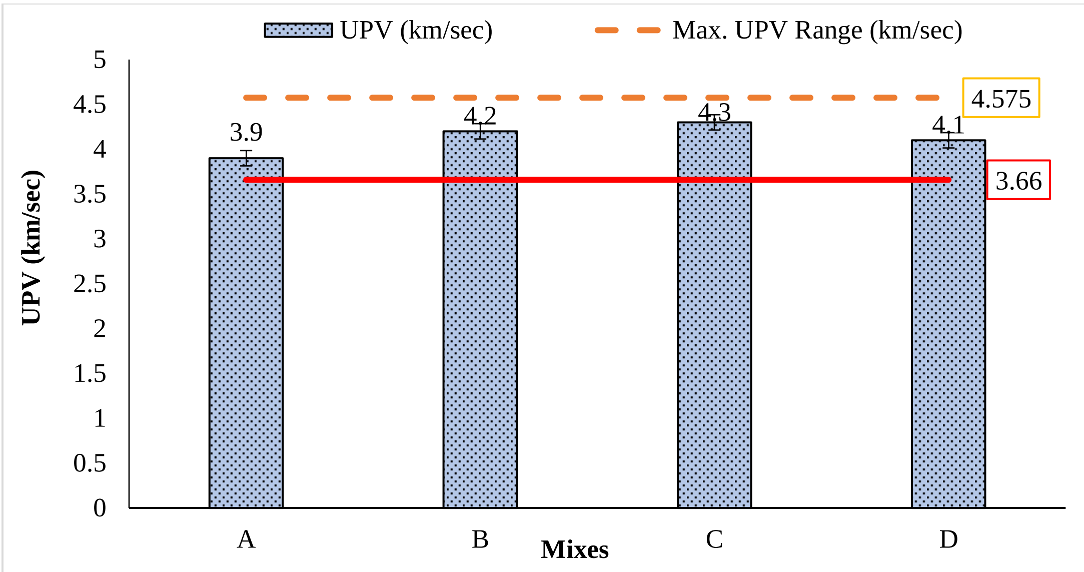

Figure 7: UPV test values of SFRC and FGC mixes

4 Conclusion

The experimental investigation conducted on the mechanical performance of Steel fibres reinforced concrete (SFRC) and functionally graded concrete (FGC) yielded the following conclusion.

- The mix PPC+SFRC and RCA+SFRC exhibit higher flexural strength compared to SFRC. While the flexural performance of RPAC+SFRC is lower than SFRC.
- The FGC combination of PCC+SFRC has a 5.5 % higher strength compared to the traditional SFRC.
- As compared to conventional SFRC, the FGC mix of RCA+SFRC has 1.8 % higher flexure strength, and the RPAC + SFRC mix has 13.3 % lower flexure strength.
- The strongest FGC mix combination is PCC+SFRC, which offers 5.5 % more flexure strength than traditional SFRC. Therefore, the FGC mix possessing PCC+SFRC is more effective and cost-efficient in bending members by reducing the fibres content.
- The ultrasonic pulse velocities of all FGC mixes are higher than the SFRC mix which ensures the concrete's consistency and uniformity.
- The FGC method, on the other hand, allows us to use fibres in one layer and cast the second layer from recycled aggregates concrete (RCA, RPA). It can support us in recycling everyday plastic waste and reusing demolished concrete as an aggregate substitute in new concrete in a cost-effective (environmentally friendly) manner.

In comparison to traditional SFRC, functionally graded concrete (FGC) is more efficient in flexural strength. As a result, FGC is suggested for the flexural member. However, utilizing different fibres, waste materials, and aspect ratios need to be examined along with the cost analysis to assess the FGC's performance.

Acknowledgment

For the successful completion of the study experimental work, the authors would like to thank the concrete research laboratory staff of the department of civil engineering, University of Engineering and Technology (U.E.T) Taxila.

References

[1] Y. Choi and R. L. Yuan, "Experimental relationship between splitting tensile strength and compressive strength of GFRC and PFRC," *Cem. Concr. Res.*, vol. 35, no. 8, pp. 1587–1591, 2005.

[2] L. Li, D. Gao, Z. Li, M. Cao, J. Gao, and Z. Zhang, "Effect of high temperature on morphologies of fibers and mechanical properties of multi-scale fiber reinforced cement-based composites," *Constr. Build. Mater.*, vol. 261, 2020.

[3] L. Li, M. Cao, C. Xie, and H. Yin, "Effects of CaCO 3 whisker, hybrid fiber content and size on uniaxial compressive behavior of cementitious composites," *Struct. Concr.*, vol. 20, no. 1, pp. 506–518, 2019.

[4] G. Meng, B. Gao, J. Zhou, G. Cao, and Q. Zhang, "Experimental investigation of the mechanical behavior of the steel fiber reinforced concrete tunnel segment," *Constr. Build. Mater.*, vol. 126, pp. 98–107, 2016.

[5] M. G. Alberti and A. Enfedaque, "On the prediction of the orientation factor and fi bre distribution of steel and macro-synthetic fi bres for fi bre-reinforced concrete," vol. 77, 2017.

[6] M. Koizumi, "FGM activities in Japan," vol. 8368, pp. 1–4, 1997.

[7] P. M. Subramanian, "Plastics recycling and waste management in the US," vol. 28, pp. 253–263, 2000.

[8] I. Almeshal, B. A. Tayeh, R. Alyousef, H. Alabduljabbar, A. Mustafa Mohamed, and A. Alaskar, "Use of recycled plastic as fine aggregate in cementitious composites: A review," *Constr. Build. Mater.*, vol. 253, p. 119146, 2020.

[9] P. Mikhailenko, M. Rafiq Kakar, Z. Piao, M. Bueno, and L. Poulikakos, "Incorporation of recycled concrete aggregate (RCA) fractions in semi-dense asphalt (SDA) pavements: Volumetrics, durability and mechanical properties," *Constr. Build. Mater.*, vol. 264, p. 120166, 2020.

[10] G. H. Loh, E. Pei, D. Harrison, and M. D. Monzón, "An overview of functionally graded additive manufacturing," *Addit. Manuf.*, vol. 23, no. June, pp. 34–44, 2018.

[11] O. Access, "We are IntechOpen , the world ' s leading publisher of Open Access books Built by scientists , for scientists TOP 1 %."

[12] M. G. Naghibdehi *et al.*, "Behaviour of functionally graded reinforced- concrete beams under cyclic loading," vol. 67, pp. 427–439, 2015.

[13] X. Liu, M. Yan, I. Galobardes, and K. Sikora, "Assessing the potential of functionally graded concrete using fibre reinforced and recycled aggregate concrete," *Constr. Build. Mater.*, vol. 171, pp. 793–801, 2018.

[14] L. Liao, A. De Fuente, S. Cavalaro, and A. Aguado, "Design of FRC tunnel segments considering the ductility requirements of the Model Code 2010," *Tunn. Undergr. Sp. Technol. Inc. Trenchless Technol. Res.*, vol. 47, pp. 200–210, 2015.

[15] J. Lee, "Influence of concrete strength combined with fiber content in the residual flexural strengths of fiber reinforced concrete," *Compos. Struct.*, vol. 168, pp. 216–225, 2017.

[16] F. Debieb, E. Kadri, and M. Bentchikou, "Use of plastic waste in sand concrete," no. January, 2016.

[17] C. ASTM, "Standard test method for flexural strength of concrete (using simple beam with third-point loading)," in *American Society for Testing and Materials*, 2010, vol. 100, pp. 12959–19428.

[18] ASTM_C597-09, "Standard Test Method for Pulse Velocity Through Concrete," Washington DC, USA, 2010.

[19] K. Pin, W. Ashraf, and Y. Cao, "Resources , Conservation & Recycling Properties of recycled concrete aggregate and their in fl uence in new concrete production," *Resour. Conserv. Recycl.*, vol. 133, no. February, pp. 30–49, 2018.

[20] H. A. Lie, U. Diponegoro, B. S. Gan, S. Kristiawan, and U. S. Maret, "THE BEHAVIOR OF FUNCTIONALLY GRADED CONCRETE AND THE PROSPECT OF MATERIAL OPTIMIZATION," no. December, 2016.

[21] M. Herrmann and W. Sobek, "Functionally graded concrete : Numerical design methods and experimental tests of mass-optimized structural components," no. March 2016, pp. 54–66, 2017.

[22] V. M. Malhotra, *Testing Hardened Concrete : Nondestructive Methods (American Concrete Institute Monograph No. 9)*. Iowa State University Press, 1976.

[23] H. Chao-lung, B. Le Anh-tuan, and C. Chun-tsun, "Effect of rice husk ash on the strength and durability characteristics of concrete," *Constr. Build. Mater.*, vol. 25, no. 9, pp. 3768–3772, 2011.

[24] L. Li and M. Cao, "Influence of calcium carbonate whisker and polyvinyl alcohol- steel hybrid fiber on ultrasonic velocity and resonant frequency of cementitious composites," *Constr. Build. Mater.*, vol. 188, pp. 737–746, 2018.

3rd Conference on Sustainability in Civil Engineering (CSCE'21)
Department of Civil Engineering
Capital University of Science and Technology, Islamabad Pakistan

AN OVERVIEW ON COMPRESSIVE BEHAVIOUR OF COCONUT FIBER REINFORCED PLASTER

[a] Ali Rehman [b] Muhammad Adnan

a: Lecturer, Department of Civil Engineering, Comsats University Islamabad, Abbottabad Campus, engr.dr.alirehman@outlook.com
b: Structure Engineer, Faisal and Fahad Associates, Bahria Town Rawalpindi, adnan.uet.com.pk@gmail.com

Abstract- Plastering is one of the general applications of earth-based mortars used for earthlike building conservation or latest architecture. Regarding the compressive strengths, there are contrasting findings presented in past studies. It is found that the mixture of coconut fibers with cement mortar decreased its compressive strength when increasing the fiber content. The extensive research has been done on the use of natural fibers as a stabilizer in building materials. The use of fibers, or natural fibers, in the plaster does more to enhance the wall strength than fibers in blocks or mortar. This paper adds to the effort to review the properties of the coconut-reinforced paper machine by focusing directly on any changes in the changing behavior of the composite. The research and conclusions of various researchers are reviewed to better understand the combined behaviors. According to the review, the dynamic nature of the hardened coconut compounds has been greatly improved.

Keywords- Plaster, Compressive behavior, stabilizer, coconut fiber

1 Introduction

One of the basic needs of a person is accommodation. This usually comes third after meals and clothing. Housing is not enough in price and quality in many developing countries as compared to population growth. This shortage is the reason for the need for development in the construction industry, especially in stone houses [1]. Plaster is a unique material that can vary basically by chemical formulation. The main types of chemicals are gypsum cement and lime plaster. Lime plaster is prepared by burning limestone (calcium carbonate) to produce quicklime (calcium oxide). Water is added to form slaked lime (calcium hydroxide), which forms a mixture of cement. The lime reacts chemically with carbon dioxide (CO2) present in the air [2]. Bulk testing is essential because plasters are used in walls and ceilings, and their attachment to substrates depends on their weight. Plasters must be able to deform when substrate deforms, in the application of loads, thermal fluctuations or to reduce shrinkage. Therefore, it is necessary to test the defects of the earth plaster, which can be tested by a strong mode of hardness testing [3]. Natural strengthening materials can be found at low cost and low energy levels using local manpower and technology. The use of natural fiber is of unique concern in rarely improved regions where there are common building materials very expensive. In making concrete with adding threads, traditional architecture has reached new levels of performance [4]. An examination of some old and modern buildings shows that their lives have been greatly reduced since then the cement of the earth undergoes shrinking cracks. Therefore, a study on the reduction of earth plaster is important for the sustainability of such construction practice. This work investigates the decrease in erosion suspension of the earth reinforced with various fibers such as barley grass, wheatgrass, and wood-shaving under various medical conditions [5].

Mortar is usually a matrix formed by judiciously combining cement or any other cementitious material like lime or alkali activated binders with fine aggregates such as river sands or crusher rock powder sand in the existence of sufficient dose of water. Mortars are useful in bonding the bricks during the wall construction or plastering, both inside as well as outside as finishing layer. When the hydration reaction gets finalized and calcium silicate hydrate gels are formed mortar will have adequate mechanical strength [6]. An experimental study of the various types of brick structure to determine the shear volume, using diagonal pressure test and triple cutting. The result of both tests has shown that the shear volume is entirely dependent on the power of used mud [7]. The main disadvantage of plaster compared to cement products its hardness and high intimacy watering. Although gypsum hemihydrate melts slowly inside water, its use is not increased for external use due to its poor mechanical properties caused by low bonding strength between gypsum grains and lack of adhesion paths between characters that lead to higher altitudes [8]. In Table 1 properties of coconut fiber reinforced concrete (CFRC) are shown.

Table 1: Properties of Coconut Fiber Reinforced Concrete (CFRC) [8].

Fiber volume Fraction (%)	Compressive strength (MPa)	Split tensile strength (MPa)	Modulus of rupture (MPa)	Shear strength (MPa)
-	21.42	2.88	3.25	6.18
0.5	21.70	3.02	3.38	6.47
1.0	22.74	3.18	3.68	6.81
1.5	25.10	3.37	4.07	8.18
2.0	24.35	3.54	4.16	8.21

The compressive strength, splitting tensile strength, modulus of rupture, and shear strength of coconut fiber reinforced concrete with 2% fibers by volume proportion were improved up to 13.7, 22.9, 28.0 and 32.7 %, respectively as compared to those of plain concrete. Researchers also found that all these properties were also improved for coconut fiber reinforced concrete with all other tested volume proportion of fibers (0.5, 1 and 1.5 %). These properties were improved up to only 1.3, 4.9, 4.0 and 4.7 %, respectively for coconut fiber reinforced concrete with 0.5% fibers by volume proportion. Modern climatic challenges in urban areas require more practical solutions to reduce environmental degradation such as the urban temperature effect (UHI). Hot pressures caused by severe temperatures, fluctuations in temperature, as well as UV rays emitted on construction sites adversely affect the city as well house construction for thermal comfort, strength building, and durability of finishing materials. Thus, it is improving the effectiveness of external finishing materials to reduce the effects of natural loads would be beneficial in construction and urban materials [9].

2 Compressive Performance of Cement Paste

The mechanical and physical properties of reinforced cementitious material can be affected by many factors. These cementitious materials are reinforced with natural fibers. These materials are categorized by, the nature of cementitious material and the composition of composite; reinforcing fibers behavior and its types; and the characteristics of composite, chemical healing and solubility. With these aspects, the arrangement of fibers and cementitious material causing the uniform distribution of reinforcing cords and affects the material properties of these compounds. The chemical composition and surface of fiber determine the fiber-matrix compatibility. This compatibility depends upon the condition of the optical connector, the reinforcement content exposed to compact mechanical properties.

There are lots of elements that can influence the mechanical and physical properties of cement composites supplemented with coconut fibers. The grouping of such materials is based upon, the variety of the cement matrix and the composition of the composite; the category and property of the reinforcing fibers; and the classification of the composite, chemical healing and solubility. Between these specifications, the alignment betwixt the fiber and the cement matrix directing to the uniform dispensation of reinforcing cords persist as one of the strongest elements affecting the mechanical properties of these materials. Coconut fiber-matrix similarity is decided by the chemical configuration of coconut fiber, its external structures and depending on the limitations of optical connector, the reinforcement volume establishes the level of exposure to compact mechanical properties [10].

Concerning the force of compression, there are conflicting results presented in past studies. It was found that the installation of coconut fibers reduces cement target's strength (compressive strength) when fiber content increases. The researches claim that the reduction of interaction of fibers within the matrix; increase the volume of voids within the composite and was seen as the highest volume fraction of coconut fibers added, indicating a bold formation. On the other hand, some researchers found an increase in strength (compressive strength) by the insertion of coconut fibers into the cement in the mud [11]. The effect on the distribution of pressure by threads. Concerns about adding more coir fiber to cement-lime mortar, it was found that the strength (compressive strength) of the mud increases with volume fraction of coconut fiber content up to 0.5%, and high coconut fiber content decreases the compressive strength of the mud compared to the reference cement [12]. Numerous studies announce that the addition of plant fibers to the earth's mud can cause the reduction of dry piles, shrinkage and heat dissipation, which is easily remedied by the presence of fibers, which have a smaller mass, and ultimately increase the compressive strength and adhesion of plaster foundations. Moreover, the effects of compression and adherence strength require further studies [12]. In Figure 1: Coconut fiber-reinforced cement-based mortars specimens after compressive strength test and flexural strength are shown.

(a)  (b) 

Figure 1: Coconut fiber-reinforced cement-based mortars specimens after: (a) compressive strength test and (b) flexural strength.

Figure 1 presents the coconut fiber-reinforced cement-based mortars samples after compressive strength and flexural strength tests. Summarizing, the compressive strength of the coconut fiber reinforced mortar showed a decrease. Bulk testing is essential because plasters are used in walls and ceilings, and their attachment to substrates depends on their weight. Plasters must be able to deform when substrate deforms, in the application of loads, thermal fluctuations or to reduce shrinkage. Therefore, it is necessary to test the defects of the earth plaster, which can be tested by a strong mode of hardness testing [13]. In short, the installation of cables reduced the performance of the mud. Therefore, the high water content of the mix was used to achieve the intended amount of table flow. The threads in the mud showed an increase in the amount of water to the binder compared to cement reference, which can affect the solid structures of cement. It was noticed that performance decreases with the length and thickness of the fibers [14].

3 Available Measures to Improve Compressive Behavior

Cement has been used historically for hundreds of years now and brings many useful properties namely decorating, protecting the environment, thermal heating, and sound effects up to a good level among many others. Nowadays, however, the research has focused on the investigation of the structures of the long-established concrete plastering machine. While good in many respects concrete exhibits weak structures such as flexural, mechanical and compressive strengths which is the main reason why cement has not escaped its common use as decorative and plastering materials. Plaster is very natural and does not provide any resistance to cracking when applied to the connecting force. The inclusion of fibers in binding materials can often improve its structure, especially in post-crack behavior; In particular, homosexuality can be reduced by an appreciation by combining mud with natural fibers [15]. The mud supply should not show high pressure, indicative of high durability, because brittle behavior may be at risk of cracking. Therefore, the results obtained from this work can be a good addition to the dedication. On the other hand, flexibility is highly requested and must withstand structural movements and thermal variability in pressure without cracking Flexural energy is strong it has to do with other factors, such as the tendency to crack and the ability to stick to offer mud [16].

Concerning the compressive strength, there are conflicting results shown in previous studies. Hwang et al. found that the installation of coconut fibers reduces cement target's strength when fiber content increases. Researchers claim that the reduction of the interaction of fibers within the matrix; enlarge the volume of voids within the composite and was seen as the highest volume fraction of coconut fibers added, indicating a bold formation. An examination of some old and modern buildings shows that their lives have been greatly reduced since then the cement of the earth undergoes shrinking cracks. Therefore, a study on the reduction of earth plaster is important for the sustainability of such construction practice. This work investigates the decrease in erosion suspension of the earth reinforced with various fibers such as barley grass, wheatgrass, and wood-shaving under various medical conditions [17].

4 Selection of Suitable Fiber

There are many general advantages of coconut fibers e.g., they are resistant to damage by moths, repellant of fungi and decay, also coconut fibers are heat insulating and sound absorbing materials, not easy to ignite, fire resistant, uninfluenced by wetness and humidity, strong and durable, irrepressible, spring back to shape even after constant use, totally uncharged and not difficult to clean [18]. Fibers, or natural fibers, could be mixed in composite materials to upgrade firmness and flexibility, reduce weight, improve the inclination of cracked candy matrices, increase shear strength and be more secure during processing, and handling. However, the element influencing the widespread utilization of fibers is durability. The strong alkaline presence in portland cement matrix (pH> 12) is largely due to the existence of calcium hydroxide and may be due to possible interaction between fiber elements and portlandite causes the degradation of composite materials [19]. Table 2 represents the tensile strength and modulus of rupture of cement paste composite reinforced with varying volume fractions of 3.8 cm long coconut fibers ranging from 2% to 6 %.

Table 2: Mechanical properties of coconut fiber reinforced plaster with respect to fiber percentage [19].

Fiber volume fraction (%)	Tensile Strength (MPa)	Modulus of Rupture (MPa)
2	1.9	3.6
3	2.5	4.9
4	2.8	5.45
5	2.2	5.4
6	1.5	4.6

For example, take note of the fact that the 4 % volume proportion of coconut fibers had shown the outstanding mechanical properties amidst all tested volume proportion [20]. With a 4 % volume proportion, the researchers also studied the tensile strength of cement paste reinforced with different lengths of coconut fibers. The observed tensile strengths with fiber lengths of 2.5, 3.8 and 5.0 cm were 2.3, 2.8 and 2.7 MPa [21]. The maximum strength of cement paste composite was achieved with coconut fiber having length of 3.8 cm and 4% by volume fraction. Another method to combat damage and to upgrade the strength of plant-reinforced concrete cement is to change the surface of the natural fibers using hydrophobic materials that permit themselves to be painted, protected in an alkaline environment where they will be disclosed and decrease the amount of water the fiber absorbs, and thus providing more stability in the cement matrix. In this study, structural elements reinforced with coconut shell are designed to decide the effect of the defensive element, length and percentage by fiber weight on the properties of reinforced mortar machines [10].

The thermal conductivity of the building material is an important method of heating comfort within buildings. Using date palm in mortars is effective in making the environment friendly and protective; Pinto et al. show good tropical buildings where corn cobs can be added. The findings reveal the divisive areas of the day-to-day combination of palm metal compounds. Those results have already been tested and verified for other tasks. Therefore, separating the properties of vegetable fibers becomes an interesting parameter for something aimed at a powerful structure [22].

5 Conclusion

Natural fibers such as coconut fiber are effective in strengthening the manufacturing of mud type. Regarding the results obtained, there is an increase in pressure and flexibility by 84.27% and 43.32% respectively as compared to untreated mud. Treatment with paraffin upgrades the chemical aversion to fiber, minimizing the water sucking up extent and contributing best preservation as a contrast of alkaline medium of the cement. The addition of coconut fibers in minor quantities (0.5 percent by weight) is to upgrade flexural and compressive strength, as long as mixing is not being disturbed by fibers. The short fibers, i.e. 1 cm, are aligned randomly which shows homogeneous way of behaving to mechanical stresses, improves compressive and flexural strength.

Acknowledgment

The author would like to thank Engr. Prof. Dr. Majid Ali for his kind support and guidance during our research work.

References

[1] F. Qamar, T. Thomas, and M. Ali, "Improvement in lateral resistance of mortar-free interlocking wall with plaster having natural fibres," *Construction and Building Materials,* vol. 234, p. 117387, 2020.

[2] E. M. Payne, "The conservation of plaster casts in the nineteenth century," *Studies in Conservation,* vol. 65, pp. 37-58, 2020.

[3] T. Santos, P. Faria, and A. S. Silva, "Eco-efficient earth plasters: The effect of sand grading and additions on fresh and mechanical properties," *Journal of Building Engineering,* vol. 33, p. 101591, 2021.

[4] A. Aladenika, O. Olanrewaju, and S. Olaitan, "Comparative Investigation of the Mechanical Properties of Coconut Coir Fibre and Synthetic Fibre Reinforced Plaster of Paris (POP) Based Composites for Celling Applications," *Journal of Materials Science Research and Reviews,* pp. 1-6, 2021.

[5] T. Ashour and W. Wu, "An experimental study on shrinkage of earth plaster with natural fibres for straw bale buildings," *International Journal of Sustainable Engineering,* vol. 3, pp. 299-304, 2010.

[6] V. V. Rao, R. Parameshwaran, and V. V. Ram, "PCM-mortar based construction materials for energy efficient buildings: A review on research trends," *Energy and Buildings,* vol. 158, pp. 95-122, 2018.

[7] F. Qamar, T. Thomas, and M. Ali, "Use of natural fibrous plaster for improving the out of plane lateral resistance of mortarless interlocked masonry walling," *Construction and Building Materials,* vol. 174, pp. 320-329, 2018.

[8] N. Sakthieswaran and M. Sophia, "Effect of superplasticizers on the properties of latex modified gypsum plaster," *Construction and Building Materials,* vol. 179, pp. 675-691, 2018.

[9] S. Soudian, U. Berardi, and N. Laschuk, "Development and thermal-optical characterization of a cementitious plaster with phase change materials and thermochromic paint," *Solar Energy,* vol. 205, pp. 282-291, 2020.

[10] M. Monsalve, O. Higuera, P. Estrada, M. Orozco, and C. Pedraza, "Production of Structural Type Mortars Reinforced with Coconut Fibre (Coconuts nuciferas)," 2018.

[11] C.-L. Hwang, V.-A. Tran, J.-W. Hong, and Y.-C. Hsieh, "Effects of short coconut fiber on the mechanical properties, plastic cracking behavior, and impact resistance of cementitious composites," *Construction and Building Materials,* vol. 127, pp. 984-992, 2016.

[12] C. Maia Pederneiras, R. Veiga, and J. de Brito, "Physical and Mechanical Performance of Coir Fiber-Reinforced Rendering Mortars," *Materials,* vol. 14, p. 823, 2021.

[13] E. Quiñones-Bolaños, M. Gómez-Oviedo, J. Mouthon-Bello, L. Sierra-Vitola, U. Berardi, and C. Bustillo-Lecompte, "Potential use of coconut fibre modified mortars to enhance thermal comfort in low-income housing," *Journal of Environmental Management,* vol. 277, p. 111503, 2021.

[14] K. Salim, A. Houssam, A. Belaid, and H. Brahim, "Reinforcement of building plaster by waste plastic and glass," *Procedia Structural Integrity,* vol. 17, pp. 170-176, 2019.

[15] B. A. Akinyemi and C. Dai, "Development of banana fibers and wood bottom ash modified cement mortars," *Construction and Building Materials,* vol. 241, p. 118041, 2020.

[16] F. Iucolano, B. Liguori, P. Aprea, and D. Caputo, "Evaluation of bio-degummed hemp fibers as reinforcement in gypsum plaster," *Composites Part B: Engineering*, vol. 138, pp. 149-156, 2018.

[17] A. A. Belkadi, S. Aggoun, C. Amouri, A. Geuttala, and H. Houari, "Effect of vegetable and synthetic fibers on mechanical performance and durability of Metakaolin-based mortars," *Journal of adhesion science and Technology*, vol. 32, pp. 1670-1686, 2018.

[18] N. Bheel, S. K. Mahro, and A. Adesina, "Influence of coconut shell ash on workability, mechanical properties, and embodied carbon of concrete," *Environmental science and pollution research*, vol. 28, pp. 5682-5692, 2021.

[19] J. Lima, P. Faria, and A. Santos Silva, "Earth plasters: The influence of clay mineralogy in the plasters' properties," *International Journal of Architectural Heritage*, vol. 14, pp. 948-963, 2020.

[20] F. Qamar, T. Thomas, and M. Ali, "Contribution of Sisal Reinforced Plaster in out of Plane Resistance of Masonry Column," in *Key Engineering Materials*, 2018, pp. 343-348.

[21] M. Ali, "Coconut fibre: A versatile material and its applications in engineering," *Journal of Civil engineering and construction Technology*, vol. 2, pp. 189-197, 2011.

[22] B. Zhadanovsky and V. Bazanov, "Technological features of application of plaster solutions with ground quicklime," in *IOP Conference Series: Materials Science and Engineering*, 2020, p. 022080.

3rd Conference on Sustainability in Civil Engineering (CSCE'21)
Department of Civil Engineering
Capital University of Science and Technology, Islamabad Pakistan

EFFECT ON WORKABILITY, COMPRESSIVE, AND TENSILE STRENGTH OF GEOPOLYMER CONCRETE INCORPORATED WITH QUARRY ROCK DUST, FLY ASH, AND SLAG CURED AT AMBIENT AND ELEVATED TEMPERATURES

[a] Khadim Hussain, [b] Faheem Butt

a, b Department of Civil Engineering, University of Engineering and Technology, Taxila
a: hussainkhadim173@gmail.com
b: faheem.butt@uettaxila.edu.pk

Abstract-This paper presents the effect of ambient (27°C) and heat (100°C) curing on the properties viz. workability, compressive, and tensile strength of quarry rock dust (QRD) based geopolymer concrete (GPC) comprising fly-ash (FA), and slag (SG) as a binder. The SG was replaced with QRD up to 20% by weight to develop QRD-SG-FA based geopolymer concrete (QFS-GPC). A total of 12 types (6 cured at ambient and 6 cured at 100°C) of mixes were prepared and tested. The workability of the mixes was reduced by the replacement of SG with QRD. The ambient cured GPC-D27°C and oven-cured GPC-D100°C mixes with FA/SG contents of 50/35% and QRD of 15%, yielded the maximum compressive strength of 33.55MPa and 35.45MPa respectively. The strength properties i.e., compressive, and splitting tensile strengths of the above optimal mixtures have shown improved strength by curing at higher temperature and have depicted more strength than the control OPC concrete specimens.

Keywords- Ambient temperature curing, elevated temperature curing, geopolymer concrete, quarry rock dust.

1. Introduction

Nowadays, construction activities have been increasing to meet infrastructure demand. It can be observed that ordinary Portland cement (OPC) concrete is an essential and broadly used construction material in most construction activities. During the manufacturing process of OPC, a huge amount of carbon dioxide (CO2) is released into the atmosphere through the transformation of raw material and fuel consumption. The second-largest source of production of greenhouse gases in the cement industry [1]. [2]. The manufacturing of OPC contributes about 5% of CO2 emission globally [3]. Therefore, an alternative finding for OPC concrete has been a challenging task for researchers and environmentalists. It is essential to work on feasible and better solutions, which can utilize industrial solid wastes to yield alternative binder materials. Alkali activated geopolymer concrete (GPC) is a relatively new technique in the construction industry that has been becoming popular due to its mechanical properties and eco-friendly benefits. The geopolymers are good solutions to reduce and support the effective use of waste materials [4]. The geopolymers can play a significant role in reducing the low emission of CO2 in comparison to OPC in the construction industry [5]. In general, the geopolymers are classified as alumino-silicate, an inorganic polymer manufactured from the alkaline activation of different aluminosilicate constituents of geological source or industrial by-product wastes like metakaolin, slag (SG) and, fly ash [6][7].

It is described that the production of GPC with low calcium FA at elevated temperature curing resulted in superior mechanical properties [8] which restricts its usage to precast structural members only. However, at ambient curing conditions, these results are comparatively less promising. It was due to the polymerization procedure which proficiently holds at elevated temperature and directs to the development of sodium aluminate silicate hydrate (NASH) calcium aluminate silicate hydrate (CASH) [9]. In few studies, by adding calcium-rich materials such as alcofine [9], SG [10], etc. the reactivity of low calcium FA was improved at ambient curing conditions. It has been remarked that SG and FA blended GPC mixes proved good resistance to high temperature [11] and displayed heightened shrinkage [12]. It is also described in experimental work that calcium comprising ingredients accelerate the rate of geopolymrization at ambient curing conditions, minimize the pore sizes in the mixture and produce the compressed composite with better mechanical properties [13][14].

The quarry rock dust (QRD) is a dumped residue and calcium-containing substance which can be utilized as a partial alternative to filler or binder material in GPC. This can assist in the reduction of land and environmental pollution by preventing its deposition at landfills. From the previous studies, it was noticed that mostly QRD has been utilized as a partial substitute of sand in geopolymer mortar [15] and cement concrete [16][17]. However, the research studies on QRD as a partial alternative of binding material in geopolymer concrete are rather limited. Therefore, the present research study investigates the effect of QRD as partial replacement of SG on fresh and mechanical properties of QRD-FA-SG based GPC (QFS-GPC) cured at ambient (27 °C) and elevated (100°C) temperature conditions. To accomplish this, a series of GPC mixes were planned by differing the amount of QRD (to partially substitute SG) in QFS-GPC as shown in Table 1. The tests were later performed to find an optimal mix considering workability and mechanical properties viz. compressive and splitting tensile strength.

2. Experimental Methodology

A total of ten types of mixes of QFS-GPC were designed as described in Table 1, with varying dosage (0%, 5%, 10%, 15%, and 20%) of QRD, partially substituting SG (by weight of binder), while maintaining all ingredients the same in all the mixes. For the sake of comparison, two OPC concrete mix types were also considered as control mixes to observe the differences and improvements, if any. Thus, a total of 12 mix types were prepared. The engineering properties (i.e., fresh, and mechanical) of control mix (OPC) and QFS-GPC mixes were evaluated by slump test, compressive, and splitting tensile strengths tests. According to ASTM standard C143/C143M-20 [26], the workability of fresh concrete was determined by performing a slump cone test. A universal testing machine (UTM) with a load capacity of 3000 KN was used for testing of cylinders and cubes at the rate of 8 KN/s after 7, 28, and 56 days of casting to determine split tensile and compressive strengths according to ASTM C496/C496M-17 [27] and BS EN 12390-5-2019 [28] respectively.

2.1. Materials specifications and mixing of ingredients.

In the present study, the type II OPC confirming to ASTM standard C-150/C150M-20 [18] for OPC concrete; and three binders i.e., QRD, FA, and SG were used in various proportions in the preparation of QFS-GPC mixes. The low calcium FA of class F (Grey color) confirming the requirements of ASTM C618-19 [19] was used. It is a preferred source over high calcium FA due to the high calcium effect on the polymerization process [19]. The grinded QRD was sieved through a 45µm sieve confirming the finess of particles used in the GPC production as a binder [20]. The off-white processed SG justifying the ASTM C989/C989M-18a was used [21].

In the present study, the alkaline solution was prepared by mixing sodium hydroxide (SH) and sodium silicate (SS). The molar solution of SH (12M) was prepared 24 hours before use, by gradually mixing 98% pure flakes in the potable water. The solution of SS was mixed with SH solution 30 minutes before its usage. The natural river sand obtained from Lawrancepur (near Attock) was used as fine aggregates. The coarse aggregates were supplied from Margallah hills crushers. The finess modulus of sand was verified to ASTM C136/C136M-19 [22] while the water absorption and specific gravity were according to ASTM C128-15 [23]. The specific gravity of coarse aggregates was as per recommendations of ASTM C127-15 [24]. The alkaline solution is generally viscous than water, hence its usage makes the GPC mixes stickier and more viscous than OPC concrete mixes. Therefore, to increase the workability of freshly GPC mixes, a Naphthalene Sulphonate grounded superplasticizer conforming ASTM C494/C494M-19 [25] was utilized in the present study. The mix proportion for 1 kg/m^3 of OPC and GPC is shown in Table 1.

Table 1. The composition and proportions of OPC and GPC mix used in the study.

Group. No.	Group ID	Curing Temperature (°C)	Mixture proportions								Concrete mixture quantity (kg/m^3)											
			Binder																			
			C %	FA %	SG %	QRD %	AAL/B Ratio	W/C Ratio	Molarity of SH (M)	SS/SH Ratio	B	C	FA	SG	QRD	SH	SS	S	CA (10 mm)	CA (20mm)	SP	Water
1	OPC-27 °C	27 °C	100	-	-	-	-	0.35	-	-	400	400	-	-	-	-	-	680	751	340	10	140
2	OPC-100 °C	100 °C	100	-	-	-	-	0.35	-	-	400	400	-	-	-	-	-	680	751	340	10	140
3	GPC-A 27 °C	27 °C	-	50	50	0	0.50	-	12	1.5	400	-	200	200	0	80	120	680	751	340	10	35
4	GPC-A 100 °C	100 °C	-	50	50	0	0.50	-	12	1.5	400	-	200	200	0	80	120	680	751	340	10	35
5	GPC-B 27 °C	27 °C	-	50	45	5	0.50	-	12	1.5	400	-	200	180	20	80	120	680	751	340	12	35
6	GPC-B 100 °C	100 °C	-	50	45	5	0.50	-	12	1.5	400	-	200	180	20	80	120	680	751	340	12	35
7	GPC-C 27 °C	27 °C	-	50	40	10	0.50	-	12	1.5	400	-	200	160	40	80	120	680	751	340	14	35
8	GPC-C 100 °C	100 °C	-	50	40	10	0.50	-	12	1.5	400	-	200	160	40	80	120	680	751	340	14	35
9	GPC-D 27 °C	27 °C	-	50	35	15	0.50	-	12	1.5	400	-	200	140	60	80	120	680	751	340	14.5	35
10	GPC-D 100 °C	100 °C	-	50	35	15	0.50	-	12	1.5	400	-	200	140	60	80	120	680	751	340	14.5	35
11	GPC-E 27 °C	27 °C	-	50	30	20	0.50	-	12	1.5	400	-	200	120	80	80	120	680	751	340	14.5	35
12	GPC-E 100 °C	100 °C	-	50	30	20	0.50	-	12	1.5	400	-	200	120	80	80	120	680	751	340	14.5	35

***Note*:** W (Water): B (Binder); C (Cement): OPC (Ordinary Portland Cement); AAL (Alkaline Activator Solution); QRD (Quarry Rock Dust); SG (Ground Granulated Blast Furnace Slag); FA (Fly Ash); SH (Sodium Hydroxide); SS (Sodium Silicate); M(molarity); SP (Superplasticizers); S (Sand); CA (Coarse Aggregates).

For the preparation of mixes, all the ingredients including aggregates (fine and coarse), and binders (OPC or QRD, FA, and SG) were dry mixed uniformly in the mechanical mixer having the capacity of 0.15m3 and speed of 20 rev/m for 2 minutes. Before the mixing, the saturated surface dry (SSD) condition of fine and coarse aggregates was obtained. The solution of SH was prepared 24 hours before its application [9] due to exothermic reaction produced during its preparation and mixed 30 min before with SS solution at a required ratio of 1.5 to enhance the reactivity of the solution [10]. Afterward, the premixed alkali-activated solution was added progressively, and mixing continued for another 2-3 minutes to ensure the uniformity of the mixture. Finally, the extra water and superplasticizer (SP) were added to the fresh mixture to achieve the required workability.

The moulds of cubes (150mm x 150mm x 150mm), and cylinders (150mm x 300mm) were filled in three layers with the freshly prepared concrete mix. A vibrator was used for compaction. The freshly casted specimens were placed in the laboratory at ambient and in an oven at 100°C temperature for 24 hours. After demoulding, the OPC and QFS-GPC specimens were kept in a water tank and direct sunlight for water and air curing respectively for 7, 28, and 56-days for testing. Three samples for any test of a mixed type were cast and the average value was used in the results.

3. Results and Discussions

The results of workability, compressive, and splitting tensile strengths are discussed in the following subsections.

3.1. Workability

The ease of positioning and placement of freshly made concrete is known as workability. The slump test on freshly prepared OPC and QFS-GPC mixes was performed according to ASTM standard C143/C143M-20 [26]. The values of the slump test are shown in Figure 1. The workability of QFS-GPC mixes was observed lower than OPC mixes due to the sticky and viscous properties of SH and SS solution [28]. In the present study, the target medium workability standard (50 to 89 mm) [29] was followed. The workability decreases by replacement SG with QRD in the QFS-GPC mixes due to the angular shape of QRD [15] than SG and FA particles that increase water requirement. The target medium workability standard was maintained by an equal amount of extra water for all QFS-GPC mixes and a varying amount of super-plasticizer [25]. The results of workability achieved for OPC and QFS-GPC mixes are shown in Figure 1.

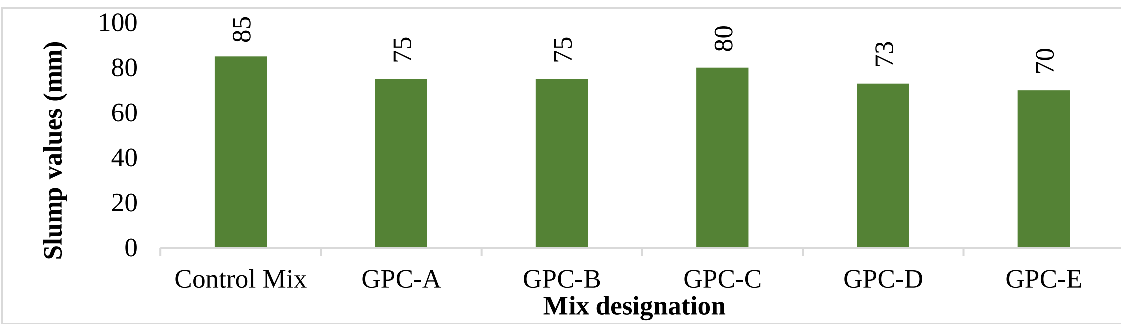

Figure 1: The slump values of control (OPC) and QFS-GPC mix to the target slump (medium workable) after supplementing varying quantities of SP.

3.2. Compressive strength

The compressive strength results of OPC and QFS-GPC mixes cured at ambient (27°C) and elevated temperature (100°C) are shown in Figure 2. From the Figure 2, it can be observed that the 56- days cured OPC, GPC-A, GPC-B, GPC-C, GPC-D and GPC-E specimens at elevated temperatures have 7.97%, 14.45%, 4.27%, 7.76%, 5.67%, and 19.82% respectively better compressive strengths than at ambient cured specimens. It is also observed that the compressive strength of QFS-GPC mixes increases as the replacement levels of QRD contents increase but up to 15%, after which it decreased. It can be due to the increasing quantity of calcium-rich materials which hasten the rate of the polymerization process at room temperature (ambient) as well as at elevated temperature (100°C) and lessen the pore sizes. The specimens cured at elevated temperatures have higher strength due to better polymerization than the ones cured at ambient temperature. The effect of calcium-rich materials on the strength properties has also been described by other researchers at ambient [10,13-14] and elevated temperatures [8,11]. The increase in compressive strength is due to higher calcium oxide contents (in QRD) [13]. When the QRD contents increased from 15% to 20% (as in GPC-E27°C and GPC-E100°C), the QFS-GPC mix becomes least workable. The decrease in compressive strength can be due to excess lime quantity and an incomplete polymerization process [30]. The maximum strength was achieved by the GPC-D mix with 50% FA, 35% SG, and 15% QRD contents. After 56-day testing, the optimal mix GPC-D27°C and GPC-D100°C has 11.35% and 8.9% more compressive strength than the control mix (OPC mix) cured at ambient (27°C) and elevated (100°C) temperature respectively due to better polymerization process.

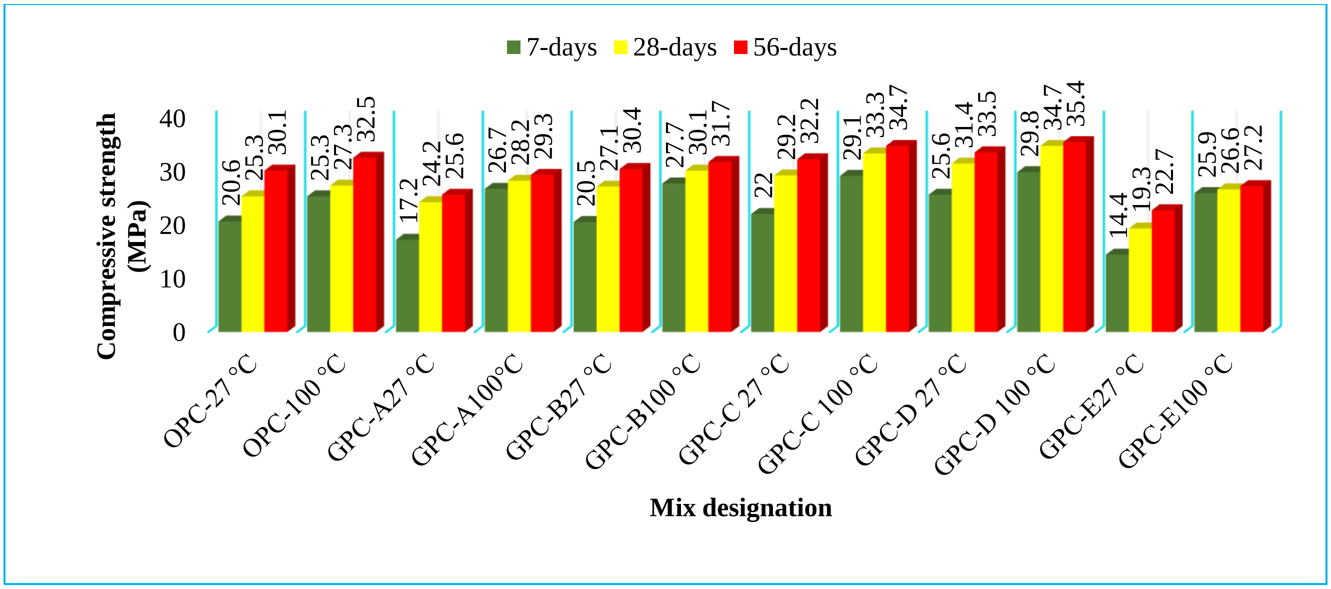

Figure 2: The compressive strength results of OPC and QFS-GPC mix at ambient and elevated temperatures

3.3. Splitting tensile strength

The results of split tensile strength are shown in Figure 3. From the figure, it can be noticed that the trend of increase in split tensile strength behavior is the same as was observed for the compressive strength results. The split tensile strength has improved as QRD contents increased in the QFS-GPC mixes up to 15%. The replacement level of SG with QRD beyond 15% has caused the reduction of split tensile strength. The increase of calcium-carrying blends (mostly CaO with an increase in QRD up to 15%)in the binders has caused improvement in the strength of QFS-GPC specimens at all ages which produced a reaction product for both FA and SG [32].The replacement levels of QRD beyond 15% have caused the reduction of tensile strength due to the deficient polymerization process [14]. After 56-day testing, the ambient cured GPC-D27°C and elevated temperature cured GPC-D100°C mix have slightly more i.e., 1.43% and 1.89% tensile strengths than the control mix specimens respectively. The mix GPC-D27°C and GPC-D100°C with the tensile strength of 2.12 MPa and 2.15 MPa were considered as the optimal QFS-GPC mixes cured at ambient and elevated temperatures respectively.

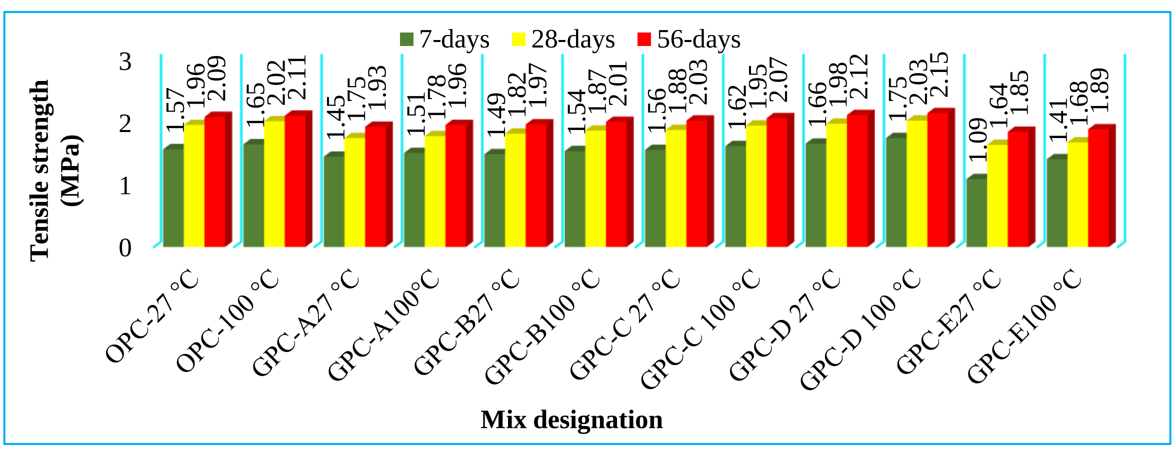

Figure 3: The splitting tensile strength results of OPC and QFS-GPC mix at ambient and elevated temperatures

4. Practical Applications

In general, GPC has restricted field applications due to heat curing for accomplishing a superior and better strength. Due to this reason generally, the precast structural units of GPC have been manufactured and applied in field applications. However, with the inclusions of calcium-rich materials (binders) like QRD, SG, and lime, the production of GPC at ambient curing conditions with better strength properties has become possible. The ambient curing conditions also lessen the energy consumed and costs related to heat curing.

5. Conclusions

The following conclusions can be drawn from the present study:

- The workability of QFS-GPC mixes decreases as the incorporation of QRD contents increases.
- The mechanical properties of QFS-GPC mixtures usually increased by incorporating the QRD content from 0% to 15% and beyond this replacing level i.e., 20% with SG, strength was reduced.
- The optimum (maximum) strength properties i.e., compressive, and split tensile strength of specimens cured at 27°C and 100°C were obtained by GPC-D27°C and GPC-D100°C with 15% QRD contents by weight of total binder respectively.

References

[1] V. M. Malhotra and P. K. Mehta, "High-performance, high-volume fly ash concrete: materials, mixture proportioning, properties, construction practice, and case histories," 2002.
[2] M. Abdullahi, "Effect of aggregate type on compressive strength of concrete," *Int. J. Civ. Struct. Eng.*, vol. 2, no. 3, p. 782, 2012.
[3] C. D. Lawrence, "The production of low-energy cements," *Lea's Chem. Cem. Concr.*, vol. 4, 1998.
[4] L. K. Turner and F. G. Collins, "Carbon dioxide equivalent (CO2-e) emissions: A comparison between geopolymer and OPC cement concrete," *Constr. Build. Mater.*, vol. 43, pp. 125–130, 2013.
[5] K.-H. Yang, J.-K. Song, and K.-I. Song, "Assessment of CO2 reduction of alkali-activated concrete," *J. Clean. Prod.*, vol. 39, pp. 265–272, 2013.
[6] J. Davidovits, "Geopolymer chemistry & application. 16 rule Galilee," *F-02100 Saint-Quentin, Fr. Inst. Géopolymèr*, 2008.
[7] C. B. Cheah, L. E. Tan, and M. Ramli, "Recent advances in slag-based binder and chemical activators derived from industrial by-products–A review," *Constr. Build. Mater.*, p. 121657, 2020.
[8] M. T. Junaid, A. Khennane, O. Kayali, A. Sadaoui, D. Picard, and M. Fafard, "Aspects of the deformational behaviour of alkali activated fly ash concrete at elevated temperatures," *Cem. Concr. Res.*, vol. 60, pp. 24–29, 2014.
[9] D. Singhal, M. T. Junaid, B. B. Jindal, and A. Mehta, "Mechanical and microstructural properties of fly ash based geopolymer concrete incorporating alccofine at ambient curing," *Constr. Build. Mater.*, vol. 180, pp. 298–307, 2018.
[10] P. Nath and P. K. Sarker, "Effect of GGBFS on setting, workability and early strength properties of fly ash geopolymer concrete cured in ambient condition," *Constr. Build. Mater.*, vol. 66, pp. 163–171, 2014.
[11] M. Guerrieri and J. G. Sanjayan, "Behavior of combined fly ash/slag-based geopolymers when exposed to high temperatures," *Fire Mater. An Int. J.*, vol. 34, no. 4, pp. 163–175, 2010.
[12] M. Chi and R. Huang, "Binding mechanism and properties of alkali-activated fly ash/slag mortars," *Constr. Build. Mater.*, vol. 40, pp. 291–298, 2013.
[13] J. v Temuujin, A. Van Riessen, and R. Williams, "Influence of calcium compounds on the mechanical properties of fly ash geopolymer pastes," *J. Hazard. Mater.*, vol. 167, no. 1–3, pp. 82–88, 2009.
[14] D. Dutta and S. Ghosh, "Effect of lime stone dust on geopolymerisation and geopolymeric structure," 2012.
[15] T. V. Madhav, I. V. R. Reddy, V. G. Ghorpade, and S. Jyothirmai, "Compressivestrength study of geopolymer mortar using quarry rock dust," *Mater. Lett.*, vol. 231, pp. 105–108, 2018.
[16] B. K. Meisuh, C. K. Kankam, and T. K. Buabin, "Effect of quarry rock dust on the flexural strength of concrete," *Case Stud. Constr. Mater.*, vol. 8, pp. 16–22, 2018.
[17] K. S. Prakash and C. H. Rao, "Strength characteristics of quarry dust in replacement of sand," in *IOP Conference Series: Materials Science and Engineering*, 2017, vol. 225, no. 1, p. 12074.
[18] ASTM C150 / C150M-20, Standard Specification for Portland Cement, ASTM International, West Conshohocken, PA, 2020, www.astm.org
[19] ASTM C618-19, Standard Specification for Coal Fly Ash and Raw or Calcined Natural Pozzolan for Use in Concrete, ASTM International, West Conshohocken, PA, 2019, www.astm.org

[20] G. F. Huseien *et al.*, "Waste ceramic powder incorporated alkali activated mortars exposed to elevated Temperatures: Performance evaluation," *Constr. Build. Mater.*, vol. 187, pp. 307–317, 2018.
[21] ASTM C989 / C989M-18a, Standard Specification for Slag Cement for Use in Concrete and Mortars, ASTM International, West Conshohocken, PA, 2018, www.astm.org.
[22] ASTM C136 / C136M-19, Standard Test Method for Sieve Analysis of Fine and Coarse Aggregates, ASTM International, West Conshohocken, PA, 2019, www.astm.org
[23] ASTM C128-15, Standard Test Method for Relative Density (Specific Gravity) and Absorption of Fine Aggregate, ASTM International, West Conshohocken, PA, 2015, www.astm.org
[24] ASTM C127-15, Standard Test Method for Relative Density (Specific Gravity) and Absorption of Coarse Aggregate, ASTM International, West Conshohocken, PA, 2015, www.astm.org
[25] ASTM C494 / C494M-19, Standard Specification for Chemical Admixtures for Concrete, ASTM International, West Conshohocken, PA, 2019, www.astm.org
[26] ASTM C143 / C143M-20, Standard Test Method for Slump of Hydraulic-Cement Concrete, ASTM International, West Conshohocken, PA, 2020, www.astm.org.
[27] ASTM C496 / C496M-17, Standard Test Method for Splitting Tensile Strength of Cylindrical Concrete Specimens, ASTM International, West Conshohocken, PA, 2017, www.astm.org
[28] BS EN 12390-5:2019 standard Testing hardened concrete. Flexural strength of test specimens.
[29] G. Fang, W. K. Ho, W. Tu, and M. Zhang, "Workability and mechanical properties of alkali-activated fly ash-slag concrete cured at ambient temperature," *Constr. Build. Mater.*, vol. 172, pp. 476–487, 2018.
[30] M. T. Junaid, O. Kayali, A. Khennane, and J. Black, "A mix design procedure for low calcium alkali activated fly ash-based concretes," *Constr. Build. Mater.*, vol. 79, pp. 301–310, 2015.
[31] J. Temuujin and A. Van Riessen, "Effect of fly ash preliminary calcination on the properties of geopolymer," *J. Hazard. Mater.*, vol. 164, no. 2–3, pp. 634–639, 2009.
[32] T. Phoo-ngernkhama, P. Chindaprasirt, V. Sata, and T. Sinsiri, "High calcium fly ash geopolymer containing diatomite as additive," 2013.

3[rd] Conference on Sustainability in Civil Engineering (CSCE'21)
Department of Civil Engineering
Capital University of Science and Technology, Islamabad Pakistan

EVALUATING THE MECHANICAL AND DURABILITY PERFORMANCE OF CONCRETE UTILIZING PLASTIC FINE AGGREGATE

[a] Kiffayat Ullah*, [a] Dr. Irshad Qureshi, [b] Tahir Ahmad, [c] Afnan Ahmad

a: Civil Engineering, UET Taxila, Pakistan, kiffayat8@gmail.com & irshad.qureshi@uettaxila.edu.pk
b: College of Civil and Transportation Engineering, Hohai University, China, tahirahmad667@gmail.com
c: civil and Environmental Engineering, Universti Technologi Petronas (UTP) Perak, 32610, Malaysia, afnan_19001642@utp.edu.my
* Irshad Qureshi: Email ID: irshad.qureshi@uettaxila.edu.pk

Abstract- This study evaluates the mechanical and durability characteristics of eco-friendly concrete comprising of electronic plastic waste (EPW) as partial replacement of fine aggregate. Such an approach not just only reduces the negative effects of EPW on the surrounding world, but also helps in avoiding excessive quarrying for the production of natural aggregate. For this purpose, four M20 grade concrete mixes were prepared, substituting natural fine aggregates with plastic fine aggregates (PFA) using 0%, 10%, 15%, and 20% substitution levels. The mechanical efficiency of EPW concrete was evaluated based on the compressive strength while some of the durability properties were assessed through, sorptivity coefficient and alternate wetting and drying. The findings showed that by 10%, 15%, and 20% PFA replacement, compressive strength decreased by 2.6%, 9%, and 13.6%, respectively. Conversely, EPW concrete provided acceptable to excellent performance in the workability, and also shows positive results for required durability properties such as sorptivity coefficient, and alternate wetting and drying.

Keywords- Eco-friendly concrete; Electronic plastic waste; Natural aggregates; Plastic fine aggregate (PFA).

1 Introduction

Concrete is one of the most prominent and frequently used construction materials on the earth. Its global production is approximately 5.3 billion cubic meters per year, The world's second most utilized material in the universe after water[1]. Besides that, increased urbanization is driving the market growth for infrastructure, which in turn is going to increase the utilization of concrete. The extreme utilization of concrete is draining natural aggregate resources, which is thought to be a disastrous exercise as it harms watersheds and other ecosystem functions[2]. But on the other hand, Plastic materials, have become a significant environmental threat and are discarded in substantial volumes day after day. Every year, approximately 30 million tons of solid waste are generated in Pakistan[3], and 299 million tons of plastic waste were produced worldwide in 2013 [4]. A fraction of this plastic waste is recycled, whereas the remainder is frequently tossed aside in landfills, rivers, and seas, or burnt. All such mitigation strategies pollute the land and harm aquatic organisms, while burning emits toxic fumes.

Electronic plastic waste (EPW) comprises the plastic from dismantled household items, machines, televisions, freezers, radio equipment, etc. In Pakistan, the total amount of electronic waste produced is roughly 433 kilograms per capita, and 44.7 million tons of Electronic waste (E-waste) were noted globally in 2016[5]. Only around 12.5 percent of E-waste is effectively recycled globally, while the remaining portion is thrown away or burned. [6]. EPW's negative environmental impacts necessarily require its recycling and potential use in the construction industry.

Several attempts were made to study the effectiveness of EPW aggregates as a partial alternative to natural aggregates. Plastic waste (electronic and PET products) has been shredded into fine aggregates to evaluate its potential in concrete. K.

Alagusankareswari et al. [7] substituted fine aggregates by 0%, 10%, 20%, and 30% of EPW aggregates in concrete. About 3.8%, 7.25%, and 10.96% reduction in the self-weight were observed replacing 10%, 20%, and 30% fine aggregates. Likewise, the compressive strength was decreased by 7.6%, 21.47%, and 26.11%, and tensile strength was reduced by 1.67%, 20.98%, 38.98%, respectively with the increment of EPW replacement ratio. Similarly, the effect of EPW fine aggregate in partial replacement of natural sand was assessed by Basha et al. on concrete properties [8]. They recommended a 20% replacement ratio by obtaining the compressive strength of 32.2 MPa and split tensile strength of 4.8 MPa at 28 days of curing. Some author also studied the thermal performance of PFA concrete,as shown in Figure 1 Such as It is important to mention that the ABS plastic is heated to the melting point only to reshape it and is not burned. The corresponding author have performed the TGA analysis of concrete with this particular plastic type and it was observed that up to 2000 C, the change in weight of the sample is negligible compared to control sample meaning the release of substances and gases is at minimum. Furthermore, if this plastic is not reused using only the melting process, it may be burned, land filled or thrown into sea which would create more serious environmental problems[9]. Lili et al. replaced fine aggregate with coal bottom ash (CBA) in roller compacted concrete (RCC), and the results of compressive strength, deformation, stress strain curve, and splitting tensile strength indicate a decreasing trend with CBA material. However, in the case of uniaxial compressive strength, the disruption growth process is delayed[10]. Similarly, li et al. has also used Aragonite and calcite calcium carbonate whisker (CW) for improving the mechanical properties of cementitious composites. It has been added as a high-performance, low-cost, micro fiber material. Which showed a significant decrease in the heat of hydration of cement and the total amount of non-evaporable water. Also an increase in the yield stress and plastic viscosity of cement past was observed[11] Also, Lili et al. investigates the effect of high temperature on the microstructure of CW reinforced cement paste using nanoindentation and a mercury intrusion porosimetry test. The result shows that the fractal component of calcium carbonate whisker reinforced cement paste increased with increasing temperature and porosity[12]Other plastic types like high-density polyethylene (HDPE) plastic have also been utilized in concrete as a fine aggregate substitute by Amalu et al. [13]. The results indicate that for all concrete mixes and at all curing ages, the compressive strength decreased from 24.44 MPa (controlled) to 17.55 MPa (25% HDPE substitution). Choi et al. [14] used PET waste from plastic jugs as a fine aggregate substitute in concrete for the fresh and mechanical properties assessment. About 21% reduction in the compressive strength was found utilizing 75% PET waste plastic as natural fine aggregate replacement. But in our case with the replacement of PFA in concrete the compressive strength decreased by 13.6% which represents the positivity of using PFA in concrete.

Past studies investigated the use of various plastics (PVC, HDPE) as a fine aggregate substitute in concrete. However, only a few studies have been published on EPW as a fine aggregate substitute in concrete, reviewing its mechanical and durability properties. As a result, this research looks into the mechanical and durability properties of EPW concrete that uses manufactured PFA as a natural fine aggregate substitute. It is intended to develop durable lightweight concrete, ensuring a feasible replacement ratio, and reducing the reliance of the construction industry on natural fine aggregate. For this purpose, PFA was used as a replacement of natural sand with substitution levels of 0%, 10%, 15%, and 20% of natural fine aggregate. The compressive strength test was performed to assess the mechanical properties of EPW concrete while sorptivity coefficient and alternate wetting and drying tests were adopted to evaluate the durability properties.

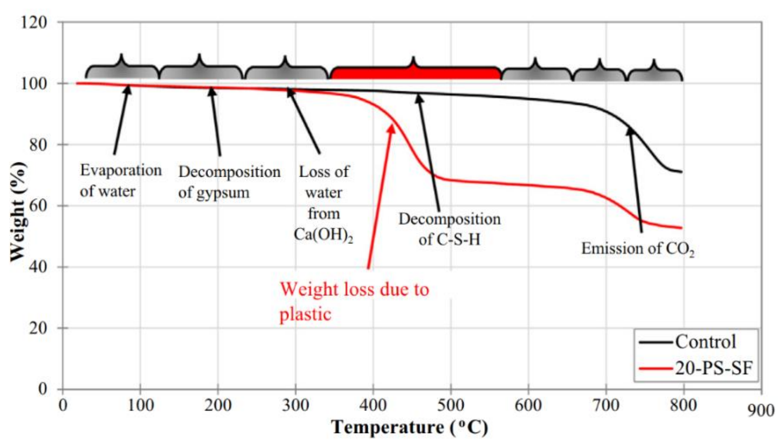

Figure 1 TGA analysis of EW[9]

2 Experimental Detail

The Fauji Cement Company Limited's Ordinary Portland Cement (OPC) of grade 53 is used as a binding agent. The OPC used is a general-purpose Type-I cement according to ASTM C150/C150M. In Table 1 Both the physical and chemical properties of OPC provided by the vendor are listed. The concrete mixture was made with potable water appropriate for drinking.

Table 1. General properties of Portland cement

Chemical properties	Results (%)	Physical properties	Results
SiO_2	22.5	Fineness modulus	93.4%
SO_3	5	Specific gravity	322
Loss on ignition	1.70	Initial setting time	110min
Al_2O_3	2.80	Final setting time	180min
MgO	1.76	28-day compressive strength	47MPa

2.1 Aggregates

To develop a concrete mix, natural sand of the Lawrencepur quarry was utilized as a fine aggregate. It has a fineness modulus of 2.73, is dark in color, and is classified as medium sand. In this study, coarse aggregates from the local market were used, which were processed by grinding rocks with a maximum size of 20mm. The EPW is depicted shown in Figure 2, had been bought from the Rawalpindi local store and was composed of scrap computer equipment such as computer mouses, keyboards, printers, and so on, which have been processed in three stages before being altered into a manufactured plastic fine aggregate (PFA). The process initiates with the washing of EPW using ordinary tap water followed by shredding the plastic into smaller pieces in a mechanical shredder. To remove other similar objects such as wires, steel, etc., all the broken EPW was then screened out in the second stage. After screening, the shredded EPW was melted in a kiln at a high temperature (200° C), followed by cooling in water to turn it into plastic rocks. The plastic rocks were eventually crushed and ground to turn into plastic fine aggregates (PFA) in the last stage. The detail process of preparation of EW is shown in Figure 3. The general properties of all aggregates (fine, coarse, and PFA) are enlisted in Table 2.

Figure 2. Dumped electronic wastes (E-waste)

Figure 3 Detail process of preparation of PFA

Table 2.General properties of aggregates (coarse, fine, and PFA)

Properties	Coarse aggregate	Natural fine aggregate	Plastic fine aggregate
Maximum nominal size(mm)	20	4.73	4.72
Minimum nominal size(mm)	4.75	0.074	0.149

Fineness modulus	7.21	2.73	3.18
Specific gravity	2.71	2.61	1.21
Saturated surface dry water	1.08	0.49	0

2.2 Mix composition:

Four different types of concrete mixes were produced incorporating plastic fine aggregate (PFA) in partial replacement of natural sand by adopting the M20 concrete mix. The number of samples tested is listed in table. while the mix composition is demonstrated in table

Table 3 Detailed summary of all tests

Properties	Dimensions of specimens	No of Specimens			
		P0	P10	P15	P20
Slump	Standard cone size	3	3	3	3
Compressive strength (28 days)	100 ×100 ×100 mm^3 (cubic)	3	3	3	3
Sorptivity coefficient (28 days)	100× 50 mm (Disk)	3	3	3	3
Alternate wetting & drying	100 ×100 ×100 mm^3 (cubic)	3	3	3	3

Table 4 Mix composition of PFA concrete

Mix ID	PFA (%)	Cement (kg/m^3)	Water (kg/m3)	Coarse aggregate (kg/m^3)	Sand (kg/m^3)	PFA (kg/m^3)
P0	0	424	212	44.13	676	-
P10	10	424	212	44.13	608	52
P15	15	424	212	44.13	575	79
P20	20	424	212	44.13	541	105

3 Results

3.1 Fresh property

3.1.1 Slump

The slump test, which is a measure of concrete consistency and fluidity, was used to assess EPW concrete's workability. Figure *4* depicts the results of the slump test performed on EPW concrete. An increasing trend was observed in the workability of EPW concrete mix with the increasing amount of PFA. The enhancement in the workability by 30.16% with 10% replacement of natural fine aggregate with the PFA and an almost 10% increment in the slump value was reported for every 5% further increment in substitution of PFA in EPW concrete mix as shown in Figure *5*.

The increase in workability of EPW concrete mix with the addition of PFA may be due to PFA's extremely low water absorption. As observed and reported in previous experiments, the excess water in the mix aids in increasing workability [13]–[15]. However, the workability of concrete depends upon numerous factors including aggregate size, water absorption capacity, and shape. The size of PFA was regulated during processing, but a higher slump value is due to the excess of free water in EPW concrete.

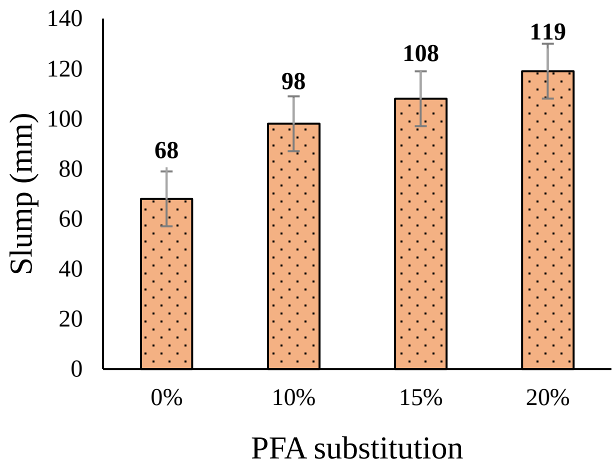

Figure 4. The slump of EPW concrete mixes

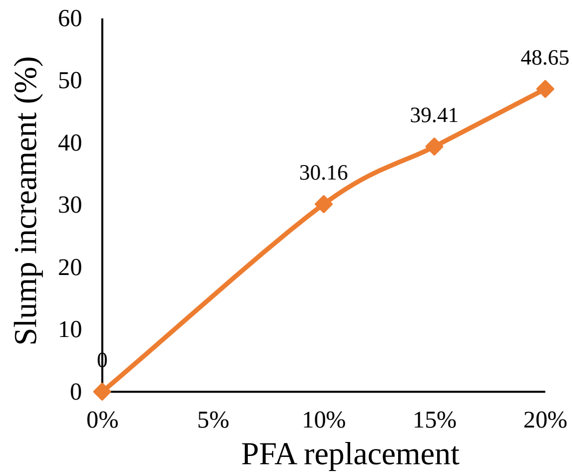

Figure 5.Slump % increased with PFA substitution

3.2 Mechanical property

3.2.1 Compressive strength

The compressive load carrying capacity of EPW concrete is assessed by performing Compressive strength tests for cubes of 100mm. The 28-day compressive strength test results of P0, P10, P15, and P20 are shown in Figure 6. It has shown that the compressive strength of EPW concrete decreases with an increasing percentage of PFA. About 2.6%, 9%, and 13.6% decrease in the compressive strength was noticed for P10, P15, and P20 samples, in Figure 7 respectively.
The decrease in compressive strength is because of the PFA's smooth surface texture, which produces a weak interfacial bond between PFA and cement paste [16]. Furthermore, the plastic aggregates have hydrophobic nature, which produces excess water in the mixture and reduces the strength of EPW concrete. However, some studies relate the decrease in compressive strength to the imbalanced moduli, which occurs when PFA particles have a lower elastic modulus than the adjacent cement paste, resulting in small cracks. The outcomes of EPW concrete compressive strength support the previous work [7], [10], [11], performed on the plastic waste utilization as partial replacement of natural aggregates.

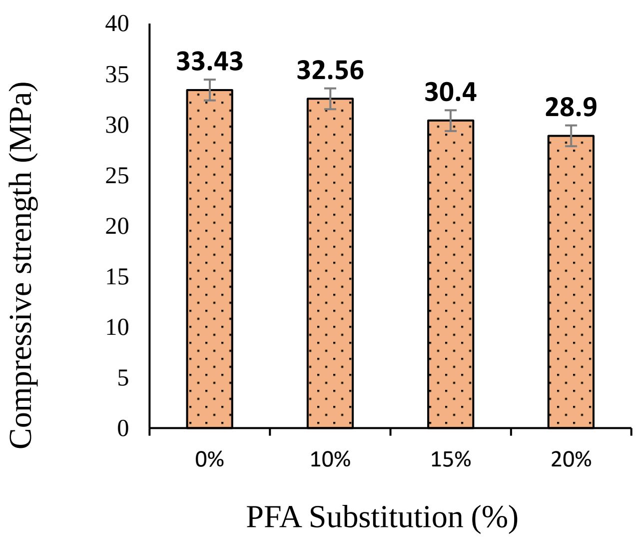

Figure 6. Compressive strength of EPW concrete at 28 days

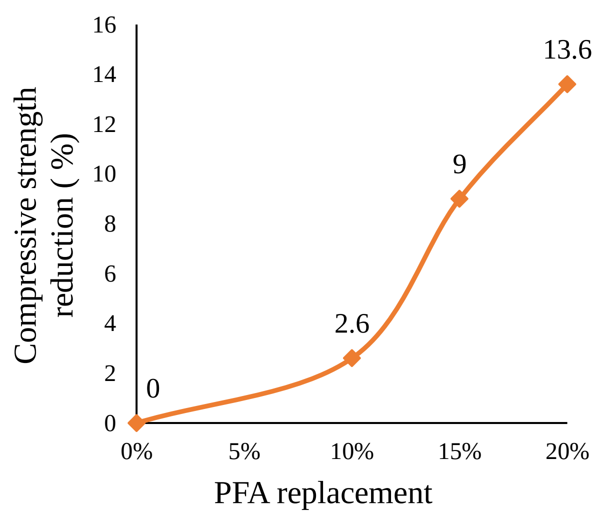

Figure 7 Compressive strength decrease with PFA replacement.

3.3 Durability property

3.3.1 Sorptivity coefficient

The amount of water absorbed by a substance through capillary action per unit area is known as the sorptivity coefficient (SC). Materials with a high sorptivity coefficient are more vulnerable to degradation, which affect durability adversely. The sorptivity coefficient of the specimen was measured by taking the weight gain of a specimen after immersing it in water for 6 hours. Figure 8 shows the experimental results of the sorptivity coefficient for all mixes of EPW concrete (P0, P10, P15, and P20). For SC 100mm*50mm disk was prepared and tested. It can be seen in Figure 9 that the sorptivity coefficient decreases with the increasing percentage of PFA substitution. Water absorption cumulative reduction reaches up to 57.25% for P20, highlighting the role of PFA in sorptivity coefficient reduction. The cumulative reduction in sorptivity coefficient shown in Figure **9** eventually adds to the EPW concrete durability enhancement. This significant decrease in water absorption can be attributed to the impervious nature and non-absorbent behavior of plastic aggregates [18].

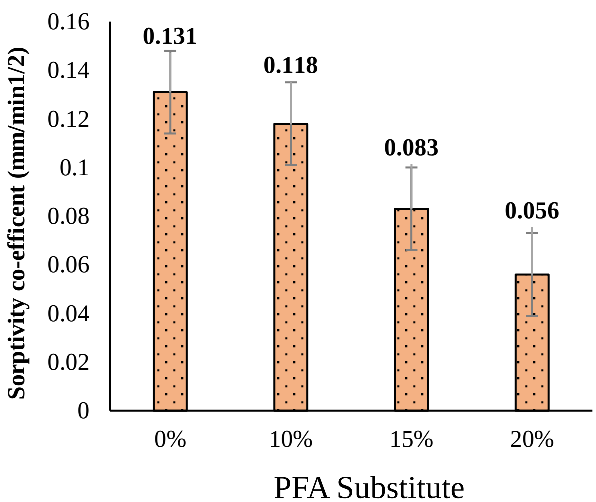

Figure 8 *The sorptivity coefficient of EPW concrete*

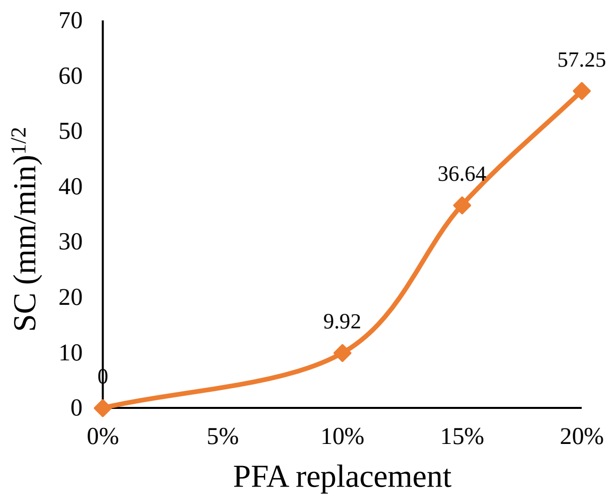

Figure 9 SC reduction with PFA replacement

3.3.2 Alternate wetting and drying

This experiment reflects the ability of concrete to degrade when subjected to alternate wetting and drying cycles, such as sea tidal waves. In this test EPW concrete samples were exposed to alternate wetting and drying procedure for 25 cycles. The compressive strength reduction of EPW concrete upon exposure to 25 alternate wetting and drying conditions in addition to the average loss in compressive strength is shown in Table 5. While Figure 10 illustrate the comparative compressive strength of all percentages with PFA incorporation after 0 and 25 cycles of alternate wetting and drying. The results show that the compressive strength is affected negatively while resistance to strength degradation in 25 cycles is significantly increased with the incorporation of PFA. When compared to P0, the higher percentage of PFA (P20) generates additional resistance to alternative wetting and drying cycles. This progress is attributed to PFA's non-absorbent nature as compared to natural fine aggregates. In the control mix, compressive strength degradation is 24.3% for PO. Likewise, the compressive strength reduction for P10, P15, and P20 is approximately 21.3%, 8.88%, and 14.1%, respectively.

Table 5. Compressive strength of EPW concrete after 25 cycles of alternate wetting and drying.

Mix Id	Compressive strength (MPa)	Compressive strength reduction (%)
	25 cycle	25 cycle
PO	25.3	24.3
P10	25.6	21.4
P15	27.7	8.88
P20	28.0	3.11

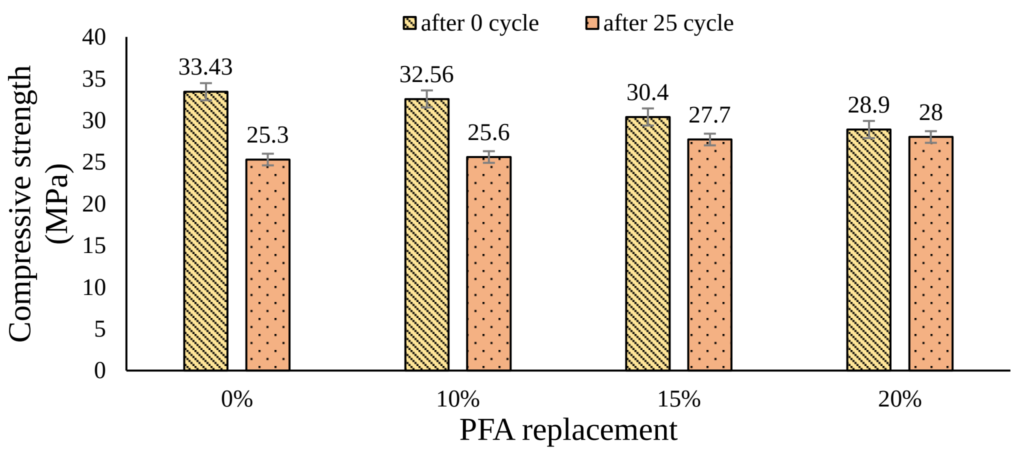

Figure 10 Alternate wetting and drying before and after 25 cycles.

4 Conclusion

The research provides a review of the effect of PFA inclusion on EPW concrete results. The influence of increasing replacement levels (10%, 15%, and 20%) of natural fine aggregates by PFA on the fresh, mechanical, and durability properties of EPW concrete is demonstrated. Increasing the substitution level of sand by PFA leads to the following conclusions:

•The workability of EPW concrete significantly improved due to the non-absorbent smooth surface texture of PFA.

• The mechanical properties (compressive strength) of EPW concrete were substantially decreased as a result of poor and ineffective bonding of PFA with the cement paste to remain firm. However, EPW concrete is still preferred to utilize for construction purposes because the minimum compressive strength accomplished by EPW concrete is greater than the minimum pressure required (17.5 MPa).

•The sorptivity coefficient values significantly reduced due to the non-absorbent nature of PFA in EPW concrete. Minimizing the water absorption capability of EPW concrete mitigates several issues e.g., concrete spalling, reinforcement corrosion, etc., improving the durability properties of EPW concrete.

•The percentage reduction in compressive strength after 25 cycles of alternate wetting and drying tends to decrease with increasing PFA percentage as the PFA has lower water absorption and does not permit the smooth swelling and shrinkage of concrete, making the EPW concrete suitable for offshore construction activities.

This study demonstrates the production of PFA from raw electronic waste and its suitability for use as a natural fine aggregates substitute in concrete mixes. The negative impact of PFA on mechanical properties limits the use of EPW concrete in projects where concrete strength is critical. However, the increased durability of EPW concrete in respective properties extends its usage in other applications such as coastal or offshore structures, etc.

Further research works are suggested to elevate the mechanical characteristics of EPW concrete using pozzolanic materials i.e., silica fume, nanoparticles, etc. Moreover, it is important to examine some other durability characteristics such as freezing and thawing, chloride migration, wear resistance, ultrasonic pulse velocity, temperature resistance, etc. along with the chemical and microstructural properties of EPW concrete for the proper application of PFA concrete

Acknowledgment

First of all, the authors would like to thank the editor and all the reviewers for suggesting improvements for the manuscript. The following line is also added in acknowledgements as an appreciation for the anonymous reviewers.The authors would like to express their gratitude to the entire staff of the Civil Department's concrete research laboratory at the University of Engineering and Technology (UET) for their continuous experimental support.

References

[1] C. Roskos, D. Cross, M. Berry, and J. Stephens, "Identification and Verification of Self-Cementing Fly Ash Binders for ' Green ' Concrete," *2011 World Coal Ash Conf.*, 2011, [Online]. Available: http://www.flyash.info/.

[2] D. Padmalal and K. Maya, "Introduction," *Environmental Science and Engineering (Subseries: Environmental Science)*, no. 9789401791434. Springer Berlin Heidelberg, pp. 1–7, 2014, doi: 10.1007/978-94-017-9144-1_1.

[3] "The Looming Plastic Pollution Crisis | Pakistan Today." https://www.pakistantoday.com.pk/2019/03/14/the-looming-plastic-pollution-crisis/ (accessed Sep. 23, 2020).

[4] D. K. A. Barnes *et al.*, "Accumulation and fragmentation of plastic debris in global environments Accumulation and fragmentation of plastic debris in global environments," no. June, 2009, doi: 10.1098/rstb.2008.0205.

[5] H. Bin Hameed, Y. Ali, and A. Petrillo, "Environmental risk assessment of E-waste in developing countries by using the modified-SIRA method," *Sci. Total Environ.*, vol. 733, p. 138525, 2020, doi: 10.1016/j.scitotenv.2020.138525.

[6] T. Haque, "Introduction to Electronics (E-Waste) Recycling," *The balance small bussiness*, 2019. .

[7] K. Alagusankareswari, S. Sandeep Kumar, K. B. Vignesh, and K. Abdul Hameed Niyas, "An experimental study on E-waste concrete," *Indian J. Sci. Technol.*, vol. 9, no. 2, pp. 3–7, 2016, doi: 10.17485/ijst/2016/v9i2/86345.

[8] M. Basha S, B. Reddy Ch, and V. K, "Strength behaviour of geopolymer concrete replacing fine aggregates by M-sand and E-waste," *Int. J. Eng. Trends Technol.*, vol. 40, no. 7, pp. 401–407, 2016, doi: 10.14445/22315381/ijett-v40p265.

[9] K. Ali, M. I. Qureshi, S. Saleem, and S. U. Khan, "Effect of waste electronic plastic and silica fume on mechanical properties and thermal performance of concrete," *Constr. Build. Mater.*, vol. 285, p. 122952, May 2021, doi: 10.1016/j.conbuildmat.2021.122952.

[10] R. C. Using, C. Bottom, and A. Entirely, "Constitutive Model of Uniaxial Compressive Behavior for," 2021.

[11] L. Li, M. Cao, and H. Yin, "Comparative roles between aragonite and calcite calcium carbonate whiskers in the hydration and strength of cement paste," *Cem. Concr. Compos.*, vol. 104, no. June, 2019, doi: 10.1016/j.cemconcomp.2019.103350.

[12] L. Li, Z. Li, M. Cao, Y. Tang, and Z. Zhang, "Nanoindentation and porosity fractal dimension of calcium carbonate whisker reinforced cement paste after elevated temperatures (up to 900◦C)," *Fractals*, vol. 29, no. 2, pp. 1–16, 2021, doi: 10.1142/S0218348X21400016.

[13] R. . Amalu, Azeef Ashraf, Muhammad Hashim, Rejith.K.U, Vijitha.V, "Use of Waste Plastic As Fine Aggregate Substitute in," *Int. J. Sci. Eng. Res.*, vol. 7, no. 4, pp. 172–177, 2016.

[14] Y. W. Choi, D. J. Moon, J. S. Chung, and S. K. Cho, "Effects of waste PET bottles aggregate on the properties of concrete," *Cem. Concr. Res.*, vol. 35, no. 4, pp. 776–781, 2005, doi: 10.1016/j.cemconres.2004.05.014.

[15] E. del R. Castillo, N. Almesfer, O. Saggi, and J. M. Ingham, "Light-weight concrete with artificial aggregate manufactured from plastic waste," *Constr. Build. Mater.*, vol. 265, p. 120199, 2020, doi: 10.1016/j.conbuildmat.2020.120199.

[16] Z. Z. Ismail and E. A. AL-Hashmi, "Use of waste plastic in concrete mixture as aggregate replacement," *Waste Manag.*, vol. 28, no. 11, pp. 2041–2047, 2008, doi: 10.1016/j.wasman.2007.08.023.

[17] S. Akçaözoğlu, C. D. Atiş, and K. Akçaözoğlu, "An investigation on the use of shredded waste PET bottles as aggregate in lightweight concrete," *Waste Manag.*, vol. 30, no. 2, pp. 285–290, 2010, doi: 10.1016/j.wasman.2009.09.033.

[18] B. T. A. Manjunath, "Partial Replacement of E-plastic Waste as Coarse-Aggregate in Concrete," *Procedia Environ. Sci.*, vol. 35, pp. 731–739, 2016, doi: 10.1016/j.proenv.2016.07.079.

3rd Conference on Sustainability in Civil Engineering (CSCE'21)
Department of Civil Engineering
Capital University of Science and Technology, Islamabad Pakistan

EXPERIMENTAL INVESTIGATION OF THE INFLUENCE OF NANO GRAPHITE PLATELETS ON THE COMPRESSIVE STRENGTH OF CONCRETE WITH RECYCLED PLASTIC AGGREGATES

[a]Farhan Ahmad, [b]Muhammad Irshad Qureshi*

a: Department of Civil Engineering, University of Engineering and Technology, Taxila, Pakistan.
Email: engrfarhan51@gmail.com
b: Department of Civil Engineering, University of Engineering and Technology, Taxila, Pakistan.
Email: irshad.qureshi@uettaxila.edu.pk
* Corresponding author: Email ID: irshad.qureshi@uettaxila.edu.pk

Abstract- The rapid increase in industrialization, population, and modern life style has significantly increased the rate of waste production. As a result of technological advancement and up gradation of technological innovations, the rate of obsolescence in the electronic equipment's has also increased making it one of the fastest growing waste streams in the world. The current annual production rate of Electronic or E-waste is 3-4% in the world. E-waste will be increased approximately to 55 million tons per year by 2025. This E-waste significantly damages the environment because of its non-biodegradable nature. In order to diminish this problem one of the ways is to utilize this E-waste in the concrete production. Past works have used the E-waste plastic as a raw material for production of plastic aggregate to be used as a substitute for natural aggregates. However, the results have shown the plastic aggregate reduces the compressive strength of resulting concrete. In order to enhance the strength properties, different dosages of nano graphite platelets (NGPs) (i.e. 1, 3 and 5%) have been introduced into concrete with replacement of 25% coarse aggregates by plastic aggregates. Dispersion test is carried and a ratio of 0.6:1 (surfactant/NGPs) is found to yield maximum dispersion. NGPs are nanofillers which significantly improve the density and hardness of the cementitious composite due to reduction in porosity and reinforcement in microstructure. The specimen that contained 25% (by volume) of E-waste as an aggregate, and 5% of NGPs (by weight of cement) was proved effective in increasing compressive strength by 13.56%.

Keywords- E-waste, nano graphite platelets, dispersion, compressive strength.

1 Introduction

Concrete is considered to be the second most extensively utilized material in construction industry. This can be attributed to its properties, accessibility to its raw materials, low price in conjunction with increasing industrialization and urbanization. This led to increasing natural rocks exploitation which resulted in deterioration of the landscape and escalation in environmental pollution. The rapid increase in industrialization, urbanization and population growth significantly increased the amount of waste generation. The use of modern electrical and electronic appliances turns out to be an essential part of our everyday life enabling us with more convenient, secure, comfortable, easy and swift procurement. As a result of technological advancement and continuous up gradation of technological products, the rate of waste generation in the electrical and electronic equipment also increased, making it one of the fastest increasing waste streams in the world. E-waste significantly damages the environment and its disposal process is relatively more difficult compared to other waste streams. To prevent the environment from the adverse and hazardous effect of E-waste, proper utilization is required along with its disposal. In order to tackle this problem one of the ways is to utilize this waste in concrete production. To minimize the adverse impacts on environment and diminishment of natural resources [1, 2], the preservation of raw materials needs to be emphasized. In concrete, coarse aggregates occupy 65-70% of volume. Large scale use of concrete ingredients especially use of coarse aggregates from rocks causes depletion of natural resources thus welcoming disasters in the form of global warming, land sliding and depletion of ozone layer. Nowadays, many countries around the globe are facing a deficiency of natural resources, and depend on the imports to meet their needs[3]. Efforts are required to take important steps in order to save the nature without compromising on the overall performance of concrete. Various attempts has been carried out in the past with the ambition of substituting natural aggregate with recycled aggregate[3, 4]. Therefore, several other alternatives in concrete to natural aggregates like demolition waste, plastic waste, paper etc. has gained momentum.

Zeeshan et al. [5] conducted an extensive investigation by utilizing manufactured E-waste as a partial substitute of coarse aggregate. The substitution ratio of E-waste aggregate was 10 to 20%. It was revealed that by substituting coarse aggregate by 10 and 20% of E-waste, the mechanical properties decreased while an improvement in durability and workability properties were reported. Needhidasan et al. [6] studied the effect of grinded E-waste on the concrete performance. The range of substitution ratio used was 0 to 20% of coarse aggregate by volume. It was reported that the decrement in compressive and flexural strength occurs with the increments of E-waste but the tensile strength increased. Also, the utilization of E-waste plastic in concrete production not only prevented the environmental degradation but also reduced the cost and unit weight of concrete. M.Chougan et al. [7] studied the variation of density, microstructure, compressive strength, flexural strength and permeability properties of concrete with different commercial nano graphite content (i.e. 0.01, 0.1 and 0.2%) and found that there is significant increase in mechanical characteristics and density up to 30% and 16%, respectively and a significant decrease in permeability. W.Meng el al.[8] investigated the effect of different nanomaterials like carbon nanofibers (CNFs) and graphite nanoplatelets (GNPs) on the mechanical performance of ultra-high performance concrete (UHPC). The dosage of nanomaterials ranged from 0 to 0.3% and it was found that the compressive strength increases from 5 MPa to 8 MPa. It was also reported that 59%, 276% and 56% enhancement was observed in flexural strength, toughness and tensile strength, respectively. However, no work has been reported to date where nano materials are used to enhance the strength properties of concrete with plastic aggregates. In this research, an attempt is made to enhance the compressive strength properties of E-waste incorporated concrete with the addition of nano graphite platelets (NGPs).

2 Materials and Experiments

Ordinary Portland cement (OPC) Type-I, meeting the guidelines as per ASTMC150 was utilized as a binder. Table 1 indicates different characteristic of Type-1 cement. Commonly used tap water with a PH range between 6.5 and 7 is used. Fine aggregate utilized in this research was "Lawrence Pur sand" with maximum particle size of 4.75mm in compliance with ASTM C566. Coarse aggregate utilized was obtained from Margalla brand in Taxila, Pakistan with maximum particle size of 20mm. Properly manufactured E-waste plastic aggregate by heating process of required shape and size comparable to coarse aggregate was utilized in this research work as shown in Figure 1(a). Table 3 indicates the physical properties of fine and coarse aggregates as well as manufactured E-waste plastic aggregates. Nano graphite platelets (NGPs) were commercially purchased in powder form and its elemental composition obtained from EDX spectroscopy is listed in Table 2. The surface texture and morphology of NGPs were determined using SEM which indicates that the NGPs have rough texture and irregular shape as shown in Figure. 1(b). Acacia gum (AG) was utilized as a natural surfactant for effective dispersion of NGPs.

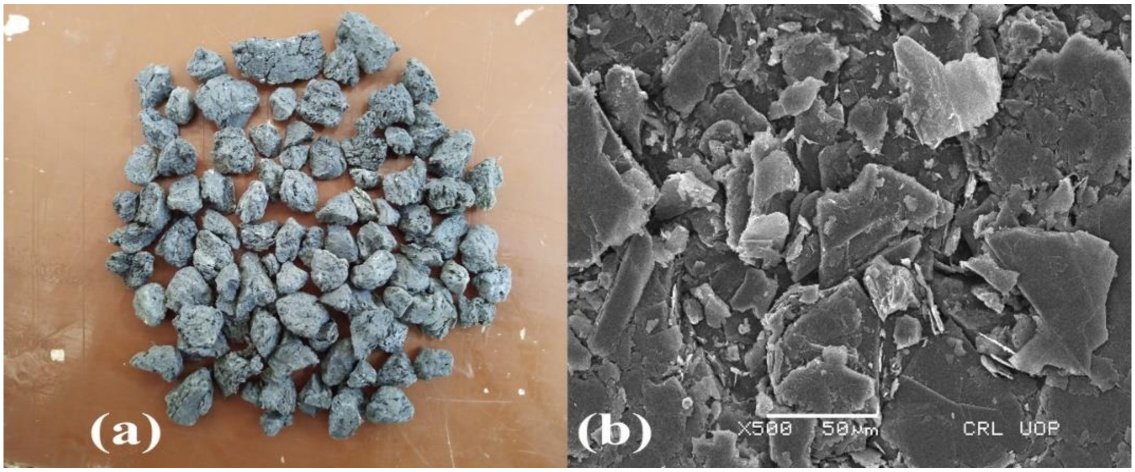

Figure 1: (a) Manufactured E-waste aggregate and (b) SEM micrograph of NGPs

Table 1-Features of OPC

Chemical composition	Content (%)
CaO	63.58
SiO_2	21.9
Al_2o_3	5.1
Fe_2O_3	4.1
MgO	2.56
SO_3	2.74
Na_2O	0.23
K_2O	0.88
Ignition loss	0.63

Table 2-Elemental Detail of NGPs

Elements	Nano graphite platelets (NGPs)	
	Weight(%)	Atomic (%)
C	83.77	90.45
O	7.83	6.35
Mg	0.62	0.33
Al	0.64	0.31
Si	2.97	1.37
S	0.32	0.13
Ca	1.81	0.59
Fe	2.03	0.47
Total	100	100

Table 3-Physical properties of fine and coarse aggregates, and manufactured E-waste aggregates

Property	Coarse Aggregate	E-waste aggregate	Fine Aggregate
Max. nominal size(mm)	20	19	4.75
Min. nominal size (mm)	4.74	4.75	0.074
Specific Gravity	2.71	1.21	2.78
SSD water Absorption (%)	1.08	0	0.5
Color	Dark	Black brown	Dark
Shape	Angular	Angular	_
Aggregate impact value (%)	25.43	8.108	NIL
Aggregate Crushing value	27.42	1.3	NIL
Fineness Modulus	Nil	Nil	2.27
Bulk Density(lb./ft^3)	94.05	30.43	100

1.1 Concrete mix proportions

In this research, M25 grade concrete was followed and the mix ratio was 1:2.14:3.08[9]. The maximum size of coarse and fine aggregate was 20 and 4.75 mm, respectively and water cement ratio was kept at 0.49. In this research, about 25% of E-waste aggregate by volume of coarse aggregate was incorporated in concrete along with different percentages of nano graphite platelets (NPGs) (i.e., 0%, 1%, 3% and 5%). Tilting drum revolving with speed of 35rev/min was utilized for concrete mix preparation. Five different concrete mixes with one control mix and the other four of E-waste incorporated concrete with different percentages of NGPs were prepared. Each E-waste incorporated concrete mix contained 25% of E-waste by volume of coarse aggregate with 0, 1, 3 and 5 % NGPs respectively. The mixing of concrete was done in three stages. Firstly, the NGPs along with specified amount of acacia gum (AG) was dispersed in water with the help of ultra sonicator. Secondly, the coarse, fine and E-waste aggregates were mixed along with 75% of total water (containing dispersed NGPs) for four minutes. Thirdly, the remaining 25% of water with cement were also added and mixed for the next four minutes. 30 cylinders of dimension (150mmx300mm) were prepared and tested at 7 and 28 days. Table 4 indicates the details of concrete mixes.

Table 4-Details of concrete mix proportions

Mix ID	Cement (Kg/m^3)	Water (Kg/m^3)	W/C	Fine aggregate (Kg/m^3)	Coarse aggregate (Kg/m^3)	E-waste (kg/m^3)	NGPs (kg/m^3)
Control Mix	367.34	180	0.49	789	1133.3	___	___
E.W25%NGP0%	367.34	180	0.49	789	850.0	126.51	—
E.W25%NGP1%	367.34	180	0.49	789	850.0	126.51	3.67
E.W25%NGP3%	367.34	180	0.49	789	850.0	126.51	11.02
E.W25%NGP5%	367.34	180	0.49	789	850.0	126.51	18.37

3 Results and Discussion

3.1 Dispersion of NGPs

NGPs consist of graphite which is closely packed and has an affinity to agglomerate because of its large surface area and fine particle size. The Van der Waals forces resist its dispersion into the cementitious matrix. Therefore, it is needed to homogeneously disperse NGPs in cementitious composites. For the dispersion of NGPs, the use of natural surfactant or chemicals with mechanical sonication is required in order to reduce the impact of powerful Van der Waal forces [10]. In this research, a natural surfactant i.e., Acacia gum (AG) was utilized to disperse NGPs effectively by breaking the Van der Waals interactions among NGPs [11, 12]. Initially, NGPs to surfactant ratios from 1:0 to 1:1 was chosen. To obtain dispersed solution, the surfactant-ultrasonication method was used and then it is further diluted to the amount of water required for concrete preparation. After that a prototypical sample was collected, to examine the effectiveness of dispersion. The absorbance of dispersed aqueous solution is generally examined at 500nm (whereas 500nm is the wavelength to be adjusted on UV spectroscopy apparatus), which remains least affected at the ambient conditions [11]. The absorbance of dispersed aqueous solution for each ratio of NGPs/surfactant (1:0 to 1:1) with increment of 0.2 was examined. Finally, Graph is plotted between Surfactant/NGPs ratios and absorbance at each corresponding ratio. The results indicated that the ratio of 0.6:1 (surfactant**:** NGPs) shows maximum absorption and is optimum to obtain uniform dispersion aided with 45 min of mechanical sonication as given in Figure 2.

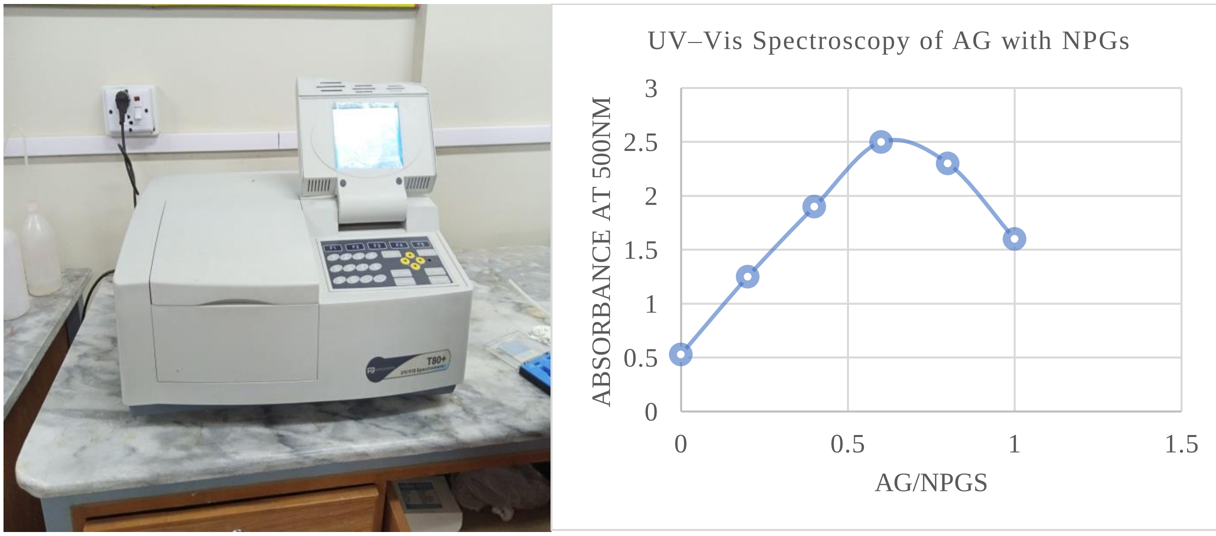

Figure 2: UV-Vis Spectroscopy of AG with NGPs

3.2 Compressive strength

In the design of reinforced cement concrete (RCC) structures, concrete compressive strength is considered as one of the fundamental property. In the present study, cylindrical compressive strength of concrete containing E-waste is determined in compliance with ASTM C39 [13]. Before testing, both ends of the cylinder were provided with rubber pads to prevent any surface irregularity to effect the result as well as the ends to be orthogonal to the sides of specimen as shown in Figure 3. Compressive strength was measured with the help of universal testing machine (UTM) having 1000 kN capacity. Figure 4(a) reported the results of cylindrical compressive strength at 7- and 28-days curing. The results show that the compressive strength of E-waste incorporated concrete significantly declines which is in compliance with the past works [14, 15]. This reduction in strength is because of the smooth texture of E-waste aggregates thereby yielding a weak adhesion with the cement paste. Also, because of the hydrophobic nature of plastic aggregate, it may prevent the intrusion of requisite quantity of water during curing which is necessary for the process of hydration. Another reason of strength decrement may be because of low water absorption/non-absorbent behavior of E-waste aggregates thereby causing excess content of water in concrete mixes. Besides, E-waste aggregates have less unit weight, density, strength and rigidity in contrast to natural coarse aggregates thereby generating a high stress region facilitating the spread of damage which may be the cause of strength decrement [16, 17]. The results shown in Figure 4(a**)** also reported that by incorporating NGPs in concrete containing plastic aggregate, increase in compressive strength was observed as compared to E-waste concrete without NGPs. This increase in compressive strength is a result of the inclusion of NGPs which strengthened the composites at nano level thereby resulting in an improvement in the strength. Previous studies mentioned that incorporating nanofillers (GNPs, GONPs, NGPs, nG etc.) in cementitious composites significantly improve their density and hardness due to the reduction in porosity and reinforcement in microstructure of cementitious composites[7, 18].

The results reported that the strength of concrete comprising 25% partial substitution of coarse aggregate via E-waste aggregate decreased by 26.3% after 28 days curing compared to control samples. Also, the results reported that compressive strength of E-waste concrete containing 1, 3 and 5% NGPs has been improved compared to E-waste concrete without NGPs. Figure 4 (a) and (b) indicates the assessment in compressive strength and the rate of strength gain at various curing ages. It has been observed that the regular rise in compressive strength occur with increasing dosage of NGPs in the E-waste concrete composites at various hydration period. After 28 days curing, the mix with 5% NGPs shows the maximum compressive strength with 13.56% enhancement compared to E-waste concrete without NGPs. The mix with 1% NGPs was examined to have lowest increase in strength of 1.95%. Hence, it was concluded that incorporating NGPs in E-waste concrete significantly enhanced its compressive strength. Thus, a substitution proportion up to 25% can be utilized with manufactured E-waste coarse aggregate as the compressive strength achieved is more than the minimum compression capacity required for usually implemented concrete which is assessed to be 17.24 MPa [19].

Figure 3: Compression test Assembly a. Cylinder before test and b. Cylinder After test

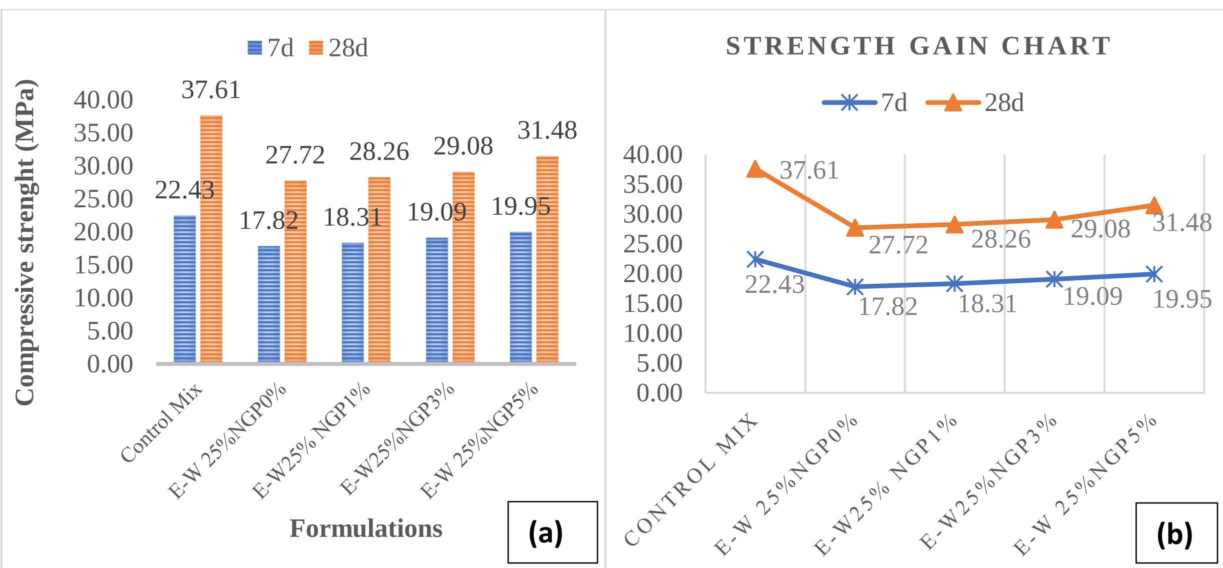

Figure 4: (a) Compressive Strength of NGPs composites incorporated with 25% E-waste and (b) Strength gain chart

4 Conclusions

From the research study, the following results regarding the NGPs reinforced composites containing the 25% E-waste aggregates has been drawn.

- Dispersion of nano graphite platelets (NGPs) in water along with surfactant (AG) yield maximum dispersion at ratio of 0.6:1 (surfactant/NGPs ratio).
- The compressive strength of E-waste incorporated concrete without NGPs was decreased by 26.3% after 28 days curing as compared to control samples. This is because of the weak bond formation between E-waste aggregate and cement paste. Also, it can be examined that the gradual increase in compressive strength was observed with increase in concentration of NGPs in the E-waste concrete mixes. The mix with 5% NGPs exhibits 13.56% higher compressive strength after 28 days curing as compared to E-waste concrete without NGPs. This increase in strength is due to the inclusion of NGPs which significantly improved density, hardness and reduced porosity thereby resulting an enhancement in the strength property.
- A substitution of E-waste up to 25% can be utilized with manufactured E-waste coarse aggregate with reasonable compressive strength.

Acknowledgement

The careful review and constructive suggestions by the anonymous reviewers are gratefully acknowledged.

References

1. Ragaert, K., L. Delva, and K. Van Geem, *Mechanical and chemical recycling of solid plastic waste.* Waste Management, 2017. **69**: p. 24-58.
2. Paul, S.C., B. Šavija, and A.J. Babafemi, *A comprehensive review on mechanical and durability properties of cement-based materials containing waste recycled glass.* Journal of Cleaner Production, 2018. **198**: p. 891-906.
3. Suchithra, S., M. Kumar, and V. Indu, *Study on replacement of coarse aggregate by E-waste in concrete.* International Journal of Technical Research and Applications, 2015. **3**(4): p. 266-270.
4. Alagusankareswari, K., et al., *An experimental study on e-waste concrete.* Indian Journal of Science and Technology, 2016. **9**(2).
5. Ullah, Z., et al., *An experimental study on the mechanical and durability properties assessment of E-waste concrete.* Journal of Building Engineering, 2021. **38**: p. 102177.
6. Santhanam, N., B. Ramesh, and F.K. Pohsnem, *Concrete blend with E-waste plastic for sustainable future.* Materials Today: Proceedings, 2020. **22**: p. 959-965.
7. Chougan, M., et al., *High performance cementitious nanocomposites: The effectiveness of nano-Graphite (nG).* Construction and Building Materials, 2020. **259**: p. 119687.
8. Meng, W. and K.H. Khayat, *Mechanical properties of ultra-high-performance concrete enhanced with graphite nanoplatelets and carbon nanofibers.* Composites Part B: Engineering, 2016. **107**: p. 113-122.
9. Kumar, K.S. and K. Baskar, *Recycling of E-plastic waste as a construction material in developing countries.* Journal of Material Cycles and Waste Management, 2015. **17**(4): p. 718-724.
10. Meng, W. and K.H. Khayat, *Effect of graphite nanoplatelets and carbon nanofibers on rheology, hydration, shrinkage, mechanical properties, and microstructure of UHPC.* Cement and Concrete Research, 2018. **105**: p. 64-71.
11. Baloch, W.L., R.A. Khushnood, and W. Khaliq, *Influence of multi-walled carbon nanotubes on the residual performance of concrete exposed to high temperatures.* Construction and Building Materials, 2018. **185**: p. 44-56.
12. Iqbal, H.W., et al., *Influence of graphite nano/micro platelets on the residual performance of high strength concrete exposed to elevated temperature.* Construction and Building Materials, 2020. **253**: p. 119029.
13. ASTM, C., *Standard test method for compressive strength of cylindrical concrete specimens*. 2012.
14. Vickers, N.J., *Animal communication: when i'm calling you, will you answer too?* Current biology, 2017. **27**(14): p. R713-R715.

15. Prasanna, P.K. and M.K. Rao, *Strength variations in concrete by using E-waste as coarse aggregate.* International Journal of Education and applied research, 2014. **4**(2).
16. Ahirwar, S., et al., *An experimental study on concrete by using E-waste as partial replacement for course aggregate.* IJSTE-International Journal of Science Technology & Engineering, 2016. **3**(04).
17. Osei, D.Y., *Experimental investigation on recycled plastics as aggregate in concrete.* Int. J. Struct. Civ. Eng. Res, 2014. **3**(2): p. 168-174.
18. Devi, S. and R. Khan, *Effect of graphene oxide on mechanical and durability performance of concrete.* Journal of Building Engineering, 2020. **27**: p. 101007.
19. Ismail, Z.Z. and E.A. Al-Hashmi, *Use of waste plastic in concrete mixture as aggregate replacement.* Waste management, 2008. **28**(11): p. 2041-2047.

3rd Conference on Sustainability in Civil Engineering (CSCE'21)
Department of Civil Engineering
Capital University of Science and Technology, Islamabad Pakistan

PREDICTING THE IMPACT OF CHEMICAL AND PHYSICAL VARIABILITY IN BINARY AND TERNARY CEMENTITIOUS BLENDS

[a] Vireen Limbachiya*, [b] Rabee Shamass,

a: Civil and Building Services Engineering, London South Bank University, limbachv@lsbu.ac.uk
b: Civil and Building Services Engineering, London South Bank University, shamassr@lsbu.ac.uk
* Corresponding author: Email ID: limbachv@lsbu.ac.uk

Abstract- To reduce the quantity of CO_2 emitted within the construction industry, cementitious by-products will need to be implemented on a larger scale. In relation to the use of by-products, one of the biggest disadvantages is that not only from source to source, obtaining a by-product from the same source could result in a variation in the chemical and physical properties which will then impact the mechanical properties. Therefore, the paper reviewed binary and ternary cementitious pastes that were produced from 7 different by-products and predicted the impact of variation in the chemical and physical properties on the 14-day compressive strength. The predictions and analysis were done with the use of artificial neural networks (ANN). Overall, ANN successfully derived an accurate prediction which correlated with the trends that were expected. This study noted that if parameters of the overall mix were taken into consideration, the increase in SiO_2 will have a negative impact while increase in CaO would have a positive impact on the 14-day strength. The most accurate form of understanding the impact of chemical and physical variability of cementitious replacements, took into consideration both Ca/Si ratio and the average particle size.

Keywords- ANN, Cement Replacements, Predicting Compressive Strength, Binary and Ternary Cementitious Pastes.

1 Introduction

Studies have reviewed many combinations of cementitious by-products that can be used as an alternative for Ordinary Portland Cement (OPC) [1,2]. The impact of Pulverised Fuel Ash (PFA) and By-Pass Dust (BPD) obtained over a 6-month period from the same source was analysed by Limbachiya et al [3]. The results showed a clear variation in the chemical and physical properties and the correlating impact on strength development. Shi et al. [4] reported on four different forms of glass powder being used as a cementitious replacement. They noted that the particle size has a large effect on the compressive strength of concrete, as replacements containing larger particles size produced lower strengths at 28 days. Overall results showed one of the biggest disadvantages of using by-products is that not only from source to source, obtaining a by-product from the same source could result in a variation in the chemical and physical properties, which thereafter will result in a variation in concrete strength.

When there is variation in OPC, Bogues equations are used to predict the quantity of compounds that will be produced during the hydration process and therefore, an indication of strength development. Bogues equations use the oxide composition of OPC to determine the level of alite, belite, tricalcium aluminate and tetracalcium aluminoferrite [5], which are responsible for different properties within concrete. As well as the individual oxide values, oxide ratios are known to help predict the behaviour of concrete. In a review of the influence of the Ca/Si ratio on the compressive strength of cementitious calcium–silicate–hydrate binders, it was concluded that as Ca/Si ratio decreases the compressive strength increase [6]. It was reported that the diffraction peaks' intensity of calcite became stronger as the Al/Si ratio decreases [7]. It is assumed that as the Al/Si ratio increases the calcite decreases, therefore, greater formation of strength gaining compounds. Finally, it was concluded that for lower ratios of Mg/Si, unreacted silica remained and for higher ratios brucite precipitated. Therefore, greater forms of deterioration are likely to occur at higher ratio levels [8].

When it comes to a variation of properties in cement replacements, there are no such tools that can be used to help understand the impact on strength development. Studies have used artificial neural networks (ANN) to predict the strength of concrete using more sustainable materials. ANN was used to understand the effect of Nano and Micro Silica on the compressive and flexural strength of cement mortar [9]. The variables in this case were the quantity of different components used in the mortar mixture. The study concluded that the ANN model was able to predict the compressive strength to a high level of accuracy. Alongside ANN, Fuzzy Logic (FL) models have been used by previous studies to help predict the behaviour of concrete [10,11]. Although both models can provide high levels of accuracy, both studies concluded that ANN provided a greater level of statistical accuracy in comparison to FL. Currently, there are very few studies that have looked at a range of chemical and physical variations in by-product combinations and the impact of this on the strength of cementitious mixes consisting of binary and ternary blends. Therefore, the aim of this study is to use ANN to predict the impact of chemical and physical variability in cementitious by-products. The objectives are to firstly, produce ternary and binary cementitious pastes. Secondly, use the chemical and physical properties of these mixes as input parameters to help predict and determine the parameters that have an impact on the compressive strength. The significance of this work is that it will allow for a better understanding on the impact of chemical and physical variability when using binary and ternary cementitious pastes and determine how ANN can be used to help predict this behaviour.

2 Research Methodology

2.1 Cementitious materials

The OPC fulfilled the requirements of BS EN 197-1 CEM I [12]. The cementitious materials used in this study were obtained from a variety of sources. Ground Granulated Blast Furnace Slag (GGBS), (PFA), Metakaolin (MK), BPD and Silica Fume (SF) came in powder form to be used within the cementitious binders, while Basic Oxygen Slag (BOS) and Glass Powder (GP) came in a crushed form and required further grinding before adequate levels of fineness were achieved. Table 1 provides the physical and chemical properties using of Hydro 2000/Mastersizer 2000 and X-Ray Fluorescence (XRF) respectively.

Table 1 Chemical and physical properties of OPC and Cement Replacements.

Composition	SiO_2 (%)	TiO_2 (%)	$Al2O_3$ (%)	Fe_2O_3 (%)	MnO (%)	MgO (%)	CaO (%)	Na_2O (%)	K_2O (%)	P_2O_5 (%)	SO_3 (%)	Average Particle Size (µm)
OPC	19.42	0.36	4.55	2.49	0.02	1.03	60.60	0.22	0.57	0.2	3.62	38
PFA	45.85-52.29	0.98-0.82	24.43-19.76	10.38-7.55	0.16-0.06	2.09-1.44	6.13-2.81	0.91-0.63	2.75-2.02	0.51-0.22	0.84-0.48	55-32
GGBS	33.28	0.57	13.12	0.32	0.32	7.74	37.16	0.33	0.48	0.01	2.21	20
SF	94.21	0.01	0.48	0.71	0.01	0.55	0.37	0.35	1.15	0.04	0.17	0.7
BOS	13.94	0.7	2.98	25.99	3.17	6.56	39.57	0.06	0.03	1.51	0.28	30
GP	69.56	0.07	2.01	0.65	0.32	1.19	10.61	12.28	0.98	0.03	0.18	100
MK	54.06	0.02	40.65	0.77	0.01	0.23	0.03	0.17	1.89	0.16	0.02	7
BPD	17.34-12.79	0.23-0.19	4.26-3.47	2.36-1.88	0.05-0.04	1.11-0.82	53.6-44.03	1.16-0.5	10.06-4.28	0.25-0.12	12.22-6.25	67-32

2.2 Mix Design and Fabrication

130 cementitious pastes were produced, tested, and analysed by the author in the laboratory for this study. All cementitious pastes were produced as a semi dry mix with constant w/c ratio of 0.2, therefore the variability in the results could only be due to the difference in the chemical and physical properties of the materials used. To produce samples, the binary//ternary mixtures were mixed thoroughly before water was added and compaction was applied. Thereafter, the samples were cured and tested following guidance in BS EN1338:2003. The paste cubes had a dimension of 50x50x50mm, and the compressive strength was obtained at 14 days. The mixes produced had varying levels of OPC and by products. OPC, PFA, BPD, GGBS, GP, SF, BOS and MK was used to produce the cement pastes by up to 60%, 80%,10%, 80%, 15%, 15%, 45% and 30% by weight respectively. All mixes can be found in Appendix A.

3. Artificial Neural Network setup

3.1 Input and target parameters

Input properties were based on the combined oxide properties of ternary and binary mixes, which were obtained by using Equation 1 that was developed for this study. Table 2 provides the actual oxide compositions determined using XRF for 11 ternary and binary mixes, as well as the predicted oxide compositions using Equation 1. Based on these results, Equation 1 was determined to provide an accurate assumption on the combined oxide percentage and therefore be used in the ANN models.

$$\mathrm{Input_n} = \left(\frac{\%\mathrm{OPC}}{100} * \mathrm{OPC_n}\right) + \left(\frac{\%\mathrm{CR1}}{100} * \mathrm{CR1_n}\right) + \left(\frac{\%\mathrm{CR2}}{100} * \mathrm{CR2_n}\right) \qquad \textit{(Equation 1)}$$

Where $\mathrm{Input_n}$ is the input parameter for the ANN model, %OPC is the percentage of OPC used in the mix, n represents the chemical or physical property, OPC_n is the quantity of n in OPC, %CR1 and %CR2 are the percentages of cement replacements used in the mix and $CR1_n$ and $CR2_n$ are the quantity of n in the cement replacement.

Table 2 Accuracy of Predicted Ternary and Binary oxides

	SiO_2 (%)		CaO (%)		Al_2O_3 (%)		Fe_2O_3 (%)	
Mix	Actual	Predicted	Actual	Predicted	Actual	Predicted	Actual	Predicted
1	24.53	24.96	50.49	51.22	6.73	7.98	1.69	1.62
2	31.25	32.22	45.57	45.91	5.16	5.76	1.74	1.69
3	20.62	21.10	50.27	51.71	5.33	5.95	6.31	6.76
4	23.42	24.14	50.96	52.05	6.40	7.53	1.77	1.72
5	23.96	24.71	49.23	50.52	6.69	7.94	1.64	1.61
6	16.51	17.23	51.21	52.19	3.64	3.92	11.18	11.89
7	27.98	30.75	38.42	37.66	10.19	12.38	4.65	5.58
8	35.49	37.72	37.62	37.23	7.55	8.83	3.60	4.16
9	33.91	34.10	44.82	45.71	5.76	6.08	1.56	1.68
10	31.60	31.06	46.25	47.55	5.72	6.71	1.63	1.66
11	28.94	29.53	48.75	48.46	5.94	7.03	1.70	1.65

3.2 Neural Network setup.

Figures 1 and 2 show the ANN models developed in this study, namely NN 5-7 and NN 4-7. Seven neurons in the hidden layer were chosen as they provided accurate predictions. The five input parameters for NN 5-7 were based on the combined chemical properties that form alite, belite, tricalcium aluminate and tetracalcium aluminoferrite, as well as the average particle size. The four input parameters for NN 4-7 were ratios that are known to have a direct impact on hydration compounds and formation of calcium silicate hydrate (CSH) as well as the average particle size.

To have a more effective ANN setup, the input and target parameters are normalised [13]. The calculated output will then also provide a normalised value, which will require it to be reverse transformed to obtain the actual target value. To normalize the input and output parameters, Equation 2 was applied to all values. Where a_{min} and a_{max} are constants, b_{max} is the greatest value of that parameter, b_{min} is the lowest value of that parameter, b is the actual value and a is the normalised value. Table 3 provides the values required to de-normalise the values.

$$a = (a_{max}-a_{min})*(b-b_{min})/(b_{max}-b_{min}) + a_{min} \qquad \textit{(Equation 2)}$$

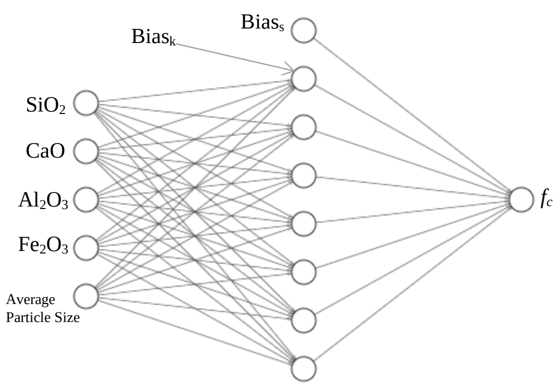

Figure 1 NN 5-7 Model

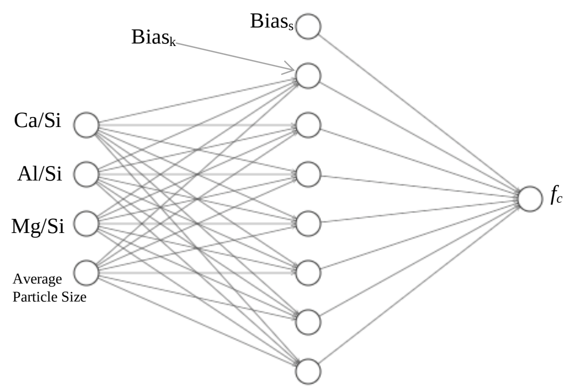

Figure 2 NN 4-7Model.

Table 3 Parameters used to normalise input and target values

Input/Target Parameter	a_{max}	a_{min}	b_{min}	b_{max}
SiO_2	1	-1	16.12	53.30
CaO	1	-1	5.69	60.23
Al_2O_3	1	-1	3.61	26.34
Fe_2O_3	1	-1	0.49	16.59
Ca/Si	1	-1	0.11	3.15
Al/Si	1	-1	0.18	0.58
Mg/Si	1	-1	0.02	0.28
Average Particle Size (µm)	1	-1	18.01	58.9
f_c(MPa)	1	-1	0	70.40

Once the input and output parameters were determined, the next step was to define the neural network. A pre-installed neural network fitting app in Matlab was used in this study. The neural network fitting app solves an input-output fitting problem with a two-layer feedforward neural network. The network was a two-layer feed-forward network with sigmoid hidden neurons and linear output neurons and trained with Levenberg-Marquardt backpropagation algorithm, unless there is not enough memory, in which case scaled conjugate gradient backpropagation will be used [13]. The backpropagation algorithm involves two phases. Firstly, the forward phase where the activations are propagated from the input to the output layer [11]. Secondly, the backward phase where the error between the observed actual value and the desired nominal value in the output layer is propagated backwards to modify the weights and bias values [11]. Equations 3 and 4 provide the calculations that includes the transfer function required to determine the normalised target value based on the inputs provided [14]. Where, O_s is the normalised ouput value, q is the number of input parameters; r is the number of hidden neurons; s is the number of output parameters; $Bias_s$ and $Bias_k$ are the biases of s^{th} output neuron and kth hidden neuron (H_k), respectively; with j,k is the weights of the connection between I_j and are the weights of the connection between H_k and O_s

$$O_s = Bias_s + \sum_{k=1}^{r} w_{k,l}^{ho} \cdot \frac{2}{(1+ e^{(-2\,x\,H_k)})-1} \qquad \textit{(Equation 3)}$$

$$H_k = Bias_k + \sum_{j=1}^{q} w_{j,k}^{ih}.I_j \quad \text{(Equation 4)}$$

For training, validation and testing the data sets were divided into 70%, 15% and 15% respectively. To assess the accuracy of the output the regression (R^2), Root Mean Square Error (RMSE), Mean Absolute Percentage Error (MAPE) and Mean Square Error (MSE) were calculated using equations 5, 6, 7 and 8 respectively.

$$R^2 = 1 - \left(\frac{\sum_{i=1}^{N}(ti - Oi)^2}{\sum_{i=1}^{N}(ti - tm)^2}\right) \quad \text{(Equation 5)}$$

$$RMSE = \sqrt{\frac{\sum_{i=1}^{N}(Oi - ti)^2}{N}} \quad \text{(Equation 6)}$$

$$MAPE = \frac{1}{N}\sum_{i=1}^{N}\left|\frac{Oi - ti}{ti}\right| \times 100 \quad \text{(Equation 7)}$$

$$MSE = \frac{\sum_{i=1}^{N}(Oi - ti)^2}{N} \quad \text{(Equation 8)}$$

Where t_i is the actual compressive strength of concrete mixes, t_m is the mean compressive strength of concrete mixes, O_i is the predicted value and N is the total number of data points in each set of data.

3.3 Impact of Individual Input

As well as assessing the accuracy of the models with Equations 5 and 6, it is also important to understand the impact of input parameters on the output value. This will allow for further validation of the ANN model and algorithms, as it will have the potential to be used for values outside of those used in this model. It is important to note that the values will still have to remain within the ranges stated in Table 3. To determine the impact of each input parameter, the connection weight approach was adopted. The connection weight approach uses raw connection weights, which accounts for the direction of the input–hidden–output relationship and results in the correct identification of variable contribution [15]. Based on this approach, Equation 9 was used to determine impact of each input parameter. A negative value will mean that an increase in this parameter will decrease the output value, a positive value will mean that an increase in this parameter will increase the output value and those values with the largest value are those with the largest impact.

$$Input_x = \sum_{Y=A}^{E} Hidden_{XY} \quad \text{(Equation 9)}$$

3 Results

3.1 Predicting the impact of chemical and physical variability

Figure 3 provides the predicted vs experimental strengths for the NN 5-7 model. Equation 10 is derived from algorithms used in the ANN model for predicting the 14-day compressive strength. The R^2, RMSE, MSE and MAPE values were 0.95,4.36, 18.98 and 17.97, respectively. Overall, the results show that ANN can predict compressive strength to a high level of accuracy when oxide values are considered using Equation 1. It is assumed that the accuracy is closely related to the input parameters behaving in the way that is expected. Figure 4 provides the impact that each input parameter has on the output value. Results show that as SiO_2, Al_2O_3 and Average particle size increases, there will be a negative impact on the output and that as CaO and Fe_2O_3 increases, there is a positive impact on the output. Studies [16][17][18] have previously noted that cement replacements with a high SiO_2 content provide greater strength development through secondary reaction with $Ca(OH)_2$. However, when SiO_2 is determined using Equation 1, results show that overall, as SiO_2 increases the strengths tend to decrease and that as CaO increases there is an increase in strength. This therefore correlates with result that you would expect to occur in OPC hydration in which the ratio of Ca/Si dictates the formation of compounds and therefore strength development. Fe_2O_3 is the input that is responsible for the greatest strength gain.

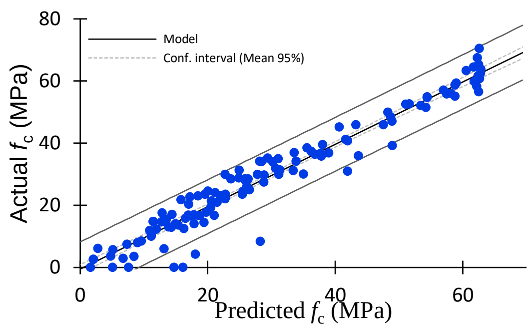

Figure 3 Regression of Actual fc vs predicted fc for NN 5-7

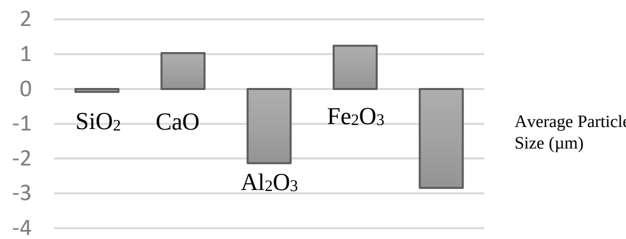

Figure 4 Influence of each input for NN 5-7

$$f_c = -0.84 - 1.47\left(\frac{2}{(1+e^{(-2H_1)})} - 1\right) - 0.29\left(\frac{2}{(1+e^{(-2H_2)})} - 1\right) - 0.74\left(\frac{2}{(1+e^{(-2H_3)})} - 1\right) + 1.86\left(\frac{2}{(1+e^{(-2H_4)})} - 1\right) - 1.89\left(\frac{2}{(1+e^{(-2H_5)})} - 1\right) - 0.25\left(\frac{2}{(1+e^{(-2H_6)})} - 1\right) + 0.55\left(\frac{2}{(1+e^{(-2H_7)})} - 1\right) \qquad \textit{(Equation 10)}$$

Where:
H_1= -1.80 + 0.29SiO_2 + 0.20CaO + 1.90 Al_2O_3- 4.06Fe_2O_3 + 1.49 Average Particle Size (µm)
H_2= 1.97 + 0.52SiO_2 – 1.01CaO + 2.29Al_2O_3 + 0.15Fe_2O_3 -0.63 Average Particle Size (µm)
H_3= -0.03 + 1.22SiO_2 - 0.71CaO – 2.74Al_2O_3 + 0.22Fe_2O_3 – 1.19 Average Particle Size (µm)
H_4= -0.87 + 0.25SiO_2 + 0.43CaO + 1.68Al_2O_3 – 2.27Fe_2O_3 + 0.35 Average Particle Size (µm)
H_5= 1.08 – 0.42SiO_2 + 0.23CaO + 1.96Al_2O_3 - 0.38Fe_2O_3 – 0.42 Average Particle Size (µm)
H_6= 1.84 + 2.71SiO_2 – 4.00CaO + 0.46Al_2O_3 – 1.37Fe_2O_3+ 3.03 Average Particle Size (µm)
H_7= -2.42 + 1.47SiO_2 – 1.56CaO – 0.07Al_2O_3 – 2.45Fe_2O_3 – 4.36 Average Particle Size (µm)

Although studies [19] have reported on the positive impact of Nano Fe_2O_3 on the compressive strength of concrete, the strength development in concrete is primarily down to the formation of Calcium silicate (Ca_3SiO_5) and Larnite (Ca_2SiO_4). Overall, the biggest impact on strength development was the average particle size. Results show that as average particle size increases the strength decreases. This correlated with conclusions made is previous studies [4] and is assumed to be due to the water not being able to react with the oxides within the inner particle of the material.

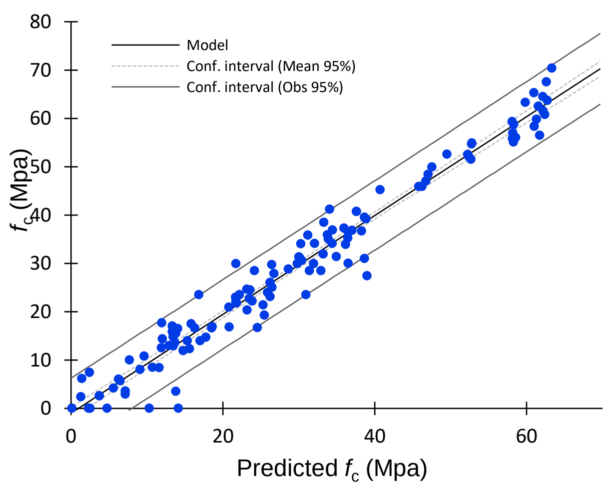

Figure 5 Regression of Actual fc (MPa) vs predicted fc (MPa) for NN 4-7

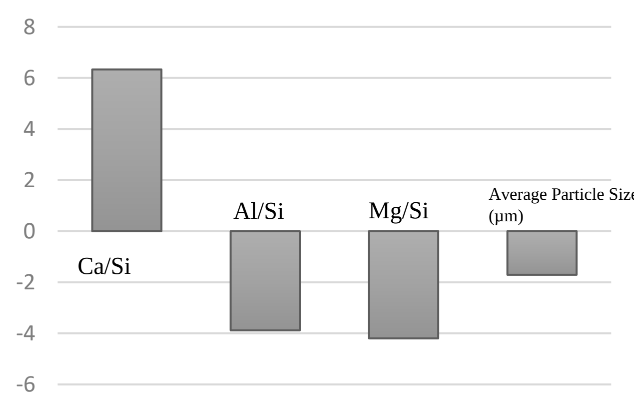

Figure 6 Influence of each input for NN 5-7-1

$$f_c = 1.04 + 0.67\left(\frac{2}{(1+e^{(-2H_1)})}-1\right) + 0.38\left(\frac{2}{(1+e^{(-2H_2)})}-1\right) - 0.36\left(\frac{2}{(1+e^{(-2H_3)})}-1\right) + 0.64\left(\frac{2}{(1+e^{(-2H_4)})}-1\right) + 0.73\left(\frac{2}{(1+e^{(-2H_5)})}-1\right) + 1.72\left(\frac{2}{(1+e^{(-2H_6)})}-1\right) + 1.00\left(\frac{2}{(1+e^{(-2H_7)})}-1\right)$$

(Equation 11)

Where:
H_1= 1.79 + 0.34Ca/Si – 1.79Al/Si - 1.86 Mg/Si – 0.29 Average Particle Size (μm)
H_2= 1.20 – 0.43Ca/Si – 2.36Al/Si – 0.26 Mg/Si – 0.15 Average Particle Size (μm)
H_3= 0.31 – 0.66Ca/Si + 2.31Al/Si + 2.17 Mg/Si + 3.15 Average Particle Size (μm)
H_4=0.02 – 1.16a/Si + 0.12Al/Si + 1.10 Mg/Si + 1.41 Average Particle Size (μm)
H_5= -0.74 + 0.89Ca/Si + 1.92Al/Si + 0.37 Mg/Si – 0.64 Average Particle Size (μm)
H_6=1.76 + 2.61Ca/Si + 0.08Al/Si - 1.77 Mg/Si – 0.18 Average Particle Size (μm)
H_7= 3.96 – 1.50Ca/Si – 1.67Al/Si + 1.43 Mg/Si + 0.26 Average Particle Size (μm)

Figure 5 provides the predicted vs experimental strengths for the NN 4-7 model. Equation 11 is derived from algorithms used in the ANN model for predicting the 14-day compressive strengths. The R^2, RMSE, MSE and MAPE values are 0.96,3.61, 13.05 and 14.92, respectively. In comparison to oxide percentages, oxide ratios predict output with a higher level of accuracy and a greater level of confidence. It is assumed R^2, RMSE, MSE and MAPE provide a greater level of accuracy as the ratios correlate to the formation of compounds that are responsible for strength development. Therefore, ANN can correlate more accurately with the output parameter. Figure 6 shows that the only ratio that contributes to strength development is Ca/Si, while Al/Si, Mg/Si and average particle size all have a negative impact. Overall, these results show that when taking into consideration the combined oxide values, the trends follow those that are noted for OPC hydration. Alite has a Ca/Si ratio of 3:1 and C-S-H has a Ca/Si ratio of approximately 2:1, so excess lime is available to produce $Ca(OH)_2$ [20]. Alite is responsible for early age strength development as well as formation of $Ca(OH)_2$ and results show that as Ca/Si increases, the trend is that strength properties will also increase. When reviewing Al/Si, trends show a decrease in strength as the ratio increases. This correlates with the results that were obtained, in which it was concluded that depending on the Al_2O_3/SiO_2 ratio, the ye'elimite and gehlenitephases were formed in different proportions [21]. It is therefore assumed that in the mixes reviewed, at lower ratios of Al/Si, content of gehlenite exceeds the ye'elimite content therefore decreasing strength properties.

4 Conclusion

The overall the aim of this study was to produce an ANN system that can be used to predict the compressive strength of cement paste at 14 days and to help in gaining a better understanding of the chemical and physical properties of by-products that impact strength. Based on the report the following conclusions can be made:

- Cementitious replacements for OPC come from a variety of sources with varying chemical and physical properties. Based on the level of replacement, the use of these materials will have an impact on the hydration compounds produced and therefore, strength.
- Although previous studies have noted that a high SiO_2 content in the cement replacement would allow for an enhancement in strength with secondary hydration of $Ca(OH)_2$. This study noted that if parameters of the overall mix as shown in Equation 1 were taken into consideration, the increase in SiO_2 will have a negative impact on strength.
- When reviewing oxide values, oxide ratios provided the most accurate trendlines. Results showed when taking all parameters in consideration, the trend was like that of OPC hydration alone, in which Ca/Si determined the early age strength.
- Overall, results showed that the most accurate form of understanding the impact that chemical and physical variability of cementitious replacements would have, took into consideration both Ca/Si and the average particle size.
- ANN is a powerful tool in helping us gain a better understanding of the impact that each input has in relation to the target and allowing accurate prediction of the strength of concrete which incorporates cement replacements.
- ANN was successfully used in this study to provide an accurate prediction which correlated with the trends that were noted in the oxide analysis.

Acknowledgment

The authors gratefully appreciate and acknowledge the financial support from the 2 Engineering and Physical Sciences Research Council who had sponsored the PhD programme. The authors also acknowledge the support and facilities that were provided at Coventry University and London South Bank University.

References

[1] Qureshi, L., Ali, B. and Ali, A. (2020). Combined effects of supplementary cementitious materials (silica fume, GGBS, fly ash and rice husk ash) and steel fiber on the hardened properties of recycled aggregate concrete, Construction and Building Materials, 263, 120636.

[2] Gehlot, T., Sankhla, S. and Parihar, S. (2021). Modelling compressive strength, flexural strength and chloride ion permeability of high strength concrete incorporating metakaolin and fly ash. Materials Today Proceedings, in press.

[3] Limbachiya, V., Ganjian, E. and Claisse, P. (2015). The impact of variation in chemical and physical properties of PFA and BPD semi-dry cement paste on strength properties, Construction and Building Materials, 96, pp. 248-255

[4] Shi, C., Wu, Y., Riefler, C., and Wang, H. (2005). Characteristics and Pozzolanic Reactivity of Glass Powders. Cement and Concrete Research, 35 (5),pp. 987-993

[5] Neville, A. (1996) Properties of Concrete. Fourth Edition, Wiley.

[6] Kunthur, W., Ferreiro, S. and Skibsted,J. (2017). Influence of the Ca/Si ratio on the compressive strength of cementitious calcium–silicate–hydrate binders, Journal of Materials Chemistry A, 5, pp. 17401-17412.

[7] Li, J., Yu, Q., Huang, H. and Yin, s. (2019). Effects of Ca/Si Ratio, Aluminum and Magnesium on the Carbonation Behavior of Calcium Silicate Hydrate, Materials. 12, 1268.

[8] Nied, D., Enemark-Rasmussen, K., L'Hopital, E., Skibsted, J., & Lothenbach, B. (2016). Properties of magnesium silicate hydrates (M-S- H). Cement and Concrete Research, 79, pp. 323-332

[9]] Azimi-Pour, M. and Eskandari-Naddaf, H. (2018) ANN and GEP prediction for simultaneous effect of nano and micro silica on the compressive and flexural strength of cement mortar, Construction and Building Materials, 189 , pp. 978-992.

[10] Ozcan, F., Atis, C., Karahan, O., Uncuoglu, E. and Tanyildizi, H. (2009). Comparison of artificial neural network and fuzzy logic models for prediction of long-term compressive strength of silica fume concrete. Advances in Engineering Software, 40 (9), pp.856-863.

[11] Golafshani, E.M., Rahai, A., Sebt, M.H. and Akbarpour, H. (2012). Prediction of bond strength of spliced steel bars in concrete using artificial neural network and fuzzy logic. Construction and Building Materials, 36, pp.411-418.

[12] British Standard Institution, BS EN 197-1 Cement Composition, specifications and conformity criteria for common cements BSI, London (2011)

[13] MATLAB and Statistics Toolbox Release 2019a, The MathWorks, Inc., Natick, Massachusetts, United States.

[14] Gupta, T., Patel, K. A., Siddique, S., Sharma, R. K. and Chaudhary, S. (2019) Prediction of mechanical properties of rubberised concrete exposed to elevated temperature using ANN, Measurement, 147, pp. 106870.

[15] Olden, J. D., Joy, M. K. and Death, R. G. (2004) An accurate comparison of methods for quantifying variable importance in artificial neural networks using simulated data, Ecological Modelling, 178 (3), pp. 389-397.

[16] Behnood, A. and Ziari, H. (2008). Effects of Silica Fume Addition and Water to Cement Ratio on the Properties of High-Strength Concrete After Exposure to High Temperatures. Cement and Concrete Composites 30 (2), 106-112

[17] Papadakis, V. G. (1999) Effect of Fly Ash on Portland Cement Systems: Part I. Low- Calcium Fly Ash. Cement and Concrete Research ,29 (11), 1727-1736

[18] Köksal, F., Altun, F., Yiğit, İ., and Şahin, Y. (2008) Combined Effect of Silica Fume and Steel Fiber on the Mechanical Properties of High Strength Concretes. Construction and Building Materials 22 (8), 1874-1880

[19] Zhang, A., Ge, A., Yang, W., Cai, X. and Du, Y. (2019). Comparative study on the effects of nano-SiO2, nano-Fe2O3 and nano-NiO on hydration and microscopic properties of white cement. Construction and Building Materials, 228 ,116767.

[20] Winter, N. (2012). Understanding Cement. Woodbridge: WHD Microanalysis Consultants Ltd.

[21] Berrio, A., Rodriguez, C. and Tobon, J. (2018). Effect of Al2O3/SiO2 ratio on ye'elimite production on CSA cement. Construction and Building Materials, 168, pp.512-521.

Appendix A

1	OPC20/PFA80*	44	OPC20.63/PFA68.12/SF11.25	87	OPC5/GGBS60/BOS25
2	PFA80/MK20	45	OPC5/PFA80/SF15	88	OPC30/GGBS40/BOS30
3	OPC14/PFA56MK30	46	OPC12.5/PFA80/SF7.5	89	OPC35/GGBS20/BOS45
4	OPC14/PFA66/MK20	47	OPC60/PFA25/SF15	90	OPC45/GGBS40/BOS15
5	OPC24/PFA66/MK10	48	OPC48.13/PFA48.12/SF7.5	91	OPC45/GGBS20/BOS35
6	OPC44/PFA26/MK30	49	OPC60/PFA32.5/SF7.5	92	OPC25/GGBS60/BOS15
7	OPC60/PFA40	50	OPC28.13/PFA68.12/SF3.75	93	OPC15/GGBS40/BOS45
8	OPC60/MK40	51	OPC36.25/PFA56.25/SF7.5	94	GGBS40/BOS60
9	OPC27/PFA46/MK10	52	OPC15/PFA80/SF5	95	GGBS60/BOS40
10	OPC28/PFA52/MK20	53	OPC48.13/PFA40.62/SF11.25	96	OPC47.5/PFA47.5/GP5
11	OPC60/GGBS40	54	OPC20.63/GGBS68.12/SF11.25	97	OPC30/PFA50/GP20
12	OPC14/GGBS56/MK30	55	OPC5/GGBS80/SF15	98	OPC27.5/PFA67.5/GP5
13	OPC14/GGBS66/MK20	56	OPC12.5/GGBS80/SF7.5	99	OPC47.5/PFA37.5//GP15
14	OPC44/GGBS46/MK10	57	OPC60/GGBS25/SF15	100	OPC35/PFA55/GP10
15	OPC28/GGBS52/MK20	58	OPC48.13/GGBS48.12/SF7.5	101	OPC60/PFA20/GP20
16	OPC24/GGBS66/MK10	59	OPC60/GGBS32.5/SF7.5	102	OPC10/PFA80/GP10
17	OPC44/GGBS26/MK30	60	OPC28.13/GGBS68.12/SF3.75	103	OPC17.5/PFA67.5/GP15
18	OPC20/GGBS80	61	OPC36.25/GGBS56.25/SF7.5	104	OPC60/PFA30/GP10
19	OPC37.5/PFA57.5/BPD5	62	OPC48.13/GGBS40.62/SF11.25	105	OPC47.5/GGBS47.5/GP5
20	OPC23.75/PFA68.75/BPD2.5	63	OPC43/PFA38/GGBS19	106	OPC30/GGBS50/GP20
21	OPC28.75/PFA68.75/BPD25	64	OPC24/PFA58/GGBS18	107	OPC27.5/GGBS67.5/GP5
22	OPC15/PFA80/BPD5	65	OPC24/PFA18/GGBS58	108	OPC47.5/GGBS37.5//GP15
23	OPC60/PFA30/BPD10	66	OPC14/PFA28/GGBS58	109	OPC35/GGBS55/GP10
24	OPC48.75/PFA48.75/BPD2.5	67	OPC26/PFA37/GGBS37	110	OPC40/GGBS60
25	OPC60/PFA35/BPD5	68	OPC14/PFA58/GGBS28	111	OPC60/GGBS20/GP20
26	OPC10/PFA80/BPD10	69	OPC44/PFA18/GGBS38	112	OPC10/GGBS80/GP10
27	OPC48.75/PFA43.75/BPD7.5	70	OPC5/PFA60/BOS25	113	OPC17.5/GGBS67.5/GP15

28	OPC37.5/GGBS57.5/BPD5	71	OPC30/PFA40/BOS30	114	OPC60/GGBS30/GP10
29	OPC23.75/GGBS68.75/BPD2.5	72	OPC35/PFA20/BOS45	115	OPC90/PFA-JUL10*
30	OPC28.75/GGBS68.75/BPD25	73	OPC45/PFA40/BOS15	116	OPC90/PFA-AUG10*
31	OPC15/GGBS80/BPD5	74	OPC45/PFA20/BOS35	117	OPC90/PFA-SEP10*
32	OPC60/GGBS30/BPD10	75	OPC40/BOS60	118	OPC90/PFA-OCT10*
33	OPC48.75/GGBS48.75/BPD2.5	76	OPC25/PFA60/BOS15	119	OPC90/PFA-NOV10*
34	OPC60/GGBS35/BPD5	77	OPC15/PFA40/BOS45	120	OPC90/PFA-DEC10*
35	OPC10/GGBS80/BPD10	78	OPC60/BOS40	121	OPC80/PFA-JUL20*
36	OPC48.75/GGBS43.75/BPD7.5	79	OPC40/PFA60	122	OPC80/PFA-AUG20*
37	OPC70/PFA-NOV30*	80	OPC90/BPD-JUL10*	123	OPC80/PFA-SEP20*
38	OPC70/PFA-DEC30*	81	OPC90/BPD-AUG10*	124	OPC80/PFA-OCT20*
39	OPC95/BPD-JUL5*	82	OPC90/BPD-SEP10*	125	OPC80/PFA-NOV20*
40	OPC95/BPD-AUG5*	83	OPC90/BPD-OCT10*	126	OPC80/PFA-DEC20*
41	OPC95/BPD-SEP5*	84	OPC90/BPD-NOV10*	127	OPC70/PFA-JUL30*
42	OPC95/BPD-OCT5*	85	OPC90/BPD-DEC10*	128	OPC70/PFA-AUG30*
43	OPC95/BPD-NOV5*	86	OPC95/BPD-DEC5*	129	OPC70/PFA-SEP30*
				130	OPC70/PFA-OCT30*

*OPC20/PFA80- 20%OPC and 80%PFA in the cementitious paste

3rd Conference on Sustainability in Civil Engineering (CSCE'21)
Department of Civil Engineering
Capital University of Science and Technology, Islamabad Pakistan

EFFECT OF JUTE FIBER AND RECYCLED COARSE AGGREGATES ON THE COMPRESSIVE STRENGTH AND POROSITY OF CONCRETE

[a]Hafiz Kamran Jamil*, [b]Faisal Shabbir

[a, b] Department of Civil Engineering, University of Engineering and Technology, Taxila, Pakistan.
kamranjamil894@gmail.com faisal.shabbir@uettaxila.edu.pk
*Corresponding author: Email ID: kamranjamil894@gmail.com

Abstract- In construction, concrete is mostly used for different projects. The drawback of plain cement concrete is that it is strong in compression but weak in tension. Nowadays, a lot of effort is made to minimize this problem by using additives e.g. fibers and cementitious material. Moreover, recycled coarse aggregates (RCA) are seeking more attention towards substituting natural coarse aggregate (NCA) because of their related economic benefits and sustainable development. Hence, this paper examines the combined influence of jute fiber (JF) and recycled coarse aggregates (RCA) on the concrete properties. In this investigation, the length of JF is kept at 10 mm. Two types of mixes are investigated i.e. with 0% RCA (control mix) and 100% RCA. In each of these mixes, 0%, 0.30%, and 0.60% of jute fiber (JF) by volume of concrete are used. The mechanical and durability properties are evaluated by compressive strength test and porosity test respectively. This investigation shows that the addition of 0.30% of JF has a positive influence whereas the addition of 0.60% has a negative influence on the mechanical property of concrete in both 0% RCA and 100% RCA cases. In both cases (0% RCA and 100% RCA), the compressive strength is slightly improved up to 0.30% of fibers but upon further increase of the fibers, the compressive strength is decreased. While in the durability test, the concrete porosity increases with the increasing quantity of JF and RCA in both 0% RCA and 100% RCA cases. In a higher dosage of fibers (0.60%), the effect of porosity is more as compared to lower dosages.

Keywords- Durability properties, Jute fiber, Mechanical property, Recycled coarse aggregates.

1 Introduction

Concrete is mostly used in structures due to its high compressive strength, low maintenance, and economical as compared to other materials. To improve its construction (mechanical and durability) properties, many researchers have been working on the addition of cementitious materials and natural fibers. This composite material is called fiber reinforced concrete. These natural fibers can be divided into three groups i.e. plant, mineral, and animal fibers. Plant fibers possess higher strength than other fibers and are investigated by different researchers [1]. According to Banthia [2], the compressive strength of concrete is increased by the addition of plant fiber. In this paper, jute fiber (JF) is used to increase the mechanical and durability properties of concrete. Islam et al. [3] used different amounts of JF and concluded that the small amount (0.25%) of JF has a positive effect on concrete properties. Dayananda N et al. [4] uses different dosages and different curing ages of JF and concluded that the addition of 0.4% JF has a positive effect on concrete and with the increase in curing age, the mechanical properties of JF reinforced concrete mix increase.

Recently, many countries are facing problems with the dumping of construction and demolition (C&D) waste due to a shortage of land. According to Akhtar [5], 3 billion tons of C&D waste are generated in 40 major countries. The volume of natural coarse aggregates (NCA) in concrete is 50-75% normally. So recycled coarse aggregates (RCA) derived from C&D waste are used to minimize the problem and to lessen the dependence on the NCA. The partial or full replacement of NCA with RCA can assist to solve the problems related to the shortage of landfills and pollution. Kwan et al. [6] indicated that the compressive strength of concrete is almost identical in the case of concrete which is made of 30% RCA and NCA concrete, and compressive strength is decreased by 20% when 100% RCA is used. In China, Li et al. [7] used RCA successfully in different structural and pavement applications and shown the positive response of RCA in civil engineering. Hoffman et al. [8] also showed the RCA sustainability in different concrete structures applications and indicated the corresponding variation in concrete properties.

The literature shows that there are rare studies on the effect of JF with RCA keeping the mechanical and durability aspects into account. For this purpose, this paper shows the behavior of JF reinforcement on the performance of concrete with RCA. In this research, two different types of mixes are made from 0% RCA (reference mix) and 100% RCA, and in every mix, 0%, 0.30%, and 0.60% of JF by volume of concrete are used. The results show that 0.30% JF has a positive effect on the properties of concrete in all cases.

2 Experimental Procedures

2.1 Materials

2.1.1 Binder

Ordinary portland cement (OPC) of grade 53 was used as a binder in this investigation. This OPC is according to ASTM C150 [9] and it is type 1. The general characteristics of OPC are given in table 1.

Table 1. General properties of OPC

Chemical composition	**Percentage (%)**	**Physical characteristics**	**Results**
SiO_2.	22.7	(SG) Specific gravity	3.13
Al_2O_3	5.15	(SS) Specific surface	318 (m^2/kg)
Fe_2O_3	3.95	Consistency	28.75 (%)
CaO	63.85	Initial setting time	175 (min)
MgO	2.71	Final setting time	240 (min)
SO_3	3.03	Soundness	No
Na_2O	0.23	28 days f_c' (compressive strength)	43.95 MPa
K_2O	0.85	Fineness	94%
Ignition loss	0.65	--	--

2.1.2 Aggregates

Originally Lawrencepur natural siliceous sand was used as fine aggregates (FA) in all mixes. Locally available natural coarse aggregate (NCA) of Margalla brand natural crush was used in this research. The chemical and physical properties of fine and coarse aggregates are given in table 2. RCA was obtained manually by crushing concrete cylinder having compressive strength in the range of 30-35 MPa. After crushing, these recycled coarse aggregates were sieved according to the size of NCA. The maximum and minimum sizes of NCA and RCA were kept constant as shown in figure 1. The gradation curve of aggregates is shown in figure 2. All aggregates (fine and coarse) used in this experiment follow the ASTM standard specification [10]. The general properties of aggregates are given in table 2.

Figure 1: Recycle coarse aggregates (RCA) and natural coarse aggregates (NCA)

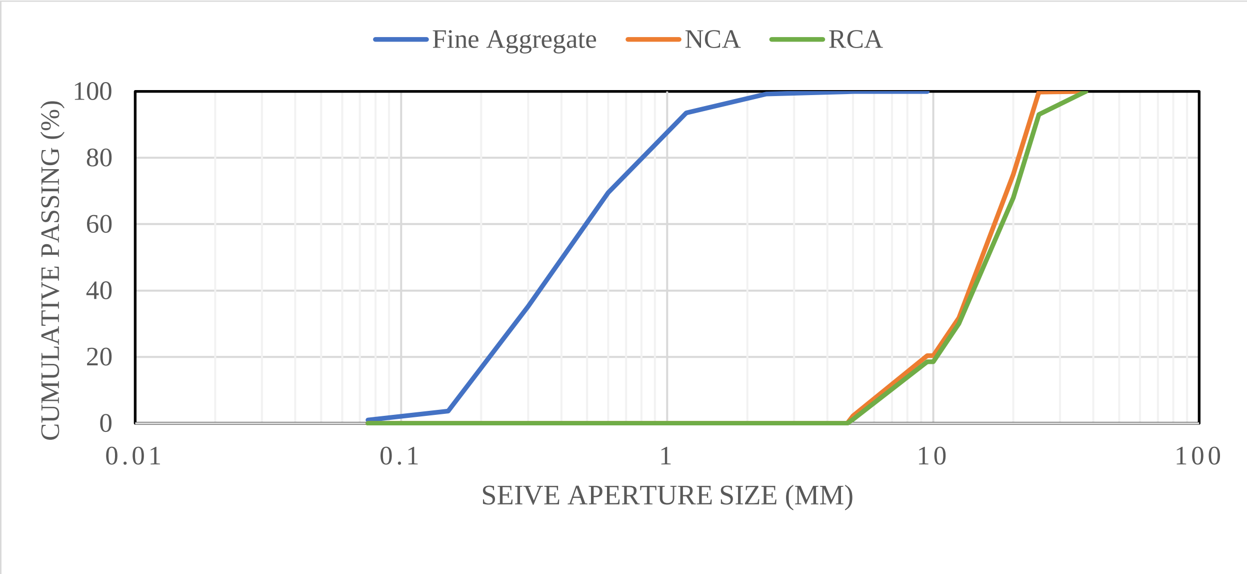

Figure 2: Gradation curve of aggregates

Table 2. General Properties of aggregates

Properties	**FA**	**NCA**	**RCA**
Max. nominal size (mm)	4.75	25	25
Min. nominal size (mm)	0.075	4.75	4.75
Saturated surface dry water absorption (%)	0.62	1.04	6.5
Bulk Density (kg/m^3)	1638	1602	1360
Specific gravity	2.67	2.73	2.27

2.1.3 Jute fibers

Locally available jute fibers were used in this experiment. The jute fibers were cut into 10 mm length as shown in figure 3. Table 3 shows the typical properties of JF.

Table 3. Typical properties of JF

Parameters	Results
Fiber length (mm)	10
Fiber diameter (mm)	0.02-0.05
Bulk density (kg/m^3)	1450
Ultimate tensile strength (MPa)	490
Young Modulus (GPa)	26

Figure 3: Jute fiber (JF)

2.1.4 Water and plasticizer

Fresh tap water was used in all the concrete mixes. High-range plasticizer Sikament 515 was used to attain the required slump in all mixes. This plasticizer contains the properties of type F according to ASTM C494 [11] standard.

2.2 Concrete mixes composition

In this analysis, two cases have been studied i.e., with 0% RCA and 100% RCA. A total of six mixes were prepared with three various fractions of JF (0%, 0.30%, and 0.60%) having 0% RCA and three various fractions of JF (0%, 0.30%, and 0.60%) having 100% RCA. The first mix is the control mix (reference mix), which contains 0% JF and 0% RCA. The 0% RCA mixes are made according to ACI 211-91[12] for 30 MPa cylinder compressive strength, while 100% RCA mix cases, the RCA is used as a substitution of the volume of NCA. The value of slump and the water-cement ratio is 75-100 mm and 0.45 respectively for all the mixes. Table 4 shows the details for all concrete mixes.

Table 4. Detail of mix proportion

Mixture	RCA	JF (kg/m^3)	OPC (kg/m^3)	Sand (kg/m^3)	NCA (kg/m^3)	RCA (kg/m^3)	Water (kg/m^3)	Slump (cm)
R0JF0(Ref)	0	0	439	660	1107	0	193	88
R0JF0.30	0	4.35	439	660	1107	0	193	98
R0JF0.60	0	8.7	439	660	1107	0	193	82
R100JF0	100	0	439	660	0	940	193	85
R100JF0.30	100	4.35	439	660	0	940	193	80
R100JF0.60	100	8.7	439	660	0	940	193	91

The mixing is carried out into two stages in a mechanical mixer. In the first stage, aggregates are mixed with the help of half of the water for 4 min, then fibers, cement, and the remaining half of water are inserted in the next stage, and the mixing is continued for 6 min. The total time of mixing is 10 min. Kurad et al. [13] adopted a similar method of mixing. After completion of mixing, the value of the slump is recorded by the slump cone apparatus. Table 4 reveals that the range of slump values is 75-100 mm.

3 Specimen Preparation and Testing Method

In all mixes, the mechanical property is calculated by compressive strength test while durability property is calculated by porosity test. For the compressive strength test, cylinder specimens of (150 mm diameter × 300 mm height) sizes were cast according to the ASTM C39/C39M-14 [14] standard. In the case of the porosity test, concrete discs of 50 mm thickness and 100 mm diameter were cast according to ASTM C642 [15] standard. These types of discs were produced from cylinders of 100 mm diameter and 200 mm height with the help of a stone cutter after curing. All the cylinders were left to be set in molds for 48 hours after casting. After de-molding, the curing of these cylinders is done for 28 days in normal water. After curing, these cylinders were cut into discs using a stone cutter and subjected to testing. Three specimens of each mix are cast and the average of these three is used to determine the results.

4 Results

4.1. Mechanical Property

4.1.1. Compressive strength test

The compressive strength test is conducted after curing as shown in figure 4. Figure 5 shows the values of the compressive strength test of all mixes with different quantities (0%, 0.30%, and 0.60%) of JF. With the increasing percentage of fibers in the case of 0% RCA and 100% RCA, a similar trend in compressive strength has been observed. As the fiber percentage increases, the compressive strength is increased in both cases of RCA. Similar observations have been observed by [3] [14]. Ali et al. [16] show that by adding fibers, the compressive strength is increased up to a certain limit then the compressive strength is decreased. In this paper, the compressive strength is increased up to 0.30% of fibers but upon further increases of fibers, the compressive strength is decreased in both cases as shown in figure 5. This is because of the addition of excessive fibers, honeycombing, and voids are created in the case of 0.60% of fibers. These types of defects decrease the internal strength of concrete. At 0.30% JF, the compressive strength of concrete made with 0% RCA is greater than the reference mix (R0JF0). Compared to reference (R0JF0), the compressive strength is increased by 8% at R0JF0.30. However, by looking at the standard distribution of the results, it can be noted that the strength increase is not much significant. Therefore, it can be said that compressive strength is not compromised up to 0.30 % of JF in the concrete as compared to the control mix.

The value of compressive strength in the case of R100JF0 is lower than the reference mix (R0JF0). Compared to reference (R0JF0), the compressive strength is reduced by around 22% at R100JF0. This shows that the recycled coarse aggregates (RCA) have less strength than natural coarse aggregates (NCA). The maximum compressive strength achieved at R0JF0.30 is 31 MPa but in the case of R100JF0.30, it was 25 MPa.

It is concluded that as the jute fiber (JF) percentage increases, the compressive strength is not compromised up to 0.30% of jute fibers (JF) in both cases but on further percentage increases, the compressive strength is decreased. The average maximum compressive strength is achieved at R0JF0.30. Therefore, 0.30% of JF quantity is the optimum quantity for the compressive strength of concrete. It is also observed that the RCA mixes have less compressive strength than the NCA mixes. This is because of the lesser density of RCA than NCA, therefore compressive strength is affected negatively by equal volume replacement with NCA.

Figure 4: Compressive strength test

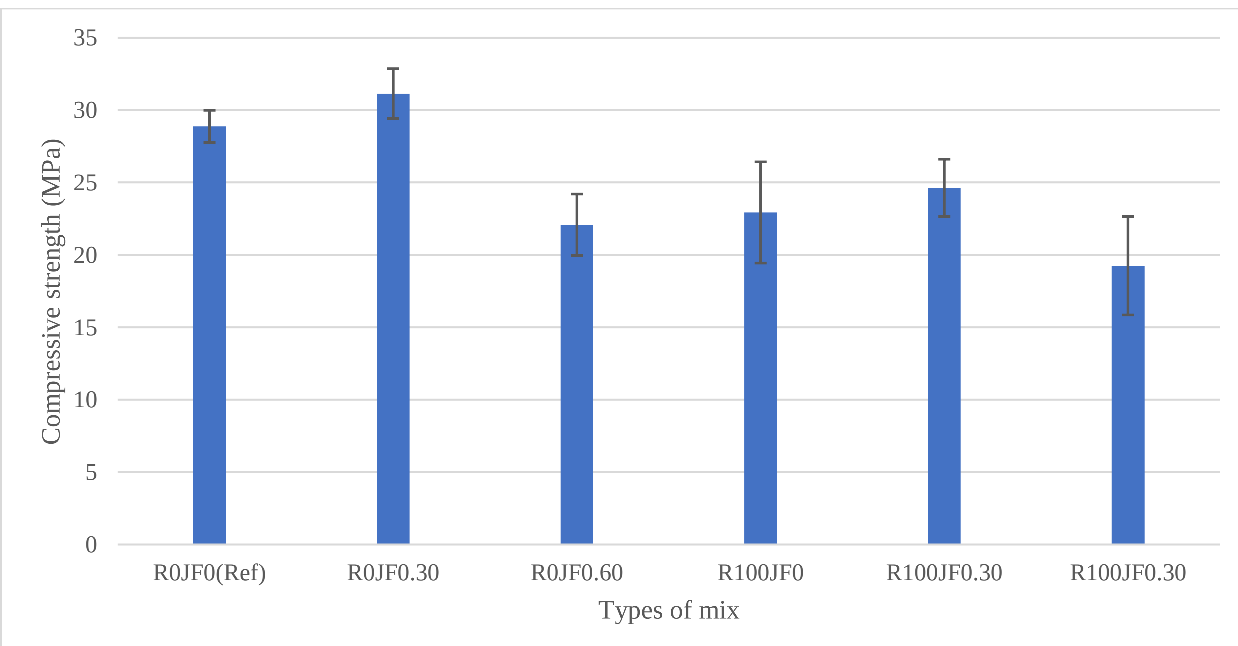

Figure 5: Graph between compressive strength and type of mix

4.2. Durability Property

4.2.1. Porosity

The porosity of concrete is the measurement of void spaces in concrete. Figure 6 shows that the porosity of concrete mixes increases as the JF and RCA content increases. This is because of the presence of mortar which is adhered to RCA and the high volume of free water in RCA is the major cause of higher porosity. The porosity is significantly increased in higher dosages of JF (>0.30%) in both cases. A similar trend was also shown in the research performed by Ali et al. [16] This is because as the percentages of fibers increase, the compression is not effective due to fibers accumulation.

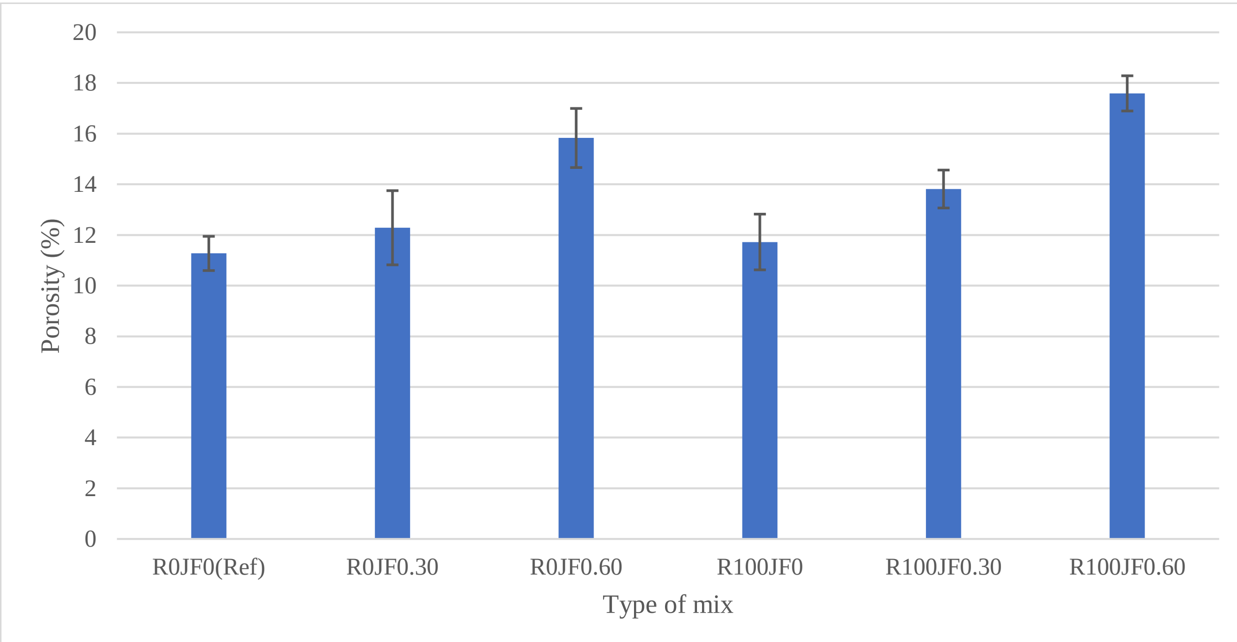

Figure 6: Graph between porosity and type of mix

5 Conclusion

This research topic investigates the effect of JF on the performance of concrete with RCA. The following conclusion can be drawn as,

- The average compressive strength of the concrete mixes is slightly increased in both cases (0% RCA and 100% RCA) due to the addition of JF as compared to reference mixes. The maximum compressive strength is increased up to 0.30% of fibers but upon a further increase in the percentage of fibers, the compressive strength is decreased.
- The values of porosity increase with the increase of JF and RCA. This is attributed to the fact that as the percentages of fibers increase, the compression is not effective due to fibers accumulation. In the higher dosage of fibers (0.60%), the effect of porosity is more when compared to lower dosages.
- It is concluded that 0.30% is the optimum dosage of fiber for compressive strength of concrete and RCA can be used in concrete where low strength is desired.

Acknowledgment

The author would like to thank his supervisor Prof. Dr. Faisal Shabbir.

References

[1] K. L. Pickering, M. G. A. Efendy, and T. M. Le, "A review of recent developments in natural fibre composites

and their mechanical performance," *Compos. Part A Appl. Sci. Manuf.*, vol. 83, pp. 98–112, 2016.

[2] O. Onuaguluchi and N. Banthia, "Plant-based natural fibre reinforced cement composites: A review," *Cem. Concr. Compos.*, vol. 68, pp. 96–108, 2016.

[3] M. S. Islam and S. J. U. Ahmed, "Influence of jute fiber on concrete properties," *Constr. Build. Mater.*, vol. 189, pp. 768–776, 2018.

[4] N. Dayananda, B. S. K. Gowda, and G. L. E. Prasad, "A study on compressive strength attributes of jute fiber reinforced cement concrete composites," in *IOP Conference Series: Materials Science and Engineering*, 2018, vol. 376, no. 1, p. 12069.

[5] A. Akhtar and A. K. Sarmah, "Construction and demolition waste generation and properties of recycled aggregate concrete: A global perspective," *J. Clean. Prod.*, vol. 186, pp. 262–281, 2018.

[6] W. H. Kwan, M. Ramli, K. J. Kam, and M. Z. Sulieman, "Influence of the amount of recycled coarse aggregate in concrete design and durability properties," *Constr. Build. Mater.*, vol. 26, no. 1, pp. 565–573, 2012.

[7] X. Li, "Recycling and reuse of waste concrete in China. Part II. Structural behaviour of recycled aggregate concrete and engineering applications," *Resour. Conserv. Recycl.*, vol. 53, no. 3, pp. 107–112, 2009.

[8] C. Hoffmann, S. Schubert, A. Leemann, and M. Motavalli, "Recycled concrete and mixed rubble as aggregates: Influence of variations in composition on the concrete properties and their use as structural material," *Constr. Build. Mater.*, vol. 35, pp. 701–709, 2012.

[9] A. ASTM, "C150/C150M-17, Standard Specification for Portland Cement," *Am. Soc. Test. Mater. West Conshohocken, PA, USA*, 2017.

[10] A. C33/C33M, "Standard specification for concrete aggregates." ASTM international West Conshohocken, PA, 2013.

[11] C. ASTM, "Standard specification for chemical admixtures for concrete," *Annu. B. ASTM Stand.*, 2013.

[12] M. C. Nataraja and L. Das, "Concrete mix proportioning as per IS 10262: 2009–Comparison with IS 10262: 1982 and ACI 211.1-91," *Indian Concr. J.*, pp. 64–70, 2010.

[13] R. Kurad, J. D. Silvestre, J. de Brito, and H. Ahmed, "Effect of incorporation of high volume of recycled concrete aggregates and fly ash on the strength and global warming potential of concrete," *J. Clean. Prod.*, vol. 166, pp. 485–502, 2017.

[14] "ASTM C 39/C 39M – 01. Standard Test Method for Compressive Strength of Cylindrical Concrete Specimens." .

[15] ASTM C642, "Standard Test Method for Density, Absorption, and Voids in Hardened Concrete, ASTM International, United States," *Annu. B. ASTM Stand.*, no. March, pp. 1–3, 1997.

[16] B. Ali and L. A. Qureshi, "Influence of glass fibers on mechanical and durability performance of concrete with recycled aggregates," *Constr. Build. Mater.*, vol. 228, p. 116783, 2019.

3rd Conference on Sustainability in Civil Engineering (CSCE'21)
Department of Civil Engineering
Capital University of Science and Technology, Islamabad Pakistan

INFLUENTIAL ASSESSMENT OF MACRO SYNTHETIC FIBERS ON MECHANICAL PROPERTIES OF CONCRETE CONTAINING E- WASTE COARSE AGGREGATES

[a] Zeeshan Ahmad*, [b] Muhammad Irshad Qureshi

a: Department of Civil Engineering, University of Engineering and Technology Taxila, Pakistan, zeeshanlaskani@gmail.com
b: Department of Civil Engineering, University of Engineering and Technology Taxila, Pakistan, irshad.qureshi@uettaxila.edu.pk
* Corresponding author: Email ID: zeeshanlaskani@gmail.com

Abstract- In this modern era, concrete has become a basic construction material whose production on large scale, is leading towards the huge usage of natural resources. That is why, the natural resources are going on depletion consistently. To overcome this fact, it has become essential to find out alternate resources for the ingredients of concrete. Usage of non-biodegradable waste items is one of the sustainable solutions. However, some researchers are working on the fruitful utilization of electronic waste in concrete as a partial substituent for coarse or fine aggregates. Basically, electronic wastes or E-wastes are any electronic appliances that have paid off their effective working life e.g. discarded old computers, CDs, VCRs, TVs, radios. In this experimental-based investigation, shredded electronic waste materials are utilized as coarse aggregates in concrete with a constant volume replacement of 30%. Moreover, to overcome the brittle nature of concrete, polypropylene macro synthetic fibers are used in concrete. Results show that the fibrous materials have a better effect on the mechanical performance of E-waste aggregated concrete. The addition of 0.75% fibrous material in concrete increases the compressive strength of E-waste aggregated concrete about 30% while tensile strength increases about 75% as compared to the reference specimen. Main purpose of this research work is to reduce the high consumption of natural resources of ingredients of concrete by the utilization of E- waste material as coarse aggregates in concrete.

Keywords- macro synthetic fiber, reference specimen, relative density, shredded E-waste.

1 Introduction

In the construction industry, concrete is a highly used building material. High compressive strength and adorable durability of concrete are the basic reasons behind its immense usage in the construction industry. Conventional concrete is a mixture of cement, sand, crushed stones, and water. That is why the huge consumption of concrete is leading towards the depletion of natural resources around the globe [1]. Being a citizen of this global village, it is our responsibility to save the natural resources for maintaining the matchless beauty of our planet.

In this undeniable scenario, several researchers are struggling to seek out new suitable resources for the ingredients of concrete. Effective utilization of recycled aggregates, by-products of various industries, waste materials, synthetic aggregates, etc. in concrete production, is the fruitful effort of researchers. Usage of those waste materials makes our environment healthy. Since from last few decades, many researchers are working on the effective usage of electronic waste materials in concrete production [2]. Electronic waste is the non-biodegradable waste that consists of discarded old computers, CDs, VCRs, TVs, radios etc – basically, any electronic appliances that have completed their working life.

Manjunath et al. [3] replaced the coarse aggregate of conventional concrete with electronic waste coarse aggregate upto 30% by volume. It is observed that compressive strength of concrete reduces with the increase of percentage of E-waste aggregate. But its split tensile strength increases upto 17% at 20% replacement. Kalpana [4] replaced the fine aggregate of conventional concrete with electronic waste in powdered form upto 30% by volume. It is observed that all strengths of modified concrete become optimum at 20% replacement of fine aggregate of E-waste material. It is also observed that use of E-waste in conventional concrete somehow reduces its brittle nature by improving its ductility.

Roy et al. [5] stated that the workability of concrete increased by adding E-waste coarse aggregate. Compressive strength reduces by increasing the percentage of E-waste. But, the compressive strength can be improved by using fly ash as a substitute of cement. So, there are multiple advantages of using fly ash in the e-waste aggregated concrete. On one side, it improves the strength of concrete while simultaneously on the other side; it causes a reduction in usage of cement and gives economical results as compared to conventional concrete.

Khubaib et al. [6] stated that the use of polypropylene fiber in concrete causes reduction in the workability as well as in compressive strength of concrete. At 0.5% (by concrete volume) usage of polypropylene fiber in concrete, the compressive strength reduced about 10% while split tensile strength improved about 8% as compared to conventional concrete. Guerini et al. [7] investigated the influence of polypropylene macro synthetic fiber and steel fiber usage in concrete. In that work, it is observed that the usage of steel fibers in concrete causes more bleeding as compared to macro synthetic fiber. Moreover, macro synthetic fibers highly improve all the strengths of concrete as compared to steel fiber. Results become optimum at the usage of 1% of fibers in concrete.

In this experimental-based investigation, shredded electronic waste materials are utilized as coarse aggregates in concrete with a constant volume replacement of 30%. Shape, size, and roughness of shredded electronic waste aggregates are relatively matching with that of the natural coarse aggregates. Shredded electronic waste coarse aggregates are much lighter than the natural coarse aggregates and have relative density (ratio of density of sample to density of reference) of 1.03 which results in the production of lightweight concrete. As, concrete is strong in compression but weak in tension, that is why polypropylene macro synthetic fibers are used to overcome the brittle nature of concrete.

2 Experimental Program

2.1 Materials

In this experimental-based research work, Ordinary Portland Cement (OPC) of grade 43 is used. Sand of Lawrance pur (local area) is used in this work. Crushed stones of Margalla hills are used as natural coarse aggregates (NCA) in concrete production. After purchasing the electronic waste from a local market from Rawalpindi, manufacturing of shredded electronic waste coarse aggregates (ECA) is performed in a nearby local factory. Gradation [8] of both NCA and ECA is kept almost the same. Their characteristics [9] are given in Table 1. Properties of MSF are given in Table 2.

Table 1 Properties of aggregates

Property	Sand	NCA	ECA
Bulk density (kg/m³)	1612	1578	524
Water absorption (%)	0.9	0.7	1.2
Specific gravity	2.66	2.69	1.04
Max. aggregate size (mm)	4.75	19	19
Min. aggregate size (mm)	-	4.75	4.75

Table 2 Properties of macro synthetic fiber (MSF)

Property	Result
Shape of fiber	Crimped
Fiber length (mm)	50
Fiber diameter (mm)	0.8
Modulus of elasticity (MPa)	> 5000
Tensile strength (MPa)	> 450
Specific gravity	0.91
Melting point (°C)	160

Clean potable water is used for concrete production. In order to keep the slump value 80 mm – 100 mm, a high range water reducing admixture (sika viscocrete – 20 he) is used [10]. Gradation curves of fine aggregates and both types of coarse aggregates are shown in Figure 1. Overview of shredded E-waste coarse aggregates and MSF is given in figure 2.

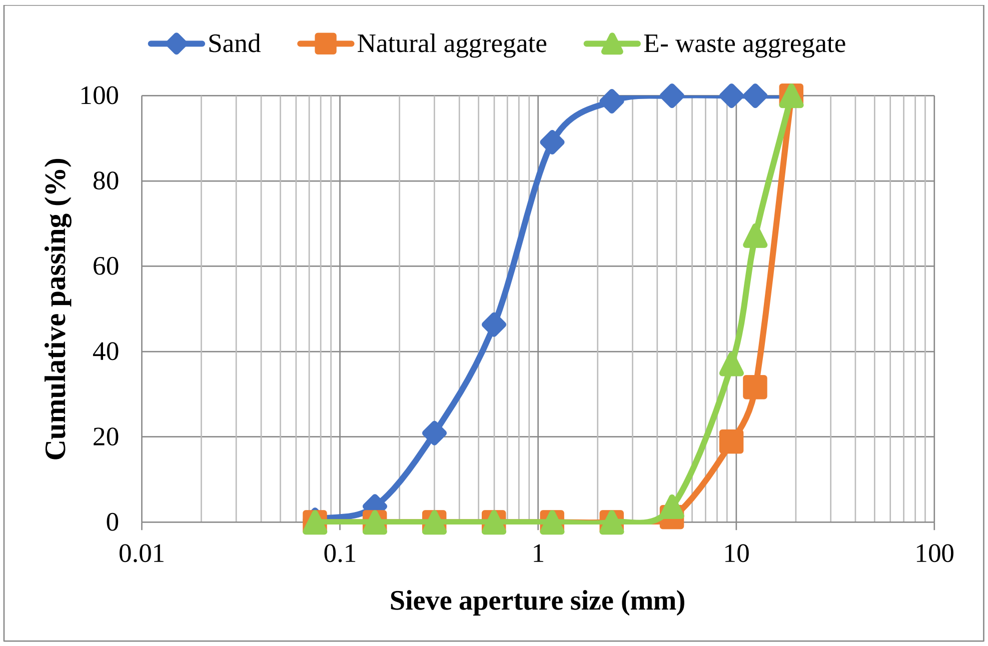

Figure 1: Gradation curves of aggregates

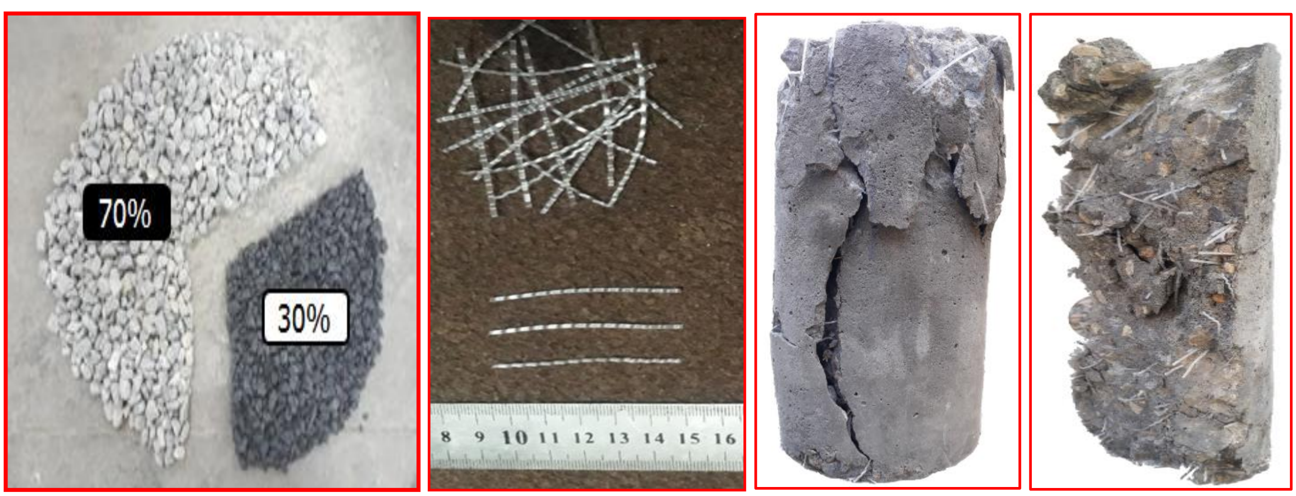

a) b) c) d)

Figure 2: a) 30% E- waste aggregate b) Macro synthetic fiber (MSF) c) Compressive tested d) Split tensile tested cylinder

2.2 Composition of concrete mixes

In this experimental-based research work, total of 14 mixes are prepared by using 0% and 30% of E-waste coarse aggregates as shown in Table 3. First mix that contains no E-waste and no fiber is taken as control or reference specimen in the whole research work. Amount of macro synthetic fiber is used at 0.25%, 0.5%, 0.75%, 1.0%, 1.25%, and 1.5% by volume of concrete. Effect of each amount of fiber on concrete is studied by conducting various tests. Moreover, a constant water-cement ratio of 0.4 is used for all mixes. To keep the workability same, a high range water reducing admixture is used. For all mixes, the slump value is kept in the range of 80 – 100 mm. To design the composition of ingredients of concrete mix, ACI 211.1-91 [11] is used. Detail of all mix proportions, is presented in Table 3.

Table 3- Details of mix proportions (1:1.6:2.3)

Mixture ID	E-waste (%)	Fiber (%)	OPC (kg/m³)	Sand (kg/m³)	NCA (kg/m³)	E-waste (kg/m³)	Fiber (kg/m³)	Water (kg/m³)	Super-plasticizer (kg/m³)
E0 (Ref.)	0	0	430	690	990	0	0	172	1.72
E0MSF0.25	0	0.25	430	690	990	0	2.27	172	1.72
E0MSF0.5	0	0.5	430	690	990	0	4.55	172	1.72
E0MSF0.75	0	0.75	430	690	990	0	6.82	172	1.72
E0MSF1.0	0	1.0	430	690	990	0	9.11	172	2.15
E0MSF1.25	0	1.25	430	690	990	0	11.38	172	2.15
E0MSF1.5	0	1.5	430	690	990	0	13.65	172	2.15
E30	30	0	430	690	720	105	0	172	2.15
E30MSF0.25	30	0.25	430	690	720	105	2.27	172	2.58
E30MSF0.5	30	0.5	430	690	720	105	4.55	172	2.58
E30MSF0.75	30	0.75	430	690	720	105	6.82	172	2.58
E30MSF1.0	30	1.0	430	690	720	105	9.11	172	3.02
E30MSF1.25	30	1.25	430	690	720	105	11.38	172	3.02
E30MSF1.5	30	1.5	430	690	720	105	13.65	172	3.02

3 Research Methodology

3.1 Preparation of concrete specimens

A mechanical mixer of 0.15 m^3 capacity is used for the mixing of concrete ingredients. First of all, fine and coarse aggregates are mixed in the mixer in the presence of half water. After 4 minutes, cement and fibers are added to the revolving mixer with the addition of remaining half water. Whole mixing phenomenon is completed within 10 minutes.

3.2 Testing of concrete specimens

Mechanical performance of each concrete mix is verified on the basis of compressive strength test and split tensile strength. To perform the compressive strength test, 150 mm diameter x 300 mm height cylinders are cast and tested according to the specification of ASTM C39/C39M [12]. To perform the split tensile test, 150 mm diameter x 300 mm height cylinders are cast and tested by obeying the specification of ASTM C496/C496M [13]. For each concrete mix, three specimens are cast and tested.

4 Results and discussions

4.1 Density

By investigating the density of concrete mix designs, it is observed that the addition of 30% E-waste coarse aggregate is causing reduction in density of concrete about 15% as compared to that of conventional concrete. Density values of all mix designs, under investigation, are shown in the graph below. Actually, the density value of E-waste coarse aggregate is 524 kg/m^3 which is much lower as compared to natural coarse aggregates (1578 kg/m^3). Due to this reason, the density of E-waste aggregated concrete is relatively low as compared to conventional concrete.

However, the addition of fibrous material is impacting different effects on the density values of conventional concrete mixes and E- waste aggregated concrete mixes. It is evident from the following graph that the addition of macro synthetic fiber (MSF) is causing reduction in the density value of conventional concrete but enhancing the density value of E-waste aggregated concrete. Main reason behind this phenomenon is density of MSF which is 910 kg/m^3. So, density value of MSF is greater than that of the E-waste coarse aggregate (524) but less than that of natural aggregates (1578).

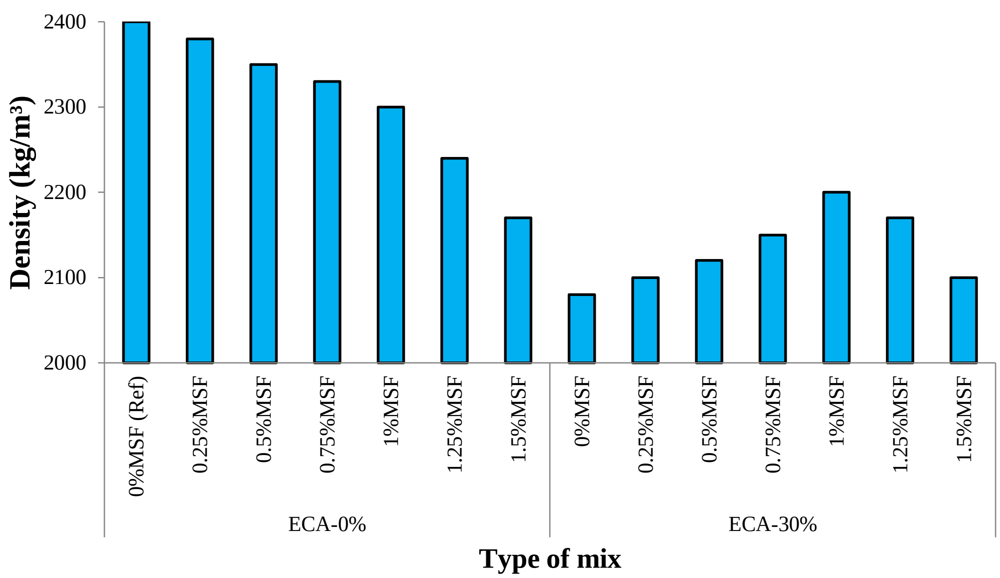

Figure 3: Density values for all type of mixes with varying volume fractions of MSF

4.2 Compressive strength

Compressive strength values of all mix designs, under investigation, are shown in graph below. It is observed that 30% replacement of E-waste coarse aggregates with natural coarse aggregates in conventional concrete is causing reduction in compressive strength about 15%. However, it is evident from the graph that addition of macro synthetic fiber (MSF) is causing high increment in compressive strength value of both conventional and E-waste aggregated concrete specimens.

It is evident from figure 2(c), macro synthetic fibers are trying to hold together the concrete matrix in a well manner. Being in 3D random orientations in concrete matrix, the macro synthetic fibers are strengthening the concrete core matrix and confronting the disintegrating force acting from any direction. That is why, the fibrous material is causing increment in the compressive strength value of both conventional concrete and E- waste aggregated concrete about 30% at 0.75% amount of MSF by volume. However, after 0.75% amount, the compressive strength of both of the concrete goes on reduction. Because after that specific amount of fibrous material, the fibrous material creates hurdles to achieve proper compaction and finally that heavy fibrous concrete have to face segregation which results reduction in its strength.

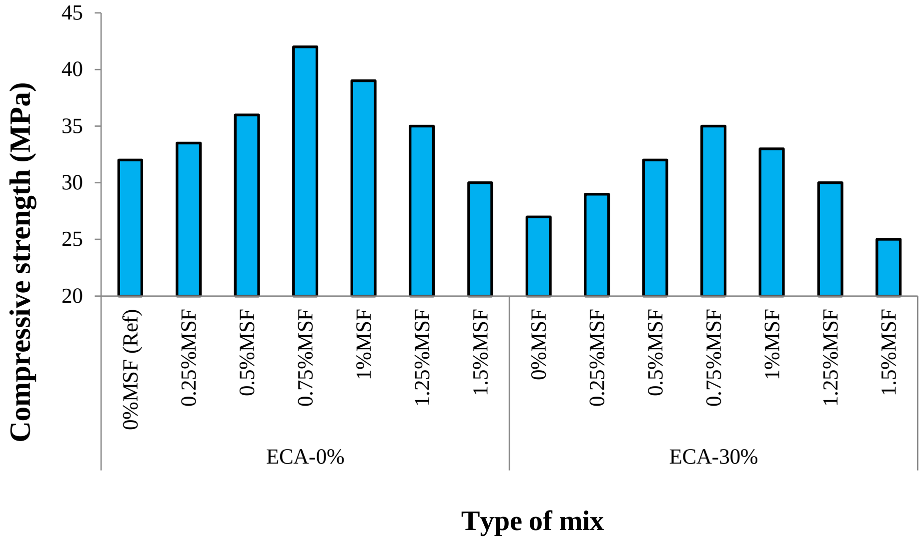

Figure 4: Compressive strength values for all type of mixes with varying volume fractions of MSF

4.3 Split tensile strength

Split tensile strength values of all mix designs, under investigation, are shown in graph below. It is observed that the 30% replacement of E-waste coarse aggregates with the natural coarse aggregates in conventional concrete is causing reduction in split tensile strength about 10%. However, it is evident from the graph that the addition of macro synthetic fiber is causing a huge increment in split tensile strength value of both conventional and E-waste aggregated concrete. It is evident from figure 2(d), macro synthetic fibers are trying to hold together the concrete matrix in well manner. Half portion of cylinder is showing the 3D random orientation of macro synthetic fibers in concrete matrix. Due to their high elasticity and random orientation, the macro synthetic fibers are highly confronting the splitting force. That is why, the fibrous material is causing tremendous increment in the tensile strength value of both conventional concrete and E- waste aggregated concrete about 150% at 1% amount of MSF by volume. However, after 1% amount, the tensile strength of both of the concrete goes on reduction. Because after that specific amount of fibrous material, the fibrous material creates hurdles to achieve proper compaction and finally leads toward segregation which results in reduction in strength.

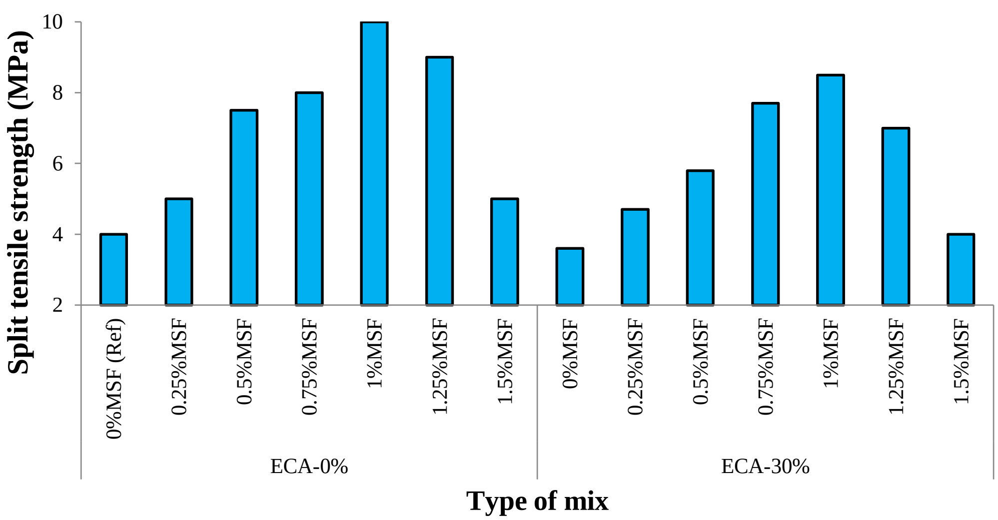

Figure 5: Split tensile strength values for all type of mixes with varying volume fractions of MSF

5 Conclusion

In this experimental-based study, the mechanical performance of conventional concrete and the concrete incorporated with E-waste coarse aggregate is studied. Amount of E-waste coarse aggregate is kept 30% by volume of natural coarse aggregate. Following conclusions can be made by this experimental based investigation:-

- Electronic waste (E- waste) coarse aggregates are much lighter in weight as compared to natural coarse aggregate. They have density about 1.04 which leads to the production of lightweight concrete.
- Density of concrete is reduced, by replacing natural coarse aggregate with 30% E-waste coarse aggregate, about 15%. Addition of fibrous material also reduces the density of conventional concrete but increases in the case of E- waste aggregated concrete mixes.
- 30% replacement of E- waste coarse aggregate with the natural coarse aggregate is causing reduction in compressive strength value of concrete about 15% as compared to conventional concrete. However, the addition of fibrous material has been increasing the compressive strength upto 30% of both conventional and E- waste aggregated concrete. Compressive strength of both type of concrete becomes optimum at 0.75% of macro fiber.
- 30% replacement of E- waste coarse aggregate with the natural coarse aggregate is causing reduction in split tensile strength value of concrete about 7% as compared to conventional concrete. However, the addition of fibrous material has been hugely increasing the split tensile strength upto 150% of both conventional and E-waste aggregated concrete. Split tensile strength of both types of concrete becomes optimum at 1% of fiber.

References

1. Monteiro, P.J., S.A. Miller, and A. Horvath, *Towards sustainable concrete.* Nature materials, 2017. **16**(7): p. 698-699.
2. Raut, S.R., R.S. Dhapudkar, and M.G. Mandaokar, *Experimental study on utilization of E-waste in cement concrete.* The International Journal of Engineering and Science (IJES), 2018.
3. Manjunath, B.A., *Partial replacement of e-plastic waste as coarse-aggregate in concrete.* Procedia Environmental Sciences, 2016. **35**: p. 731-739.
4. Kalpana, M., D. Vijayan, and S. Benin, *Performance study about ductility behaviour in electronic waste concrete.* Materials Today: Proceedings, 2020. **33**: p. 1015-1020.
5. Roy, P., D. Jain, and V. Meshram, *Use Of Electronic Waste As A Partial Replacement Of Coarse Aggregate In Concrete.* International Journal Of Engineering Research-Online, 2015. **3**(4): p. 132-138.
6. Jan, A., M. Khubaib, and I. Ahmad, *Evaluation of Effect of Polypropylene on the Mechanical Properties of Concrete.* Int. J. Innov. Sci. Res. Technol, 2018. **3**: p. 194-202.
7. Guerini, V., et al., *Influence of steel and macro-synthetic fibers on concrete properties.* Fibers, 2018. **6**(3): p. 47.
8. Standard, A., *C136/C136M-14.(2014).* Standard Test Method for Sieve Analysis of Fine and Coarse Aggregates, 2014.
9. C33/C33M, A., *Standard specification for concrete aggregates*. 2013, ASTM international West Conshohocken, PA.
10. Standard, A., *C494/C494M, 2015.* Standard Specification for Chemical Admixtures for Concrete. ASTM International, West Conshohocken, PA. **29**.
11. 211, A.C.I.C. *Standard Practice for Selecting Proportions for Normal, Heavyweight, and Mass Concrete:(ACI 211.1-91)*. 1991. American Concrete Institute.
12. ASTM, C., *Standard test method for compressive strength of cylindrical concrete specimens*. 2012.
13. Standard, A., *C496/C496M (2011) Standard Test Method for Splitting Tensile Strength of Cylindrical Concrete Specimens.* Annual Book of ASTM Standards, 2004. **9**.

3rd Conference on Sustainability in Civil Engineering (CSCE'21)
Department of Civil Engineering
Capital University of Science and Technology, Islamabad Pakistan

RETROFITTING OF REINFORCED CONCRETE COLUMNS BY NSM REINFORCEMENT

[a] Adam Khan, [b] Shahzad Saleem*

a: M.Sc Student, Department of Civil Engineering, UET Taxila, adamislamian712@gmail.com
b: Assistant Professor, Department of Civil Engineering, UET Taxila, shahzad.saleem@uettaxila.edu.pk
* Corresponding author: Email ID: shahzad.saleem@uettaxila.edu.pk

Abstract- Near surface mounted (NSM) method is one of the promising solutions for increasing the flexural and shear strength of deficient reinforced concrete (RC) members. It has also been used to increase the load-carrying capacity and ductility of poorly detailed RC columns. This paper presents the results of an experimental program aiming to study the compressive behavior of small sized RC column specimens strengthened with different configurations of near-surface mounted (NSM) steel reinforcement. The parameters considered were the number of stirrups added at (48mm and 96mm), diameter of stirrups (6.35mm and 9.5mm), bonding material (grout and epoxy), and type of confining material (steel rebar and wire). Test results indicated that both the peak and post-peak strengths were significantly increased by all the different configurations considered. NSM steel reinforcement also changed the failure mode from brittle to ductile. In general, providing additional steel stirrups to poorly detailed RC columns can significantly improve the post-peak behavior without changing the member sizes.

Keywords- Near surface mounted reinforcement; retrofitting; RC columns; stirrups.

1 Introduction

Recent earthquakes have proven the vulnerability of existing reinforced concrete (RC) columns to seismic loading. In a structure, columns are the critical members which may fail due to the crushing of concrete, rebar buckling, shear, flexural or the bond at lap-splice as a result of poor detailing. Retrofitting of RC columns may be addressed successfully by using externally bonded fiber reinforced polymer (FRP) composite materials. FRPs in the form of jackets provided in circumferential direction are quite effective in taking shear stresses and providing confinement to concrete which results in increasing deformational capacity of columns [1]. However, these FRPs are expensive for large scale applications in Pakistan, as these materials are not locally manufactured and imported from abroad. Secondly, a considerable amount is further required to cover and protect the retrofitted surfaces against fire. Previously, strengthening of RC columns was mostly achieved by providing RC or steel jacketing which is covered by shotcreting. RC or steel jacketing needs intensive labor work and artful detailing which increases the dimensions and weight of existing member resulting in substantial obstruction of occupancy and making the building more vulnerable to an earthquake. Moreover, due to an increase in stiffness, RC or steel jacketed members may attract more forces. Therefore, the development of low cost and minimal obstruction strengthening technique for RC columns is still a challenging task.

Near surface mounted (NSM) reinforcement, also named "grouted or embedded reinforcement", involves creating a series of grooves in the concrete cover and inserting reinforcing bars or strips inside to improve the strength of the members. Previous studies so far on NSM reinforcement for RC structures have focused on flexural strengthening of beams or slabs with an emphasis on bond aspects [2-4], and on flexural strengthening with prestressed NSM FRP bars [5-6]; the most recent studies in this area is reported in [7]. Hassan et al. presented both experimental and analytical investigations undertaken to evaluate bond characteristics of near surface mounted carbon FRP (CFRP) strips [8]. In another study by Jalalai et al. [9] they observed the effectiveness of NSM method by using innovative technique which involved manually made FRP rod for enhancing the shear strength of RC beams. They discussed the results of a series of tests conducted on simply supported RC beam with and without the proposed anchors. The proposed manually made fiber reinforced polymer (MMFRP) rods and end anchorage increased the shear capacity of beam from 25% to 48% along with significant increase in ductility.

Previous literature shows that very little work is done on the use of NSM steel reinforcement to strengthen the poorly detailed RC columns. The concept of providing additional steel stirrups without changing the column cross section has not been paid much attention in the past. Therefore, in this paper, findings of an experimental study are presented to explore the effectiveness of NSM steel stirrups in enhancing the poorly detailed RC column specimens.

2 Experimental Program

A total of sixteen small sized square RC column specimens were manufactured and tested under axial compression. All specimens had same dimensions which is 150×150mm, with 300mm height. In all specimens 4 #3 (9.5mm diameter) deformed longitudinal bars were used with two stirrups of #2 (6.35mm diameter) at the two ends to represent poorly detailed columns with a length-to-diameter ratio of about 20 for longitudinal bars. The parameters considered were the number of stirrups added at (48mm and 96mm), diameter of stirrups (6.35mm and 9.5mm), bonding material (grout and epoxy), and type of confining material (steel rebar and wire). Descriptions of specimens are given in Table 1.

Table 1- Specimen details

Specimen notation	Stirrup spacing (mm)	Number of specimen	Type of NSM reinforcement	Bar size	Binder
S_nU_{200}	200	2	Nil	Nil	Nil
S_nU_{96} R_2	96	2	Steel bars	6.35mm	Cement grout
S_nU_{48} R_2	48	2	Steel bars	6.35mm	Cement grout
S_nU_{96} R_3	96	2	Steel bars	9.5mm	Cement grout
S_nU_{48} R_3	48	2	Steel bars	9.5mm	Cement grout
S_nU_{48} W_{10}	48	2	Binding wire	0.82 mm	Cement grout
S_n U_{48} R_2E	48	2	Steel bars	6.35mm	Epoxy resin
S_nU_{96} R_2E	96	2	Steel bars	6.35mm	Epoxy resin

In Table 1, specimens' notation is as follows: the first symbol "S_n" denotes the specimen number, the second symbol "U" denotes the external stirrup spacing in mm, "R" denotes the reinforcement with number of bar in subscript, "W" denotes the binding wire, and "E" denotes the epoxy resin. For example, specimens $S_nU_{96}R_2$ and $S_nU_{48}R_2$ were strengthened with NSM stirrup at spacing of 96 and 48mm, respectively, using 6.35mm bar, while in specimens $S_nU_{96}R_3$ and $S_nU_{48}R_3$, 9.5mm bars were used. Specimen $S_nU_{48}W_{10}$ was strengthened with steel binding wire having diameter equivalent to that of 9.5mm. Similarly, for specimen $S_nU_{48}R_2$, high strength cement grout was used to fill the groove whereas for specimen $S_nU_{96}R_2E$, groove was filled with epoxy resin.

2.1 Material properties

Concrete with a mix ratio of 1:2:4 (cement: sand: aggregate) was used to cast the column specimens and cylinders. The 28-days concrete strength obtained by testing two cylinders was about 20 MPa. Sikagrout-114 was used as a filling material for grooves. Sikagrout-114 is a high-performance cementitious material that is free-flowing and general-purpose grout with a 65MPa ultimate strength at 28 days. For NSM steel stirrups, two sizes of deformed steel bars were used: #2

(6.35mm diameter) and #3 (9.5mm diameter) having yield strength of 422 and 450MPa, respectively. In one specimen, binding wire was used as NSM reinforcement in place of steel stirrups. The wire diameter was 0.82mm and it was wrapped 62 times around the specimen as an equivalent to 9.5mm. In some specimens, epoxy resin was used for NSM bar embedment having 7-day strength of 30MPa.

2.2 Specimen preparation

A total of sixteen specimens were prepared along with control specimens. Firstly, molds of required dimensions were prepared from plywood sheets. The steel cages were then prepared along with spacers which were connected to steel cage to maintain a 25mm clear cover, as shown in Figure 1.

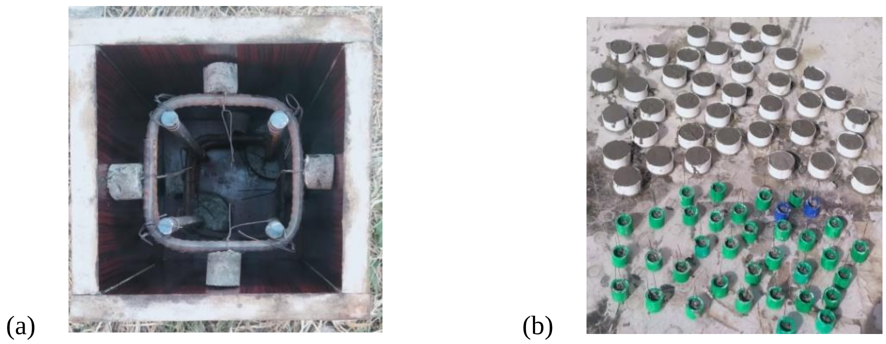

Figure 1: a. Mould of specimen with spacer of 25mm, b. 25mm spacer for both side and bottom cover

After 28 days of concrete casting, RC specimens were grooved 20mm wide and 20mm deep using concrete grinding machine. When the surface preparation was completed, the NSM reinforcement was placed as shown in Table 1 and Figure 2. The steel stirrups were in C shape which were then welded at the center of flat sides of square specimen. The grooves were filled by cement grout or epoxy resin, accordingly, as shown in Figure 2.

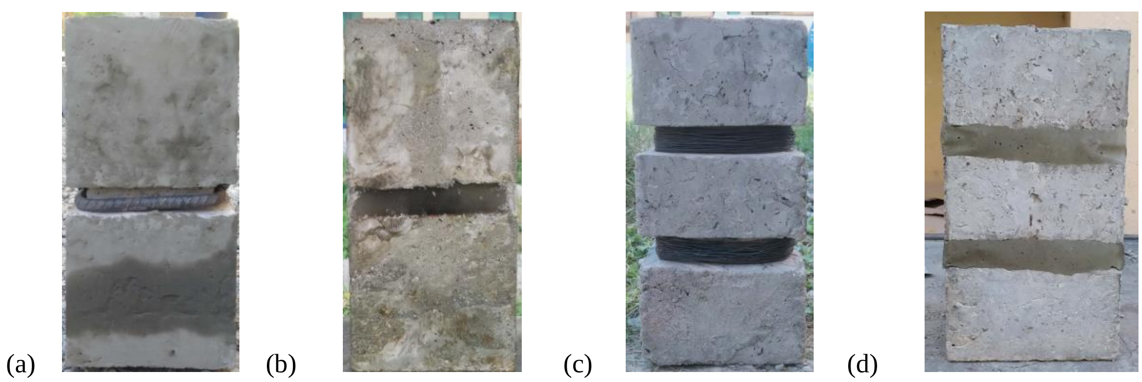

Figure 2: Grooved specimen, a. specimen with one horizontal groove, b. specimen (a) with epoxy resin, c. binding wire along with two horizontal grooves, d. specimen (c) with cement grout

2.3 Testing setup

All the specimens were tested under compression in a universal testing machine (UTM) of CONTROLS with a maximum capacity of 5000KN. The specimens were tested under displacement-controlled manner with a speed of 1 mm/min. Axial deformation of specimens was recorded through a dial gauge mounted on the specimen with a run of 50 mm. It is to be noted that in this paper only the strength results are presented. The load was obtained from the built-in load cell of UTM.

3 Results and Discussion

3.1 Failure modes

In control specimens with no NSM stirrups, small vertical cracks were developed near the peak strength at the specimen corners. These small cracks grew faster and projected towards the mid height in the post-peak region. The onset of buckling of longitudinal bars then resulted in the formation of major vertical cracks around the corners and spalling of concrete cover, as can be seen in Figure 4a. Because of large stirrup spacing i.e., 200 mm, central concrete core was poorly confined and was observed to be damaged badly. In specimens with one NSM stirrup and grout filling, comparatively less damage was observed at the central concrete core and cover. Buckling of longitudinal bars was reduced because of reduced stirrup spacing i.e., 96mm. Stirrups were remained closed, and no weld failure was observed. The grout filling in the grooves performed well and allowed only major cracks to be developed on surface, see Figure 4b. The addition of two NSM stirrups further reduced the buckling length of longitudinal bars i.e., 48mm, which resulted in even less damage both in the concrete core and cover. Figure 4c shows the damaged specimen with NSM steel binding wires. It is interesting to note that no wire failure was observed until the end of test. Furthermore, no appreciable major corner cracks and concrete cover spalling was observed at higher deformation level. Binding wire wrapped specimens had shown better result in ductility as well as in crack pattern, as shown in Figure 4c. Specimens with epoxy resin as filling material also showed better results by showing an obstacle to crack path which did not allow cracks to extend in their respective path. In these specimens, vertical cracks above and below the epoxy resin were observed, see Figure 4d.

(a)


Figure 4: Cracked specimen, a. controlled specimen, b. specimen with one stirrup, c. wire wrapped specimen, d. specimen with epoxy as a bonding agent

3.2 Effect of number of NSM stirrups

Figure 5 shows the effect of NSM stirrup spacing on the peak and post-peak ultimate residual strengths of poorly detailed square RC column specimens. The post-peak ultimate residual strength is the strength in post-peak region when no further drop is observed, and the curve becomes almost horizontal. It can be observed in Figure 5a and 5b that both the peak and post-peak residual strengths were improved significantly with an increase in NSM stirrups. For example, the peak strength was increased from 434.4 to 570 and 639kN when control specimen was retrofitted with one and two NSM 6.35mm steel stirrups, respectively, see Figure 5a. It can be concluded that with the addition of NSM stirrups, not only the buckling length of longitudinal steel bars was reduced, but the central concrete core was also more effectively confined which resulted in higher peak and post-peak strengths.

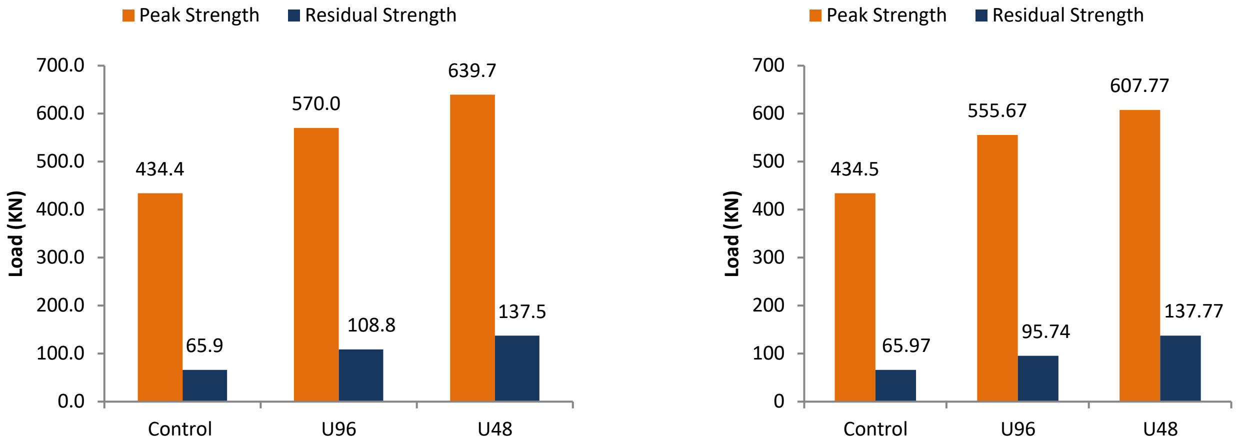

(a) (b)

Figure 5: Effect of stirrup spacing, a. 6.35mm stirrup, b. 9.5mm stirrup

3.3 Effect of NSM stirrup diameter

Figure 6 shows the effect of NSM stirrup diameter for a particular spacing on the load caring capacity of square RC column specimens. It is interesting to note that the strength increment for NSM 6.35mm steel stirrups is more than that for 9.5mm both for 96 and 48mm spacings. For example, in specimens with 96mm stirrup spacing, compared to the peak strength of 569.9 kN for 6.35mm stirrups, strength was increased from 434.4 to 555.7kN for 9.5mm stirrups. It was observed during the testing that 9.5mm stirrup was fractured near the bent in the post-peak region which indicated its brittleness compared to 6.35mm stirrups. Similar observation was recorded for specimens with 48mm stirrup spacing.

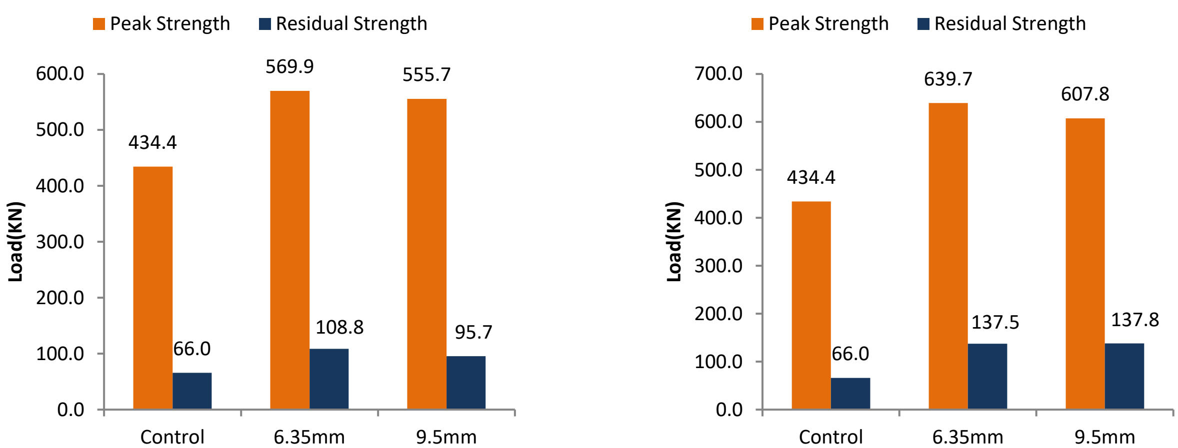

(a) (b)

Figure 6: Effect of diameter of stirrup, a. 96 mm spacing, b. 48 mm spacing

3.4 Effect of bonding material

Figure 7 depicts the effect of groove bonding material on the peak and residual strengths of RC square specimens. In case of specimens with 96mm stirrup spacing, peak strength is higher for grout filling compared to the epoxy filling, however, the residual strength is higher for specimens with epoxy resin, see Figure 7a. On the other hand, in specimens with 48mm stirrup spacings, both the peak and residual strengths were higher for specimens with epoxy resin compared to the specimens with grouting, see Figure 7b. Higher strengths of specimens with epoxy resin could be due to better tensile properties of epoxy resin which did not allow cracks to pass through it and increased the effective confinement of stirrups. The high peak strength of specimens with 96mm stirrup spacing and grout filling in Figure 7a needs further investigation.

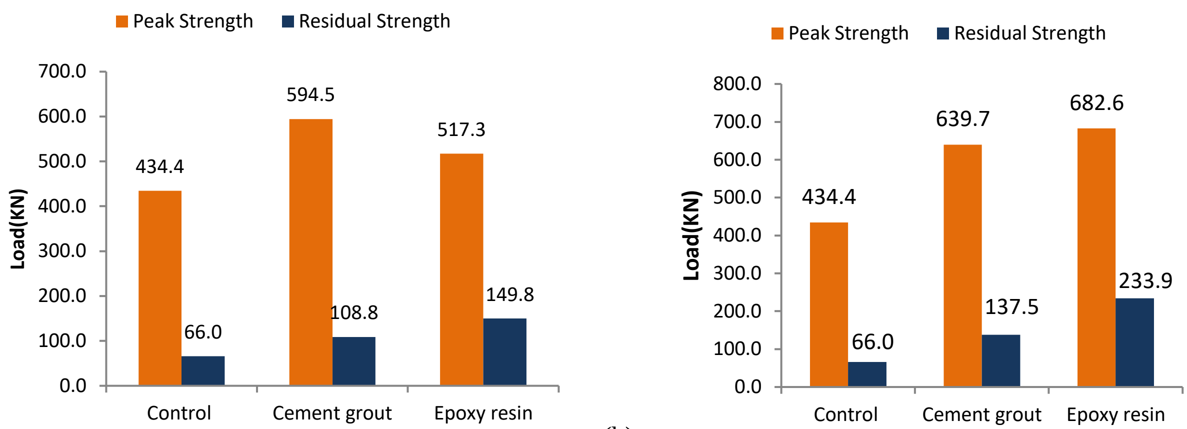

(a) (b)

Figure 7: Effect of bonding material, a. 96 mm stirrup spacing, b. 48 mm stirrup spacing

3.5 Effect of stirrup type

Figure 8 shows the comparison of NSM binding wire and steel bar as a stirrup. The peak load capacity of specimen with steel bar is more than that of specimen with binding wire. The reason could be the less flexural stiffness of small diameter wires compared to the steel bars, however, the difference in strength is only 4%. Interestingly, the residual strength in case of binding wires is 167.9kN which is significantly higher than 137.8kN in case of steel stirrups. The reason could be the high tightness of binding wire achieved during wrapping compared to steel bar which were not so tight to the core.

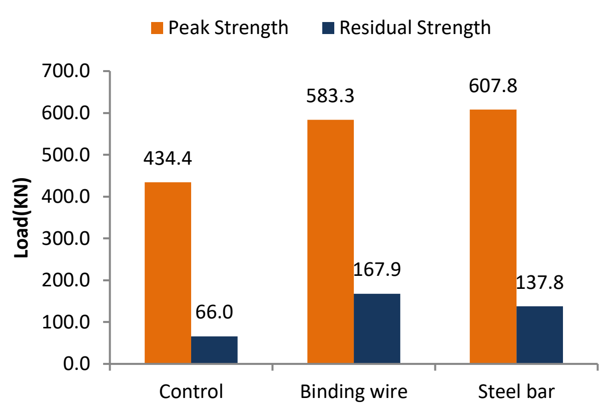

Figure 8: Effect of stirrup type at 48mm spacing

4 Conclusion

The main goal of this research work is to observe the effect of NSM steel stirrups on the axial compressive behavior of RC column specimens. The influence of NSM reinforcement type (steel stirrups/steel wires) and bonding material on the compressive behavior of reinforced concrete was is investigated. From the test results the following conclusions can be drawn:

- The peak and post-peak strengths of poorly detailed RC column specimens can be increased by providing confinement through NSM stirrups. In general, the overall compressive behavior improves with an increase in number of NSM stirrups.
- There is no significant impact of bar diameter on peak and ultimate strengths. The performance of 6.35mm stirrups is better than that of 9.5mm stirrups.
- Filling of grooves by epoxy resin is more effective for post-peak response because of its better tensile properties compared to grout.
- Binding wire, if used as NSM stirrup, has significant effect on the post-peak strength because of its high ductility and progressive nature of failure.
- In general, NSM steel stirrups are very effective in shifting the brittle failure mode of poorly detailed columns to ductile one.

Acknowledgment

The careful review and constructive suggestions by the anonymous reviewers are gratefully acknowledged.

References

[1]. N.A Siddiqui, S.H Alsayed, Y.A Al-Salloum, R.A Iqbal, and H. Abbas, (2014). Experimental investigation of slender circular RC columns strengthened with FRP composites. Construction and Building Materials, 69, 323–334. doi:10.1016/j.conbuildmat.2014.07.053

[2]. L. De Lorenzis, J.G. Teng "Bond between Near-Surface Mounted Fiber- Reinforced Polymer Rods and Concrete in Structural Strengthening", ACI Structural Journal, V. 99, No. 2, 2002, pp. 123-132.

[3]. T. Hassan and S. Rizkalla "Investigation of Bond in Concrete Structures Strengthened with Near Surface Mounted Carbon Fiber Reinforced Polymer Strips", ASCE Journal of Composites for Construction, V. 7, No. 3, 2003, pp. 248-257.

[4]. TG Harmon, YJ Kim, J Kardos, T Johnson. "Bond of Surface- Mounted Fiber-Reinforced Polymer Reinforcement for Concrete Stuctures", ACI Structural Journal, V. 100, No. 5, 2003, pp. 557-564.

[5]. H Nordin, B Täljsten, "Concrete Beams Strengthened with Prestressed Near Surface Mounted CFRP", ASCE Journal of Composites for Construction, V. 10, No. 1, 2006, pp. 60-68.

[6]. P. Casadei, N Galati, G. Boschetto, K.Y Tan, and A. Nanni, "Strengthening of Impacted Prestressed Concrete Bridge I-Girder using Prestressed Near Surface Mounted C- FRP Bars", Proceedings of the 2nd International fib Congress, Naples, Italy, 2006 (CD-ROM, paper ID 10-76).

[7]. T. C. Triantafillou, editor, Fiber-Reinforced Polymer Reinforcement for Concrete Structures - Proceedings of the 8th International Symposium on Fiber Reinforced Polymer Reinforcement for Concrete Structures, University of Patras, Greece, 2007 (www.frprcs8.upatras.gr).

[8]. T. Hassan and S. Rizkalla (2003). Investigation of Bond in Concrete Structures Strengthened with Near Surface Mounted Carbon Fiber Reinforced Polymer Strips. Journal of Composites for Construction, 7(3), 248–257. Doi:10.1061/(asce)1090-0268(2003)7:3(248).

[9]. M. Jalali, M.K Sharbatdar, J.-F Chen, and F. Jandaghi Alaee (2012). Shear strengthening of RC beams using innovative manually made NSM FRP bars. Construction and Building Materials, 36, 990–1000. doi:10.1016/j.conbuildmat.2012.06.068.

3rd Conference on Sustainability in Civil Engineering (CSCE'21)
Department of Civil Engineering
Capital University of Science and Technology, Islamabad Pakistan

MECHANICAL PROPERTIES OF NATURAL FIBER REINFORCED CONCRETE

[a] Muhammad Saqib, [b] Shahzad Saleem*

a: Department of Civil Engineering, U.E.T, Taxila, msaqib642@gmail.com
b: Department of Civil Engineering, U.E.T, Taxila, shahzad.saleem@uettaxila.edu.pk
*Corresponding author: Email ID: shahzad.saleem@uettaxila.edu.pk

Abstract- It is well known that the mechanical properties of concrete can be improved by incorporating discrete fibers to produce more durable and sustainable concrete for construction industry. The purpose of the current research work is to investigate the effect of locally available mazri plant leaves in concrete to improve its mechanical properties. Mazri leaf straw of an average length of approximately 20 mm were mixed with concrete at a percentage of 0.5 and 1.0 by mass of wet concrete. For compressive and split tensile tests, standard cylindrical specimens were prepared, while flexural strengths were obtained from small beams. Test results showed that compared to the plain concrete the compressive strength was decreased with an increase in content of mazri leaf straw. On the other hand, both the split tensile and flexural strengths were found to be increased with the addition of natural mazri leaf straw. It is also interesting to note that the cracking pattern of mazri leaf straw reinforced concrete (MLSRC) exhibited improved ductile behavior compared to the reference specimens, however, in most of the cases pullout of straws was observed which needs further investigation on fiber-concrete bond behavior. In general, mazri leaf straw has the potential to be used in cement concrete composites for different non-structural applications.

Keywords- Mazri leaf straw reinforced concrete (MLSRC), Mechanical properties, Natural fiber.

1 Introduction

Conventional concrete shows less tensile strength and brittle failure. In order to enhance its tensile strength, adding fibers in concrete has proved to be very successful which not only improves its tensile strength but also imparts ductility to it. Previously, different fibers such as glass, steel, polypropylene and many other synthetic fibers have been added in concrete for this purpose. These fibers act as a crack-arresters to enhance the tensile behavior of concrete [1]. In recent decades, emphasis has been given to look for new materials based on renewable resources because of the increasing problem of resource reduction and global pollution. Also, the increase in cost of construction materials and environmental side effects made it necessary to think of new materials lower in cost and environmentally friendly. For this purpose, the development of natural fiber reinforced composites is based on the strategy of preventing the demolition of forest resources as well as producing good economic returns for the cultivation of these fibers [2].

Many natural fibers have been used in concrete for different applications which include sisal, coir, hemp, elephant grass, coconut fibers, wheat straw, jute, roselle fibers, palm oil, and date palm leaf [3-7]. The effect of wheat straw and hemp on the fracture energy of concrete was studied by [3] in which 40 mm long and 0.19% (by concrete mass) fibers were used. An increase of 70 and 2%, respectively, in fracture energy of hemp and wheat straw reinforced concrete was observed compared to plain concrete. The effect of different wheat straws i.e. SWSRC, BWSRC, and NWSRC was also studied by [5] in which 25 mm long wheat straw were added by 1, 2 and 3% of mass of wet concrete. An increase of 91, 92 and 105% in compressive, flexural and splitting tensile toughness indices, respectively, were observed. Roselle fibers in volume fractions of 0 to 4% were studied by [7]. The results indicated that the tensile strength was increased about 53% while compressive strength was reduced with an increase in fiber content. Palm oil fiber as discrete reinforcing fiber in concrete was studied by [8]. It was concluded that fiber reduces workability and compressive strength while splitting tensile strength is increased.

The overall aim of the present research program is to develop an economically efficient concrete for the improvement of pavements like parking pavements, footpaths and shoulders by using locally available natural fibers in concrete. For this purpose, the mazri plant leaf fiber which is abundantly available in the region of Kohat is used. The reason for using this fiber in concrete composites is its low price, local and abundant availability. The other reasons for using these fibers in concrete are their good tensile properties and rapid degradation of their plant forests. The mazri leaf are used in making mats, ropes, hats, baskets and are also used in roofs and huts [9]. Due to the introduction of polythene products in markets the farmers have lost their interest in cultivation of mazri plants leading to the rapid degradation of mazri plants forests. Thus, using these fibers in concrete will again open the markets for the farmers, hence it will also help to sustain mazri plant forests. To the best of authors' knowledge, no study has been carried so far on mazri plant leaf fibers for structural applications. Therefore, a pilot study is conducted to determine the effect of locally available mazri plant leaf fibers on the mechanical properties of concrete composites.

2 Experimental Program

2.1 Materials

The constituents used in the preparation of plain concrete (PC) and mazri leaf straw reinforced concrete (MLSRC) are ordinary Portland cement (OPC), locally available sand, aggregates, tap water and straw from mazri plant leaves available locally in southern regions of Pakistan (i.e. Karak).The maximum size of aggregates used is 19.5 mm.

2.2 Preparation of mazri leaf straws

The natural fibers used were extracted from the leaves of mazri palm trees. Firstly, the leaves were cut from the plant and were air dried for 4-5 days. Secondly, the dried leaves were split into fibers by hand tools locally used for making such fibers. After that the fibers were cut manually into an average length of 20mm, width of 3mm and thickness of 1-1.2mm. Finally, before mixing into the concrete the fibers were dipped in water for an hour to remove the dust on the surface of the straws. After that, the straws were air dried for 10-15 minutes. Figure 1 shows the straws obtained from the mazri plant.

a) b) c)

Figure 1: a. Mazri plant [9], b. dried mazri leaves, and c. prepared mazri straw

2.3 Mix proportions and casting procedure

The mix proportion for PC was 1:2:4 (cement: sand: aggregate). For making MLSRC, the straw contents were added in 0.5 and 1% by mass of wet concrete. The w/c ratio of 0.6 is kept same for both PC and MLSRC. For the preparation of PC mix all the ingredients were simultaneously put into the drum type mixer and the mixer was rotated for one minute.

The water in required quantity was then poured into the mixer and the mixer was rotated again for five minutes until a homogeneous mixture was obtained. In case of MLSRC, one-third of cement, sand, aggregates and straw were put in the mixer in four layers. The remaining quantities were then added using the same layering technique. After that, two-third of water was added, and the mixer was rotated for about four minutes. The one-third of the remaining water was added, and the drum mixer was again rotated for two minutes. Slump test was performed for both PC and MLSRC; values of slump noted are 75, 25 and 5mm for 0, 0.5 and 1% straw reinforced concrete. The less value of slump for MLSRC is due to absorption of water by the straws which resulted in reduced workability. For preparation of MLSRC specimens, the prepared homogeneous mixture is then poured in the respective molds. Each mold is filled in three layers with compaction of 25 blows per layer with the help of temping rod.

2.4 Specimens

For compressive and split tensile strength tests, cylinders with height of 300mm and diameter of 150mm were cast for both PC and MLSRC. However, for flexural strength test, 100 mm wide, 100 mm deep and 500 mm long beams/prisms were cast. Table 1 shows details of specimens cast for different testing.

Table 1-Details of specimens cast

S.no	**Testing**	**Number of specimens casted**		
		0% Fiber	**0.5% Fiber**	**1.0% Fiber**
1	Compressive	3	3	3
2	Split tensile	3	3	3
3	Flexure	2	2	2

3 Test Methodology

Ultra-sonic pulse velocity (UPV) test is one of the non-destructive tests used to check the quality of concrete and estimate the strength without damaging the concrete. UPV test was performed following the standard procedure of ASTM C597 [10]. For determination of compressive strength of concrete cylinders, universal testing machine (UTM) of CONTROLS with a capacity of 5000 kN was used following the ASTM C39 [11]. Since the finished surfaces of MLSRC specimens were not smooth, all cylinders were capped with plaster of paris to ensure uniform compression. PC and MLSRC concrete cylinders for split tensile strength were tested conforming to ASTM C494/496M-11 standard [12]. ASTM C78/C78M standard is adopted for performing flexural strength using small sized beams with third point loading [13]. Testing setup for above mentioned tests is shown in Figure 2.

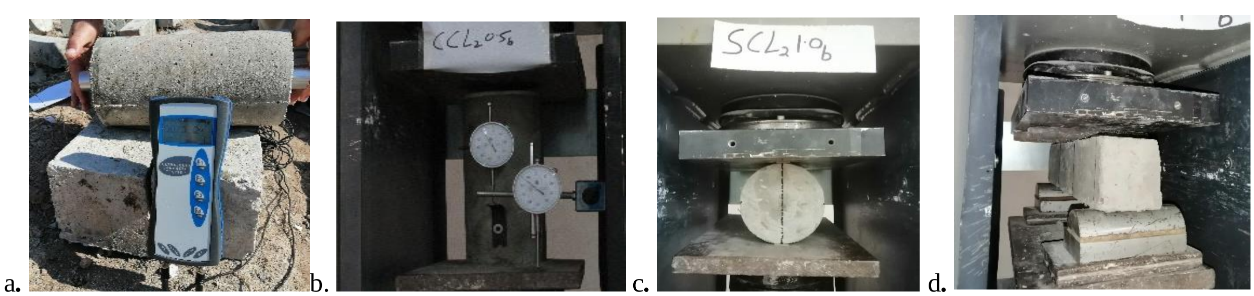

Figure 2: Testing setup, a. ultra-sonic pulse velocity test (UPV), b. compressive strength test, c. split tensile strength test, and d. flexural strength test

4 Results and Discussion

4.1 Ultra-sonic pulse velocity

Figure 3 shows the average of four readings of UPV for cylinders and three readings for beams. Several studies had concluded that there is a relation between UPV and compressive strength [14,15]. The present results of UPV indicate a decrease in the UPV with the addition of discrete fibers, however, the overall difference is small. The maximum value of 4 km/sec at 0 and 0.5% fiber content indicates that the concrete is of excellent quality while all the values in case of beams are greater than 3.5 km/sec showing overall good quality of concrete.

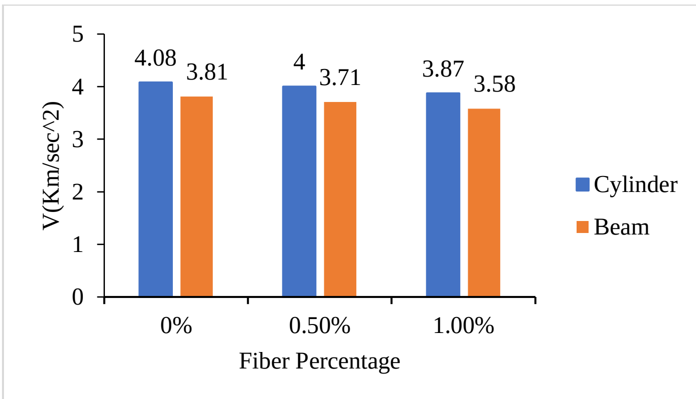

Figure 3: Results of ultrasonic pulse velocity in cylinders and beams

4.2 Compressive strength

It can be observed in Figure 4 that the compressive strength of MLSRC was decreased with an increase in content of mazri palm fibers. Similar observation of strength reduction in natural fiber reinforced concrete had also been reported in many other studies [5,7,8]. For specimens with 0.5% content of mazri fibers, the compressive strength was observed to be reduced by 10% compared to the control specimen. Similarly, a decrease of about 31% was observed in specimens with 1% fiber content. This strength loss might be due to the weak bonding between fibers and concrete as the fibers were easily pulled out from the failed specimens. However, it needs further investigation into the bonding behavior of mazri fibers with concrete.

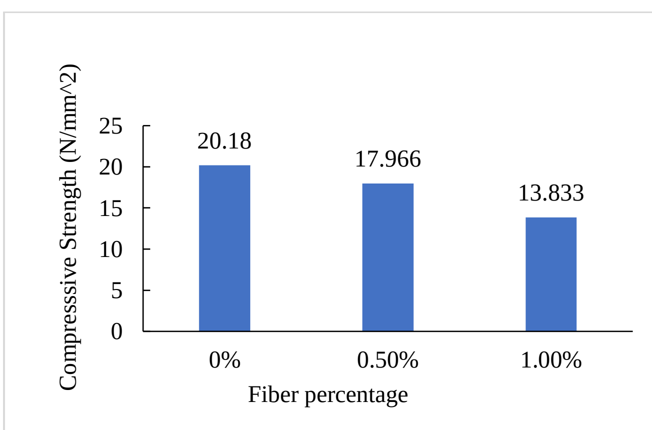

Figure 4: Average compressive strengths at 28 days

4.3 Splitting tensile strength

Figure 5 shows that the tensile strength of MLSRC was increased by 23.5 and 5.7% for 0.5 and 1.0% fiber content, respectively, compared to PC. This increase in tensile strength of MLSRC might be due to the better tensile properties of mazri leaf straws. During the test, it was observed that unlike the splitting of PC specimens into two halves, MLSRC specimens did not exhibit sudden brittle failure mode and only cracks are observed as the maximum load is reached. It shows that the mazri fibers performed well a bridging action among the cracks. Similar observation was also reported by [5].

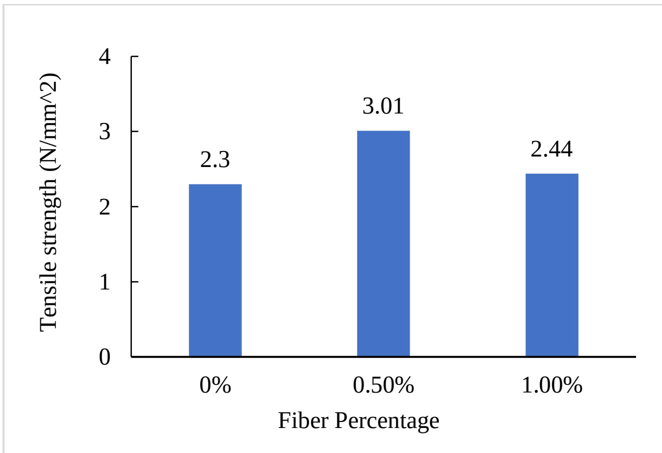

Figure 5: Average split-tensile strength of cylinders at 28 days

4.4 Flexural strength

The results of flexural strength test are shown in Figure 6 which show that the flexural strength of MLSRC was increased by 9.6 and 6.6% for 0.5 and 1.0% fiber addition, respectively. This increase in flexural strength might be due to the tensile properties of the mazri leaf fibers and better interlocking between concrete and straw. It was also observed from the cross section of failed specimens that a proportion of 80:20 existed in fiber pull out and fracture failure. The pull out of straw was observed where less straw length was embedded in concrete. A similar behavior was also observed by [5].

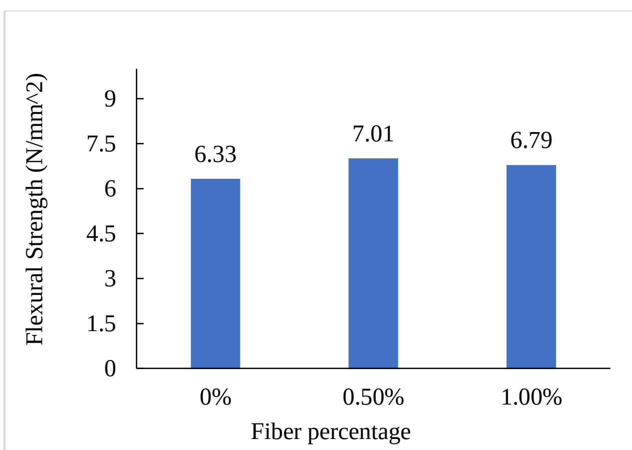

Figure 6: Average flexural strength of concrete beams at 28 days

5 Implemenation of Current Research

Results of current study shows that these fibers has the potential to be used to increase the tensile and flexural strength of concrete, however further research is required to improve the bonding of these fibers with concrete by surface treatment using different techniques.

6 Conclusions

An experimental work was done to study the effect of mazri leaf straw on the mechanical properties of concrete. The following conclusions were made from the results obtained:

- The ultrasonic pulse velocity was slightly decreased by the presence of natural mazri plam fibers.
- The compressive strength was reduced with an increase in fiber content which might be due to the presence of low-density straws causing improper compaction and making concrete less workable.
- Incorporation of mazri leaf straw increased the tensile strength of concrete due to the bridging behavior. A higher increment was observed for 0.5% fiber content compared to 1.0%.
- Like tensile strength, flexural strength is also improved. A higher increment was observed for 0.5% fiber content than for 1.0%.

Acknowledgment

The authors are grateful to every person who provided support thorough out the research work and the staff of Concrete Lab. The careful examination and positive feedbacks by the unknown reviewers are gratefully acknowledged.

References

[1] S. Yin, R. Tuladhar, F. Shi, M. Combe, T. Collister, and N. Sivankugan. "Use of Macro plastic fibers in concrete; A review," *construction and Building Materials*, vol. 93, pp. 180-188, 2015.

[2] N. K. Krishna, M. Prasanth, R. Gowtham, S. Karthic, and K. M. Mini. "Enhancement of properties of concrete using natural fibers," *Materials Todays: Proceedings*, vol. 5, pp. 23816-23823, 2018.

[3] I. Merta, E. K. Stanzl-Tschegg, A. Kolbitsch. "Fracture Mechanics of concrete reinforced with hemp, straw and elephant grass fibers.," in *18th International Conference on Composite Materials*, Jeju Island, Korea, 2011.

[4] M. Ali, A. Liu, H. Sou, and N. Chouw. "Mechanical and dynamic poperties of cocunut fiber reinforced concrete," *Construction and Building Materials*, vol. 30, pp. 814-825, 2012.

[5] M. U. Farooqi and M. Ali, "Efffect of pre-treatment and content of wheat straw on energy absorption capability of concrete," *Construction and Building Materials*, vol. 224, pp. 572-583, 2019.

[6] M. A. Mansur and M. A. Aziz, "A study of jute fiber reinforced cement composites," *International Journal of cement composite and light weight concrete*, vol. 4, 1982.

[7] M. A. Ismail, "Compressive and tensile strength of natural fiber-reinforced cement based composites," *Al-Rafdain Engineering*, vol. 15, no. 2, pp. 42-51, 2007.

[8] M. H. Ahmad and N. H. Noor, *Mix Design of palm oil fiber concrete*, Malasyia: MSc Thesis Department of Structural and Materials Engineering, Faculty of Civil and Enviromental Engineering. , 2012.

[9] A. Latif, S. Begum, M. Adnan, K. Hussain, and, M. Waseem. et al, *Challenges Faced to Mazri Palm (Nannorhops ritchieana) : A Case Study of Jhandy, District Mardan- Pakistan*, Ethnobotanical Leaflets, 2004.

[10] C597 A, "Standard test method for pulse velocity through concrete," ASTM International west Conshohocken, PA, 2009.

[11] ASTM C39/C39M-03, "Standard test method for compression strength of cylinder specimens." West

Conshohocken, PA, 2003.

[12] ASTM C494/496M, "Standard test method for split tensile strength of cylindrical specimens." ASTM International West Conshohocken, PA.

[13] ASTM C78/78M, "Standard test method for flexural strength of concrete (using simple beam with third-point loading), ASTM International West Conshohocken, PA.

[14] Y. Tanigawa, K. Baba, and H. Mori, "Estimation of concrete strength by combined nondestructive testing method," *ACI Special Publication,* vol. 83, pp. 57-76, 1984.

[15] P. Turgut, "Research into the correlation between concrete strength and UPV values," *NDT.net,* vol. 12, no. 12, pp. 1-9, 2004.

3[rd] Conference on Sustainability in Civil Engineering (CSCE'21)
Department of Civil Engineering
Capital University of Science and Technology, Islamabad Pakistan

AXIAL COMPRESSIVE BEHAVIOR OF NON-BONDED NATURAL FIBER ROPE-CONFINED CONCRETE: EXPERIMENTAL STUDY

[a] Muhammad Waqas Khan, [b] Muhammad Hamza, [c] Ibrahim khader, [d] Shahzad Saleem*

a: Department of Civil Engineering, U.E.T, Taxila, waqas3768@gmail.com
b: Department of Civil Engineering, U.E.T, Taxila, muhammadhamza1601@gamail.com
c: Department of Civil Engineering, U.E.T, Taxila, ibra.653@gamail.com
d: Department of Civil Engineering, U.E.T, Taxila, shahzad.saleem@uettaxila.edu.pk
* Corresponding author: Email ID: shahzad.saleem@uettaxila.edu.pk

Abstract- In this research, an experimental investigation was carried out to determine the compressive behavior of normal (20 MPa) and medium (40 MPa) strength plain concrete confined by non-bonded cotton fiber rope reinforced polymer (FRRP). For this purpose, a total of 20 circular concrete cylinders were tested monotonically under axial compression. The study parameters covered the number of FRRP layers, strength of concrete and FRRP spiral spacing. Experimental results showed that the non-bonded manually wrapped cotton FRRP significantly enhanced the axial deformation of both normal (20 MPa) and medium (40 MPa) strength concrete, although less improvement was observed in the ultimate strength. The results also indicated that the effectiveness of cotton FRRP decreases with an increase in strength of concrete, increases with an increase of the FRRP layers and decreases with an increase of spiral spacing. Overall, the use of non-bonded manually wrapped cotton fiber ropes can result in improving the axial load and deformation capacity of concrete specimens.

Keywords- Axial stress-strain behavior, cotton FRRP layers, strength of concrete and cotton FRRP spacing.

1 Introduction

The reinforcement of old concrete buildings is needed by modification in demands regarding its use and loading conditions [1]. To date, numerous approaches have been used in a successful way to reinforce a given structure [2]. In the early stages of retrofitting, steel and concrete jacketing was widely used for the confinement of concrete columns. However, these confining materials have some serious issues including their physical properties such as weight, corrosion problems, enlarging the column sizes and long casting period due to their curing requirements.

In recent decades, synthetic fiber reinforced polymer (FRP) composites have been introduced. Various features and advantages regarding the application of these FRPs on RC columns, beams etc. have been thoroughly investigated, both in analytical and experimental way [3-4]. The benefits of these FRPs are high resilience, high tensile properties, lightness in weight, and straightforward application. Different types of synthetic FRPs such as carbon, aramid etc. have been used systematically for the repairing of structures and strengthening of RC components [5-8]. Typically, these FRPs are applied to the structural members externally by mixing enough resin with it. Rochette and Labossiere [9] studied the strengthening performance of the aramid and carbon FRPs for the enhancement in compressive stress-strain behavior of both rectangular and square concrete columns. A remarkable increase in compressive strength and strain of these FRP-confined square and concrete columns was reported.

The proposal to use natural fiber reinforced polymer (NFRP) to strengthen the concrete structures was given by Triantafillou et al. in 2006 [10]. The axial compressive behavior of concrete confined by NFRP composite [11-12] was recently studied by Pimanmas et al. [11] and Yan [12]. It was concluded that NFRP composites were very successful in altering the confined concrete's behavior. The main advantages of NFRP are that these materials are eco-friendly, sustainable, and cheap, along with reduced respiratory disorder. Despite the fact that these NFRPs have been shown to be effective in enhancing the ultimate stress, strain and ductility of concrete members [13-15], in many countries of the globe the production of these natural fibres particularly in the fabric's form, is still a problem.

In contrast to the above-mentioned studies in which the concrete columns were usually confined by fabric sheets of FRPs, the use of non-bonded vinyl and polypropylene fiber ropes as external confinement was explored by Rousakis [16-17]. The widespread features of rope confinement are readily accessible, easy to use, affordable and friendly in environment. The research findings showed that these non-bonded fiber ropes were very effective in improving the confined concrete's ultimate stress and strain. The use of epoxy bonded natural and synthetic fiber ropes (hemp, cotton, and polyester) as an external confinement was also explored by Hussain et al. [18]. It was observed that these ropes exhibited high efficiency in enhancing the ultimate compressive stress, strain and ductility of the confined concrete.

The aim of present study is to extend the study of concrete confinement in which non-bonded natural fiber (cotton) ropes are used as a confining material. In this regard, the effect of concrete strength, number of FRRP layers and spiral spacing on the stress-strain response is observed in detail. The research findings can be helpful in developing retrofitting schemes in which locally manufactured low-cost cotton fiber ropes can be satisfactorily used instead of imported and costly synthetic FRPs which also require high skilled labor.

2. Experimental Program

In this study, a total of 20 concrete cylindrical specimens were prepared out of which 12 specimens were confined with cotton FRRPs and remaining were the control specimens. The parameters used in this study were the compressive strength of concrete, the number of FRRP layers and the pitch distance in case of spiral wrapping. Table 1 gives the details of research specimens. The diameter and height of the specimens was 150 and 300 mm, respectively, as shown in Figure 1. All the specimens were prepared in 4 batches. The concrete specimens that were prepared in first 2 batches had compressive strengths of (20 MPa) and the specimens of remaining 2 batches had compressive strength of (40MPa). After fulfilling the curing requirements at 28 days, the top and bottom sides of the cylinders were made smooth and flat with the help of concrete cutting machine. The labeling of specimens is done as XNYM in which X represents the type of rope used as FRRP (C for cotton); N indicates concrete's compressive strength (20 for 20 MPa and 40 for 40 MPa); Y represents the type of wrapping (F for Full and S for spiral); and the last alphabet M indicates the number of rope layers. For example, C40F2 designates that this specimen has compressive strength of 40 MPa and is fully wrapped with two layers of cotton rope. The controlled specimens are simply labeled as XN, in which X represents control and N represents the compressive strength of the concrete.

Table 1-Details of experimental test matrix

Sr. no.	Designation	Identical specimens	Confining material	Wrapping type	No. of layers	Pitch distance (cm)
1	X20	4	-	-	-	-
2	X40	4	-	-	-	-
3	C20F1	2	Cotton	Full	1	0
4	C20F2	2	Cotton	Full	2	0
5	C20S1	2	Cotton	Spiral	1	1
6	C40F1	2	Cotton	Full	1	0
7	C40F2	2	Cotton	Full	2	0
8	C40S1	2	Cotton	Spiral	1	1

2.1 Concrete

The details of the concrete mix proportions are given in Table 2 and Table 3. Concrete cylinders of two different strengths were prepared in the laboratory. The ingredients of concrete were mixed by using mechanical mixer. Due the limited mixing capacity of the mixer, concrete cylinders were prepared in four different batches. In the first two batches, ten concrete specimens of strength 20 MPa were cast and in the last two batches, remaining concrete specimens of strength 40 MPa were cast. For each batch, two similar control specimens were also prepared and tested along with their confined parts to find their unconfined compressive strength f_{co}.

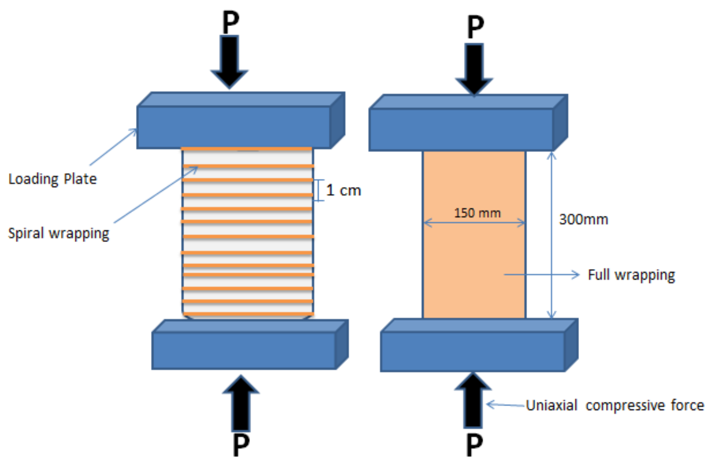

Figure 1: Schematic diagram of concrete specimens showing spiral and full FRRP wrapping

2.2 Cotton FRRP wrapping

After having prepared the concrete cylinders, the specimens were confined with cotton ropes. The diameter of the cotton rope, used as an external confinement, was 3 mm. The specimens were wrapped fully and spirally, as shown in Figure 2a. A pitch distance of 1 cm was used in case of spiral wrapping. To avoid premature failure of the confined specimens during the test, the top and bottom ends of the cylinders were additionally wrapped by providing 25 mm strip of the cotton rope bonded with high strength epoxy resin.

2.3 Test setup

In this experimental study, all the concrete specimens were tested under monotonic axial compression with the help of universal testing machine (UTM) having a capacity of 2000 kN, as shown in Figure 2b. Due to limited instrumentation available, axial deformation was noted with the help of two dial gauge meters. Load was applied axially at the rate of 2.5 kN/sec and the deformation was recorded after every 10 sec.


a

b

Figure 2: Specimens wrapping and instrumentation details, a. cotton FRRP wrapped specimens, and b. instrumentation and loading setup

Table 2-Concrete mix proportion for 20MPa

Item	Value
Cement (kg/m^3)	301.47
Sand (kg/m^3)	772.194
Coarse aggregates (kg/m^3)	1020
Water (kg/m^3)	195.95
Water/cement ratio (kg/m^3)	0.65
Maximum aggregate size (mm)	20

Table 3- Concrete mix proportion for 40MPa

Item	Value
Cement (kg/m^3)	500
Sand (kg/m^3)	609.654
Coarse aggregates (kg/m^3)	1020
Water (kg/m^3)	250
Water/cement ratio (kg/m^3)	0.5
Maximum aggregate size (mm)	20

3. Research Methodology

The casting and preparation of concrete specimens was done in the initial stage of the research. These specimens were then wrapped manually with the cotton FRRPs without using any epoxy coating for its binding with concrete surface. To avoid stress concentration, 25 mm cotton strip along with high strength epoxy was provided on top and bottom ends of the cylinders. After preparation, testing of all cylinders was done by applying pure compressive load with the help of UTM. Experimental results of the confined specimens including stress-strain curves were obtained. At the last, analysis and comparative study of the stress-strain curves obtained by testing these specimens was done using various research parameters.

4. Test Results

4.1 Stress-strain response

Initially, for both the normal strength (20 MPa) and medium strength (40 MPa) concrete, the stress- strain curve followed an ascending branch reaching up to the unconfined concrete strength, f_{co}. After reaching f_{co}, a sudden significant drop in axial strength was observed because of growth of concrete cracks and inadequate confinement of cotton FRRPs at this moment. After reaching the maximum drop when concrete core dilated enough to engage the FRRP confining pressure, the curve of normal strength concrete ascended almost linearly depending on the number of FRRP layers, while curve of medium strength concrete followed an almost a uniform straight plateau. In case of spiral wrapping, the curve for both normal and medium strength concrete descended gradually after the maximum stress drop point. In general, the overall response of non-bonded cotton FRRP confined concrete can be classified as trilinear.

4.2 Effects of FRRP layers

The stress-strain response of both normal and medium strength FRRP confined concrete cylinders are shown in Figure 3. For both types of concrete strength, it was observed that the last part of the curve greatly enhanced with an increase in FRRP layers. In the normal concrete strength specimens confined by one or two FRRP layers, a similar drop in strength after the unconfined peak strength was observed which shows that the external confinement of non-bonded ropes is not sufficiently activated yet. After the maximum drop, curves of both specimens ascended again indicating that the ropes are strained enough to provide enough confining pressure until their failure. For double layer of FRRP, the ultimate stress was about 18 MPa compared to the 12 MPa of single FRRP. Similarly, in case of specimens confined with single layer of FRRP the ultimate strain was 10%, whereas in specimens with two layers of FRRPs the ultimate strain was observed to be 18% (Figure 3a). In case of medium strength concrete specimens, the external confinement of single FRRP layer was not enough to maintain the load after the sudden drop. In these specimens, the strength was observed to be continuously decreased at a slow rate with an increase in axial deformation until their failure. In specimens confined by two FRRPs layers, a long approximately horizontal plateau is observed indicating that the strength is efficiently sustained even at high axial deformation of about 24% (Figure 3b). In contrast, Hussain et al. observed relatively less strength softening in epoxy bonded cotton rope confined circular specimens [18]. A significant drop in strength after the peak load was also observed by Rousakis for specimens confined by three full layers of non-bonded polypropylene fiber ropes [17]. In case of spiral confinement, the strength could not be sustained after the maximum drop; however, the specimens failed at high axial deformation compared to the control specimens. Effect of FRRP layers on ultimate axial stress and strain is shown in Figures 4 and 5, respectively.

4.3 Effect of concrete strength

It can be observed from Figure 6 that the effectiveness of FRRP confinement is less for medium strength concrete specimens compared to the normal strength concrete specimens. This observation agrees with the previous findings of Ozbakkaloglu and Vincent (2014) for carbon FRP confined concrete [19] and Wahab et al. (2019) for their specimens confined by jute and polyester hybrid confinement [20]. In general, a higher drop after the peak strength is observed for specimens with medium concrete strength. In specimens confined by single layer of FRRP, the curve after the maximum drop slightly ascended again in normal strength concrete, whereas in specimen with medium strength concrete the curve descended gradually until the FRRP failure (Figure 6a). In case of two layered specimens, the curve in normal concrete specimens ascended near to the peak strength, whereas in specimens with medium strength concrete the load was efficiently sustained at high axial deformation (Figure 6b). Interestingly, the specimens with medium concrete strength exhibited higher axial deformation compared to the normal strength concrete specimens. In case of spiral wrapping, a similar response is observed in both concrete specimens except that a higher drop is observed for medium strength concrete specimen, see (Figure 6c). Effects of concrete strength on ultimate axial stress and strain are shown in Figures 7 and 8, respectively.

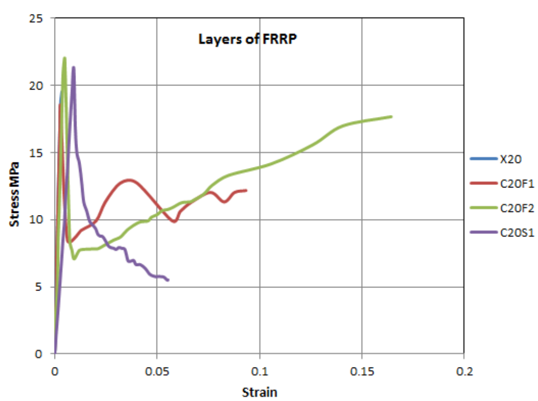

a)

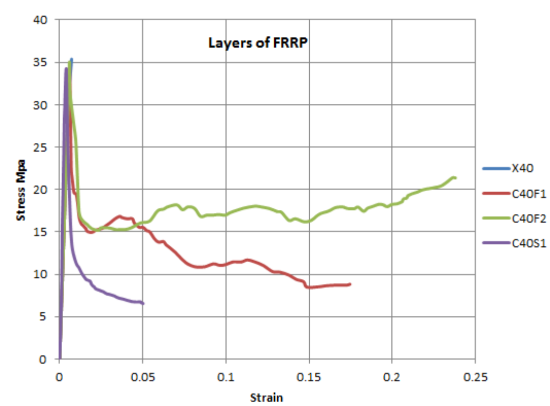

b)

Figure 3: Effect of FRRP layers on stress-strain response, a. normal strength concrete, 20MPa, and b. medium strength concrete, 40MPa

4.4 Effect of FRRP spacing

Figures 9a and b represent the effect of FRRP spacing on the stress-strain response of normal and medium strength concrete. For 20 MPa concrete, the reduced effective confinement of spiral FRRP could not sustained the load after drop in peak strength and exhibited a descending branch until failure at about 5%, whereas in specimens with full FRRP wrapping the confining pressure was enough to sustain the load even at higher axial deformation of about 9% (Figure 9a). On the other hand, for 40 MPa concrete, although full wrapping of FRRP could not sustained the load after the sudden drop, however, it exhibited a gradual strength softening and failed at high axial strain of 17% compared to the 5% failure strain of spirally confined concrete (Figure 9b). Effect of FRRP spacing on ultimate axial stress and strain is shown in Figures 10 and 11, respectively.

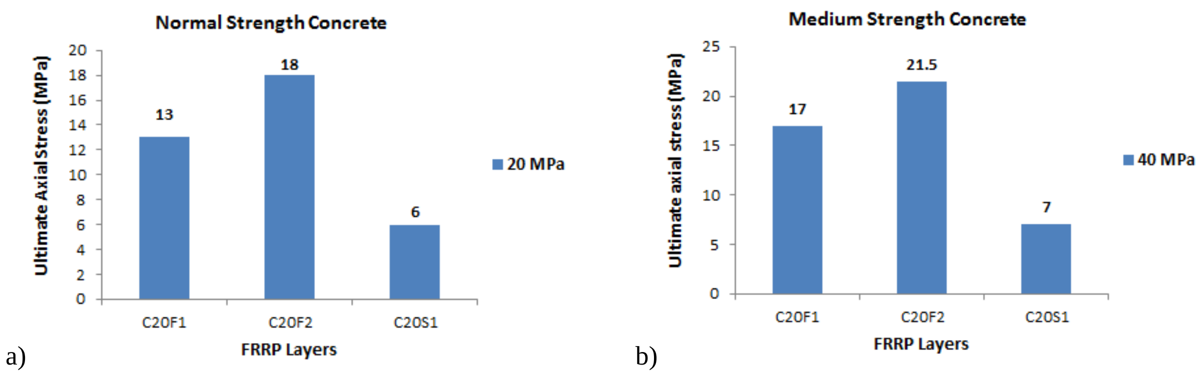

Figure 4: Effect of FRRP layers on ultimate axial stress, a. normal strength concrete, and b. medium strength concrete

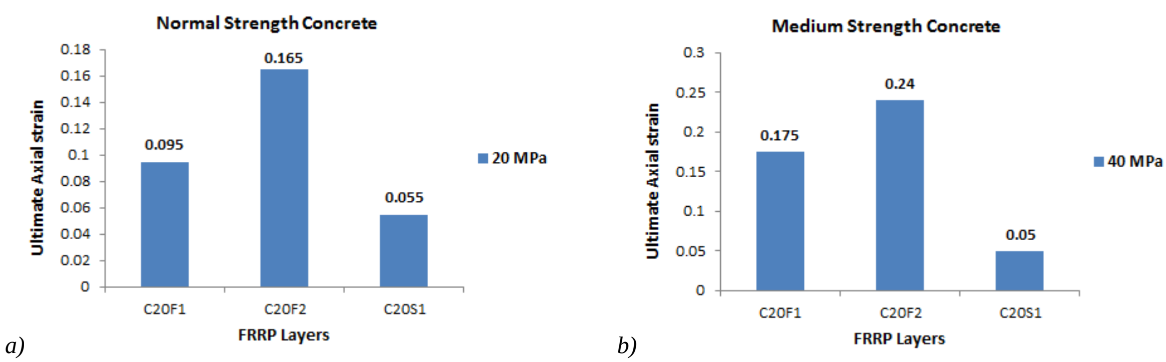

Figure 5: Effect of FRRP layers on ultimate axial strain, a. normal strength concrete, and b. medium strength concrete

4.5 Ultimate failure modes

The ultimate failure modes of the unconfined and FRRP confined concrete specimens are shown in Figures 12 and 13. The un-strengthened specimens failed in a conventional way by concrete crushing at peak compressive stress. Whereas the cotton FRRP strengthened specimens were failed by the tensile rupture of cotton FRRPs. The tensile rupture of the cotton FRRPs started in the periphery of epoxy bonded cotton strips provided at the top and the bottom, and then the splitting of FRRPs was very gradual during the ultimate failure. The failure was very quiet even in case of double FRRP layers for both normal and medium strength concrete.

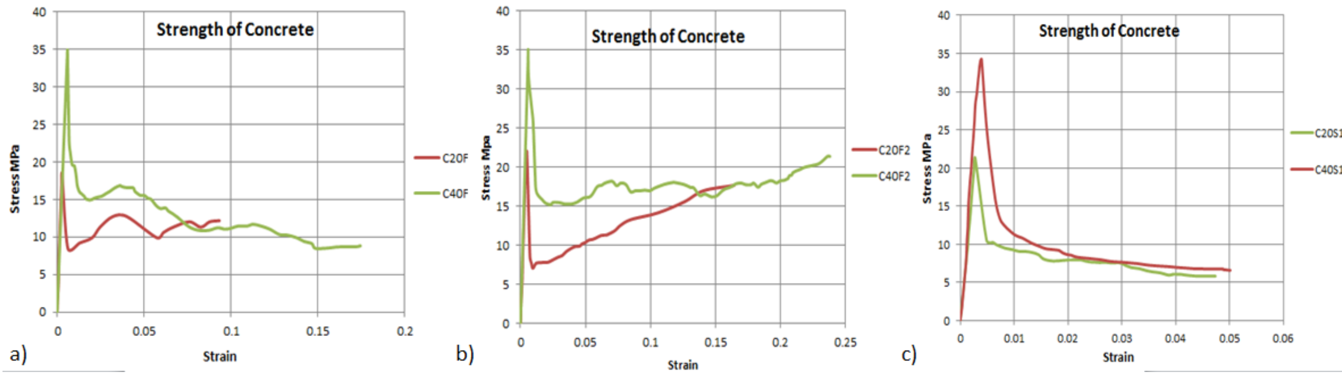

Figure 6: Effect of concrete strength on stress-strain response, a. single layer of FRRP, b. double layer of FRRP, and c. spiral layer

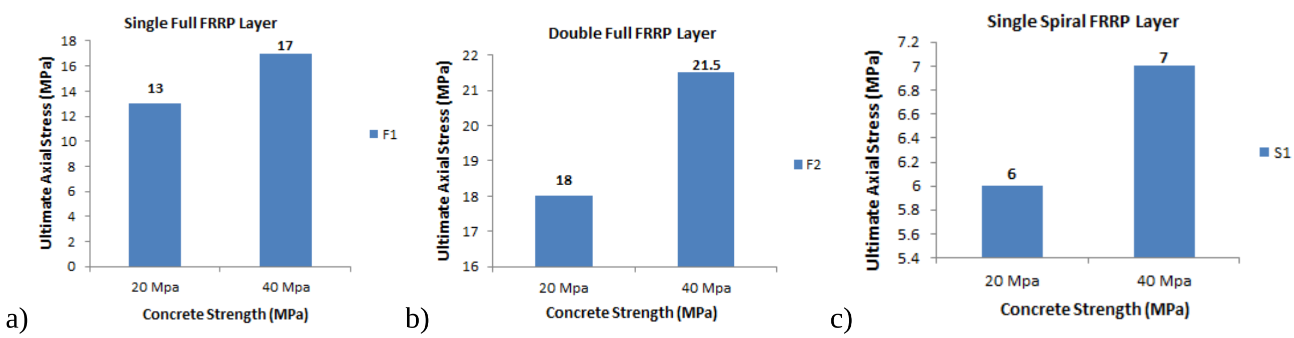

Figure 7: Effect of concrete strength on ultimate axial stress, a. single layer of FRRP, b. double layer of FRRP, and c. spiral layer

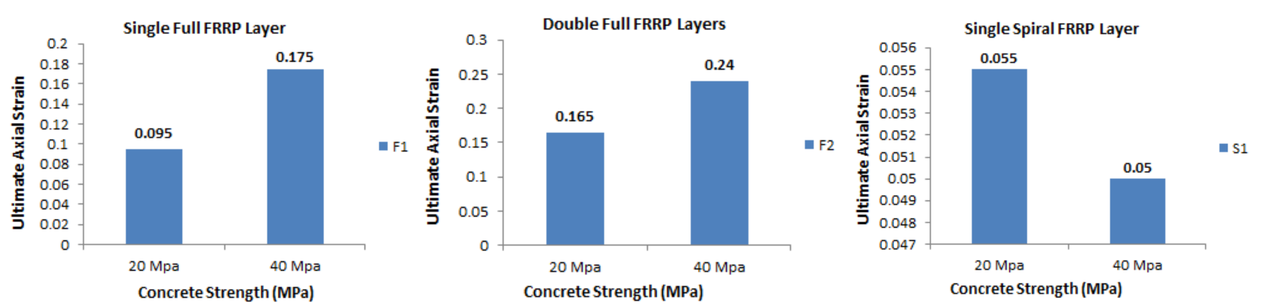

Figure 8: Effect of concrete strength on ultimate axial strain, a. single layer of FRRP, b. double layer of FRRP, and c. spiral layer

5 Conclusions

This research study includes an experimental work to comprehend the compressive behavior of both normal and medium strength concrete confined with non-bonded cotton FRRP in circular columns. For this purpose, a total of 20 specimens were tested under monotonic axial compressive. The parameters used were number of FRRP layers, concrete strength and FRRP spiral spacing. The conclusions are being summarized as follows:

- Axial stress-strain behavior of non-bonded FRRP confined concrete is trilinear in which the post-peak response was improved with an increase in the FRRP layers.

- For medium strength concrete, the FRRP confinement is less effective compared to normal strength concrete. For a particular number of FRRP layers, higher strength softening was observed in medium strength concrete specimens compared to the normal strength concrete.
- FRRP spiral wrapping technique is found not effective in enhancing the post peak behavior for both normal and medium strength concrete, however, it prevented the brittle collapse of concrete up to high axial deformation

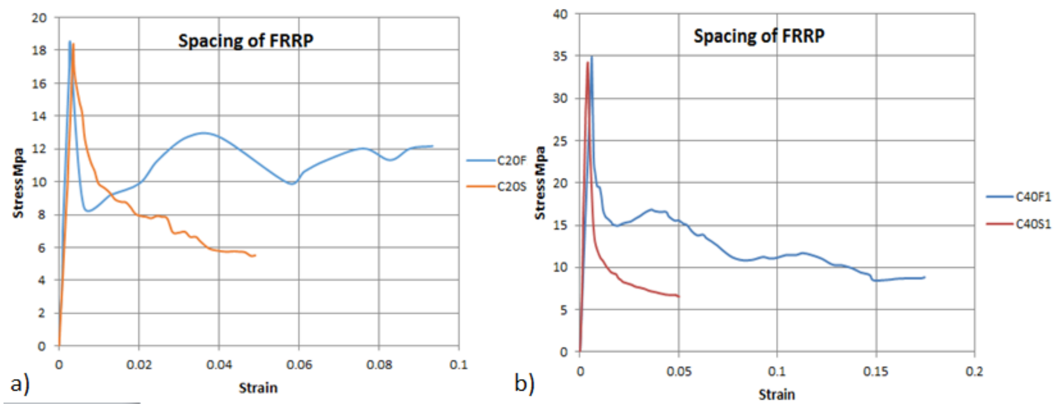

Figure 9: Effect of FRRP Spacing on stress-strain response, a. normal strength concrete, and b. medium strength concrete

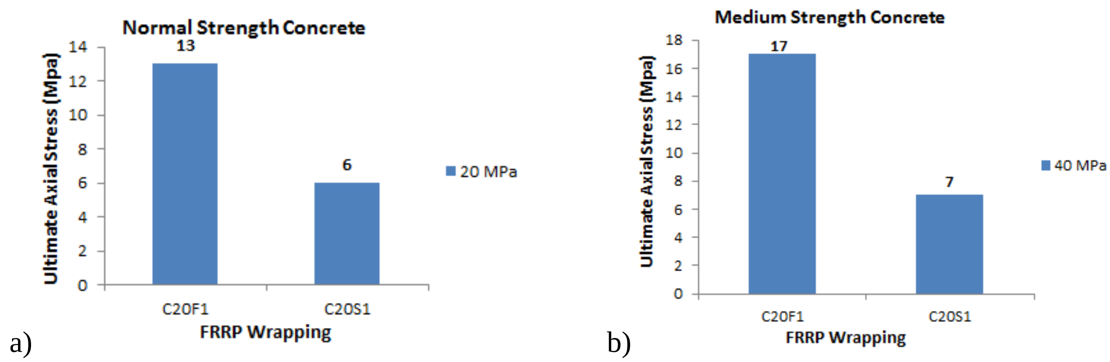

Figure 10: Effect of FRRP Spacing on ultimate axial stress, a. normal strength concrete, and b. medium strength concrete

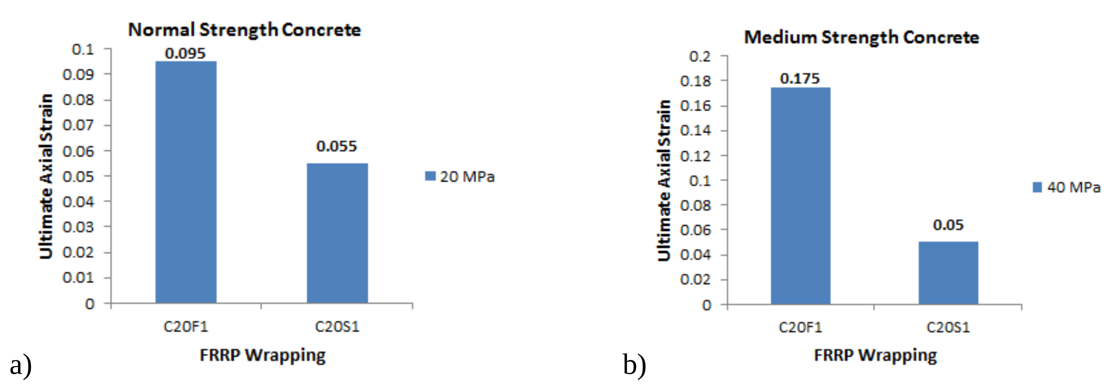

Figure 11: Effect of FRRP Spacing on ultimate axial strain, a. normal strength concrete, and b. medium strength concrete

a b c d

Figure 12: Typical failure modes of 20 MPa FRRP specimens, a. control specimen, b. full single layer, and c. full double layers and d) spiral layer.

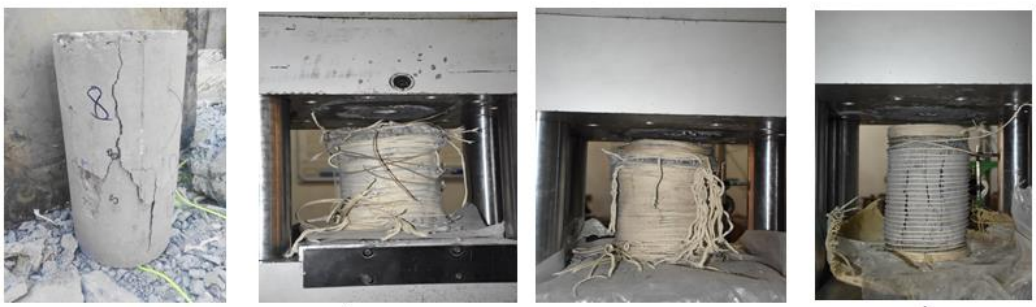

a b c d

Figure 13: Typical failure modes of 40 MPa FRRP specimens, a. control, b. full single layer, c. full double layers, and d. spiral layer.

Acknowledgment

The authors are grateful to every person who provided support thorough out the research work and the staff of Strength of Materials Lab. The careful examination and positive feedbacks by the unknown reviewers are gratefully acknowledged.

References

[1] T. C. Triantafillou, "Shear strengthening of reinforced concrete beams using epoxy-bonded FRP composites," *ACI Structural Journal*, vol. 95, pp. 107–115, 1998.

[2] N. M. Barkoula, B. Alcock, N. O. Cabrera, and T. Peijs, "Flame-retardancy properties of intumescent ammonium poly (phosphate) and mineral filler magnesium hydroxide in combination with graphene," *Polymer Compsoites*, vol. 16, pp. 101–113, 2008.

[3] M. Z. Naser, R. A. Hawileh, and J. A. Abdalla, "Fiber-reinforced polymer composites in strengthening reinforced concrete structures: A critical review," *Engineering Structure*, vol. 198, p. 109542, 2019.

[4] C. E. Chalioris, A. G. Zapris, and C. G. Karayannis, "U-jacketing applications of fiber-reinforced polymers in reinforced concrete t-beams against shear-tests and design," *Fibers*, vol. 8, p. 13, 2020.

[5] S. Saleem, Q. Hussain, and A. Pimanmas, "Compressive behavior of PET FRP–confined circular, square, and rectangular concrete columns," *Journal of Composites for Construction*, vol. 21, p. 04016097, 2017.

[6] B. N. Plevris and T. C. Triantafiuou, "Time-dependent behavior of RC members strengthened with FRP laminates," *Journal of Structural Engineering*, vol. 120, pp. 1016–1042, 1994.

[7] M. A. Adam, M. Said, A. A. Mahmoud, and A. S. Shanour, "Analytical and experimental flexural behavior of concrete beams reinforced with glass fiber reinforced polymers bars," *Construction and Building Materials*, vol. 84, pp. 354–366, 2015.

[8] R. A. Hawileh, A. Abu-Obeidah, J. A. Abdalla, and A. Al-Tamimi, "Temperature effect on the mechanical properties of carbon, glass and carbon-glass FRP laminates," *Construction and Building Materials*, vol. 75, pp. 342–348, 2015.

[9] B. S. Chan and J. Gu, "Exact tangent stiffness for imperfect beam-column members," *Journal of Structural Engineering*, vol. 7, pp. 129–136, 2000.

[10] T. C. Triantafillou, C. G. Papanicolaou, P. Zissimopoulos, and T. Laourdekis, "Concrete confinement with textile-reinforced mortar jackets," *ACI Structural Journal*, vol. 103, pp. 28–37, 2006.

[11] A. Pimanmas, Q. Hussain, A. Panyasirikhunawut, and W. Rattanapitikon, "Axial strength and deformability of concrete confined with natural fibre-reinforced polymers," *Magazine of Concrete Research*, vol. 71, pp. 55–70, 2019.

[12] L. Yan, "Plain concrete cylinders and beams externally strengthened with natural flax fabric reinforced epoxy composites," *Materials and Structures*, vol. 49, pp. 2083–2095, 2016.

[13] T. Sen and H. N. Jagannatha Reddy, "Efficacy of bio derived jute FRP composite based technique for shear strength retrofitting of reinforced concrete beams and its comparative analysis with carbon and glass FRP shear retrofitting schemes," *Sustainable Cities and Society*, vol. 13, pp. 105–124, 2014.

[14] Y. Li, Y. Mai, and L. Ye, "Sisal fibre and its composites : a review of recent developments," *Composites Science and Technology*, vol. 60, pp. 2037–2055, 2000.

[15] T. Sen and H. N. J. Reddy, "Flexural strengthening of RC beams using natural sisal and artificial carbon and glass fabric reinforced composite system," *Sustainable Cities and Society*, vol. 10, pp. 195–206, 2014.

[16] T. C. Rousakis, "Reusable and recyclable nonbonded composite tapes and ropes for concrete columns confinement," *Composites Part B Engineering*, vol. 103, pp. 15–22, 2016.

[17] T. C. Rousakis, "Hybrid Confinement of Concrete by Fiber-Reinforced Polymer Sheets and Fiber Ropes under Cyclic Axial Compressive Loading," *Journal of Composites for Construction*, vol. 17, pp. 732–743, 2013.

[18] Q. Hussain, A. Ruangrassamee, S. Tangtermsirikul, and P. Joyklad, "Behavior of concrete confined with epoxy bonded fiber ropes under axial load," *Construction and Building Materials*, vol. 263, p. 120093, 2020.

[19] T. Ozbakkaloglu, and T. Vincent, "Axial compressive behavior of circular high-strength concrete-filled FRP tubes." *Journal of Composites for Construction*, vol 18, p. 04013037, 2014.

[20] N. Wahab, P. Srinophakun, Q. Hussain, and P. Chaimahawan, "Performance of Concrete Confined with a Jute–Polyester Hybrid Fiber Reinforced Polymer Composite: A Novel Strengthening Technique." *Fibers*, vol. 7, pp 1-26, 2019.

3rd Conference on Sustainability in Civil Engineering (CSCE'21)
Department of Civil Engineering
Capital University of Science and Technology, Islamabad Pakistan

EFFECT OF CARBON NANOTUBES AND FLY ASH ON MECHANICAL AND MICROSTRUCTURAL PROPERTIES OF CEMENT MORTARS

[a]Raja Wajahat Zahoor Khan, [a]Dr.Muhammad Yaqub, [a]Tariq Ali, [b]Raja Shujahat Zahoor Khan

* Corresponding author: Raja Wajahat Zahooor Khan. Email ID: wajahatzahoor12@gmail.com
[a] Department of Civil Engineering, University of Engineering and Technology, 47050 Taxila, Pakistan
[b] Department of Civil Engineering, Mirpur University of Science and Technology, 10250 Mirpur, Pakistan

Abstract: This paper aims to evaluate the effect of various dosages of carbon nanotubes (CNTS) and fly ash (FA) on the mechanical and microstructural properties of mortar cubes. Cement was replaced with varying dosages of fly ash (5%, 10%, 15%, 20% and 25%) and CNTS (0.125%, 0.25%, 0.137% and 0.5%). In addition 10% fly ash was added independently with 0.125%, 0.25%, 0.137% and 0.5% carbon nanotubes. The addition of 10% fly ash in cement as an optimum dosage increased the compressive strength by 21.9%, 17.4%, and 80.2%, however, increase in fly ash dosage (25%) led to a decrease in mortar strength by 50.8%, 56.9% and 55.1% when specimens were subjected to compressive strength test at 7,28 and 90 days respectively. The study shows that the addition of 0.125% CNTS as an optimum dosage increased mortar strength up to 12.7%, 62.6%, and 48.7% at 7, 28, and 90 days respectively due to the bridging effect of CNTS. Similarly, the introduction of 10% fly ash with 0.25% CNTS as an optimum dosage led to an increase in compressive strength by 8.2%,20%, and 21.4% at 7,24, and 90 days respectively, however higher dosages of CNTS decreased mortar strength. Microstructural analysis shows improvement in bonding between matrix and aggregates due to the filling and bridging effect of fly ash and carbon nanotubes.

Keywords: Carbon Nanotubes, Fly ash, Mortar, Mechanical properties, Compressive strength, Microstructural properties

1. Introduction

The use of nanomaterials in the construction industry has got prime importance due to their peculiarity in physical and chemical properties. Materials having a size equal to or less than 100 nanometers are usually associated with nanomaterials. Apart from being sustainable, these materials show resilience against fire, cracking, corrosion, and water penetration [1]. Eloquent research carried out in past shows the potential use of carbon nanotubes in enhancing various properties of cementitious materials [2], [3]. Due to the high aspect ratio, high young modulus, and availability of nanoparticles like nano-Fe_2O_3 and nano-SiO_2 in CNTS increase both compressive and tensile strength of cement mortars [4],[5]. Results of various researchers show that the use of carbon nanotubes acts as a filling agent which consequently leads to an increase in the density of microstructure and its strength by reducing permeability [6],[7].[8]. The study carried out by A. Chaipanich et al. [4] indicates that the use of 0.5% CNTS and 1% fly ash significantly increased the density of mortar at 28 days (2.29g/cm^3) as compared to mix without CNTS (2.19g/cm^3). Optimum dosage (0.01%) of carbon nanotubes increased led to an increase in compressive strength and stiffness of cement mortars [9].

The introduction of by-products as cementitious material such as fly ash produced by industrial expansion has also got warm attention. Early research carried out by (Haque, 1984) lead the way to introduce high volume fly ash in concrete. He found that 50% replacement of cement with fly ash could result in better performance without affecting its initial and final setting time. It is reported that the addition of 70% fly ash with 5% nano-silica substantially increased compressive strength up to 90% when used in cement mortars [10]. On contrary, the research carried by [11] shows a decrease in compressive strength by 76.98% when cement was replaced by 70% with fly ash. Furthermore, the study of [12] reflects that introduction of a high amount of fly ash in cement mortars (50,60, and 70%) decreases 28 days compressive strength by 40%, 46.57%, and 74.29% respectively.

When a building is subjected to high temperature or environmental changes, the building materials deteriorate and its mechanical properties become more dynamic. The unprotected concrete may lead to severe damage. Literature shows that extensive research has been carried out to analyze the behavior of fly ash in concrete but the use of fly ash and carbon nanotubes as an emerging material is still needed to be explored through various perspectives that could help to reinforce mortar to protect buildings and finished surfaces. In this study, different dosages of carbon nanotubes and fly ash were added to the cement. Mechanical properties such as compressive strength and microstructural properties of mortar are evaluated that would help to design optimum mix ratio to reinforce mortars which would provide an economical and sustainable solution.

2. Experimental Program

2.1 Materials & Mix Proportions

Locally available *Fauji* Cement originated at (Fauji Cement Company Limited, n.d.) was used in this research. The cement (ASTM Type I) follows the requirements of (ASTM C150) [13]. Black-colored multi-walled carbon nanotubes having an outer diameter of 20-40nm and length of 5-15nm were used in this study as shown in Fig.1 (b). The CNTS were mixed with 0.1% plasticizer (poly-carboxylate) by using sonicator as shown in Fig.1 (c). The specific surface area of CNTS is 90-120 m^2g^{-1} having 97% purity. Locally processed class F fly ash meeting the standard of ASTM C 618 manufactured at 'Port Qasim Power Plant Karachi Pakistan' was used in research as shown in Fig.1. (a). The maximum nominal size of fine aggregates is 4.75mm which follows the specifications of ASTM C778 [14]. The amount of fly ash and CNTS is calculated by weight (Kg/m^3) and volume (%) of the total mix. The casting, drying, and testing of mortar cubes having the size of ($70\times70\times70$ mm^3) was done carefully.

Table.1 Mix proportion of mortar mixtures.

Batch No.	Mixture	w/c	Water Kg/m^3	Cement Kg/m^3	Sand Kg/m^3	Fly Ash		CNTS	
						Kg/m^3	%	Kg/m^3	%
1	Control	0.5	234	468	1414	0	0	0	0
	F1	0.5	234	445	1414	23	5	0	0
	F2	0.5	234	421	1414	47	10	0	0
	F3	0.5	234	398	1414	70	15	0	0
	F4	0.5	234	374	1414	94	20	0	0
	F5	0.5	234	351	1414	117	25	0	0
2	C1	0.5	234	467.4	1414	0	0	0.6	0.125
	C2	0.5	234	466.8	1414	0	0	1.2	0.25
	C3	0.5	234	466.2	1414	0	0	1.8	0.375
	C4	0.5	234	465.6	1414	0	0	2.3	1
3	CF1	0.5	234	419	1414	47	10	2	0.125
	CF2	0.5	234	418	1414	47	10	3	0.25
	CF3	0.5	234	416	1414	47	10	5	0.375
	CF4	0.5	234	414	1414	47	10	7	1

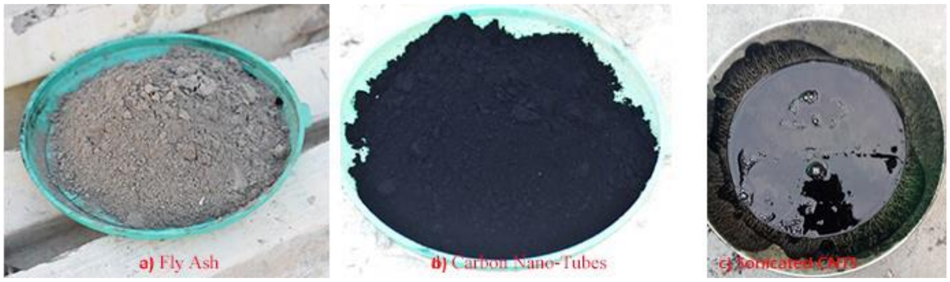

Fig 1. (a). Fly Ash (b). Dry CNTS (c). Sonicated CNTS.

3. Testing Program

3.1. Compressive strength test

The compressive strength of cubes was found according to the guidelines of ASTM C109. Cubes were subjected to the compressive testing machine having a loading capacity of 3000KN to determine the compressive strength of cubes. Tests at 7,28 and 90 days were performed to evaluate mortar strength. The loading rate and reference load was fixed as 1.8KN/sec and 1000KN respectively.

3.2. Microstructural analysis

The microstructural analysis was performed by spectral electron microscopy (SEM) to determine the structure of hydration products. SEM images were taken at different resolutions ranging between 5-50 µm.

4. Results and discussions

4.1. Compressive strength

The results of 7, 28 and, 90 days compressive strength of mortars having fly ash are shown in Fig.2. Compressive strength was determined by replacing cement with 5%,10%,15%,20% and 25% fly ash. Results showed slight variation in compressive strength at 7 days but become more evident at 28 and 90 days. The gradual increase in compressive strength was noticed when cement was replaced by 10% FA which was followed by the reduction in strength at higher dosages of fly ash. At 10% replacement of fly ash, an increase of 5.2, 17.4, and 80.2% increase in compressive strength was noticed when specimens were tested at 7, 28, and 90 days respectively. The findings of Nasser et al. [15] show that 10% replacement of fly ash leads to higher compressive strength at 7 and 28 days. A higher dosage of fly ash leads to a decrease in compressive strength both at an early and late age. The addition of 25% fly ash brought to 55.% and 56.1% decrease in strength when mortars were tested at 28 and 90 days respectively. A similar trend of results was reported by S.W.M Supit [16] showing that reduction in 28 days compressive strength of mortar was 40%,54.29%, and 74.29% when cement was replaced with 50%, 60%, and 70% of fly ash respectively. Mortar cubes containing different proportions of carbon nanotubes were also tested for compressive strength at 7, 28, and 90 days as graphed in Fig.3. In general addition of CNTS by 0.125%, 0.25%, 0.375% and 0.5% showed marked difference in strength when tested at 7, 28 and 90 days. At an optimum dosage of CNTS an increase of 39.5, 62.6, and 48.7% compressive strength was recorded at 7, 28, and 90 days respectively. The addition of CNTS more than 0.125% of cement lead to a decrease in compressive strength. The strength exhibited by mortar specimens containing 0.25%, 0.375% and 0.5% CNTS was 62.6%, 30.1%, and 21.9% with respect to control sample which shows a considerable decrease in strength as compared to optimum mix. Similarly the tests performed at 90 days on specimens containing 0.5% CNTS shows that compressive strength of mortar became equivalent to control sample which reflects that higher dosage of CNTS leads to decrease in compressive strength. The research carried out by Amin et al. [17] shows that replacement of composite cement with 0.1% CNTS gives higher compressive strength and 0.2% CNTS leads to a decrease in strength. Another study shows that the introduction of 0.5% multi-walled CNTS in cement paste significantly lead to a decrease in compressive strength [18].

The combined behavior of carbon nanotubes and fly ash on compressive strength was also determined in this study as presented in Fig.4. In each mix of the third batch 10% fly ash was added with varying dosages of CNTS like 0.125, 0.25, 0.137, and 0.5%. In general addition of fly ash improved late strength but increasing concentration of CNTS led to a decrease in strength. The optimum dosage of CNTS (0.25%) with 10% FA increased mortar compressive strength by 8.2%, 20%, and 21.4% when subjected to loading at 7, 28, and 90 days. On the contrary increase in CNTS dosage by 0.5% showed only 5.7% and, 4.8% increase in strength at 28 and 90 days which reflects that the overall compressive strength of mortar has reduced as compared to the optimum mix named CF1 due to agglomeration of CNTS and incomplete hydration reaction. The addition of 0.5% CNTS with 10% FA reduced 7 days compressive strength by 20.2% which shows that the high dosage of CNTS with fly ash retard hydration reaction and increases the setting time of the mortar. The average compressive strength of all mixes having different dosages of CNTS with 10% fly ash was greater than the controlled mix. Similar results reported by R. Siddique [19] indicate that the addition of 1% multi-walled CNTS with 20% fly ash gives higher strength and the same trend is found for other mixes having CNTS and FA when tested at 60 days. This is also confirmed by [4] that the use of fly ash with CNTS leads to an increase in the compressive strength of mortars. The comparison of compressive strength between mixes of batch 2 containing CNTS and batch 3 having CNTS with fly ash is performed in Fig 5, Fig 6, and Fig 7 which reflects that mortar mixes containing CNTS showed greater strength as compared to mixes having CNTS and FA at both 7 and 28 days. Results show that optimum dosage of CNTS in mix C1 lead to an increase in 7, 28, and 90 days compressive strength by 36%, 42%, and 38% respectively as compared to optimum mix CF1 having CNTS and FA which indicates that use of fly ash with CNTS gives lower strength which is also uneconomical as compared to mixes only having CNTS. The mixing of CNTS with FA drives to decrease in mortar compressive strength but overall strength remains greater than control sample.

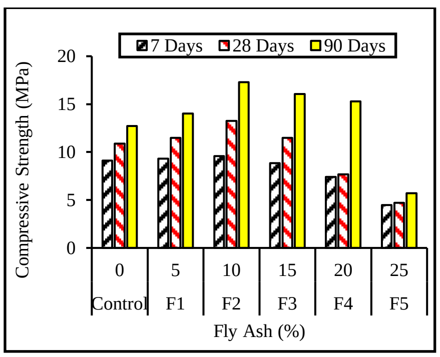

Fig.2. Compressive strength of specimens containing fly ash at 7, 2,8 and 90 days.

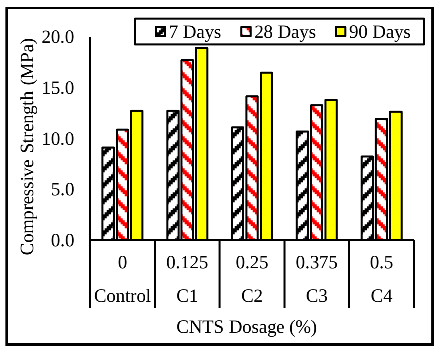

Fig.3. Compressive strength of specimens containing CNT's at 7, 28, and 90 days.

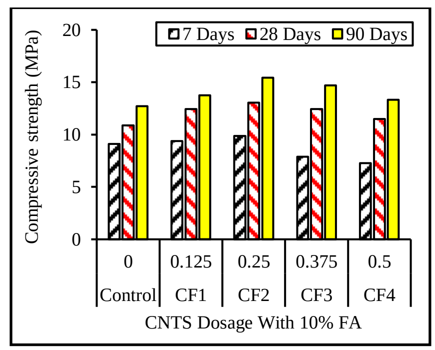

Fig.4. Compressive strength of specimens containing CNT's with 10% FA at 7, 28, and 90 days.

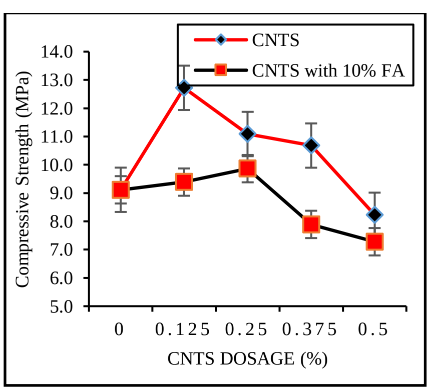

Fig.5. Strength comparison of specimens containing CNT's and CNT's+ 10% FA at 7 days.

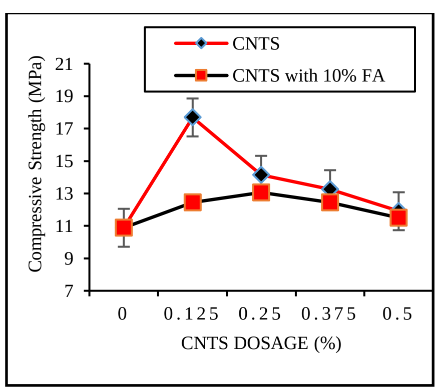

Fig.6. Strength comparison of specimens containing CNT's and CNT's+ 10% FA at 28 days.

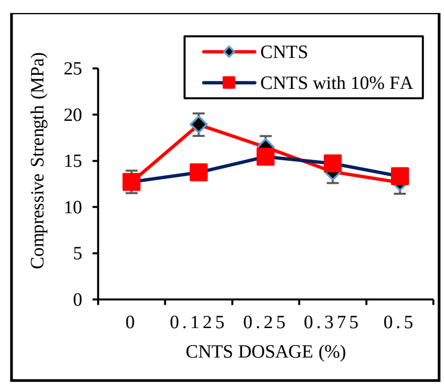

Fig.7. Strength comparison of specimens containing CNT's and CNT's+ 10% FA at 90 days.

4.2. Microstructural Analysis

The analysis of the control sample of mortar shows needle-shaped crystals of ettringite and prismatic crystals of calcium hydroxide, however, there has been the formation of micro-cracks and voids as shown in Fig.8. The addition of 10% fly ash accelerated ettringite formation and C-S-H gel which reinforced the matrix in some ways by binding the hydration products as shown in Fig.9. Similarly, the addition of CNT's enhanced the interfacial interaction between hydration products and carbon nano-tubes which lead to the formation of stable and denser microstructure. The nano-sized reinforcements of CNT's interacted intimately with C-S-H gel creating bridges between matrix and fine aggregates which provided sufficient resistance to cracks and enhanced the load-carrying capacity of mortar specimens. The bridging of CNTS is evident from Fig.10.

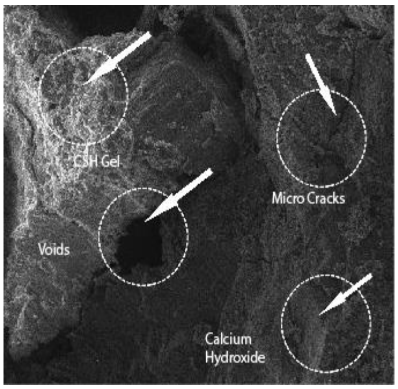

Fig.8. SEM image of control specimen at 50µm.

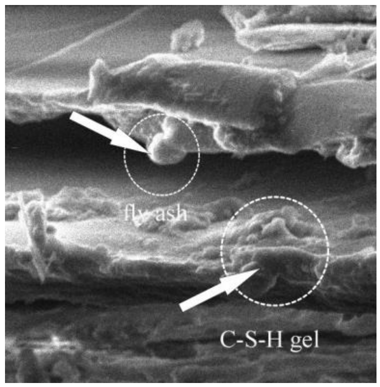

Fig.9. SEM image of specimen containing fly ash at 10µm.

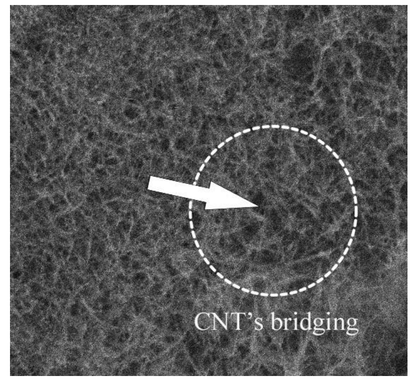

Fig.10. SEM image of specimen containing CNT's at 5µm.

5. Conclusion

In this study the cement was replaced with varying dosages of fly ash (5%, 10%, 15%, 20% and 25%) and CNTS (0.125%, 0.25%, 0.137% and 0.25%). Similarly, 10% fly ash was mixed with different dosages of CNTS (0.125%, 0.25%, 0.137%, and 0.25%). Following conclusions are made from this study.

- The use of 10% fly ash as an optimum dosage has increased 7, 28, and 90 days compressive strength by 9.7%, 21.9%, and 35.7% respectively. On contrary, an increase in fly ash dosage by 25% led to a decrease in strength by 50.8%, 56.9%, and 55.1% on the same days due to incomplete hydration reaction.
- The addition of CNTS showed improvement of compressive strength in general but higher dosage reduced strength slowly. The addition of 0.125% CNTS significantly increased in strength by 21.6%,27.6%, and 29.4% due to bridging action when the mix was tested and compared at 7,28, and 90 days separately.
- The early strength of mortar both at 7 and 28 days considerably increased due to the incorporation of fly ash as compared to fly ash which contributed to late strength (at 90 days) due to the formation of ettringite and hydration products.
- The study showed that the addition of 10% fly ash with 0.25% CNTS in mortars raised its strength to 8.2%, 32.4%, and 21.4% due to the bridging and filling effect of CNTS and fly ash at 7,28 and 90 days respectively.
- The development signifies that even small replacements with CNTS and fly ash significantly improves mortar compressive strength which suggests their use to reinforce mortar to protect structures in extreme loadings and environmental conditions.

6. Further Work

The addition of carbon nanotubes and fly ash imparted a positive effect on strength but other parameters such as workability and the impact resistance of various mixes are still needed to be studied further.

References

[1] D. Vollath and D. V. Szabó, "Synthesis and Properties of Nanocomposites," *Advanced Engineering Materials*. 2004, doi: 10.1002/adem.200300568.

[2] G. Y. Li, P. M. Wang, and X. Zhao, "Mechanical behavior and microstructure of cement composites incorporating surface-treated multi-walled carbon nanotubes," *Carbon N. Y.*, 2005, doi: 10.1016/j.carbon.2004.12.017.

[3] S. Parveen, S. Rana, and R. Fangueiro, "A review on nanomaterial dispersion, microstructure, and mechanical properties of carbon nanotube and nanofiber reinforced cementitious composites," *Journal of Nanomaterials*. 2013, doi: 10.1155/2013/710175.

[4] A. Chaipanich, T. Nochaiya, W. Wongkeo, and P. Torkittikul, "Compressive strength and microstructure of carbon nanotubes-fly ash cement composites," *Mater. Sci. Eng. A*, 2010, doi: 10.1016/j.msea.2009.09.039.

[5] A. Anvari, "The Influence of CNT Structural Parameters on the Properties of CNT and CNT-Reinforced Epoxy," *Int. J. Aerosp. Eng.*, 2020, doi: 10.1155/2020/4873426.

[6] C. Redondo-Gómez, R. Leandro-Mora, D. Blanch-Bermúdez, C. Espinoza-Araya, D. Hidalgo-Barrantes, and J. Vega-Baudrit, "Recent Advances in Carbon Nanotubes for Nervous Tissue Regeneration," *Adv. Polym. Technol.*, 2020, doi: 10.1155/2020/6861205.

[7] Ö. Güler, Ö. Başgöz, S. H. Güler, C. A. Canbay, Ş. Açıkgöz, and M. Boyrazlı, "The synergistic effect of GNPs + CNTs on properties of polyester: comparison with polyester–CNTs nanocomposite," *J. Mater. Sci. Mater. Electron.*, 2021, doi: 10.1007/s10854-021-06275-w.

[8] A. Nieto, A. Agarwal, D. Lahiri, A. Bisht, and S. R. Bakshi, "Mechanics of CNT-MMCs," in *Carbon Nanotubes*, 2021.

[9] R. Hamzaoui, S. Guessasma, B. Mecheri, A. M. Eshtiaghi, and A. Bennabi, "Microstructure and mechanical performance of modified mortar using hemp fibres and carbon nanotubes," *Mater. Des.*, 2014, doi: 10.1016/j.matdes.2013.10.084.

[10] V. C. Khed, B. S. Mohammed, and M. F. Nuruddin, "Effects of Nano-Silica modified Self-Compacted, High Volume Fly Ash Mortar on Slump Flow and Compressive Strength," *Madridge J. Nanotechnol. Nanosci.*, 2016, doi: 10.18689/mjnn-1000104.

[11] L. Jiang and Y. Guan, "Pore structure and its effect on strength of high-volume fly ash paste," *Cem. Concr. Res.*, 1999, doi: 10.1016/S0008-8846(99)00034-4.

[12] F. U. A. Shaikh and S. W. M. Supit, "Mechanical and durability properties of high volume fly ash (HVFA) concrete containing calcium carbonate (CaCO3) nanoparticles," *Constr. Build. Mater.*, 2014, doi: 10.1016/j.conbuildmat.2014.07.099.

[13] "Standard Specification for Portland Cement C150/C150M," 2019.

[14] ASTM, "Standard Specification for Standard Sand C778 − 17."

[15] A. A. K. F. K. I. K. Z. Nasser, "Effect the Local Fly Ash on Cement Mortar Properties," *J. Univ. Babylon, Eng. Sci.*, vol. 26, no. 5, pp. 11–12, 2018.

[16] S. W. M. Supit, F. U. A. Shaikh, and P. K. Sarker, "Effect of ultrafine fly ash on mechanical properties of high volume fly ash mortar," *Constr. Build. Mater.*, 2014, doi: 10.1016/j.conbuildmat.2013.11.002.

[17] M. S. Amin, S. M. A. El-Gamal, and F. S. Hashem, "Fire resistance and mechanical properties of carbon nanotubes - Clay bricks wastes (Homra) composites cement," *Constr. Build. Mater.*, 2015, doi: 10.1016/j.conbuildmat.2015.08.074.

[18] S. Musso, J. M. Tulliani, G. Ferro, and A. Tagliaferro, "Influence of carbon nanotubes structure on the mechanical behavior of cement composites," *Compos. Sci. Technol.*, 2009, doi: 10.1016/j.compscitech.2009.05.002.

[19] R. Siddique and A. Mehta, "Effect of carbon nanotubes on properties of cement mortars," *Construction and Building Materials*. 2014, doi: 10.1016/j.conbuildmat.2013.09.019.

3rd Conference on Sustainability in Civil Engineering (CSCE'21)
Department of Civil Engineering
Capital University of Science and Technology, Islamabad Pakistan

TO STUDY THE BEHAVIOR OF FIBER REINFORCED CONCRETE AGAINST FIRE BY USING SIKAFIBER®12

[a] Muhammad Abu Bakar*, [b] Dr. Muhammad Yaqub

a: Department of Civil Engineering, University of Engineering and Technology Taxila,abubakkar7810@gmail.com
b: Department of Civil Engineering, University of Engineering and Technology Taxila,muhammad.yaqub@uettaxila.edu.pk
* Corresponding author: Email ID: abubakkar7810@gmail.com

Abstract- Concrete has not very much resistance against fire because of its brittle behavior therefore to check improvement in crack resistance and compression strength against fire, SikaFiber®12 with dosage (0, 0.4,0.8,1.5,2.5,3 % by weight of cement) was used as polypropylene fiber with addition of superplastisizer ("Sika Viscocrete 3110" used 0.70% by weight of water for workability) and w/c of 0.45 to cast 60 M25 Grade standard size cylinders (150 x 300 mm) of fiber reinforced concrete tested against fire under compression according to ASTM C39 (cured in water for 28 days) for duration of 0.5,1,1.5&2 hours in gas furnace using infrared thermometer to maintain a temperature of 200,400,600&700°C respectively to find optimum dosage of SikaFiber®12. Six series of concrete mixes (each with 10 cylinders) including five series of SikaFiber®12 and one series of plain concrete cylinders were tested at an age of 28 days after exposure to fire and cooled down. Reinforcement of SikaFiber®12 increased compressive strength of FRC cylinders after exposed to fire for 2 hours at 1.5% dosage and minimized splitting and crack width, delaying the appearance of concrete fragmenting. The addition of polypropylene beyond optimum value decreased the workability of concrete which results in rapid compression strength loss. At 1.5% dosage using SikaFiber®12 increase of 25.39% compressive strength was obtained and strength remained same at 0.4% dosage.

Keywords- Compression strength, cylinders, fire, SikaFiber®12.

1 Introduction

Safety against fire is an important part of the look of concrete structures, which avoid harm in fireplace [***1***]. To control cracks in concrete Polypropylene fiber are added. The addition of fibers within the matrix has several vital effects. One in all the first reasons for the intensive use of Polypropylene fiber in concrete is improving fatigue [***2***]. The behavior of concrete at elevated temperature is stricken by many factors like, most temperature and exposure time and cooling methodology [***3***].

Polypropylene fibers don't absorb water so mixed long enough to insure dispersion. To decrease shrinkage and cracks in concrete, length of the fiber should be double than the diameter of the coarse aggregate [***4***]. Addition of PPF in concrete prevents micro cracks making concrete ductile thus gradual failure will occur [***5***]. Many thousands of little Fibers are distributed in every direction and improve properties throughout the concrete cylinders [***6***]. SikaFiber®12 specimen showed nested behavior in reinforced concrete resulting in good ductility by decreasing number of cracks and crack length, enhancement of compression strength and resistance to fire.

2 Experimental Materials

2.1 Cement

The cement used was Fauji Ordinary Portland cement of Grade 53 satisfying ASTM C150-04 standards with 28 days strength of 10000 Psi and having specific gravity of 3.11. Initial and final setting times of the cement were 68 minutes and 210 minutes, respectively.

a) 

b) 

Figure 1: Concrete cylinders casting, a. SikaFiber®12 transparent & Sika Viscocrete 3110, and b. Casted concrete cylinders

2.2 Fine Aggregates

Good quality Lawrence Pur sand was used as fine aggregate. Specific gravity of 2.68 and its grading fell within ASTM.

2.3 Coarse Aggregates

The coarse aggregate used in this experimental work are of 3/4" size crushed angular in shape with specific gravity of 2.70.

2.4 SikaFiber®12

Addition of Polypropylene fibers to concrete increases life span of the structure by controlling micro cracks due to shrinkage when concrete is cured. SikaFiber®12 is chemical base 100 % polypropylene transparent of 12mm length & 32 µm diameter having 0.91 g/cm^3 density, 160 °C Melting Point and belongs to Class 1a: Mono filamented EN 14889-2 is shown in Figure 1a. SikaFiber®12 improves durability, impact resistance and reduces shrinkage, cracking and splintering of concrete at high temperatures.

Table 1-Design mix quantities for M25(1:1:2) concrete with SikaFiber®12

Cylinders	Percentage Dosage	SikaFiber®12(Grams)	Cement(Kg)	Sand(Kg)	Aggregate(Kg)
10	**0.4**	122	30.58	32	74
10	**0.8**	244	30.58	32	74
10	**1.5**	458	30.58	32	74
10	**2.5**	764	30.58	32	74
10	**3.0**	917	30.58	32	74

2.5 Superplasticizer

To maintain good workability of concrete Superplastisizer used is "Sika Viscocrete 3110" with dosage of 0.7% by weight of water is shown in Figure 1a.

3 Research Methodology

For preparation of M25 (1:1:2) concrete all concrete materials weighed on a weighing balance. The total cement content for six batches was 183.39 kg, fine aggregate taken 192 kg and coarse aggregate taken 444 kg. The water to cement ratio was kept constant as 0.45, Super plasticizer (Sika Viscocrete 3110) content was 0.7% by weight of water to maintain a slump of (60-95 mm) for all concrete mixes. Cement was replaced in percentages of 0%, 0.4%, 0.8%, 1.5%, 2.5%, 3% with SikaFiber®12.Cement, sand, coarse aggregates and SikaFiber®12 were first dry mixed then added with 11.2 liter of water containing 254 ml of dissolved liquid superplastisizer for each batch. After the materials were mixed, the slump test was performed on fresh concrete to find out the workability of the mixture as per ASTM C143. Right away after the completion of slump test, the fresh concrete was added into the oiled molds to form 60 standard 150 x 300 mm cylinders as per ASTM C 192. Casted concrete cylinders were demolded after 24 hours as shown in Figure 1b. Metal Cylinder molds were used for casting. Compression test was conducted at age of 28 days, cylinders were placed out of curing tank and placed in brick furnace using gas tank to burn concrete cylinders for maximum of 2 hours then cooled down to normal temperature by natural air. Two Sample cylinders from all dosages were tested for compression at different temperatures and from each batch two sample cylinder were tested without exposure to fire then the result obtained was compared, Optimum percentage dosage of fiber addition in concrete was determined.

3.1 Compression Strength Test

Compression strength test performed at 28 days concrete cylinders after burning in fire is shown in Figure 2b. Compressive test was performed by using the digital display pressure testing system which has a maximum load capacity of 2500 KN is shown in Figure 3a. The loading rate was 8 KN/Sec, and cylinders were loaded until failure. 60 Concrete cylinders of 150mm diameter and 300mm height, both heated and non-heated at the age of 28 days were tested in UTM according to ASTM C39 to obtain the compression strength. These tests were carried out 1 day after heating.

3.2 Heating

After the completion of 28 days curing, cylinders were dried in natural air for 24 hours before heating. A gas fire furnace with top cotton fiber blanket and refractory bricks wall was used for heating the concrete cylinders is shown in Figure 2a.Total seventeen kg of gas was used to burn cylinders in brick furnace for 2 hours. Four target temperatures of 200, 400, 600 and 700 °C were selected for heating period of 2 hours and then cylinders were left to cool down naturally. During heating process the temperature of burning cylinders was checked using an infrared thermometer.

a) b)

Figure 2: Heating process, a. Brick furnace, and b. Cylinders under fire showing temperature

4 Results

Test results showed that SikaFiber®12 are of great use in long lasting structures as they have increased both strength of concrete and reduced cracking length and showed more ductile behavior than plain concrete in compression. By adding polypropylene fibers to the concrete, risk of explosive fracturing in fire is also reduced considerably.

a) 

b) 

Figure 3: Lab testing, a. Cylinders under process in compression testing machine after fire, and b. Compression test results

4.1 Compression Strength Results

Compression strength result showed that as we increase SikaFiber®12 dosage compressive strength of FRC first increases and then decreases. Graphical comparison shows that strength of concrete cylinders with 2.5% and 3% fibers against fire is very lower than those of ordinary concrete as shown in Figure 5a. Maximum compression strength of concrete after fire with 1.5% dosage was obtained 38.427 Mpa which is 18.506% increase of 32.462 Mpa that is for same dosage without fire having difference 0f 6.001 Mpa.

Table 2-Compression strength results of concrete cylinders after failure

Dosages	**Control**		**0.4**		**0.8**	
Sample Strength	**Sample 1 Mpa**	**Sample 2 Mpa**	**Sample 1 Mpa**	**Sample 2 Mpa**	**Sample 1 Mpa**	**Sample 2 Mpa**
No Fire	25.408	26.484	26.823	27.106	26.88	28.351
0.5 Hr Fire 200°C	22.239	23.088	26.88	26.993	20.089	20.202
1 Hr Fire 400°C	23.711	22.353	23.541	23.145	22.635	21.221
1.5 Hr Fire 600°C	17.599	17.146	22.805	23.088	28.351	28.86
2 Hr Fire 700 °C	16.524	16.354	19.919	20.428	29.03	28.917

4.2 Visual Observation

In addition to partial splintering of concrete, plain concrete also bear harsh cracking after heating. Fiber reinforced cylinders showed less cracking and cracks were shallower and shorter than that of plain concrete. Increase of PPF dosage from 0.8 to 1.5 % showed extreme decrease in cracking as shown in Figure 4a. After undergoing compression test, SikaFiber®12 augmentation still holds together concrete components after failure like a fibers mesh showing ductile behavior. Thousands of SikaFiber®12 transparent fibers can be seen on casted concrete cylinders surface which is shown in Figure 4b. These fibers prevent concrete fragmenting during fire.

a)

b)

Figure 4: Concrete lab tested cylinders, a. Cylinders after failure, and b. View of SikaFiber®12 fibers reinforced in cylinder

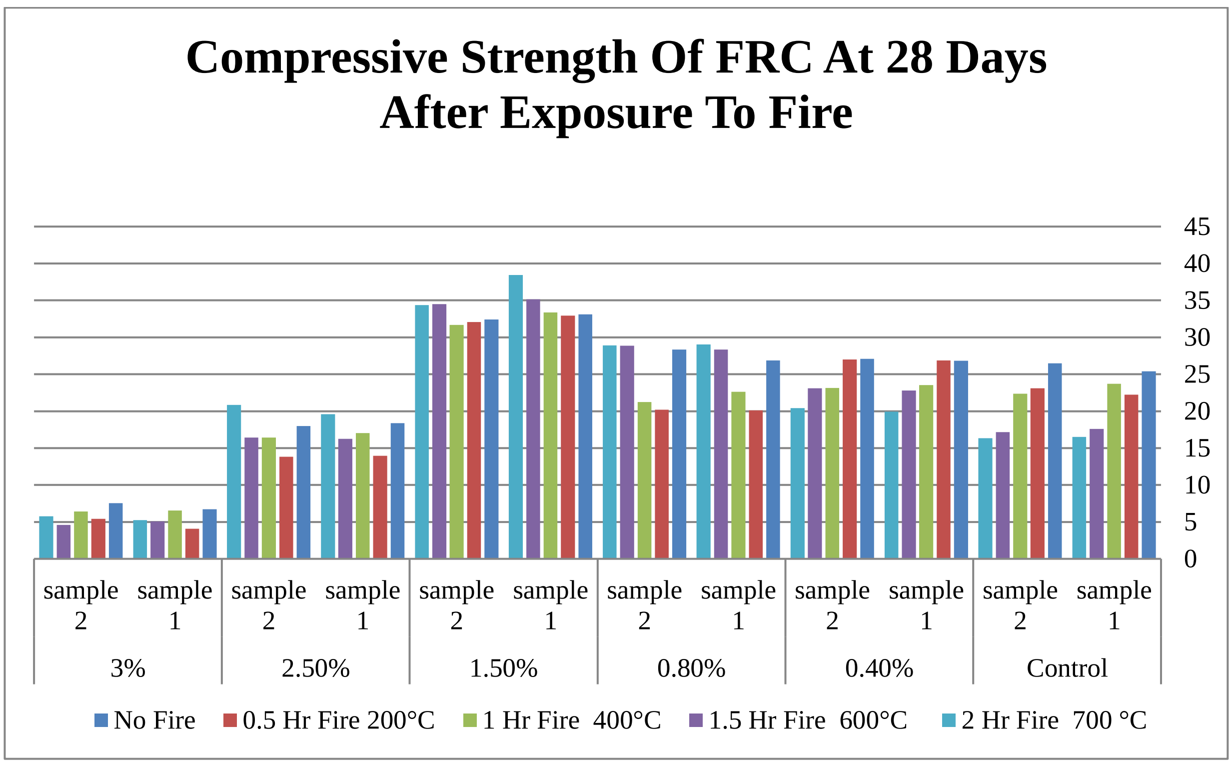

a)

Figure 5: Graphical comparison of results, a. Compression results with and without fire

Table 3-Compression strength results of concrete cylinders after failure

Dosages	**1.5**		**2.5**		**3.0**	
Sample Strength	**Sample1 Mpa**	**Sample 2 Mpa**	**Sample 1 Mpa**	**Sample 2 Mpa**	**Sample 1 Mpa**	**Sample 2 Mpa**
No Fire	33.105	32.426	18.391	17.995	6.734	7.526
0.5 Hr Fire 200°C	32.933	32.087	13.977	13.807	4.074	5.432
1 Hr Fire 400°C	33.352	31.691	17.033	16.411	6.564	6.394
1.5 Hr Fire 600°C	35.163	34.502	16.241	16.411	5.093	4.583
2 Hr Fire 700 °C	38.427	34.37	19.58	20.825	5.262	5.772

Computer linked to compression testing machine gave the digital results of FRC cylinders after failure is shown in Figure 3b. This Compression test results also showed that SikaFiber®12 also enhances compression strength when tested without fire while increasing fibers dosage till 1.5%.

5 Implementation of SikaFiber®12 Results in Construction Industry

These test results of SikaFiber®12 are useful in implementation of this research in real field for engineers and designers to design structure safer and durable against fire hazards, saving more people lives and increasing structure lifespan. When Concrete is exposed to fire the vapor pressure in concrete is generated which is dangerous to structure causing concrete splintering. The reason behind implementation in field work is that these fibers have low melting point of 160°C and doesn't absorb H_2O, which means they will gradually melt and create a capillary system through which the evaporating water can escape, without any damage to concrete.

6 Conclusion

Following are the interpretations of work done on SikaFiber®12 FRC against fire.

- When SikaFiber®12 reinforced concrete cylinders were exposed to elevated temperature up to 700°C, strength of the fiber reinforced concrete cylinders increased with increasing fiber dosage and exceeded that of ordinary concrete till optimum dosage that is 1.5%.
- SikaFiber®12 reinforced concrete shows the highest compression strength and increase in bond strength at 1.5% than those of cylinders having more or less and no fiber content after heating to 700°C.
- The addition of SikaFiber®12 has increased the 28 days compressive strength of FRC by 25.39% than concrete without fibers.
- Compressive strength decreased with the increase of SikaFiber®12 content beyond 1.5% because the mix become fibrous which results in difficulty in handling and therefore compression strength of 2.5 and 3 % dosage is very poor near about 90-105 KN.
- Compressive strength of concrete cylinders without fibers at 28 days before fire was 26.484 Mpa which decreased rapidly to 16.524 Mpa as fire temperature was increased for duration of two hours.
- Concrete containing SikaFiber®12 with 0.4% dosage tried to resist compression strength against fire but could gain only 20.4 Mpa after exposure to 700 °C heating.
- Increase of 18.5% compression strength after fire exposure is obtained which is 32.462 Mpa.
- Dosage of 0.8% maintained compressive strength of 28.86 Mpa after fire exposure for 1 to 2 hours having strength of 28.35 Mpa without fire.

Further research work should be done on polypropylene fibers so that results obtained should be utilized in construction industry to improve construction methods and robustness of concrete against fire risk.

Acknowledgment

The author would like to thank Prof. Dr. Muhammad Yaqub (Director ASR&TD, UET Taxila) who helped thorough out the research work. The careful review and constructive suggestions by the anonymous reviewers are gratefully acknowledged.

References

[1] A. Kohoutková J. Novák, "Fire response of hybrid fiber reinforced concrete high temperature," *Proc. Eng*, vol. 172 , pp. 784–790, 2017.

[2] M.B. Waris, A.H. Al-Saidy K.S. Al-Jabri, "Effect of aggregate and water to cementratio on concrete properties at elevated temperature," *Fire Mater*, vol. 40, pp. 913–925, July 2016.

[3] D.N. Crook, "Regain of strength after firing of concrete," *Mag. Concr*, vol. 72, no. 22, pp. 149–154, (1970).

[4] Shakir A and Maha , "Effect of polypropylene fibers on properties of mortar containing crushed brick as aggregate," *Eng. And Tech*, vol. 26, pp. 1508-1513, 2008.

[5] G.P. Lee J. Kim, "Evaluation of Mechanical Properties of fibre-reinforced Concrete Exposed to High Temperatures ," *Construction and Building Materials* , vol. 79, pp. 182-191, 2015.

[6] B. Chen, "Residual strength of fiber-reinforced high-strength concrete after exposure to high temperatures," *Cement and Concrete Research* , vol. 34, pp. 1065 – 1069, 2004.

3rd Conference on Sustainability in Civil Engineering (CSCE'21)
Department of Civil Engineering
Capital University of Science and Technology, Islamabad Pakistan

PERFORMANCE EVALUATION OF AMBIENT CURED QUARRY ROCK DUST (QRD) INCORPORATED GEOPOLYMER CONCRETE (GPC) BEAMS

[a] Abdul Ghafar*, [b] Faheem Butt,

a: Department of Civil Engineering, University of Engineering and Technology Taxila,
withabdulghafar32@yahoo.com
b: Department of Civil Engineering, University of Engineering and Technology, Taxila,
faheem.butt@uettaxila.edu.pk
* Corresponding author: Email ID: withabdulghafar32@yahoo.com.com

Abstract- Geopolymer concrete (GPC) an alternative of Ordinary Portland Cement concrete (OPC) is prepared by mixing three waste/by-products that are Fly-ash (FA), ground granulated blast furnace slag (GBS) and quarry rock dust (QRD) at the rate of 50%, 35% and 15% of binder respectively. Since GPC has gained interest of many researchers due to the harm that OPC is causing to the environment. However, GPC exhibit somewhat brittle behavior. To improve this property of GPC the steel fibers (SF) and natural fibers called sisal fibers (SsF) are incorporated into the GPC both separately and in hybrid form. The purpose of this research work is to prepare natural fiber (i.e SsF) reinforced GPC which can be a potential sustainable construction material having good mechanical properties and lesser environmental impact. The SsF is used individually and also in hybrid form with SF for purpose of replacing the SF with natural counterpart. The control sample with no fibers and fibers reinforced matrices with increasing content of SsF (varying from 0.8 to 2.4 %) and novel hybrid SsF and SF (by keeping SF fixed at 0.5% and increasing the amount of SsF from 0.5 to 1.5%) were casted and mechanical tests were performed for optimum values. Then the four types of shear deficient GPC beams were casted that are unreinforced control GPC and GPC reinforced with optimum values already calculated which are SF at 0.75%, SsF at 2.4% and hybrid fiber reinforcement at 0.5% and 1% of SF and SsF respectively. To ensure shear is dominant mode of failure moderate shear reinforcement along with required flexural reinforcement were provided. The load carrying capacity through four point loading was then checked for GPC and fiber reinforced GPC beams. The load carrying capacity of simple GPC versus 2.4% SsF reinforced GPC, hybrid fibers reinforced GPC (having 0.5% SF and 1% SsF) and 0.75% SF reinforced GPC beams was found to have increased by 22.22%, 38.89% and 75% respectively.

Keywords- geopolymer, steel fibers, sisal fibers, ambient curing

1 Introduction

In the present world cement concrete is most widely used man made material. Large amount of natural resources are consumed during the production process of this binding material i.e ordinary Portland cement (OPC). Also during the production of OPC the CO_2 produced is key contributor in causing environmental pollution [1]. The CO_2 is produced during the chemistry of OPC production (calcination of limestone) but not during the use of OPC. Consequently, the need of some environmental friendly material that can replace the cement has gained attention of many researchers. Fly-ash (FA) and ground-granulated blast furnace slag (GBS) are the industrial waste/by products which are supplementary binding materials widely used for partial replacement of OPC. Their use has gained attention because of their low cost and good binding or pozzolanic properties. The widely available low calcium FA is considered to be a suitable material because of its pertinent silica, alumina composition and very low water requirement. Also the geopolymer concrete

(GPC) incorporated with heat cured low calcium FA when tested in fresh and hard state has shown excellent mechanical properties and durability [2]. The quarry rock dust (QRD) is a residue and calcium rich material which can also be used as partial replacement of binder or filler material in GPC [3]. This can help in reducing the environmental and land pollution by avoiding its deposition at landfills [4].

Researcher have found that these waste or by-products (FA, GBS and QRD) have great potential to be used as innovative replacement of OPC [5]. Therefore, the GPC can be a sustainable and green solution for construction industry because of its excellent properties. However, GPC has shown comparatively brittle behavior than OPC concrete [6]. But with the addition of fibers, GPC has improved behavior not only in splitting tensile strength, flexural strength and flexural toughness but also in the post-peak behavior i.e the stress-strain response in comparison from brittle to ductile [7]. Therefore, these fibers had gain attention of researchers for making GPC less brittle material. There are many options of fibers for researchers such as steel fibers (SF), synthetic fibers and natural fibers [29]. Tung T. Tran [18] found in its research that ultimate load carrying capacity of fiber reinforced GPC beams increased with increase of SF content with showing optimum value at 0.75%, he also concluded that fibers length of 60 mm has approximately 10% lesser load carrying capacity than fibers having length of 35 mm. The SF are widely used fibers since they show excellent properties both in OPC and GPC under fracture toughness, splitting tensile and flexural strengths [19]. However, according to Food and Agriculture Organization of the United Nations (FAO), natural fibers are considered to be the future fibers because no harm is done to the environment while using these fibers [13,30]. It has been found that 11 tons of oxygen is produced, and 15 tons of CO_2 is consumed during one hector cultivation of jute fibers plant. Also the SsF plant absorb more CO_2 than the oxygen they produce, and the organic wastes which are produced during preparation of SsF can be used in the feeding the animals, bioenergy generations and fertilizer production. [8].

It is therefore a wise solution to add natural fibers as a reinforcing material to the composites based on GPC matrix. The growing environmental awareness and the need to ensure sustainability of construction materials have led many researchers to look for some alternative fibers to reinforce GPC [20]. In this respect natural fibers (like SsF) are attractive because they are reproducible, have low density, high specific strength and are cheap to obtain. They do not pose any problems in terms of closing important life cycles (especially CO_2) of the products based on natural fibers [8]. The replacement of SF with SsF is not only important because of its low cost but also due to environmental concern, because the production of SF is energy consuming process while the production of SsF is natural process which involve emission of oxygen along with the consumption of CO_2. Therefore, in this study, composites with GPC matrices reinforced with SF and natural fibers i.e. SsF are studied and compared. The use of SsF with GPC is very limited especially its hybridization with SF is a novel work, the intention of this combination is to replace the SF with natural fibers to promote the use of more environment friendly construction materials. The hybridization method used in the initial trials to find out optimum values consist of fixing the SF at 0.5% and increasing the SsF content like 0.8%, 1.2% and 2.4% [27, 28]. The performance of these new composites is investigated by a series of laboratory experiments which are explained in the following sections.

2 Experimental Program

The experimental program comprises two stages (this manuscript is a part of parallel research work). In the first stage, a mix design study was carried out for finding the optimum ratio of SsF and hybrid with SF for mixing in the GPC composites. The optimum value of SF was taken as 0.75% by weight of concrete from the previous study [9]. For strength tests cubes, cylinders and prisms were casted for finding out mechanical properties (three specimens for each test and mix type, mix types are shown in table 1).

In the second stage, based upon the results from the first stage, the optimum values of fibers were identified and beams of size 150mm (W), 150mm (H) and 1000mm (L) were cast for evaluating the flexural performance of beams. The types and optimum mix proportions for casting of beams are shown in table 2. To ensure that the shear is the dominant mode of failure in the beams, moderate shear reinforcement was provided along-with the required flexural reinforcement in the tension and compression zone [22]. In order to make shear deficient beams, 2 nos 12mm bars are used as main bars and 2 nos 9mm bars are used as anchor bars with shear reinforcement of 6mm diameter bars @ 150 mm c/c. For each mix type (table 2) three beams along with three cubes and cylinders were cast.

Table 1: The Mix types for initial trials

SsF-R-GPC		**Hybrid SF and SsF R-GPC**	
Mix ID	**Mix Composition**	**Mix ID**	**Mix Composition**
GPC	GPC without Fibers	0.5SF+0.5SsF-R-GPC	GPC with 0.5% SF and 0.5% SsF
0.8SsF-R-GPC	GPC with 0.8% SsF only	0.5SF+1SsF-R-GPC	GPC with 0.5% SF and 1% SsF
1.2SsF-R-GPC	GPC with 1.2% SsF only	0.5SF+1.5SsF-R-GPC	GPC with 0.5% SF and 1.5% SsF
2.4SsF-R-GPC	GPC with 2.4% SsF only		

Note: SsF=sisal fibers, R-GPC= reinforced with fibers geopolymer concrete, SF=steel fibers

Table 2: The types and mix proportions for casting the fiber-reinforced GPC beams

Mix ID	**AL/B Ratio**	**W/B Ratio**	**SS/SH Ratio**	**B**	**Binder**			**CA 20mm**	**CA 10 mm**	**S**	**Alkaline Solution**		**SP**	**SF**	**SsF**	**W**
					FA	**GBS**	**QRD**				**SH**	**SS**				
GPC (control mix)	0.5	0.45	1.5	400	31.3	21.9	9.4	53.3	117.6	106.5	12.5	18.8	3.8	-	-	9.1
0.75SF-R-GPC	0.5	0.45	1.5	400	31.3	21.9	9.4	53.3	117.6	106.5	12.5	18.8	4.6	9.2	-	9.1
0.5SF+1SsF-R-GPC	0.5	0.45	1.5	400	31.3	21.9	9.4	53.3	117.6	106.5	12.5	18.8	5.7	6.1	2.3	9.1
2.4SsF-R-GPC	0.5	0.45	1.5	400	31.3	21.9	9.4	53.3	117.6	106.5	12.5	18.8	7.8	-	5.5	9.1

Note: AL=Alkaline solution, B =binder, W/B= water/binder ratio, SH= Sodium hydroxide, SS=Sodium silicate, FA= Fly-ash, GBS=Ground granulated blast furnace slag, QRD=Quarry rock dust , CA=Coarse aggregates, S= Sand, SP= Super plasticizer, SF= Steel fibers, SsF= Sisal fibers, W=Water

2.1 Materials and mixing of ingredients

The Low Calcium FA is used for manufacturing of GPC since high calcium FA has poor performance in polymerization process. The QRD was collected from Margalla, Taxila, and was grinded to cement size at Pakistan Council of Scientific and Industrial Research (PCSI) Peshawar, by ball Mill Machine. The Molarity of sodium hydroxide (SH) used for GPC is 12M in pallets forms and was mixed in water 24 hours prior to be used for concrete preparation. The sodium silicate (SS) was purchased from commercial manufacturer from Islamabad in the liquid form and was mixed with SH 30 minutes prior to mix them with the other ingredients. The sand (S) and coarse aggregates (CA) were taken from Margallah quarries and Lawrencepur respectively. The fineness modulus of fine aggregate was conforming to ASTM-C-136-06 [10], whereas specific gravity and water absorption was conforming to ASTM-C128-15 [11]. The specific gravity of coarse aggregate was conforming to ASTM-C127-07 [12]. The sisal (Agave Sisalana) fibers (SsF) were purchased from Ayub Research Centre (ARC) Faisalabad which have water absorption capacity of 120% [8]. The SsF is mainly composed of cellulose, hemicellulose and lignin and have a density around 1.45g/cm^3 [8]. The SsF were cut into size of 10 mm length with an average diameter of 137µm resulting in an aspect ratio of 73. The 10 mm length of SsF were used because it is considered to have shown better results than 20 mm or 30 mm due to workability problems [8]. The SF used were both end hooked with length 35 mm, diameter 0.55 mm (aspect ratio 65 mm) and having tensile strength of 1350 MPa.

The SH pallets are mixed in water for 24 hours prior to be mixed with the concrete. The SS is added into solution of SH 30 minutes prior to add them into the other ingredients [21]. The CA, S, binder consisting of FA, GBS and QRD are mixed in dry condition for 2 minutes. The FA, GBS and QRD were mixed in the ratio of 50%, 35% and 15% of the binder. This ratio of binder was taken from an already published study of the second author [9]. The SF or/and SsF are then added and mixed for another 2 minutes in concrete mixer drum for homogenous dispersion of fibers. Then solution of SH, SS along with water is added into the mixer. The remaining water (amount of water already present in SH and SS is 47.08 kg/m^3 and 75 kg/m^3 respectively) is added to maintain 0.45 W/Binder ratio and slump was checked.

2.2 Testing of specimens

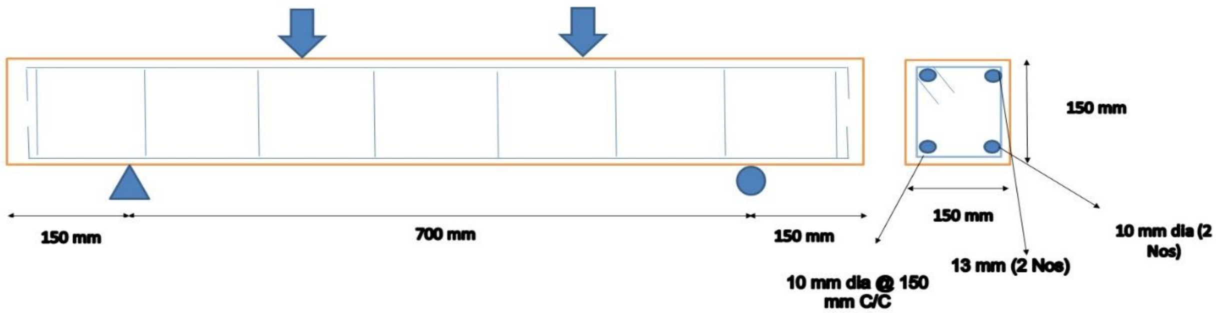

Figure 1: Reinforcement detail and four point loading of beam

Figure 2: Shear failure of the beams

The mixing procedure was carried out according to ASTM C-143M-15a [14]. A universal testing machine (UTM) was used for performing compressive, split cylinder and flexural strengths according to ASTM C39/39M-03 [15], C496/C496M-11 [16] and 1609/C1609M-19a [17] respectively. In the second stage of experimental program, the load bearing capacity of GPC beams was checked by four point loading test. The four point loading of beams with reinforcement detail are shown in figure 1 and beams after loading/failure are shown in figure 2. The loading arrangement consist of a load cell with hydraulic jack. The maximum load applying capacity of reaction frame was 2000 KN. The load was applied with the help of hydraulic jack whose capacity was 200 KN. The hydraulic jack was placed over steel plate and it was connected to load cell over the top of it.

3 Results and Discussion

3.1 *Workability.*

The workability of mixes was checked using slump cone test. An effort was made to maintain the slump value in between 70 and 90 mm by varying the quantity of superplasticizer (SP) for a workable mixture. The slump value was dependent on both the percentages and type of fibers. It was noted that along with increase of percentage of SsF there was decrease in the slump value in both type of fiber reinforcement with showing minimum slump value at 2.4% SsF. This decrease is due to large water absorption capacity of SsF. The slump values for GPC, 0.8SsF-R-GPC, 1.2SsF-R-GPC, 2.4SsF-R-GPC, 0.5SF+0.5SsF-R-GPC, 0.5SF+1SsF-R-GPC and 0.5SF+1.5SsF-R-GPC were calculated to be 84, 81, 78, 70, 78, 75 and 73 mm respectively.

3.2 *Mechanical Properties*

The mechanical properties of the mixes were evaluated using cube (150 mm), cylinder (dia 150mm, H 300 mm) and prisms (150x150x750mm) specimens for each mix type given in table 1. The uniaxial compression strength test was performed to determine cube strength after 28 days of casting and results are shown in figure 3. From the figure it is clear that the compressive strength of GPC (20.5 MPa) versus 2.4SsF-R-GPC (28.56 MPa) and 0.5SF+1SsF-R-GPC (29.5 MPa) has shown maximum increase of 39.31% in case of SsF incorporation and 43.90% in case of hybrid fibers respectively, similar trend was also observed by Guido silva [8]. The addition of 0.8% SsF has shown greater increase in compression strength than the addition of a mixture of 0.5% SsF and 0.5% SF, this may be due improper dispersion of fibers among the mix since less quantity of fibers are used in earlier case than in the later one.

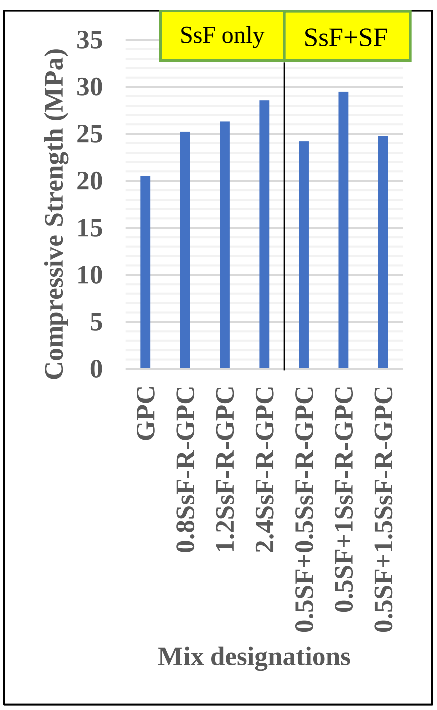

Figure 3: Compressive strength

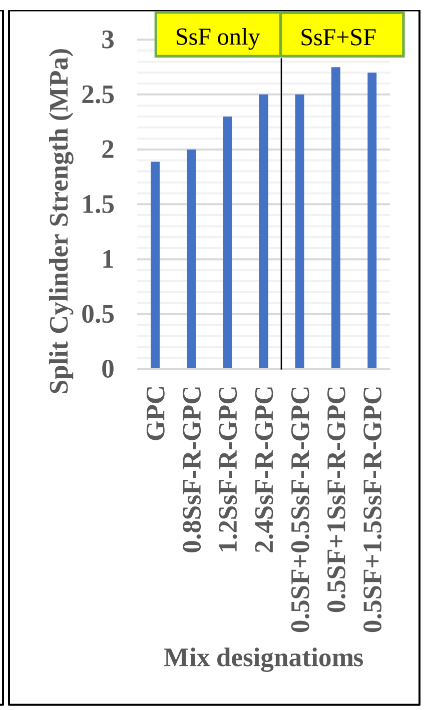

Figure 4: Split cylinder strength

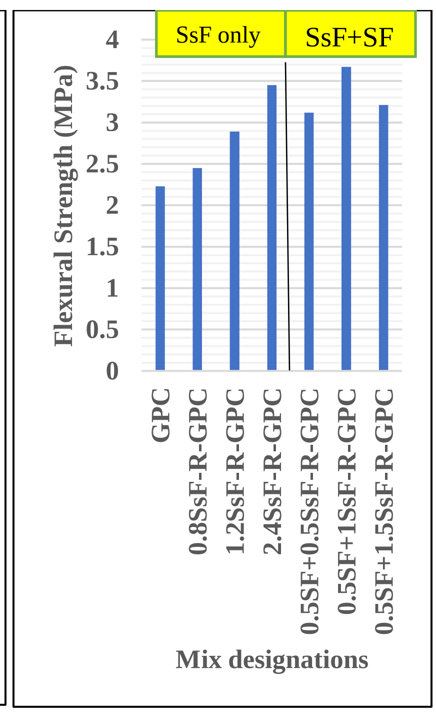

Figure 5: Flexural strength

Also with the increase of fibers content in 0.5SF+1.5SsF-R-GPC there is decrease in the compressive strength. This decrease in the strength is also due to low workability in case of higher fiber content which resulted in uneven distribution of fibers among the mix.

The results of split cylinder are reported in the figure 4. From the figure it is clear that tensile strength also follow similar trend that was observed for compressive strength with showing maximum value of 2.5 MPa for 2.4SsF-R-GPC which is 32.27% more than unreinforced GPC. Similarly maximum value of hybridized fiber reinforcement was observed for 0.5SF+1SsF-R-GPC of 2.75 MPa which is 45.5% more than control mix. Also the fiber reinforced GPC showed more ductile failure as compared to the control mix. The failure of fiber reinforced GPC was accompanied by the multi cracking due to fact that fibers allow load transference from the cracked area to the other parts of the specimen. These results are in same pattern with what observed by the other researchers [23].

The results of three point bending test are shown in the figure 5. Like above the flexural strengths also show similar trend with the increase of values along with increase of fiber content. The maximum value of 3.45 MPa was observed for 2.4SsF-R-GPC which is 54.70% more than the control mix. For hybridized fiber reinforced GPC the maximum value was noted for 0.5SF+1SsF-R-GPC of 3.67 MPa (64.57% more than GPC). It may be noted that for tensile and compression strength tests nearly same amount of increase in strengths is noted with addition of fibers however this increase is more dominant in case of flexural tests, this my be due to fact that the fibers pulling and stretching is not tested as in the flexural strength test also observed by Sun et al. [23] and Chen et al. [24]. The standard deviation of compressive, split cylinder and flexural strength results are calculated to be 2.970 MPa, 0.341 MPa and 0.525 MPa respectively.

3.3 Load carrying capacity of beams

The shear deficient beams for each mix types having optimum values in initial trials and 0.75% SF-R-GPC selected from earlier research [9] along with control GPC (all mix types are shown in Table 2) were casted and tested for maximum load under four point loading arrangement as shown in figure 1. The sample of beams after the tests are shown in figure 2. From the figure 2 it is clear that all the beams failed by the formation of diagonal cracks near the supports, no tensile splitting was noticed along the main reinforcement. Such failure was also observed by Shoaib et al. [25].

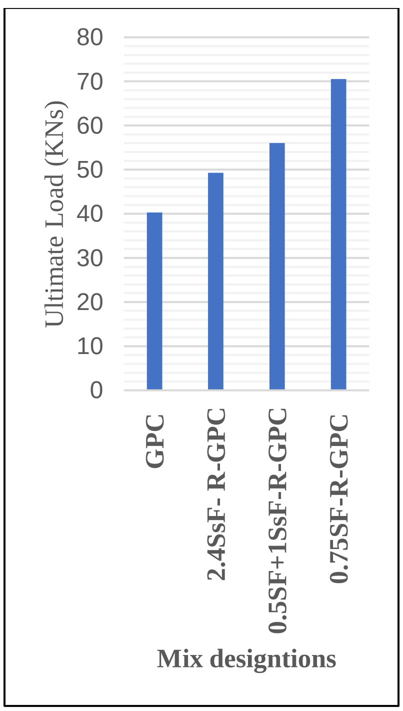

Figure 6: Ultimate load capacity of beams

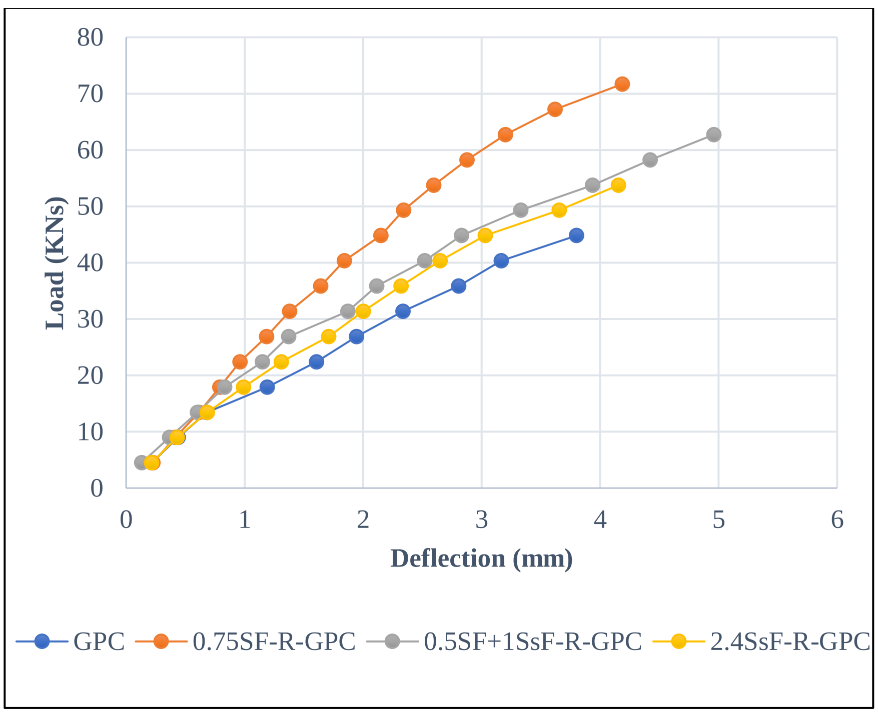

Figure 7: Load Deflection Curve

It was found that fibers addition enhanced the ultimate load carrying capacity of the beams with 2.4SsF-R-GPC showing 49.28 KNs (22.22% more than unreinforced GPC), 0.5SF+1SsF-R-GPC having 56 KNs (38.89% increase) and 0.75SF-R-GPC showing maximum value of 70.56 KNs (75% more than its counterpart GPC) value of ultimate load. Unlike the specimens without fibers (GPC) which failed at once, fibers reinforced GPC (both SsF and SF) having fibers stitching the cracks showed more ductile failure by resisting opening of crack with pulling out of fibers from concrete through the crack. The load carrying capacity of beams are shown in figure 6 (the values has standard deviation of 12.75 KNs).

3.4 Load deflection curve of beams

Figure 7 shows the load deflection curve of the beams having size of 150x150x1000 mm. According to ASTM C1018 the flexural toughness is the area under load deflection curve. From figure 7 it is quite obvious that fibers addition has enhanced the flexural toughness. The greater the flexural toughness more will the capacity of the beams to absorb the energy. During the pulling out of fibers in crack propagation has led to more energy/load absorption than normal GPC, which resulted in more ductile failure of fiber reinforced concrete as also observed by other author [26]. The SF-R-GPC has shown maximum toughness however the SsF both individually and in hybridized form has shown improved results than their counterpart unreinforced GPC. The stiffness is the ratio of load applied and deflection in the beam. The stiffness of beams is also observed to increase with incorporation of fibers especially with hybrid fibers having SF has shown maximum stiffness. However, from the figure it can also be observed that that SsF reinforced GPC also has more stiffness than its counterpart GPC.

4 Practical Implementation

The SsF with GPC in both form that is individually and in hybridized form at optimum rate can prove to be a environment friendly, economical and efficient construction material for important structure. Since incorporation of SsF into calcium rich FA, GBS and QRD based GPC at ambient curing has yielded excellent results. However its behavior in concrete for longer period of time is still needed to be found.

5 Conclusion

Following conclusions can be drawn from the conducted study:

- Natural fiber (SsF) reinforced GPC which can be a potential sustainable construction material is developed having good mechanical properties and lesser environmental impact. The SsF addition into QRD incorporated GPC at various fraction has yielded improved performance in mechanical properties and flexural strength with having maximum values at 2.4SsF-R-GPC.
- The novel hybrid natural fibers (SsF) and SF has also shown increased results (maximum values are observed for 0.5SF+1SsF-R-GPC). In case of hybrid fibers for higher fiber content the decrease in the strength is due to less workability that resulted in uneven dispersion of fibers among the mix.
- The fiber incorporation into GPC has resulted in increased ultimate load carrying capacities of beams with 0.75SF-R-GPC showing maximum values however the SsF both individually and in hybridized form has shown improved results than their counterpart unreinforced GPC.
- The fibers addition into GPC in both of the cases has promoted more prolonged failure than their counterpart GPC with the fact that fibers stitching and resisting the opening of cracks during the application of loads.

References

[1] J. Davidovits, Properties of geopolymer cements, in: *First International Conference on Alkaline Cements and Concretes*, 1994, pp. 131–149.
[2] Nath, P. and P. K. Sarker (2014). "Effect of GGBFS on setting, workability and early strength properties of fly ash geopolymer concrete cured in ambient condition." *Construction and Building Materials* 66: 163-171.
[3] Cohen, E., Peled, A., & Bar-Nes, G. (2019). Dolomite-based quarry-dust as a substitute for fly-ash geopolymers and cement pastes. *Journal of Cleaner Production*, 235, 910-919.
[4] Zhao, Y., Qiu, J., Xing, J., & Sun, X. (2020). Recycling of quarry dust for supplementary cementitious materials in low carbon cement. *Construction and Building Materials*, 237, 117608.

[5] Huseien GF, Sam AR, Mirza J, Tahir MM, . Waste ceramic powder incorporated alkali activated mortars exposed to elevated Temperatures: Performance evaluation. *Const and Build Mat*. 2018 Oct 30;187:307-17.
[6] Thomas RJ, Peethamparan S Engg properties and stress–strain behavior. *Constr Build Mater* 2015;93:49–56.
[7] Khan MZN, Hao Y, Hao H, Shaikh FUA. Mechanical properties of ambient cured high strength hybrid steel and synthetic fibers reinforced geopolymer composites.*Cem Concr Compos* 2018;85:133–52..
[8] Guido Silva, Suyeon Kim (2020). Optimization of a reinforced geopolymer composite using natural fibers and construction wastes. *Construction and Building Materials* 258 (2020) 119697
[9] Muhammad Ibraheem, Faheem Butt. Fresh and Mechanical Properties of Ambient Cured Ternary Blended Geopolymer Concrete Reinforced With Steel Fibers. *(CSCE'20), CUST Islamabad*.
[10] ASTM C136-06, "Standard Test Method for Sieve Analysis of Fine and Coarse Aggregates," ASTM Int., 2006.
[11] ASTM C128-15, "Standard Test Method for Density, Relative Density (Specific Gravity), and Absorption of Fine Aggregate," *ASTM Int.*, 2015.
[12] ASTM C127-07, "Standard Test Method for Density, Relative Density (Specific Gravity), and Absorption of Coarse Aggregate," *ASTM Int*., 2007
[13] Food and Agriculture Organization of the United Nations (FAO), Future Fibers, *http://www.fao.org/economic/futurefibers/home/en/, 2010*.
[14] ASTM C-143M-15a "Standard Test Method for Slump of Hydraulic Cemnet Concrete" *ASTM Int*., 2015
[15] ASTM C39/39M-03 " Standard Test Method for Compressive Strength of Cylinderical Concrete Specimen" *ASTM Int*., 2008
[16] ASTM C496/C496M-11 "Standard Test Method for Spliting Cylinder Strength of cylinderical Concrete Specimen" *ASTM Int* 2011
[17] ASTM 1609/C1609M-19a" Standard Test Method for Fiber reinforced concrete (Using beam with three point loading) *ASTM Int* 2005
[18] Tung T. Tran "Experimental and analytical investigation on flexural behaviour of ambient cured geopolymer concrete beams reinforced with steel fibers", *Engineering Structures* 200 (2019) 109707
[19] Ali Nazari, "Flexural strength of plain and fiber-reinforced boroaluminosilicate geopolymer", *Const and Build* Mat 76 (2015) 207–213
[20] K. Korniejenko*, E. Fraczek, E. Pytlak, M. Adamski," Mechanical properties of geopolymer composites reinforced with natural fibers", *Procedia Engineering* 151 (2016) 388 – 393
[21] Parveen, D. Singhal, M. T. Junaid, "Mechanical and microstructural properties of fly ash based geopolymer concrete incorporating alccofine at ambient curing," *Constr. Build. Mater*., vol. 180, pp. 298–307, 2018.
[22] Abdul Saboor Karzad, Moussa Leblouba," Repair and strengthening of shear-deficient reinforced concrete beams using Carbon Fiber Reinforced Polymer", *Composite Structures* 223 (2019) 110963
[23] P. Sun, H. Wu, Transition from brittle to ductile behavior of fly ash using PVA fibers, Cem. *Concr. Compos*. 30 (1) (2008) 29–36
[24] R. Chen, S. Ahmari, L. Zhang, Utilization of sweet sorghum fiber to reinforce fly ash-based geopolymer, *J. Mater. Sci.* 46 (6) (2014) 2548–2558
[25] A. Shoaib, A.S. Lubell, V.S. Bindiganavile, Shear response of lightweight steel fiber reinforced concrete members without stirrups, *Mater. Struct*. 48 (10) (2015) 3141–3157.
[26] Kim Hung Mo, Khai Hung Yeoh, Shear behaviour and mechanical properties of steel fiber-reinforced cement-based and geopolymer OPS lightweight aggregate concrete, *Const and Build Mat* 148 (2017) 369–375
[27] Li L, Cao M, Xie C, Yin H. Effects of CaCO3 whisker, hybrid fiber content and size on uniaxial compressive behavior of cementitious composites. *STRUCT CONCRETE*. 2019;20(1):506-518.
[28] Cao M, Li L. New models for predicting workability and toughness of hybrid fiber reinforced cement-based composites. *CONSTR BUILD MATER*. 2018;176:618-628.
[29] N. Ranjbar, M. Zhang, Fiber-reinforced geopolymer composites: A review, *Cem. Concr. Compos*. 107 (2020) 103498
[30] G. Silva, S. Kim, R. Aguilar, J. Nakamatsu, Natural fibers as reinforcement additives for geopolymers – a review of potential eco-friendly applications to the construction industry, *Sustain. Mater. Technol*. 23 (2020).

3rd Conference on Sustainability in Civil Engineering (CSCE'21)
Department of Civil Engineering
Capital University of Science and Technology, Islamabad Pakistan

STRENGTHENING OF AMBIENT CURED QUARRY ROCK DUST INCORPORATED GEOPOLYMER CONCRETE BEAMS

[a]*Muhammad Awais**, [b] *Faheem Butt,*

a: Department of Civil Engineering, University of Engineering and Technology Taxila,
engineerawais81@gmail.com
b: Department of Civil Engineering, University of Engineering and Technology, Taxila,
faheem.butt@uettaxila.edu.pk
* Corresponding author: Email ID: engineerawais81@gmail.com

Abstract- Geopolymers concrete (GPC) has gained attraction in construction field due to low-carbon, cement less composite materials possessing considerably high mechanical properties and being used in numerous structural applications. On the other hand strengthening the structural members using advanced materials is a contemporary research in the field of repairs and rehabilitation. Carbon fiber reinforced polymer (CFRP) composite is becoming prominent in strengthening and rehabilitation to improve the flexure and shear strength of the structural members due to ease of installation, lower cost and time saving, strength and confinement gain and long-term durability. Most of the research works depicts the properties of GPC at elevated temperature which is costly and limit the field application but in this research work the beams were casted using quarry rock dust (QRD) which helps to improve the properties at ambient temperature. Very limited literature is available to improve the shear capacity of fiber reinforced GPC beams using CFRP. The purpose of this paper is to strengthen the pre-damaged shear deficient ambient cured GPC beams incorporated different combination of steel fibers (SF) and Sisal fibers (SsF) in mix design, with externally bonded CFRP composites. This paper also discuss the effect of natural fibers (i.e SsF, which has less environmental effect, used individually and in hybrid form) on fresh and mechanical properties of GPC and compare the ultimate load bearing capacity of strengthened and unstrengthen GPC beams. For this purpose a total of twenty four beams spanning 1000x150x150 mm were cast and tested under four point loading. Twelve of the beams were tested to failure while the remaining twelve were partially damaged by applying 60% of the ultimate load. The damaged beams were strengthened by applying CFRP strip at soffit of beams and U-shaped CFRP sheet near supports. The results showed that by applying CFRP strips and sheets, the ultimate load carrying capacity has increased significantly up to 45% relative to load capacity of the unstrengthen beam. The results demonstrated that the application of CFRP is an effective way to repair and strengthen the shear deficient/damaged GPC beams.

Keywords- Geopolymer beams, strengthening, sisal fibers, steel fibers, CFRP strips and sheets.

1 Introduction

The geopolymer concrete has gained attraction now days due to its remarkable capability of being able to replace cement concrete and possessing enhanced mechanical and serviceability criteria as compare to OPC based construction materials. In terms of global warming, the GPC could diminish the emission of CO2 to the atmosphere produced by the cement industries. Fly-ash (FA) and ground-granulated blast furnace slag (GBS) are the industrial waste/by products which are supplementary binding materials widely used for partial replacement of OPC due to their low cost and good binding or pozzolanic properties. The GPC incorporated with heat cured low calcium FA when tested in fresh and hard state has shown excellent mechanical properties and durability [1]. The quarry rock dust (QRD) is a residue and calcium rich material which can be used as a partial replacement of binder or filler material in GPC. This can help in reducing the environmental and land pollution by avoiding its deposition at landfills.

GPC has shown comparatively brittle behavior than OPC concrete [2]. But with the addition of fibers, GPC has improved behavior not only in splitting tensile strength, flexural strength and flexural toughness but also in the post-peak behavior i.e the stress-strain response in comparison from brittle to ductile [3]. There are many options of fibers for researchers such as steel fibers (SF), synthetic fibers and natural fibers. The SF are most widely used fibers since they show excellent properties both in OPC and GPC under fracture toughness, splitting tensile and flexural strengths [4] According to Food and Agriculture Organization of the United Nations (FAO) natural fibers are considered to be the future fibers due to the benefits to the environment [5]. The SsF plant absorb more CO2 than the oxygen they produce, and the organic wastes which are produced during preparation of SsF can be used in the feeding the animals, bioenergy generations and fertilizer production. [5]. It is therefore, a wise solution to add natural fibers as a reinforcing material to the composites based on geopolymer matrix.

During last three decades, different methods have been presented for strengthening and rehabilitation of structural elements but the application of CFRP is the most effective methods in the field of strengthening/rehabilitation due to its numerous advantages such as high strength-to-weight ratio, ease of installation, very high tensile strength and high modulus of elasticity, immunity from corrosion and durability of the CFRP composites [6]. CFRP significantly improve the shear and flexure capacity of damaged structural element which greatly extend their useful life [7].

The externally bonded CFRP strengthening method is an effect way to for strengthening the damaged beams to enhance their load bearing capacity [8]. Many researchers have recommended that the strengthening method with CFRP laminates can improve the behavior of the shear deficient beams effectively and increased their capacity upto 37% [7]. Using CFRP strips on bottom surface of elements and U-shaped on sides of element ascertained to be very effective way to increase the load carrying capacity and stiffness of strengthened element. Therefore, use of CFRP strengthening technique is gaining popularity in the construction filed and considered as a better choice for retrofitting/strengthening of structures [17]. Although there are many studies available to strengthening the beams but limited literature is available to the behavior associated with shear deficient GPC beams strengthened with CFRP.

The main objective of this paper is to study the behavior of fiber reinforced shear deficient and partially damaged GPC beams strengthened with CFRP laminates. The combination of binder materials and different percentage of fibers used in this study is quite new and there is no literature available on strengthening of beams casted using this combination at ambient cured condition. This paper also shed light on fresh and mechanical properties of GPC concrete using SF and SsF both individually and in hybrid form.

2 Experimental Program

In the first stage of experimental program, a mix design study was carried out for finding the optimum ratio of SsF and hybrid with SF for mixing in the GPC composites. The optimum value of SF was taken as 0.75% by weight of concrete from the previous study [9]. The mix ratios of the binders i.e. FA, GBS and QRD are taken as 50%, 35% and 15% respectively by weight from another study of the second author [9]. After identifying optimum ratios of fibers from the first stage, four mix types were considered as shown in Table 1. In the second stage of experimental program, 24 GPC beams were cast, six for each mix type. All beams have dimensions of 1000mm (L), 150mm (W), 150mm (H). In order to make shear deficient beams, 2 Nos 12mm bars are used as main bars and 2 Nos 9mm bars are used as anchor bars with shear reinforcement of 6mm dia bars @ 150 mm c/c.

All the beams were tested under four point loading following ASTM 78/C78M-21 [14] as shown in Figure 1. Out of the 24 beams, 12 beams were partially damaged by applying about 60% of the ultimate load while the remaining twelve beams were tested to failure. In the third and final stage of experimental program, the partially damaged beams were strengthened by CFRP strips and wraps as shown in Figure 2 to determine the enhancement in the load carrying capacity of the GPC beams.

Table 1. The types and mix proportions for casting the fiber-reinforced GPC beams

Concrete Quantities (Kg/m^3)																	
Samples	**Mix ID**	**AL/B Ratio**	**W/C Ratio**	**Molarity of**	**SS/SH Ratio**	**B**	**Binder**			**CA 20mm**	**CA 10 mm**	**S**	**Alkaline Solution**		**SP**	**SF**	**SsF**	**W**
							FA	**GBS**	**QRD**				**SH**	**SS**				
GPC beams without Fibers	GPC	0.5	0.5	12.0	1.5	400	31.3	21.9	9.4	53.3	117.6	106.5	12.5	18.8	3.8	-	-	9.1
GPC beams with 0.75% Steel Fibers	0.75SF-R-GPC	0.5	0.5	12.0	1.5	400	31.3	21.9	9.4	53.3	117.6	106.5	12.5	18.8	4.6	9.2	-	9.1
GPC beams with 0.5% Steel Fibres+1% Sisal Fibers	0.5SF+1SsF-R-GPC	0.5	0.5	12.0	1.5	400	31.3	21.9	9.4	53.3	117.6	106.5	12.5	18.8	5.7	6.1	2.3	9.1
GPC beams with 2.4% Sisal Fibers	2.4SsF-R-GPC	0.5	0.5	12.0	1.5	400	31.3	21.9	9.4	53.3	117.6	106.5	12.5	18.8	7.8	-	5.5	9.1

Note: AL=Alkaline solution, B =Binder, W/C= water/cement ratio, SH= Sodium hydroxide, SS=Sodium silicate, FA= Flyash, GBS=Ground granulated blast furnace slag, QRD=Quarry rock dust , CA=Coarse aggregates, S= Sand, SP= Super plasticizer, SF= Steel fibers, SsF= Sisal fibers, W=Water

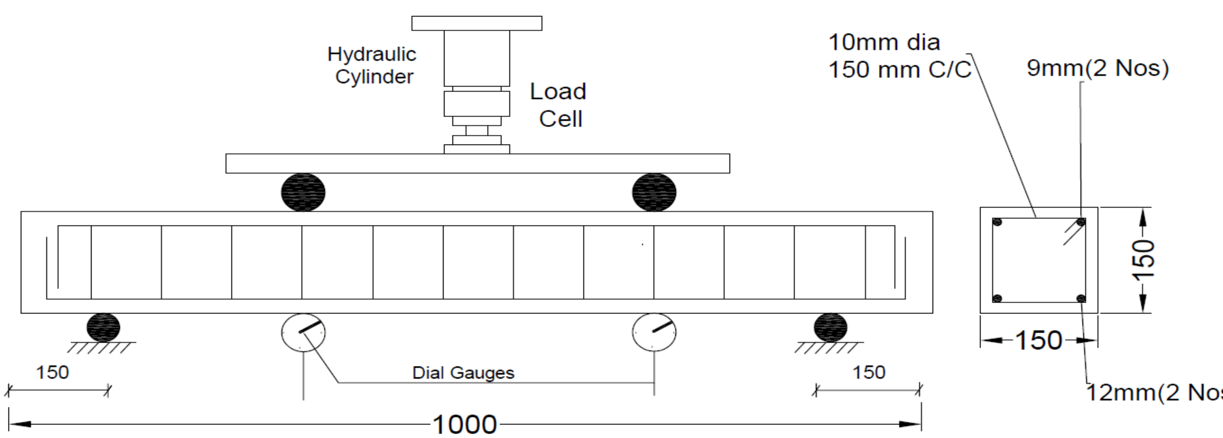

Figure 1: Test set up and reinforcement details (dimensions are in mm)

2.1 Materials used in the study

The commercially available FA of class-F is used for manufacturing of GPC. The QRD was collected from Margallah quarries in Taxila and grinded to cement size at Pakistan Council of Scientific and Industrial Research (PCSI) Peshawar, by ball Mill Machine. The GBS used as one of the binder material was obtained from Dewan steel mill Karachi. The alkaline liquid preparation materials used in this study were sodium silicate (SS) solution which is available in liquid form and sodium hydroxide (SH) which is in the form of pellets. The 12M SH solution was prepared by dissolving SH pallets with tap water, 24 hours before using it. The SS is added into solution of SH, 30 minutes prior to be added into the other materials. The coarse aggregate (CA) of varying size from 7mm to 20mm, from Margallah quarries was used. The aggregate crushing value and the aggregate impact value were found to be 22.7 and 19.48 respectively. The sand (S) used was clean dry Lawrancepur sand. The fineness modulus of sand was conformed to ASTM-C-136-06 [10] whereas specific gravity and water absorption was conforming to ASTM-C128-15 [11]. The Specific gravity of CA was conforming to ASTM-C127-07 [12]. The sisal fibers (SsF) were obtained from Ayub Research Centre (ARC) Faisalabad which has a water absorption capacity of 120% [13]. The SsF were cut into a size of 10 mm length with an average diameter of 137 µm resulting in an aspect ratio of 73. The both end hooked SF were used of a 35mm length, diameter of 0.50mm aspect ratio of 65 and tensile strength of 1350MPa.

A high strength, high elastic modulus, carbon fiber reinforced polymer (CFRP) wrap and strips by SIKA® were used for strengthening the damaged beams. The strips and wraps were bonded to concrete surface using epoxy adhesive. Table 2 presents the properties of the CFRP wrap and strips, as provided in the material's specifications of the manufacturer.

Table 2. The properties of CFRP laminates

Material	Width (mm)	Thickness (mm)	Elastic Modulus (GPA)	Tensile Strength (MPA)	Elongation at break (%)
CFRP strip (S812)	80	1.2	165	3100	1.69
CFRP wrap (230 C)	300	0.129	225	3500	1.59

2.2 Strengthening procedure.

To apply the CFRP strips and sheets, first the soffit and sides of damaged beams were grinded to make the surface levelled by removing the undulations and any adhered material. Next, the two parts of the epoxy adhesive Sikadur-30 were mixed to form epoxy paste. A layer of epoxy paste having thickness of 1.5mm was applied on concrete surface and CFRP strip. After the CFRP strip was placed on the concrete surface. The laminate is pressed until the adhesive is forced out on both sides as per recommended procedure. The CFRP strip is fixed throughout the length of beams and then confined with u shaped wrap near support using adhesive sikadur 330 in order to avoid the premature bond failure and strengthen the shear portion. Finally, grooved rollers were used on the attached CFRP sheets and left the beams undisturbed for 7 days. The beams were retested after strengthening till ultimate failure load as shown in Figure 2 (e) and (f).

a) Application of epoxy   b) Fixing of CFRP strip   c) Fixing of CFRP wrap

d) Completion of applying CFRP strip and wrap   e) The four point loading arrangement   f) The strengthen GPC beam at ultimate failure load

Figure2: The steps followed for strengthening the GPC beams and testing arrangement

3 Results and Discussion

3.1 Workability

The workability of mixes was checked using slump cone test. The slump value was maintained between 70 and 90 by varying the quantity of super plasticizer (SP) for a workable mixture. The slump vales for GPC, 2.4SsF-R-GPC, 0.5SF+1SsF-R-GPC and 0.75SF-R-GPC were calculated to be 84, 78, 75 and 78 mm respectively. The mixes with SsF has shown least slump value owing to their higher water absorption capacity and hollow cylindrical nature

3.2 Mechanical Properties

In order to obtain the optimum values of sisal fibers both individually and in hybrid form, the cube, cylinder and prism specimen were casted with mix proportion as mentioned in Table 3, and their mechanical properties were evaluated. The uniaxial compression strength test was conducted to determine cube strength after 28 days of casting following BS EN 12390-2:2009/EN 12390-3 and results are shown in Table 3. The maximum values were obtained in case of 0.5%SF+1%SisalF-R-GPC and 2.4%SisalF-R-GPC which are 44% and 39% more than the control mix respectively. The compressive strength has increase due to addition of fibers both individually as well as in hybrid but with the increase of fibers content in hybrid form (0.5SF+1.5SsF-R-GPC), there is decrease in the compressive strength due to low workability because of higher fiber content.

The split cylinder strength is checked with cylinders after 28 days of casting following ASTM C496/496M and the results are shown in Table 3. The maximum results were achieved in case of 0.5%SF+1%SisalF-R-GPC and 2.4%SisalF-R-GPC which are 43% and 32% more as compare to the control mix respectively. The failure of fiber reinforced GPC was accompanied by the multi cracking due to fact that fibers allow load transference from the cracked area to the other parts of the specimen. These results are in same pattern with what observed by the other researchers [15] as far mode of failure is concerned.

Like the compressive and tensile strength the flexural strength has also shown similar trend with the increase of fiber content with maximum values at 0.5%SF+1%SisalF-R-GPC and 2.4%SisalF-R-GPC which are 65% and 55% more relative to the control mix respectively. It is observed that the increase in strength is more dominant in case of flexural behavior due to the fact that fibers help to bear more load across the cracks, resist the penetration of the cracks and fibers stretching and elongation is observed especially in case of flexural testing of specimens as also observed by Sun et al. [15] and Chen et al. [16].

Table 3. The mechanical properties of mix design with different combination of fibers

Material	Compressive Strength (MPA)	Split Cylinder Strength (MPA)	Flexure Strength (MPA)	Increase in Compressive Strength	Increase in Split Cylinder Strength	Increase in Flexure Strength
GPC (Control mix)	20.5	1.89	2.23	-	-	-
0.5%SF+0.5%SisalF-R-GPC	24.2	2.5	3.12	18%	32%	40%
0.5%SF+1%SisalF-R-GPC	29.5	2.75	3.67	44%	46%	65%
0.5SF%+1.5%SisalF-R-GPC	24.8	2.7	3.21	21%	43%	44%
0.8%SisalF-R-GPC	23.24	2	2.45	13%	6%	10%
1.2%SisalF-R-GPC	26.340	2.300	2.89	28%	22%	30%
2.4%SisalF-R-GPC	28.560	2.500	3.45	39%	32%	55%

4 *Load Carrying Capacity of Strengthened GPC Beams*

A total of twenty four beams were tested under four point loading as shown in Figures 1 and Figure 2. Out of 24 beams, 12 beams were partially damaged and remaining 12 beams were tested to failure. The substantially damaged beams were strengthened and re-tested till failure to find out the ultimate load bearing capacity. The results showed that the ultimate load carrying capacity of strengthened beams is higher relative to the control unstrengthen beams in all cases. The average increase in ultimate strength of retrofitted GPC beams viz. GPC, 0.75SF-R-GPC, 0.5SF-1SsF-R-GPC, and 2.4SsF-R-GPC was 20%, 24%, 43% and 45% respectively as compared to non-strengthened beams. The comparison of ultimate load carrying capacity of original beams and retrofitted beams is shown in Figure 3. All the strengthened beams failed due to formation shear cracks and same behavior is observed in unstrengthen beams. However the significant increase in load bearing capacity and high ductile behavior of the strengthened beams observed due to usage of CFRP composites. The ductile behavior is obtained due to high tensile strength of CFRP which can provide ample warning before the ultimate failure. The use of CFRP helped to delay the initial cracks and their further propagation in the beam resulting the increase in load bearing capacity.

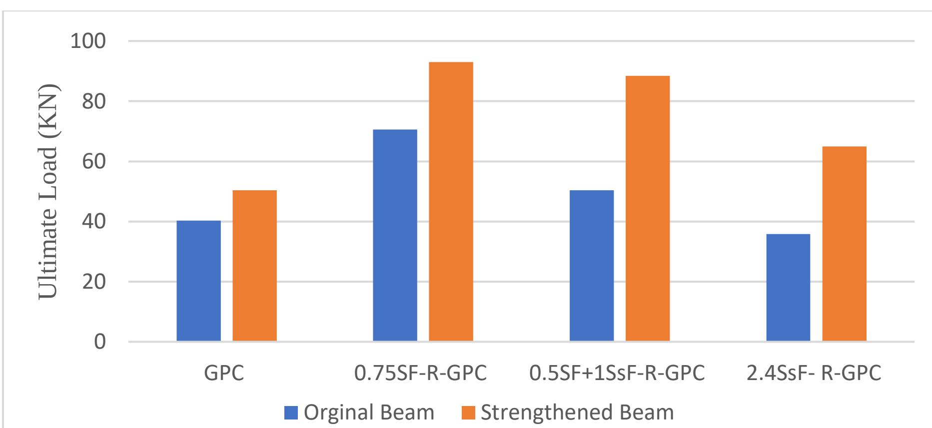

Figure 3: The comparison of ultimate load capacity of original and strengthened beams

5 *Load Deflection Curve*

Two dial gauges were used under the test specimens in order to observe the deflection values. The curve was plotted using mid deflection values with respect to load which is termed as load deflection curve. The strengthened beams have steeper load-deflection curve and higher load bearing capacity due to enhanced stiffness provided the CFRP strengthening system as shown in Figure 4. The same behavior was observed by Lavorato, D.,A [7]. The stiffness has increased due to high tensile strength of CFRP laminates which delays and prevent the cracks propagation by transferring the load from beam to CFRP strengthening system.

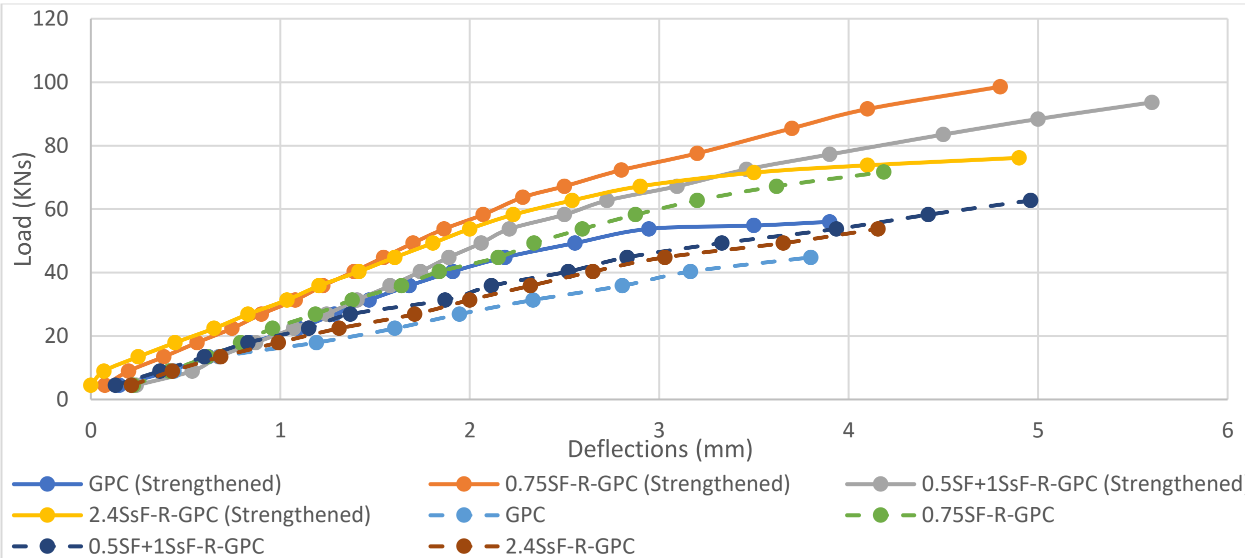

Figure 4: The load deflection curve of strengthened unstrengthen GPC beam

6 Practical Application

The use of GPC concrete is gaining popularity in construction field and but there are limited studies available to strengthen the shear deficient fiber reinforced GPC beams cured at ambient temperature. The CFRP strengthening regime of shear deficient GPC beams will not only improve/restore the load bearing capacity but also save the time and cost required to dismantle and reconstruct the structural element. This will help to repair and improve the capacity of structural elements and increase the serviceability of the structures.

7 Conclusion

Following conclusions can be drawn from the conducted study:

- Sisal fibers have good having good mechanical properties and lesser environmental impact. The addition of Ssf both individually and in hybrid form with SF into QRD incorporated GPC at various fraction has yielded improved performance in mechanical properties and flexural strength relative to control specimen.
- The addition of fibers both individually and in hybrid form has increased the load bearing capacity of all GPC beams and the maximum value is obtained at 0.75% steel fiber which is 75% higher than the counterpart GPC.
- The pre-damaged GPC beams strengthened with CFRP strips and CFRP wraps has increased the ultimate load capacity relative to control unstrengthen beams.
- The ultimate load carrying capacity has increased significantly up to 45% relative to load capacity of the unstrengthen beam due to high tensile strength of CFRP laminates.
- The strengthened beam with 0.75% SF has shown maximum load capacity. The other strengthened beams has also shown improved results and significantly enhanced the load bearing capacity relative to the control beams
- The mode of failure in all beams is due to formation of cracks near supports which travelled towards point of impact. However in case of strengthened beams the CFRP delays the initial cracks and further propagation which results in increased load bearing capacity of beams.

- The strengthened beams have steeper load deflection curve due to high tensile strength of CFRP laminates which can give us enough warning before ultimate failure.

References

[1] Nath, P. and P. K. Sarker (2014). "Effect of GGBFS on setting, workability and early strength properties of fly ash geopolymer concrete cured in ambient condition." Construction and Building Materials 66: 163-171.
[2] Thomas RJ, Peethamparan S Engg properties and stress–strain behavior. Constr Build Mater 2015;93:49–56.
[3] Khan MZN, Hao Y, Hao H, Shaikh FUA. Mechanical properties of ambient cured high strength hybrid steel and synthetic fibers reinforced geopolymer composites.Cem Concr Compos 2018;85:133–52.
[4] Ali Nazari, "Flexural strength of plain and fibre-reinforced boroaluminosilicate geopolymer", Const and Build Mat 76 (2015) 207–213
[5] Guido Silva, Suyeon Kim (2020). Optimization of a reinforced geopolymer composite using natural fibers and construction wastes. Construction and Building Materials 258 (2020) 119697.
[6] Danraka, M. N., H. M. Mahmod, O.-k. J. Oluwatosin and P. Student (2017). "Strengthening of Reinforced Concrete Beams using FRP Technique: A Review." International Journal of Engineering Science 7(6):13199.
[7] Lavorato, D., A. V. Bergami, G. Fiorentino, A. Fiore, S. Santini and C. Nuti (2018). "Experimental tests on existing RC beams strengthened in flexure and retrofitted for shear by C-FRP in presence of negative moments." International Journal of Advanced Structural Engineering: 1-22.
[8] Osman, B. H., et al. (2019). Effect of reinforcement ratios on shear behavior of concrete beams strengthened with CFRP sheets. HBRC Journal,14(1), 29–36.
[9] Muhammad Ibraheem, Faheem Butt. Fresh and Mechanical Properties of Ambient Cured Ternary Blended Geopolymer Concrete Reinforced With Steel Fibers. 2nd Conference on Sustainability in Civil Engineering (CSCE'20), CUST Islamabad.
[10] ASTM C136-06, "Standard Test Method for Sieve Analysis of Fine and Coarse Aggregates," ASTM Int., 2006.
[11] ASTM C128-15, "Standard Test Method for Density, Relative Density (Specific Gravity), and Absorption of Fine Aggregate," ASTM Int., 2015.
[12] ASTM C127-07, "Standard Test Method for Density, Relative Density (Specific Gravity), and Absorption of Coarse Aggregate," ASTM Int., 2007
[13] Tung T. Tran "Experimental and analytical investigation on flexural behaviour of ambient cured geopolymer concrete beams reinforced with steel fibers", Engineering Structures 200 (2019) 109707
[14] Abdul Saboor Karzad, Moussa Leblouba," Repair and strengthening of shear-deficient reinforced concrete beams using Carbon Fiber Reinforced Polymer", Composite Structures 223 (2019) 110963
[15] P. Sun, H. Wu, Transition from brittle to ductile behavior of fly ash using PVA fibers, Cem. Concr. Compos. 30 (1) (2008) 29–36
[16] R. Chen, S. Ahmari, L. Zhang, Utilization of sweet sorghum fiber to reinforce fly ash-based geopolymer, J. Mater. Sci. 46 (6) (2014) 2548–2558
[17] Salama, A. S. D., Hawileh, R. A., & Abdalla, J. A. (2019). Performance of externally strengthened RC beams with side-bonded CFRP sheets. Composite Structures,212, 281–290.

3rd Conference on Sustainability in Civil Engineering (CSCE'21)
Department of Civil Engineering
Capital University of Science and Technology, Islamabad Pakistan

EVALUATION OF PERFORMANCE OF SELF COMPACTING CONCRETE WITH MINERAL ADMIXTURES BY ARTIFICIAL NEURAL NETWORKS

[a] Nauman Shahid*, [b] Ayub Elahi, [c] Sarmad Mahmood

a: Department of Civil Engineering, University of Engineering and Technology, Taxila, 47050, Pakistan
naumanshahid121@gmail.com
b: Department of Civil Engineering, University of Engineering and Technology, Taxila, 47050, Pakistan
ayub.elahi@uettaxila.edu.pk
c: Swedish College of Engineering and Technology, Wah Cantt, 47050, Pakistan
sarmadmahmood8@gmail.com
* Corresponding author: Email ID: naumanshahid121@gmail.com

Abstract- Bentonite a natural pozzolan can reduce the amount of CO_2 produced as an output of cement production. The mechanical properties of cementitious materials used in concrete can be enhanced using bentonite. Durability of structures has become a critical issue in management of reinforced concrete structures. This research work emphasis on analyzing the performance of self-compacting concrete (SCC) using mineral admixtures such as BASF manufactured Super Plasticizer (SP), silica fume and bentonite. Total 16 samples by adding bentonite and silica fume in binder and using 0.8% super plasticizer ultimately have developed SCC. Artificial Neural Network (ANN) model is used for the prediction of mechanical properties of SCC using Levenberg Marquardt (LM) Algorithm having certain inputs/variables and compression strength at 28 and 91 days as output. The ANN model results show overall accuracy of 97%. It was concluded that the bentonite in addition with constant silica fume used in SCC increases the compressive strength of concrete by reduces the chloride ion diffusion, but excess of Bentonite reduces the w/c too much and causes decrease in compressive strength and in workability.

Keywords- Artificial neural network, Bentonite, Self-compacting concrete (SCC), Super Plasticizer (SP)

1 Introduction

In the late 1990s the use of self-compacting concrete was introduced and studied in Asian countries such as Japan as a material with maximum workability without compromising its compressive strength, so that it can be effortlessly casted, without further effort of compacting, in difficult formwork, congested reinforced structural elements and areas with difficult access. Due to several advantages and structural configuration Self-compacted concrete has gained wide-ranging consumption in many countries [1]. Concrete is one of the most vital element of construction industry. Durability of concrete is the most critical problem for the construction of reinforced concrete structures with protracted service life and to improve construction knowledge due to various economic as well as environmental reasons in recent few years, it is significant to yield well-designed concrete as a construction material with lifelong services. However, production of concrete relies on huge extents of natural sources such as water, sand, gravel particles and cement which are widely used in concrete manufacturing. Also, about 2.99 billion tons of fine as well as coarse materials are used every year for cement manufacturing in the world and, around 2.6% of CO2 emissions are result of cement manufacturing in Industrial sources[2, 3]. The use of mineral admixtures such as fly ash, silica fume or ground granulated blast furnace etc., can effectively reduce the ecological effect as a partly cement replacement. The amount of permeability, pore structure and compressive strength of concrete can be enhanced by the use of admixtures such as fly ash, blast furnace in concrete manufacturing plants, this is credited to the pozzolanic reaction. [4, 5]. The main criterion of self-compacting technology is achieving a highly plastic conduct while avoiding draining and mixture components segregation. While casting fresh plastic Self-compacting concrete (SCC) the compaction needs are eliminated. This decreases overall cost, increases working environment by saving time and opens the way for the mechanization of the concrete structure. Because of these remarkable advantages, SCC is anticipated to progressively change most of the ordinary concrete currently produced worldwide. Particularly the development and evolution of the self-compacting concrete by considerably contribution of super plasticizer technology. Different from the ordinary Portland cement concrete design, the self-compacting concrete desires the super plasticizers, addition of viscosity increase and pozzolanic admixture additions in bulk amount all together or moderately[6, 7]. The quantifiable constituents of SCC are mostly the same as: water, mineral, chemical admixtures, cement, fine as well as coarse aggregates. The material components contains the main modification in comparative quantities of each of the component constituents[8]. The use of SSC in building industry does not only propose speed due to the lack of constraints on concrete amount to be placed in one shot for proper consolidation, it also makes workability easier without comprising compressive strength of CVC[9]. The resistance to segregation of SCC and its plasticity yields a meticulously compacted material of uniform configuration with great surface appearances. The proper compaction converses greater bond strength and durability. The non-requirement of vibration removes some of the high construction noise which is one of the notable distinguishing feature of CVC[10]. The void filling property of SCC provides an abundant advantage of labor as well as mechanical compactor use reduces for the compaction which enables better attention on accuracy rather than being worried with monitoring the crowd masses handling concrete on site[11]. It is very important for Asian as well as countries beyond Asia to adopt the SCC with several mineral admixtures due to its exceptional attributes and should be adopted worldwide.[12]. Therefore, there is a huge space of data available to be filled concerning unsuitability of SCC as a construction material, with reference to usability of raw materials available locally and production cost with respect to ordinary Portland concrete of comparable strength and toughness features[13].

With certain advances in technology, civil engineers tend to focus on software/models to predict properties of concrete without testing. For this, Artificial Neural network models became the priority these days. An artificial neural network (ANN) is a mathematical model or computational model that is inspired by the structure and/or functional aspects of biological neural networks. It can learn from experiences to develop its performance. Same as human brain, Artificial Neural Network obtains information through learning [14]. ANN consists of three different steps of training, validation and Test. In training step, model is repeated as long as it got the desired output. The errors of the validation step are monitored during the training step [15]. Generally, an ANN model comprises of different layers, Input and Output consists of input and output data. Between these layers, there are one or more hidden layers depending upon the model. It includes neurons and are connected by weights. Each neuron has an activation function to determine the output. There are many kinds of activation functions. Usually, nonlinear activation functions such as sigmoid, step are used [16].

The aim of this study is to construct ANN model as well as to develop environment friendly SCC by utilizing locally available mineral admixtures/waste materials and compare the result obtained from software with experimental results of experimental work. The current research work addresses the alternative to both fundamental alteration on the mix proportions used to keep away from conditions where cement does not accomplish the required compressive strength or by staying away from substantial that is needlessly durable and furthermore for more economic utilization of raw material and less construction disappointments, subsequently decreasing development cost and environmental effects. Thus, prediction of compressive strength and different important parameters of cement has been a functioning space of this research study.

2 Experimental procedure

2.1 Materials

The Portland cement used for experimental work is having a registration code of ISO 9001:2000 meeting the requirements of ASTM 150 [17]. The physical as well as chemical properties of Portland cement are listed in Table 3. The maximum size of coarse aggregate was selected as 19mm (meeting requirement of ASTM C33M) to avoid blocking of SSC. The fine aggregates used in this research having size less than 4.75mm and meeting the requirement of ASTM C33 [18]. The physical properties of coarse as well as fine aggregates are listed in Table 1. BASF manufactured Super plasticizers is used as admixture in concrete and its amount is kept constant which gives us optimum workability at 0.8% use and reducing the excess water requirement of concrete workability. Furthermore, Bentonite is also used to increase the pore structure of cementitious materials, thereby increasing the durability of structure. An excess of bentonite reduces the compressive strength of cement concrete. The chemical properties of Bentonite and Silica fume are listed in Table 3.

Table 1: Physical Properties of Coarse and Fine aggregates

Properties	Coarse Aggregates	Fine Aggregates
Surface Texture	Rough	Smooth
Particle Shape	Angular	Rounded
Specific Gravity	2.58	2.61
Fineness Modulus	6.2	2.4

2.2 Mix Proportions

Design mix was done based on Self compacting concrete codes by keeping Silica Fume fix at 5% and 10% and bentonite varies from 2.5 – 20 %. Total of 17 design mixes were made and are given in Table 2.

2.3 Preparation of Specimen and Testing

After self-compatibility was controlled by new substantial analyses cements were poured from a point at the highest point of the form and set in moulds without vibration. The compressive strength tests were performed on cube sizes of 100x100x100mm (4x4x4in.) after demoulding the test specimens and curing using tap water.

2.4 Concrete Tests

2.4.1 Fresh Concrete

Slump flow, L-Box and V-Funnel tests were performed on fresh concrete to check the filling and passing ability of SCC.

2.4.2 Hardened Concrete

To check the compressive strength of concrete after completion of curing in tap water, compressive strength tests are performed.

Table 2: Mix Design

Sr No.	MIX ID	Cement	Silica Fume	Bentonite	C.A	F. A	water (0.45)	Sp (% of binder)
		kg/m3	kg/m3	kg/m3	kg/m3	kg/m3	kg/m3	kg/m3
1.	Control	500	0	0	629	721.5	225	0.8
2.	SF5B2.5	462.5	25	12.5	629	721.5	225	0.7
3.	SF5B5	450	25	25	629	721.5	225	0.7
4.	SF5B7.5	437.5	25	37.5	629	721.5	225	0.7
5.	SF5B10	425	25	50	629	721.5	225	0.7
6.	SF5B12.5	412.5	25	62.5	629	721.5	225	0.7
7.	SF5B15	400	25	75	629	721.5	225	0.7
8.	SF5B17.5	387.5	25	87.5	629	721.5	225	0.7
9.	SF5B20	375	25	100	629	721.5	225	0.7
10.	SF10B2.5	437.5	50	12.5	629	721.5	225	0.8
11.	SF10B5	425	50	25	629	721.5	225	0.8
12.	SF10B7.5	412.5	50	37.5	629	721.5	225	0.8
13.	SF10B10	400	50	50	629	721.5	225	0.8
14.	SF10B12.5	387.5	50	62.5	629	721.5	225	0.8
15.	SF10B15	375	50	75	629	721.5	225	0.8
16.	SF10B17.5	362.5	50	87.5	629	721.5	225	0.8
17.	SF10B20	350	50	100	629	721.5	225	0.8

Table 3: Physical and Chemical properties of Cementitious material

Physical Properties	Cement	Silica Fume	Bentonite
Specific Gravity	3.063	2.1	1.65
VICAT Initial settling time (min)	150	-	-
VICAT Final settling time (min)	240	-	-
Compressive Strength at 28th day (MPa)	17.2	-	-
Le-Chatelier Expansion (mm)	1.66		-
Chemical Properties %		80	
SiO_2	19.15	1.12	70.10
$AI2O_3$	4.80	1.4	12.18
Fe_2O3_3	3.20	0.5	5.12
CaO	60.90	0.4	3.51
MgO	2.01	0.6	3.14
Na_2O_3	0.32	0.50	5.02
K_2O	0.80	-	0.54
TiO_2	-	-	0.14
MnO	-		0.06

3 Research Methodology

Self-compacting Concrete was developed according to mix design by hit and trail method and after developing, fresh properties were determined. Figure 1 is attached below. In evaluating hardened properties of SCC, total of 9 cube samples were used for each age. The samples were prepared and cured a day after at 23 ± 2°C using mineral admixtures as mentioned before. The samples were used to measure the compressive strength after 28 and 91 days, figure 2 is attached below. The compressive strength of each sample is measured using UTM with a capacity of 200KN with a loading rate of 0.3MPa/s. An artificial neural networks study was carried out to predict the compressive strength of SCC. Several inputs and outputs of conducted experiments are defined. The compressive strength of SCC is evaluated using ANN Testing network comparing predicted values and actual values.

Figure 1: Evaluating Fresh properties of developed SCC.

Figure 2: Compression Strength Test

4 Experimental Results

4.1 Fresh Properties

4.1.1 Slump Flow Test

Slump flow test is used to check the workability of concrete and is considered 1st workability test. Slump flow values fall in the range given by EFNARC i.e., 650 mm – 800 mm. Results are shown in fig. 3.

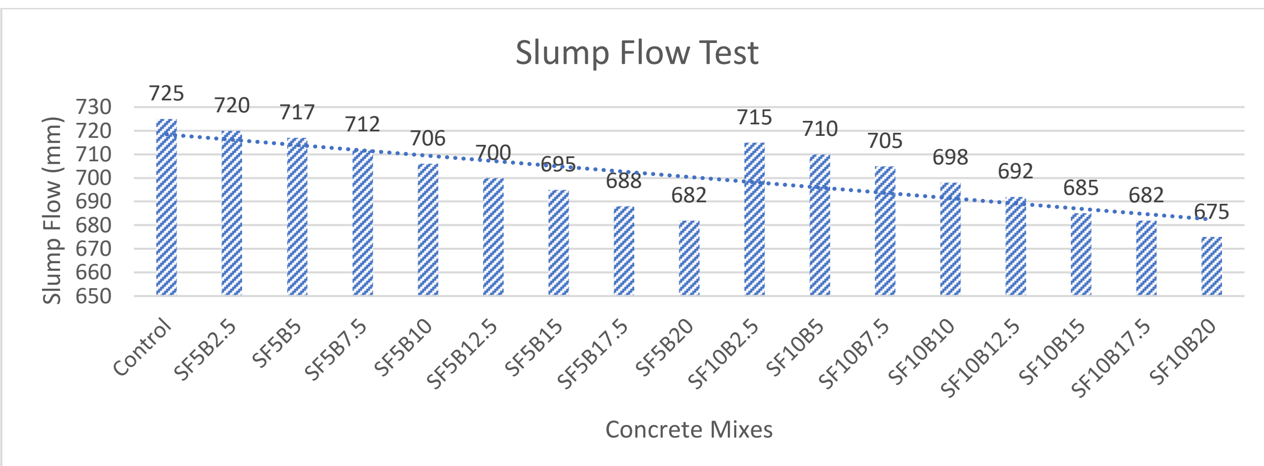

Figure 3: Slump Flow Test Results

4.1.2 V – Funnel Test

V-funnel test is considered a second workability test performed on fresh concrete to check the flow ability of SCC. Results obtained after experimentation fall in the range given by EFNARC i.e., 6-12 sec. Results are shown in Fig. 4.

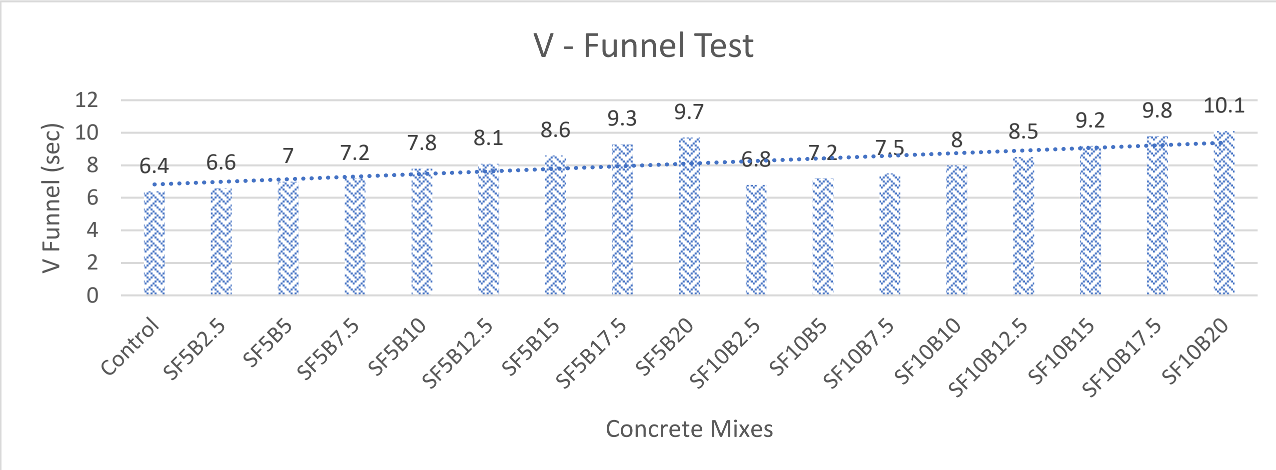

Figure 4: V-Funnel Test Results

4.1.3 L – Box Test

L-Box test is used to check the passing ability and blockage ratio (h2/h1) of SCC and considered as a third workability test. Blockage ratio obtained from L-Box test lies within acceptable range given by EFNARC i.e., 0.8-1.0. Results are shown in Fig. 5.

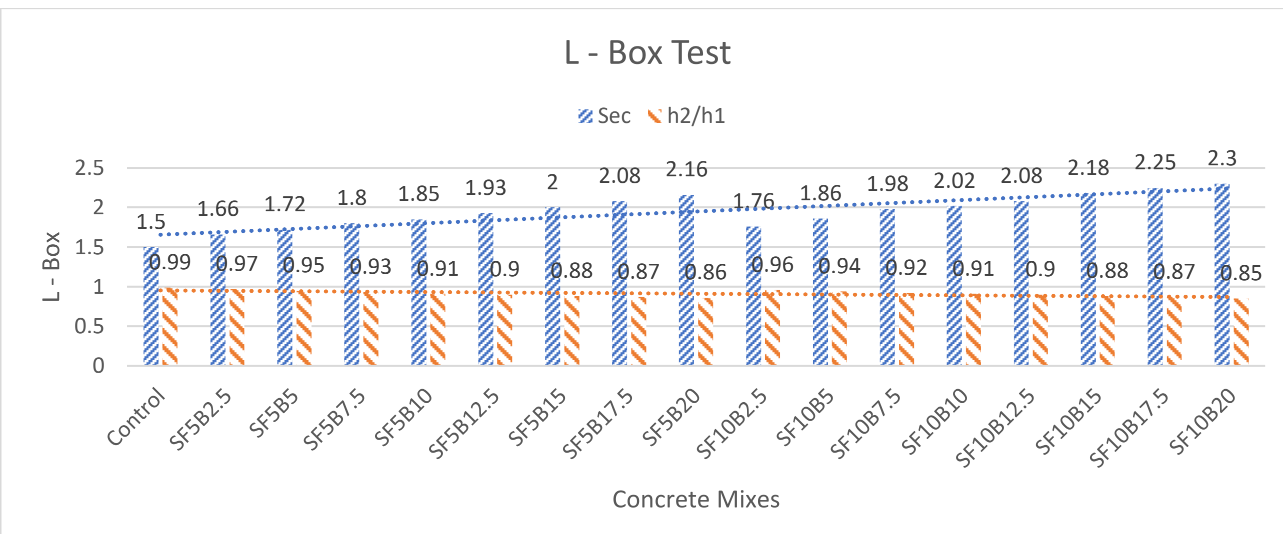

Figure 5: L-Box Test Results

4.2 Hardened Properties

4.2.1 Compressive Strength

Compressive strength test was performed fulfilling the requirements of ASTM C39 [19] on hardened concrete after 28 and 91 days and their results are shown in Figure 6. It is noted that the value of compressive strength is maximum for sample #08 because by increasing the value of bentonite the amount of W/C decreases and workability increases ultimately decreeing the value of compressive strength. Results shows that the 0.8% super plasticizer and 17.5% use of bentonite having constant 10% silica fume gives us maximum compressive strength values of 27.0 and 27.3 MPa for 28 days and 91 days, respectively.

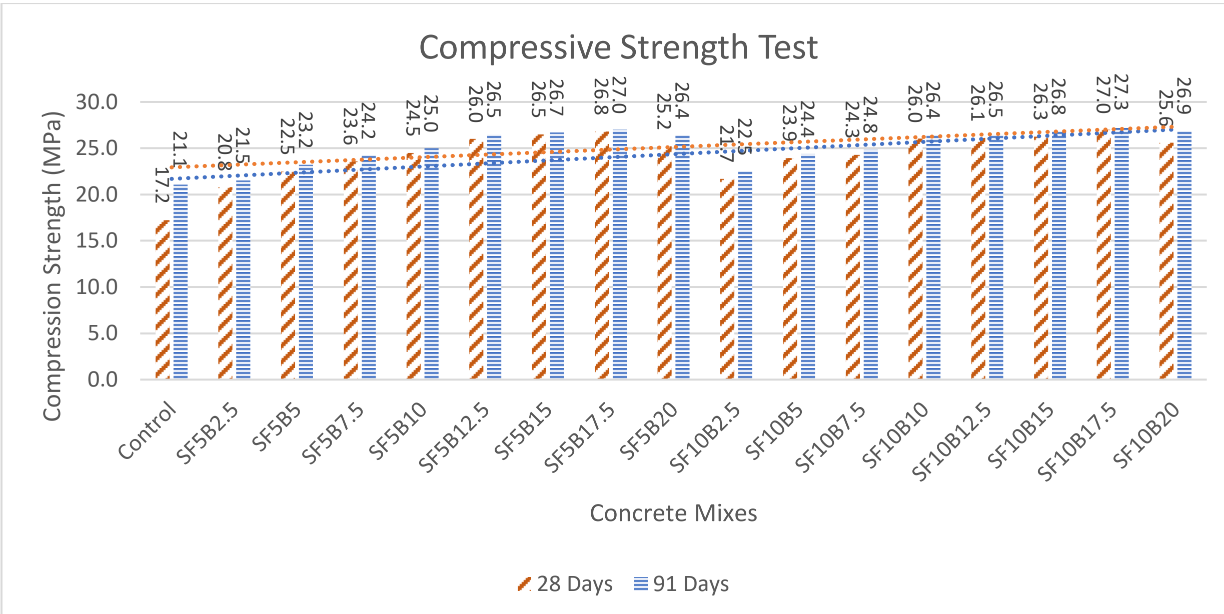

Figure 6: Compressive strength test results for mixes at different ages using mineral admixtures.

4.3 Prediction of Experimental Results using Artificial Neural Network (ANN)

In this investigation total 7 input variables such as Cement, Silica fume, Bentonite, coarse and fine aggregates, water/cement ratio and superplasticizer are used. The compressive strength at 28 and 91 days were the output. Number of hidden neurons are set as 10. MATLAB was used for modelling. The structure of the ANN model is shown in Figure 7.

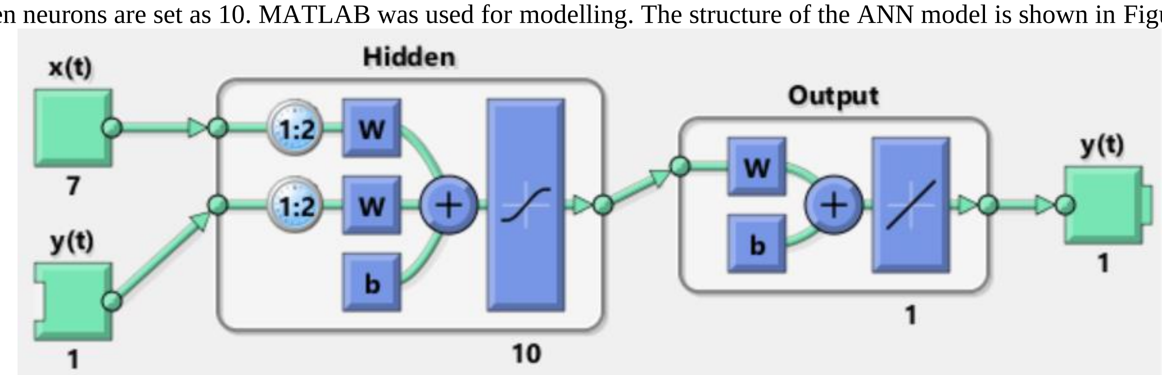

Figure 7: Structure of ANN Model

ANN model is based on back propagation technique using Levenberg-Marquardt Algorithm. The data set is divided into three categories such as training, validation, and testing with percentages 70, 20 and 20, respectively. The results of 28 days strength and 91 days strength by ANN modelling are shown in Figure 8 and 9. Graphs shows that ANN model was developed for 28 days and 91 days compression strength with an overall accuracy of 93% respectively proving LM algorithm to be a good learning algorithm for this research study despite limited data.

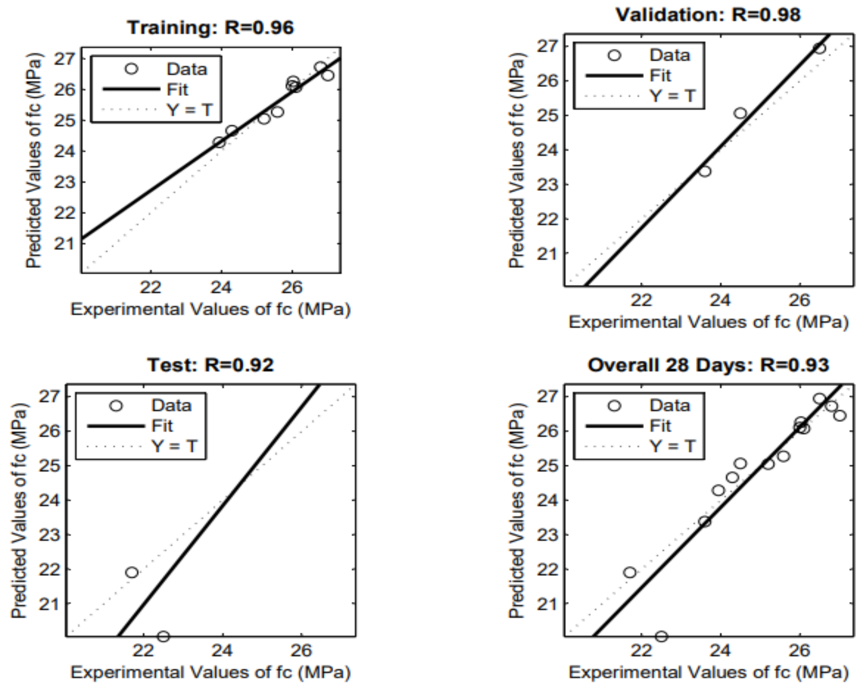

Figure 8: Artificial Neural Network ANN) Modelling on MATLAB for experimental and predicted compression strength at 28 days.

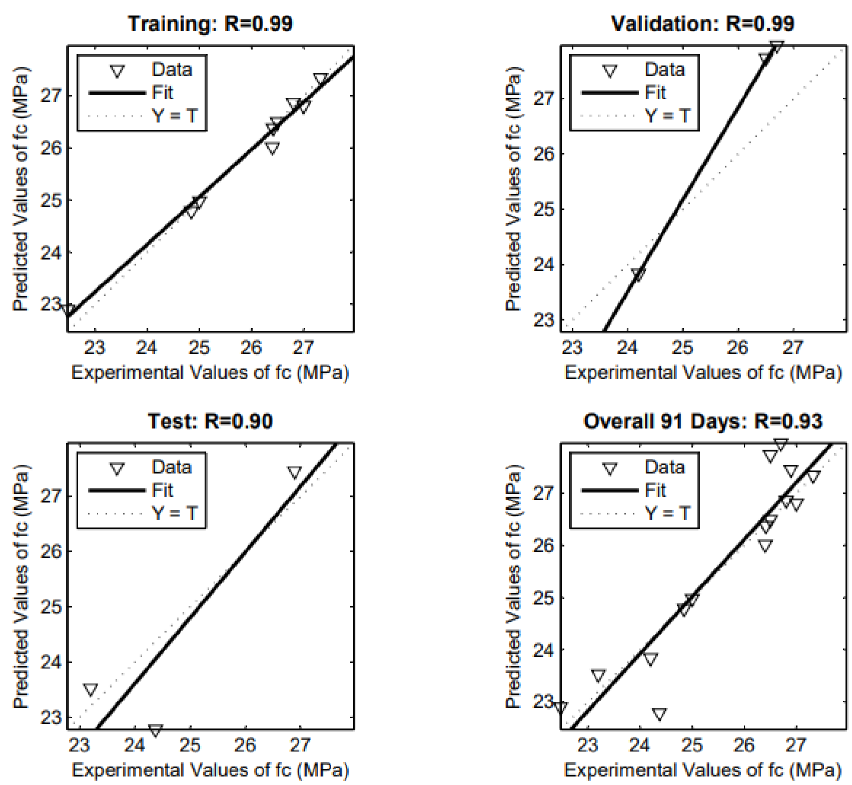

Figure 9: Artificial Neural Network ANN) Modelling on MATLAB for experimental and predicted compression strength at 91 days.

5 Conclusion

The following findings of our investigations are as:

1. It is concluded that the SCC can be developed using fixed amount of Super Plasticizer (0.8%) and using control quantity of bentonite and silica fume.
2. In examining fresh properties of SCC, it is demonstrated that Slump flow, L-Box and V-Funnel decreasing by addition of Bentonite but well within the range of EFNARC.
3. The presence of excessive amount of bentonite causes decrease in workability.
4. Compressive Strength of SCC Mixes increased up to addition of 17.5% Bentonite, however, strength loss was observed beyond 17.5% addition of Bentonite.
5. Based on compressive strength development tendency, some further research is needed to find out the optimum amount of bentonite for developing optimum strength SCC changing other parameters.
6. ANN model shows overall accuracy of 93% despite limited data proving LM algorithm to be a good learning algorithm for this research study. Therefore, to predict the compressive strength of concrete with high reliability, instead of using costly experimental investigation, ANN model can be replaced.

References

1. Su, N., K.-C. Hsu, and H.-W. Chai, *A simple mix design method for self-compacting concrete.* Cement and concrete research, 2001. **31**(12): p. 1799-1807.
2. Bilim, C., et al., *Predicting the compressive strength of ground granulated blast furnace slag concrete using artificial neural network.* Advances in Engineering Software, 2009. **40**(5): p. 334-340.
3. Bui, D.-K., et al., *A modified firefly algorithm-artificial neural network expert system for predicting compressive and tensile strength of high-performance concrete.* Construction and Building Materials, 2018. **180**: p. 320-333.
4. Dehn, F., K. Holschemacher, and D. Weiße, *Self-compacting concrete (SCC) time development of the material properties and the bond behaviour.* Selbstverdichtendem Beton, 2000. **5**: p. 115-124.
5. Dinakar, P., M.K. Reddy, and M. Sharma, *Behaviour of self compacting concrete using Portland pozzolana cement with different levels of fly ash.* Materials & Design, 2013. **46**: p. 609-616.
6. Khayat, K.H., J. Assaad, and J. Daczko, *Comparison of field-oriented test methods to assess dynamic stability of self-consolidating concrete.* Materials Journal, 2004. **101**(2): p. 168-176.
7. OUCHI, M., et al., *A Quantitative Evaluation Method for the Effect of Superplaticizer.* Transactions of the Japan Concrete Institute, 2001. **22**: p. 15-20.
8. Kapoor, Y., C. Munn, and K. Charif. *Self-Compacting Concrete-An Economic Approach*. in *7th International Conference on Concrete in Hot & Aggressive Environments, Manama, Kingdom of Bahrain*. 2003.
9. Ramsburg, P., et al. *Durability of Self-Consolidating Concrete in Precast Application*. in *Proceedings, Third International Symposium on High Performance Concrete, PCI National Bridge Conference, Orlando, FL*. 2003.
10. Zhu, W. and P.J. Bartos, *Permeation properties of self-compacting concrete.* Cement and Concrete Research, 2003. **33**(6): p. 921-926.
11. Persson, B., *Chloride migration coefficient of self-compacting concrete.* Materials and Structures, 2004. **37**(2): p. 82-91.
12. Goodier, C.I., *Development of self-compacting concrete.* Proceedings of the Institution of Civil Engineers-Structures and Buildings, 2003. **156**(4): p. 405-414.
13. EFNARC, S., *Guidelines for self-compacting concrete.* London, UK: Association House, 2002. **32**: p. 34.
14. Nikoo, M., et al. (2015). "Prediction of concrete compressive strength by evolutionary artificial neural networks." Advances in Materials Science and Engineering 2015.
15. Khademi, F. and S. M. Jamal (2016). "Predicting the 28 days compressive strength of concrete using artificial neural network." i-manager's Journal on Civil Engineering 6(2).
16. Bilim, C., et al. (2009). "Predicting the compressive strength of ground granulated blast furnace slag concrete using artificial neural network." Advances in Engineering Software 40(5): 334-340.
17. ASTM C150 / C150M - 20 *"Standard Specification for Portland Cement"*
18. ASTM C33 / C33M - 18 *"Standard Specification for Concrete Aggregates"*
19. ASTM C39 / C39M - 21 *"Standard Test Method for Compressive Strength of Cylindrical Concrete Specimens"*

3rd Conference on Sustainability in Civil Engineering (CSCE'21)
Department of Civil Engineering
Capital University of Science and Technology, Islamabad Pakistan

MECHANICAL AND DURABILITY PROPERTIES OF POLYPROPYLENE CONCRETE CONTAINING BENTONITE AND SILICA FUME

[a] Inzimam Ul Haq*, [b] Ayub Elahi, [c] Syed Aamir Qadeer Shah, [c] Malik Ahmad Ghaffar

a: MSc student, Department of Civil Engineering, University of Engineering and Technology Taxila. inzimamsafi@gmail.com
b: Professor at Department of Civil Engineering, University of Engineering and Technology Taxila. ayub.elahi@uettaxila.edu.pk
c: Dy. Chief Engineer (Civil), OGDCL Islamabad. aamirqadeer@ogdcl.com

Abstract- This paper reports the mechanical and durability properties of bentonite and silica fume (SF) concrete containing fibrillated micro polypropylene fibers (PPF). The fresh property was investigated by slump test and mechanical property was investigated by compressive strength and ultrasonic pulse velocity (UPV) tests. For durability properties, permeability test was performed. This research is based on the previous published research and selected the optimum percentages of supplementary cementing material (SCMs) for bentonite and SF. The concrete mixture consists of total of nine mixes: control mix (CC), two binary mixes (i.e., 10% bentonite (B10SF0P0), 10% SF(B0SF10P0)), ternary mix (B10SF10P0), also known as ternary control mix (TCC) and then additional mixes by adding polypropylene fiber equal to 0%, 0.25%, 0.50%, 0.75%, 1% and 1.25% in TCC. It was concluded that all the binary and ternary mixes showed decrease in the workability. The UPV test indicated good quality of concrete for binary mixes and ternary mixes up to the PPF content equal to 0.75%. It was observed that compressive strength and permeability properties of concrete were improved for both the binary mixes and ternary mixes up to addition of PPF equal to 0.5%. PPF increased the deformability properties and completely changed the failure pattern of concrete as compared to ternary mix without PPF.

Keywords- Workability, supplementary cementing material, bentonite, compressive strength, ultrasonic pulse velocity, permeability.

1 Introduction

In the current era, Pakistan is trying to boost their economic state and provide best standard of life to the inhabitant of the state. To facilitate the public and provide standard of living, different projects are on their track line, like housing, highway, dam and the most important CPEC projects. For all these infrastructure of development projects, concrete is one of the abundantly used construction material. Cement is the important constituent of concrete responsible for binding all other ingredients. All these projects increase the demand of cement [1]. Recently Govt of Pakistan announced to increase the cement manufacturing industries to fulfil the current huge demand required for infrastructure development. Cement industry is responsible for consuming large amount of energy and CO_2 emission that ultimately causes climatic problem [2]. Supplementary cementing material (SCMs) is one of the solutions to minimize the consumption of natural raw material for cement, energy consumption and reduce the negative impacts on the environment. Different researchers used SCMs to investigate fresh properties and hardened properties to study mechanical and durability performance of concrete [3] [4]. The pozzolanic material can also be added during the manufacturing process of cement at different proportion. Uzal et al [5] studied the manufacturing laboratory based blended Portland cement by addition of natural volcanic pozzolanic material. Experimental study was limited to material from two volcanic sources by 55% replacement at different grinding time. The blended cement improved compressive strength and reduced the ability of alkali silica expansion.

Bentonite is a pozzolanic material abundantly available in Pakistan. Different researchers worked on bentonite as a partial replacement of cement [6] [7]. Memon at al., observed that the particle size of bentonite is flaky and elongated, which tends to reduce the workability [8]. SF is being used as partial replacement of cement at a certain proportion to increase certain mechanical and durability properties. From the scanning electron microscopy, it was observed in past research that the use of silica fume in concrete significantly reduced the porosity and provide dense concrete, which ultimately reduced the permeability [9]. In another study, SF increased both mechanical and durability properties of concrete due to the formation calcium silicate hydrate gel (C-S-H) in the result of pozzolanic reaction [10]

The addition of PPF and polyester fibers improved mechanical properties and ductility. In addition, PPF showed greater ductility than polyester fiber [11]. PPF significantly reduced workability, increased air content, improved ductility of mortar. Increase in the proportion of PPF, permeability was increased [12]. The combine effect of SCMs improved the mechanical and durability properties of concrete and different fibers were added to improve the ductility properties [13]. Akbar et al studied the combine effect of Pakistani bentonite and SF on various aspects of high-performance concrete [3].

The use of Bentonite and SF as a partial replacement of cement increased the mechanical, durability properties of concrete along with reducing the emission of global warming gases and reduced the cost of concrete. Further addition of SF in Bentonite concrete increased the mechanical and durability properties of concrete due to the preformation of C-S-H gel. The addition of PPF further increased certain properties of concrete.

However, there is limited and contradictory data available in the literature regarding effect of PPF on binary and ternary mixes of concrete with Bentonite and SF. The proposed study will help the stakeholders of construction industry in using SCMs and PPF without any hesitation for the intended purpose.

2 Experimental Work

2.1 Materials used

Ordinary Portland cement (OPC) of type-I was used as the main binding material followed by ASTM C150 [14]. Specific gravity of OPC was 2.99, initial and final setting time was 109min and 285 min respectively. Bentonite and SF was used as a SCMs. Properties of OPC, Bentonite and SF are shown in the Table 1.

Table 1Properties of OPC, Bentonite and SF

Chemicals	**SiO_2**	**TiO_2**	**Al_2O_3**	**Fe_2O_3**	**MnO**	**MgO**	**CaO**	**Na_2O**	**K_2O**	**P_2O_3**	**LOI**
OPC	17.4	-	10.2	3.6	-	1.8	62.3	0.9	1.4		0.9
Bentonite	56.8	1.45	15.45	12.27		3.71	0.55	-	-	-	6.89
Silica fume	92.2										2.7

Tap water was used both for mixing and curing of the concrete samples. The addition of both SCMs caused reduction in the workability. Water- cement ration was kept constants for all mixes. In order to get the required slump, dosage of superplasticizer was adjusted. Fine aggregate (FA) was used from Lawrencepur source in Pakistan. Coarse aggregate (CA) from Margalla hills source was used in concrete. The maximum size of coarse aggregate was 19mm. The properties of FA and CA are shown in the Table 2. PPF of length 19mm was used. Its properties, as reported by manufacturer [15], are shown in the Table 3.

Table 2. Properties of inert materials

	FA	**CA**
Specific gravity	2.7	2.65
Water absorption (%age)	1.3	0.54
Loose density (Kg/m^3)	-	1412
Rodded density (Kg/m^3)	-	1550
Fineness modulus	2.99	-

Table 3. Properties PPF (Matrixx Company).

Tensile Strength at breakage (MPa)	31-41 [16]
Elongation at break (%)	100-600 [16]
Tensile modulus (MPa)	1137-1551 [16]
Specific gravity	0.9-0.91 [17]

2.2 Mix Proportions

Total nine different mix proportion were used to investigate the mechanical and durability properties of concrete. The optimum percentage for partial replacement of Bentonite and SF was selected on the basis of previous research [18] [7]. A total of nine mixes were prepared with a constant water to binder ratio of 0.5. Mixes include CC mix, 10% bentonite(B10SF0P0), 10% SF (B0SF10P0), ternary mix (B10SF10P0). PPF was then added into the ternary mix with varying percentages up to 1.25% with an interval of 0.25%.

2.3 Sample preparation

Yielding of all the batches of ingredients were done by weight. The ingredients were mixed in an electric concrete mixer and revolved at a rate of 30 rev/min. To get desired workability, Visconcrete 3110 superplasticizer (SP) was used in the concrete mixes. Different sample were prepared for different tests. To get the average value of each testing results, three sample were prepared and tested. Cube of 150x150x150mm was used for compressive strength, whereas, 100x100x150mm size samples were prepared and tested for permeability results. Fresh property was observed through slump test. Hardened properties of concrete were investigated by performing mechanical and durability tests. For mechanical properties, compressive strength was investigated by preparing cubes and ultrasonic pulse velocity test was also performed. For durability property, permeability test was conducted. The coefficient of permeability was calculated by the following formula;

$$k = \mathrm{Qxh/AxtxP}$$

Where Q=discharge from sample; P is hydrostatic pressure; A is sample top surface area; h is sample height and t is permeability time.

3. Results and discussion

3.1 Fresh properties

3.2.1. 3.1.1. Workability

Workability of each mix (with constant water-cement ratio) was determined using slump test according to ASTM C143 [19]. Slump values for varying percentage of Bentonite, SF and PPF were tried to keep constant. Dosage of SP (by %age weight of binder) reflected that workability was reduced by adding Bentonite and SF. It was concluded from the results that the addition of bentonite, SF and PPF significantly reduced the workability. Required dosage of SP for Bentonite binary mix was more as compared to that of SF binary mix, showing comparatively severe effect of Bentonite as compared with that of SF in reducing workability. However, TCC mix, being highest replacement value among unstrengthen mixes used combatively high dosage of SP. For other mixes achieved by adding PPF, there was no improvement, even at maximum permissible dosage of SP. Therefore, Workability results of all the PPF strengthened ternary mix were discarded in the Figure 1. Because of the fine particle size of bentonite and SF compared to cement particle, reduced slump value was experienced. The particle shape of bentonite and SF was flaky and spherical respectively. Due to spherical nature, SF showed better workability than that of Bentonite which is in accordance with other studies [12].

3.2. Mechanical properties

3.2.2. Compressive strength

It is one of the important properties widely used to determine the uniaxial load carrying capacity of concrete. It was determined on cubes according to BS [20]. The results of compressive strength of cubes are shown in the Figure 2. It was concluded that PPF increased the ductility properties of concrete. The addition of Bentonite and SF increased the compressive strength, and PPF showed slightly improvement in the strength up to 0.5% its addition as compared to that of TCC mix, but further increase in the proportion of PPF caused reduction in the compressive strength which is in accordance with previous work [21]. Increase in strength by adding PPF up to 0.5% is due to effective bond of PPF with the cement paste. However, further addition in optimum content of PPF caused decrease in compressive strength. The addition of PPF completely changed the failure pattern of concrete. It was observed with naked eye that there was about half inch deformation without crushing of concrete. However, this deformation was not experienced by control mix, rather crushing was noted. The compressive strength of the TCC mix was improved by about 8% as that of control mix at 90 days. PPF content up to 0.5% addition, showed optimum compressive strength results but further increase in PPF proportion caused decrease in the compressive strength and the mix containing maximum PPF (1,25%) reduced the strength by 44% as compared to the CC mix. It might be due to poor bond between PPF and concrete ingredients. Up to 0.5% addition of PPF, parameter of interlocking was dominate on any adverse effect due to bond between two different materials. When cracks became visible in the sample, there was no reduction in applied load, but the load became constant and only the strain was increased, after a short period of time again the load started increasing due to the bond interlocking capacity of the PPF in concrete.

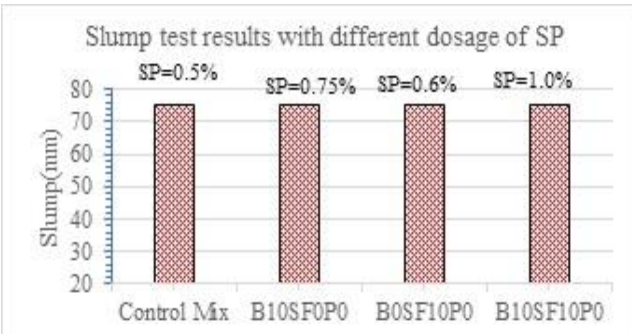

Figure 2. Slump test results

Figure 1. Compressive strength test results

3.2.3. Ultrasonic Pulse Velocity (UPV) Test

The quality of concrete was determined by a non-destructive UPV test by using direct method. A direct pulse transit time was calculated between the two opposite transducers emitter and receiver by passing sound pulse from one transducer to receive by other. The propagation of signal was directly noted and velocity was determined by putting the distance between the transducers. The pulse time taken depends on the uniformity, porosity and cracks availability [22]. From the pulse transit time, velocities were calculated by dividing the pulse distance by transit time. It was performed for cubes in all the three planes of the cube to get the average value of the stable pulse time. From this test quality of concrete was investigated from the velocity of waves. The results of UPV are shown in the Figure 3. From the results it was observed that the addition of bentonite and SF increased the velocity of signals and PPF reduced its value due to porous nature. All the mixes up to 0.75% PPF showed good quality of concrete because its UPV value lies in the range 3660-4575m/s [23]. Greater the addition of PPF fiber, greater was the time to pass the waves in concrete body. It was because of the greater absorption of pulse wave by PPF and voids developed due to PPF and ultimately it reduced the quality of concrete as compared to CC.

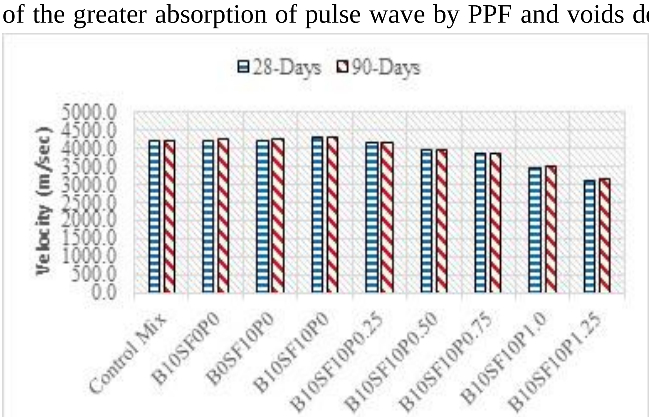

Figure 3. UPV test results

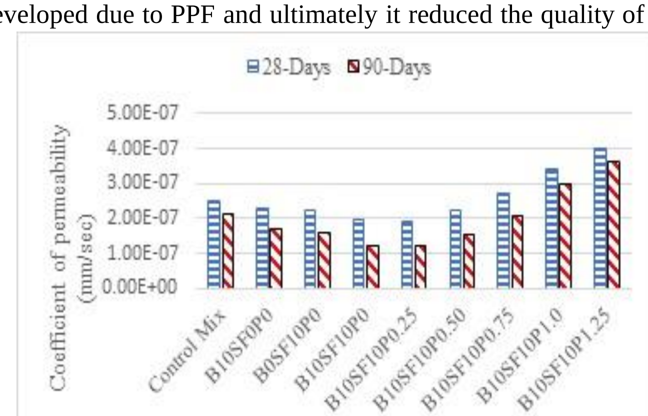

Figure 4. Permeability coefficient of concrete

4. Durability properties

4.1 Permeability

It was observed by an apparatus specially design for permeability test was performed according to Indian Standard [24]. Samples with sizes of 100x100x150 were prepared and cured in water for 24 hours and then cured in room temperature in hessian cloth till 72 hours before the age of testing at 28 days and 90 days. The samples were then oven dried by placing it in oven for a period of 48 hours before performing test on it. The oven dried samples were placed in open air to bring its temperature to atmospheric level and after that they were painted from all the four sides to retain the penetration of water from the sides and water was made to flow from the top and bottom side only. Samples were fitted in the machine and open spaces were closed by silicon abrasive to maintain constant pressure of water and hindering the water to flow out from the sides. After complete dry of silicon, machine was fixed for performing the test [25]. The results of each mix are shown in the Figure 4. From the results it was observed that the TCC mix reduced the penetration of water by 42% compared to CC. It was due to dense structure of concrete and the fine particle of pozzolana. The addition of PPF up to 0.5% contributed in the reduction of permeability and further addition of PPF in concrete increased the permeability due increased in porosity of concrete [12]. The mix containing maximum PPF (B10SF10P1.25) increased permeability by 41.5% as compared to CC mix at 90 days curing.

4.2 Correlation between compressive strength and coefficient permeability

The compressive strength and coefficient of permeability of concrete are inter-related and are dependent on each other. As Bentonite and SF were added into concrete, both compressive strength and coefficient of permeability of concrete were improved, while the addition PPF contributed further improvement in the properties up to the content of PPF equal to 0.5%. There is a linear relationship between compressive strength and coefficient of permeability of concrete at both the ages (28 days as well as 90 days) and these results are in agreement with previous study [7] as shown in the

Figure 5. The results at 90-days for PC as well as RC mixes showed better performance as compared to those obtained at 28-days. It was due to the consumption of free calcium hydroxides produced during the hydration reaction, which make

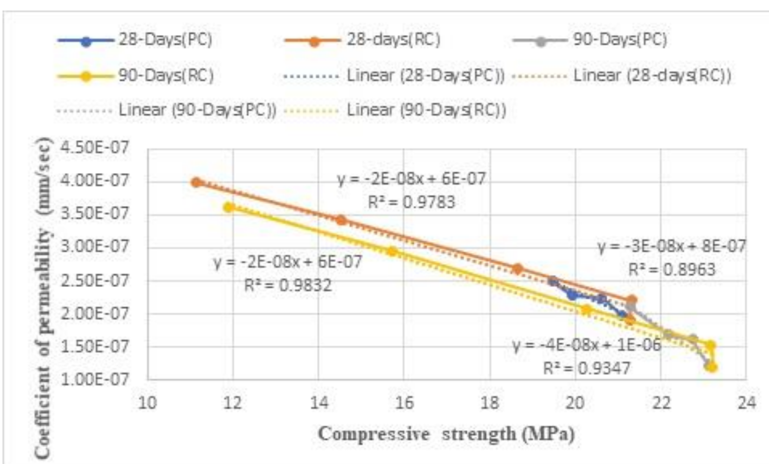

C-S-H gel. This C-S-H gel formation contributed in the strength, durability improvement and made concrete denser.

Figure 5. correlation between compressive strength and Coefficient of permeability

5. Conclusion

This study investigated the partial replacement of cement by bentonite and silica fume on PPF concrete. the effect of SCMs and PPF on various parameter of concrete properties such as compressive strength, UPV, permeability was studied. From the experimental results it was concluded that,

- Compressive strength was increased by addition of SCMs, both Bentonite as well as SF mixes. The ternary mix (B10SF10P0) increased the strength by 8% as compared to CC mix at the age of 90 days.
- Coefficient of permeability of concrete of both binary and ternary mixes were decreased as compared to CC mix. Coefficient of permeability of ternary mix was reduced by 42% as compared with CC mix at 90 days.
- PPF strengthened ternary mixes, containing PPF up to 0.5%, showed reduction in the coefficient permeability PPF content as compared to CC mix. Further addition of PPF increased the coefficient of permeability and ternary mix by 42% as compared with CC mix.
- The addition of PPF increased the ductility and completely change the failure pattern of concrete during compression test.
- There was a linear relationship between compressive strength and permeability as the dosages of PPF increased both at 28 days and 90 days curing.

References

[1] P. K. Mehta, "Greening of the concrete industry for sustainable development," *Concrete International,* 2002.

[2] T. R. W.-J. Da-YoungOh, "CO2 emission reduction by reuse of building material waste in the Japanese cement industry," *Renewable and Sustainable Energy Reviews 38,* vol. 38, p. 796–810, 2014.

[3] B. A. M. A. Junaid Akbar, "Combined effect of Bentonite and Silica Fume properties of High Performance Concrete," *International Journal of Advanced Structures and Geotechnical Engineering,* vol. 02, 2013.

[4] A. E. Muhammad Hamza Irshad, "Effect of rice hush ash on properties of Self compacting concrete containing marble powder," in *International Civil Engineering Conference (ICEC 2020)*, Karachi, 2020.

[5] L. T. B. Uzal, "Studies on blended cements containing a high volume of natural pozzolans," *Cement and Concrete Research 33,* p. 1777–1781, 2003.

[6] I. J. a. H. U. Shams ul khaliq, "Evaluating permeability and mechanical properties of waste marble dust mix concrete and bentonite mix concrete," *ISEC,* 2018.

[7] M. Y. Safi Ur Rehman, "The Influence of Thermo-Mechanical Activation of Bentonite on the Mechanical and Durability Performance of Concrete," *Applied Science,* 2019.

[8] R. A. S. K. T. Y. L. Shazim Ali Memona, "Utilization of Pakistani bentonite as partial replacement of cement in concrete," *Construction and Building Materials,* p. 237–242, 2011.

[9] K. B. M. Rostami, "The effect of silica fume on durability of alkali activated slag concrete," *Construction and Building Materials,* p. 262–268, 2016.

[10] S. D. ,. a. C. I. Ali Hamza, "The effects of silica fume and hydrated lime on the strength development and durability characteristics of concrete under hot water curing condition," in *ASCMCES-17,* 2017.

[11] M. Z. M. K. S. M. M. A. Rohallah Rostami, "The effect of concrete alkalinity on behavior of reinforcing polyester and polypropylene fibers with similar properties," *Cement and Concrete Composites,* 2018.

[12] K. S. M. T. N. Bilal Zaman Afridi, "Mechanical properties of polypropylene fibers mixed cement-sand mortar," *Journal of Applied Engineering Science,* 2019.

[13] B. A. b. A. A. Liaqat Ali Qureshi, "Combined effects of supplementary cementitious materials (silica fume,GGBS, fly ash and rice husk ash) and steel fiber on the hardened properties of recycled aggregate concrete," *Construction and Building Materials,* p. 120636, 2020.

[14] "ASTM C150 / C150M-20, Standard Specification for Portland Cement, ASTM International, West Conshohocken, PA, 2020".

[15] M. Company, "http://matrixxco.net/downloads/duracrete/DURACRETE%20BROCHURE.pdf," 2021.

[16] "ASTM D638 Standard Test Method for Tensile Properties of Plastics".

[17] "ASTM D792 Standard Test Methods for Density and Specific Gravity (Relative Density) of Plastics by Displacement".

[18] A. J. a. U. M. Liaqat A. Qureshi, "Effect of Cement Replacement by Silica Fume on Compressive Strength of Glass Fiber Reinforced Concrete," *International Journal of Structural and Civil Engineering Research,* vol. 7 No 3, 2018.

[19] "ASTM C-143 Standard Test Method for Slump of Hydraulic-Cement Concrete".

[20] "BS EN 12390-3:2019 Testing hardened concrete, Compressive strength of test specimens," 2019.

[21] A. A. M. A. R. S. Z. Tuqa Waleed Ahmed, "Properties of high strength polypropylene fiber concrete containing recycled aggregate," *Construction and Building Materials,* p. 118010, 2020.

[22] "ASTM C597-16 Standard Test Method for Pulse Velocity Through Concrete," 2016.

[23] V. M. Malhotra, Testing Hardened Concrete: Nondestructive Methods, 1976.

[24] "Indian Standard 3085 (1965): Method of test for permeability of cement mortar and concrete," 2002.

[25] A. A. Ayub Elahi, "Experimental investigation of fibre reinforced self-compacting concrete containing marble powder," *ned university journal of research - structural mechanics,* vol. XIV, 2017.

[26] A. E. Bilal Masood, "Mechanical and durability performance of recycled aggregate concrete incorporating low calcium bentonite," *Construction & building material,* pp. 1-8, 28 November 2019.

3rd Conference on Sustainability in Civil Engineering (CSCE'21)
Department of Civil Engineering
Capital University of Science and Technology, Islamabad Pakistan

WORKABILITY OF RICE HUSK REINFORCED CONCRETE FOR EASY POURING

Hafiz Muhammad Bilal

HH Robertson Pak Pvt. Limited m.bilal@robertson.com.pk.
Corresponding author: Email ID: engr.hafizbilal95@gmail.com

Abstract- In the construction industry, the universally used material is reinforced concrete, because of its best durability and cost effectiveness compared to others. The fibre reinforced concrete is also produced by adding fibres and different kinds of fibre in concrete gets importance nowadays. The factor of strength and the quality of the concrete directly depend on the workability property. In this work, in addition to the workability, the compressive strength of the rice husk fibre reinforced concrete is investigated experimentally. The properties of plain cement concrete used as a reference to evaluate the effect of rice husk fibre. It is noted that the workability of the rice husk fibre reinforced concrete is reduced by 8% and the compressive strength is also reduced as compared to the plain cement concrete. Furthermore, the concrete handling becomes harder when the mix is less workable.

Keywords- Rice Husk (RH), Fibres, Concrete Workability, Fibre Reinforced Concrete

1 Introduction

In the construction industry utmost universally used material is reinforced concrete, because of its best durability and cost effectiveness compared to others [1]. Globes world faces very serious environmental and sustainability issues just because of concrete use. The concrete is best in compression but weak in tension. Due to the weak tensile behavior of concrete, its application is limited. The fibre reinforced concrete is produced by adding the different kinds of fibre in concrete to overcome this drawback and to improve the durability and impact resistance of concrete [2]. The addition of natural and artificial fibres in the concrete is developed by the researchers for the structural application [3]. Workability is a very significant property of concrete, which mainly discourses properties such as consistency, flow-ability and compaction of the green concrete [4]. The size of the course aggregate is also effected the workability of fresh concrete. Kronlof et al. [5] Reported that the water requirement reduced with the fine aggregate powder and observed that the better workability achieved by consistent mixing. By adding the fibre, slump value reduced and reported that more water is required if the fibre particles are short [6]. Mehran Khan and Majid Ali, reported that the workability of different fly ash-SPC and fly ash-SCFRC mixes are reduced up to 66%-100% as to that of a PC and CFRC, respectively [7].

Thomas A. Bier et al. [8] Studied that the course aggregate having lower weight and round in shape helped to minimize the workability issue, which is a more common problem in FRC (fibre reinforced concrete). In order to increase the workability of the fibre reinforced concrete the volume of course aggregate should be reduced [9]. As, in the conventional reinforced structures, steel fibre are used, nowadays many researchers used plant fibre as a substitute of steel fibre. There are number of natural fibre used by researchers such as sisal, coconut fiber, jute fibre, hibiscus cannabinus fibre, eucalyptus grandis pulp fibre, Malva fibre, ramie bast fibre, pineapple leaf fibre, kenaf bast fibre, abaca leaf fibre, vakka, date fibre, bamboo fibre, palm fibre, banana fibre, hemp fibre, flax fibre, cotton and sugarcane fibres etc. Natural fibres are locally available in many countries due to which it is very cheap as well. Fibres are used in the construction industry will reduce the overall cost of the project. Handling of the natural fibres are very easy due to their flexibility properties when compared with the steel [10]. The workability of the concrete mix may reduce by adding the fibre and in the FRC use lesser amount of water to avoid honeycombing and bleeding [11]. As, the ration or the content of the fibre increased the workability of the FRC gets reduced significantly [12]. In spite of the fact that whatever the fibre type, workability of concrete reduce significantly by adding the fibre [13].

The applications of agriculture waste like sugarcane bagasse and rice husk ash (RHA) were investigated by many researchers [14] and the utilization of RHA into the concrete are encourages in the construction industry [15].A Million tons of rice are harvested every year in all over the world and approximately 160 tons of rice husk are produced every year, that causes environmental pollution problems and cover a large area of land fill [16]. The quantities of production of rice for the top rice producing country's production in metric ton (Mt) in the years of 2002, 2009, 2010, 2013 and in 2017 are shown in Table 1 [17] and for the year of 2018, 2019, 2020 and for 2021 are shown in Table 2 [18].The Rice husk ash produced by combusting the rice husk and the utilization of rice husk ash in the construction industry provides great advantages by addressing both environmental and commercial concerns. Paddy rice seed is carved with the hard shell of the rice husk, which protects the seeds from the attack of insects, pests, physical damages and delivers nutrient throughout the development of grain [19]. The RH structural layer divided into four parts that are (1) concentration of silica is high, on the rough outer skin with surface hairs, (2) sclerenchyma, (3) spongy parenchyma cells and (4) inner skin. The composition of the rice husk organic compound and chemical composition of the rice, shown in the Table 3 [20].

Table 1: Quantities of rice paddy production [17]

Country	**Rice Production (Mt)**				
	2002	**2009**	**2010**	**2013**	**2017**
China	**177.6**	196.70	197.2	200	210
India	**123**	133.75	120.6	160	163
Indonesia	**48.7**	64.45	66.4	90	74
Bangladesh	**39**	47.7	49.4	45	53
Vietnam	**31.3**	40	40	40	44
West Africa	**10.7**	-	-	13.54	-
Brazil	**10.5**	-	-	12.3	11.9
Pakistan	**5.8**	-	-	9	10.3

Table 2: Quantities of rice paddy production [18]

Country	**Rice Production (1000 MT)**			
	2018	**2019**	**2020**	**2021**
China	148490	146730	148300	149000
India	116480	118870	122000	121000
Indonesia	34200	34700	35200	35300
Bangladesh	34909	35850	34600	35330
Vietnam	27344	27100	27100	26900
West Africa	-	-	-	-

Brazil	7140	7602	7899	7820
Pakistan	7202	7414	8184	8200

Table 3-The composition of rice husk organic compound [20]

Content (%)	C	H	O	N
	36.74	5.51	42.55	0.28

An ample literature is available on concrete with different types of fibre like coconut fibre, bagasse fibre, sugar cane fibre etc. as a substitute of steel reinforcement. The applications of agriculture waste like sugarcane bagasse and RHA were investigated [14]. But, very limited literature is available in which Rice husk used as a fibre in the concrete mix, numerous researchers used rice husk for the removal of heavy metal [21] and in most of the cases, rice husk ash used as partial replacement of cement [22,23,24,25,26]. RH has been utilized in several sectors as construction material in a concrete production and as fuel in power plants [27].

The objective of the present study is to investigate the properties of fresh concrete and hardened concrete experimentally. For this purpose the rise husk fibre having length 0.5cm to 1cm was added in the concrete mix and then slump core test was performed to evaluate the workability of fresh RHFRC. Compressive tests performed to check the properties of hardened concrete and then compared with the value of plain cement concrete to evaluate the effect of fibre. Hence, the addition of rice husk fibre reduced the workability and compressive strength of the concrete.

2 Experimental Procedure

This part of the research shows properties of used material and experimental procedure in this study.

2.1 Raw Materials

The rice husk fibre used in this research was brought from the Sialkot region, where more than 280 tons rice produced every year. In the beginning the rice husk fibres particle size varied in the range of 0.01cm to 3cm. The particles were passed through the sieve number 10, 40, and 100 to remove the dust and small particles and then select the rice husk particle having length 0.5cm to 1cm as shown in Figure 1a, 1b and 1c respectively. The experimental procedure consists the test parameter, preparation of specimens and testing as well. In this research, slump test and compressive test was performed to check the workability and compressive strength of RHFRC respectively.

Figure 1: a. Dust remove from the rice husk, b. small particles, c. selected rice husk particles for test

Ordinary Portland cement, Margalla crush and the locally available sand were used, the sand passed through the sieve number 4 to remove the larger particles of stone. The size of the aggregate varied from 20mm to 30 mm, were used for the preparation of both types of concrete, rice husk fibre reinforced concrete (RHFRC) and plain cement concrete (PCC). Drinkable tap water used and water temperature was normal. Water cement (W/C) ratio was constant for the production of both types of concrete that was 0.5.

2.2 Concrete Mix Design

For the manufacturing of the rice husk fibre reinforced the mix design ratio is 1:2:4 in which 1 part of cement, 2 part of sand and 4 parts of aggregate are used and same mix design is used for the manufacturing of the plain concrete. While 200 grams rice husk having the length 0.5cm to 1cm added into the RHFRC mix and the water cement W/C ratio is 0.5 as shown in Figure 2a.Table 4 represents mix design of rice husk fibre reinforced concrete (RHFRC) and plain cement concrete (PCC).

Table 4- Mix design of RHFRC and PCC

		Content (%)					
Samples	**W/C ratio**	**Cement (Kg)**	**Water (Kg)**	**Sand (Kg)**	**Aggregate (Kg)**	**RH(g)**	**Cylinders**
RHFRC	0.5	4	1.4	8	16	200	2
PCC	0.5	4	1.4	8	16	00	1

2.3 Casting of Sample

The procedures which were adopted during the casting of the 3 cylinders in which 2 is for RHFRC and 1 for PCC for the given study is given as under.

To ensure the uniformity in the material and greatest possible blending, cement is mixed thoroughly by dry hand. Aggregate is air dried for each batch before using in the mix. Portable water having room temperature is used. Electronic weight balance is used for proportioning of the material and the weight of material done by the weight per cubic foot concrete. The sequence of the material placed in the mixer machine is followed by the standards. First of all ¼ of the aggregated placed in the mixer machine, then ¼ sand, ¼ fibre and then ¼ cement placed respectively, and repeats this for four times as shown in figure 2b. Then the mixed machine on for 1 minute without adding the water so that fibre mixed uniformly into the material. Water is added in three portions to avoid the bleeding phenomenon and mixed the material for 3 minutes. For RHFRC and PCC, 3 cylinders of 150x300mm (6 x 12 inches) was poured in which 2 cylinders are for RHFRC and 1 is for PCC. The average strength of RHFRC specimens is taken. The concrete filled into the mold in layers having an approximate height equal to 5cm and given 25 strokes per layers with the tamping rod of 10x300mm. After initial setting time, all the sample of PCC and RHFRC are labeled for identification.

a) *b)*

Figure 2: a. Material used in the RHFRC, b. placement of material in the mixer machine by parts

3 Testing Methods

3.1 Slump cone test

The workability of the manufactured RHFRC and RHFRC investigated by using the slump core test. As, according to the best knowledge of the author there is no specific method of mixing of fibre reinforced concrete is available, so the methodology for filling of slump core by layers is adopted. A slump core test is performed to check the workability of the fresh concrete, as per the ASTM standards C143/C143M-15a [28]. The slump core is open at the both ends and have handles to carry and the slump cone typically has an internal diameter of 100 mm, at the top and 200mm at the bottom, with the height of 305mm is used to perform the slump test. The cone is placed on the cleaned surface. The cone is filled in three stages with the fresh concrete. Each layer, each time is tamped for 25 times with the metal rod which have standard dimensions. The extra concrete is cleaned out from the molds at the end of the third layer as well.

a) b)

Figure 3: a. Measuring the slump value of the RHFRC, b. Compressive test of the RHFRC

The mold is vertically lifted upward carefully, so as not to disturb the concrete's cone, then the concrete will slump as shown in Figure 3a. The cone is placed upside down near the concrete cone. The tamping rod is placed over the slump cone in such way that the rod other edge reaches the concrete cone. Then the slump value measured by measuring the distance from the top level of the slump cone to the slump concrete top. The slump test is significantly suitable and acceptable, having a slump of median to low workability. The suitable slump range varied from 5mm to 260 mm.

3.2 Compressive Strength Test

The 14 days compressive strength of the RHFRC and PCC samples was determined by using ASTM C-39 [29] procedures. Cylinders having dimensions 150mmx300mm were placed in water at normal temperature for 7 days, and then the samples were placed in a room for 7 days, where the temperature was maintained at 27 Celsius and the relative humidity at 50%. The 0.25 MPa/sec pressure rate was maintained throughout the test.

4 Results and discussion

4.1 Workability of fresh concrete

The slump values of RHFRC and PCC are 15mm and 40mm respectively. It is observed that the slump value is significantly reduced by adding the rice husk fibre in the concrete. Although the concentration of the RH has been just 200 grams. Hence the water absorbed by the fibre is greater which disturbed the water cement ratio (W/C), so to maintain the workability free water is not available. Figure 3a represents the slump value of the rice husk fibre reinforced concrete and it is observed that too much variation is noted by adding just 5% rice husk fibre in the concrete when compared with the plain cement concrete. The overall drop in the slump value of the plain cement concrete is about 25 mm which has significant value. If the length and the ratio of the fibre increases the slump value will also decreases.

4.2 Compressive strength of hardener concrete

It is observed that the compressive strength of the rice husk fibre reinforced concrete is 4.8MPa while the compressive strength of the plain cement concrete is 5.231MPa. Although, the concentration of the rice husk fibre is very low, but it is observed that by the addition of the rice husk fibre into the concrete mix decreased the compressive strength, when compared with the plain cement concrete. It can be noted that in case of PCC spalling of concrete were observed while only cracks were developed in case of RHFRC. The crushed RHFRC cylinder specimen which consists fibre content as shown in Figure 3b.

4.2 Ease with concrete handling.

Easy to transport and place of the concrete means easy to handle the concrete and it depends on the workability and consistency of concrete. The size of the aggregate and water cement ratio (W/C) play a vital role in the easy handling of the concrete. Plain cement concrete (PCC) is easy to handle and transport when compared with the rice husk fibre reinforced concrete (RHFRC). This is just because the slump value is reduced and effected by adding the rice husk fibre in the concrete mix and observed that the placing of the RHFRC is little bit harder as compared to the PCC. Moreover, the handling with the RHFRC become difficult when the time passed compared with the PCC. This difficulty is observed due to water absorption capacity of the fibre. This observation shown that the addition of the fibre into the mix made it harder to transport, place and handle.

5 Conclusion

An experiment was conducted to investigate, inspect and evaluate the workability and the compressive strength of the rice husk fibre reinforced concrete and the plain cement concrete. For the manufacturing of RHFRC and the PCC the mix design ratio is constant. While 200 grams rice husk fiber having length 0.5cm to 1cm added into the RHFRC mix and the water cement W/C ratio is 0.5. Slump test performed to evaluate the workability. It is noted that the workability of the rice husk fibre reinforced concrete is reduced by 8% when compared with the plain cement concrete. The compressive strength of the RHFRC is 4.78MPa which is less than the compressive strength of the plain cement concrete that is 5.23MPa. So, the addition of the fibre will reduce the compressive strength of concrete as compared to the plain concrete. Concrete handling become harder, as much as the mix is less workable. The handling and placement of the PCC is easier as compared to RHFRC.As, the workability helps in the proper placement of the concrete as well.

From the results, it is observed that the addition of the natural fibre in the concrete mix imposes significant effect in the reduction of the compressive strength and the workability. The handling of the concrete, highly affects from the workability. The use of rice husk fiber resultantly decreases the workability, and difficult to handle and place as well. So, a greater water cement (W/C) ratio is required to get high workability while incorporating rice husk (RH) fibre into the concrete mix.

Acknowledgment

The authors would like to thank every person/department who helped thorough out the research work, particularly to the Prof. Dr. Majid Ali. The careful review and constructive suggestions by the anonymous reviewers are gratefully acknowledged.

References

[1] Lingling Hu, Zhen He and Shping Zhang, " Sustainable use of rice husk ash in cement-based materials: Environmental evaluation and performance improvement," *Journal of Cleaner Production*", Vol. 264, pp. 121744, 2020.

[2] F. Liu, W. Ding, Y. Qiao and Yafei Qiao, " Experimental investigation on the flexural behavior of hybrid steel-PVA fibre reinforced concrete containing fly ash and slag powder," *Construction and Building Materials*", Vol. 228, pp. 116706, 2019.

[3] Kene, K. S., Vairagade, V. S., & Sathawane, S. (2012). Experimental study on behavior of steel and glass fibre reinforced concrete composites. *Bonfring international journal of industrial engineering and management science*, *2*(4), 125-130.

[4] Choudhary, Harish, A. M. Siddique, and Dauji Saha. "Effect of clay fines on strength and workability of concrete." In *Proceedings of International Conference on Architecture, Civil and Environmental Engineering (ACEE2019), Jawaharlal Nehru University, New Delhi, India*. 2019.

[5] Kronlöf, Anna. (1994). "Effect of very fine aggregate on concrete strength". Materials and Structures, 27, 15-25.

[6] ACI Committee 544, 1999, Measurements of Properties of Fibre Reinforced Concrete, ACI 544-2R-89.

[7] Khan, Mehran, and Majid Ali. "Improvement in concrete behavior with fly ash, silica-fume and coconut fibres." *Construction and Building Materials* 203 (2019): 174-187.

[8] Ali, Ahsan, Shahid Iqbal, Klaus Holschemacher, and Thomas A. Bier. "Effect of fibres on bond performance of lightweight reinforced concrete." *Periodica Polytechnica Civil Engineering* 60, no. 1 (2016): 97-102.

[9] Khayat, Kamal H., Fodhil Kassimi, and Parviz Ghoddousi. "Mixture design and testing of fibre-reinforced self-consolidating concrete." *ACI Materials Journal* 111, no. 2 (2014): 143.

[10] Ali, Majid, Anthony Liu, Hou Sou, and Nawawi Chouw. "Mechanical and dynamic properties of coconut fibre reinforced concrete." *Construction and Building Materials* 30 (2012): 814-825.

[11] Mohod, Milind V. "Performance of steel fibre reinforced concrete." *International Journal of Engineering and Science* 1, no. 12 (2012): 1-4.

[12] Mohod, Milind V. "Performance of steel fibre reinforced concrete." *International Journal of Engineering and Science* 1, no. 12 (2012): 1-4.

[13] Vafaei, Davoud, Reza Hassanli, Xing Ma, Jinming Duan, and Yan Zhuge. "Sorptivity and mechanical properties of fibre-reinforced concrete made with seawater and dredged sea-sand." *Construction and Building Materials* 270 (2021): 121436.

[14] A. A. Dayo, "Use of sugarcane bagasse ash as a fine aggregate in cement concrete", Engineering Science and Technology International Research Journal, Vol. 3, No. 3, pp. 8-11, 2019.

[15] Naraindas Bheel, Muneer Ali Jokhio and Javed Ahmed Abbasi, "Rice Husk Ash and Fly Ash Effects on the Mechanical Properties of Concrete," *Engineering, Technology & Applied Science Research*", Vol. 10, pp.5402-5405, 2020.

[16] Cristina Barris, Pau Sala, Javier Gómez and Lluís Torres, "Flexural behaviour of FRP reinforced concrete beams strengthened with NSM CFRP strips",*Composite Structures*",Vol. 241, pp.11205,2020.

[17] Mohammad A. Mosaberpanaha and Sadiq A. UMAR, "Utilizing Rice Husk Ash as Supplement to Cementitious Materials on Performance of Ultra High Performance Concrete – A review", *Materials Today Sustainability*",Vol. 7–8, pp. 100030, 2020.

[19] Yanping Zou and Tiankui Yang, "Rice Husk, Rice Husk Ash and Their Applications", *Rice Bran and Rice Bran Oil, Chemistry, Processing and Utilization*, pp. 207-246, 2019.

[20] Mohiuddin, Obaidullah, Abdullah Mohiuddin, Madina Obaidullah, Humayun Ahmed, and Samuel Asumadu-Sarkodie, "Electricity production potential and social benefits from rice husk, a case study in Pakistan." *Cogent Engineering* 3,2016.

[21] Zou, Yanping, and Tiankui Yang. "Rice husk, Rice husk ash and their applications." In *Rice Bran and Rice Bran Oil*, pp. 207-246. AOCS Press, 2019.

[22] Muthukrishnan, Souradeep Gupta and Harn Wei Kua,"School of Design and Environment Architecture," *Department of Building,National University of Singapore*", 2019.

[23] Pokpong Rattanachu, Prajak Toolkasikorn, Weerachart Tangchirapat, Prinya Chindaprasirt and Chai Jaturapitakkul," Performance of recycled aggregate concrete with rice husk ash as cement binder," *Cement and Concrete Composites*",Vol. 108, pp. 103533, 2020.

[24] Farshad Ameri, Parham Shoae, Nasrollah BahramLi, *et al.*,"Optimum rice husk ash content and bacterial concentration in self-compacting concrete," *Construction and Building Materials*",Vol. 222, pp. 796-813, 2019.

[25] Peter A. Adesinaa and FestesA.," Structural properties of sustainable concrete developed using rice husk ash and hydrated lime," *Journal of Building Engineering*",Vol. 25, 2019.

[26] Sung-Hoon Kanga, Sung-Gul Honga and Juhyuk Moonc," The use of rice husk ash as reactive filler in ultra-high performance concrete," *Cement and Concrete Research*",Vol.115, pp. 389-400, 2019.

[27] Azat, S., A. V. Korobeinyk, K. Moustakas, and V. J. Inglezakis. "Sustainable production of pure silica from rice husk waste in Kazakhstan." *Journal of cleaner production* 217 (2019): 352-359.

[28] Standard, A. S. T. M. "Standard test method for slump of hydraulic-cement concrete." *ASTM Annual Book of ASTM Standards*, 2015.

[29] Standard, A. S. T. M. "Standard test method for compressive strength of cylindrical concrete specimens." *ASTM C39*, 2010.

3rd Conference on Sustainability in Civil Engineering (CSCE'21)
Department of Civil Engineering
Capital University of Science and Technology, Islamabad Pakistan

WORKABILITY OF BANANA FIBERS REINFORCED CONCRETE FOR EASY POURING

[a] *Muhammad Abrar*

a: Department of Civil Engineering, University of South Asia Lahore, abrar19125@gmail.com

Abstract- Concrete is the most widely used construction material in construction industry. Workability is the property of concrete which is directly related to the strength factors and quality of work. Workability of concrete is determined to ensure ease of handling. Natural Fibers are added in concrete to achieve desired properties and results in reduction of cost and light weight structures. The purpose of this study is to check the workability of specimen having banana fibers of 50 mm length for easing pouring and handling. For the study of workability banana fiber reinforced concrete (BFRC) slump cone test is performed. Banana fiber is added 2.5% by mass of cement content. The value of BFRC slump test is compared with the value obtained by the slump test of plain concrete (PC). The results revealed that by the addition of banana fibers the value of slump decreased. It is concluded that the workability depends upon the ingredients of concrete as well as the additional materials which are used to enhance or achieve desired properties.

Keywords- Banana Fibers, Banana Fibers Reinforced Composites. Slump Test.

1 Introduction

Concrete is the back bone of construction industry [1]. By the passage of time the utilization of concrete is growing day by day. This can be due to increase of urbanization rate in developing countries and even developed countries. Concrete has adverse ecological affects and there is always need to reduce the impacts of concrete on environment. Sustainable material is always needed to reduce the cement content of concrete resulting in reduction of air pollution due to less emission of carbon dioxide (Co_2) in air. Concrete is a brittle material which is stronger in compression phase and weaker in tension [2] [3].The natural fibers have gained popularity for using in concrete due to their eco-friendly nature, economical and good physical properties. The utilization of natural fibers in concrete lead to reduction of workability of concrete [4]. Workability is the property of concrete which is directly related to the strength factors and quality of work. By the addition of fibers the workability is reduced [5]. Banana fiber is lignocellulose natural fiber so by addition of banana fiber (BF) the concrete become less workable. This is due to the increase of water absorption because of presence of banana fiber [6]. Owing to the fact of increased water absorption property of concrete the slump test value is decreased.

Therefore, not only banana fibers, the usage of all agricultural natural fibers may lead to reduction in workability [7]. By the increment of quantity of fibers in concrete the value of slump test performed on fresh concrete is decreased [8] [9] [10]. Slump test is performed both on site and in laboratory for determination of workability of concrete [11] [12]. Workability of concrete is related with the value of slump test. If the slump value is high then the material is considered as more workable and vice versa. Raw materials and additional fibers have great influence on workability. Hence, workability is controlled by these ingredients and water to cement ratio (W/C) in concrete. Less water cement ratio results in reduction of workability i.e. slump cone test value. To overcome this flaw different types of plasticizers and super-plasticizers are used [13]. These admixtures help in increment of workability. Many researchers reported the influence of agricultural natural fiber on properties of concrete when they are used in concrete composites [14]. Jute is also a natural fiber and it is used by researchers to enhance the mechanical, dynamic and absorption proprieties of concrete. It is also found that by the use of jute natural fibers, there is increases in resistance against the impact loadings [15]. With the popularity of use of admixtures in concrete, it has been observed that the fibers in concrete enhanced the properties when used with admixtures. Admixtures solely may not perform better than the combination of fibers with them [16]. Numerous studies are being conducted by different researchers on the effect of fibers on workability and mechanical properties of concrete [17] [18] [19].

There are a number of studies present on the workability of artificial fibers [20]. But the literature on the workability of agricultural natural fibers is very less. Workability plays a vital role in the hardened properties of concrete. So, there is need to investigate the workability of natural fibers reinforced composites (NFRC). For this purpose banana fiber reinforced composite (BFRC) is casted with 2.5% content of banana fiber by the mass of cement content. Slump cone test is performed to check the workability of BFRC for easy pouring and handling. If the value of workability test is undesirable it may deviate from the required properties of concrete. Lower value of slump means the concrete is less workable and it will cause difficulty in handling and pouring, can lead to decreased in strength. The study will help to understand the workability of PC and BFRC. It will also help to understand the usage of agricultural waste like banana fiber in concrete and its effects towards the workability of fresh concrete but the determination of water absorption is not included in this work.

2 Methodology

2.1 Raw materials.

For the production of PC, Ordinary Portland cement (OPC) and Margalla crush were used along with locally available sand. The max. size of aggregate was taken as 20 mm for production of both PC and BFRC. For the preparation of fiber reinforced composite (FRC), banana fiber was used. Banana fiber used in slump cone test is shown in figure 1. The length of banana fiber was kept fixed as 5 cm (50mm). Tap water of normal temperature was used for the preparation of both PC and BFRC. PC was prepared by the water cement ration (W/C) of 0.6 and 0.7 W/C was used for preparation of BFRC.

Figure 1: Combed banana fibers of 50mm length.

2.2 Mix design and concrete preparation.

For plain concrete preparation, cement, sand and course aggregates ratio for mix design was 1, 2 and 4 respectively. The water to cement ratio (W/C) was 0.6 for PC. Same mix design was executed for the production of BFRC. To the best of the author's knowledge there is no standard present for mixing of BFRC so, layer method was adopted. The W/C was increased to 0.7 for BFRC because of presence of fiber. This increment was also for making it workable and for good compaction because poor compaction may lead to reduction in strength. The addition of water was carried out stepwise to avoid bleeding. All materials were added in a way that they may mixed efficiently. To prepare PC, all materials were added in concrete mixer along with water and mixer was rotated for three minutes. For the preparation of BFRC, one third of the aggregates were spread in concrete mixer followed by the one third of BF content. Then one third of sand and the same content of cement were placed and spread in mixer. Same procedure was adopted for three layers of each, aggregates, fibers, sand and cement. After the addition of one third water content, concrete mixer was rotated for three minutes. The remaining water was added in increments to make BFRC workable.

2.3 Workability test

Slump test is performed to find out the consistency or workability of concrete. This test is performed both in laboratory and at construction site before pouring of concrete into testing moulds. ASTM standard C143/C143M-15a states that slump test is the method which provides a procedure to investigate the slump of plastic hydraulic concrete [21]. The slump cone is used in test has top diameter of 100 mm and bottom diameter of 200 mm. The length of temping rod used for compacting is 600 mm and it's both ends are hemispherical with diameter of 16 mm. The first concrete layer is placed in 1/3 volume of cone. Compaction is performed by dropping temping rod at random places in the cone from a height of 25mm. Remaining two layers are also filled and efficiently compacted by earlier described way. By rolling and screeding, surface can be made smooth. Cone is lifted vertically up and placed besides the concrete which is moulded by slump cone. Ensure upside down before placing it besides the moulded concrete. Temping rod is placed over the upper surface of cone in such a way that half of the temping rod length may cover concrete mould. Ruler is use to read the slump value of concrete as shown in figure 2.

Figure 2: Measuring the slump value of BFRC

3 Results and Analysis

3.1 Slump of fresh concretes

The values of slump for plain concrete and BFRC, addition of BF to produce BFRC and W/C are present in table 1. Values of slump for PC and BFRC are 40mm and 10 mm respectively. It can be noticed that there is considerable decrease in the value of slump for BFRC having 2.5% BF. The W/C ratio is increased for BFRC but even after increment of water content there is huge decrease of 75% in value of BFRC. The decrease of slump value for BFRC is may be due to the water absorption of banana fiber. The water absorption of natural banana fibers reduce the water content in other ingredients of concrete. The addition of fiber may reduce the workability of concrete.

Table:1-Water cement ratio (W/C) and slump of PC and BFRC

Mix	BF addition (%)	W/C (ratio)	Slump (mm)
PC	0	0.6	40
BFRC	2.5	0.7	10

3.2 Ease with concrete handlings.

The transportation and pouring of concrete depends upon the workability of concrete. The water cement ratio has great influence on the workability of concrete. If concrete does not meet the required water cement ratio then it results in reduction of slump value. BFRC is less workable as compared to PC as it has less value of slump test. Greater is the slump value, more is the workability and vice versa. PC has more workability i.e. slump value of BFRC is reduced by the addition of natural banana fibers in it. So, as a result of this the handling of BFRC is difficult as compared to PC. This is due to water absorption property of BF. The water provided in concrete during mixing is absorbed by fiber content present in mixture and other ingredients get less amount of water. Due to the reduced content of water in ingredients, it becomes harder and difficulty is faced during its transportation and pouring. The concrete with reduced slump value is also difficult to compact during compaction of concrete in molds.

4 Conclusions

The Plain concrete (PC) and banana fibers reinforced composite (BFRC) are evaluated in terms of workability. For this purpose, slump test is performed on both PC and BFRC. The fiber content by mass of cement and length are kept as 2.5% and 50 mm respectively. By conducting this study following conclusions can be drawn.

- By the addition of banana fiber there is huge decrease in workability of BFRC as compared to PC.
- Workability of BFRC is reduced to 75% as compared with PC.
- Less value of slump leads towards the difficulty of the concrete handling and concrete matrix becomes less workable.
- PC is more convenient to handle and transport as compared to BFRC.

The above mentioned outcomes indicated that the difficulty of handling is caused by less workability. The banana fibers have drawbacks towards the workability of BFRC. More amount of W/C as compared to PC is required to BFRC to make it more workable. Plasticizers and super plasticizers may also be used to enhance workability.

Acknowledgment

The author would like to thank every person/department who helped thorough out the research work, particularly CE department and Engr. Prof. Dr. Majid Ali whose hand of kindness remained present at every step.

References

[1] H. Tian, Z. Zhou, Y. Zhang, Y. Weic, "Axial behavior of reinforced concrete column with ultra-high performance concrete stay-in-place formwork," Engineering Structures, 2020.
[2] F. Aslani, B. Samali, "High Strength Polypropylene Fibre Reinforcement Concrete at High Temperature," Fire Technology, 2014.
[3] M. Khan, M. Ali, "Improvement in concrete behavior with fly ash, silica-fume and coconut fibres," Construction and Building Materials, 2019.
[4] M. Ali, N. Chouw, "Coir Fibre and Rope Reinforced Concrete Beam," Australian Earthquake Engineering Society Conference, Newcastle , 2009.
[5] W. Huanga, W. Quan, P. Ge, "Orthogonal tests investigation into hybrid fiber-reinforce recycled aggregate concrete and convolutional neural network prediction," Journal of Asian Architecture and Building Engineering, 2021.
[6] J. R. Aseer, K. Sankaranarayanasamy, S. R. Elsen, A. K. Thakur, "Experimental studies on water absorption properties of acetic acid treated banana fiber composites," Materials today: Proceedings, 2021.
[7] A. Wongsa, R. K. watwong, S. Naenudon, V. Sata, P. Chindaprasirt, "Natural fiber reinforced high calcium fly ash geopolymer mortar," Construction and Building Materials, vol. 241, 2020.
[8] S. Guler, B. Öker, Z.F. Akbulut, "Workability, strength and toughness properties of different types of fiber-reinforced wet-mix shotcrete," Structures, pp. 781-791, 2021.

[9] W. Ahmad, S. H. Farooq, M. Usman, M. Khan, A. Ahmad, F. Aslam, Rayed Al Yousef, Hisham Al Abduljabbar, Muhammad Sufian, "Effect of Coconut Fiber Length and Content on Properties of High Strength Concrete," Materials, 2020.

[10] M. A. Faris, M. M. A. B. Abdullah, R. Muniandy, M. Firdaus, A. Hashim, K. Błoch, B. Jeż, S. Garus, P. Palutkiewicz, N. Aida, M. Mortar, M. F. Ghazali, "Comparison of Hook and Straight Steel Fibers Addition on Malaysian Fly Ash-Based Geopolymer Concrete on the Slump, Density, Water Absorption and Mechanical Properties," Materials, 2021.

[11] Y., I. Cheng, " Exploring Concrete Slump Model Using Artificial Neural Networks," Journal of Computing in Civil Engineering, pp. 217-221, 2006.

[12] I. C. Yeh, "Modeling slump flow of concrete using second-order regressions and artificial neural networks," Cement and Concrete Composites, pp. 474-480, 2007.

[13] M. Nematzadeh, A. Maghferat, M. Rezaei, Z. Herozi, "Mechanical properties and durability of compressed nylon aggregate concrete reinforced with Forta-Ferro fiber: Experiments and optimization," Journal of Building Engineering, 2021.

[14] M. Ali. M. U. Farooqi, "Contribution of plant fibers in improving the behavior and capacity of reinforced concrete for structural applications," *Construction and Building Materials*, pp. 94-107, 2018.

[15] T. Hussain, M. Ali, "Improving the impact resistance and dynamic properties of jute fiber reinforced concrete for rebars design by considering tension zone of FRC," Construction and Building Materials, 2019.

[16] J., G. Peng, X. Wang, S. Hu, C. Ran, P. Sun, K. Zeng, L., "Influence of magnesium slag as a mineral admixture on the performance of concrete," Construction and Building Materials, vol. 295, 2021.

[17] K. F. Li, C. Q. Yang, W. Huang, Y. B. Zhao, Y. Wang, Y. Pan, F. Xu, "Effects of hybrid fibers on workability, mechanical, and time-dependent properties of high strength fiber-reinforced self-consolidating concrete," Construction and Building Materials, 2021.

[18] C. Li, L. Miao, Q. You, S. Hu, H. Fang, "Effects of viscosity modifying admixture (VMA) on workability and compressive strength of structural EPS concrete," Construction and Building Materials, 2018.

[19] Z. Pan, Y. Zhu, D. Zhang, N. Chen, Y. Yang, X. Cai, "Effect of expansive agents on the workability, crack resistance and durability of shrinkage-compensating concrete with low contents of fibers," Construction and Building Materials, 2020.

[20] D. Gao, Z. Gu, Y. Pang, L. Yang, "Mechanical properties of recycled fine aggregate concrete incorporating different types of fibers," Construction and Building Materials, 2021.

[21] AMERICAN SOCIETY FOR TESTING AND MATERIALS. ASTM C143, "Standard Test Method for Slump of Hydraulic-Cement Concrete," Astm C143/C143M-20, pp. 1–2, 2020.

3rd Conference on Sustainability in Civil Engineering (CSCE'21)
Department of Civil Engineering
Capital University of Science and Technology, Islamabad Pakistan

EFFECT OF CARBON BLACK ON PROPERTIES OF STEEL FIBER-REINFORCED CONCRETE

[a] *Abasal Hussain**, [b] *Zahoor Hussain*

a: Department of Civil and Environmental Engineering, The Hong Kong Polytechnic University, Kowloon, Hong Kong, China, abasal.hussain@connect.polyu.hk
b: Department of Civil Engineering, Zhengzhou University, Zhengzhou, Henan 450001, China, dutian17@outlook.com
* Corresponding author: Email ID: abasal.hussain@connect.polyu.hk

Abstract- In this research work, hybrid conductive materials like carbon nano black (CNB) and macro steel fiber (SF) are integrated into the cementitious composite to investigate the mechanical properties and self-sensing properties of the conductive concrete flexural members. For that purpose, 70 kg/m^3 steel fiber with three different dosages of carbon black is evaluated. The mechanical properties like compressive strength, flexural strength and toughness are evaluated. Furthermore, the relationship of fractional change in resistance (FCR) and crack opening displacement (COD) has been determined to study the effect of different types of conductive materials on the gauge factor. The results reveal that the mechanical properties (compression strength, toughness, and flexural strength) are improved with diphasic conductive admixture. Furthermore, the gauge factor is enhanced with the addition of CNB.

Keywords- Self-sensing concrete; steel fiber; carbon nano black; the fractional change in resistance**.**

1 Introduction

Concrete civil infrastructures throughout their service life are pregnable to different loadings, fatigue, erosion, or aging, which leads to the collapse of concrete infrastructures [1]. Therefore, the proper maintenance and monitoring system is required for long-term durability. Structural health monitoring (SHM) in civil infrastructure is an emerging technology in the past few decades. SHM of concrete structures is applied to give information about structural conditions regarding durability and contribute to the extent of their service life [2], [3]. For this purpose, different health monitoring systems are utilized in civil infrastructure. Different sensors are attached, which are expensive, short lifetime and all above incompatibility with concrete structure. Therefore, it is not the permanent and filed deployable solution for SHM.

These are some of the reasons which lead to the development of conductive concretes. The conductive (piezoresistive behaviour) concrete is fabricated by adding a different conductive fiber and fillers. Piezo resistivity can be described as the physical property of materials that changes electrical resistivity when the material is subjected to mechanical strain [5], [6]. The hybrid use of different conductive materials improves not only the conductive properties but also the mechanical properties of the cementitious matrix. For this purpose, micro and/or nano-scale fiber and conductive fillers are normally used to produce structural conductive concrete. Numerous types of conductive fillers have been explored i.e., carbon fibers[7]–[9], carbon nanotubes[10]–[12], steel fibers [13], [14], and carbon black [15]–[17].

Hybrid use of different conductive materials such as fiber and filler would be more effective for improving mechanical and electric conductivity of cementitious matrix by facilitating the conductive matrix and crack bridging by macro fibers. Steel fiber (SF), with its strong electric and mechanical properties, is an ideal material for concrete flexural members. In addition, it shows deflection-hardening behaviour relatively large energy absorption capacity by bridging the cracks with a considerable volume fraction of SF. On the other hand, carbon nano black (CNB) has high chemical and thermal stability, low cost, permanent electrically conductive properties, and a filling effect potentially be employed as ideal materials for the conductive behaviour of concrete.

2 Research significance

Carbon nano tubes and CF have also improved the conductive properties, but the unit cost of the materials is very high as compared to carbon black and they need very extensive dispersion techniques to ensure the proper dispersion. Therefore, this study investigates the carbon nano black with steel fiber to improve the mechanical properties and sensing behaviour of the concrete beam, which is a very cost-effective and field-deployable solution for structural health monitoring in civil infrastructure. The effect of steel fiber and carbon black on the energy absorption capacity of concrete beams is also investigated. Also, the correlation between crack opening displacement (COD) and the fractional change in electrical resistance (FCR) has been examined.

3 Experimental Procedure

3.1. Material properties and base mix design

The mix design of conductive concrete strength grade C30 was used to fabricate the conductive concrete. Ordinary Portland cement 42.5R, class F fly ash. The particle size of quartz sand is 0 ~ 5mm; coarse aggregate size is 5 ~ 10mm and a high-water reducing agent from Sika polycarboxylate superplasticizer (SP) is used.

Table 1-The dosage of conductive materials in a mix design (kg/m^3)

Mix ID	Steel Fibre (SF)	Carbon nano Black (CNB)
PC	-	-
SF70	70	-
SF70CNB2	70	02
SF70CNB4	70	04
SF70CNB6	70	06

SF and CNB stand for macro steel fiber and carbon nano black, respectively. The number shows the content of conductive materials in kg/m^3; For example, SF70CNB6 implies that the specimen with 70 kg/m^3 steel fibers and 6 kg/m^3 carbon nano black.

The conductive materials, carbon nano black (CNB) (Fig. 1(a)) having a particle size of 30-90 nm, a density of 0.5 g/cm^3 and the volumetric resistivity is 2.30 ohm-cm. The steel fibers (SF) (Fig. 1(b)) with a length of 35 mm and diameter of 0.55 mm are added. The density is about 7.85 g/cm^3 and aspect ratio of steel fiber is 65, and the volumetric resistivity is 10-5 Ω-cm. The dispersion of a nano carbon black is done by dry mixing cementitious materials and aggregated with CNB, which will help the carbon black to disperse at an accepted level. The second thing, SP is also helpful to disperse the carbon nano materials. Table 1 shows the specimens with different amounts of materials.

a) b)

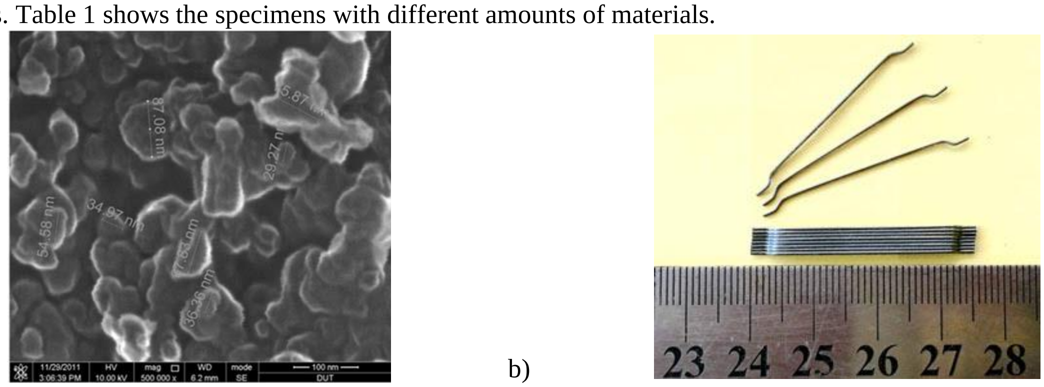

Fig. 1 (a) Show the average carbon nano black particle size by using SEM and (b) macro steel fiber.

3.2 Test methods

According to ASTM C1609, the flexural load is applied on fiber-reinforced concrete beam specimens of 400 x 100 x 100 mm under third-point loading using a closed-loop, servo-controlled testing system are evaluated [18]. According to the four-electrode electric resistance measurement system, four copper meshes are used as an electrode. The displacement rate is 0.2 mm/min at mid-span until the specified deflection is reached. One LVDT on the front and one on the rare side is used to measure the deflection of the mid-span. In addition, an extensometer is attached at the mid-span of the beam to measure the crack opening displacement during the test.

The following equation calculates FCR.

$$FCR = \frac{R - R_0}{R_0} \qquad (1)$$

R is representative of the resistance value at any point during the test, R_0 is the initial value of the resistance before the test and the unit of R and R_0 is Ω.

4 Experimental results and discussion

4.1 Effect of conductive material on workability

The Effect of carbon nano black and steel fiber on fresh properties are also investigated. The addition of conductive admixture has greatly reduced the workability of concrete. It is the nature of nano materials to absorb too much water due to nano size. The specific surface area of the nano materials is high, which would lead to adsorbed more free water and superplasticizer onto the surface of nanomaterials[19]. Therefore, it decreased free water content and thus decreased the workability of the mix and increased the water demand. In this investigation, the SF and CNB have greatly decreased, as shown in Table 2. With respect to plain concrete, the steel fiber 70 kg/m^3 has decreased up to 8% of the slump. But the CNB has decreased up 49% of the slump with 6kg/m^3.

4.2 Effect of conductive material on compressive strength

The CNB and carbon fiber increases the compressive strength (f_{cu}) with various dosages of materials, as described by Ding et al. [20]. It can be noticed that the compressive strength of specimens containing diphasic conductive materials (SF+CB) has improved up to 23.85% that of plain concrete (PC). The improvement of compressive strength by the addition of SF70 is 5.02% concerning PC, as shown in Table 2. In diphasic conductive mixes, the increment in compressive strength is linear with an increasing amount of CNB up to 6kg/m^3. With the addition of carbon nano black by 2, 4 and 6 kg/m^3 compressive strength is improved by 7.86%, 15.52% and 23.85%, respectively, compared to plain concrete. It can be explained that CNB shows its filler effect, which fills nano-level pores of the matrix. The more filled voids, the more dense and consolidated concrete, which ultimately increase compressive strength.

4.3 Effect of conductive materials on flexural strength

The flexural strength (f_P) of the specimen with carbon nano black and steel fiber conductive materials has been investigated through ASTM C1609. The comparison of f_P of the conductive concrete beams to PC is illustrated in Table 2.

It can be seen from the data in the table, the flexural strength of the conductive concrete beam with SF 70 kg/m^3 (SF70) is increased by 32.09 % as compared to plain concrete. The flexural strength of 70 kg/m^3 SF content with hybrid conductive admixture, SF70CNB2, SF70CNB4 and SF70CNB6 (beams with SF 70 kg/m^3 and CNB 2 - 6 kg/m^3) are increased by 72.73%, 78.76% and 86.24% respectively to PC. In hybrid conductive mixes of SF70, the 02 kg/m^3 CNB dosage doesn't improve well than 04 kg/m^3 and 06 kg/m^3. It can be attributed that a lower amount of CNB may not significantly affect the flexural strength performance of the beam, but, with 4 kg/m^3 and 6 kg/m^{3,} CNB content has dramatically improved the flexural strength. The reason behind this increment would be the nanopore filling effect of the CNB, which enhances the bond behaviour of steel fiber to the matrix.

Table 2-Details of the Compressive strength, Flexural strength, Toughness and FCR with different conductive materials

Specimen	**Compressive strength f_{cu} (N/mm^2)**	**Flexural strength f_P (kN)**	**Toughness T^D_{150} (J)**	**FCR (%)**	**Slump (mm)**
PC	38.66	7.10	-	-	200
SF70	40.60	9.37	38.43	42.10	186
SF70CNB2	41.70	12.26	39.14	50.14	169
SF70CNB4	44.66	12.69	48.65	51.32	153
SF70CNB6	47.88	13.22	53.51	59.67	134

Where, FCR at COD =5.0mm

4.4 Effect of conductive materials on toughness

The experimental data evaluation of the toughness parameter (post crack energy absorption capacity) is carried out based on ASTM C1609. T^D_{150} is the toughness of the beam and is calculated by the area of the Load-displacement curve up to a net deflection of L/150 (2.0 mm), where L stands for the span length of the beam. Fig. 2 shows the Load-displacement diagram of PC, SF70 with 2-6 kg/m^3 CNB conductive materials. The T^D_{150} values of monophasic and diphasic conductive materials are shown in Table 2. It can be noticed that the PC flexural member does not demonstrate any flexural toughness because the PC beam does not have any fiber, so it shows strong brittle behaviour.

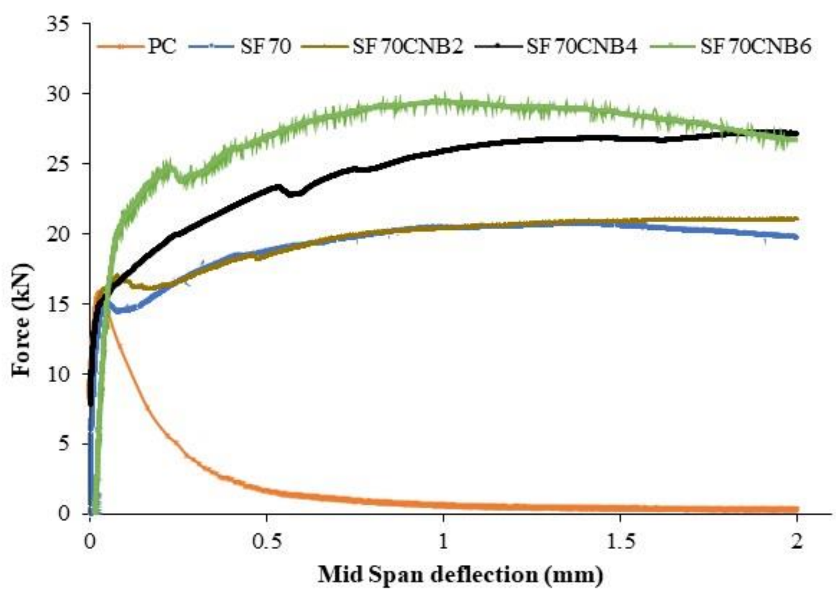

Fig. 2 The Load-displacement curve of solo and hybrid conductive materials and PC

Compared to the plain concrete beam, the addition of steel fiber has shown significant improvement in the toughness of the concrete beam. The toughness (T^D_{150}) of diphasic conductive materials specimens SF70CNB2, SF70CNB4 and SF70CNB6 toughness values are increased by 1.9%, 26.6% and 39.3%, respectively, concerning SF70. Therefore, it can be concluded that the CNB with 2-6 kg/m^3 shows a positive effect. The improvement in toughness can also be counter checked by compressive strength results that as the CNB increased, the compressive strength is also increased. So, the bond between the matrix and steel fiber is improved by the more compacted and consolidated matrix which will lead a higher energy absorption capacity.

4.5 Effect of hybrid conductive materials on FCR-COD

The effects of CNB and SF conductive materials on the relationships of the fractional change in resistance (FCR) and the crack opening displacement (COD) of concrete flexural members are demonstrated in Table 2. Generally, it is believed that above the percolation threshold of conductive material, the FCR values value does not show any noticeable improvement as the SF content increased. The percolation threshold is classified as the dosage of the conductive admixtures, where they make a conductive path to flow electric charges. Higher the FCR means higher the resistance change with the strain, which is the gauge factor. The gauge factor of SF 70 is 41.26 and the gauge factor of carbon black with 6 kg/m^3 59.67 at COD 5mm. The improvement in gauge factor is about 45% by the addition of 6 kg/m^3 due to the synergetic effect of both conductive materials. The conductive carbon nano black improves the conductivity of the matrix at the nano level. The SF 70 kg/m^3 provides a maximum number of fibers to bridge the cracks and the moments of the electrons are more stable and resilient. The diphasic conductive phase SF70CNB2, SF70CNB4 and SF70CNB6, have higher FCR values than solo SF 70 by 19.1%, 21.9% and 30.8%, respectively. PC does not show any FCR because it is a pure insulator with no conductive admixture. The FCR-COD is improved with the addition of CNB. The FCR values are increased by the addition of steel fiber with 70 kg/m^3. Moreover, the addition of CNB has further improved the FCR by 45% concerning solo use of SF. It means that the carbon nano black has a clear effect on the conductivity of the member, which will lead the higher sensitivity for the crack of the member. The CNB with 6 kg/m^3 have the higher FCR values which could be attributed that the higher amount of the CB has a permanent and strong conductive path by tunnelling effect of the CNB particles, so the change in resistivity with initiation of the crack is higher.

This work is a to study for the self-sensing and self-diagnosing of single and multiple cracking behavior of concrete flexural members. The hybrid use of the nano carbon black and steel fiber is beneficial for both mechanical and self-sensing properties of concrete beam. It will be a very cost-effective field deployable solution. It would replace the very expensive and complicated structural health monitoring techniques.

5 Conclusion

This study investigates the use of carbon nano black (CNB) and macro-steel fiber (SF) as a hybrid electric conductive material for the self-sensing ability of the beam. A series the experimental and analytical investigations, the results lead to the conclusions as follows:

- The fresh properties like workability have decreased nut the combined use of macro-SF and CNB has shown an improvement in compressive strength, and flexural strength up to 23.85% and 86.24%, respectively, with respect to PC.
- The compressive strength and flexural strength of 2 to 6 kg/m^3 CNB show a clear improvement of 17.93% and 41.00 %, respectively, concerning SF 70 kg/m^3.
- The toughness of hybrid uses of the SF and CNB compared to solo use of steel fiber is improved by 39.3%, respectively.
- The gauge factor of the conductive admixture is highly improved by adding carbon nano black up to 6 kg/m^3 by 45% compared to solo use of SF.

Recommendation

- The followings are some recommendations for future studies
- The dispersion of the carbon black is not studied properly. It is recommended an extensive investigation on carbon black dispersion is needed.
- Durability parameters of the carbon black incorporated concrete are recommended to investigate further.

Acknowledgement

The authors would like to thank all the people/organizations who helped throughout the research.

References

[1] J. Ou, "Research and practice of intelligent sensing technologies in civil structural health monitoring in the mainland of China," *Nondestruct. Eval. Heal. Monit. Aerosp. Mater. Compos. Civ. Infrastruct. V*, vol. 6176, p. 61761D, 2006, doi: 10.1117/12.663993.

[2] G. Song, Y. L. Mo, K. Otero, and H. Gu, "Health monitoring and rehabilitation of a concrete structure using intelligent materials," *Smart Mater. Struct.*, vol. 15, no. 2, pp. 309–314, 2006, doi: 10.1088/0964-1726/15/2/010.

[3] H. N. Li, D. S. Li, and G. B. Song, "Recent applications of fiber optic sensors to health monitoring in civil engineering," *Eng. Struct.*, vol. 26, no. 11, pp. 1647–1657, 2004, doi: 10.1016/j.engstruct.2004.05.018.

[4] B. Han and J. Ou, "Embedded piezoresistive cement-based stress/strain sensor," *Sensors Actuators, A Phys.*, vol. 138, no. 2, pp. 294–298, 2007, doi: 10.1016/j.sna.2007.05.011.

[5] A. O. Monteiro, P. B. Cachim, and P. M. F. J. Costa, "Self-sensing piezoresistive cement composite loaded with carbon black particles," *Cem. Concr. Compos.*, vol. 81, pp. 59–65, 2017, doi: 10.1016/j.cemconcomp.2017.04.009.

[6] S. Wen and D. D. L. Chung, "Effect of moisture on piezoresistivity of carbon fiber-reinforced cement paste," *ACI Mater. J.*, vol. 105, no. 3, pp. 274–280, 2008.

[7] A. Dehghani and F. Aslani, "Piezoresistive sensing of cementitious composites reinforced with shape memory alloy, steel, and carbon fibres," *Constr. Build. Mater.*, vol. 267, no. xxxx, 2021, doi: 10.1016/j.conbuildmat.2020.121046.

[8] L. Wang and F. Aslani, "Mechanical properties, electrical resistivity and piezoresistivity of carbon fibre-based self-sensing cementitious composites," *Ceram. Int.*, vol. 47, no. 6, pp. 7864–7879, 2021, doi: 10.1016/j.ceramint.2020.11.133.

[9] Z. Zhou *et al.*, "Electrical properties of low dosage carbon nanofiber/cement composite: Percolation behavior and polarization effect," *Cem. Concr. Compos.*, vol. 109, no. January, 2020, doi: 10.1016/j.cemconcomp.2020.103539.

[10] M. S. Konsta-Gdoutos *et al.*, "Effect of CNT and CNF loading and count on the corrosion resistance, conductivity and mechanical properties of nanomodified OPC mortars," *Constr. Build. Mater.*, vol. 147, pp. 48–57, 2017, doi: 10.1016/j.conbuildmat.2017.04.112.

[11] F. Azhari and N. Banthia, "Cement-based sensors with carbon fibers and carbon nanotubes for piezoresistive sensing," *Cem. Concr. Compos.*, vol. 34, no. 7, pp. 866–873, 2012, doi: 10.1016/j.cemconcomp.2012.04.007.

[12] A. Naqi, N. Abbas, N. Zahra, A. Hussain, and S. Q. Shabbir, "Effect of multi-walled carbon nanotubes (MWCNTs) on the strength development of cementitious materials," *J. Mater. Res. Technol.*, vol. 8, no. 1, pp. 1203–1211, 2019, doi: 10.1016/j.jmrt.2018.09.006.

[13] Y. Ding, G. Liu, A. Hussain, F. Pacheco-Torgal, and Y. Zhang, "Effect of steel fiber and carbon black on the self-sensing ability of concrete cracks under bending," *Constr. Build. Mater.*, vol. 207, pp. 630–639, 2019, doi: 10.1016/j.conbuildmat.2019.02.160.

[14] L. Shi, Y. Lu, and Y. Bai, "Mechanical and Electrical Characterisation of Steel Fiber and Carbon Black Engineered Cementitious Composites," *Procedia Eng.*, vol. 188, pp. 325–332, 2017, doi: 10.1016/j.proeng.2017.04.491.

[15] A. Hussain, Y. Ding, G. Liu, and A. Naqi, "Study on self-monitoring of multiple cracked concrete beams with multiphase conductive materials subjected to bending," *Smart Mater. Struct.*, vol. 28, no. 9, 2019, doi: 10.1088/1361-665X/ab2cfe.

[16] A. O. Monteiro, P. B. Cachim, and P. M. F. J. Costa, "Electrical Properties of Cement-based Composites Containing Carbon Black Particles," *Mater. Today Proc.*, vol. 2, no. 1, pp. 193–199, 2015, doi: 10.1016/j.matpr.2015.04.021.

[17] A. O. Monteiro, A. Loredo, P. M. F. J. Costa, M. Oeser, and P. B. Cachim, "A pressure-sensitive carbon black cement composite for traffic monitoring," *Constr. Build. Mater.*, vol. 154, pp. 1079–1086, 2017, doi: 10.1016/j.conbuildmat.2017.08.053.

[18] C. C. Test, T. Drilled, C. Concrete, and S. T. Panels, "C 1609/C 1609M-05 Standard Test Method for Flexural Performance of Fiber-Reinforced Concrete (Using Beam With Third-Point Loading) 1," *Astm*, vol. i, no. C 1609/C 1609M-05, pp. 1–8, 2005, doi: 10.1520/C1609.

[19] Z. Wu, C. Shi, K. H. Khayat, and S. Wan, "Effects of different nanomaterials on hardening and performance of ultra-high strength concrete (UHSC)," *Cem. Concr. Compos.*, vol. 70, pp. 24–34, 2016, doi: 10.1016/j.cemconcomp.2016.03.003.

[20] Y. Ding, Z. Han, Y. Zhang, and J. B. Aguiar, "Concrete with triphasic conductive materials for self-monitoring of cracking development subjected to flexure," *Compos. Struct.*, vol. 138, pp. 184–191, 2016, doi: 10.1016/j.compstruct.2015.11.051.

3rd Conference on Sustainability in Civil Engineering (CSCE'21)
Department of Civil Engineering
Capital University of Science and Technology, Islamabad Pakistan

ELECTRICAL PROPERTIES OF CARBON NANOTUBE AND CARBON FIBER REINFORCED CEMENTITIOUS COMPOSITES

[a] Oğuzhan Öztürk*, [b] Arife Akın,

a: Civil Engineering Department, Konya Technical University, oozturk@ktun.edu.tr
b: Civil Engineering Department, Konya Technical University aakin@ktun.edu.tr
* Corresponding author: Email ID: oozturk@ktun.edu.tr

Abstract- The addition of nano/micro scale carbon-based materials into cement-based composites is of significance for achieving reliable electrical properties in different civil engineering practices. The present study aims to disperse carbon-based materials homogenously for the improved electrical performance for non-structural functionalities. The investigation addresses the different mixing methods of carbon nanotubes (CNT) and carbon fibers (CF) on the electrical properties of cement mortars. To do this, two mixing methods for each carbon-based material were applied and the electrical properties of cement mortars were evaluated via alternating current (AC) measurements. Although both carbon-based materials were able to improve the electrical properties, CFs were more pronounced in terms of reducing the electrical resistivity values of specimens compared to CNT-based and reference specimens. It is worth noting that proposing different methods may also further enhance the electrical properties for the specific mixture design of cement-based composites.

Keywords- Carbon fibers, carbon nanotubes, cementitious mortars, electrical properties.

1 Introduction

Despite the debate over the environmental effect of Portland cement [1], civil engineering industry is still in the necessity of huge amount of concrete production to sustain economic development. For different purposes, mechanical and durability performance of traditional concrete has been widely studied by researchers in terms of strength, ductility, toughness, impact resistance, environmental factors. Recently, additional efforts are given to design cement-based composites with different non-structural functionalities through maintaining or improving structural performance. For example, strain sensing, deicing, anti-static component, electromagnetic shielding applications can be integrated with the cement-based composites [2-5]. Achieving reliable non-structural functionalities is very interdependent with the best use of conductive materials. However, incorporation of the inert carbon-based materials is the initial challenge for the effective capturing of aforesaid non-structural properties. Carbon-based materials having nano/micro-scale physical properties are inert and they are in the need of homogeneous distribution within the cement matrix [6]. Unless uniform distribution is provided, pre-targeted non-structural functionalities may be improbable and weak zones may lead to inadequate mechanical performance. Several studies reported on the mechanical/electrical characterization of the cement-based composites [7-9] and the common conclusion is initially concentrated on the dispersion characteristics of the conductive fillers prior to tailoring electrical performance.

Dispersion of the nanoscale conductive fillers is interrelated with the van-der Waals forces acting upon the materials. Furthermore, synthesis of the nano conductive fillers results in entangled form, and this is more prevalent for the carbon nanotubes (CNT) [10]. Besides synthesis methods, the high aspect ratio of CNTs possesses difficulties in multiphase composites such as cement-based matrices and disentanglement of CNTs becomes further challenge for efficient electrical performance. On the other hand, effective dispersion of the microscale carbon fibers (CF) is generally attributed to disentanglement instead of bundling in cement matrix. In the current study, effects of carbon fibers (CF) and carbon nanotubes (CNT) on the electrical properties of cementitious composites were investigated at curing age of 28 days. In experiments, different mixing methods were examined for each conductive filler aiming to obtain effective dispersion methods in comparison to reference mixtures. Investigations were performed basically on the electrical resistance of the specimens. Instead of laborious mixing, proposing a more practical and cost-effective mixing methods was aimed to achieve desirable electrical performance. The potential modification of the electrical performance may support the reliable use of cement-based composites having structural and non-structural abilities endowed through different carbon-based materials. For the multifunctional ability of cement-based materials, the current study deal with the novel dispersion methods for the carbon-based materials which is the initial step of the pre-targeted electrical performance. In comparison with the literature studies [8, 11-12], the current study presents new data with proposed methods comprising CNT and CF materials.

2 Experimental Procedures

2.1 Materials

Two conductive fillers used during the experimental study were carbon nanotubes (CNT) and carbon fibers (CF). CNTs had a diameter of ~10-20 nm, length of 10-30 μm and surface area of more than 200 m^2/g with the purity of %90. CFs had an aspect ratio of 800, tensile strength of 4200 MPa, elongation of 1.8% and density of around 1.76 g/cm^3. Scanning electron microscope (SEM) images of the carbon-based materials were given in Figure 1. On the other hand, traditional ingredients of the cement mortars were CEM I 42.R (PC) similar to ASTM type I, F-class fly ash (FA), silica sand having maximum aggregate 0.4 mm, and high range water reducing admixture (polycarboxyl ether-based). Nano-SiO_2 and calcium carbonate and methylcellulose-based dispersive agents were also used during the employed mixing methods. Chemical and physical properties of the PC, FA and silica sand were given in Table 1.

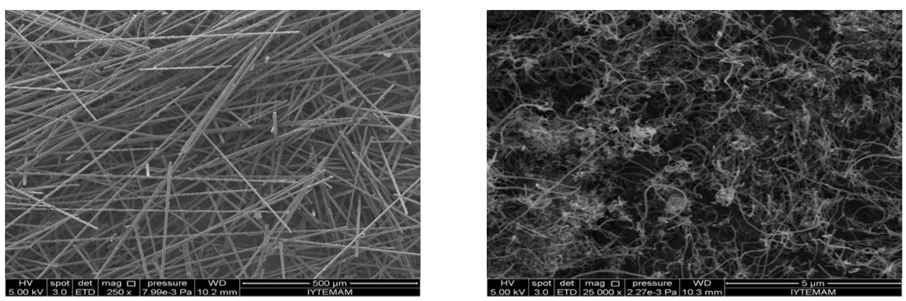

a) b)

Figure 1: Carbon-based materials, a. carbon fibers, and b. carbon nanotubes

Table 1. Chemical and physical properties of PC, FA and silica sand

Chemical composition	**PC**	**FA**	**Silica sand**
CaO (%)	61.43	1.64	34.48
SiO_2 (%)	20.77	56.22	38.40
Al_2O_3 (%)	5.55	25.34	10.96
Fe_2O_3 (%)	3.35	7.65	0.81
MgO (%)	2.49	1.80	7.14
SO_3 (%)	2.49	0.32	1.48
K_2O (%)	0.77	1.88	0.86
Na_2O (%)	0.19	1.13	0.18
Loss on ignition (%)	2.20	2.10	3.00
SiO_2+Al_2O_3+Fe_2O_3	29.37	89.21	50.17
Physical properties			
Specific gravity (g/cm^3)	3.10	2.31	2.60

2.2 Mixture proportions and sequence

In mixtures, water to total cementitious materials (PC+FA) ratio (W/C) and F-class fly ash to Portland cement (FA/PC) ratio were 0.26 and 1.2. In each mixture, HRWRA was used to provide adequate workable properties having 14-15 cm of mini-slump flow rate. Mixture proportions of the specimens were given in Table 2.

Table 2. Typical matrix mix design (ratios by weight)

Cement (PC)	Water	Silica Sand	F-Class Fly ash	HRWRA*	CNT	CF**
1.00	0.58	0.80	1.20	-	0.25	0.5

*: HRWRA was used based on the similar workability properties of each mixture.
**: by volume.

Two different mixing methods were performed for each carbon-based material type. In the preparation of CNT-based and CF-based cement mortars, 1st and 2nd mixing methods comprised the following sequence together with reference mixture:

- *CM/Ref:* Raw materials (PC, FA and silica sand) were mixed for 5 minutes in mortar mixer and then water and HRWRA were added gradually and 10 minutes of mixing was conducted additionally.
- *CM/CNT1:* Initially, dry mixing of raw materials (PC, FA and silica sand) was employed for 5 minutes. Then water and HRWRA were added and mixed for 10 minutes. In the separate homogenizer, 1st mixing method for the CNT-based cement mortars covered the mixing sequence of separate mixing of nano SiO_2 with CNT for 5 minutes. Then, separate mixing of CNTs was added to traditional mixing and 10 minutes of additional mixing was conducted.
- *CM/CNT2:* A separate mixing was prepared with CNT, water, HRWRA and calcium carbonate in nano/micro scale material homogenizer for 5 minutes. Then, the prepared suspension was added into ongoing dry mixing (PC, FA and silica sand) in mortar mixer and additional 10 minutes of mixing was performed in the 2nd of mixing method proposed for the CNT-based cement mortars.
- *CM/CF1:* Carbon fibers having 12 mm of length were mixed with dry raw materials (PC, FA and silica sand) for 10 minutes at 100 round per minute (rpm). Then water was added during 10 seconds into ongoing mixing and mixing speed was increased to 300 rpm after adding of HRWRA within 30 seconds. 10 minutes of mixing at 300 rpm was conducted additionally.
- *CM/CF2:* Carbon fibers having same properties in previous method were first mixed with the methylcellulose-based dispersive agent used by 0.2% of total binder. Mixing was made for 5 minutes at 100 rpm. The prepared mixing was added to ongoing raw material mixing (PC, FA and silica sand) and additional 10 minutes of mixing at 300 rpm was employed by gradual adding of HRWRA.

2.3 Testing

Produced fresh mortars reinforced with CNTs and CFs was poured into cylindrical mould having dimensions of 100^{mm} diameter and 200^{mm} length. After completion of casting, specimens were kept in molds at 50±5 relative humidity, 23±2 °C for 24 hours. After first day of curing, specimens were removed from the molds and kept in isolated bags until the curing ages of 7 and 28 days at 95±5 relative humidity, 23±2 °C. Cylindrical specimens having dimensions of 100^{mm} diameter and 200^{mm} length were cut into smaller cylindrical specimens having 100^{mm} diameter and 80^{mm} length for the electrical testing configuration. Electrical resistivity (ER) measurements were conducted using a concrete resistivity meter with uniaxial configuration similar to studies in the literature [13]. In this configuration, specimens were put into testing device and pre-saturated sponges were placed between the plates of the resistivity meter to sustain adequate electrical contact (Figure 2). The alternating current (AC) was employed with working frequency of 1 kHz to minimize the polarization effect [14]. Electrical measurements were made by calculating impedance and phase angle values and then resistivity values were made by using geometrical factors according to equation (1) given below;

$$\rho = Z * \cos(\theta) * \frac{A}{L} \qquad (1)$$

where, ρ, Z, θ, A and L stand for resistivity (Ω.m), electrical impedance (Ω), phase angle (°), cross-sectional area (m^2) and length (m) of the specimen, respectively.

Figure 2: Concrete resistivity meter (AC) and testing of the specimen

3 Results and Discussions

ER measurements of CNT and CB reinforced cement mortars are presented in Table 3. In addition to raw data given in Table 3, comparative results were also given for each carbon-based material modified cement mortars in Figure 3-4. As presented in Table 3 and Figure 3-4, ER values of the specimens showed a continuous increase from 7 days to 28 days without regard to mixing method and conductive filler type. The reason was related to the changes in the microstructure of the specimens resulting from porosity, tortuosity of pore network and pore solution [13]. The progress of hydration and pozzolanic reactions induced by fly ash may have led a substantial change in microscale level such as reducing pore solution and densification of matrix. Diminished conductive ions could be influential on the increase of the ER between 7 to 28 days of curing.

Table 3. Electrical resistivity measurements of cement mortars reinforced with CNT and CF

Mixture	7 days (Ω.m)	28 days (Ω.m)
CM/Ref	29.17	175.31
CM/CNT1	37.86	174.33
CM/CNT2	26.81	156.65
CM/CF1	13.60	41.50
CM/CF2	12.62	36.83

Figure 3 and Figure 4 indicate that incorporation of carbon-based materials was influential on the modifying of electrical properties of cement mortars. On the other hand, only CM/CNT1 mixture was not in this line at 7 days of curing compared to value of reference mixture. However, ER values of CM/CNT1 were able to present comparable results with the reference specimens at further curing (28 days). CM/CNT2 mixture had lower ER values compared to reference specimens both at 7 and 28 days. For the CF reinforced cement mortars (CM/CF1 and CM/CF2), a considerable reduction of ER values were obtained in comparison with the CNT reinforced cement mortars at 7 and 28 days. As seen from the results, CNT-bearing specimens had higher ER values and the reason can be attributed to hypothesis of nucleation occurred on the very fine surface of CNTs (around 200 m^2/g) that accelerate the formation of dense hydration products. It was likely that specimens reinforced with CNTs exhibiting higher ER values were due to lesser abundance of porosity, pore solution and tortuosity in the matrix system. On the other hand, another explanation can be given about the dispersion difference of the CNTs followed in the mixtures of CM/CNT1 and CM/CNT2. The clustering of CNTs during the mixing method of CM/CNT1 mixture may have been a disadvantage for the modifying electrical properties. For this reason, mixing method of the CM/CNT2 seemed to have more convenient dispersion for lowering the electrical resistivity of the reference specimens. (Figure 3). However, further microstructural analysis may be favorable for the precise interpretation of this finding and comparative analysis would then be possible especially between CM/CNT1 and reference mortars.

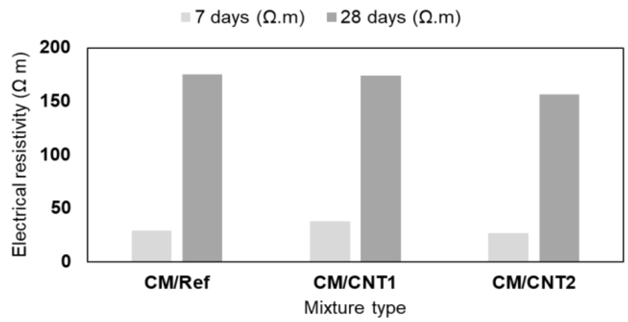

Figure 3: Electrical resistivity values of CNT reinforced cement mortars at 7 and 28 days

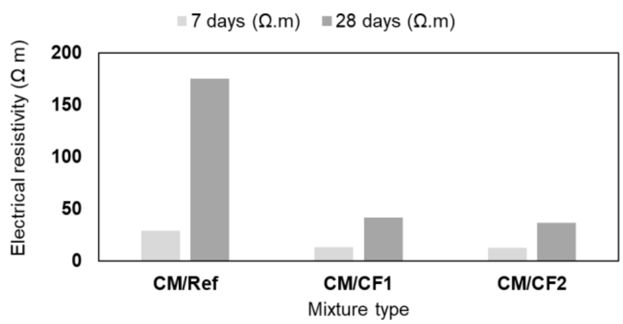

Figure 4: Electrical resistivity values of CF reinforced cement mortars at 7 and 28 days

For the CF-based cement mortars (Figure 4), it is clearly obtained that CFs were more promising in the modification of electrical performance. For example, an average of the both 7 day-old CF-based mixture (CM/CF1 and CM) was 13.11 Ω.m while it was 32.33 Ω.m and 29.17 Ω.m for the CNT-based and reference mixtures, respectively. The results imply that CF-modified specimens were able to present 55% and 59.4% lower electrical resistivity values compared to CNT reinforced and reference specimens. Similarly, average ER value of both CF-based mixtures was 76.30% and 77.66% lower than the CNT-based and reference specimens at 28 days, respectively. The advantage use of CFs can be related to longer CF fibers (aspect ratio of 1600 [12 mm]) may have provided a continuous conductive path by creating fiber-to-fiber contact [6]. Similar explanations are also available in the literature [15]. However, it is worth noting that similar testing should be addressed especially for the shorter CF fibers (3-6 mm) available in the market. The outcome of the study implies that electrical modification of the cement mortars is the first step of developing multifunctional cementitious composites which can be used in strain sensing, anti-static, thermal energy storage and deicing applications.

4 Conclusion

Following conclusions can be drawn from the conducted study:

- Two different mixing methods were applied for each mixture reinforced with CNT and CF. For the CNT-based specimens, CM/CNT2 mixing method was more promising compared to CM/CNT1 type both at 7 and 28 days. On the other hand, CNT/CM1 mixture had comparable ER values compared to reference specimens.

- Mixing methods proposed for the CFs were very promising without regard to both mixture types. A significant reduction of ER values was obtained for the CF reinforced cement mortars in contrast to CNT-based mixtures. The reduction is more pronounced particularly for CM/CF2 mixture type.

- Instead of elaborate mixing methods followed for the nanoscale carbon-based materials (herein CNT), employed mixing methods for the CFs provided practical and efficient benefits in the modification of electrical performance.

Acknowledgment

The study hereby presents the data and findings of the first author's Master of Science Thesis Defense in Selçuk University in the Program of ÖYP (Academic Staff Training Program) supervised by Assist. Prof. Arife Akın and co-supervised by Prof. Dr. Mustafa Şahmaran. The authors also gratefully acknowledge the financial assistance of the Scientific and Technical Research Council (TUBITAK) of Turkey provided under project: MAG-114R043.

References

[1] R.B. Andrew, "Global CO_2 emissions from cement production," *Earth System Science Data*, vol. 10, pp.195-217, 2018.

[2] D.D.L. Chung, "Carbon materials for structural self-sensing, electromagnetic shielding and thermal interfacing," *Carbon*, Vol. 50, pp. 3342-3353, 2012.

[3] D.D.L. Chung, "Electrically conductive cement-based materials," *Advances in Cement Research*, Vol. 16, pp. 167-176, 2004.

[4] V.K. Sachdev, S.K. Sharma, S. Bhattacharya, K. Patel, N.C. Mehra, V. Gupta, R.P. Tandon, "Electromagnetic shielding performance of graphite in cement matrix for applied application" *Advanced Material Letters*, Vol 6, pp. 965-972, 2015.

[5] H. Zhao, Z. Wu, S. Wang, J. Zheng, G. Che, Concrete pavement deicing with carbon fiber heating wires'', *Cold Regions Science and Technology*, Vol. 65, pp. 413-420, 2011.

[6] O. Öztürk, Effects of different types of carbon based materials on electrical properties of cementitious composites, Selcuk University, Master Thesis, 2015.

[7] O. Öztürk, "Multifunctional behavior of CNT- and CB-based composite beams". *Construction and Building Materials*, 296, 123456, 2020.

[8] O.Öztürk, Ü.S. Keskin, M. Şahmaran "Self-sensing Fiber Reinforced Cement Mortars for the Monitoring of Critical and Transport Infrastructures" *EGU General Assembly Conference Abstracts*, 2018.

[9] V. W. J, Lin, M. Li, J. P. Lynch, V. C. Li, "Mechanical and electrical characterization of self-sensing carbon black ECC'', *Proc of SPIE* Vol. 7983, 798316–7983, 2011.

[10] R. Atif, F. Inam "Reasons and remedies for the agglomeration of multilayered graphene and carbon nanotubes in polymers'' *Beilstein Journal of Nanotechnology*, Vol. 7, pp.1174–1196, 2016.

[11] A. Al-Dahawi, O. Öztürk, F. Emami, G. Yıldırım, M. Şahmaran (2016). "Effect of mixing methods on the electrical properties of cementitious composites incorporating different carbon-based materials". *Construction and Building Materials*, 104, 160-168.

[12] A. Al-Dahawi, M. H. Sarwary, O. Öztürk, G. Yıldırım[5], A. Akın, M. Şahmaran and M. Lachemi. "Electrical percolation threshold of cementitious composites possessing self-sensing functionality incorporating different carbon-based materials". Smart Mater. Struct., 25, 10, 2016.

[13] R. Spragg, Y. Bu, K. Snyder, D. Bentz, J. Weiss, "Electrical testing of cement-based materials: role of testing techniques, sample conditioning, and accelerated curing'', *Publication FHWA/IN/JTRP-2013/28. Joint Transportation Research Program*, Indiana Department of Transportation and Purdue University, West Lafayette, Indiana, 2013.

[14] T. C. Hou, "Wireless and electromechanical approaches for strain sensing and crack detection in FRC materials'', *PhD dissertation*, Civil and Environmental Engineering, University of Michigan, Ann Arbor, MI. 2008.

[15] B. Chen, K. Wu, W. Yao, "Conductivity of carbon fiber reinforced cement-based composites'', *Cement and Concrete Composites*, Vol. 26, pp. 291-297, 2004.

STRUCTURAL ANALYSIS

3rd Conference on Sustainability in Civil Engineering (CSCE'21)
Department of Civil Engineering
Capital University of Science and Technology, Islamabad Pakistan

MODERN METHODS OF RESIDUAL STRENGTH ASSESSMENT OF FIRE DAMAGED RC STRUCTURE-A REVIEW

[a] Muhammad Sultan Sikandar

a: Civil Engineering Department, Lahore Leads University,sultansikandar618@gmail.com

Abstract- Structures have been severely damaged by fire. As far as fire safety is concerned, it is necessary to build cost-effective but fire-resistant constructions. Reinforced concrete (RC) buildings do not sink during fire exposures, and the building may be able to be used again after the fire. Despite this, fire can cause a permanent loss of concrete strength. Following a fire assessment, many researchers are looking at post-fire assessments; however, they haven't yet looked at recent residual strength evaluation methodologies. The focus of this research is on current methodologies for determining the residual strength of fire-damaged reinforced concrete (RC) structures. As a result of the findings, it has been determined that current methods for determining residual strength are required. The purpose of this research is to determine future directions for investigating new methods of residual strength assessment to improve the utilization of fire-damaged structures.

Keywords- Reinforced concrete (RC) buildings, Residual strength assessment.

1 Introduction

Built infrastructure plays an important role in the socioeconomic development of a country. Many buildings are designed for several decades and provide residential or commercial operations throughout their design life. Buildings are subjected to many hazards i.e. Earthquake etc. and manmade hazards i.e. Fire, explosion etc. These hazards can cause partially or fully damage to buildings. Rapid development across the world make a significant transformation in the form of severity from the fire hazard. The researchers revealed that in the past two decades (1935-2015) a total of 86.4 million fire events have caused greater than one million fire deaths. It is reported that annual loss from the fire hazard about 1 per cent of the world GDP. The researchers revealed that every year in developed and developing countries with an average of 3.8 million fires caused 44,300 fire deaths. Developing countries i.e. India and Pakistan experience the highest number of fire events (10,000-25,000 per year) and fires deaths (100,000-600,000 per year) [1]. The importance of structural fire engineering increased day by day with the increased population.

Pre fire assessment and post-fire assessment are the main concern of structural fire engineering. Pre fire assessment is conducted before a fire event in the buildings and a post-fire assessment is conducted after the fire events in the building. Post-fire assessment is necessary for further use of the fire affected building. There is a need to develop modern methods in the residual strength assessment of fire-damaged reinforced concrete (RC) structure. Because public health and safety is the priority. Modern methods of residual strength assessment of fire-damaged reinforced concrete (RC) structures have recently drawn importance for structural health assessment. The performance of concrete in the fire mainly depends on its ACI design. Normal concrete strength and high concrete strength gives results almost similar at high temperatures while ultra-high-strength concrete behaves differently [2]. The performance of structural members at high temperature could find out by testing [3]. Fire resistance of a reinforced concrete structure could be evaluated under high temperature by a standard time-temperature curve. Many materials and analytical models have been prepared for finding the residual strength of concrete after fire [4].

Post-fire assessment is carefully considered in damaged reinforced concrete (RC) structure. Keep in mind the exterior condition of the building before entering the building for assessment. If the exterior condition of the building is acceptable damaged then enter into the building for further investigation. On the other side if the exterior condition of the damaged building is not well then use modern techniques for residual strength assessment from the outside. There is a need to develop innovative and cost-effective building models that also take fire safety into account. Many researchers work on the post-fire assessment of fire-damaged buildings because it's important to used already constructed building than newly constructed building from a sustainability point of view. The age of the building must necessary to be considered during the assessment. Chemical changes occurred in the cement and concrete when the temperature is significantly increased. The density decreases as the temperature rises, as shown in Figure 1. So there is a need to develop modern methods for the residual strength assessment of fire-damaged structures.

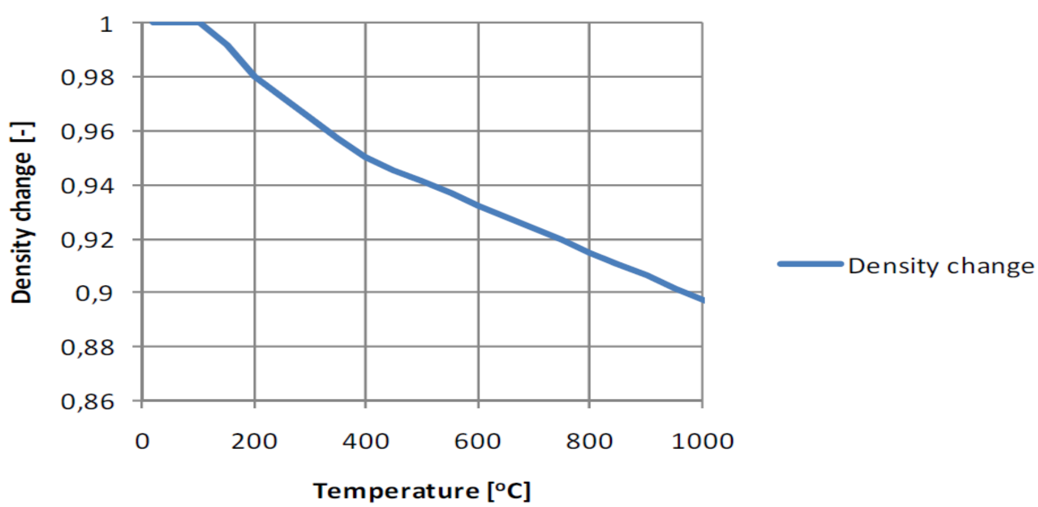

Figure 1: Reduction in density with temperature [5]

2 Fire Risks In Rc Structure

A structural fire is a fire that requires the structural components of many types of residential, commercial or industrial buildings [5]. There is always risks of fire in the reinforced concrete (RC) structure. It is impossible that there are no risks of fire in the reinforced concrete (RC) structure. Always deal to reduce the risks in the reinforced concrete (RC) structure. Fire is the most important potential risks for the buildings and reinforced concrete (RC) structures [6]. And for this reason during the design of a building fire safety codes must be considered. Buildings have many sources to start a fire. Active fire protection system i.e. heat and smoke detectors etc. And passive fire protection system i.e. Structural and nonstructural components of the buildings are capable to resist fire. When fire exposed at a high temperature for a longer duration then changes occurred in cement, sand and aggregate and due to these changes mechanical deformation occurred in the concrete [6]. When fire breaks out in reinforced concrete (RC) structure the structural members i.e. Columns starts to rise because of their lower thermal conductivity and high specific heat of concrete [7].

At the initial stages of fire outer faces of concrete is much hotter than internal concrete. When the fire continued for a certain time then internal concrete also starts to heat up. The increase in temperature disturbs the strength and modulus properties of steel and concrete. Fire causes a severe hazard in developing and developed countries all over the world [7]. And it disturbs the structure and environment. In the buildings, there are many reasons to start a fire. A massive fire erupted in Pakistan (Lahore) Hafeez plaza on 18-10-20 morning. The fire started from the second floor in the building but gradually travelled to the fourth floor. The reason for the fire is a short circuit. When a detailed study conducted on Hafeez centre there are no safety rules to be followed in the building. Figure 2 shows the methods to reduce fire risks.

Fire protection features, regulation and enforcement, common or civic sense and technology and firefighting resources are shown in Figure 2.

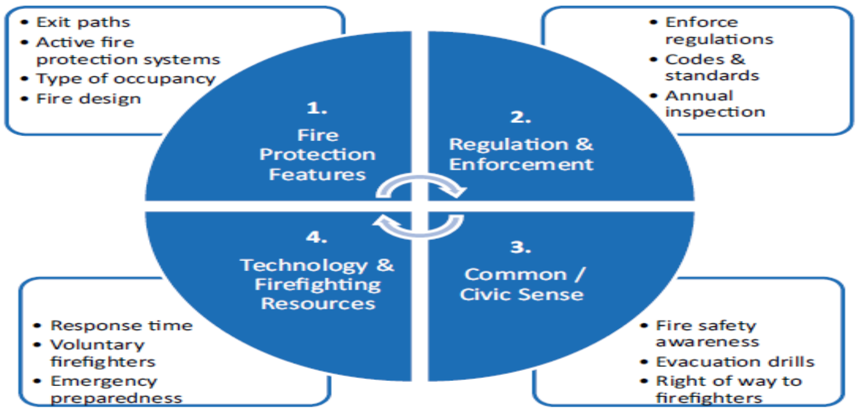

Figure 2: Methods to reduce Fire Risks [1]

3 Post-Fire Assessment

Reinforced concrete (RC) structure inherent Fire can nevertheless result in a permanent loss of concrete strength. The post-fire assessment is necessary for deciding to further use the affected building or not. Post-fire assessment of reinforced concrete (RC) structure describes what is the current condition of the affected building after the fire. At high temperatures, the micro-structural properties of concrete are exposed [8]. Concrete is mostly used construction material worldwide. The performance of concrete in fire event is better than other kinds of construction materials [9]. At high temperature, the mechanical and physical properties of concrete changed [9]. Reinforced concrete (RC) structure shows better performance under fire exposures [10]. When the temperature of concrete is increased then the water vapour pressure in the concrete also increased and creates cracks and spalling in the concrete [10]. The results of high temperature are mostly deformation, disintegration and fracturing [11]. The concept of fire resistance applied to the structural elements not on the materials but the properties of the material affect the structural performance. After fire exposures, there is a need to check the technical condition of the reinforced concrete structure [12]. First of all, inspect the affected building from the outside that is the right way to enter the damaged building for the assessment or not.

Check the affected area concrete strength and unaffected area concrete strength. If the damages are too high in the building then detail specialized analysis are to be performed. If building design live load of 100 Psi and residual strength of concrete remain 60 psi. Then there is another method to deal residual strength for use of the damaged building to reduce the live load i.e.60 Psi. For further use the affected building according to concrete strength. The aim of the post-fire assessment is to repairing a structure after a fire and restore it to condition before the fire. During assessment collect valuable information regarding fire and its temperature on particular places of structure. Classify the damages and their impact on the safety level of the building. Find out mechanical properties of material i.e. concrete and steel by adopting destructive or nondestructive testing. Check there is a need to strengthening of structure or retrofitting of structure. Moderate cracks are (> 0.5 mm) and the concrete chippings are greater than 10mm in size. If the 25% exposed reinforcing bars the surface colour is pink-red. If the reinforcing bars are exposed to greater than 50% then the pink surface is converted to red or whitish-grey [11].

For this checking, there is a need to select the damaged and undamaged parts of the structure. Concrete at the temperature of 500-600 °C is not suitable for further use in the structure [12]. At higher temperatures, the loss of strength is more severe; for example, at 650 °C, just 20% of the original strength remains. Cold drawn bars, wires, and strands are more vulnerable to high temperatures than hot-rolled bars. At 400 degrees Celsius, the strength is reduced by half, and at 650 degrees Celsius, just 10% of the original strength remains. The initial yield strength of cold wrought steel will be regained after cooling if the temperature is less than 450 °C. 650 °C is the corresponding temperature for hot-rolled steels. The residual yield and fire load are not possible [13]. The study revealed that post-fire tests on material show degrading of mechanical properties of concrete [14]. Fire damages decrease the load-bearing capacity of the reinforced concrete structure [14]. After being d strength will diminish as the temperature rises over these levels. The researchers revealed that the effect of dynamic loading subjected to fire, the shear capacity and stiffness of the RC beams both decreased [15]. The researchers studied that fire exposure reduced the lateral/seismic load capacity and ductility of the two reinforced concrete column specimens significantly [16]. Table 1 shows that some research on post-fire curing.

Table 1- Some studies on the post-fire curing [9]

Authors	**Year**	**Materials**	**Exposed temperature (C^0)**
Crook and Murray	1970	Concrete	620
Lin et al.	1996	Concrete	900
Poon et al.	2001	Concrete	600, 800
Henry et al.	2013	Paste & Concrete	600
Henry et al.	2014	Concrete	600

4 Modern Methods Of Residual Strength Assessment

Repairing is restoring structural components that have damaged to an honest condition for further use. Repairs are performed to regain the strength of structural members after a fire disaster. Modern methods of residual strength assessment increase the efficiency of the affected buildings. Root cause analysis is conducted for now the defects in design, material or construction. Destructive testing and nondestructive testing are known for modern methods. Within the destructive testing, the material is broken and can't be further used. Nondestructive testing is a technique for determining material qualities without causing harm. [17].Detecting delamination in concrete by ultrasonic pulse ECHO, Infrared thermal imaging and Eddy current. Find out concrete strength or quality by rebound hammer (with calibration) (ASTMC805), ultra-sonic pulse velocity (UPV) (ASTM597), Windsor probe test and Impact Echo. To estimate thickness cover and rebar spacing use GPR scanning (ASTM 6432) and impact echo (ASTM C1383).For evaluating corrosion use half-cell potential and resistivity [18]. These all are included within the nondestructive testing. According to the ACI 562-16, section 6.4.3.2 non-destructive strength testing to judge in situ strength of concrete shall be permitted if a legitimate correlation is established with core sample compressive strength test results and nondestructive test results. Quantifications of concrete compressive strength by nondestructive testing alone shall not be permitted as a substitute for core sampling and testing.

Within the concrete destructive testing concrete core and pull out the test (ASTM C 900) are used for compressive strength. Rebar sample extraction is additionally destructive testing. Load test is nondestructive testing but it can destructive testing if it ends up in failure. Strengthening of structure and retrofitting are known for the trendy methods of residual strength assessment. Strengthening of structure applied individual members i.e. slabs, columns by using different techniques i.e. jacketing, replacement of spalled concrete. Retrofitting technique is employed for damaged areas to create more proof to loads. The rebound hammer, ultrasonic pulse measurements, and microscope procedures are among the traditional assessment methods included in the experimental section of the report. These are compared to full-field optical strain measurements on drilled cores during a compressive load cycle, i.e. the new approach proposed to quantify the degree of damage in a fire-exposed cross-section. The first step is to conduct an inspection to identify the fire's progression, size, and spread pattern (if possible). A visual mapping of damage, such as spalling, cracking, delamination, deformations, and other physical effects from the fire, should also be included. It's helpful to have a hammer and a chisel on hand for your initial inquiry so you can identify very valuable items.

Ultrasonic pulse measurements on different depths from the fire exposed side of the core can be done on-site immediately after drilling to gain a basic picture of the depth of damage. On the drilled cores, optical full-field strain measurements during a compressive load cycle can be done to get a direct linkage to mechanical properties. The true mechanical response of the material in the cross-section may be estimated, and the most damaged regions would deform more under load due to reduced stiffness. Different microscopy approaches can be used in the lab to study the cores. For estimating acceptable concrete strength of recent structures use the ACI 318 code and for estimating the concrete strength of existing structures use ACI 562 or ACI 214 code. In keeping with ACI 562 section 6.4.2.1, it shall be permitted to see the compressive strength of sound concrete by taking cores from the members being evaluated. Located steel reinforcement before locating the cores to be extracted [19]. The cores shall be selected, tested and removed under ASTM C42 and ASTM 823. Predetecting fire temperatures by visual inspection i.e. if windows aluminium are melted it means temperature exceeds 450-500 ºC. It's also done by petrographic analysis and using standard curves. Concrete cores are used for testing of actual properties of concrete in existing structures like strength, permeability, chemical analysis, carbonation etc. [20].

5 Conclusion

This work sought to introduce post-fire assessment of fire-damaged reinforced concrete structures as well as new methodologies for determining the residual strength of fire-damaged reinforced concrete (RC) structures. The following conclusions are derived based on the literature.

- The buildings have suffered extensive damage as a result of the fire. There is a need to develop techniques for making buildings safer from a fire standpoint.
- When designing reinforced concrete structures, adhere to the building code.
- There is a need to introduce modern methods of residual strength assessment of fire-damaged reinforced concrete (RC) structure.
- There is a need for individuals to be more conscious of fire safety.
- The government makes the policies and strategies regarding fire safety and such policies are strictly followed by everyone.
- A current approach of determining residual strength aids in the reuse of a damaged structure.

The above conclusion demonstrates the importance of fire safety during the design process. Furthermore, contemporary methods of residual strength assessment aid in the reuse of afflicted structures as well as the creation of long-term sustainability.

6 Recommendations

- Investigating new approaches for post-fire evaluation to repurpose fire-damaged structures.
- To assess the concrete/reinforcement strength, consider using a visual scanning method in the future.

Acknowledgement

The author special thanks to Prof. Engr. Dr Majid Ali for his guidance and help in this study.

References

[1] V.Kdour and P.Kumar, "Fire hazard in buildings: review, assessment and strategies for improving fire safety, "*Fire Safety Journal*, 2019.

[2] A. Aseem, W. Baloch, R.A.Khushnood, A.Mushtaq, "Structural health assessment of fire-damaged building using non-destructive testing and micro-graphical forensic analysis: A case study, "Case Studies in Construction Materials, vol.11, 2019.

[3] T.T. Lie and V.K.R. Kodur, "Thermal and mechanical properties of steel-fibre-reinforced concrete at elevated temperatures, "*Canadian Journal of Civil Engineering*, 2014.

[4] J. u. Hwang and H .g. Kwak, "Evaluation of post-fire residual resistance of RC columns considering non-mechanical deformations, "*Fire Safety Journal*, 2018.

[5] <https://en.wikipedia.org/wiki/Structure_fire> [accessed 7.12.20].

[6] A.Bilotta, A.Compagnone, L.Esposito and E.Nigro, "Structural behaviour of FRP reinforced concrete slabs in fire, "*Engineering Structures*, Vol.221, 2020.

[7] M.Z.Naser and A.Seitllari, "Concrete under fire: an assessment through intelligent pattern recognition, "*Engineering with Computers*, 2019.

[8] J. d. A.Oliveir , J. C. L. Ribeiroa , L.Pedroti, C. S.d. Faria, G. H.Nalon and A. L. d. O. Júniora, "Durability of Concrete After Fire Through Accelerated Carbonation Tests, "*Materials Research*, vol. 22,2019.

[9] L. Li, L. Shi, Q Wang Liu, J Dong, H Zhang, G. Zhang, "A review on the recovery of fire-damaged concrete with post-fire-curing, "*Construction and Building Materials*, vol. 237,2020.

[10] S. Ni and T. Gernay, "Predicting residual deformations in a reinforced concrete building structure after a fire event, "*Engineering Structures*, vol.202, 2020.

[11] F. Mistretta and F Stochino, "Thermal Path Reconstruction for Reinforced Concrete under Fire, "*Fire Technology*, 2019.

[12] P. Knyziak, R.Kowalski and J.R.Krentowski, "Fire damage of RC slab structure of a shopping centre, "*Engineering Failure Analysis*, vol.97, 2019.

[13] L.Jin, R. Zhang, G.Dou and X.Du, " Fire resistance of steel fibre reinforced concrete beams after low-velocity impact loading, "*Fire Safety Journal*, vol. 98,2018.

[14] S.Ni, A.C and Birely, "Post-fire seismic behaviour of reinforced concrete structural walls, "*Engineering Structures*, vol. 168,2018.

[15] C. Jiang , J.yu, L. Li, X. Wang and J. Liao, "Experimental study on the residual shear capacity of fire-damaged reinforced concrete frame beams and cantilevers, " *Fire safety journal*, Vol.100, 2018.

[16] H.Mostafaci, F. J. Vecchio and N. Benichou, "Seismic resistance of fire-damaged reinforced concrete columns," *Conference papers*, 2009.

[17] <https://www.tec-science.com/material-science/material-testing/non-destructive-material-testing-ndt/> [accessed 7.12.20].

[18] <https://www.youtube.com/watch?v=Jrgt8_9c0v0> [accessed 7.12.20].

[19] Concrete Structures (ACI 562-19) and Commentary.

[20] <https://www.engineeringcivil.com/testing-concrete-cores.html.> [accessed 8.12.20].

3rd Conference on Sustainability in Civil Engineering (CSCE'21)
Department of Civil Engineering
Capital University of Science and Technology, Islamabad Pakistan

FIRE DAMAGE ASSESSMENT OF REINFORCED CONCRETE STRUCTURES A-REVIEW

[a] ***Ali Rehman***

a: Lecturer, Department of Civil Engineering, Comsats University Islamabad, Abbottabad Campus, alirehman@cuiatd.edu.pk.

Abstract- Event of fire is major hazard come across in civil engineering structures, and consequently given that suitable fire safety methods is a key constraint in a design of building for guaranteeing of safety to the occupants. Fire is the supreme destructive factor that creates deterioration of reinforced concrete structures (R-C-S). Even that the concrete is a not explosive construction material, when R-C-S are in contact to elevated temperature, their mechanical, chemical and physical properties weaken. The fire damage levels of R-C-S considerably depends upon dimension and fire time period. Intensity of fire is minor and small, the loss is expected to be lesser in R-C-S elements. Overall aim of this research is to explore the behavior of R-C-S for high rise (H-R) buildings after the sever event of fire, firefighting (F-F) deficiencies and implementation of precautions for recovering the severe effect of damage by fire. The current study is review of previous studies related to fire damage for reinforced concrete structures. Several case studies have also been reported in this work. After detail literature review results shows that the popularity of fire damages to R-C-S. It was found that the main incorporated fire source occurrence is electric defects, fire detection system not in active condition and lack of firefighting equipment's, barriers in emergencies exits way and due to human mistakes. Further study should be carried out in detail, because of limited scope of this work for fire related apprehensions of H-R building.

Keywords- Damages due to fire, damaged reinforced concrete structures, safety measures for high rise buildings.

1 Introduction

According to world fire data, around 1 million deaths were caused by fires between 1993 to 2014, and nearly 40% of all fires surrounding the world initiated from structures [1]. In this modern world, the fire hazards are arriving as a threat to reinforced concrete structures (R-C-S) buildings. The main components for fire are oxygen, fuel and heat. The fire calamities happening in the R-C-S building causes damage to the R-C-S elements. The key causes for these threats are explosive materials, electric equipment, human wrongdoings and house hold appliances. These rationales direct them to damage of the R-C-S building. Also this may be affect the life lines of living mortals and treasure damages [2]. Many studies show that the decrease of the strength occurred in concrete of R-C-S at elevated temperatures, be governed by some aspects such as: specimen measurement, loading condition, strength of concrete, temperature stages, cooling method, and heating period [3], [4]. The comparative review of case studies of four fire accidents occurred in the different places were reported. The massive fire adversities arisen in case study, and have discussed almost the planning of the R-C-S building, represents the cause for the happening of the fire event, materials that can be sources for fire to the next phases, occurrence of failure to R-C-S, causes behind the life sufferers and treasure loss and helpful measure taken for each R-C-S building are also estimated. The foremost aspect behind the failure of R-C-S is unsuitable design of the high rise (H-R) buildings; the passive and active remedial measures are recommended to minimize the damage of the structure R-C-S [2]. In Figure 1 various phases during the enlargement of a natural fire are shown.

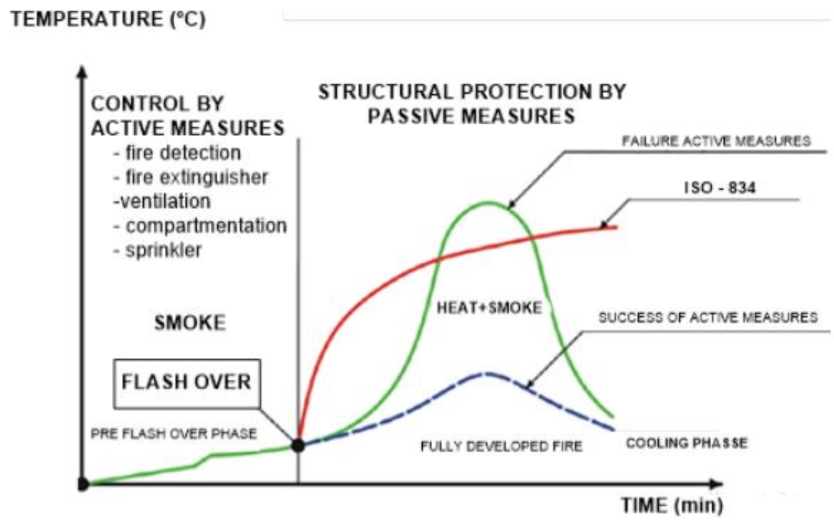

Figure 1. The various phases during the development of a natural fire [5].

In this research work a detailed literature review related to fire damages to reinforced concrete structures, firefighting deficiencies for high rise buildings, and remedial measure adopted for fire prevention in reinforced concrete structures of high rise buildings. Some of case studies also investigated for effect of intensity of fire on structural elements of buildings. Stability of concrete and steel structures in sever event of fire are also identified.

2 Evaluation of reinforced concrete structure of high rise buildings by fire intensity

One of the greatest severe probable hazards for R-C-S building is fire, and because of this international codes provide specific guiding principle to taking into account fire in R-C-S design. In many kingdoms (i.e. Greece, Spain, Turkey, Portugal in the Mediterranean area and Italy), where seismic activity is an event with extraordinary danger for physical grievance and harm to items and assets, national codes are leading more guideline for the risk of fire, by considering that human activities are in constant development and evolution and can be more dangerous than natural events. Amongst the building materials, the concrete is commonly considered by adequate performance for fire. Concrete exposed to long duration of elevated temperature, mechanical loss due to the transformations of microstructure in cement paste and aggregates occurring and changes in volume persuaded by thermal stresses [6]. Fire exposures resulting an earthquake may be noteworthy because of improved possibility ignition of fires, firefighting resources demand increased, and probable barriers to suitable reaction. Ignitions increment and extensive flame duration have substantial structural effects on R-C-S which are generally considered to have advanced performance in events of fire [7]. The Grenfell Tower fire occurred on 14 June 2017, killing 72 people. The pattern and speed of vertical and horizontal fire spread characterize this catastrophic event. After the façade ignited at the fourth floor, vertical propagation over time is linear, with a vertical fire spread rate of around 3.5 m/min until the fire reached the sixth floor. Then fire propagation decelerated [8]. Hotel Aseman Fire, Iran Building features: 22-storey Concrete building Fire occurred on Aug. 3, 2019 No deaths significant structural damage to slabs & shear walls need repair and retrofitting Fire cause occurred during renovation work [9]. Figure 2 shows the damaged reinforced concrete structural elements expose to fire.

(a) (b) (c)

Figure 2. Destruction in slab soffit: (a) Slab#1, (b) Slab#2 and (c) Slab#3 [10].

Exposure to fire can cause R-C-S deterioration, even lead to the collapse of building. Depends upon the fire period and on the structural details i.e. concrete cover, R-C-S elements to be able to bear the effect of fire and stay stable afterward cool down. In the latter case, a structure cannot be bent during a fire, it can still undergo from weakening of the steel and concrete because of higher temperatures. Structural property of reinforced concrete is the flexural ductility i.e. ratio between deformations at state of ultimate and at tension steel yield [11]. Minimum duration to resist the fire in R-C-S shown in Table 1.

Table 1. Minimum fire resistance time period of building in minutes [12].

Category		**Fire resistance time period of building in minutes**			
		Height of building			
		Up to 5m	Up to 18m	Up to 30m	Above 30m
		Minutes	Minutes	Minutes	Minutes
Residential flats	Non-Sprinkler	30	60	90	120
Offices	Non-Sprinkler	30	60	90	Not permitted
	Sprinkler	30	30	60	120
Commercial	Non-Sprinkler	60	60	90	Not permitted
	sprinkler	30	60	60	120
Industrial	Non-Sprinkler	60	60	120	Not permitted
	Sprinkler	30	90	90	120

2.1 Effect of fire damage on strength of reinforced concrete structures

Fire event exposed to a particular raised temperature, concrete is usually lesser defenseless to fire as compare to steel [13]. Most of the fires in R-C-S, structural destruction was detected due to the deterioration of the materials i.e. as concrete and reinforcement of steel. Furthermore guidelines of design R-C-S cannot provide any of reliable estimation of structural performance afterward event of fire, so as a result the level of fire safety against the risk of structural collapse is just unknown [14]. On the behalf of researchers studies concluded that high temperature effect on R-C-S indicate that the calculation of fire resistance is basically depends on tabularized data having the dimensions of R-C-S elements cross-sections and cover of concrete. Buckling mode is noticed at a temperature of 500°C and a crushing failure mode is at lesser temperatures [15]. In addition the creation of non-uniform thermal strain and pore pressure cause in concrete spalling and thermal stresses [16]. Damaged reinforced concrete due to fire with variation of temperature is shown in Table 2.

Table 2. Composition of concrete damage with varying temperatures [17].

Temperature	**Damage Level**	**Grade**
~300 ◦C	No damage	I
	Finishing material damage (soot, surface exfoliation)	II
300~600 ◦C	Concrete damage without steel damage (small cracks in concrete or spalling)	III
600~950 ◦C	Bond damage of steel bars (large cracks in concrete or exposure of steel bars)	IV
950~1200 ◦C	Damage or buckling of steel bars (large damage or deformation of structural members, heavy exposure of steel bars in a wide area)	V
~1200 ◦C	Concrete melting	

Thus the residual capacity of R-C-S members is lesser as per original residual capacity, so that for which these were designed and constructed. The feature exposed to fire were inspected by numerous researchers, assessment of the residual-bearing-capacity of R-C-S next to the event of fire. [18], [13]. Consequently, the importance of variance between the change in properties of materials against pre-fire and post-fire event, reduced the load-bearing capacity, however after the event of post fire reduced capacity because of the concrete deterioration [19]. Reinforcement of steel, the property i.e. residual once, depending upon type of steel, yield strength, young modulus of cold-worked rebar's that are subject to high temperatures ~300oC reduced significantly, for hot-rolled rebar's decrease capacity starts after exposure to ~500oC [20]. So review revealed that steel and residual properties of concrete materials are severely damaged by contact up to~200 temperature, although temperatures cooling ranges from 400oC to 800oC, goes to reduction of residual compressive strength of concrete of with comparison to original strength [21], [22]. It was concluded that the reliability reduced non-linearly with time, whereas the most effective factors influencing the dependability of R-C-S elements were cover of reinforcement, load ratio, exposure of fire and boundary conditions [23].

3 Imperfections in firefighting systems for reinforced concrete structures

In 2009-2013, U.S. fire departments responded to an average of 14,500 R-C-S on fires per year in H-R buildings. These fires initiated yearly usually of: 40 civilian fire deaths, 520 civilian fire harms, and $154 million in direct property destruction. 5 property use groups responsible for just about 3 quarters (73%) of H-R fires: Multi-family housing/Apartments i.e. 62% of all H-R fires, Hotels i.e. 4% of H-R fires, Dormitories i.e. 4% of H-R fires, Offices i.e. 2% of H-R fires, Conveniences that attention for the sickening i.e. 2% of H-R fires [24]. The Shanghai Tower is a mega-tall skyscraper in Lujiazui, Shanghai. The Tower consists minimum of 3 hours fire resistance withstand fire persuaded advanced failure. The R-C-S elements have minor residual displacements reference with steel elements. It is recommended that, reinforced concrete and related structures design, that effective for protection of fire, should be provided for the outrigger trusses to assurance the assembly between the central and mega columns [25]. The World Trade Center (WTC) New York, the United States in 2001, which murdered 2,451 persons, and destruction amount is 33.4 $ billion. It is defined that the separation of the building into fire sections in the vertical for the case was purely nominal [26], [27],[28]. Pictorial view of R-C-S of H-R buildings are shown in Figure 3.

(a) *(b)* *(c)* *(d)*

Figure 3. Pictorial view of fire on:: a) Skyscraper Transport-Tower, Astana; b) Hotel Mandarin Oriental, Beijing; (c) Building in Odessa; (d) Madrid building [29].

3.1 Deficiencies in firefighting systems case studies

Bashundhara City, Dhaka the first biggest commercial complex in Bangladesh. A fire starting through short circuit broke out on 18th floor of the office tower. In addition, the fire-plug could not be used because it was installed inside of an office. The building was not equipped with a sprinkler system but have fire alarms and smoke detectors. The fire hose was installed only in an office area on the standard floor, not compartmented by fire rated walls [30]. Odessa in 2015, paneling on the top floors of the incomplete buildings of the complex Arcadia. The fire was extinguished by two tall ladders 30m and 50 m. However the issue was that the sleeves not have sufficient pressure, and not provide interior fire extinguishing system in building. In 2005 event of fire occur in 106m and 32-storey Vidzor building of office, firefighters reached just over two hours. The building was combination of central reinforced concrete core and outer frame is steel, as an outcome the fire come into contact with 6 upper floors. A fire event occurred in government 32-storey skyscraper Transport Tower in the Kazakh capital Astana in 2006. The fire was convoyed by the scattering to glass-façade shards. In event of fire happened in Mandarin Oriental hotel building, Beijing 2009, fire quickly blow down to the front. Continuation of fire almost to five hours [29]. In Los Angeles 1988, a fire arisen in 62-storey building, although the point is that effectively the whole H-R building area was sprinkler system equipped. Simply through the optimal fire defense of load-bearing components, construction of skyscraper of steel with stood three hours contact with fire intensity. [31].

4 Prevention of fire damage to reinforced concrete structures of high rise buildings

Subsequently the tragedy of WTC, New York, United States in 2001, several criterions have been revised on the behalf of fire event occurrence information manual. As earlier happened fires in H-R buildings cannot lead to whole damage of R-C-S buildings, more or less, the guidelines in many kingdoms permit the evacuation plan by just the fire floor and adjacent floors below and above [32]. Modern H-R policies within the UK requires a minutest fire safety standard as prescribed in the current building regulations "Part B" which can be accomplished through passive and active performance based fire protection methodologies [33]. The remedy for issues in the design of new and renovated H-R structures applied through following procedures: actions for well-timed evacuation and safety contrary to smoky; alarm devices for fire and management evacuation; procedures to protect lives and bound the risk of fire to the materials, buildings and structures. Active Protection System for H-R structures to prevent fire damage: alarm devices for fire and F-F; strong-hold of the fire; Central remote control device systems for fire defense of H-R buildings [29]. In Figure 4 shown some of the F-F equipment's for R-C-S of H-R buildings.

(a) *(b)* *(c)*

Figure 4. Pictorial view of: (a) Fire detection and alarm systems; (b) Internal and external (above ground) hydrants; (c) Sprinkler head [34].

The American National Fire Protection Association (NFPA, 2003) has developed a framework for evaluating fire safety, so called Fire Safety Concepts Tree [35]. The leading cause of serious fatalities in fires event is smoke suffocation i.e. the number of smoke casualties ranges 80% to 90%, whereas a considerably fewer people die due to collapse of building. On the contrary, all buildings must be designed in such a way as to maintain their structural integrity during the fire and thus enable safe evacuation of people and provide a certain level of protection for firefighters. Time duration before the structural collapse should be minimal of 15 minutes, for lightweight wooden/steel structures, including roofs, 1 hour for: small buildings and 3 hours: for H-R buildings [36].

4.1 Standards of fire safety measures for reinforced concrete structures

Fire detectors and alarm systems are the basic fire protection components of each building whose installation and use can considerably decrease the losses of human lives and property after fire. The types of detectors almost usually used in H-R buildings, particularly when human lives are exposed, are heat and smoke detectors, and detectors of other fire phenomena, as well as combined detectors. Control of smoke is compulsory because of difficulties produced by the toxic matters existent in it as well as due to the widespread disorientation effect, due to decreased visibility. [34]. F-F evacuation directions for reinforced concrete structures of H-R building are shown in Figure 5.

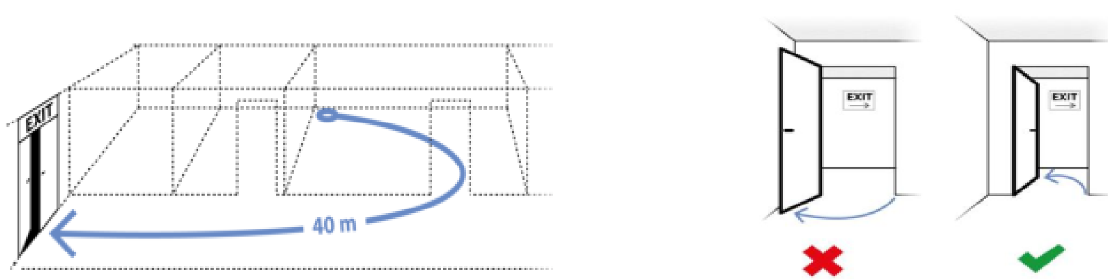

(a) *(b)*

Figure 5. Pictorial view of: (a) Maximum travel distance; (b) Exits opening direction [34].

There are obvious negative significances of interaction between ventilation devices and sprinkler systems. The issues recognized are produced by effect of the water cooling the smoke, which prevents its upward buoyance [37]. A number of tests 34 have been conducted in connection with this phenomenon and design guidelines have been published [38]. Evacuation is one of the most essential problems in fire, and each building must be designed so that occupants can escape on their own or with the help of rescuers/other persons. In all rooms where more than 20 occupants can be accommodated, the exit door must be provided and must be opened in the direction of the exit path. All the width of the stair-way and the corridors must be suitable for the estimated number of people. This also applies to external access to the balcony when people are used primarily for way out. Buildings must be equipped with a backup light with a standby battery to confirm safe evacuation in situation of power failure [34].

5 Conclusion

Numerous important information for structural assessment of a fire damaged building can be, categories of building elements and materials, fire initiated point, exposure condition, necessary data required, expected temperature of fire and time period of fire. Fire ignition can take its peak level because of the limited numbers of fire prevention equipment's and other parameters. The study further shown the requirement to advancement on fire safety actions carry out for the owner of property and designers. The review results show the popularity of survey and case study in fire damage related to reinforced concrete structures. It was found that major corporate source of fire occurrence is faults in electric system, fire detection system not in active condition and lack of firefighting equipment's and barriers in emergencies exits way.

6 Future recommendation

Further study should be carried out in detail for control on fire ignition and fire related concerns of H-R building due to limited scope of this research. Following are some suggestion for R-C-S of H-R buildings to fight with fire disasters and all these are in active and operational condition:

a) Educate all workers and other staff regarding to save their life from fire disaster. Install fire hydrant surrounding the high rise building. Fire control room and assembly area. Emergency stairs are need to be opened all time, tag instruction poster and hang key near the stairs exit door.

b) Increase the numbers of smoke detectors, fire extinguishers, automatic fire alarms, fire proof electric circuit boxes.

c) Posters of emergency phone numbers (i.e. help from university and outside sources), emergency response guidelines (i.e. personal injury response and fire), first aid kit, evacuation plan and fire exits are placed on walls with different locations, of each floor of reinforced concrete structure buildings. Make sure that availability of stock of full face masks on every floor, to avoid the effects of fire and smoke in an emergency condition.

Acknowledgment

The author would like to thank Engr. Prof. Dr. Majid Ali for his kind support and guidance. Also thankful to Engr. Dr. Mehran Khan for his guidance.

References

[1] N. Brushlinsky, M. Ahrens, S. Sokolov, and P. Wagner, "World fire statistics," *Center of fire statistics.-2006.-Report,* 2016.
[2] C. Aravindhan and S. Nayannathara, "Behaviour of Concrete Structure Subjected to Open Fire-State of Art," EasyChair 2516-2314, 2020.
[3] C. Eurocode, "2: Design of concrete structures," *British Standards Institution,* 1992.
[4] J.-C. Dotreppe, J.-M. Franssen, and Y. Vanderzeipen, "Calculation method for design of reinforced concrete columns under fire conditions," *ACI Structural Journal,* vol. 96, pp. 9-18, 1999.
[5] J. Schleich, "Fire Actions in Buildings," *Leonardo Da Vinci Project CZ/02/B/F/PP-134007, Development of Skills Facilitating Implementation of Eurocodes, Handbook,* vol. 5, 2005.
[6] A. Bilotta, A. Compagnone, L. Esposito, and E. Nigro, "Structural behaviour of FRP reinforced concrete slabs in fire," *Engineering Structures,* vol. 221, p. 111058, 2020.
[7] S. Ni and A. C. Birely, "Post-fire seismic behavior of reinforced concrete structural walls," *Engineering Structures,* vol. 168, pp. 163-178, 2018.
[8] E. Guillaume, V. Dréan, B. Girardin, F. Benameur, and T. Fateh, "Reconstruction of Grenfell Tower fire. Part 1: Lessons from observations and determination of work hypotheses," *Fire and Materials,* vol. 44, pp. 3-14, 2020.
[9] C. Thornton, *Descendants of Cyrus: Travels Through Everyday Iran*: U of Nebraska Press, 2019.
[10] T. Ha, J. Ko, S. Lee, S. Kim, J. Jung, and D.-J. Kim, "A case study on the rehabilitation of a fire-damaged structure," *Applied Sciences,* vol. 6, p. 126, 2016.
[11] Y. M. Shachar and A. N. Dancygier, "Assessment of reinforced concrete slabs post-fire performance," *Fire Safety Journal,* vol. 111, p. 102932, 2020.
[12] C. Industry, "Assessment, design and repair of fire-damaged concrete structures," *The Concrete Society,* 2008.

[13] Y. Wang, W. Guo, Z. Huang, B. Long, G. Yuan, W. Shi, *et al.*, "Analytical model for predicting the load–deflection curve of post-fire reinforced-concrete slab," *Fire Safety Journal,* vol. 101, pp. 63-83, 2018.
[14] U. Demir, C. Goksu, G. Unal, M. Green, and A. Ilki, "Effect of Fire Damage on Seismic Behavior of Cast-in-Place Reinforced Concrete Columns," *Journal of Structural Engineering,* vol. 146, p. 04020232, 2020.
[15] V. Kodur, "Properties of concrete at elevated temperatures," *International Scholarly Research Notices,* vol. 2014, 2014.
[16] H. K. Chinthapalli and A. Agarwal, "Effect of Confining Reinforcement on Fire Behavior of Reinforced Concrete Columns: Experimental and Numerical Study," *Journal of Structural Engineering,* vol. 146, p. 04020084, 2020.
[17] H.-C. Cho, D. H. Lee, H. Ju, H.-C. Park, H.-Y. Kim, and K. S. Kim, "Fire damage assessment of reinforced concrete structures using fuzzy theory," *Applied Sciences,* vol. 7, p. 518, 2017.
[18] V. Kodur and A. Agrawal, "An approach for evaluating residual capacity of reinforced concrete beams exposed to fire," *Engineering Structures,* vol. 110, pp. 293-306, 2016.
[19] K. D. Hertz, *Design of Fire-resistant Concrete Structures*: Ice Publishing, 2019.
[20] V. Kumar, U. K. Sharma, B. Singh, and P. Bhargava, "Effect of temperature on mechanical properties of pre-damaged steel reinforcing bars," *Construction and Building Materials,* vol. 46, pp. 19-27, 2013.
[21] Y.-F. Chang, Y.-H. Chen, M.-S. Sheu, and G. C. Yao, "Residual stress–strain relationship for concrete after exposure to high temperatures," *Cement and concrete research,* vol. 36, pp. 1999-2005, 2006.
[22] B. Eurocode, "2: Design of Concrete Structures-Part 1–2: General Rules-Structural Fire Design," *Brussels: European Concrete Platform,* 2004.
[23] R. K. Chaudhary, T. Roy, and V. Matsagar, "Member and structural fragility of reinforced concrete structure under fire," *Journal of Structural Fire Engineering,* 2020.
[24] M. Ahrens, "High-rise building fires," *NFPA (National Fire Protection Association): Quincy, MA, USA,* 2016.
[25] J. Jiang, L. Chen, S. Jiang, G.-Q. Li, and A. Usmani, "Fire safety assessment of super tall buildings: A case study on Shanghai Tower," *Case Studies in Fire Safety,* vol. 4, pp. 28-38, 2015.
[26] M. Gravit, A. Vaititckii, M. Imasheva, D. Nigmatullina, and A. Shpakova, "Classification of fire-technical characteristic of roofing materials in European and Russian regulation documents," in *MATEC Web of Conferences*, 2016, p. 01031.
[27] A. Krivtcov, M. Gravit, S. Zimin, O. Nedryshkin, and V. Pershakov, "Calculation of limits of fire resistance for structures with fire retardant coating," in *MATEC Web of Conferences*, 2016, p. 01032.
[28] M. Gravit, V. Gumenyuk, M. Sychov, and O. Nedryshkin, "Estimation of the pores dimensions of intumescent coatings for increase the fire resistance of building structures," *Procedia engineering,* vol. 117, pp. 119-125, 2015.
[29] V. Pershakov, A. Bieliatynskyi, I. Popovych, K. Lysnytska, and V. Krasheninnikov, "Progressive Collapse of High-Rise Buildings from Fire," in *MATEC Web of Conferences*, 2016, p. 01001.
[30] S. i. Sugahara, H. Yoshioka, and S. Barua, "Case Studies of High-Rise Building Fires in Dhaka City with Reference to Building Fire Code of Japan," *Fire Science and Technology,* vol. 30, pp. 69-80, 2011.
[31] R. W. Archibald, J. J. Medby, B. Rosen, and J. Schchter, "Security and safety in Los Angeles high-rise buildings after 9/11," RAND CORP SANTA MONICA CA2002.
[32] F. Building, "Fire Safety Investigation of the Word Trade Center Disaster: Final Report of the National Construction Safety Team on the Collapses of the World Trade Center Towers," *NIST, NIST NCSTAR,* vol. 1, 2005.
[33] A. J. Baker, "'Suitable and sufficient'? UK regulation of post-construction fire safety," 2019.
[34] M. Laban, S. Draganić, and I. Džolev, "FIRE SAFETY IN BUILDINGS," 2020.
[35] M. J. Karter, *Fire loss in the United States during 2002*: National Fire Protection Association Quincy, MA, 2003.
[36] UNOPS, "Design Planning Manual for Buildings," *Technical framework for minimum requirements for infrastructure design.,* vol. 1.1, 2014.
[37] A. Heselden, *The interaction of sprinklers and roof venting in industrial buildings: the current knowledge*: Department of the Environment, Building Research Establishment, Fire …, 1984.
[38] P. Hinkley and P. Illingworth, "The Ghent fire tests; observations on the experiments," *Colt International, Havant, Hants, UK. Murs séparatifs coupe-feu et façades à function d'écran thermique en béton (B67), CIMbéton, Paris, France,* 1990.

3rdConference on Sustainability in Civil Engineering (CSCE'21)
Department of Civil Engineering
Capital University of Science and Technology, Islamabad Pakistan

ASSESSING DAMAGE GRADES OF BUILDINGS AND THEIR RELATIONSHIP WITH SEISMIC RISK PERCEPTION, A CASE STUDY OF PABBI, KHYBERPAKHTUNKHWA

[a]Riazud din*, [b]Faheem Butt

a: Department of Civil Engineering, UET Taxila, meetriaz22@yahoo.com
b: Department of Civil Engineering, UET Taxila, faheem.but@uettaxila.edu.pk
*Corresponding author: Email ID: meetriaz22@yahoo.com

Abstract- The aim of the study is to accomplish seismic vulnerability appraisal of buildings in the town of Pabbi (Nowshera district) of Khyber Pakhtunkhwa (KPK) province and to observe the relationship between risk perception and vulnerability assessment, if any. The paper describes building structures, damage grades and their relationship with people risk perception, based on the current physical condition of buildings. The vulnerability assessment of the existing buildings was carried out using customized FEMA P-154 form. The investigation of the present condition of buildings revealed that due to old age, plan and vertical irregularities, unplanned settlement, rapid urbanization, buildings constructed on soft soil and no implementation of seismic design codes; most of the buildings were vulnerable to earthquake loading. It was observed that most of the buildings (>50%) fall in damage grade 3 and 4, implying strong probabilities of heavy structural and non-structural damages and require detail evaluation. The people risk perception study was carried out using face to face interviews which revealed that the people perceive the chances of earthquake in future. An empirical relationship between damage grades and people seismic risk perception were developed using regression analysis. The results revealed that people risk perception and damage grades of their buildings have a reasonably good relationship with an R^2 value of 0.57. The study is an important step for the institutions, policy makers, designers and researchers to reduce the risk associated with earthquake and thereby reducing loss of lives and assets.

Keywords- Damage grades, Earthquake risk perception, Rapid visual screening, Vulnerability assessment.

1 Introduction

The intrinsic vulnerability to seismic action of unreinforced brick masonry structure is perceived as deficient despite several decades of academic research. The seismic activities are considered one of the most destructive natural disaster and damages associated has significantly increased[1]. There are various methods and procedures are available in the literature for determining earthquake vulnerability of the existing building structures[2]. The procedures vary from complex finite element analysis of each building to the simple ones based upon Rapid Visual Screening (RVS) which can help in predicting the future vulnerability of structures[3]. The former is a computationally expensive, laborious and time consuming exercise, while the latter is a simple sidewalk survey which can be completed for a building stock with a significantly less effort and time [4].

The term risk refers to probable degree of damage and associated injury likely to occur over a specified period of time from the exposure of people and property. The risk perception directly alters one's action before and during a hazard[5].

The earthquake risk assessment is the estimation of maximum loss i.e. infrastructural, economical, and social which can help in developing earthquake risk maps[6].The perception of risk from hazard relationships have been studied by various researchers and it was concluded that perceived risk from natural hazard is influenced by many factors such as age, gender, education[7] location of residence[8] and duration of stay[9]etc.

The objective of the study is to carry out seismic vulnerability assessment of buildings; people risk perception survey and their inter-relationship in the city of Pabbi of Nowshera district in the KPK province. The study can be used for mitigation of future earthquake hazards through awareness and preparedness.

2 Methodology

2.1 Case study area and sample size

Pabbi is tehsil of Nowshera district of Khyber Pakhtunkhwa province of Pakistan. It is located at Grand Trunk (GT) road around 20km from Peshawar. It has a latitude of 34^0 00’ 34” N and has a longitude of 71^0 47’ 40” S. The Pabbi tehsil has an urban population of 55,255 according to Pakistan Bureau of statistics[10]. In the past, the city was basically a residential dominant area; however in the recent past due to rapid urbanization it has grown into zones of commercial, semi commercial and residential areas. For conducting the vulnerability assessment of buildings using RVS procedure, 400 samples as per Yamane formula[11]have been selected and investigated from the area as shown in Figure 1.

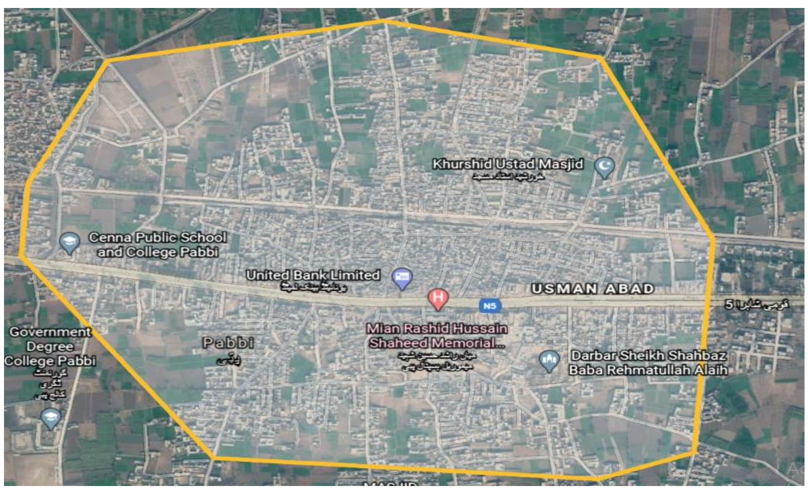

Figure 1: Arial view of the surveyed area

2.2 Vulnerability assessment of buildings using RVS procedure

A building’s response to earthquake is associated to earthquake intensity and duration along-with building’s lateral load resisting system, materials and construction quality, soil strata, plan and vertical irregularities, wall opening, damage from past hazards etc. Following are the factors which are considered for RVS survey for vulnerability assessment:

Earthquake hazard intensity─ Damage to building is directly associated to this and it is a part of RVS.

Building type─ Building response to earthquake mainly relies on its lateral load resisting system[12].

Building height─ It is proved that low rise buildings are generally less vulnerable than high rise building[13].

Vertical irregularity─ Since vertical irregularity has adverse effect on seismic performance and its score modifier is taken as negative for all building types[14].

Plan irregularity─Buildings having plan irregularities are considered more vulnerable that of regular one[15].

Construction quality─ Poor construction quality exhibits poor performance during earthquake[16].

Soil type─Structural damage associated with amplitude and duration of shaking and soil types has major influence upon these[17]. To classify soil type during planning stage if sufficient data are not available then soil type E should be assumed[18].

Pre code construction─ Buildings constructed before the adaptation of seismic codes are vulnerable and have poor performance during an earthquake[19].

2.3 Risk perception assessment

Focusing on the issues associated to risk appraisal the field of risk analysis has developed expeditiously. The risk perceived covers the factors such as vulnerability, character and cognition[20] .The basis of the risk research can be traced back at the time of initial nuclear debate in 1960. The analysis of earthquake risk perception in Pakistan is vital in drafting the earthquake risk communication plan. The scheme needs to address the current risk perception of the community on the land of Pabbi city district Nowshera. Risk perception and awareness is not only rely upon individual risk and risk past events. To introduce risk awareness, another way is by establishing and promulgating information and communication tools and coordinating risk alertness campaign.

Using an extensive literature review, based on the nine selected indicators shown in Table 1, risk perception index has been developed. The indicators include like probability of earthquake occurrence in future, probability of future harm by an earthquake, loss of lives, ability to cope, level of last seismic event harming, your structure resistance etc. A value of 1 and 0 has been assigned to each indicator representing no risk and maximum risk respectively. Mean Risk perception index (RPI) value has computed using the following equation for each indicator.

Table 1 The details of earthquake risk perception indicators

S. No	Attributes	Category	Weightage	Explanation	Proof
1.	How likely an earthquake will occur in future?	Very high High Medium Low Very low	1 0.8 0.6 0.4 0.2	Those perceiving likelihood of an earthquake would perceive more risk.	[21-24]
2.	The probability of future harms by an earthquake.	Very high High Medium Low Very low	1 0.8 0.6 0.4 0.2	Those perceiving likelihood of destruction of an asset by earthquake would perceive more risk.	[25]
3.	How much are you afraid of an earthquake?	Very high High Medium Low Very low	1 0.8 0.6 0.4 0.2	Those afraid relatively more from an earthquake would perceive more risk.	[22, 26]
4.	The level of understanding of emergency protocols.	Very high High Medium Low Very low	1 0.8 0.6 0.4 0.2	The knowledge about emergency protocols would perceive low risk.	[22, 25]
5.	The level of loss of lives in earthquake.	Very high High Medium Low Very low	1 0.8 0.6 0.4 0.2	Those who believe loss of lives in future earthquake perceive more risk.	[21, 22, 27, 28]

6.	The ability to cope with a future earthquake.	Very low Low Medium High Very high	1 0.8 0.6 0.4 0.2	A better economy of households with high capability perceives low risk.	[29, 30]
7.	The level of harm/damage in the last seismic event.	Very high High Medium Low Very low	1 0.8 0.6 0.4 0.2	The people affected from past earthquake will Perceive more risk.	[28]
8.	The structure resistance to an earthquake.	Very high High Medium Low Very low	1 0.8 0.6 0.4 0.2	The perceived more building resistance will have low risk perception.	[21, 24, 26, 31]
9.	The age of the respondent.	>35 31—35 26—30 21—25 <25	1 0.8 0.6 0.4 0.2	The risk perception increases with age.	[7]

$$RPI = \Sigma(W1 + W2 + W3 + \cdots W9)/9 \qquad (1)$$

3 Results and discussions

3.1 *Building vulnerability assessment and grading*

Based on lateral load resisting system, base score is assigned to each building which reflects probability of damage if exposed to maximum considered earthquake (MCE) ground motion. The basic structural hazard score, score modifier and final structural score (SS) has been calculated on RVS data collection form and then correlated with damage grades (DG). The recommended minimum score was encircled in case of the SS less than the minimum score. A value of 1 for SS means that at MCE the calculated probability of building collapse is 10^{-1} i.e. 1 in 10. Similarly, a value of 2 or 3 for SS means that at MCE the calculated probability of building collapse is 10^{-2}or 10^{-3} respectively[32].

The final structural score (SS) as mentioned above is correlated with damage grades (DG).The researchers have used different relationships for correlating SS score with DG[33]. The short period spectral acceleration (S_s) and long period spectral acceleration (s_1) values for the selected region have been obtained from a previous study[34]. The MCE level ground motion values are not available; therefore these were determined from design basis earthquake (DBE) values by multiplying with 1.5 as a standard practice. Based upon the values of spectral accelerations (S_s and S_1), the current study area has been placed in moderately high seismicity region according to FEMA P-154[18].According to the European macro seismic scale, damage to buildings have been categorised in various grades as shown in Table 2. This classification helps in evaluation of seismic intensity and is used in RVS to predict probable damage to a building.

Table 2- **Structural score along corresponding damage potential[35]**

Rapid Visual screening score	**Potential Damage Grade (G)**
S < 0.3	High chance of G5 damage; very high likelihood of G4 damage
0.3 < S < 0.7	High chance of G4 damage; very likelihood of G3 damage
0.7 < S < 2	High chance of G3 damage; very high likelihood of G2 damage
2 < S < 2.5	High chance of G2 damage; very high likelihood of G1 damage
S > 2.5	Possibility of Grade 1 damage

During the field survey, plan and vertical irregularities, poor materials and construction quality, lack of implementation of seismic design codes and diaphragm insufficient thickness were observed in the study area. These factors influence seismic performance of structures[16].

The surveyed buildings have been categorized into four classes, viz. residential, commercial, educational and other. The other building structures in the study area found were semi commercial and health centres etc. Most of the investigated buildings were unreinforced masonry and ordinary moment resistance frame structures. The overwhelming majority of the investigated fall into damage grade 3 (DG3) and 4 predicting high structural and non structural damage. The result in Figure 2 revealed that 56% of residential, 42% of commercial, 56% of educational and 52% of other buildings fall under DG3 and 4.

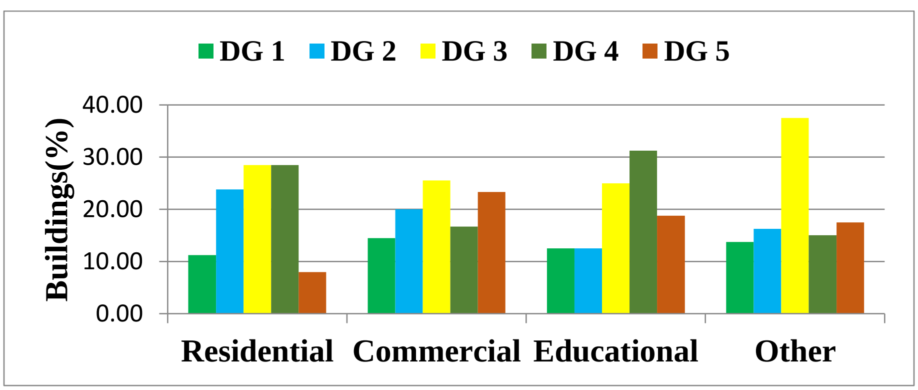

Figure 2: The building categories with determined damage grades

A detail evaluation of a structure is determined on the basis of final structure score SS. The buildings with SS value less than 2 should need to be assessed in detail. However, this figure varies from country to country[35, 36]. The result from Figure 3 revealed that more than fifty percent of buildings of all categories in the study area required detail evaluation. From the study, 137 out of 217 (63.13%) residentail, 58 out of 89 (65.16%) commercial, 12 out of 16 (75%) educational and 55 out of 78 (70.51%) other buildings required detail evaluation due to low final score. Such low final score was mainly due to plan and vertical irregularities, buildings constructed on soft soil and pre code construction.

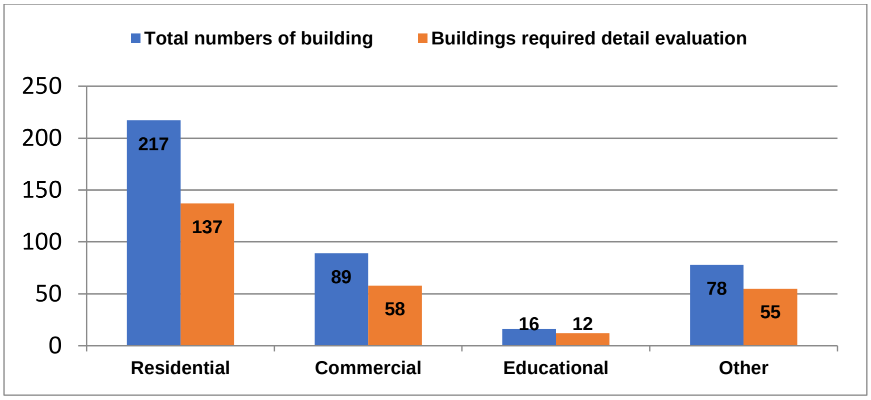

Figure 3: The buildings of all categories which require detail evaluation

3.2 People risk perception results

The risk perception is an important element of comprehensive disaster risk evaluation. The risk perception index was calculated for each household using face to face interview. The results revealed that perceived risk increases with increase in seismic vulnerability of buildings. In risk perception, the majority of variations observed was due to past earthquake losses, fear from seismic events, emergency protocol understanding level, capability to cope with future earthquake and supplies disruption.

3.3 Relationship between damage grades and people risk perception

A relationship has been developed between people risk perception and damage grades of their buildings using linear regression analysis. The result shown in Figure 4 disclosed that there is a positive relation between people risk percpetion and damage grades. The value of R^2 is 0.572, this means that the relationship accounts for 57.2% of the total variation. It reflects that community house hold risk percpetion increases with increase in damage grade (DG) of building. A possitive correlation between both assessment imply that people are comprehensive of the vulnerability of the stucture and may take precustionary and preparedness measures against future earthquak hazard. There are other factors as well which influence the relationship between people risk perception and damage grades and the results presented here may not be considered conclusive here. As a measure of eathquke hazard mitigation, pople risk perception can be considered a reasonable substitue in case of missing hard data.

$$RPI = 0.485 + 0.432 * DG \qquad (2)$$

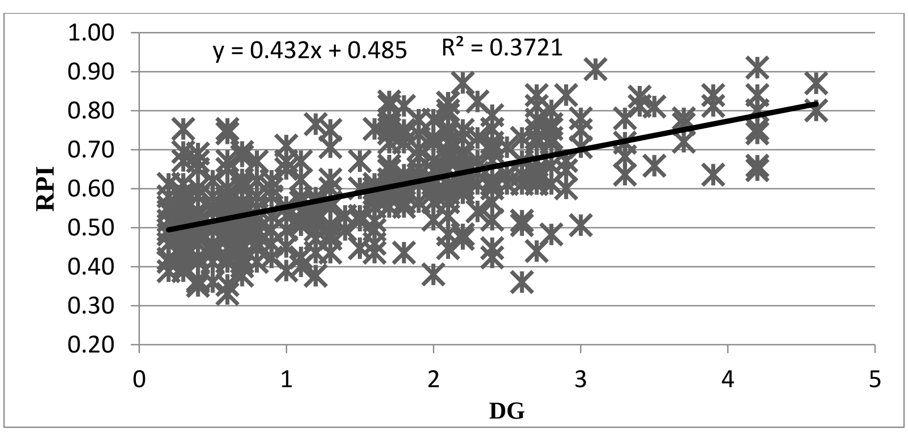

Figure 4: The corelation between damage grades and people risk perception

4 Conclusions

In this paper RVS has been used to collect data of 400 buildings in Pabbi City of District Nowshera KPK. The vulnerability assessment has been carried out using latest modified FEMA P-154 form. The percentage of various buildings categories with different damage grades recorded for the study area gives an idea of buildings requiring detail assessment. Over all maximum percentage of buildings lie in DG3 and DG4, representing moderate to heavy structural and non-structural damage. The results in term of damage grades disclosed that more than fifty percent of building of all categories require retrofitting or need to be replaced. Most of the surveyed buildings were unreinforced masonry residential structures. It has concluded and is rational that people risk perception increases with increase in damage grade of their buildings.

People customarily spend in their buildings maintenance and on advanced decoration; however by warning them about the situation large numbers would coincide care with retrofitting. During the survey it was observed that the recent seismic events caused momentous damages to unconfined brick masonry buildings. Severe vertical irregularities, heavy overhangs, short column, vertical setback and plane irregularity were noticed in reinforced concrete structures.

5 Practical implementation

The adverse impacts of earthquakes on a community can be minimized using buildings vulnerability assessment and developing correlation between damage grades and people risk perception which the current study addressed. For mitigation of earthquake disaster, the concern authorities must ensure alertness amid communities regarding protected building construction methods and implementation of building regulations in the area.

6 Appendix Acknowledgment

The support of locals during the field survey for their friendly agreement and the conduction in the surveyed area is gratefully acknowledged.

References

[1] K. M. Allen, "Community-based disaster preparedness and climate adaptation: local capacity-building in the Philippines," *Disasters*, vol. 30, no. 1, pp. 81-101, 2006.
[2] G. M. Calvi, R. Pinho, G. Magenes, J. J. Bommer, L. F. Restrepo-Vélez, and H. Crowley, "Development of seismic vulnerability assessment methodologies over the past 30 years," *ISET journal of Earthquake Technology*, vol. 43, no. 3, pp. 75-104, 2006.
[3] V. Patil and M. S. SM, "Rapid Visual Screening of Buildings for Potential Seismic Hazards: A Case Study of Chiplun City," 2017.
[4] G. Castori, A. Borri, A. De Maria, M. Corradi, and R. Sisti, "Seismic vulnerability assessment of a monumental masonry building," *Engineering Structures*, vol. 136, pp. 454-465, 2017.
[5] D. Dominey-Howes and D. Minos-Minopoulos, "Perceptions of hazard and risk on Santorini," *Journal of Volcanology and Geothermal Research*, vol. 137, no. 4, pp. 285-310, 2004.
[6] N. Frolova, V. Larionov, J. Bonnin, S. Sushchev, A. Ugarov, and M. Kozlov, "Seismic risk assessment and mapping at different levels," *Natural Hazards*, vol. 88, no. 1, pp. 43-62, 2017.
[7] I. Armaş, "Earthquake risk perception in Bucharest, Romania," *Risk Analysis*, vol. 26, no. 5, pp. 1223-1234, 2006.
[8] J.-C. Gaillard, "Alternative paradigms of volcanic risk perception: The case of Mt. Pinatubo in the Philippines," *Journal of volcanology and geothermal research*, vol. 172, no. 3-4, pp. 315-328, 2008.
[9] K. Burningham, J. Fielding, and D. Thrush, "'It'll never happen to me': understanding public awareness of local flood risk," *Disasters*, vol. 32, no. 2, pp. 216-238, 2008.
[10] P. Statistics, "of Pakistan Bureau of Statistics," ed: Pakistan: Government of Pakistan, 2017.
[11] T. Yamane, *Statistics: an introductory analysis NY, Harper & Row*. 1967.
[12] K. Subramanian and M. Velayutham, "Seismic performance of lateral load resisting systems," *Structural Engineering and Mechanics*, vol. 51, no. 3, pp. 487-502, 2014.

[13] H. B. Ozmen, M. Inel, and E. Meral, "Evaluation of the main parameters affecting seismic performance of the RC buildings," *Sadhana*, vol. 39, no. 2, pp. 437-450, 2014.
[14] C. Repapis, C. Zeris, and E. Vintzileou, "Evaluation of the seismic performance of existing RC buildings II: A case study for regular and irregular buildings," *Journal of earthquake engineering*, vol. 10, no. 03, pp. 429-452, 2006.
[15] R. G. Herrera and C. G. Soberón, "Influence of plan irregularity of buildings," in *The 14th world conference on earthquake engineering*, 2008.
[16] A. Naseer, A. N. Khan, Z. Hussain, and Q. Ali, "Observed seismic behavior of buildings in northern Pakistan during the 2005 Kashmir earthquake," *Earthquake Spectra*, vol. 26, no. 2, pp. 425-449, 2010.
[17] J. D. Bray and R. Luque, "Seismic performance of a building affected by moderate liquefaction during the Christchurch earthquake," *Soil Dynamics and Earthquake Engineering*, vol. 102, pp. 99-111, 2017.
[18] F. E. M. Agency, *Rapid visual screening of buildings for potential seismic hazards: A handbook*. Government Printing Office, 2017.
[19] C. Briceño, S. Moreira, M. F. Noel, M. Gonzales, E. Vila-Chã, and R. Aguilar, "Seismic vulnerability assessment of a 17th century adobe church in the Peruvian Andes," *International Journal of Architectural Heritage*, vol. 13, no. 1, pp. 140-152, 2019.
[20] I. Armaş and E. Avram, "Patterns and trends in the perception of seismic risk. Case study: Bucharest Municipality/Romania," *Natural Hazards*, vol. 44, no. 1, pp. 147-161, 2008.
[21] S. Ainuddin, J. K. Routray, and S. Ainuddin, "People's risk perception in earthquake prone Quetta city of Baluchistan," *International Journal of Disaster Risk Reduction*, vol. 7, pp. 165-175, 2014.
[22] B. K. Paul and R. H. Bhuiyan, "Urban earthquake hazard: perceived seismic risk and preparedness in Dhaka City, Bangladesh," *Disasters*, vol. 34, no. 2, pp. 337-359, 2010.
[23] G. NAEEM and K. OKAZAKI, "EARTHQUAKE RISK PERCEPTION OF STAKE HOLDERS INVOLVED IN HOUSING SAFETY IN PAKISTAN," *Bulletin of the International Institute of Seismology and Earthquake Engineering*, vol. 43, pp. 91-96, 2009.
[24] T. R. Paradise, "Perception of earthquake risk in Agadir, Morocco: A case study from a Muslim community," *Global Environmental Change Part B: Environmental Hazards*, vol. 6, no. 3, pp. 167-180, 2005.
[25] S. Tekeli-Yeşil, N. Dedeoğlu, C. Braun-Fahrlaender, and M. Tanner, "Earthquake awareness and perception of risk among the residents of Istanbul," *Natural hazards*, vol. 59, no. 1, pp. 427-446, 2011.
[26] A. Taylan, "Factors influencing homeowners' seismic risk mitigation behavior: a case study in Zeytinburnu district of Istanbul," *International journal of disaster risk reduction*, vol. 13, pp. 414-426, 2015.
[27] K. Okazaki, A. Ilki, N. Ahmad, R. Kandel, and H. Rahayu, "Seismic risk perception of people for safer housing," in *Proceedings of The 14th World Conference on Earthquake Engineering*, 2008, pp. 1-8.
[28] A. Y. Lo and L. T. Cheung, "Seismic risk perception in the aftermath of Wenchuan earthquakes in southwestern China," *Natural Hazards*, vol. 78, no. 3, pp. 1979-1996, 2015.
[29] M. T. Azim and M. M. Islam, "Earthquake preparedness of households in Jeddah, Saudi Arabia: a perceptual study," *Environmental hazards*, vol. 15, no. 3, pp. 189-208, 2016.
[30] K. Nicoll, T. Cova, L. Siebeneck, and E. Martineau, "Assessing "Preparedness Elevated": Seismic Risk Perception and Household Adjustment in Salt Lake City, Utah," *J Geogr Nat Disast*, vol. 6, no. 168, pp. 2167-0587.1000168, 2016.
[31] I. Armaş, "Social vulnerability and seismic risk perception. Case study: the historic center of the Bucharest Municipality/Romania," *Natural hazards*, vol. 47, no. 3, pp. 397-410, 2008.
[32] Y. Yang and K. A. Goettel, *Enhanced Rapid Visual Screening (E-RVS) Method for Prioritization of Seismic Retrofits in Oregon*. Citeseer, 2007.
[33] P. Rautela, G. C. Joshi, B. Bhaisora, C. Dhyani, S. Ghildiyal, and A. Rawat, "Seismic vulnerability of Nainital and Mussoorie, two major Lesser Himalayan tourist destinations of India," *International journal of disaster risk reduction*, vol. 13, pp. 400-408, 2015.
[34] N. PMD, "Seismic hazard analysis and zonation of Pakistan, Azad Jammu and Kashmir," *Pakistan Meteorological Department and Norway Report*, 2007.
[35] R. P. Nanda and D. R. Majhi, "Rapid seismic vulnerability assessment of building stocks for developing countries," *KSCE Journal of Civil Engineering*, vol. 18, no. 7, pp. 2218-2226, 2014.
[36] G. Grünthal, "European macroseismic scale 1998," European Seismological Commission (ESC)1998.

3rd Conference on Sustainability in Civil Engineering (CSCE'21)
Department of Civil Engineering
Capital University of Science and Technology, Islamabad Pakistan

MODERN REPAIRING TECHNIQUES OF RC BUILDINGS DAMAGED DUE TO EARTHQUAKE DISASTER –A REVIEW

[a] ***Muhammad Abrar***

a: Department of Civil Engineering, University of South Asia Lahore, abrar19125@gmail.com

Abstract- Earthquake is the natural hazard which is caused by movement of tectonic plates underneath the earth and has severe impact like collapse of buildings, bridges and roads. Due to these characteristics it has a great influence on economy, social life of humans of a country as natural hazard. Reinforced concrete (RC) buildings get damaged by the high intensity earthquakes along with the loss of life of occupants. The purpose of the study is the impact of earthquake on human life, damages due to earthquake and its influence towards economy. The aim of this paper is to study the modern techniques that are being used to repair and strengthen earthquake damaged RC buildings. The state of the art literature is reviewed and it has been observed that retrofitting is widely used in strengthening and repairing of RC building. This paper focuses on the damages of RC buildings due to earthquake in Pakistan and different types of retrofitting for repairing and strength enhancing. Since there are limited techniques present to rehabilitate the earthquake damaged RC building so there is a need of experimental work to find out new ways of repairing.

Keywords- Earthquake, Fiber reinforced polymer (FRP), Repairing techniques, Retrofitting.

1 Introduction

An earthquake is a hazard which may become disaster when there is a vulnerable society present in risk area. It is a phenomenon of large intensity with limited time duration, causes loss of lives and economical damage along with disruption of social life. If earthquake becomes disaster, it exceeds the local capacity and resources so sometimes external aid is needed to cope this disaster. Earthquake may cause the damages of roads, collapse of buildings and bridges. During the earthquake in Pakistan in 2005 about 400,000 buildings were collapsed or damaged. About 79,000 injured, 90,000 died and more than 3.5 million were homeless. Govt. reported that more than 19,000 children died under school buildings collapse [1]. Due to the damage of these structures and hospitals the emergency treatment centers were established in timber houses. As earthquake damaged this huge number of structures so social life of humans was highly affected. To accommodate these earthquakes affected homeless people, there was a need of vast re-construction for fully damaged buildings, rehabilitation, and repair of partially damaged building to make them suitable for living.

Most of the damages in RC buildings occurs due to short columns, large and heavy overhangs, defects due to workmanship, discontinuity of beams, and lack of control [2]. Seismic hazard assessment is important factor to take part to the efforts towards increasing the resilience of cities [3]. Different types of data bases are present that records damages due to worldwide hazards. It has been observed that the ratio of loss has been considerably increase after 1970. There are many factors that are responsible for this change in trend of loss in terms of damages of buildings, economy and loss of human life. Urbanization is the important factor with growing population. Due to this factor the vulnerability against hazard has considerably increased. Hence population in danger zone areas related to earthquake has considerably increased. The damages due to earthquake has to be compensated by means of repairing of damaged buildings and reconstruction. Reconstruction cost is much higher than repairing that's why repairing is often accomplished to strengthen the earthquake partially damaged structures [4]. Retrofitting is most popular technique for repairing and strengthening [5] [6].

The purpose of this paper is to provide a comprehensive overview to the damages due to earthquake. Damages due to earthquake in Pakistan during earthquake of 2005 are mainly focused. The loss of life, number of homeless people, damages of houses and impact of these factors is on overall economy and rehabilitation costs is studied. Damages due to earthquake, failure pattern and methods to repairing and strengthening of RC structures are discussed.

2 Earthquake Disaster impacts in Pakistan

Earthquake is a natural phenomenon caused by ground motion due to movement of tectonic plates underneath of earth [7]. It has some triggering point from which it generates and spread to a vast area in short time. An earthquake was recoded on 8th of October 2005 in Pakistan. It was the strongest earthquake of the history of Pakistan. The main center of this earthquake was northern area of Muzaffarabad district with depth 26 km and had magnitude of 7.6. High seismic activity was noticed in terms of aftershocks after main event of earthquake. About 12,909 aftershocks were recorded by Pakistan meteorological department and 59 aftershocks had magnitude of 5.0 or greater than this value [1] [8]. The most affected areas due to earthquake in Khyber Pakhtunkhwa were Abbottabad, Shangla, Kohistan, Mansehra, and Batagram. Some areas of AJK were also affected i.e. Poonch, Bagh and Muzaffarabad.

2.1 Socio-economic loss due to earthquake

There were about 5.1 million people affected due to earthquake in 2005. People of Pakistan experienced many earthquakes which are present on record. A number of people died and huge economy loss was noticed during study of literature. As a result of this inflation also increased in Pakistan. A number of people became homeless and it was a big challenge to provide new home to those affected persons. Table 1 provides comprehensive data of causalities due to earthquake excluding tsunami, number of homeless people and total number of affected people in a year along with damages in US dollar (USD) from 1935 to 2019. Impact of damage on consumer price index (CPI) is also given [9]. Asian development and World Bank published a report in which they claim that 787,583 houses were affected. 203,579 housed were completely collapse down during 2005 earthquake.

Total economic loss of Pakistan was calculated as $5 billion. Table 2 shows the economic loss in terms of restoration of livelihood, re-construction cost, relief package, death/injury compensation and percentage of total loss. It was noticed that there was huge loss of lives during earthquake of 2005 as compared to other earthquake of Pakistan. The number of yearly deaths from 1980 to 2014 due to earthquake are present in Fig 1. The causalities during earthquake in 2005 are nearly 39,000. The ratio of deaths registered is quite low [10]. On the other hand EM-DAT system recorded 73,338 deaths. It is clear from this two databases that the values of recorded causalities are different by different disaster data base resources. This can be due to lack of database management or due to unreliable data gathering means and missing data cards.

Table 1-Total loss due to earthquake in Pakistan [9]

Year	Total Deaths	Injured	Homeless	Total Affected	Total Damages ('000 US$)	CPI
1935	60000	25000		25000		5.37
1945	4000				25000	7.06
1972	100			5000		16.36
1974	4700	15000	5200	50200	3255	19.29
1981	250	2000		2000	5000	35.57
1981	6	12		237		35.57
1983	24	543		543	3000	38.96
1984	4	12		12		40.63
1985	5	38		12038	2000	42.07
1986				750		42.87
1990	11	250		250		51.11

1990	11	40		40	1000	51.11
1990		6		6		51.11
1991	300	574	29465	204794	10000	53.27
1992	4					54.88
1992	36	100	2000	2100		54.88
1997	50	100	10000	10100		62.79
1998	1	11	600	611		63.76
2001	12	100		914292	500	69.26
2002	17	65	4000	15065		70.36
2002	19	40		140782		70.36
2002	3					70.36
2004	24	63	2320	13148		73.88
2005	73338	128309	5000000	5128309	5200000	76.39
2008	166	320		75320	10000	84.22
2011	2			1000		87.98
2013	41	175		15175		91.12
2013	399	599		185749	100000	91.12
2013	22	50		50		91.12
2015	280	1745	133900	502590		92.71
2015	3	85		85		92.71
2016	6	42		142		93.88
1909	231					3.52
1955	12					10.47
2019	39	746		130398	17000	100.00

Table 2- Loss of economy due to earthquake of 2005 in Pakistan [1]

Category	**US $ M**	**Percentage of total**
Death and injury compensation	205	3.9
Relief	1,092	21.0
Restoration of livelihoods	97	1.9
Early recovery	301	5.8
Short-term reconstruction	450	8.7
Long-term reconstruction	3,053	58.7
Reconstruction	3,503	66.4
Total	5,198	100.0

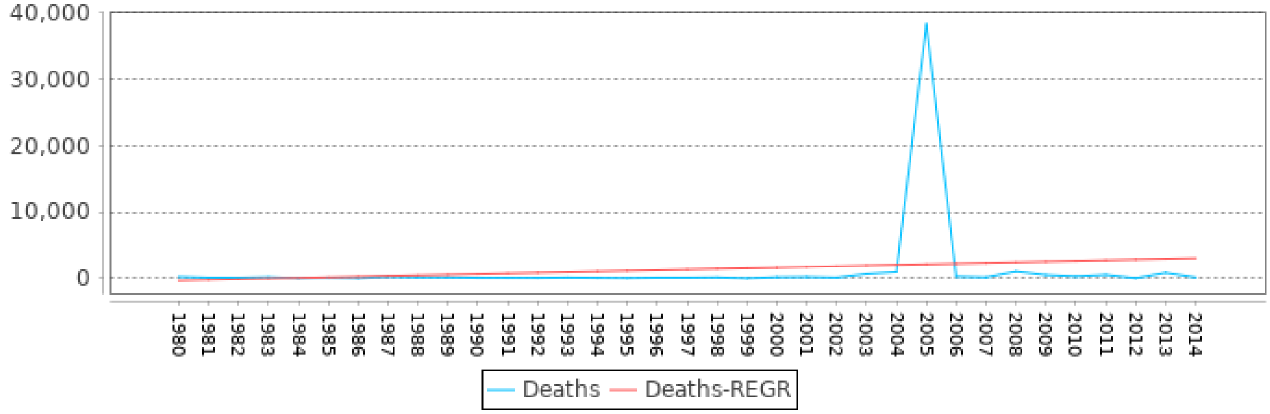

Figure 1: Number of people died due to earthquake from 1980 to 2014 [10]

3 Properties of earthquake damaged RC buildings

Earthquake causes partially damage or total collapse of RC buildings. It has been observed that while designing, building code of earthquake safety provisions is not followed properly that may cause severe damage to RC buildings. Due to this fact a large number of buildings collapsed in Pakistan under earthquake loading. Figure 2 shows the number of houses damaged due to earthquake from 1980 to 2014. Usually cracks are present on the surface of columns, beams and other components of RC structures. The nature, depth and opening of cracks can be observed so that it may be concluded, either cracks are present in concrete cover or they are at full depth. [11] Conducted a series of experiments to understand the failure pattern of Elliptical hollow section (EHS) beams and columns under seismic loading. This study revealed that it was local buckling failure in EHS columns and under combined cyclic and compression bending. There was a diverse failure in case of concrete filled columns including local buckling. Energy dissipation performance and ductility can be enhanced by applying concrete in fill or by improving compactness of steel section.

Columns are the compressive members of RC structure. RC columns must have sufficient ductility and rigidity in earthquake resistance design framework. Under seismic load, columns cannot fulfil the displacement demand hence expected performance cannot be achieved. The phenomenon mostly occurs in case of short columns where stiffness is quite high due to shorter in length than other floor columns [12]. The seismic motion cause lateral load effect whereas short columns try to compensate it by stiffness. Hence short columns do not show the desired ductile behavior. In this scenario, to increase ductility, shear reinforcement is increased [13]. Figure 3 shows the short column shear failure in RC building structure [1]. The failure of beam and column joint can be happened due to insufficient length of development (see figure 4). The development of full strength happens when length of embedment is sufficient.

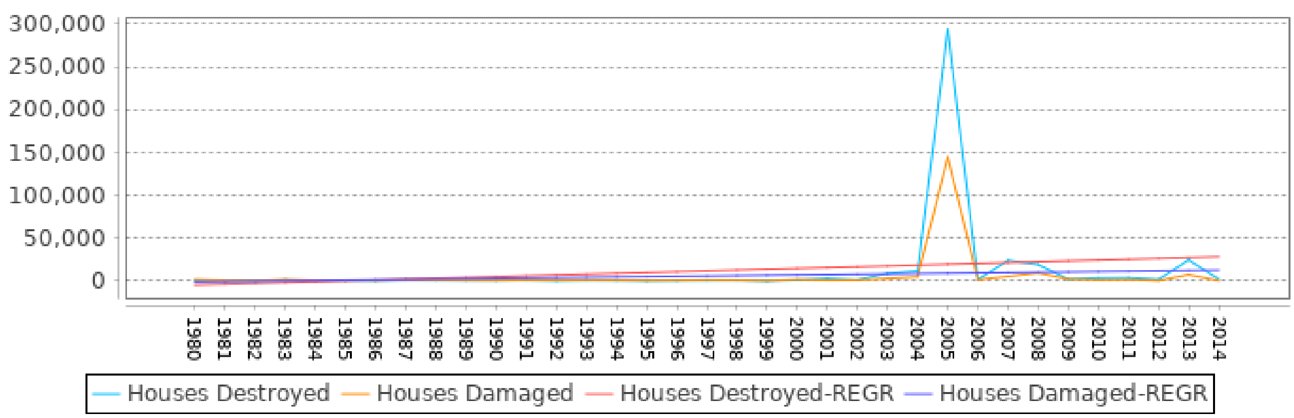

Figure 2: Houses destroyed due to earthquake during 1980 to 2014 [10]

Figure 3: Shear failure in RC short column [1]

Figure 4: Anchorage failure [1]

4 Modern repairing techniques

Earthquake damaged structures needs a repairing and strengthening for rehabilitation and reuse. For post-earthquake re-construction structure stiffness, site selection, beams columns joints and integrity of structures load transformation pattern is analyzed [14]. Fiber reinforced polymers (FRP) and its derivative wraps are most widely used materials in strengthening and repairing of RC buildings. External jacketing technique is also use to enhance the strength of columns. Steel jacketing is the most commonly used against gravity and seismic loads [15]. Due to increase of displacement demand, low flexural stiffness weakens the jacketing effectiveness. To overcome this flaw external collars are applied. For enhancing the performance of short columns external collars are found successful. An investigation was carried out to compare the performance of carbon fiber reinforced polymers (CRFP) wrapped columns and externally collar column to reference columns with no external strengthening. Results indicates that shear cracks are limited due to both strengthening techniques. These columns are more ductile than the reference column and energy absorption is higher than reference columns. If aspect ratio is same the increase in cross-section increased the strength [13].

Since shear failure and diagonal rupture is the failure pattern in short columns under seismic loads. Carbon fiber-reinforced polymer sheets and glass fiber-reinforced polymer bars as diagonal, transverse hybrid techniques are used to enhance strength [16]. Studies indicated that the wrapping of short columns by FRP prevents the buckling. Moreover it leads to a hinge on top and bottom of the column. The wrapping changes the failure from shear to flexure failure [17]. The performance of short columns is considerably increased because energy dissipation is increases to 800% and ductility up to 125% by use of corner strip-batten full wrapping technique [18]. In another study, Polyvinyl chloride tube (PVCT) with high-strength concrete (HC) was used to check the seismic behavior of short columns. HC-PVCT short columns strength degradation was slower and ductility was increased significantly as compared to HC short columns [19].

4.1 Retrofitting technique of strengthening RC buildings

Retrofitting is most widely used to strengthen and repair damaged structures [20]. Buckling-restrained-braces (BRBs) is an efficient technique of retrofitting to enhance strength of RC building present in high seismic zone areas. An experimental study was carried out to check the effectiveness of BRBs. The RC building seismic performance was observed before and after retrofitting with BRBs under incremental dynamic analyses and non-linear static analyses. The model with BRBs retrofitting found more effective under seismic ground motion [21]. Selection of suitable retrofitting rely upon the structural considerations, economy and usage of that particular structure [22]. The available and required shear resistance is calculated by multi-degree-of-freedom. Hence the difference of available and required is fulfilled by steel bracing as additional elements (retrofitting).The retrofit interventions are made to mitigate main structural deficiencies to meet current building code requirement. These building code requirements confined the damage to non-structural elements and provide and way to non-ductile failure mechanism. By increasing the ground motion intensities, retrofit alternatives are evaluated. Mean annual frequency and expected yearly loss of collapse is quantified by risk based decision variables. The retrofit alternatives were then evaluated through increasing ground shaking intensities to quantify risk-based decision variables, such as the expected annual loss and mean annual frequency of collapse. Cost-benefit analysis is also done to check economic feasibility [23].

5 Conclusion

By conducting this study following conclusions can be drawn:

- There was local buckling failure in EHS columns under combined cyclic and compression bending whereas there was a diverse failure in case of concrete filled members including local buckling.
- The bending section governed the failure mode and abrupt failure of concrete section having no buckling failure was noticed.
- Suitable retrofitting depends upon the type of building, failure and economy. Cost-benefit analysis is done to check economic feasibility.
- HC-PVCT short columns strength degradation was slower and ductility was increased significantly as compared to HC short columns.

The conclusion illustrate that columns fail in buckling failure when undergo seismic loading. Failure patterns are different for different type of failure, hence retrofitting is applied according to need of RC buildings. FRP and steel braces retrofitting is most suitable for most of the RC buildings.

Acknowledgment

The author would like to thank every person/department who helped thorough out the research work, particularly CE department and Engr. Dr. Usman Farooqi whose hand of kindness remained present at every step. The careful review and constructive suggestions by the anonymous reviewers are gratefully acknowledged.

References

[1] S. T. Maqsood, J. Schwarz, "Analysis of Building damage during the 8 October 2005 earthquake in Pakistan," *Seismological Research Letters*, pp. 163-17, 2008.

[2] R. Temür, E. Damcı, S. Öncü-Davas, C. Öser, S. Sarğın, Ç. Şekerci, "Structural and geotechnical investigations on Sivrice earthquake (Mw = 6.8), January 24, 2020," *Natural Hazards*, pp. 713-744, 2021.

[3] E. Riga, A. Karatzetzou, S. Apostolaki, H. Crowley, K. Pitilakis, "Verification of seismic risk models using observed damages from past earthquake events," *Bulletin of Earthquake Engineering*, pp. 713-744, 2021.

[4] G. Ramesh, D. Srinath, D. Ramya, B. Vamshi Krishna, "Repair, rehabilitation and retrofitting of reinforced concrete structures by using non-destructive testing methods," *Materials today: Proceedings*, 2021.

[5] W. Ahmed, M. Asif, "A critical review of energy retrofitting trends in residential buildings with particular focus on the GCC countries," *Renewable and Sustainable Energy Reviews*, 2021.

[6] L. D. Pereira, V. Tavares, N. Soares, "Up-To-Date Challenges for the Conservation, Rehabilitation and Energy Retrofitting of Higher Education Cultural Heritage Buildings," *Sustainability*, 2021.

[7] P. Oggu, K. Gopikrishna, "Assessment of three-dimensional RC moment-resisting frames under repeated earthquakes," *Structure*, pp. 6-23, 2020.

[8] P. M. Department. [Online]. Available: https://www.pmd.gov.pk/en/.

[9] T. i. d. database, "EM-DAT," [Online]. Available: https://public.emdat.be/data. [Accessed 23 04 2021].

[10] UNDRR, "SENDAI FRAMEWORK FOR DISASTWER RISK REDUCTION," [Online]. Available: https://www.desinventar.net/DesInventar/profiletab.jsp. [Accessed 23 04 2021].

[11] C. Fang, M. F. Zhou, Z. Wu, F. Wang, "Concrete-Filled Elliptical Hollow Section Beam-Columns under Seismic Loading," *Journal of Structural Engineering*, 2020.

[12] X. Gu, J. Hua, M. Cai, "Seismic responses of reinforced concrete intermediate short columns failed in different modes," *Engineering Structures*, 2020.

[13] T. Dirikgil, "Experimental investigation of the contributions of CFRP and externally collar strengthening to the seismic performance of RC columns with different cross-sections," *Structure*, pp. 266-281, 2020.

[14] C. Liu, D. Fang, L. Zhao, "Reflection on earthquake damage of buildings in 2015 Nepal earthquake and seismic measures for post-earthquake reconstruction," *Structure*, pp. 647-658, 2021.

[15] F. D. Trapani, M. Malavisi, G. C. Marano, A. P. Sberna, R. Greco, "Optimal seismic retrofitting of reinforced concrete buildings by steel-jacketing using a genetic algorithm-based framework," *Engineering Structures*, 2020.

[16] B. Duran, O. Tunaboyu, Ö. Avşar, "Structural Failure Evaluation of a Substandard RC Building due to Basement Story Short-Column Damage," *Journal of Performance of Constrcued Facilities,* 2020.

[17] A. Kargaran, A. Kheyroddin, "Experimental investigation of seismic strengthening of reinforced concrete short columns using externally bonded reinforcement, near surface mounted, and hybrid techniques," *Journal of Composite Materials,* 2019.

[18] S. M. Hosseini, D. Mostofinejad, A. Saljoughian, B. N. Tehrani, "Seismic Retrofit of Square RC Short Columns with Shear-Flexural Failure Mode via CFRP Composites Using Different Confinement Techniques," *Journal of Composites for construction,* 2020.

[19] J. Xue, X. Zhao, F. Zhang, X. Ke, L. Ma, D. Xu, "Investigation on seismic performance and shear strength of high-strength concrete-filled polyvinyl chloride tube short columns," *Structural Design of Tall and Special Buildings ,* 2019.

[20] D. A. Pohoryles, J. Melo, T. Rossetto, H. Varum, D. D'Ayala, "Effect of slab and transverse beam on the FRP retrofit effectiveness for existing reinforced concrete structures under seismic loading," *Engineering Structures,* 2021.

[21] P. Castaldo, E. Tubaldi, F. Selvia, L. Gioiella, "Seismic performance of an existing RC structure retrofitted with buckling restrained braces," *ElSEVIER Journal of Building Engineering,* 2021.

[22] W. W. C. Gallo, D. Gabbianelli, R. Monteiro, "Assessment of Multi-Criteria Evaluation Procedures for Identification of Optimal Seismic Retrofitting Strategies for Existing RC Buildings," *Journal of Earthquake Engineering,* 2021.

[23] D. W. Carofilis, D. Perrone, G. J. O'Reilly, R. Monteiro, A. Filiatrault, "Seismic retrofit of existing school buildings in Italy: Performance evaluation and loss estimation," *Engineering Structures,* 2020.

3rd Conference on Sustainability in Civil Engineering (CSCE'21)
Department of Civil Engineering
Capital University of Science and Technology, Islamabad Pakistan

EARTHQUAKE RISK ASSESSMENT FOR SINGLE STOREY RESIDENTIAL BUILDINGS- AN OVERVIEW

Muhammad Sultan Sikandar

Civil Engineering Department, Lahore Leads University,sultansikandar618@gmail.com

Abstract- Earthquake is the most dangerous natural hazard as compared to other natural hazards. New methods and technologies are being explored for earthquake risk assessment. Many scholars have looked into earthquake risk assessment for high-rise buildings, but none have looked into earthquake risk assessment for single-story residential buildings. This study focuses on earthquake risk assessment for single storey residential buildings. Many researchers investigated that single storey buildings have more ability to stand against earthquake than high rise buildings. The results have established that buildings are designed to bear shaking along horizontal X and Y direction to counter earthquake inertia force. This study determines the future directions for exploring the earthquake risk assessment for single storey residential buildings to reduce the consequences of the earthquake.

Keywords- Earthquake risk assessment, Inertia force, Natural hazard, Residential buildings

1 Introduction

The systematic recording of weather, stream heights, and then earthquakes began the process of risk estimation in the late 19th century. A detached section that consists of a ground storey only, with a roof to which only repair or maintenance access is provided may be classified as a single storey building. To achieve design strategies and risk levels that are consistent with tenant expectations and social objectives, building design and construction procedures should address the entire risk to residential construction from many hazards. According to a 2000 study by the Federal Emergency Management Agency FEMA 2000a, hurricanes and earthquakes are among the most costly natural hazards that affect residential construction in the United States, with annual economic losses averaging $5.4 billion for hurricanes and $4.4 billion for earthquakes [1]. Intensity measures (IMs) provide a link between probabilistic seismic hazard analysis and probabilistic structure response analysis in the performance-based earthquake engineering (PBEE) framework created by the Pacific Earthquake Engineering Research (PEER) Center. Mean annual rates of exceedance of different levels of IMs are estimated for the site of interest in the probabilistic seismic hazard analysis, whereas the seismic response of the structure subjected to different levels of IM is investigated in the probabilistic structural response analysis [2].

The number of casualties is directly proportional to the damage to civil engineering structures such as buildings. The frequent occurrence of damaging earthquakes highlights the urgent need for research into earthquake risk assessment (ERA) methods for buildings to effectively reduce earthquake impact in the city. Buildings are typically categorized based on a mix of building attributes (for example, structural system, height, or the number of floors) as well as the type of occupation (e.g., residential structures, hospitals, offices, schools). Single-family dwellings with one and two stories have traditionally been bundled together by the insurance business. Regional risk analyses were also based on the insurance practice [3]. An earthquake is known as a natural disaster. Earthquake risk assessment for single storey residential buildings are also very important. An earthquake occurs when two earth blocks unexpectedly slip past each other. The surface where the earth surface slips are known as the fault plane. In the literature, earthquake is declared second dangerous natural disaster. Earthquake is an out of control natural disaster and can cause much destruction to human beings.

2 Causes of earthquake

Earthquake is the main problem in the modern age and not clears any acceptable solution. Today's world discovered many technologies but we cannot prevent natural disasters and their dangerous effects [4]. The earthquake occurred in turkey in 2020 with a magnitude of 6.8 and caused serious damages to human life and property [5]. It is reported that change in groundwater can cause some sizable earthquakes. It is reported that if the time window is 90 days and the correlation coefficient is higher than 0.10 then sizable earthquakes occurred with the $M \geq 5$ During the 45 days with 200 kilometres while all the conditions are the same but correlation coefficient is higher than 0.65 than earthquakes occurred with 150killometer during the 45 days [6]. It is reported that more than 50 % of death happened in an earthquake than other types of disasters [7]. The earthquakes that occurred by the crack of rock zones are known as shortcomings. Seven large lithospheric plates and smaller plates in the earth crust. These plates moved towards each other are known as convergent boundary and when these plates' moves apart then they are called divergent boundary. If these plates are passed each other then they are called transform boundary.

In the earth crust when suddenly released stress toward faults occurred then an earthquake happened. The motion of tectonic plates developed a built-up pressure in the rock strata on sides of the fault and the stress is great which produced jerk movement. The waves which are produced through these situations propagate through the ground and its surface and these shaking we take as an earthquake. Earthquakes caused by tectonic plates are known as tectonic quakes. In the world, most earthquakes occurred on the boundaries of tectonic plates. Induced earthquakes are caused by human activities because of major technological activity i.e. mining, open pit mining etc. performed by the human and small earthquake occurred on the surface. It is reported that water can also cause earthquakes because water seeps into the subsoil increased the pore pressure and reduced internal friction so the strength of the rock decreased and rock breaks and earthquakes occurred. Volcanic earthquakes are caused by active volcanism. Figure 1 shows different tectonic plates around the globe.

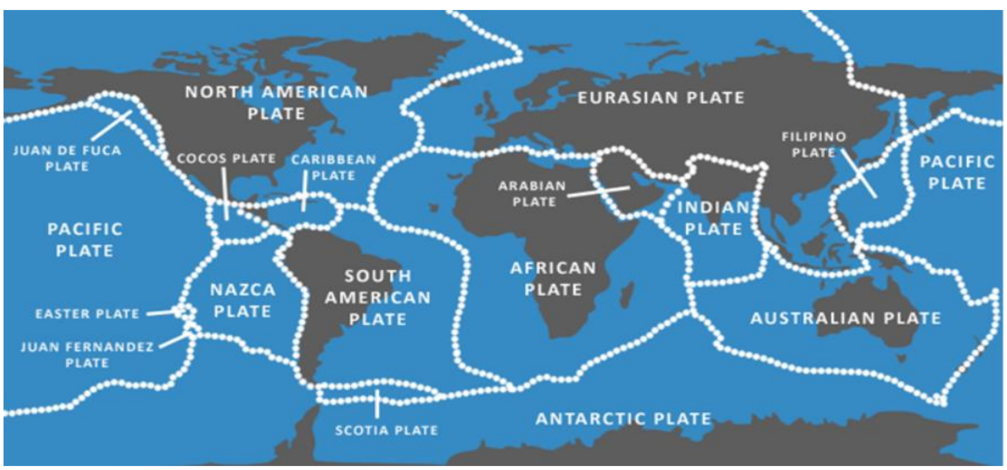

Figure 1: Boundaries of tectonic plates [8]

3 Earthquake risk assessment for single storey residential buildings

The purpose of a seismic risk assessment (SRA) is to forecast the likelihood of building and infrastructure damage, as well as economic losses, in the event of a hypothetical seismic hazard or scenario earthquake. In general, it consists of two steps: assessing structural vulnerability and analyzing seismic hazard. SRA's main focus is on assessing structural vulnerability. Open SEES was used to create nonlinear structural models for single-story industrial steel buildings, which were then used in static and dynamic seismic assessments. The following modelling criteria were used i.e. adoption of simple yet generic methodologies based on accessible data, such as geometry and material qualities and avoidance of empirical models requiring calibration based on experimental tests as much as possible. The seismic performance of various design parameters (geometry, seismic hazard, soil typology) and modelling assumptions (bare-frame model, frame including cladding panels, effect of vertical accelerations, and influence of uncertainties in the steel yield stress and brace equivalent imperfections) was evaluated using multi-stripe analyses [9]. The probabilistic seismic hazard analysis and the probabilistic structure response analysis are linked by ground motion intensity measures (IMs). IMs that are well correlated with the structural reaction enable a low-risk (high-efficiency) calculation of the structure's seismic reaction, minimizing the computational effort required for structural response analysis.

A spatial correlation model must be available to employ an IM for regional seismic risk assessments. These studies look at the seismic risk of a group of structures that are spread out throughout a region. As a result, during an earthquake, the analyst must take into account the link between IMs affecting various areas. The regional seismic risk of high-consequence events may be drastically underestimated if the spatial link is either ignored or undervalued. The HAZUS is an earthquake risk assessment instrument created in the United States that assesses the impact of earthquakes on the built environment and population in urban settings. MunichRe, Risklink (RSM), CAT MAP (Air), CATEX, EPEDAT (Early post-earthquake damage assessment tool, Image Cat), RADARS (Risk from earthquake damage to highway system), and risk management solutions are among the software's used in the commercial approaches for risk assessment [10]. Using simple models and first principles, this researcher assesses the relative seismic risk of 1- and 2-story houses. Simulated lumped-mass models are used to evaluate the impact of the fundamental period of vibration, lateral stiffness in each storey, mass distribution, and nonlinear effects on the seismic response of 1- and 2-storey houses for this purpose.

As a result, 2-story residences have a much higher risk of damage and predicted losses than 1-story buildings. This result is in line with the damage seen following other historical earthquakes, where two-story houses have performed worse than their one-story counterparts. Quantifying predicted losses from natural catastrophes and creating appropriate risk management strategies require structural reliability-based methodologies that explain natural hazard and structural system response probabilistically. It is reported that for the earthquake probability assessment data availability required i.e. slope, elevation, magnitude density, depth density, epicentre density, proximity to fault and geology [11]. Earthquake risk assessment of single-story residential buildings necessitates the consideration of Triggering factors of single-storey residential buildings, spatial occurrence, Duration of the event, Time of onset, Frequency, Magnitude/intensity, Derived/secondary events. Table 1 shows that vulnerability is categorized as very high, high, moderate, low and very low. The percentage of high vulnerability is 28.28 % because of the greater population at risk as shown in table 1.

Table 1- The details of earthquake based population at risk, percentage and number of families [12]

Vulnerability	**Percentage**	**Population at risk**	**Number of Families**	**Area (m 2)**
Very High	25.39	15415	4596	10728300
High	28.28	45162	13772	11949800
Moderate	22	75592	22513	9297200
Low	12.88	67818	21322	5445600
Very Low	11.45	130846	41564	4837900

4 Effects of earthquake on residential buildings

The earthquake occurred at Zagreb in March 2020 with a magnitude of 5.5 which cause serious damages to the architectural achievements and historical centre of Zagreb [13]. The research revealed that earthquake directly affects severe damages to structures and also indirectly cascade the results of infrastructure damages [14]. It is reported that aftershocks increased the losses by around 10 % [15]. The researchers revealed that the seismic response on the masonry structures and near and far-fault records are different. It is reported that near-fault earthquakes have the potential to more damages the structures than far fault records [16]. It is reported that small stories have more capacity to stand against earthquakes than large stories buildings. Level of shaking by earthquake cause minor damages, major damages, and interior finishes cracking, nonstructural damages i.e. plumbing and heating etc. It is reported that ground shaking intensities are very important against building response [17]

In structures destruction, the most dangerous natural hazard is an earthquake. When an earthquake hits the structure then it generates inertia of forces which caused destruction and horizontal and vertical shaking. The capacity of any roof structure to remain in its original position is known as inertia. Greater mass i.e. high rise building have the inertia of force so a single story or two stories building has a better capacity to stand against earthquake. It is reported that when an earthquake occurs and ground shaking occurred then the base of the structure also moved with the shaking. This movement creates internal forces in the columns of the buildings. These internal forces are also known as stiffness forces. It is investigated that the stiffness forces are higher as column height increased. The earthquake caused shaking the building in three directions X, Y and Z. In common practice buildings are designed for vertical loads and buildings to stand against earthquake to vertical loads by safety factor in the design. But horizontal shaking of the building in X and Y direction caused lateral displacement and inertial forces. Tsunami, landslides and liquefaction are the indirect effects on the structure [18].

5 Consequences of earthquake

It is reported in the literature that the consequences of the earthquake have positive and negative interactions. The researchers revealed that the earth not only damaged the structure but also creates problems for the living conditions of survivors. It is reported that the consequences of an earthquake can not only be evaluated by structural damages but also evaluated residual damages [19]. A consequence of earthquake includes loss of life and both social and economic loss. For finding the consequences of an earthquake for a nation or country, city and individual the common term used seismic risk assessment instead of earthquake loss estimation. Seismic risk assessment finds out the economic and social results of an earthquake will be equal or greater values in areas where the earthquake occurred. The main purpose of earthquake loss estimation is to find out not only the physical expected damages and social and economic losses that are connected direct or indirect way by the earthquake [20].

In any assessment, the consequences of earthquakes include the cost of repair of the buildings, causalities and downtime. It is reported that earthquake destroys the economy of any country. The earthquake occurred at any time and without any warning and can be caused damaged structure and human lives. It is reported that if the epicentre of the earthquake is in populated areas then they create a large disturbance. These earthquakes are known as urban earthquakes. The rescue operation can be very complex and reduced the capacity to reduce the consequences [21]. Table 2 shows the consequences of the different earthquake in Pakistan from 2005-2019. Deaths in 2005 and total affected are very high as compare to other earthquakes as shown in table 2. Dis mag value is same in 2005, 2013 and 2015 but total damaged that occurred in the 2005 earthquake is much higher than earthquakes.

Table 2-Consequences of different earthquakes in Pakistan 2005-2019 [22]

Year of Earthquake	Dis Mag Value	Total Deaths	Total Affected	Total Damages ('000 US$)
2005	8	73338	5128309	5200000
2008	6	166	75320	10000
2011	7	2	1000	-
2013	8	41	15175	-
2013	8	399	185749	100000
2013	7	22	50	-
2015	8	280	502590	-
2015	6	3	85	-
2016	7	6	142	-
2019	6	39	130398	17000

6 Conclusion

The purpose of this study is to provide an overview of earthquake risk assessment for single-story residential buildings, as well as earthquake effects on residential buildings and earthquake repercussions. The following conclusions are obtained from the literature.

- Single-story buildings can withstand earthquakes significantly better than high-rise structures.
- Residential buildings in urban areas much need more attention.
- A seismic vulnerability map for single-story residential buildings will be created to help mitigate the effects of earthquakes.
- The design of high-rise buildings includes a safety factor for horizontal shaking in both the X and Y directions.

As a result of the preceding conclusion, earthquakes are a significant natural hazard; therefore earthquake risk maps for residential buildings are essential.

Acknowledgement

The author special thanks to Engr. Dr Muhammad Usman Farooqi for his guidance and help in this study.

References

[1] Y.Li, M. Asce, B.R. Ellingwood, F. ASCE, "Framework for multi-hazard risk assessment and mitigation for wood-frame residential construction, DOI: 10.1061/_ASCE_0733-9445_2009_135:2_159_.
[2] P. Heresi and E. Miranda, "Intensity measures for regional seismic risk assessment of low-rise wood-frame residential construction, *American society of civil engineers*, 2020.
[3] E. Miranda and P. Heresi, "Seismic risk comparison between 1- and 2-story houses for performance-based earthquake engineering, *Earthquake engineering*, 2018.
[4] M. Yadav S. Chaudhary and A. Agarwal, "bio-info-sensors image processing approach: disaster pre-alarm for earthquake, *Advances in System Engineering*, pp.859-867, 2021.
[5] R. Temur, E. Damci, S. O. Davas, C. Osar, S. Sargin and C. Seerci, "Structural and geotechnical investigations on sivrice earthquakes (Mw = 6.8), *Journal of natural disasters*, Vol. 106, pp. 401-434, 2021.
[6] G. Lai, C. Jiang, W. Wang, L. Han and S. Deng, "Correlation between the water temperature and water level data at the Lijiang well in Yunnan,China, and its implication for local earthquake prediction, *The European Physical Journal Special Topics*, Vol. 230, pp. 275-285, 2021.
[7] H. Li, F. Wang, h. zhang, N. Cui and P. Zhong, "Analysis of catastrophic earthquakes characteristics and countermeasures in china, *Earth and Environmental Science*, 2021.
[8] <http://www.seismo.ethz.ch/en/knowledge/things-to-know/causes-of-earthquakes/general/> [assessed 23.4.21].
[9] F. Scozzese, G. Terracciano, A. Zona, G. D. Corte, A. D. Asta and R. Landolfo, "Modelling and seismic response of Italian code-conforming single-storey steel buildings, *Journal of earthquake engineering*,2018.
[10] B. Gulati, "Earthquake risk assessment of buildings: Applicability of hazus in Dehradun, India, 2006.
[11] P. Yariyan, H. Zabihi, I. D. Wolf, M. Karami and S. Amiriyan, "Earthquake risk assessment using an integrated fuzzy analytic hierarchy process with artificial neural network based on GIS: A case study of Sanandaj in Iran, *International Journal of Disaster Risk Reduction*, 2020.
[12] M. Stepinac, P. B. Lourenco, J. atalic, T. Kisicek, M. Uros, M. Banicek and M. S. Novak," Damage classification of residential buildings in historical downtown after the M L5.5 earthquake in Zegreb,croatiain 2020, *International Journal of Disaster Risk Reduction*, Vol. 56, 2021.
[13] C. Y. Lam and T. Shimizu, "A network analytical framework to analyze infrastructure damage based on earthquake cascades: A study of earthquake cases in Japan, *International Journal of Disaster Risk Reduction*, Vol.54, 2021.
[14] F. A. arifin, T. J. Sullivan, g. macrae, M. kurata and T. takeda, "lessons for loss assessment from the canterbury earthquakes: a 22-storey building, *Bulletin of Earth Engineering*, 2021.
[15] H. Bilgin and M. hysenlliu," Comparison of near and far-fault ground motion effects on low and mid-rise masonry buildings, *Journal of Building Engineering*, Vol. 30,2020.
[16] R. E. Chase, A. B. Liel, N. Luco and B. W. Baird, "Seismic loss and damage in light-frame wood buildings from sequences of induced earthquakes, *Earthquake engineering and Structural Dynamics*, 2019.

[17] <https://theconstructor.org/structural-engg/earthquake-effects-structures/2704/> [accessed 23.4.21].
[18] Z. Cui, A. Alipour and B. Shafei, "Structural performance of deteriorating reinforced concrete columns under multiple earthquake events, *Engineering Structures*, Vol. 191, pp. 460-468, 2019.
[19] A. Majdi and R. s. Vacareanu, "state of the art regarding quantifying the consequences associated with building response to an earthquake shaking, *Web of Conferences*, 2019.
[20] D. Jurukovski, "earthquake consequences and measure for the reduction of seismic risk, 2009.
[21] H. Bilgin and M. hysenlliu," Comparison of near and far-fault ground motion effects on low and mid-rise masonry buildings, *Journal of Building Engineering*, Vol. 30,2020.
[22] <https://public.emdat.be/> [accessed 23.4.21].

3rd Conference on Sustainability in Civil Engineering (CSCE'21)
Department of Civil Engineering
Capital University of Science and Technology, Islamabad Pakistan

A STATE OF THE ART REVIEW, IMPACT OF WINDSTORM ON STEEL STRUCTURE IN EAST ASIA

Hafiz Muhammad Bilal

HH Robertson Pak Pvt. Limited m.bilal@hhrobertson.com.pk
Corresponding author: Email ID: engr.hafizbilal95@gmail.com

Abstract- Damages, losses and social problems occurs every year due to the natural disaster in all over the world. The range of the damages caused by the windstorm on the build environment increase gradually. A number of the commercial and residential steel structure are collapse just because these building are not design to resist the high speed wind. In this work, more than 35 papers of different authors are reviewed on the windstorm related disasters. Although, the literature related to steel structure, which are collapse or partially damages due to the windstorm are very limited. Numerous authors focus on the design parameters and some of them studied the effects of high speed wind on the structure and their losses when the event happened. In results, it is found that due to extreme wind pressure roof and wall cladding of the structure damages, and it is observed that numerous buildings are not designed against the high speed wind load, design engineer should be consider the impact of high speed wind load, surrounding trees, anchoring, outdoor equipment and the direction of wind during design phase to mitigate or minimize the losses due to windstorm.

Keywords- Windstorm, steel structure, wind load, Natural disaster

1 Introduction

Damages, losses and social problems occurs every year due to the natural disaster in all over the world. The range of the damages caused by the windstorm on the build environment increases [1]. The most dangerous natural disaster on the earth surface are severe rainstorms, tornadoes, and also the hurricanes, and destructive damages and disturbance of societies are due to the tropical windstorm were reported. A number of the commercial and residential steel structure are collapse just because these building are not design to resist the high speed wind that many accrue particularly in the extreme events and the wind loading starting point on any structure is basically measure near surface wind speed [2]. Mehrshad Amini et al, [3] review the coastal domestic building performance w.r.t the direct and indirect damages, and discussed the mitigation techniques by considering the hurricanes and flood related hazards and concluded that the wood structure system shows weaker resistance as compared to other building system against the windstorm. N. Kishore et al, [4] studied that in the Atlantic, Indian and pacific ocean windstorm damages and discussed that the windstorm play vital role in the damages, losses, settlement of the build environment and the human live are also on high risk. The losses in the public and private properties and death rate lead to increase due to windstorm events. Damages and losses due to the storm event increase in 2017 as compared to the previous year according to the Centre for Research on the Epidemiology of Disasters (CRED) in Emergency Events Database (EM-DAT).

N. H. Zakaria et al, [5] used the NCEP FNL Operational Model Global Tropospheric Analyses and Meteorological Operational (MeTOP) datasets to regain the direction and the wind speed by analyzing the pattern of the wind speed in Peninsular Malaysia, and concluded that the southeast monsoon were the highest wind speed event and finds that the 5.96 m/s to 6.23 m/s were the highest wind speed from norhtsouth. A.C. Khanduri et al, [6] discussed the building vulnerability to windstorm and the property losses due to the hurricane hazards. It is very important to consider the wind load during the design phase of structure [7]. The cold rolled steel structure are also very common in these day in all over the world and Na Yang et al, studied that in recent years many of the modern cold formed steel structure are damages ranging from the roof, wall cladding to complete collapse, because of the light weight and other components. The cold rolled formed steel structure are more vulnerable to windstorm as compare the hot-rolled steel structure [8].

Seonwoong Kim et al, [9] discussed that in the summer season typhoons with the strong wind are frequent in the Korean peninsula and the Maximum wind speed measured in the korea is about 63.7 m/s due to which the design of the elastic seismic of some of the building structure may be acceptable based on the slenderness ratios in all wind exposures. The risk of the wind pressure increase as we increase the height of the structure [10]. As the wind act on the building surface, it creates the inward and outward pressure, which depends upon the orientation and location of the building and the pressure which act on the building try to uplift that building and if the building is week to resist the wind pressure, then the pressure forcing the building part [11].

As for the steel building structure are very common now a days, so many of the bridges are also constructed in the steel. Yan Han et al, [12] studied the typical long span steel-truss suspension bridges which is under the combine loading of the random traffic and wind and present an effective framework for fatigue reliability assessment and observed that the fatigue reliability have certain effect of random traffic and wind load. Most of the cases in the urban area tall and highest buildings are constructed which are highly vulnerable for windstorm, but now a days many rural areas are also subjected the extreme loads and the natural hazards such as earthquake, hurricanes, and tornados [13]. Just like the commercial and residential steel structure the steel towers can also affects from windstorm. M. Pavan Kumar et al, [14] compared the monopole and self-support type towers against the for basic wind speeds of 33m/s, 47m/s and 55m/s for the different height of the towers like 30m, 40m and 50m and concluded that under same height and same amount of loading monopole towers have higher lateral displacements compared to the self-support towers. Windstorm caused damages and collapse of the structure, because of which financial and human live losses are found all around the world [15]. N. O. Nawari, [16] observed that most of the cases build environment and their occupancies threaten by the windstorm/high speed wind, airborne projectiles, wind-driven water, sea surges, and flooding.

2 Limitations

The available literature related to steel structures, which were collapsed or partially damages due to the windstorm are very limited. Many authors focus on the design parameters and some of them studied the effects of high speed wind on the structure and their losses when the event happened.

3 Steel Structure and Windstorm Anatomy

Windstorm is the combination of air and water in turbulent flow, although the windstorm is complicated phenomenon, the combine form of wind and air means that the individual particle of either air or water have very erratic motion which is studying storm and one of them must be concerned with the statistical direction and the speed distraction expect of physical quantity. The storm forces are must be combination of wind pressure, Windborne debris, falling objects, flood pressure and maybe in the form of rain forces when analytical model are concerned. Windstorms, hurricanes, and sandstorms are basically the wind related disaster, these are very critical and dangerous for the local citizens. Due to the failure of structural members, number of tragedies have been observed in the previous decade. Structural design engineer and the wind engineer play a vital role to save the live and economy of any country by adopting and following the building design codes during design phase of tall buildings [17] basically wind is a process which occur uncertainty without warns, and various facts are responsible for this uncertainty and this uncertainty is the core and basic components while assessing the impact of wind on the buildings [18].

On the surface of the building wind load act as a lateral load in the direction of flow of wind. Wind load changes frequently when compared with the dead load and live load, if the same magnitude of wind load was applied gradually on the built in environment, different effect of the wind load are created in this case [19]. In contrast, very rough distribution of the tornados is observed, uneven distribution of vortices were acquired just because of the alternative [20] generation of the low pressure zones on the built environment cross wind sides under the crucial condition of the high wind speed as shown in (Figure 1).

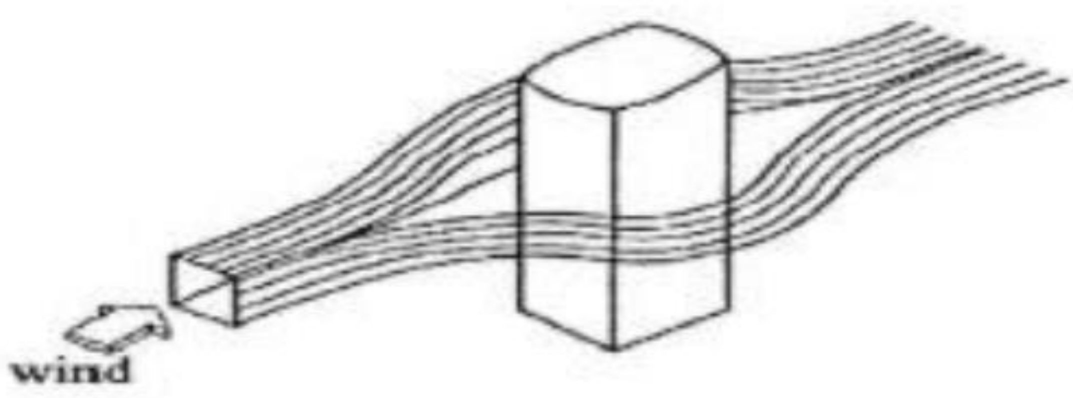

Figure 1: Built environment cross wind sides under the crucial condition of the high wind speed [20]

Windstorm, hurricanes, and tornadoes are basically wind related natural disaster which are the responsible for wind loading on the building structure significantly. Wind load impact on the building structure must be taken into under consideration during the designing of the building to control and minimize the failure of the structure and losses of the human lives [21] whenever the flow direction of the wind towards the building wind flow is separated and during the turbulent flow tornados are generated in the wake section [22].

4 Damage to buildings and structures due to windstorm in East Asia

In April 2021, in eastern Indonesia, bordering Timor-Leste tropical cyclone SEROJA formed dover the Savu Sea, as shown in Figure 2, and moving towards the Western Australia. During this event around 128 fatalities, 72 people reported missing and 8,424 people displaced according to the Indonesian national board for disaster management [23] as shown in (Figure 2a).

In 2019, a windstorm surge [23] effects the sixty seven communities of Gambia, and specifically hit the five region Jimara, Tumanna, Wuli East, Wuli West and Sandu districts and also it effects the two districts of central riven region. About 900 families are effected during this event and four deaths are reported. The wind storm surge were effected around 15,000 people and about 1,425 people were displaced. It was reported that 4 people are dead due to flying iron sheets and falling walls of the buildings. 101 people have been injured, and over 900 houses have been damaged or destroyed during this event. In china [24] during the typhoon the main resisting frame steel structures was collapsed as shown in (Figure 2b).

a)

b)

Figure 2: a. *In eastern Indonesia, bordering Timor-Leste tropical cyclone Gurney [23] and b. Main resisting frame steel structures collapsed [25]*

As reported by Tan, during the event of hurricane in southeast of china, steel structure beams buckled while the purine, girts and the connection plats remain safe [17]. In 2019, Cappucci M, reported that due to the high speed of wind a sandstorm event happened at Gurney, Penang as shown in (Figure 3a). In the nearby the toppling over of trees and tearing off of zinc roofs of houses happened, and the approximated reported speed of the wind are 80m/h. due to high wind speed debris are scattered into the air a few hundreds of meters, and approximately 50 buildings were damaged on that event [25].

The mega losses of the human societies and extreme damages of the buildings and other structure caused by the extreme wind events such as typhoons and tornadoes. Qingshan Yang et al, [26] studied the wind related disaster in East Asia, including disasters in Japan, the Philippines and China, from 2013 to 2016. They observed that the in 2008 disaster happened due to tropical cyclones was the most serious disaster in the Asian region. In this disaster about 138,000 fatalities and missing numbered happened and estimated 10 billion USD economical losses were noted. In Poland, windstorm considered most costly natural hazard. In 2017 a very strong and destructive thunderstorm happened in Poland, which caused disastrous damages in the 3 major provinces like Wielkopolskie, Kujawsko-Pomorskie and Pomorskie because of this disaster around 6 person are dead, dozens of peoples were injured and huge loss of property and buildings were noted, [27].

In 2007, inside a matter of seconds the I-35W steel Bridge over the Mississippi Stream in Minneapolis, Minnesota, collapsed as appeared in (Figure 3b).These extraordinary occasions, in any case, this occasion caused an enormous extent of wind-induced misfortunes. The later 2017 storms that affected the joined together States (Harvey, Irma, and Maria), caused $250 billion in harms to the joined together states and its domain [28]. Tropical storms Ike in 2008 and Sandy in 2012 caused almost US$29.5 billion and US$71.4 billion in harm, separately. In 2013, super storm Yolanda, too known as Storm Haiyan-caused comparable levels of harm in Southeast Asia, which were esteemed at about US$2.9 billion [29]. Kamil MuhammadKafi et al, [30] considers the harm seriousness of a windstorm that demolished more than 30 lives and thousand buildings and other basic structures inside the 2-h of its damaging span in Bauchi city in northern Nigeria. Lam, F.S. at al, [31] detailed that in 2019 alone, Temerloh area found in central Peninsular Malaysia has been hit by eccentric wind storms in restricted ranges which harmed more than 185 provincial homes.

a) b)

Figure 3: a. wind and sandstorm event happened at Gurney [25] and b. collapsed bridge center section [28]

Mehrshad Amini et al, [32] reported that during hurricane Irma and Maria (2017) residential building having the, steel roof frames faced extreme wind induced damages as shown in (Figure 4a). As the steel frame structure are light in weight so these type of structure are more vulnerable to windborne debris, and successive pressure induced due to high wind speed can also increase the chances of damage to the structure. Due to the failure of the connections between roof members and base plate for the gable end wall column complete structure as shown in (Figure 4b) collapsed during the Hurricane Charley (2004). Boback Bob Torkian et al, [33] studied the losses during the last fifty years and reported that losses due to the hurricane gradually increase of $1.3 billion US dollars per year from 1949 to1989, $10.1 billion US dollars per year from 1990 to 1995, and $35.8 billion US dollars per year from 2001 to 2006.

a) b)

Figure 4:a. Wind induces damage to steel frame structure, a. collapse of steel roof frame during hurricane Irma and Maria, 2017 [32] and b. roof frame failure and gable end wall collapse due to insufficient latera support during hurricane Hurricane Charley, 2004. [33]

From 2010 to 2021 around 7 time storm hit within the Asia region at different location or origins, due to which around 153 people are dead, 1,377 injured, 1,18,884 effected, 70,490 are homeless and 5,21,251 US dollar losses are reported in EM-DAT [34] as shown in Table 1 .

Table 1- Effects of Storm hit Asia from 2010 to 2021 [34]

Year	Disaster type	Death	No. injured	No. homeless	Total damages (US$)
2010	Storm	29	190	70000	70190
2012	Storm	05	-	490	490
2013	Storm	02	-	-	25020
2013	Storm	09	-	-	0
2103	Storm	00	67	-	3931
2016	Storm	102	1000	-	46000
2019	Storm	06	120	-	45120

5 Conclusion

Following conclusions can be drawn from the conducted study:

- This paper briefly reviewed the actual causes and evidence of damages of steel structure due to the windstorm.
- Most common failure and the mitigation techniques also discussed in connection with the windstorm related hazards and the conclusions can be drawn from the conducted study is that numerous structure are not designed against the wind load.
- Most of the structure collapse or damages due to windstorm are old or week due to rusting and due to extreme wind pressure roof and wall cladding of the structure damaged.
- It is observed that the steel structure without bracing wire suffer damages of roof and walls. During the design phase wind direction and wind load are not considered due to which most of the structure collapse from the connection point.
- Sever damage of the structure observed because of increasing the internal pressure due to pressurization. While studying the number of windstorm hit the Asia in last decade, it is observed that from 2010 to 2021 around 7 time storm hit within the Asia region at different location or origins, due to which around 153 people are dead, 1,377 injured, 1, 18,884 effected, 70,490 are homeless and 5,21,251 US dollar losses are reported.
- The wind induced damages significantly reduce by following the standardized installation methods, providing constant load-path, adopting passable connection systems and by proving the adequate wind load resisting materials for structural roofing and wall systems.
- It is observed that the structure which are designed according to the modem system and code have effective resistance against wind storm as compared to others, although they are still vulnerable, due to wind induced damages .
- Structural design engineer and the wind engineer play a vital role to save the live and economy of any country by adopting and following the building design codes during design phase of tall steel structure or buildings.

6 Recommendations

- It is very important to consider the win load during the design phase of structure
- Structure design engineer must be follow the wind design code and other relevant parameters
- During design of the building, surrounding trees, bracing, anchoring and outdoor equipment must be take into under consideration to mitigate or minimize the losses.

Acknowledgment

The authors would like to thank every person/department who helped thorough out the research work, particularly Dr. Muhammad Usman Farooqi. The careful review and constructive suggestions by the anonymous reviewers are gratefully acknowledged.

References

[1] Yum, Sang-Guk, Ji-Myong Kim, and Hsi-Hsien Wei, "Development of vulnerability curves of buildings to windstorms using insurance data: An empirical study in South Korea," *Journal of Building Engineering*, vol. 34, pp. 101932, 2019.

[2] Chmielewski, T., J. Szer, and P. Bobra, "Derecho wind storm in Poland on August 11-12, 2017: Results of the postdisaster investigation," *Environmental Hazard, Published online*, vol. 20, 2020.

[3] Amini, Mehrshad, and Ali M. Memari, "Review of literature on performance of coastal residential buildings under hurricane conditions and lessons learned," *Journal of performance of constructed facilities* vol. 34, pp. 04020102, 2020

[4] Kishore, Nishant, et al, "Mortality in puerto rico after hurricane maria," *New England journal of medicine* vol. 379.2, pp. 162-170, 2018.

[5] Zakaria, N. H., et al, "Seasonal Windstorm Pattern and Damages in Peninsular Malaysia 2018," *IOP Conference Series: Earth and Environmental Science*, vol. 385, 2019.

[6] Khanduri, A. C., and G. C. Morrow, "Vulnerability of buildings to windstorms and insurance loss estimation," *Journal of wind engineering and industrial aerodynamics, vol.* 91.4, pp.455-467, 2003.

[7] Bharvase, Shruti, and Priyanka Patil, "comparative study of vertically regular and irregular steel structure", 2019.

[8] Yang, Na, and Fan Bai, "Damage analysis and evaluation of light steel structures exposed to wind hazards," *Applied Sciences*, vol. 7.3, pp. 239, 2017.

[9] Kim, Seonwoong, "Seismic performance evaluation of high-rise steel buildings dependent on wind exposures," *Advances in Mechanical Engineering*, vol. 11.3, pp. 1687814019835111, 2019.

[10] Hatim Saleem et al, "A Comparative Study on High Rise Building for various Geometrical Shapes Subjected to Wind Load of RCC & Composite Structure using ETABS, "*International Research Journal of Engineering and Technology*, Vol. 6, pp. 2395-0056, 2019.

[11] Ahmed Sada Dheeb and Rafaa M. Abbas, "Deterministic Wind Load Dynamic Analysis of High Rise Steel Buildings Including P-Delta Effects, "*Association of Arab Universities Journal of Engineering Sciences*, vol. 26.1, pp. 129-135, 2019.

[12] Yan Han, Aff.M et al, "Fatigue Reliability Assessment of Long-Span Steel-Truss Suspension Bridges under the Combined Action of Random Traffic and Wind Loads Y J. Bridge Eng., vol. 25(3), 2020.

[13] Brito, Lianne, and Christine Wittich, "Performance of Steel Grain Silos and Rural Communities to Windstorms," *Structures Congress 2019: Blast, Impact Loading, and Research and Education*. Reston, VA: American Society of Civil Engineers, 2019.

[14] Kumar, Pavan, et al, "Effect of wind speed on structural behaviour of Monopole and self-support telecommunication towers," *Asian Journal of Civil Engineering*, vol. 18.6, pp. 911-927, 2017.

[15] Kim, Ji-Myong, Taehui Kim, and Kiyoung Son, "Revealing building vulnerability to windstorms through an insurance claim payout prediction model: a case study in South Korea," *Geomatics, Natural Hazards and Risk,* vol.8.2, pp.1333-1341, 2017.

[16] Nawari, N. O, "Analysis and prediction of building damage due to windstorms," *WIT Transactions on The Built Environment*, vol. 119, pp. 25-33, 2011.

[17] Tan, Yee Jin. *Wind Load Effects On High-Rise Building*. Diss. UTAR, 2020.

[18] Lombardo, Franklin T, "Treatment of Uncertainty for Windstorm Risk Assessment," pp. 02019001, 2019.

[19] Rajmani, A. and Guha,"Analysis of Wind & Earthquake Load For Different Shapes of High Rise Building, "*International Journal of Civil Engineering & Technology (IJCIET)*, vol. 6(2), pp.38-45, 2015.

[20] Roy, A.K. et al, "Wind Load on High Rise Buildings with Different Configurations" : A Critical Review, "*lnternational Conference on Emerging Trends in Engineering lnnovations & Technology Management*,vol. 2, pp.372–379, 2017.

[21] Dagnew, Agerneh K., Girma T. Bitsuamalk, and Ryan Merrick, "Computational evaluation of wind pressures on tall buildings," *11th Americas Conference on Wind Engineering, San Juan, Puerto Rico*, 2009.

[22] Hallebrand, Erik, and Wilhelm Jakobsson. "Structural design of high-rise buildings." *TVSM-5000*, 2016.

[23] https://reliefweb.int/

[24] Fan, B.Y.et al, "Investigation and Analysis of Public and Industrial Building Damage Caused by Typhoon" "Mujigae", In Zhanjiang Guangdong Yearbook of Disaster Prevention; Zhanjiang Municipal People's Government: Zhanjiang, China, 2016.

[25] Cappucci, M., "Massive wrong-way waterspout makes landfall in Malaysia", damaging 50 buildings - The Washington Post 21 April 2020.

[26] Yang, Qingshan, et al, "Damage to buildings and structures due to recent devastating wind hazards in East Asia," *Natural hazards*, vol. 92.3, pp. 1321-1353, 2018.

[27] Chmielewski, T., J. Szer, and P. Bobra, "Derecho wind storm in Poland on August 11-12, 2017: Results of the postdisaster investigation," *Environmental Hazard, Published online*, vol.20, 2020.

[28] NOAA National Centers for Environmental Information (NCEI). "US billion-dollar weather and climate disasters", 2018.

[29] Kim, Ji-Myong, Taehui Kim, and Kiyoung Son, "Revealing building vulnerability to windstorms through an insurance claim payout prediction model: a case study in South Korea," *Geomatics, Natural Hazards and Risk*, vol. 8.2, pp. 1333-1341, 2017.

[30] Kamil MuhammadKafi et al, "damage severity of a windstorm that ruined more than 30 lives and thousand buildings and other essential structures within the 2-h of its destructive span in Bauchi city in northern Nigeria"

[31] Lam, F.S., et al. / 8th AcE-Bs2019LangkawiIsland, Malaysia 18-19 Dec 2019 / E-BPJ, 4(12), pp.279-285.2019.

[32] Amini, Mehrshad, and Ali M. Memari, "Review of literature on performance of coastal residential buildings under hurricane conditions and lessons learned," *Journal of performance of constructed facilities*, vol. 34.6, pp. 04020102, 2020.

[33] Torkian, Boback Bob, et al, "Cost-and-benefit evaluation of windstorm damage mitigation techniques in Florida," *Natural Hazards Review*, vol.15.2, pp. 150-157, 2014.

[34] https://public.emdat.be/

3[rd] Conference on Sustainability in Civil Engineering (CSCE'21)
Department of Civil Engineering
Capital University of Science and Technology, Islamabad Pakistan

NUMERICAL ANALYSIS OF COMPRESSIVE BEHAVIOR OF GFRP REINFORCED HOLLOW CONCRETE COLUMNS

[a]Tanwir Ullah, [a]Afaq Ahmed, [a]Muhammad Yaqub, [b]Omer AlAjarmeh*

a: Civil Engineering Department, University of Engineering and Technology, Taxila, Pakistan
b: University of Southern Queensland, Centre for Future Materials (CFM), School of Civil Engineering and Surveying, Toowoomba 4350, Australia
*Corresponding Author: Email ID: engr662@gmail.com

***ABSTRACT*:** Glass-fiber-reinforced-polymer (GFRP) reinforcements provide a valuable substitute to conventional reinforcements in reinforced concrete frame structures, especially in vertical elements such as columns, due to improved anti-corrosion properties. On the other hand, the compressive behavior of GFRP-reinforced hollow concrete columns has been very rarely discovered. This purpose of this paper is to investigate the compression response of hollow concrete columns reinforced with GFRP bars and spirals. A concentric axial load of 20 KN was applied onto hollow circular columns of 250 mm external diameter and 1000mm height, having six GFRP bars of 14mm diameter each. FEA models of the columns were constructed using ABAQUS, by applying the same geometry, loading and boundary conditions. Numerical analysis of the modelled samples was performed after calibration and sensitivity analysis of the control model. The FEA analysis illustrated that hollow columns achieved greater confinement efficiency than the solid one. Moreover, hollow columns reinforced with GFRP showed higher compressive strength and deformation capacity than those reinforced with steel. The results of FEA analysis were in good agreement with the previously carried out experimental work.

Keywords- ABAQUS, GFRP columns, GFRP bars, Hollow Circular columns, Finite element modeling (FEM).

1 Introduction

Glass Fiber Reinforced Polymer (GFRP) reinforcements are increasingly being used as alternative to steel reinforcement in concrete structures, due to anti-corrosion properties [1]. Jabbar and Farid observed that in addition to higher corrosion resistance, the GFRP bars have 13% higher tensile strength and 58% higher tensile yield strain than the steel [2]. Ephraim et al. [3] reported that GFRP with 40% of fiber content showed about 25% more ductility than that recommended by ACI 440 Report [4]. Reinforced concrete columns, as structural members can be suitably reinforced with fiber reinforced polymer, for achieving greater strength [5].

Hollow RC columns are structurally more efficient in comparison to solid columns due to higher ductility and lower mass [6]. Hollow concrete columns have an obvious advantage over solid columns, owing to lesser weight, materials saving, higher axial capacity and higher resistance to bending[7]. Circular RC columns with fiber reinforcements showed more confined effect as compared to square one [8]. The longitudinal GFRP bars contribute in load carrying, upto 5% of the ultimate load in the high strength concentric columns [9]. Afifi quantified this effective share of GFRP longitudinal reinforcements in the design, to be 35% of the maximum column capacity [10]. Alajrmeh et al. found that the key factors affecting the structural axial response of hollow RC columns are the size and dia of GFRP bars, amount of lateral reinforcement, column's inner dia to outer dia ratio (i/o) and ratio of the actual load to axial capacity [11]. Kang et al. carried out FEA analysis tubular hollow composite columns with GFRP reinforcements and observed a gain in its bearing capacity by increasing the concrete strength or reducing the hollow ratio [12]. Nistico et al. developed a numerical model for solid concrete as a function of shape (circular and rectangular) and type of FRP [13]. Afaq et al. found that the performance of GFRP reinforced RC columns depends on type and shape of reinforcing material, with L-shape bars having higher capacity than round bars [14]. Raza et al. numerically investigated GFRP column with hybrid fibers and found close correlation between tests and FEM results thus validating the applicability of FEM [15].

The study of relevant literature suggests that there is a lack of numerical investigation on behavior of GFRP reinforced hollow columns. To fill this gap, the paper focuses on numerically analyzing the axial response of hollow concrete columns reinforced with GFRP bars and spirals, using ABAQUS software. The novelty of FEM study is that it is software based, instead of using cumbersome experimental tests, thus saving valuable time and effort. The GFRP reinforced hollow columns once fully applied in the structures will prove as valuable alternative to the traditional steel reinforcement, saving enormous cost and material.

2 Methodology

Numerical method was adopted to analyses the columns, using Finite Element Method (FEM). The commercial software Abaqus was utilized for the purpose of carrying out FEM analysis. Three concrete columns, each with 1000mm height and 250mm diameter, were modelled. The hollow GFRP reinforced column was used as benchmark to explore its axial behavior while a solid GFRP column and a hollow steel reinforced columns were modelled for comparison. A normal strength concrete with compressive strength of 25.6 MPa was used, with GFRP and steel bars as main reinforcement while GFRP spirals as lateral reinforcement. Material properties are tabulated in Table.

Table 1- Material Properties

Properties	Steel bars	GFRP bars	GFRP spiral	Concrete
Diameter (mm)	14	14	10	250
Area (mm^2)	153.8	153.86	70.8	-
Density (ton/mm^3)	7.85×10^{-9}	2.1×10^{-9}	2.1×10^{-9}	2.4×10^{-9}
Tensile Strength (MPa)	500	1237	1315	31.2
Modulus of Elasticity (GPa)	200	60	62.5	25.6
Poisson Ratio	0.30	0.21	0.21	0.25
Ultimate strain (%)	2.1	2.1	2.3	-

3 Finite Element Modelling (FEM)

3.1 *Geometry and Meshing*

For FEM analysis, CPD model of Abaqus was used for concrete simulation while steel and GFRP were simulated as elastic materials. In addition, steel plate, steel collars and rubber pads were applied at top and bottom surfaces for dilating load intensity. The 20mm Mesh was used for meshing GFRP and steel reinforcements with T3D2 elements whereas concrete with C3D8R elements.

3.2 *Constraints, Boundary Conditions and Loading*

"Tie" constraints using the concept of master and slave surfaces, were used to ensure smooth load transfer. The column's bottom end was fixed while top ends was let free to move. 25 KN concentric load was applied using 20 mm displacement. The initial and maximum loading increment size was 0.01, minimum as 10^{-15} and maximum number of increments was 1000.

3.3 *Control Model Calibration*

The controlled model was calibrated for various parameters by constructing a total of 58 x models. The calibrated FEA model which was produced with mesh size of 20mm, viscosity of 0.0018, shape factor of 0.667 and 36° dilation angle.

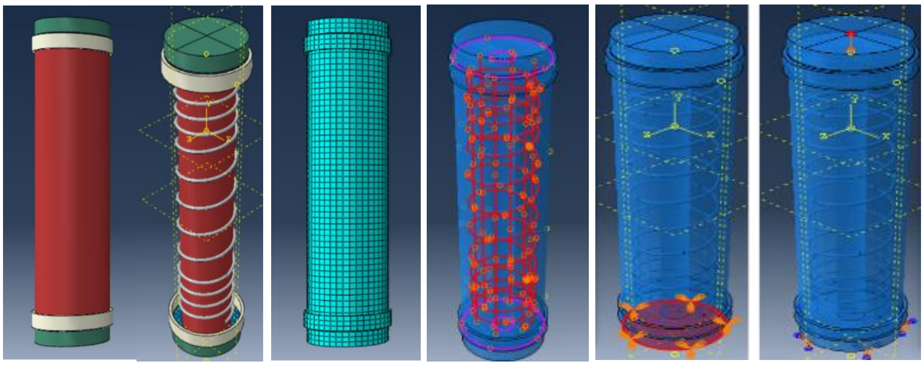

Figure 1: Column (a) assembly (b) meshing (c) constraints (d) boundry conditions (e) loading.

4 Discussions and Results

4.1 *Load-Deflection Behavior*

The modelled column showed a linear load–deflection curve in the initial phase, followed by a short nonlinear pattern just before the peak load. This brief nonlinearity is due to the initiation of cracks in the outer concrete core. The ultimate peak load of 1536 kN was obtained at an axial deflection of 9.49 mm. After the peak, an abrupt decreases in axial capacity was observed as the concrete cover spalled. However, due to the confining effect of GFRP spirals, another upward trend in the load capacity is observed in the post-peak phase. This upward increase is continued till the column finally fails when the GFRP bars and spirals reinforcements rupture. The same load-deflection pattern was observed by Alajarmeh et al. [11] by experimentally exploring the axial behavior of GFRP columns, as shown in Figure 2. Thus the numerical results are largely in agreement with the results of experimental work.

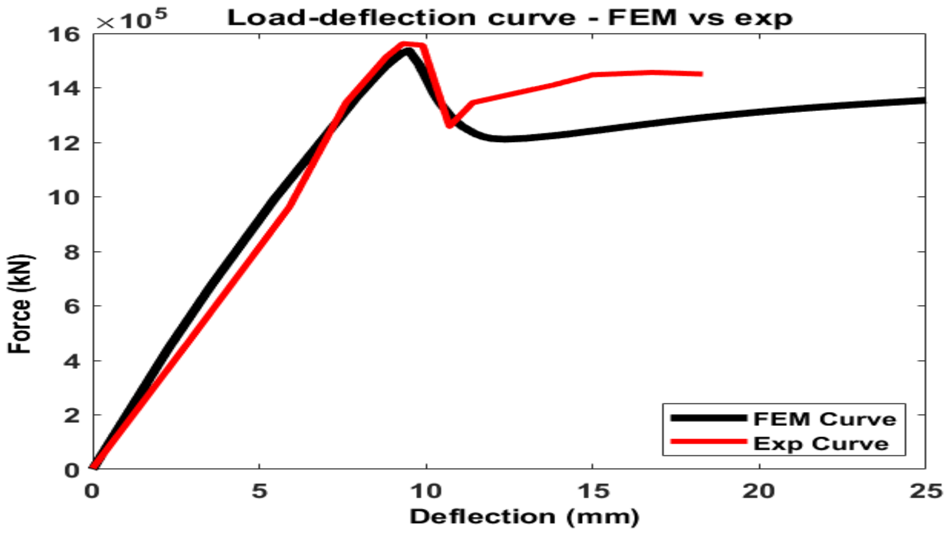

Figure 2: Load-deformation curves (FEM vs Experimental results)

4.2 *Comparison with Steel reinforced Columns*

A comparison of the axial behavior of GFRP-reinforced column was drawn with the steel reinforced column of the same dimension. For this purpose, a new model was generated having the same properties of concrete and GFRP spirals, but having steel longitudinal bars instead of GFRP. The steel reinforced column gave almost the same peak axial load as that of GFRP. However, in the post-peak phase, it showed a comparatively lower strength capacity. This shows that GFRP bars are structurally more efficient than the conventional steel bars of the same size. The comparison has been shown in the Figure 3 (a) below.

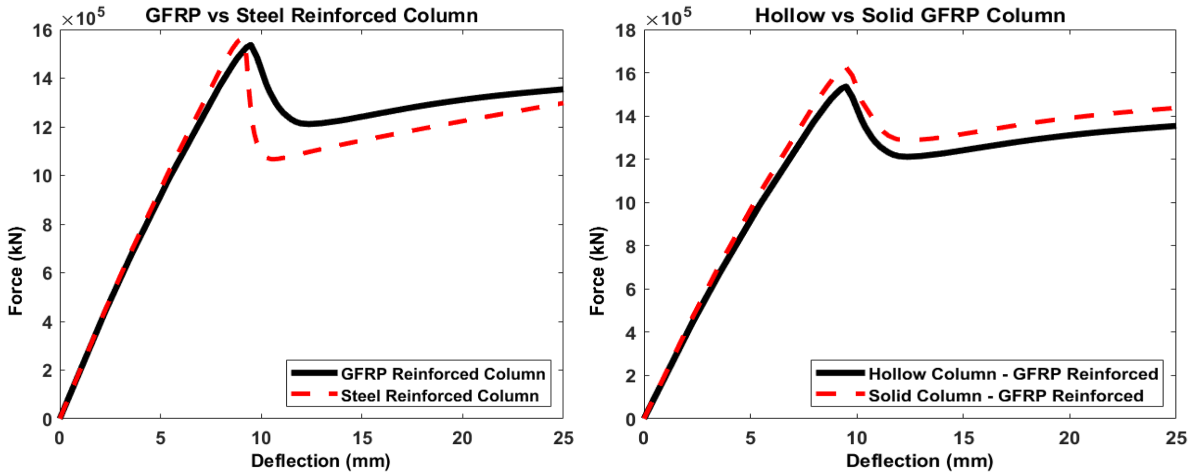

Figure 3: (a) GFRP vs Steel columns (b) Effect of Hollowness

4.3 *Effect of Inner Hollow*

To ascertain the role of inner hollow in the column, another column was simulated having the same longitudinal and spiral reinforcement but a solid cross section instead of hollow one. The load-deflection curve for both these columns have been compared in the Figure 3 (b). The solid column showed comparatively higher peak axial strength (1625000 KN vs 1536000 KN i.e. 5.8%) and more improved post-peak behavior. This can be attributed to the more confining effect provided by the inner solid concrete core. However, the relatively sharp decline in the strength after peak capacity shows that solid column is less ductile than the hollow one.

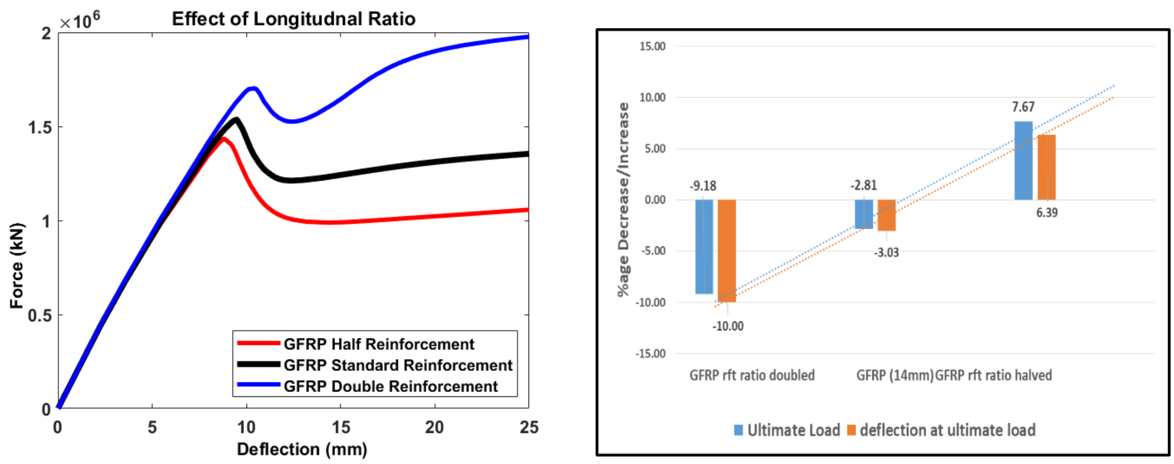

Figure 4: Effect of longitudinal ratios on load-deflection curve.

4.4 *Effect of Longitudinal Reinforcement Ratio*

The standard modelled column consisted of six 14mm GFRP longitudinal having area of 152mm^2 and reinforcement ratio of 1.86. To explore the effect of variation in GFRP reinforcement's longitudinal ratio, two more columns were modelled by doubling and halving the longitudinal ratio (one column with 10mm diameter / 76mm^2 area and second with 20mm diameter / 304mm^2 area). The increase and decrease in reinforcement ration led to a difference of +7.67 and -9.18%, respectively, in the axial load capacity of the column, thus implying a direct relationship between the axial capacity and reinforcement ratio as illustrated in Figure 4.

5 Application

The paper analyzes GFRP reinforced columns as a viable alternative to traditional steel reinforcements. FEM analysis will help all researchers to validate the results of already conducted experimental work on GFRP columns. the paper will also help designers and engineers to design and construct structurally stronger and more efficient buildings, using GFRP reinforcing materials having lesser cost and longer life than the steel reinforcements.".

6 Conclusions

This aim of the numerical study was to analyze the axial response of GFRP reinforced hollow columns, using FEM. Following are the key findings of the study:

- The load-deflection curve of FEM analysis coincided with the experimental curves of already conducted experiments, thus proving efficacy of the model.
- The GFRP-reinforced columns showed greater axial capacity and improved post-peak behavior than the steel reinforced counter-parts, thus proving GFRP reinforcement as a viable alternative to steel.
- The hollow concrete columns showed relatively lower axial capacity but considerably improved ductility than the hollow columns.
- The numerical parametric study revealed that increasing longitudinal ratio of the GFRP reinforcement, results in increased axial strength and post-peak behavior of the columns.

Acknowledgment

The authors would like to thank the advisor and all other person, who helped thorough out the research work. The careful review and constructive suggestions by the anonymous reviewers are gratefully acknowledged.

References

[1] A. Ahmad *et al.*, "Strength model for concrete columns reinforced with fiber-reinforced polymer bars and ties," *Compos. Struct.*, vol. 24, no. 1, pp. 2–3, 2020, doi: 10.1155/2020/8841795.

[2] S. A. A. Jabbar and S. B. H. Farid, "Replacement of steel rebars by GFRP rebars in the concrete structures," *Karbala Int. J. Mod. Sci.*, vol. 4, no. 2, pp. 216–227, 2018, doi: 10.1016/j.kijoms.2018.02.002.

[3] P. Ephraim M. E., Adetiloye A.Harcourt, "Mechanical Properties of Glass Fibre Reinforced Polymer Based on Resin from Recycled Plastic.," *Int. J. Sci. Eng. Res.*, vol. 6, no. 3, pp. 145–152, 2015.

[4] ACI Committee 440, *ACI 440.1R-15 Guide for the design and construction of structural concrete reinforced with Firber-Reinforced Polymer (FRP) bars*. 2015.

[5] A. M. Gora, J. Jaganathan, M. P. Anwar, and U. J. Alengaram, "Finite element analysis of rectangular reinforced concrete columns wrapped with FRP composites," *IOP Conf. Ser. Mater. Sci. Eng.*, vol. 431, no. 7, 2018, doi: 10.1088/1757-899X/431/7/072005.

[6] O. S. AlAjarmeh, A. C. Manalo, B. Benmokrane, W. Karunasena, and P. Mendis, "Effect of Spiral Spacing and Concrete Strength on Behavior of GFRP-Reinforced Hollow Concrete Columns," *J. Compos. Constr.*, vol. 24, no. 1, p. 04019054, 2020, doi: 10.1061/(asce)cc.1943-5614.0000987.

[7] A. Ahmad *et al.*, "Flexural behaviour of concrete slabs reinforced with GFRP bars and hollow composite reinforcing systems," *Compos. Struct.*, vol. 236, no. February, pp. 2–3, 2020, doi: 10.1016/j.compstruct.2019.111836.

[8] N. Tello, Y. Alhoubi, F. Abed, A. El Refai, and T. El-Maaddawy, "Circular and square columns strengthened with FRCM under concentric load," *Compos. Struct.*, vol. 255, no. September 2020, p. 113000, 2021, doi: 10.1016/j.compstruct.2020.113000.

[9] A. Hadhood, H. M. Mohamed, and B. Benmokrane, "Experimental Study of Circular High-Strength Concrete Columns Reinforced with GFRP Bars and Spirals under Concentric and Eccentric Loading," *J. Compos. Constr.*, vol. 21, no. 2, p. 04016078, 2017, doi: 10.1061/(asce)cc.1943-5614.0000734.

[10] M. Z. Afifi, H. M. Mohamed, and B. Benmokrane, "Strength and Axial Behavior of Circular Concrete Columns Reinforced with CFRP Bars and Spirals," *J. Compos. Constr.*, vol. 18, no. 2, p. 04013035, 2014, doi: 10.1061/(asce)cc.1943-5614.0000430.

[11] O. S. AlAjarmeh, A. C. Manalo, B. Benmokrane, K. Karunasena, W. Ferdous, and P. Mendis, "Hollow concrete columns: Review of structural behavior and new designs using GFRP reinforcement," *Eng. Struct.*, vol. 203, no. August 2019, p. 109829, 2020, doi: 10.1016/j.engstruct.2019.109829.

[12] K. He, Q. Lin, Y. Chen, and Z. Guo, "Compressive behavior of concrete-filled GFRP tubular stub columns after being subjected to freeze-thaw cycles," *Compos. Struct.*, vol. 255, no. May 2020, p. 112904, 2021, doi: 10.1016/j.compstruct.2020.112904.

[13] N. Nisticò, F. Pallini, T. Rousakis, Y. F. Wu, and A. Karabinis, "Peak strength and ultimate strain prediction for FRP confined square and circular concrete sections," *Compos. Part B Eng.*, vol. 67, pp. 543–554, 2014, doi: 10.1016/j.compositesb.2014.07.026.

[14] A. Ahmad and M. Iqbal, "INVESTIGATION OF DIFFERENT SHAPE OF COMPOSITE GFRP BARS IN," no. February, 2021.

[15] A. Raza, "Efficiency of GFRP Reinforcement in Concrete Columns having Hybrid Fibers : Experiments and Finite Element Analysis Efficiency of GFRP Reinforcement in Concrete Columns having Hybrid Fibers : Experiments and Finite Element Analysis," no. February, 2021.

3rd Conference on Sustainability in Civil Engineering (CSCE'21)
Department of Civil Engineering
Capital University of Science and Technology, Islamabad Pakistan

INVESTIGATION OF HIGH STRENGTH CONCRETE BRIDGE PIERS RETROFITTED WITH CFRP UNDER SEISMIC LOADING

[a] Obaid Shahid Mir*, [b] Muhammad Khalid Hafiz, [c] Dr. Qaiser-uz-Zaman Khan

a: Civil Engg. Department, University of Engineering & Technology Taxila, Pakistan, mirobaid937@gmail.com
b: Civil Engg. Department, University of Engineering & Technology Taxila, Pakistan, raokhalidhafeez@gmail.com
c: Civil Engg. Department, University of Engineering & Technology Taxila, Pakistan, dr.qaiser@uettaxila.edu.pk
*Civil Engg. Department, University of Engineering & Technology Taxila, Pakistan, mirobaid937@gmail.com

Abstract: One of the most challenging natural calamities under the umbrella of Civil Engineering, which may damage the structures and life as well is Earthquake. On 8th October 2005, a similar type of catastrophe was faced significantly in the Northern areas of Pakistan. Many Bridges got damaged due to this but some remained unaffected in various regions. It is essential to improve their strength and soundness which can be achieved with the help of Retrofitting with FRPs (Fiber Reinforced Polymers). Now a days, High strength concrete (HSC) is being employed in Bridge construction. This research targets the behavior of HSC before and after retrofitting. An experimental study was performed by applying Quasi static cyclic loadings (QSCT) with axial load applied on scaled down (1:4) RC bridge piers under different drift levels. The scaled down pier models were retrofitted with carbon fiber reinforced polymer (CFRP) sheets. The specimens were tested under QSCT against various drift levels ranging from 0 to 5%. Hysteresis loops are generated against each category of drift level which shows the lateral load carrying capacity of the Bridge pier against that specific Drift level. Results show that load carrying capacity of retrofitted bridge piers was enhanced due to the external confinement by CFRP sheets due to which the vulnerability/failure zones of structures were also upgraded. The amount of lateral load carried by the retrofitted model was more than the original or un-retrofitted model. The bridges made of HSC after the revision of building code need structural assessment and their load carrying capacity can be increased after retrofitting with single or double layer of CFRP and be brought within the safety limits as per new building code requirements. In the light of results of this research, it is considered that these bridges after retrofitting will become capable of resisting considerably more loads as per requirements of the new Building Code.

Key Words: CFRP, Energy dissipation, High strength concrete, Quasi static cyclic Loading, Retrofitting.

1 INTRODUCTION

Bridges serve as the jugular vein of the transportation system/network. Whenever an Earthquake or any other calamity occurs, Bridges are most susceptible to damage which as a result may halt the whole transportation network of the specific area. Mostly, Bridges built in Pakistan have not been structurally designed as per present seismic necessities. After the incident of 8th October 2005 in Pakistan, seismic danger maps and seismic zoning has been modified shaping a piece of the new Building Code of Pakistan (2007) known BCP-2207. But many Bridges were constructed before October 2005 and those were in accordance with the West Pakistan Highway Code (1967). An investigation was carried out for the seismic behavior of Reinforced concrete (RC) Piers wrapped with fiber reinforced plastic (FRP) composites straps. Results concluded that RC piers depicted notable improvements in strength and translational ductility [1]. Another study highlighted Short Columns investigation after wrapping with FRP composite tubes. Results indicated that wrapping was effective in enhancing the ductility, strength and energy dissipation capacity of tested concrete columns [2]. In another research, Surface mounted FRP rods were affixed in the footings and evaluated the flexural capacity of Rectangular Bridge Piers. It was found that the Flexural capacity of the Piers was increased [3]. Four low strength concrete (LSC) pier column models (1800 & 2400 Psi) scaled at 1:4

were subjected to QSCT. It was concluded that energy dissipation capacity of 1800 & 2,400 columns is almost same. Thus strength of concrete in this range does not affect the total energy absorption [4].

The columns which were damaged during the experimentation under reference[4] were retrofitted and also additional models were casted and retrofitted in undamaged state to investigate the effect of retrofitting on Load carrying capacity and Energy Dissipation of LSC (1800 Psi & 2400 Psi) RC piers. Comparison indicated that load carrying capacity of Damaged but retrofitted models was enhanced along with their strength and ductility to withstand even larger potential earthquakes [5]. A study was conducted on strengthening RC columns with a longitudinal CFRP sheet anchored to the column base. Results concluded that the use of a CFRP sheet with a CFRP anchor improved both the effective stiffness and the lateral strength of the RC columns [6]. The behavior of Non- Ductile slender reinforced concrete columns retrofitted with CFRP subjected to cyclic loading revealed significant improvement in terms of displacement ductility, load level, energy dissipation and failure mechanism [7]. Experimental work was conducted to evaluate the effectiveness of application of CFRP sheets to retrofit beams columns non-ductile joints. The load carrying capacity and number of cycles were increased. Applying two layers of CFRP sheets seemed less effective than one layer [8].

In the past, the bridges and components were constructed using High strength Concrete as per the criteria of the previous (obsolete) Building Code. But now after the revision of the Building Code and introduction of new Seismic zoning, there is a dire need to strengthen the existing bridge piers in order to withstand further events of severe earthquakes. The present research basically aims to review and reckon the lateral load carrying capacity of High strength concrete (HSC) bridge piers after these are retrofitted with CFRP. Also, the research highlights that what will be the behavior of CFRP retrofitted piers which got damaged as a result of any Earthquake event. This research also includes the comparison of performance of Bridge piers made of Low strength concrete (1800 and 2400 Psi) and High Strength concrete (6192 Psi) in terms of load carrying capacity. Research study on Low strength concrete has already been carried out vide references [4] and [5]. The test results of both these researches are obtained for comparison purposes with the test results of the present research. The results clearly depict a significant increase in load carrying capacity in HSC models the details of which are mentioned in section 3 of this research.

2 Experimental Setup

The test was conducted in the Earthquake Engineering Center (EEC) of Department of Civil Engineering UET Peshawar as adequate facilities and required equipment was available there. The Following tests were staged on the specimens:

i) Quasi-Static Cyclic loading tests (QSCT)   ii) Compressive strength tests (Concrete Cylinder tests)

The research comprises of QSC testing of Six (6) bridge pier models with the following properties:

- The pier models are scaled down to 1:4 scale with the help of similitude analysis having concrete strength of 6.192 ksi. The complete experimental setup with all the geometric details can be visualized in Figure 1. CFRP HEX 103-C is used for retrofitting with a fabric thickness of 1.016 mm, tensile strength of 153 ksi and tensile modulus of 9400 ksi. The steel used possesses yield strength of 83 ksi with modulus of elasticity 29000 ksi. The whole pier model assembly is loaded with a physical load of 42.4 kips. The models which are subjected to QSCT include two models in each of the category i-e. Control Models (CM), Damaged retrofitted columns (DRM) and Undamaged retrofitted columns (UDRM).

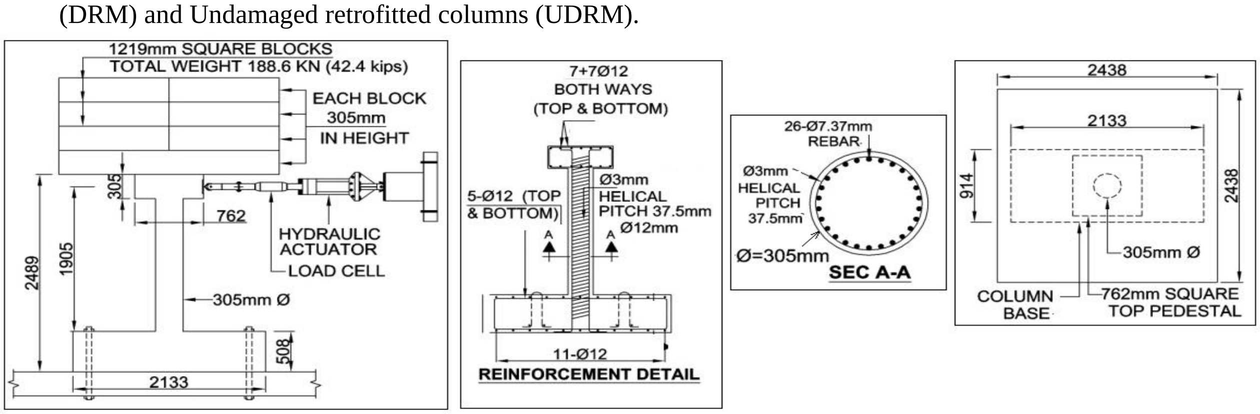

Figure 1. Experimental setup depicting all the geometric details, reinforcement details as well as loading details.

In order to predict the effects of improvements due to retrofitting on scaled down models, the model testing was carried out as per the following schedule:

a. Two test models of high strength concrete (6192 psi) were casted and both were subjected to Quasi static cyclic loading tests (QSCT) without any retrofitting and were tested up to failure. These models are referred in the research as Control Models or CM.

b. These two damaged models were repaired which constituted filling and repairing of cracks and retrofitted with CFRP. One model was retrofitted with single layer of CFRP which is referred as Damaged Retrofitted Model – Single Layer (DRM-SL), whereas the other model was retrofitted with double layer of CFRP which is referred as Damaged Retrofitted Model – Double Layer (DRM-DL). These two repaired and retrofitted models were subjected to QSCT up to failure. The tests were studied for evaluation of load carrying capacity, ductility, strength and energy dissipation of the models.

c. Two additional models of similar high strength concrete (6192 psi) were prepared and retrofitted in their original/Undamaged state and then subjected to QSCT. One model was retrofitted with single layer of CFRP which is referred as Undamaged Retrofitted Model – Single Layer (UDRM-SL), whereas the other model was retrofitted with double layer of CFRP which is referred as Undamaged Retrofitted Model – Double Layer (UDRM-DL).

d. High Strength Concrete (6192 psi) Cylinders were prepared and tested for their compressive strength.

e. QSCT were performed at different drift levels i.e. 0 to 4% and 5% in some cases. The reason that 5% drift is involved in few cases depended either upon the failure criteria set for the models or due to safety concerns as the huge physical loading of 42.4 Kips was placed over the damaged column models of one feet diameter only and was subjected to repeated reverse cyclic loading. This was a potential threat to the laboratory equipment as well as to the staff working in the laboratory. After QSCT on all the damaged models, the sequence of action was as following:

   - The data recorded on the data logger was rearranged in the format that could be managed in the spread sheets of IGOR Pro.
   - Hystereses curves were formed for each drift level separately which are attached below in Figure 1, 2 & 3. The cyclic loading of QSCT for lateral load with the change in drift levels has provided hysteresis curves for all the models. With the help of these hysteresis curves, Backbone curves are generated which give the maximum load carried by a pier under a certain drift level.

Figure 2. Test assembly setup with physical loading of 42.4 Kips.

Figure 3. Damaged Column, Cracks & Spalling of concrete.

Figure 4.Outer repair works with cementitious mix after filling of cracks

Figure 5. Grinded and Prepared surface of pier for CFRP application.

Figure 6. Application of CFRP (HEX-103-C) to pier.

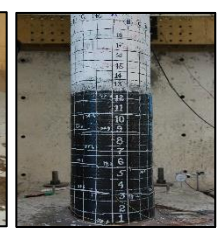

Figure 7. Final shape of pier after application of CFRP.

3 Discussion on Experimental Results:

The data obtained from the experimental results by the data logger was analyzed by using a software named IGOR Pro in which data as arranged in the form of sheets. A total of 6 Pier models were tested. Every model was subjected to QSCL at various drift levels ranging from 0 to 5%.

These graphs depict the load carried/resisted by the model. When these graphs are combined, they form a hysteresis curve as shown in Figure 1, 2 & 3. The peak values of these curves were calculated and backbone curves were made from these values. The backbone curves for Control Models, Damaged Retrofitted Models and Undamaged Retrofitted Models of Low strength concrete (1800 psi and 2400 psi) obtained from doctoral research of Ali S. M. (2009) and M. Iqbal (2012) under reference [4] and [5] were compared with corresponding models of High Strength Concrete i-e. 6192 psi.

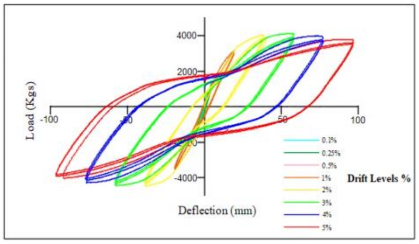

Figure 8. Hysteresis Curves – CM 6192 psi Pier Column subjected to different drift levels

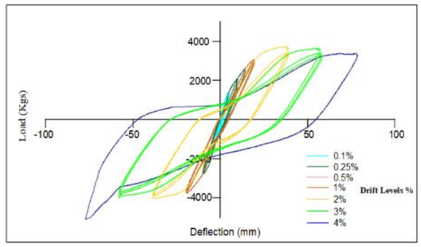

Figure 9. Hysteresis Curves - DRM 6192 psi Pier Column subjected to different drift levels.

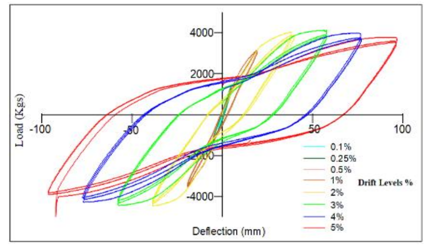

Figure 10. Hysteresis Curves - UDRM 6192 psi Pier Column subjected to different drift levels.

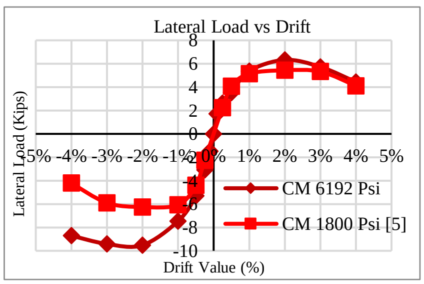

Figure 11. Control Models (CM) Backbone Curves Comparison (1800 Psi [5] vs 6192 Psi)

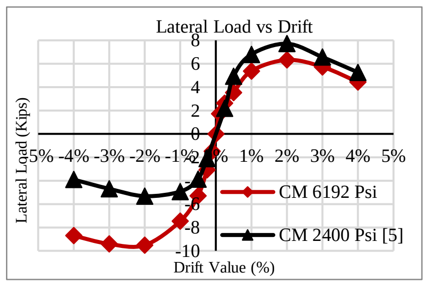

Figure 12. Control Models (CM) Backbone Curves Comparison (2400 Psi [5] vs 6192 Psi)

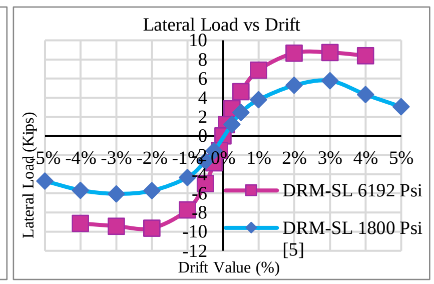

Figure 13. Damaged Retrofitted Models – Single Layer CFRP (DRM-SL) Backbone Curves Comparison (1800 Psi [5] vs 6192 Psi)

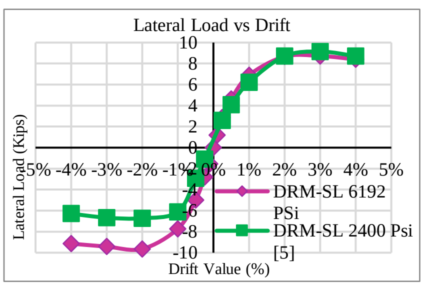

Figure 14. Damaged Retrofitted Models – Single Layer CFRP (DRM-SL) Backbone Curves Comparison (2400 Psi [5] vs 6192 Psi)

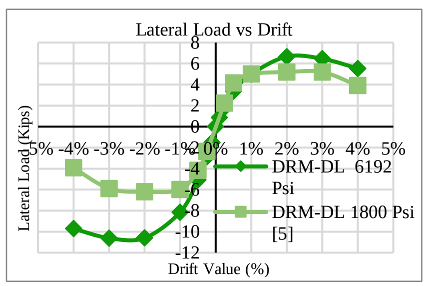

Figure 15. Damaged Retrofitted Models – Double Layer CFRP (DRM-DL) Backbone Curves Comparison (1800 Psi [5] vs 6192 Psi)

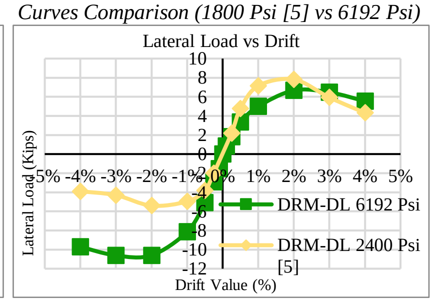

Figure 16. Damaged Retrofitted Models – Double Layer CFRP (DRM-DL) Backbone Curves Comparison (2400 Psi [5] vs 6192 Psi)

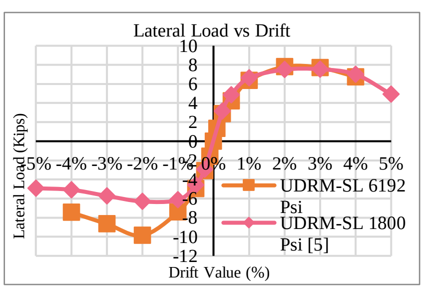

Figure 17. Undamaged Retrofitted Model- Single Layered CFRP (UDRM-SL) Backbone Curves Comparison (1800 Psi [5] vs 6192 Psi)

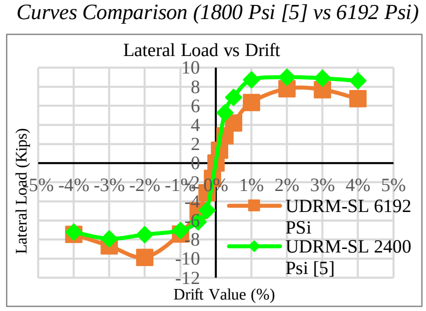

Figure 18. Undamaged Retrofitted Model- Single Layer CFRP (UDRM-SL) Backbone Curves Comparison (2400 Psi [5] vs 6192 Psi)

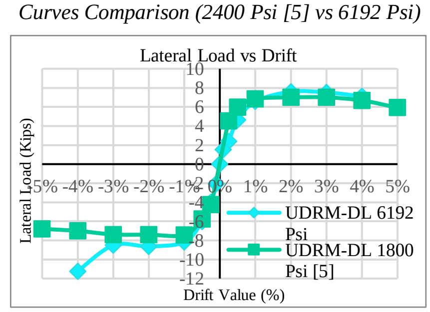

Figure 19. Undamaged Retrofitted Model- Double Layer CFRP (UDRM-DL) Backbone Curves Comparison (1800 Psi [5] vs 6192 Psi)

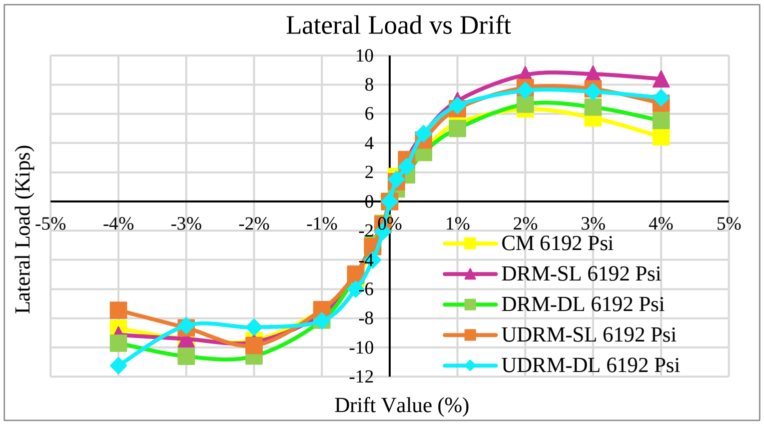

Figure 20. CM vs DRM-SL, DRM-DL, UDRM-SL &UDRM-DL (6192 psi)
Self Comparison of Backbone Curves between HSC Models.

The figures above (11 to 20) represent the behavior of Load carrying capacity of Control Models (CM), Damaged retrofitted columns (DRM) and Undamaged retrofitted columns (UDRM) in a graphical comparison between the High strength concrete models (6192 psi) and Low strength concrete (1800 & 2400 psi). It is obvious from these figures that by increasing the strength of concrete, significant increases in load carrying capacity are observed.

Table 1. Single Layered CFRP Model Results - % Increase in Load carrying Capacity (1800, 2400 vs 6192 psi)

SELF COMPARISON BETWEEN HSC MODELS (SL &DL)	**COMPARISON B/W CONTROL, DAMAGED AND UNDAMAGED MODELS OF HSC 6192 Psi**					
	Model Type	**Model Nomenclature**	**Max Lat. Force (Kips) - North**	**Max Lat. Force (Kips)-South**	**Average Lateral Force (Kips)**	**Percentage Increase**
	Damaged Models	CM-6192	6.3233	9.5174	7.9204	15.96%
		DRM-SL 6192	8.7280	9.6404	9.1842	
		CM-6192	6.3233	9.5174	7.9204	9.11%
		DRM-DL 6192	6.6691	10.6142	8.6417	
	Undamaged Models	CM-6192	6.3233	9.5174	7.9204	11.51%
		UDRM-SL 6192	7.7989	9.8658	8.8323	
		CM-6192	6.3233	9.5174	7.9204	18.95%
		UDRM-DL 6192	7.5963	11.2456	9.4210	
	COMPARISON BETWEEN CONTROL MODELS OF HSC 6192 Psi & LSC 1800 & 2400 Psi					
	Model Type	**Model Nomenclature**	**Max Lat. Force (Kips) - North**	**Max Lat. Force (Kips)-South**	**Average Lateral Force (Kips)**	**Percentage Increase**
	Control Models	CM-1800 Psi	5.4400	6.2550	5.8475	35.45%
		CM-6192 Psi	6.3233	9.5174	7.9203	
SINGLE LAYERED MODELS RESULTS		CM - 2400 Psi	7.7100	5.3250	6.5175	21.52%
		CM-6192 Psi	6.3233	9.5174	7.9203	
	COMPARISON BETWEEN DRMs- SL CFRP OF HSC 6192 Psi & LSC 1800 & 2400 Psi					
	Model Type	**Model Nomenclature**	**Max Lat. Force (Kips) - North**	**Max Lateral Force (Kips) - South**	**Average Lateral Force (Kips)**	**Percentage Increase**
	DRM-SL	DRM-SL 1800 Psi	5.7745	6.0412	5.9079	55.46%
		DRM-SL 6192 Psi	8.7280	9.6404	9.1842	
		DRM-SL 2400 Psi	9.1470	6.7230	7.9350	15.74%
		DRM-SL 6192 Psi	8.7280	9.6404	9.1842	
	COMPARISON B/W UDRMs - SL CFRP OF HSC 6192 Psi & LSC 1800 & 2400 Psi					
	Model Type	**Model Nomenclature**	**Max Lat. Force (Kips) - North**	**Max Lateral Force (Kips) - South**	**Average Lateral Force (Kips)**	**Percentage Increase**
	UDRM-SL	UDRM-SL 1800 Psi	7.5399	6.3101	6.9250	27.54%
		UDRM-SL 6192 Psi	7.7989	9.8658	8.8323	
		UDRM-SL 2400 Psi	9.0000	7.9168	8.4584	4.42%
		UDRM-SL 6192 Psi	7.7989	9.8658	8.8323	

Table 2. Double Layered CFRP Model Results - Percentage Increase in Load carrying Capacity (1800 Psi vs 2400 Psi vs 6192 psi)

DOUBLE LAYERED MODELS RESULTS						
COMPARISON B/W CONTROL, DAMAGED & UNDAMAGED MODELS OF HSC 6192 Psi						
COMPARISON BETWEEN CMs OF HSC 6192 Psi & LSC 1800 & 2400 Psi						
Model Type	**Model Nomenclature**	**Max Lat. Force (Kips) - North**	**Max Lateral Force (Kips) - South**	**Average Lateral Force (Kips)**	**Percentage Increase**	
Control Models	CM-1800 Psi	5.4400	6.2550	5.8475	35.45%	
	CM-6192	6.3233	9.5174	7.9203		
	CM - 2400 Psi	7.7100	5.3250	6.5175	21.52%	
	CM-6192	6.3233	9.5174	7.9203		
COMPARISON BETWEEN DRMs - DL CFRP OF HSC 6192 Psi & LSC 1800 & 2400 Psi						
Model Type	**Model Nomenclature**	**Max Lat. Force (Kips) - North**	**Max Lateral Force (Kips) - South**	**Average Lateral Force (Kips)**	**Percentage Increase**	
DRM-DL	DRM-DL 1800 Psi	5.2000	6.2000	5.7000	51.61%	
	DRM-DL 6192 Psi	6.6691	10.6142	8.6417		
	DRM-DL 2400 Psi	7.8200	5.4000	6.6100	30.74%	
	DRM-DL 6192 Psi	6.6691	10.6142	8.6417		
COMPARISON BETWEEN UDRMs - SL CFRP OF HSC 6192 Psi & LSC 1800 & 2400 Psi						
Model Type	**Model Nomenclature**	**Max Lat. Force (Kips) - North**	**Max Lateral Force (Kips) - South**	**Average Lateral Force (Kips)**	**Percentage Increase**	
UDRM-DL	UDRM-DL 1800 Psi	7.0000	7.4319	7.2160	30.56%	
	UDRM-DL 6192 Psi	7.5963	11.2456	9.4209		
	UDRM-DL 2400 Psi	9.8034	8.0853	8.9444	5.33%	
	UDRM-DL 6192 Psi	7.5963	11.2456	9.4209		

In Table 1, there is self-comparison of different categories of High strength concrete (6192 psi) models as well as their comparisons with the corresponding Single Layered CFRP Low strength concrete models (1800 & 2400 psi). While in Table 2, there are comparison results of High strength concrete models with the corresponding Double Layered CFRP Low strength concrete models (1800 & 2400 psi). The data in both these tables is extracted from the aforementioned backbone curves and is expressed in the form of numerical data in terms of percentage increase which gives a better understanding of results.

5 Conclusions:

After the detailed analysis of results, it was found out that:

- Upon comparison of the **CM** and **DRM – SL & DL** of HSC, Load carrying Capacity in the DRM-SL model was **increased** by **15.96%** for **SL** wrapping and **9.11% for DL** wrapping and upon comparison of the **CM** and **UDRM – SL & DL** of HSC, it was **increased** by **11.51%** for **SL** wrapping and **18.95 % for DL** wrapping.
- Upon comparison of the **CM** of LSC (1800 & 2400 Psi) and HSC Models (6192 Psi), Load carrying Capacity in the HSC model was **increased** by **35.45%** for **1800 Psi vs 6192 Psi** and **21.52%** for **2400 Psi vs 6192 Psi.**
- Upon comparison of the DRM-SL CFRP wrapped LSC models (1800 & 2400 Psi) and DRM-SL CFRP Wrapped HSC Models (6192 psi) Load carrying Capacity in HSC model was **increased** by **55.46%** for **1800 Psi vs 6192 Psi** and **15.74%** for **2400 Psi vs 6192 Psi**.
- Upon comparison of the UDRM-SL CFRP wrapped LSC models (1800 & 2400 Psi) and UDRM-SL CFRP Wrapped HSC Models (6192 Psi) Load carrying Capacity in the HSC model was **increased** by **27.54%** for **1800 Psi vs 6192 Psi** and **4.42%** for **2400 Psi vs 6192 Psi**.
- Upon comparison of the DRM-DL CFRP wrapped LSC models (1800 & 2400 Psi) and DRM-DL CFRP wrapped HSC Models (6192 Psi) Load carrying Capacity in the HSC model was **increased** by **51.61%** for **1800 Psi vs 6192 Psi** and **30.74%** for **2400 Psi vs 6192 Psi**.
- Upon comparison of the UDRM-DL CFRP wrapped LSC models (1800 & 2400 Psi) and UDRM-DL CFRP wrapped HSC Models (6192 Psi) Load carrying Capacity in the HSC model was **increased** by **30.56%** for **1800 Psi vs 6192 Psi** and **5.33%** for **2400 Psi vs 6192 Psi**.

The results clearly show that there is a significant increase in load carrying capacity of the HSC models as compared to the LSC models as well as in the load carrying capacity of the HSC retrofitted models as compared to the HSC unretrofitted/control models. The existing bridges made of High strength concrete after revision of Building code need structural improvements in order to comply with the safe provisions of revised building code. The existing bridge piers when retrofitted with CFRP will show a considerable increase in load carrying capacity as it is evident from the results of this research. This will prolong the life of the bridge as well as the structure will be saved from future earthquakes of high intensity as well.

Hence, it is recommended that the existing bridge piers of HSC be retrofitted with Single or Double layer of CFRP to meet the present codal requirements instead of demolishing a whole bridge and constructing it again as per requirements of new Building codes. This will increase its load carrying capacity and also it will fulfill the criteria of revised building codes provisions.

Acknowledgment

The authors would like to thank Engr. Aamir Jamshed and Engr. Adeel Mehmood who helped thorough out the research work, particularly Earthquake Engineering Center (EEC) staff of CED department UET Peshawar for providing laboratory assistance. The careful review and constructive suggestions by the anonymous reviewers are gratefully acknowledged.

References

[1] Saadatmanesh, H., M. Ehsani, and L. Jin, *Seismic Strengthening of Circular Bridge Pier Models with Fiber Composites.* Aci Structural Journal, 1996. **93**: p. 639-647.

[2] Saafi, M., H. Toutanji, and Z.J. Li, *Behavior of concrete columns confined with fiber reinforced polymer tubes.* ACI Materials Journal, 1999. **96**: p. 500-509.

[3] Alkhrdaji, T. and A. Nanni, *Flexural Strengthening of Bridge Piers Using FRP Composites*. 2000. 1-13.

[4] Ali, S.M. *Study Of Energy Dissipation Capacity Of RC Bridge Columns Under Seismic Demand*. 2009.

[5] Khan, Q., et al., *Seismic Evaluation of Repaired and Retrofitted Circular Bridge Piers of Low-Strength Concrete.* Arabian journal for science and engineering, 2015. **40**.

[6] Del Rey Castillo, E., J. Ingham, and M. Griffith, *Seismic strengthening of RC columns with straight FRP anchors*. 2017.

[7] Aules, W., *Behavior of Non-Ductile Slender Reinforced Concrete Columns Retrofit by CFRP Under Cyclic Loading*. 2019.

[8] Zerkane, A., Y. Saeed, and F. Rad, *Cyclic Loading Behavior of CFRP-Wrapped Non-Ductile Beam-Column Joints*. 2019.

3rd Conference on Sustainability in Civil Engineering (CSCE'21)
Department of Civil Engineering
Capital University of Science and Technology, Islamabad Pakistan

ANALYTICAL INVESTIGATION OF TYPICAL SCALE DOWN BRIDGE PIER RETROFITTED WITH CFRP UNDER SEISMIC LOADING

[a]Mustahsan Iqbal, [b]Muhammad Khalid Hafiz, [c]Dr. Qaiser-uz-Zaman Khan

a: Civil Engg. Department, University of Engineering & Technology Taxila, Pakistan, mustahsaniqbal3@gmail.com
b: Civil Engg. Department, University of Engineering & Technology Taxila, Pakistan, raokhalidhafeez@gmail.com
c: Civil Engg. Department, University of Engineering & Technology Taxila, Pakistan, dr.qaiser@uettaxila.edu.pk

Abstract: An earthquake measuring magnitude Mw 7.6 struck the Pakistan-administered part of Kashmir on 8 October 2005.As a result, many bridges experienced earthquake-associated damage of varying degree. It was essential to improve their strength and soundness. One of the modern techniques of Rehabilitating structure includes Retrofitting of bridge pier with Fiber Reinforced Polymers (FRP). This confines the concrete and cause a considerable improvement in strength of column. In order to investigate the effectiveness of Carbon Fiber Reinforced Polymers (CFRP), simulation of scaled down (1:4) High Strength Concrete (HSC) circular bridge pier models was carried out in current research using state of the art engineering simulation software "Seismostruct". The model was subjected to Quasi-Static Cyclic Tests (QSCT) and Pushover Analysis to determine improvement of strength, ductility and other dynamic properties. A load mass of 42.4 kips (19.24 tf) was added at top of model as gravity load. The model was retrofitted with CFRP wraps and analyzed till failures at their potential plastic zones. The purpose of this simulation was to evaluate seismic response of Bridge piers. The results showed that retrofitting of R.C columns with CFRP improves their strength and renders them capable to dissipate more energy.

Key Words: CFRP, High strength concrete, Quasi static cyclic Tests, Pushover Analysis, Retrofitting.

1. Introduction

Earthquake can be deadliest forces of nature that can shake the structures to their limits. Whenever an Earthquake occurs Bridges are more vulnerable to damage and if they get damaged whole system of transportation gets ceased. Usually, after any major catastrophe, the codes are revised in order to meet new challenges. So after the earthquake of 2005 in Pakistan, there was a dire need to revise the seismic zone as a result of which a new Building Code of Pakistan (2007) was formed known as BCP-2007. This new building code upgrades the zones of almost every city of Pakistan putting them into higher seismic prone zone. Many bridges were constructed before October 2005 and those were in accordance with the West Pakistan Highway Code (1967). Therefore, bridges were susceptible to damage and needed retrofitting to enhance their strength and ductility demands.

The availability of various inelastic element modeling in FEA programs have strengthen analytical techniques. A simple analytical procedure was proposed recently and is based on the ratio between displacement capacity of a structure corresponding to several limit states and displacement demand for an earthquake event as obtained from the corresponding displacement spectrum[1]. In another research, Reinforced concrete column were tested under cyclic loading. Based on results, following conclusion were made (i) The fiber element analysis which is based on cyclic constitutive models of longitudinal reinforcement and concrete confined by both CFS and ties provides good numerical simulation of experimental results (ii) The hysteric response of as-built columns can be increased by CFS jacketing which is effective at increasing lateral confinement, allowing increase in strength and ductile behavior[2]. A research study was carried out in which columns were continuously reinforced by CFRP and were tested under constant compression load combined with a horizontal quasi static cyclic load test. The results concluded that CFRP confinement completely changed the failure mode of the columns[3]. An extensive research was made on efficient rehabilitation techniques for structures damaged after historic earthquake of 2008. An experimental investigation was carried out to study the effect of retrofitting on change in dynamic properties of scale down bridge piers. Piers were tested twice, first in damaged state, then retrofitted with single layer of CFRP. Results showed that energy dissipation and ductility of retrofitted column increases as compared to control model [4].A low strength scale down concrete bridge pier model was simulated and analyzed using analytical techniques. Results show that retrofitting of undamaged state improves their ductility and made them capable to dissipate the energy more efficiently [5]. In another study, externally bonded Carbon Fiber Reinforced Polymer (CFRP) retrofit technique was implemented to improve the behavior of RC columns tested under constant axial load and cyclic lateral load. It was found that (i) CFRP retrofitting in the lateral direction at the plastic hinge region improved deformation capacity of the plastic hinge region tested under cyclic lateral load (ii) With CFRP lateral confinement, behavior of slender RC columns tested under low and moderate axial load was improved in terms of ductility, energy dissipation and failure mechanism (iii) Using longitudinal CFRP retrofitting with the lateral CFRP confinement increased both the effective stiffness and the lateral strength of the column [6]. An investigation was carried out in which plastic hinge region of FRP-confined RC Columns was studied by finite element model. The results of investigation were (i) The plastic hinge length of FRP-confined columns is very different from that of normal RC Column. Lengths of both the rebar yielding zone and curvature localization zone increases first and then decrease as the confinement ratio increases (ii) For flexural retrofitting of the RC Columns, FRP jacket needs to cover at least the length of concrete crushing zone, which is significantly affected by FRP confinement[7]. In past bridges, which were built according to specifications of old design codes do not perform well during seismic events and are considered as, insufficient in strength and ductility requirement, which in turn demands retrofitting to improve their strength and ductility. The subject research deals with the numerical evaluation and simulation of High Strength Concrete Bridge Pier retrofitted with Carbon Fiber Reinforced Polymer (CFRP) to find out its effectiveness in increasing the strength of pier.

In this research, simulation and analytical investigation of experimental research work, is carried out by using state of the art finite element software "Seismostruct". In experimental work, Quasi-Static test is performed on 1:4 scale down Bridge Pier Model having high strength of 6192 psi. The piers were first tested in their undamaged state and in next phase rehabilitation of damaged column were carried out, wrapping the damage column with carbon fiber reinforced polymer (CFRP). The pier columns after rehabilitation were again subjected to same testing and a comparison was presented in various dynamic properties of both states (Undamaged state and strengthen with CFRP state).In the current research finite element software like Siesmostruct was used to stimulate the behavior of bridge piers under seismic events. A comparison of test results of simulated model was made with experimental results of High Strength Concrete test and also with test results of low strength concrete (1800 psi and 2400 psi) model.

2. Methodology of Work:

The current research incorporates the finite element modeling of High Strength bridge pier column for assessment of their dynamic properties. The hysteretic performance and the energy dissipation capacity was assessed for the columns wrapped with CFRP Layers. The effectiveness of CFRP was estimated with high strength circular columns on term of increase in lateral load capacity. The model geometry, different dimensions, type and magnitude of applied loading are same as done through experimental work. Firstly the control specimen was modeled and analyzed through Finite Element Method (FEM) by using "Seismostruct". Then the model was retrofitted by wrapping it with layers of Carbon Fiber Reinforced Polymer (CFRP) and analyzed again using the same program. Model was retrofitted with CFRP before damaging, suggesting that the methodology adopted is pre-retrofitted.

First of all, bridge pier was scale down to 1:4 to its original dimensions. The height of pier obtained after scaling down was 6 ft and 3 in (75 in) with 1 ft (12 in) diameter. A total of 16#3 longitudinal steels bars were provided in the pier with lateral reinforcement of #1@6 in c/c spacing. Concrete cover was kept at 1.25 in. Afterwards, the same is simulated in Seismostruct for assessing the effectiveness and performance of confined concrete. A 3D solid model of bridge pier was simulated in version 2020 of Seismostruct. Element type of pier is inelastic force-based (FB) frame element. The pier has been integrated into 5 sections and is being represented by 400 fibers. Concrete used has mean compressive strength 6.192 ksi, mean tensile strength 0.382 ksi, modulus of elasticity 4453.95 ksi. Steel used has yield strength 83 ksi, modulus of elasticity 29000 ksi for longitudinal reinforcement and has mean strength value of 19.5ksi for spiral reinforcement. CFRP used have fiber thickness of 0.04 in, tensile strength 153 ksi, tensile modulus 9400 ksi. Among various sort of analysis facilities available in the software static pushover analysis was utilized to stimulate Quasi Static Cyclic Load. In addition to the lateral load, the column was subjected to gravity load of 42.2 kips in the form of concrete blocks placed at the top of column.

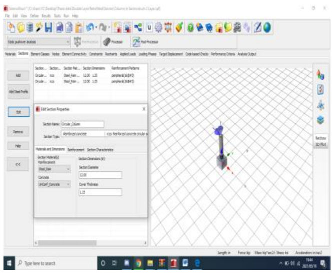

Figure 1: Numerical Modeling

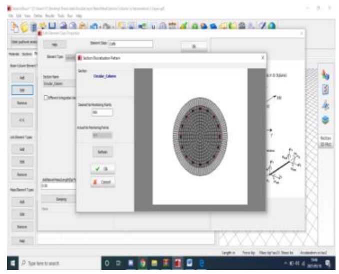

Figure 2: Meshing(Integrated into 5 sections and 400 fibers)

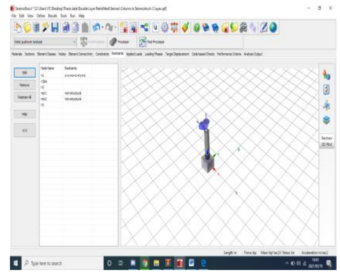

Figure 3: Boundary Conditions (Fixed at bottom)

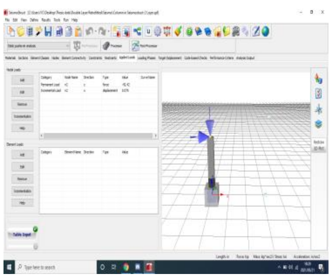

Figure 4: 3D View (Showing vertical and lateral load)

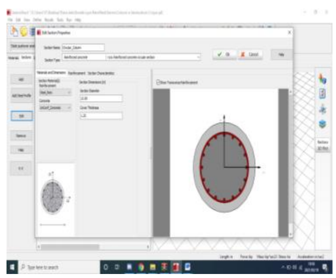

Figure 5: Cross-Section (16#3 bars, 1in diameter, 1.25in cover)

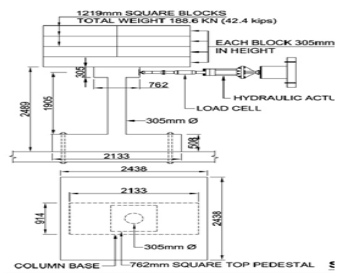

Figure 6: Plan and Elevation (6ft-3in)

The lateral load simulated on the circular column is applied in the terms of different drift levels in one particular direction and after that a restoring force in the opposite direction thus forming the hysteresis loop for each cycle. The point of application of lateral force is 75in (1905 mm) from base. Drift levels applied are 0.1%, 0.25%, 0.5%,1%.2%,3%,4%,5% of height of pier. Displacements are calculated against these drift levels like 0.1% of 1905mm is 1.9mm upto 5%. Data related to various drift level and corresponding number of cycles executed in research work are given in the Table 1.

Table 1: Different Drift Level and No. of Cycle Executed

Percentage Drift (%)	**0.1**	**0.25**	**0.5**	**1**	**2**	**3**	**4**	**5**
No. of Cycle for each Drift level	Two	Two	Two	Two	Two	Two	Two	Two
Displacement (mm)	1.9	4.8	9.6	19.2	38.4	57.6	76.8	96

3. Seismostruct Results:

Simulation of Quasi-Static Cyclic Load tests was carried out at different drift levels. Subsequent to simulating the Quasi-Static Cyclic Load Testing, the accompanying actions were taken:

a) The output data obtained after analysis of model from Seismostruct was rearranged in manageable format and transferred to spreadsheets of excel program.

b) Hysteresis loop curve at various drift level (in) against lateral load (kip) were plotted individually in excel program. The hysteresis curves for Control Model (CM), Undamaged Retrofitted Models-Single Layer (UDRM-SL) and Undamaged Retrofitted Model- Double Layer (UDRM-DL) for High Strength columns of 6192 psi have been shown from Figure 7 to Figure 9. The following information was derived from these curves:

   i. Area under each curve gives the value of energy dissipation at different drift level.

   ii. Maximum lateral load sustained by the column at each drift level shows the strength of the pier column at different drift level.

c) Once the maximum lateral load was determined for the respective drift levels, graphs were plotted for peak lateral loads against different drift value, named as backbone curve from figure 10 to figure 12.

It was observed that energy dissipation keeps on increasing with the increase in drift level. Also it is worth noticing that before 1% drift level that energy dissipation was negligible which shows that there was very less or no energy dissipation. These backbone curves of Control Model (CM), Undamaged Retrofitted Model- Single Layer (UDRM-SL) and Undamaged Retrofitted Model- Double Layer (UDRM-DL) of High Strength Concrete Bridge Pier (6192 psi) were then compare with backbone curves of Control Model (CM), Undamaged Retrofitted Model- Single Layer (UDRM-SL) and Undamaged Retrofitted Model- Double Layer (UDRM-DL) of Low Strength Concrete Bridge Pier Columns (1800 psi and 2400 psi) are shown in Figure 10 to Figure 15.

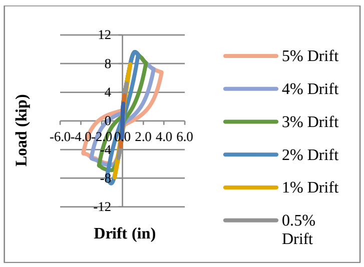

Figure 7: Hysteresis Curve of Control Models (6192 psi)

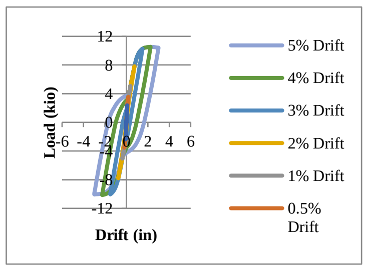

Figure 8: Hysteresis Curve of Single Layer Models (6192 psi)

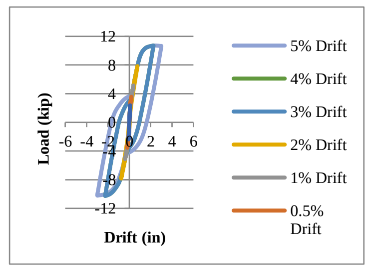

Figure 9: Hysteresis Curve of Double Layer Models (6192 psi)

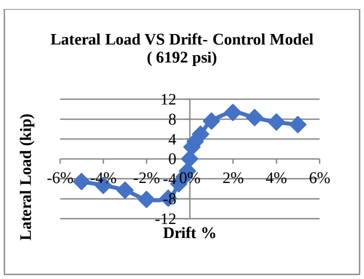

Figure 10: Backbone Curve-Control Models

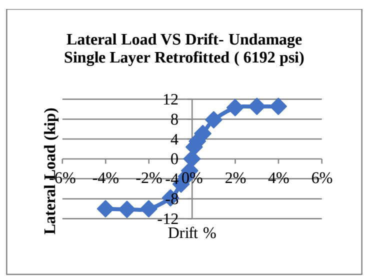

Figure 11: Backbone Curve-Single Layer Retrofitted Models

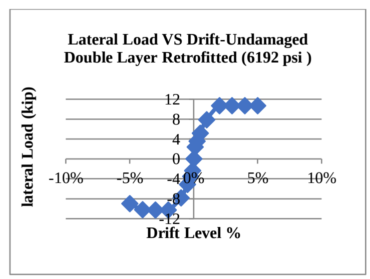

Figure 12: Backbone Curve - Double Layer Retrofitted Models

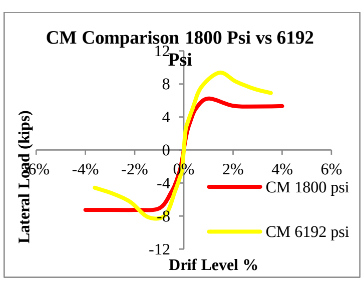

Figure 13: CM- Lateral Load VS Drift (1800 psi vs 6192 psi)

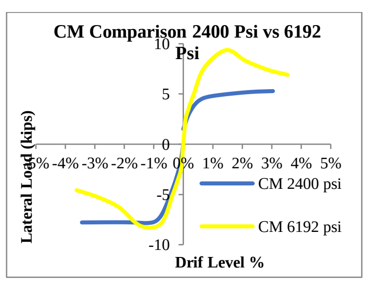

Figure 14: CM-Lateral Load VS Drift (2400 psi vs 6192psi)

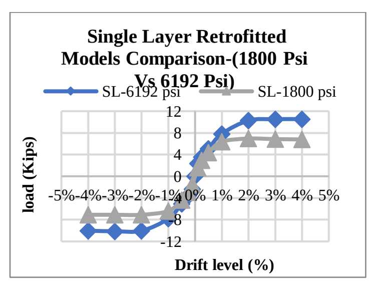

Figure 15: UDRM-SL- Lateral Load VS Drift (1800 psi vs 6192psi)

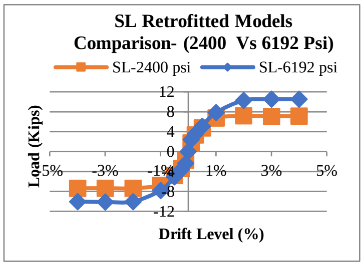

Figure 16: UDRM-SL Comparison- Lateral Load VS Drift (2400 Psi VS 6192 psi)

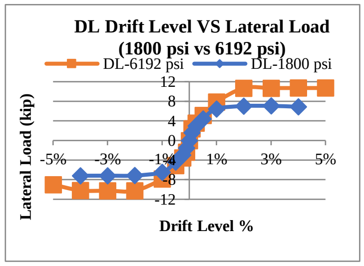

Figure 17: UDRM-DL Comparison- Lateral Load VS Drift (1800 Psi VS 6192 psi)

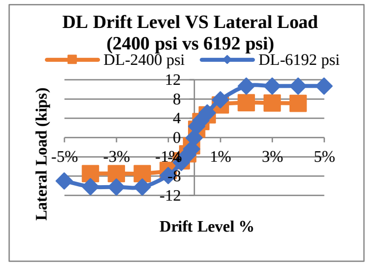

Figure 18: UDRM-DL Comparison- Lateral Load VS Drift (2400 Psi VS 6192 psi)

4. Discussion on Results:

Pier models were analyzed in their control state and undamaged retrofitted state. Quasi static cyclic loading was applied on each model at different drift levels. Graphs were drawn from the data which was obtained as a result of application of these drifts. These graphs depict the load carried/energy dissipated by the model and are known as hysteresis loop curves. The peak values of these curves were calculated both from positive and negative sides, and plotted which as a result gives the backbone curves. It was observed that energy dissipation goes on increasing with the increase in drift level and also pier is capable to dissipate significantly large amount of energy when retrofitted with CFRP as compare to control state. It was also worth noting that as number of layers of CFRP increases, energy dissipation also increases. Concrete strength also plays a key role. Energy dissipation in case of High Strength Concrete (HSC) is very huge as compare to energy dissipated in case of Low Strength Concrete (LSC). A comparison was done between backbone curves for Control Models (CM), Undamaged Retrofitted Models- Single Layer (UDRM-SL), Undamaged Retrofitted Models- Double Layer (UDRM-DL) of High strength concrete (6192 psi) and Control Model (CM), Undamaged Retrofitted Models- Single Layer (UDRM-SL) and Undamaged Retrofitted Models- Double Layer (UDRM-DL) of Low Strength Concrete (1800 psi and 2400 psi).

Following are the results of comparisons:

Table 2: Single Layered CFRP Model Results - Percentage Increase in Load carrying Capacity (1800 vs 2400 vs 6192 psi)

SINGLE LAYERED MODELS RESULTS						
COMPARISON BETWEEN CONTROL AND UNDAMAGED MODELS OF HSC 6192 Psi						
Model Type	**Model Nomenclature**	**Max Lateral Force (Kips) North Direction**	**Max Lateral Force (Kips) South Direction**	**Average Lateral Force (Kips)**	**Percentage Increase**	
Undamaged Models	CM-6192 psi	9.63	8.13	8.88		
	UDRM-SL 6192 psi	10.5282	10.1305	10.32935	16.32%	
	CM-6192 psi	9.63	8.13	8.88		
	UDRM-DL 6192 psi	10.714	10.25	10.482	18.04%	
COMPARISON BETWEEN CONTROL MODELS OF HSC 6192 Psi & LSC 1800 & 2400 Psi						
Model Type	**Model Nomenclature**	**Max Lateral Force (Kips) North Direction**	**Max Lateral Force (Kips) South Direction**	**Average Lateral Force (Kips)**	**Percentage Increase**	
Control Models	CM-1800 Psi	6.23	7.25	6.74		
	CM-6192 Psi	9.63	8.13	8.88	31.75%	
	CM - 2400 Psi	5.28	7.85	6.565		
	CM-6192 Psi	9.63	8.13	8.88	35.26%	

COMPARISON BETWEEN CONTROL AND UNDAMAGED MODELS OF HSC 6192 Psi					
Model Type	**Model Nomenclature**	**Max Lateral Force (Kips) North Direction**	**Max Lateral Force (Kips) South Direction**	**Average Lateral Force (Kips)**	**Percentage Increase**
UDRM-SL	UDRM-SL 1800 Psi	6.95	7.09	7.02	48.42%
	UDRM-SL 6192 Psi	10.5282	10.31	10.4191	
	UDRM-SL 2400 Psi	7.19	7.36	7.275	43.22%
	UDRM-SL 6192 Psi	10.5282	10.31	10.4191	

Table 3: Double Layered CFRP Model Results - Percentage Increase in Load carrying Capacity (1800 vs 2400 vs 6192 psi)

DOUBLE LAYER MODELS RESULTS

COMPARISON B/W UNDAMAGED RETROFITTED MODELS - DOUBLE LAYER CFRP OF HSC 6192 Psi & LSC 1800 & 2400 Psi					
Model Type	**Model Nomenclature**	**Max Lateral Force (Kips) North Direction**	**Max Lateral Force (Kips) South Direction**	**Average Lateral Force (Kips)**	**Percentage Increase**
UDRM-DL	UDRM-DL 1800 Psi	7.07	7.19	7.13	47.01%
	UDRM-DL 6192 Psi	10.714	10.25	10.482	
	UDRM-DL 2400 Psi	7.19	7.45	7.32	43.20%
	UDRM-DL 6192 Psi	10.714	10.25	10.482	

5. Conclusions:

After the detailed analysis of results, it was found out that:

- After comparing Control Models of Low Strength Concrete (1800 & 2400 Psi) and Control Model of High Strength Concrete Models (6192 Psi), it was found that Load carrying Capacity was increased by **31.75%** for **1800 Psi vs 6192 Psi** and **35.26%** for **2400 Psi vs 6192 Psi** in case of **Control Models**.
- After comparing Undamaged Single Layered CFRP Wrapped Low Strength Concrete models (UDRM-SL) of 1800 & 2400 Psi and Undamaged Single Layered CFRP Wrapped High Strength Concrete Models (UDRM- SL 6192 Psi) , it was found that the Load carrying Capacity was **increased** by **48.42%** for **1800 Psi vs 6192 Psi** and **43.22%** for **2400 Psi vs 6192 Psi**.
- After comparing Undamaged Double Layered CFRP Wrapped Low Strength Concrete models (UDRM-DL) of 1800 & 2400 Psi and Undamaged Double Layered CFRP Wrapped High Strength Concrete Models (UDRM-DL 6192 Psi), it was found that the Load Carrying Capacity was **increased** by **47.01%** for **1800 Psi vs 6192 Psi** and **43.20%** for **2400 Psi vs 6192 Psi**.

This clearly shows that Load Carrying capacity is increased by increasing strength of Concrete as well as wrapping of a layer of CFRP. The difference between finite element model results and experimental results depends upon factors like human error, instrumental error and realistic environmental conditions.

Acknowledgement:

The author would like to thanks Engr. Hafiz Zain Saeed and Engr. Amir Jamshed who helped throughout the research work, particularly Earthquake Engineering staff of CED department of UET Taxila. The careful review and constructive suggestions by anonymous reviewers are gratefully acknowledged.

References:

[1] Calvi∗, G.M., A DISPLACEMENT-BASED APPROACH FOR VULNERABILITY EVALUATION OF CLASSES OF BUILDINGS. Journal of Earthquake Engineering, 1999. 3(3): p. 411-438.

[2] Zafra, R. and K. Kawashima, ANALYSIS OF CARBON FIBER SHEET RETROFITTED RC BRIDGE COLUMNS. 2008.

[3] Colomb, F., et al., Seismic retrofit of reinforced concrete short columns by CFRP materials. Composite Structures, 2008. 82: p. 475-487.

[4] Khan, Q.-U.-Z., et al., Seismic Evaluation of Repaired and Retrofitted Circular Bridge Piers of Low- Strength Concrete. Arabian Journal for Science and Engineering, 2015. 40(11): p. 3057-3066.
[5] Saeed, H.Z., et al., Experimental and finite element investigation of strengthened LSC bridge piers under Quasi-Static Cyclic Load Test. Composite Structures, 2015. 131: p. 556-564.
[6] Aules, W., Behavior of Non-Ductile Slender Reinforced Concrete Columns Retrofit by CFRP Under Cyclic Loading. 2019.
[7] Yuan, F., Y.-F. Wu, and C.-Q. Li, Modelling plastic hinge of FRP-confined RC columns. Engineering Structures, 2016. 131.

3rd Conference on Sustainability in Civil Engineering (CSCE'21)
Department of Civil Engineering
Capital University of Science and Technology, Islamabad Pakistan

FEASIBILITY STUDY OF HYBRID TIMBER-CONCRETE TALL BUILDINGS

[a] Muhammad Nauman, [b] Muhammad Irshad Qureshi*, [c] Asif Iqbal, [d] Tahir Mehmood

a: Department of Civil Engineering, University of Engineering and Technology Taxila, muhammadnauman048@gmail.com
b: Department of Civil Engineering, University of Engineering and Technology Taxila, irshad.qureshi@uettaxila.edu.pk
c: Integrated Wood Design, University of Northern British Columbia, asif.iqbal@unbc.ca
d: Department of Civil Engineering, COMSATS Institute of Information Technology Islamabad, Wah Campus, drtahir.mehmood@ciitwah.edu.pk
* Corresponding author: Email ID: irshad.qureshi@uettaxila.edu.pk

Abstract- Adverse impacts of global warming are increasing worldwide. The construction industry accounts for more than 40% of CO_2 emissions worldwide. To lower the carbon footprint of the construction industry, sustainable construction methods and materials should be adopted. Timber is an alternative sustainable construction material, as timber construction produces far less CO_2 emissions during production and service life compared to conventional construction materials such as concrete and steel. Using timber alone for constructing high-rise structures has limitations due to its lightweight (higher floor accelerations), fire resistance, flexibility, etc. Also, there are disadvantages related to ductility properties to provide seismic resistance in tall timber buildings and the hesitancy on the part of designers and contractors to build high-rise timber structures. One possible solution is the use of hybrid structures, combining two or more materials by taking advantage of their individual strengths. The current work is focused on exploring the feasibility of high-rise hybrid timber-concrete structures over high-rise concrete structures in terms of their seismic and sustainability performance. The purpose of this study is to help designers and engineers towards understanding the behavior of hybrid timber-concrete tall buildings, instigating the development of more sustainable and practical design using timber.

Keywords- Sustainable construction, Green building material, Hybrid timber-concrete high rise.

1 Introduction

The increasing adverse effects of global warming due to the release of Carbon dioxide (CO_2) in the atmosphere is posing a significant threat to the environment. To contain these drastic effects, 175 countries signed a 'Paris Agreement' at the COP21 in Paris, which went into force in November 2016, and it was agreed to limit global temperature rise to well below 2 degrees centigrade in this century [1]. To achieve this ambitious target, a multifaceted approach is needed with a significant reduction of CO_2 emissions from most major industries of the world including the construction industry.

The world population has been increasing rapidly with an average estimated increase in the population of 81 million people per year [2]. This increase in population along with migration towards urban centers is causing an ever-increasing burden on the governments to build urban infrastructure including the housing units. As per UN-Habitats, 3 billion people in the world today will need a new home over the next 20 years. Constructing high-rise structures to cater to this demand is proving to be an effective solution, resulting in massive investment in infrastructure development. The carbon footprint associated with the building construction is referred to as "Embodied carbon footprint" of the building. According to a report published by United Nations Environment Program, global CO_2 emission from the building construction sector reached the highest ever level in 2019 by accounting for approximately 38% [3]. China's national CO_2 emission from the construction industry was 90% and this percentage was 66%, 82%, 51%, and 42% for USA, India, Japan, and Canada respectively for the period between 2009 and 2020 [4]. Therefore, a concerted effort is required to lower the carbon footprint of construction industry by using sustainable construction methods and materials.

A deeper look reveals that the production of materials used in the construction industry is a major contributor to the embodied carbon footprint. To lower the embodied carbon footprint of buildings, building materials that are less carbon extensive should be promoted. To lower the carbon footprint of buildings, Architecture 2030 issued a 2030 challenge in 2006 asking the global architecture and construction industry to achieve net-zero embodied carbon emission by 2030 [5]. The least carbon extensive material at our disposal is wood or timber. Wood is produced by a process called photosynthesis

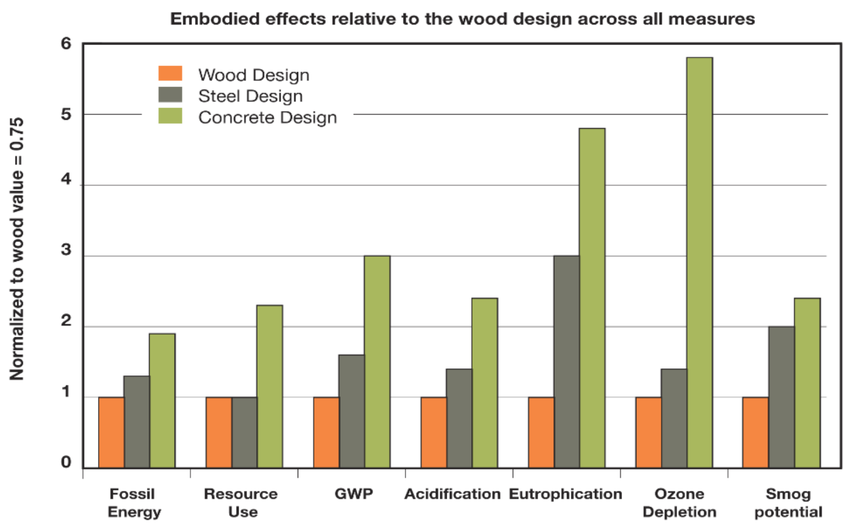

Figure 1: Comparison of environmental impacts of construction materials
Source: Dovetail Partners using the Athena Eco-Calculator (2014)

which makes it a carbon sink. Also, the process to make mass timber products take less energy than steel and concrete. The bar chart in Figure 1 clearly shows that the environmental impact of wood design is significantly lower than concrete and steel [6].

In recent decades, the development of mass timber products like glued-laminated timber, cross-laminated timber, etc., created a renewed interest in lightweight and sustainable timber structures. However, using timber alone for building high-rise structures has limitations due to its lightweight which could cause higher floor accelerations and flexibility which may cause higher displacement demand [7]. Also, there are disadvantages related to ductility requirements to provide seismic resistance in tall timber buildings [8]. The use of timber for constructing tall structures has geared up in the recent decade but design codes are still lagging behind for designing timber tall buildings, as *National building code of Canada* (NBCC) 2014 does not allow an all-timber construction above 6 stories. One possible solution is to shift to more sustainable construction materials like timber in a relatively gradual manner by first exploring the use of hybrid timber-concrete structures [9] especially as the code does not have any restriction on the maximum height of these structures. E.C Slooten et. al. [10] studied the technical feasibility of super tall hybrid timber-concrete building, and mainly focused on optimizing the wind-induced dynamic behavior. Kaushik [11] studied the feasibility of 30-story hybrid timber-concrete structure, making the gravity load resisting system as hybrid timber-concrete by introducing concrete slab at every third story, and discussed inter-story drift and base shear results. Wu k. et. al. [12] also studied the behavior of six different hybrid structural systems and compared only drift demands. Schuirmann et. al. [13] also studied the feasibility of hybrid tall timber-concrete structures with different slab types (1-way and 2-way) by performing non-iterative P-Delta analysis. However, still more work is needed including the development of codal requirements, experimental testing, design procedures, etc., to enable the designers and contractors to adopt this sustainable alternative. This research aims to assess the feasibility of high-rise hybrid timber-concrete structures over high-rise concrete structures in terms of seismic and sustainability performance, by comparing story shear, story displacement, Inter-story drift, and concrete core shear results of both structures.

2 Case study Structures

To assess the potential of using timber-concrete hybrid structures, a 20-story case study building is selected. Plan and 3-D view of the building are shown in Figure 2. The case study building consists of a core wall and stairwell (referred hereafter as core wall) in the center connected by framing on the sides. The core wall is designed to act as a lateral force-resisting system while the beams and columns are designed primarily to resist only gravity loading. Initially, the whole structure is designed as a concrete building (CB). Few works in the past have used timber as a part of the lateral force-resisting system; however, the values of force reduction and over-strength factors for such systems are still not clear and need further research. Therefore, timber structural components in this study are used for only gravity load resisting system. The second case study building is same as CB except that the beams and columns are composed of glued laminated timber while the slabs are composed of cross-laminated timber with concrete topping referred hereafter as hybrid timber-concrete building (HTCB). Structural members of both the buildings are designed using the factored loads to select the material and cross-section properties according to CSA-A23.3-14 and CSA O86-2014 for concrete and timber design, respectively. Table 1 shows the structural member properties of two buildings. Case study buildings are assumed to be located in the Vancouver area with site class C as per NBCC 2015. Values of force reduction factor (R_d) and overstrength factor (R_o) for CB are chosen as 3.5 and 1.6, respectively from the NBCC 2015. Although the HTCB is composed of both concrete and timber and both have different values of these factors, the same values of R_d and R_o are used for HTCB as the concrete core is assumed to resist all of the lateral actions. This assumption will be validated in the results section. Dead load is composed of self-weight of the structure plus the super-imposed dead load of 4kPa while the live load is 2kPa.

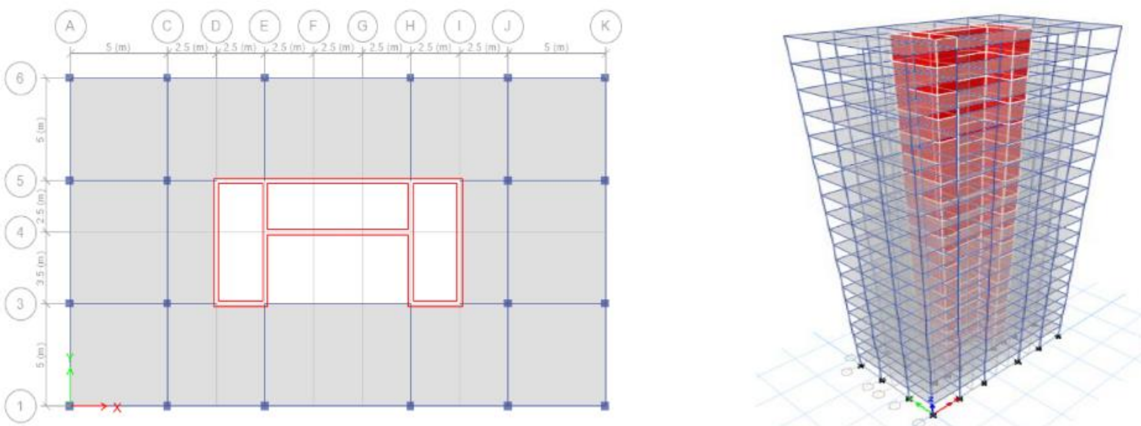

Figure 2: Typical plan and 3-D elevation of case study buildings

Table 1: Material and section properties of case study structures

Section property	CB Size/Thickness	Grade	Section property	HTCB Size/Thickness	Grade
Slab	150 mm	3000 psi	CLT slab	243 mm, 9 layers	E2
Beams	250 x 500 mm	4000 psi	Perimeter glulam beams	215 x 532 mm	24f-EX
			Interior glulam beams	365 x 874 mm	24f-EX
Columns	400 x 400 mm	4000 psi	Glulam columns	365 x 380 mm	16c-E
Concrete core	250 mm	4000 psi	Concrete core	250 mm	4000 psi

3 Modeling and Analysis

The case study buildings are modeled in commercially available software ETABS. Linear elastic modeling is done in this study. Initially, an equivalent lateral force procedure (ELFP) is performed to calculate total seismic demands and the seismic demands carried by different structural components for both buildings. The case study building has a significant torsional response and therefore, results from response spectrum analysis capable of considering higher mode effects are also discussed. The strength and stiffness properties of glued laminated and CLT timber sections are defined for different directions as timber is an orthotropic material using timber grades defined in Table 1. It is important to note here that only linear static analysis (ELFP and RSP) are performed in this study. Also, this study is focused on only the global behavior of the structures against the design basis earthquake level of seismic intensity.

4 Results and Discussion

The foremost advantage of using a hybrid structural system can be seen by looking at the self-weight of the two case study buildings as shown in Table 2. The HTCB has almost 30% lower self-weight and seismic weight compared to CB. This implies reduced shear and moment demands for beams and reduced axial load ratios for columns. Furthermore, it can also significantly reduce the forces and moments for foundation design, resulting in cost savings. Seismic weight in this study is calculated by using 100% of dead and super dead load and 25% of live load. It is important to mention here that the total lateral seismic forces acting on a structure represent a portion of a total seismic weight acting laterally described in most codes as seismic response coefficient for ELFP. So, a reduced value of seismic weight would result in lower seismic demand for same seismic response coefficient or same spectral acceleration.

Table 2: Seismic characteristics of case study buildings

Building Type	Self-weight (KN)	Seismic Weight (KN)	T_X (Sec)	T_Y (Sec)
CB	59,155	92,005	1.22	1.90
HTCB	31,630	64,480	1.04	1.74

The fundamental time periods for CB in X and Y-direction of responses are 1.22 sec and 1.9 sec, respectively which are reduced to 1.04 sec and 1.74 sec for HTCB. Time period of a structure is dependent on the ratio of mass and stiffness. Although the HTCB has reduced stiffness compared to CB, the reduction in mass is even higher, resulting in a reduced mass/stiffness ratio or time period. In a typical design spectrum as in the current study, a decrease in the time period in the concerned range results in a higher spectral acceleration value resulting in higher shear demand. HTCB has a lower time period compared to CB meaning a higher spectral acceleration ordinate however reduced seismic weight means that the shear values in the absolute terms would be lower. Figure 3 shows the shear force results for the case study buildings. Overall, the shear values for both CB and HTCB are higher in Y-direction than in X-direction. The contribution of higher modes seems to be limited as seen in the shear profile along the height. For both X and Y directions of response, HTCB is showing an almost 25% less base shear compared to CB and a similar pattern is observed along the height. This shows a significant drop in shear demand, signifying the effectiveness of hybrid solution as far as force demands are concerned.

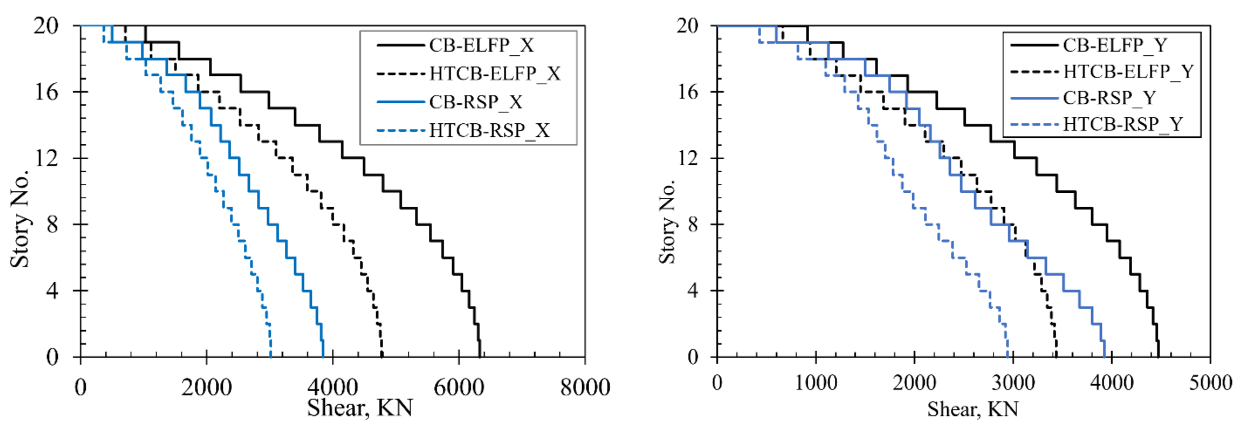

Figure 3: Shear force comparison

The relatively reduced time period for HTCB, on the other hand, has an opposite effect on the displacement and inter-story drift demands with lower spectral displacement ordinate. Figure 4 shows the displacement and inter-story drift results for both CB and HTCB, showing a reduced displacement demand for HTCB in both directions of response. This would eventually lead to better performance for HTCB with reduced residual drifts and damages. The comparison also showed that the displacements in Y-direction are nearly double than in X-direction.

Response spectrum analysis is also performed to calculate the force and displacement demands. Both force and displacement demand for CB and HTCB using RSP are less than demands from ELFP. The difference is particularly high in X direction of response due to torsional behavior. This is because in ELFP, all of the seismic weight is used to calculate the seismic forces by using fundamental time period while in RSP the seismic mass is divided into different modes and is multiplied with individual spectral acceleration for different modes against their time periods and the total response is obtained by using SRSS.

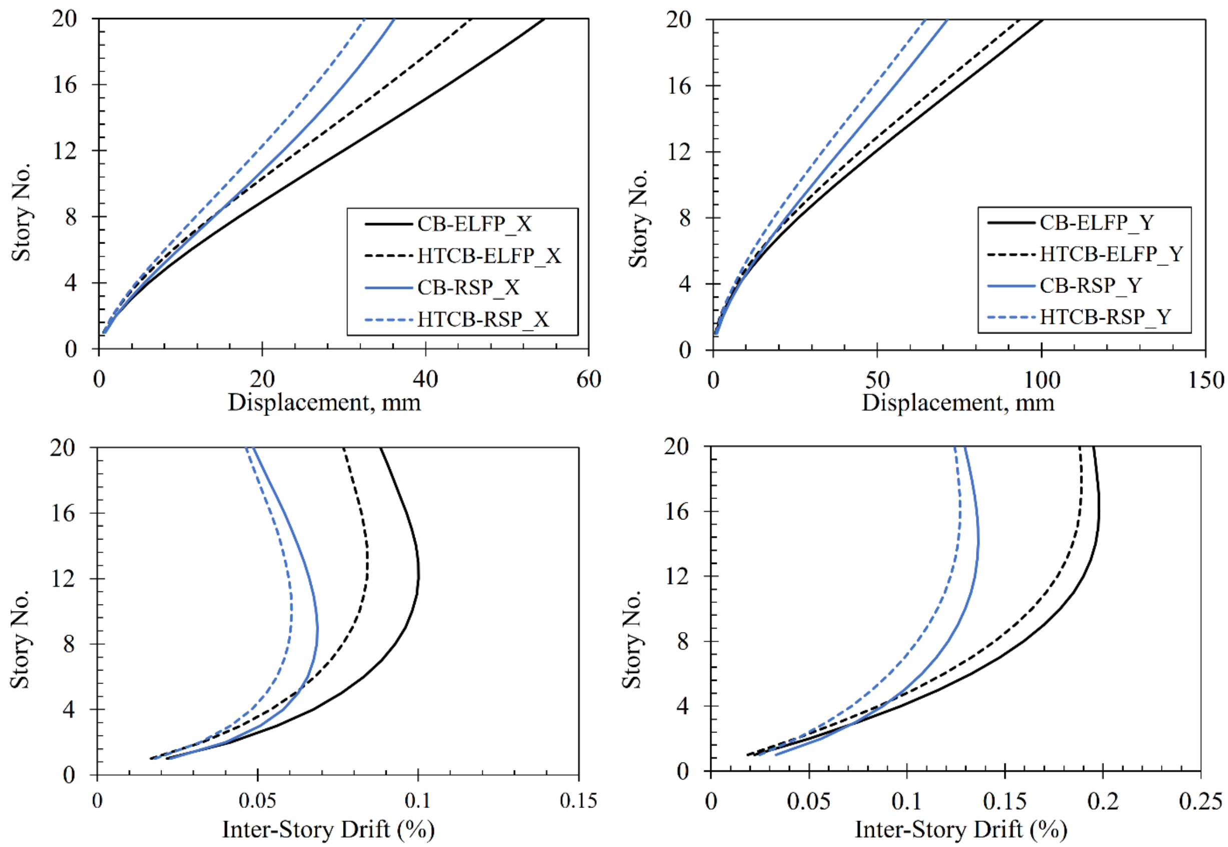

Figure 4: Displacement and Inter-story drift comparison

To evaluate the assumption that the concrete core wall is designed to resist most of the lateral load, seismic response for ELFP for individual walls is shown in Figure 5 for both directions of response it can be seen that for both HTCB and CB, the base shear carried by all the walls combined is more than 95% of the total base shear of the building in both directions, validation the assumption made in the earlier section. It also validates the use of the same values for R_d and R_0 factors for both buildings. Figure 5 also shows the seismic demands of individual walls with walls 9 and 11 taking a maximum lateral load in the X direction of response, almost all walls are contributing equally to resist the lateral load.

Designers and engineers are still hesitant to construct hybrid timber-concrete high rise as much extensive research isn't carried out in this field yet, and also the behavior of hybrid timber-concrete tall buildings is not explored in depth yet. Furthermore, values for seismic factors (R_d and R_0) are not defined in design codes for hybrid timber-concrete tall building design. Results obtained from this study would help engineers and designers to understand the behavior of hybrid timber-concrete tall structures and would provide a way to fulfill the codal requirements related to height and use of seismic factors (R_d and R_0).

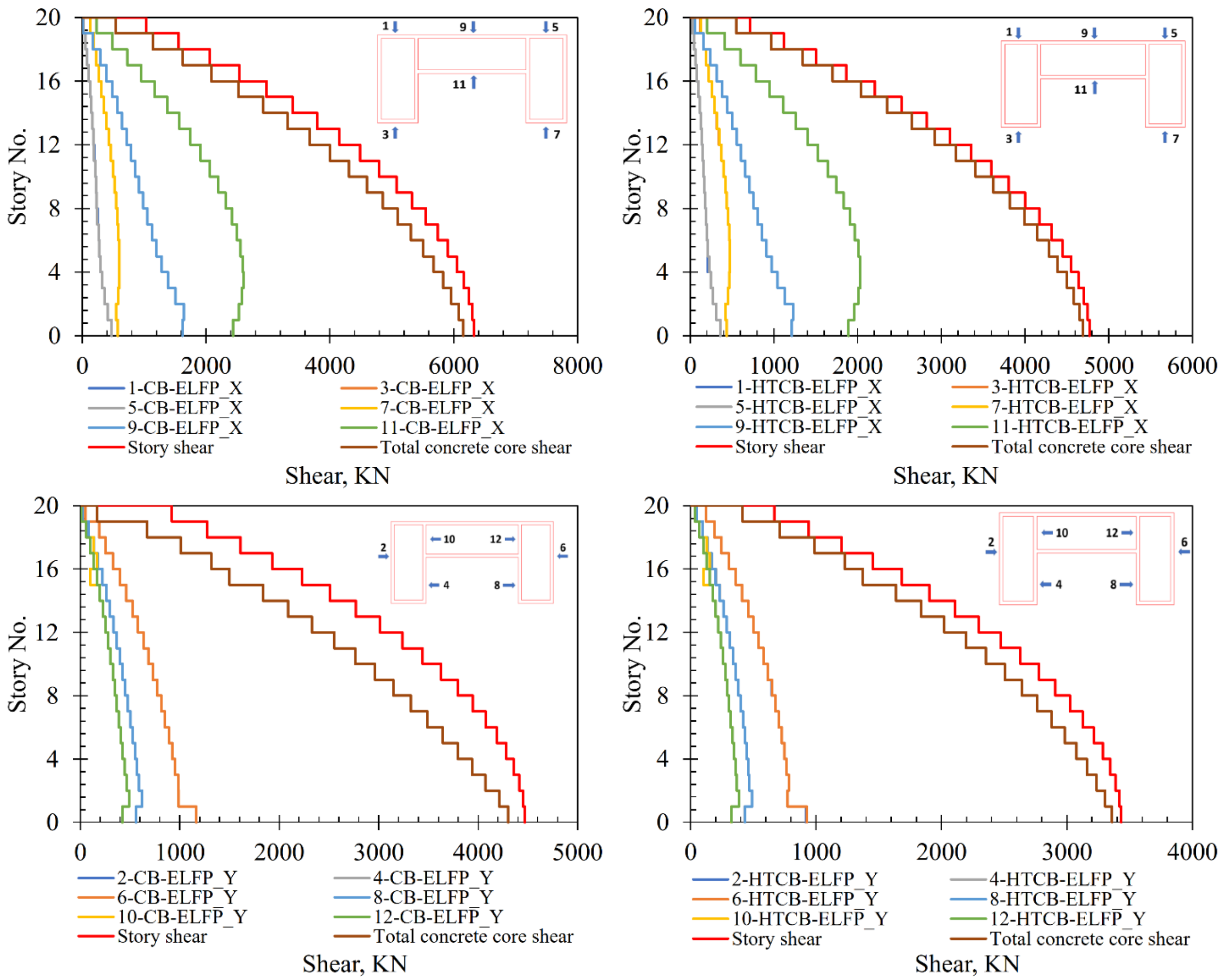

Figure 5: Concrete core shear results

A comparison of the embodied footprint of one building with another can clearly show how using different construction materials can be potentially environment friendly in terms of greenhouse gas emissions. Similar comparison of the case study structures is made in terms of CO_2 production from the usage of concrete, discussed as follows. In this comparison, only carbon footprint from the production of concrete material (Cradle-to-gate) is considered, and Life Cycle Assessment (LCA) is not made in this comparison, as only the superstructure of the two buildings is assessed excluding foundation, architectural components, and operational energy. CB would use 2541 m^3 of concrete and HTCB would use 797 m^3 of concrete, which shows that using timber in HTCB reduces the quantity of concrete by 69% compared to CB. Hong et. al. [14] found

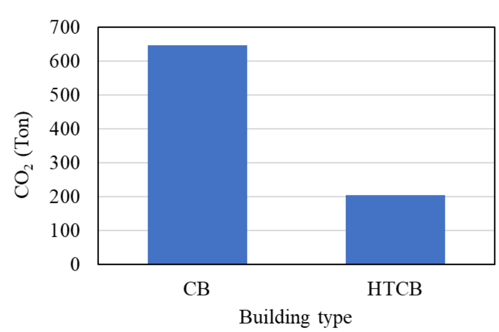

Figure 6: CO_2 production comparison

that approximately 106 kg of CO_2 is produced per ton of concrete [14]. Based on which it is found that CB would produce approximately 646 Ton CO_2 and HTCB would produce nearly 202 Ton CO_2, which is significantly less than that of CB.

5 Conclusions

In this study, a 20-story commercial concrete building (CB) and hybrid timber-concrete building (HTCB) located in Vancouver are designed and analyzed against design level seismic hazard. ELFP and RSP are performed as per *National building code of Canada (*NBCC) 2015. The case study buildings (CB and HTCB) are designed with separate lateral and gravity load resisting systems. Following conclusions are drawn from this study.

1. The results show a significant decrease of 30% in self-weight and seismic weight of HTCB compared to CB along with a 25% decrease in base shear values for HTCB.
2. In addition to this, the displacement demands are found to have a marginal decrease for HTCB, signifying a possible reduction in damages also which are closely related to displacement demand.
3. In addition, the HTCB is found to decrease the CO_2 emissions related to the construction materials and activity by a massive 68% compared to CB.

Therefore, it is concluded that the HTCB building has superior seismic and sustainability performance over CB while satisfying the different codal requirements.

Acknowledgement

"The careful review and constructive suggestions by the anonymous reviewers are gratefully acknowledged."

Refrences

[1] U. Nations. (2019). *Sustainable development goals.* Available: https://www.un.org/sustainabledevelopment/climate-change/
[2] Worldometers. (2020). *World Population: Past, Present, and Future*. Available: https://www.worldometers.info/world-population/
[3] P. Neill. (December 16th 2020). *United Nations Environment Programme*. Available: https://environmentjournal.online/articles/emissions-from-the-construction-industry-reach-highest-levels/
[4] N. C. Onat, M. J. R. Kucukvar, and S. E. Reviews, "Carbon footprint of construction industry: A global review and supply chain analysis," vol. 124, p. 109783, 2020.
[5] A. 2030. (2006, 04/29/2020). *THE 2030 CHALLENGE*. Available: https://architecture2030.org/2030_challenges/2030-challenge/
[6] R.-t. wood, "Materials Matter: Constructive Materials and Environmental Costs.," 2020.
[7] I. Smith and A. Frangi, "Overview of design issues for tall timber buildings," *Structural Engineering International,* vol. 18, no. 2, pp. 141-147, 2008.
[8] M. Fairhurst, "Dynamic analysis of the FFTT system," University of British Columbia, 2014.
[9] M. Green and E. Karsh, "The case for tall wood buildings," *Canadian Wood Council on behalf of the Wood Enterprise Coalition by Forestry Innovation Investment, North Vancouver, BC, Canada,* 2012.
[10] E. Slooten, "Feasibility study of a wood-concrete hybrid super tall building and optimization of its wind-induced behaviour," ed: Delf University of Technology, 2018.
[11] K. Kaushik, "Feasibility study of tall concrete-timber hybrid system," University of British Columbia, 2017.
[12] K. Wu, A. Iqbal, and T. Tannert, "Structural Systems for a 20-Storied Hybrid Building," ed: CSCE, 2019.
[13] A. Schuirmann, C. Loss, A. Iqbal, and T. Tannert, "Structural and environmental analyses of tall wood-concrete hybrid system," in *Proceedings of the CSCE 2019 International Specialty Conference on Engineering Mechanics and Materials, Laval, QC, Canada*, 2019, pp. 12-15.
[14] T.-H. Hong, C.-Y. Ji, M.-H. Jang, and H.-S. Park, "Predicting the CO 2 emission of concrete using statistical analysis," *Journal of Construction Engineering and Project Management,* vol. 2, no. 2, pp. 53-60, 2012.

SEISMIC VULNERABILITY ASSESSMENT AND RETROFITTING OF REINFORCED CONCRETE BRIDGE BY RC JACKETING

[a] Ahsan Khalil, [b] Muhammad Khalid Hafeez, [c] Dr. Qaiser-uz-Zaman Khan

[a, b, c] Civil Engineering Department, University of Engineering and Technology Taxila, Pakistan,
ahsankhalil455@gmail.com
raokhalidhafeez@gmail.com
dr.qaiser@uettaxila.edu.pk

Abstract- Seismic vulnerability assessment of Reinforced Concrete (RC) bridges is of paramount importance in developing countries due to poor design and construction practices, especially in an earthquake-prone zone. A case study of a typical bridge in Pakistan was carried out and results were analyzed. The overall aim of this research was to perform an equivalent static analysis of the existing bridge and measure its adequacy against existing loading conditions and new seismic requirements. This paper aims to highlight the use of SAP2000v14 in seismic analysis of the RC bridge piers, in the existing as well as post remedial measures stage. The bridge was modeled on the software as per existing structural parameters and loading was applied as per relevant seismic criteria which indicated that the bridge was under-designed. The goal was the introduction of an effective remedial measure to accommodate seismic loading in the structural design, which in this case was retrofitting in the form of RC jackets, the results were successful.

Keywords- Reinforced Concrete Bridge, Earthquake-Prone Zone, SAP2000v14, Retrofitting.

1 Introduction

Developing countries like Pakistan with high seismic hazards, poor design, and construction practices require an in-depth special seismic vulnerability assessment of their Reinforced Concrete (RC) bridge stock having different structural systems [1]. Most of the existing RC bridges in Pakistan are gravity-loaded design RC structures. A significant portion of these RC bridges is pre-stressed reinforced concrete structures [2]. Most of these bridges have low lateral load resistance and suffer from ductility issues. Low strength concrete, aging, bad design, inappropriate detailing, and poor construction practices are the components that play a substantial role in structural damages and eminent failures during an earthquake that should be addressed in vulnerability assessment [3][4].

Many recent vulnerability assessment studies focused on the bridges of the developed countries, which generally comprise good quality and code conforming RC bridges [5][6]. These vulnerability studies are not feasible for bridge stocks of the developing countries and can underestimate the damage potential of highly fragile RC bridges to a large extent [7]. The post-Kashmir earthquake seismic hazard studies have predicted higher seismic hazard in different parts of the country indicating high vulnerability of various civil infrastructure which calls for seismic vulnerability assessment of other civil infrastructure [8]. The current work focused on estimating the performance of a case bridge against the new seismic demand of the area. The bridge was found deficient and a feasible technique of retrofitting was proposed for the low strength existing RC bridge piers to meet with declared seismic hazard.

2 Research Methodology

A high-intensity earthquake was recorded in Jatlan by the Pakistan Metrological Department (PMD), in September 2019. According to the official reports, the earthquake in Jatlan caused severe damages to domestic structures including homes, multi-story buildings, and other infrastructures. A typical existing Reinforced Concrete (RC) bridge in the vicinity of the affected region in Pakistan was selected for a case study to investigate whether the considered bridge is safe or not as per the declared seismic zone requirements of the region. The bridge was modeled as per the existing structural drawings prepared by the Bridge Directorate Highway Department of Punjab, Pakistan. Material properties i.e. concrete strength, yield strength for steel, and section properties i.e. girders and piers, were selected as per the existing drawings. Static linear analysis was performed after the input of required loading conditions. Software results were analyzed and it was concluded that the structure is under-designed. Accordingly, retrofitting by RC jacketing was carried out.

2.1 Case Study.

A pre-stressed I-girder bridge located on Dina-Rohtas Road near Rohtas Fort, in the seismic zone 2B of Pakistan was selected as a case study. This bridge consists of two traffic lanes, seven spans of 103.36 ft. (31504.13 mm), and 60 ft. (18288 mm) high piers of 5.5 ft. (1676.4 mm) diameter. Bridge was modeled using SAP2000 v14 software as per the structural drawings. There were no parametric variations along the length of the bridge.

Based on Peak Ground Acceleration (PGA) values, Pakistan is divided into five seismic zones in line with the Building code of Pakistan (BCP 2007) [9]. The Building Code was revised in 2007 and seismic zoning was changed and new Zones were defined as shown in Table 1.

Table 1: Seismic Zones (BCP 2007)

Seismic Zones	Peak Horizontal Ground Acceleration
1	0.05 to 0.08g
2A	0.08 to 0.16g
2B	0.16 to 0.24g
3	0.24 to 0.32g
4	> 0.32g

The case bridge is located on the PGA intensity line of 0.2g, as per BCP 2007 PGA contours map. Therefore, the values of the seismic coefficients $\mathbf{C_a}$ and $\mathbf{C_v}$ against seismic zone factor Z, **0.2** were considered.

2.2 Modeling Details.

Modeling was done as per the structural drawings prepared by the concerned department of Pakistan. Girders, Deck slabs, and diaphragms were prestressed members. All the load combinations were taken from the Government of West Pakistan Code of Practice for Highway Bridges (WPCPHB-1967) [10]. The case bridge was designed as per the WPCPHB assuming seismic loads as 2%, 4%, and 6% of dead loads for different foundation conditions. The effect of the live load was ignored. The material properties used for the modeling of the existing bridge were according to the structural design data and the key details are shown in Table 2. Girders, Piers, and transoms were modeled by using these details.

Table 2: Properties of Materials

Concrete Strength for piers (28 days compressive cylinder strength)	3200 psi (22063.2 kPa)
Concrete Strength for prestressed members (28 days cylinder strength)	4400 psi (30336.9 kPa)
Steel Yield strength	60000 psi (413685.4 kPa)

For analysis of the case bridge, the soil profile type **S_D** (stiff soil) was considered. The values of seismic coefficients **C_a** and **C_v** for seismic zone factor Z, **0.20** relevant to the soil profile type were 0.28 and 0.40 respectively (BCP 2007). The structural ductility was considered by the Response modification factor (R) as per BCP 2007-Table 5.13 [9]. In the modeling, bearings on the pier head were considered as link elements, and bearings on the abutment sides were modeled as springs. The values of lateral, vertical, and rotational spring stiffnesses for elastomeric bearing pads on the abutment sides are shown in Table 3 [11].

Table 3: Spring Stiffnesses on the Abutment Sides

Direction	Spring stiffness, K
Lateral	1755 (KN/m)
Vertical	1143752 (KN/m)
Rotational	16270 (KNm/m)

2.3 Model.

The structural drawings of some key components of the existing bridge are shown in Figure 1.

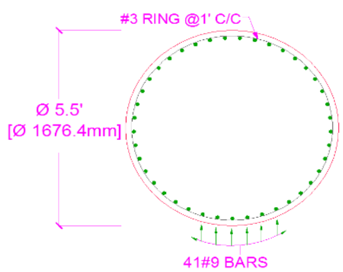

1a) Pier

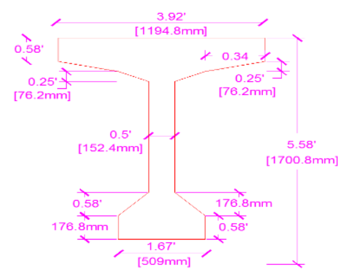

1b) I-girder

Figure 1: Cross-sections of pier and girder

After modeling all the components on SAP2000v14, the x-section of the bridge structure and perspective view of the 3-D model is shown below in Figure 2a and 2b respectively.

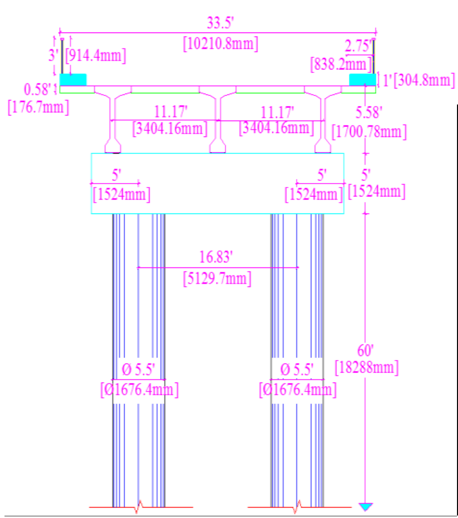

2a) X-section

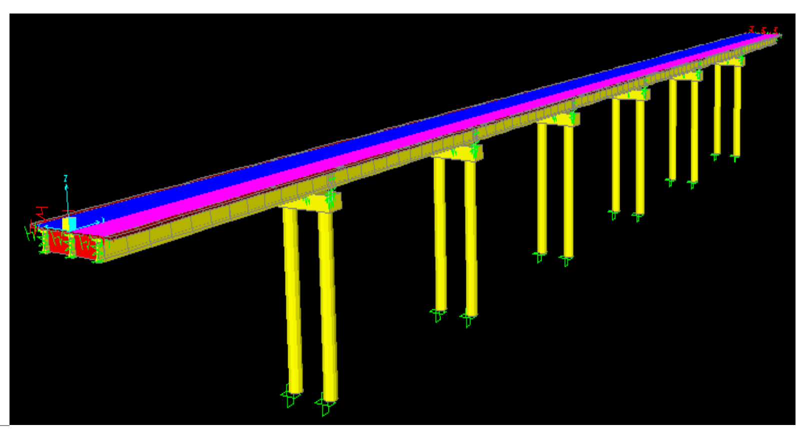

2b) 3-D Model View

Figure 2: Different Views of Bridge

3 Results and Discussion

Static linear analysis was performed and the model was checked for elastic limits. The seismic forces at the base of each bridge pier and the natural period of vibration are given below.

$$V_X = 13.55 \text{ Kips } (60.27 \text{ KN}),\ V_Y = 159.54 \text{ Kips } (709.66 \text{ KN}),\ T = 0.73 \text{ sec}$$

From the analysis of the data obtained, it was observed that against the load combination, 1.33 Dead+1.33 Earthquake, which is a static load case for seismic forces, the highlighted bridge piers failed in flexure as shown in Figure 3a. The bridge is thus under-designed and vulnerable in the existing seismic zone. It was noted that as per the requirements of WPCPHB, the bridge was designed assuming seismic loads as 2%, 4%, and 6% of dead loads for different foundation conditions. These assumptions do not match with the present seismic demand of the area as PGA estimated in BCP2007 for that area is 20 percent of dead load. The model was then run for the design of the bridge pier for the new PGA requirement. It was noted that the requirement of the longitudinal steel in the bridge pier was 61.142 square inches against the provision of 41.0 square inches in the design. The bridge thus requires additional measures to accommodate this extra demand and there is a need for retrofitting for all the critical members as shown in Figure 3c. To accommodate the required strength for critical members and to compensate for this gap provision of retrofitting through RC Jacketing was proposed.

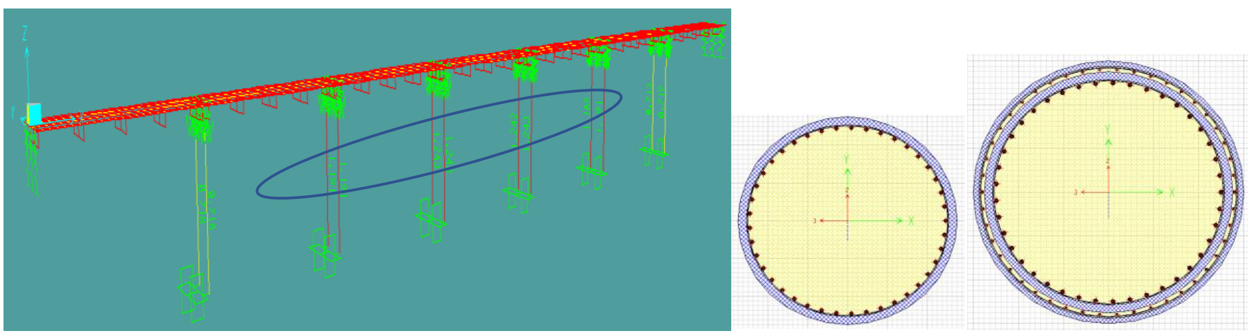

3a) Flexural Failure Model 3b) Bridge Pier 3c) Bridge Pier with Jacketing

Figure 3: Failed Model and After Retrofitting

The type of proposed retrofitting, in this case, was RC jacketing because the scale of deficiency in the structural strength required a sizeable increase in the flexural capacity of the bridge piers by increasing its cross-sectional dimensions. Further, the material used in RC jacketing is locally and readily available and no extraordinary skilled labor is required for its execution. For a trial, RC jacketing of different thicknesses (3, 4, 5, 6, and 8 inches) were considered in 15 ft lower critical part of the bridge piers and checked for its effectiveness for the case Bridge. The bridge piers were modeled for these additional thicknesses in SAP2000v14 and their efficacy was checked for each thickness of trail RC jacketing. It was concluded that the most efficient thickness of RC jacketing is 0.5 ft (6 inches) with other properties are as shown in Table 4.

Table 4: Reinforcement details for RC Jacketing

Longitudinal Reinforcement	Transverse Reinforcement (Hoops)
46 # 6	# 4 @ 6" c/c

The jacketing of 6 inches thickness when applied up to a height of 15 ft from the base, all the critical members performed well and the structure becomes safe for new seismic demand of the area as shown in Figure 4 [12][13]. The demand/capacity ratios for critical members before and after retrofitting are also shown in Table 5.

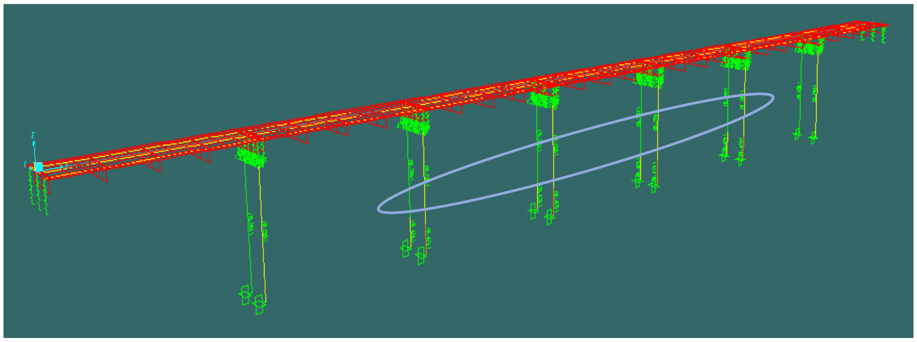

Figure 4: Model after Retrofitting

Table 5: Demand/Capacity ratios for Critical Members

Pier	Demand/Capacity ratios before retrofit	Demand/Capacity ratios after retrofit
2	1.088	0.842
3	1.322	0.886
4	1.322	0.886
5	1.088	0.842

4 Applicability of Research

In Pakistan, after the Kashmir (2005) earthquake, seismic zoning has been revised. Before this major earthquake, the bridges were designed as per the Government of West Pakistan Code of Practice for Highway Bridges (WPCPHB-1967) [10]. Therefore, most of the existing bridges are susceptible to major seismic damages and need strengthening to enhance their strength against the present seismic demand. As the existing RC bridge piers are deficient in flexural strength. The obtained results reveal that the technique for retrofitting thus used i.e, RC jacketing has a greater impact in fulfilling the required flexural strength of all critical bridge piers.

5 Conclusion

From the conducted study it has been concluded that

- The required longitudinal reinforcement area for the bridge piers in the present seismic zoning of Pakistan is more than the provided area.
- There is a need for retrofitting for all the critical members to enhance their load-carrying capacities to accommodate the revised seismic requirements of the area.
- All the critical members fulfill the required criteria when RC Jacketing of thickness 0.5 ft (6 inches) with forty-six bars of # 6 are provided to compensate for the reinforcement gap and applied up to 15 ft bottom depth of piers for case bridge.

Acknowledgment

The authors would like to thank every person/department who helped throughout the research work particularly and Engr. Irbaz Hasan. The careful review and constructive suggestions by the anonymous reviewers are gratefully acknowledged.

References

[1] S. Ahmad, K. Pilakoutas, Q. U. Z. Khan, and S. Mehboob, "Seismic Demand for Low-Rise Reinforced Concrete Buildings of Islamabad–Rawalpindi Region (Pakistan)," *Arab. J. Sci. Eng.*, vol. 43, no. 10, pp. 5101–5117, 2018.

[2] M. Waseem and E. Spacone, "Fragility curves for the typical multi-span simply supported bridges in northern Pakistan," *Struct. Eng. Mech. An Int. J.*, vol. 64, no. 2, pp. 213–223, 2017.

[3] M. Zain, M. Usman, S. H. Farooq, and T. Mehmood, "Seismic vulnerability assessment of school buildings in seismic zone 4 of Pakistan," *Adv. Civ. Eng.*, vol. 2019, 2019.
[4] H. Aryan, "Seismic Resistant Bridge Columns with NiTi Shape Memory Alloy and Ultra-High-Performance Concrete," *Infrastructures*, vol. 5, no. 12, p. 105, 2020.
[5] K. Aljawhari, F. Freddi, and C. Galasso, "State-dependent vulnerability of case-study reinforced concrete frames," in *COMPDYN 2019 Proceedings*, 2019, vol. 7.
[6] T. Rossetto and A. Elnashai, "Derivation of vulnerability functions for European-type RC structures based on observational data," *Eng. Struct.*, vol. 25, no. 10, pp. 1241–1263, 2003.
[7] M. Pregnolato, "Bridge safety is not for granted–a novel approach to bridge management," *Eng. Struct.*, vol. 196, p. 109193, 2019.
[8] A. Q. Bhatti and H. Varum, "Application of Performance Based Nonlinear Seismic Design and Simulation Static Pushover Analysis for Seismic Design of RC Buildings," in *Proceedings of the 15th World Conference on Earthquake Engineering, 15WCEE, Lisbon*, 2012, pp. 24–28.
[9] Seismic Provisions, "Building Code of Pakistan (Seismic Provisions 2007)," p. 303, 2007.
[10] "Government Of West Pakistan Highway Department Code Of Practice," 1967.
[11] C. Akogul and O. C. Celik, "Effect of elastomeric bearing modeling parameters on the Seismis design of RC highway bridges with precast concrete girders," in *Proceedings of the 14th World Conference on Earthquake Engineering*, 2008, pp. 13–28.
[12] M. Suarjana, D. D. Octora, and M. Riyansyah, "Seismic Performance of RC Hollow Rectangular Bridge Piers Retrofitted by Concrete Jacketing Considering the Initial Load and Interface Slip.," *J. Eng. Technol. Sci.*, vol. 52, no. 3, 2020.
[13] A. Reggia, A. Morbi, and G. A. Plizzari, "Experimental study of a reinforced concrete bridge pier strengthened with HPFRC jacketing," *Eng. Struct.*, vol. 210, p. 110355, 2020.

3rd Conference on Sustainability in Civil Engineering (CSCE'21)
Department of Civil Engineering
Capital University of Science and Technology, Islamabad Pakistan

STRUCTURAL PERFORMANCE OF GFRP-REINFORCED BCJ THROUGH FINITE ELEMENT ANALYSIS

[a] Anees ur Rehman, [b] Qaiser uz Zaman Khan, [c] Ali Raza*

a: Department of Civil Engineering, University of Engineering and Technology Taxila, 47080, Pakistan, engr.anees6384@gmail.com
b: Department of Civil Engineering, University of Engineering and Technology Taxila, 47080, Pakistan, dr.qaiser@uettaxila.edu.pk
c: Department of Civil Engineering, University of Engineering and Technology Taxila, 47080, Pakistan
* Corresponding author: Email ID: ali.raza@uettaxila.edu.pk

Abstract- Glass-fiber reinforced polymer (GFRP) rebars are being employed as a good substitute to steel in reinforced concrete (RC) structural elements due to their superior performance. The main objective of the present study is to evaluate the structural behavior of beam-column joints (BCJ) reinforced with GFRP rebars using non-linear finite element analysis (NLFEA) under the seismic loading. In the present study, three-dimensional NLFEA of BCJ reinforced with steel and GFRP rebars was conducted using a finite element (FE) code ABAQUS. The FE model was verified against the experimental load-deflection curves of BCJ. A sensitivity analysis of the proposed FE model was carried out to investigate the effect of different parameters, including mesh size, dilation angle (ψ), stress ratio, viscosity parameter (VP), eccentricity, and shape factor of concrete material on the load-deflection response of BCJ. The FE modeling using ABAQUS software predicted the experimental load-deflection curve of BCJ with sufficient accuracy. The results concluded that the currently proposed FE model can accurately pretend the load-deflection performance of BCJ.

Keywords- GFRP; finite element modeling; concrete damaged plasticity; BCJ; failure modes; parametric study

1 Introduction

The GFRP rebars are now utilized everywhere in the world as a viable substitution to steel in current substantial constructions particularly in such designs that may bear severe environmental conditions [1]. The majority of the past research shows that fiber-reinforced polymers (FRPs) are a functioning swap for steel while giving a few benefits like corrosion resistance, including high strength, simplicity of taking care of, high tensile strength, low self-weight, and low maintenance necessity [2-4]. In any case, brittle performance is a significant shortcoming of FRP rebars because of which they show straight elastic conduct up to rupture, which seriously influences the ductility of concrete. Considering the shortfall of ductility, FRPs portray low value of modulus when compared with ordinary steel. This performance of FRP achieves excessive deflections and large cracks that affect its functionality [5]. To look at the thermal stability of glass fiber reinforced polymer (GFRP) rebars, it was seen that mechanical characteristics like shear, flexural, and ductile improvement with the decline in temperature [6]. The external surface conditions like ribbed GFRP rebars and string-wrapped were generally influencing the bond strength and pullout behavior of GFRP rebars [7].

Various experimental studies have been carried out on the beam-column joints (BCJ) reinforced with either steel rebars or GFRP rebars under different seismic loading conditions [8-23]. These studies concluded that the structural performance of BCJ can be significantly improved by using advanced FRP composites. A detailed investigation of the role of GFRP reinforcement in the perpendicular beam of BCJ concluded that the capacity of BCJ can be enhanced when GFRP reinforcing rebars are added to the perpendicular beams [24, 25]. The GFRP reinforced columns show a smaller axial load and bending moment capacity as compared to conventional steel-reinforced columns. On the other hand, the ductility of the GFRP reinforced columns was very close to the ductility of the steel-reinforced columns [26]. Benmokrane et al. [27] experimented and concluded that the flexural conduct of beams utilizing various kinds of GFRP rebars in a 3.3 m long rebar and contrasted exploratory outcomes with the conservative steel rebars. The outcomes demonstrate that GFRP rebars are a favorable choice for steel. GFRP-RC beams display larger stiffening strain-hardening and bigger crack widths when contrasted with steel having lower stiffness of GFRP rebars [28]. A non-linear finite element analysis (NLFEA) was carried out to consider the buckling in I-beams and reasoned that because of the end bending constraints and amendment in loading capacity, the FRP rebar portray larger effects the buckling process when contrasted with steel [29, 30]. The finite element (FE) crack samples of geopolymer concrete flexural members showed a nearby concurrence with the tests, however, introduced a few deviations in the deflection results [31]. The mathematical outcomes got from NLFEA for the shear limit and crack samples of outside and inside BCJ gave a decent understanding of testing results [32]. Elflah et al. proposed a NLFEA model on hardened steel BCJ which precisely anticipated stiffness, maximum resistance, moment rotation performance, and the failure patterns [33]. A mathematical examination of non-ductile external joints has been carried out to investigate the shear breaking. Mathematical outcomes demonstrate that joint perspective proportion and rebar longitudinal support proportion were the significant boundaries that impact the joint shear behavior [34]. The performance of a BCJ was researched by utilizing ABAQUS programming. An identical T-stub strategy was utilized to demonstrate every one of the components of the tension areas of the BCJ concluding that the tension joint presented an increment in deflections [35].

The literature review depicts that the NLFEA modeling of steel and GFRP built up BCJ has not been performed in the previous studies on BCJ and, therefore, there is a need to investigate the performance of GFRP-RC BCJ to positively validate their applications in the construction industry which is the novelty of the present work. The main goal of the current examination is to propose a three-dimensional NLFEA model utilizing ABAQUS that precisely predicts the underlying performance of GFRP built-up BCJ. The subsequent goal is to execute an extensive parametric examination utilizing the proposed constitutive NLFEA model to analyze the impact of different geometric and material boundaries of BCJ. Finally, the cracking patterns and failure modes of concrete in BCJ were reviewed. This examination will be useful for designers to investigate and design the GFRP reinforced concrete BCJ utilizing the suggested NLFEA model. Furthermore, the serviceability of structures will be improved using FRP in structural elements.

2 Finite Element Analysis

Joints elements were modeled using commercial software ABAQUS 6.12 [36], a general NLFEA program is employed to verify the influence of GFRP rebars on BCJ. In the preprocessing stage, material properties, element types, geometry, and boundary conditions, and nonlinear analysis solutions are defined. There are different models in ABAQUS which are employed to define the structural performance of concrete as a quasi-brittle material, i.e., brittle and smeared cracking models. In the damage plasticity model, yield criteria, hardening rule, and flow rule are essential integrals of the model [34]. By using the experimental results of Mohammad et al. [1], this study investigated the numerical models of the BCJ by calibrating the key factors like reinforcement types and ratios. The structural dimensions of the studied BCJ, as shown in Figure 1, are summarized in having a horizontal beam with a cross-section of 350 mm ×450 mm and a vertical column with a 350 mm × 500 mm cross-section. The height of the column is 3650 mm, and the length of the beam is 2350 mm.

In the present study, the testing samples SS, GS, and GS3 were labelled as MSS, MGS, and MGS3, correspondingly [1]. The details of the longitudinal and shear reinforcement of all specimens are shown in Table 1. All test samples were made with a maximum aggregate size of 20 mm using normal weight ready mix concrete. The obtained 28-days compressive strength of concrete specimens was determined based on a standard cylinder test was 32 MPa. The properties of reinforcing rebars are shown in Table 2. Figure 2 shows the simulated FE models of BCJ.

Table 1. Reinforcement details of specimens

Specimens	Beam		Column	
	Rebars	Stirrups	Rebars	Stirrups
Specimen (MSS)	5#M20 Steel	2 legs steel hoop #10M@100 mm	8#M15 Steel	2 legs steel hoop #10M@90 mm +1 transversal crosstie #10M@90 mm
Specimen (MGS1)	5#16 GFRP	3 branches #13GFRP@100 mm	8#16 GFRP	3 branches #13GFRP@90 mm +1 transversal branch #10GFRP@90 mm
Specimen (MGS3)	8#19 GFRP	3 branches #13GFRP@100 mm	12#19 GFRP	3 branches #13GFRP@90 mm +1 transversal branch #10GFRP@90 mm

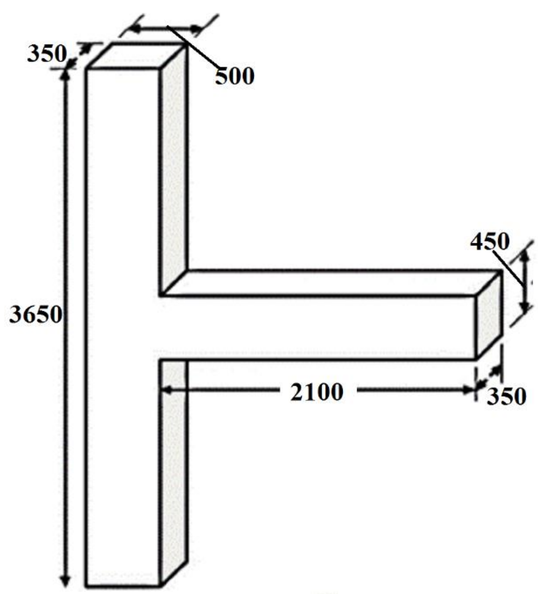

Figure 1. Overall dimensions of the specimen (all values are in mm)

Table 2. Properties of steel and GFRP Rebars

Rebar Size	Young's Modulus (GPa)	Tensile strength (MPa)
Steel #20M	200	f_y=400 (460)^a
Steel #15M	200	f_y=400 (460)^a
Steel #10M	200	f_y=400^a
GFRP #19	47.6	728
GFRP #13	46	590^b
GFRP #10	45	642^b

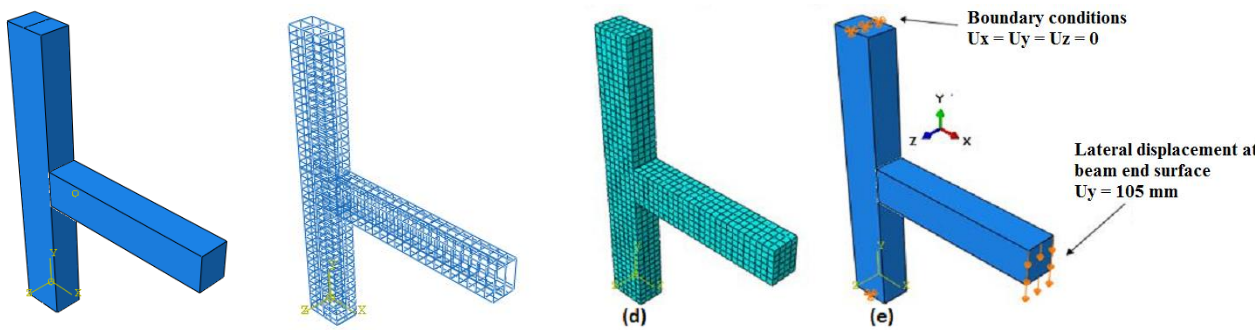

Figure 2. Simulated FE models

2.1 Concrete damage plasticity (CDP) model

The numerical simulation of concrete is a challenging task because of the complex behavior of concrete under loading. In this work, using the concept of isotropic damaged elasticity combine with compressive plasticity and isotropic tensile the inelastic behavior of concrete was presented by a CDP model. The strain hardening under compressive loading can be determined by using the CDP model based on the strain rate. The elastic behavior of confined concrete is up to 50% of peak confined loading strength. Therefore, to consider the confinement improvement effect due to GFRP ties, the models suggested by Afifi et al. [37] for the compressive stress and compressive strain of confined concrete were employed in this research as portrayed by Eq. (1) and Eq. (2).

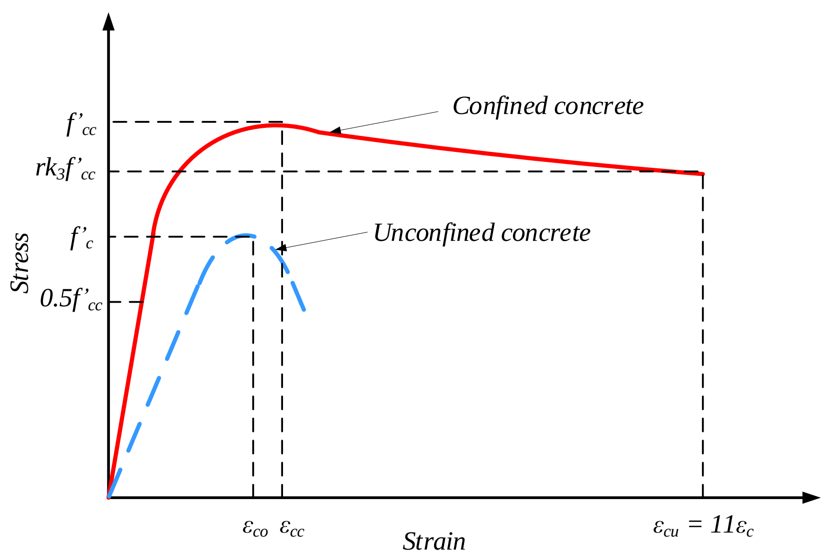

Figure 3. Stress-strain performance of confined and unconfined concrete

$$\frac{f'_{cc}}{f'_{co}} = 1.0 + 4.547\left(\frac{f_{le}}{f'_{co}}\right)^{0.723} \tag{1}$$

$$\frac{\varepsilon'_{cc}}{\varepsilon'_{co}} = 1.0 + \left(\frac{0.024}{\varepsilon'_{co}}\right)\left(\frac{f_{le}}{f'_{co}}\right)^{0.907} \tag{2}$$

where f_{le} reports the effective confinement loading strength provided by the GFRP ties which can be measured from Eq. (3) [38].

$$f_{le} = \frac{2E_f \varepsilon_{h,rup} t}{D} \quad (3)$$

where E_f describes the elastic modulus of lateral ties, $\varepsilon_{h,rup}$ describes the hoop rupture strains of lateral GFRP ties and 't' defines the thickness of lateral GFRP ties. According to the concept of elastoplasticity theory, the total strain of concrete (ε) can be divided into two parts: the elastic strain (ε^{el}) and the plastic strain (ε^{pl}) of concrete as portrayed by Eq. (4).

$$\varepsilon = \varepsilon^{el} + \varepsilon^{pl} \quad (4)$$

The uniaxial compression damage parameter (d_c) and the uniaxial tension damage parameter (d_t) are employed for the simulation of damage of concrete in the CDP model. By assuming Figure 4, the compressive (σ_c) and tensile (σ_c) strengths of concrete can be calculated as:

$$\sigma_c = (1 - d_c)E_o\left(\varepsilon_c - \varepsilon_c^{pl}\right) \quad (5)$$

$$\sigma_t = (1 - d_t)E_o\left(\varepsilon_t - \varepsilon_t^{pl}\right) \quad (6)$$

where E_o is Young's modulus of concrete, ε_c is the compression strain of concrete, and ε_c^{pl} is the plastic portion of the compression strain of concrete and ε_t^{pl} is the plastic portion of the tension strain of concrete. The factor d_c and d_t are defined by Eq. (7) and Eq. (8), correspondingly [39].

$$d_c = \frac{1}{e^{-1}/m_{c-1}}\left(e^{-\varepsilon_{c,norm}^{in}/m_c} - 1\right) \quad (7)$$

$$d_t = \frac{1}{e^{-1}/m_{t-1}}\left(e^{-\varepsilon_{t,norm}^{ck}/m_t} - 1\right) \quad (8)$$

where m_c is the compressive collapse progression speed governing parameter with a value of 0.1 and m_t is the tensile collapse evolution speed governing parameter with a value of 0.05 [40]. The parameter $\varepsilon_{c,norm}^{in}$ is the standardized compressive plastic strain that can be interpreted by the ratio of inelastic compressive strain having a value of 0.033 $\varepsilon_{c,norm}^{in}$ is the standardized tensile plastic strain of concrete having a value of 0.0033 [40].

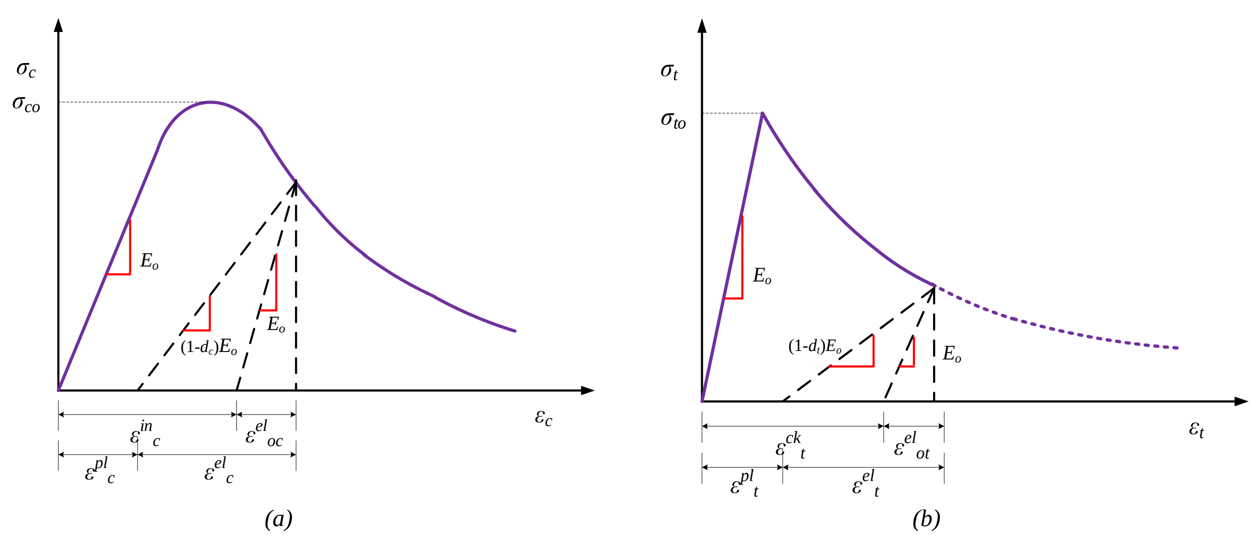

Figure 4. (a) Compressive stress-strain behavior of concrete (b) Tensile stress-strain behavior of concrete

The compressive and tensile loading strength, the Poisson's ratio v and the Young's modulus E_0 are some concrete mechanical behavior parameters. The value of Poisson's ratio $v = 0.2$ is assumed as constant for the CDP model in this work. The corrected values were taken for dilation angle (ψ) and viscosity parameter (VP) and shape factor K_c=0.667, eccentricity ε =0.1, the stress ratio σ_{b0}/σ_{c0}=1.16 are the default values employed for the CDP model in ABAQUS [41]. The non-linearity of the concrete is produced from three major causes: the ductility of the steel reinforcement, the nonlinearity of the concrete under compressive loading, and the behavior of the concrete in the tension zones [41]. The values of ultimate stress and ultimate stain and yielding are taken from experimental results [1]. The nonlinear response of reinforcing rebars was assumed to be linear elastic-perfectly plastic. The value of Poisson's ratio v was taken as 0.3.

2.2 Calibration of a model on material parameters

The calibration of the FE model is done according to the experimental test results. For the justification of the numerical model, different materials and geometric parameters were investigated to obtain a result that is closer to the experimental results. Here, specimen MSS is selected as a control sample and VP, element type, ψ, eccentricity, stress ratio, shape factor, and mesh size are the varying parameters. After calibration, the model is then employed to perform FEM analysis on other specimens. Element types C3D8R and T3D2 were employed for concrete and reinforcement, correspondingly. Concrete is usually considered a brittle material and due to inelastic strains undergo considerable volume change which is called dilatancy. By assigning the value of ψ, dilatancy can be modeled in the CPD model, according to the researcher's ψ is ranges between 31∘ to 42∘ [42-45]. A sensitive FE examination is executed to consider the impact of ψ on load-deflection performance. Figure 5 reports that the ψ somewhat influences the load-deflection curve. With the increment in ψ, the maximum load improves, and it was seen that the ψ of 35° reported a negligible effect on the load-deflection behavior of the test curves. In this way, a ψ of 35∘ was preferred for all remaining investigations with VPs and meshing sizes of 0.0075 and 80 mm, separately. Eventually, it can undoubtedly be reasoned that larger amounts depict ductile performance and small values of the ψ depict lower performance [32]. The eccentricity (ε) was validated to examine a maximum load-deflection of the BCJ as shown in Figure 5. Various values of (0.1, 0.2, 0.3 and 0.4) were chosen to examine the load-deflection curves. The outcomes show that the impact of ε on the BCJ samples is minor.

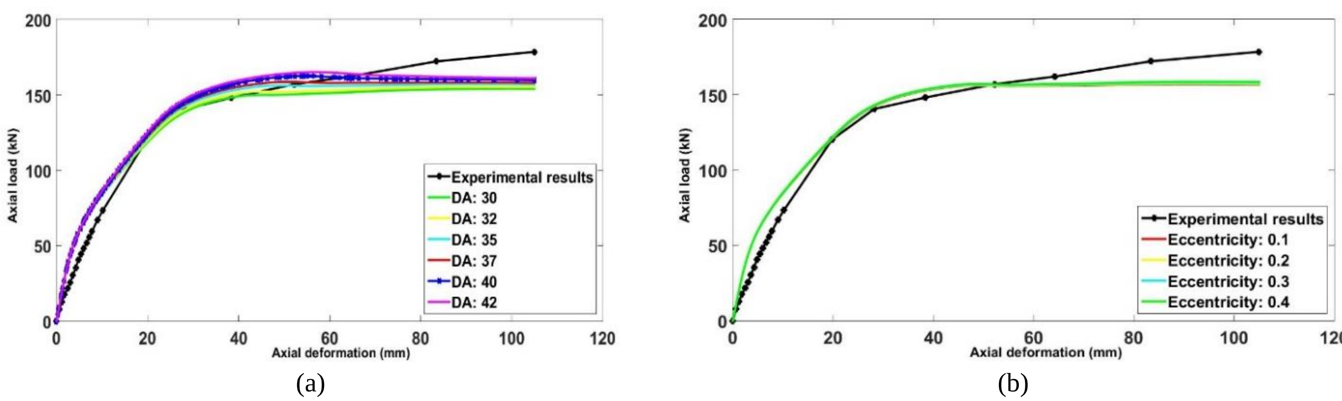

Figure 5. Calibration work (a) effect of ψ on the load-deflection performance (b) effect of eccentricity on load- deflection performance

The validation process for the stress ratio was also carried out to examine the consequence of different stress ratios σ_{b0}/σ_{c0} value. The predictions of the NLFEA model show that change of values is not showing any protruding change, so 1.16 was selected which was also the default value [46]. To explore the performance of parameter Kc, some validation works have been made. To simulate the yielding surface and shape, the Kc parameter is very important. By default, it is considered to carry a value of 0.667 although its range is between 0.5 to 1 [32]. In the current investigation, four various quantities of shape factor were selected as 0.667, 0.750, 0.822, and 1.0. Therefore, the most precise predictions can be employed as the default value of 0.667. To inspect the effect of mesh size, its values of 140 mm, 120 mm, 100 mm, 80 mm, 60 mm, and 40 mm were employed to examine the influence of various mesh sizes on the NLFEA model. Figure 6 shows that mesh size 80 mm represents a more precise outcome compared with the test load-deflection curve.

To examine the impact, various values of VP (VP) 0.0015, 0.0035, 0.0055, 0.0075, 0.0095, and 0.015 were utilized in the NLFEA model. By utilizing the VP of 0 (which is the default ABAQUS esteem), the modeling will end. The value of the VP relies on the time increase step, the scientist proposes that to increase the arrangement 15% of the time increase step value is to be selected [46]. Various amounts of the VP greatly influence the load-deflection behavior as represented in Figure 7. The best fit to experimental results is obtained unison 80 mm and 35° for mesh size and dilation of concrete, correspondingly.

3 Discussion of Results

3.1 Load-deflection response

After validating the control model for various parameters, the calibrated control model MSS was employed to remaining BCJ members to examine the performance of the load-deflection behavior as represented in Figure 8(a & b). Figure 8 shows that steel rebars portrayed a close correlation with the test outcomes as associated to GFRP rebars. But some differences are observed in the load-deflection curve at ultimate load failure as shown in Figure 8(a) because, in FEM, the concrete is considered as a homogenous type of material, but the experimental concrete is not homogenous. The specimen MGS and MGS 3 as shown in Figures 8 (a) and (c) show more stiffness than the experimental curve. This may be due to the difference in the boundary condition of actual and tested specimens and the assumption of perfect bond during FEA and the accuracy of the testing instruments. The calibration work also reported a good response for the complete load-deflection curves of the BCJ specimens.

Although the proposed numerical model reported a good prediction behavior in the elastic behavior, it portrayed some differences in the post-peak behavior of the load-deflection curves. The minor deviations between the experimental and NLFEA results can be credited to the following reasons: (1) deviations in materials properties provided by the manufacturers (2) assumptions made during NLFEA simulations for the materials definitions (3) considering the linear elastic behavior of GFRP rebars (4) assuming perfect bond between the concrete and reinforcement, and (5) assumptions of boundary conditions made in the NLFEA simulations [47-52].

3.2 Cracking patterns

In the MSS specimen cracks produced in the plastic hinges zone prolonged from the face of the column to the death of the beam and no cracks seemed in the column or joint area as represented in Figure 9(a). Figure 9(b) shows that failure occurs gradually starting with spalling of concrete. In specimen MGS the GFRP rebars portrayed rupture at the deflection of 136.5 mm of the beam. The GFRP stirrups presented the failure after the peak loading capacity when the concrete core was activated after securing the ultimate strength of concrete. In specimen MGS 3 at the joint area a larger diagonal failure look, the crack becomes wider and ongoing to proceed toward the far edge of the column as shown in Figure 9(c).

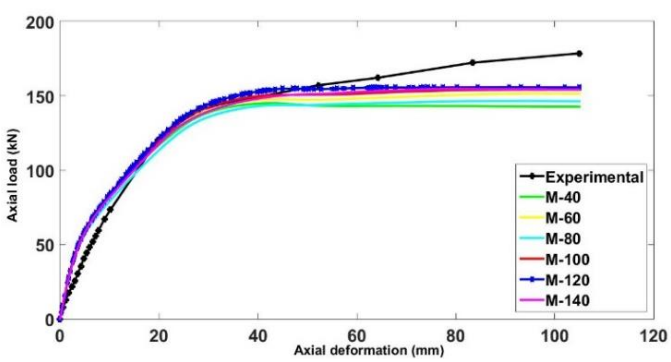

Figure 6. Lateral load deflection for various mesh values.

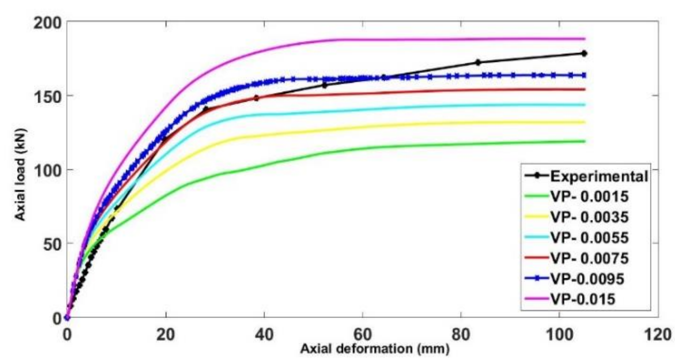

Figure 7. Load-deflection response for various values of VP.

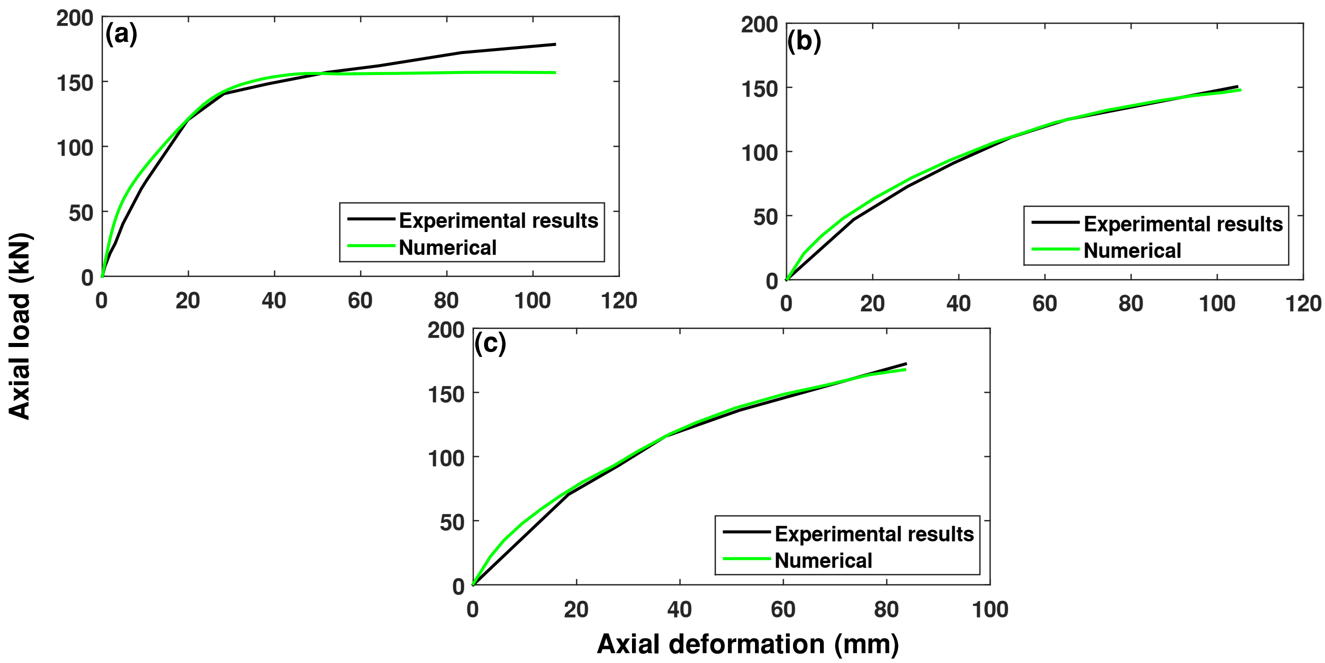

Figure 8. NLFEA and test load-deflection behavior of (a) MSS (b) MGS (c) MGS3.

By employing the CDP, the cracks performance of concrete will happen because of the positive ultimate principal plastic straining. The track of the cracks process is observed via ultimate principal plastic straining due to the reason that direction of the cracking process is considered as normal to the ultimate principal plastic straining [41, 42, 52, 53]. Crack behavior and failure modes of steel and GFRP BCJ are represented in Figure 9 which was secured from NLFEA modeling in ABAQUS. The crack patterns obtained from the proposed NLFEA model depict a good correlation with test cracks in the joint region. The failure of the specimens was mostly observed at the connection of columns to beam due to the rupture of GFRP bars in GFRP reinforced BCJ and the yeilding/buckling of steel bars in the steel rebars renforced BCJ soecimens. The brottle behavior of GFRP rebars allowed them to rupture after reaching to their ultimate tensile strength. Similar observations were depicted by the proposed NLFEA model in the present study.

4 Practical Implementation of Present Work

The beam-column joint is very important structural part that bears the stress concentrations during any uncertainty in the loading due to the earthquake or any other uncertain conditions. This study proposes a novel nonlinear finite element model that can accurately predict the structural behavior (including load-deflection response and failure behavior) of beam-columns joints reinforced with advanced fiber reinforced polymers. This study will be helpful for the structural engineers in understanding the load-deflection behavior, complex damaging behavior, and failure behavior under the cyclic loading without performing the costly experimentation. Moreover, the good outcomes of the present investigation will be helpful for the practitioners in Pakistan in implementing the corrosion-resistant and lightweight GFRP material in structural elements.

5 Conclusions

The present study aims to evaluate the structural behavior of beam-column joints (BCJ) reinforced with GFRP rebars using non-linear finite element analysis (NLFEA) under the seismic loading. The following conclusions can be drawn from the present work:

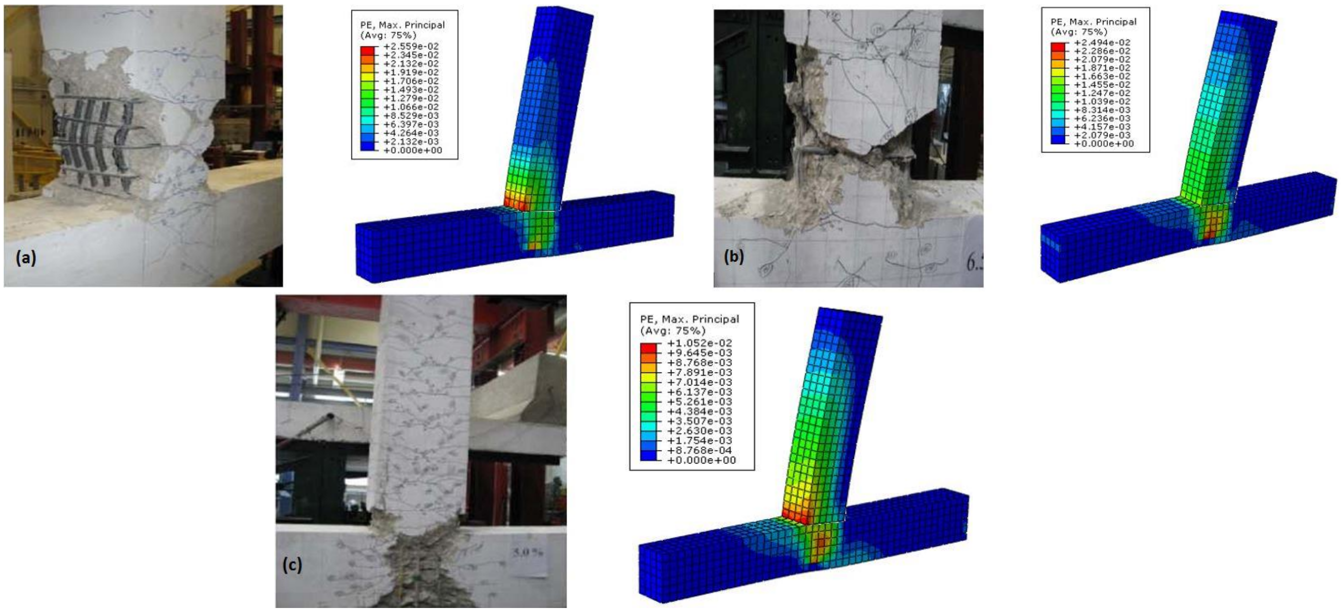

Figure 9. Crack patterns of (a) MSS (b) MGS (c) MGS3

- The results indicated that the FEA utilizing ABAQUS computer program is capable to anticipate the load-deflection curves in BCJ reinforced with steel and GFRP rebars having acceptable accuracy of 87.85%.
- Various material parameters such as mesh, dilation angle ψ, shape factor, and viscosity parameter VP have been considered for the calibration of the behavior of concrete modeling which depicted that the calibration work is very important for the NLFEA simulations to secure the better results compared with the experimentation work. Among the studied parameters, the VP reported a critical influence on concrete modeling utilizing the CPD model. The variation of VPs provides more exact results for the complete load-deflection behavior of BCJ. Mesh size ranging between 40 mm to 140 mm has signifying effect on the load-deflection curves response by affecting the computational time of the computer, the greater value of the mesh size decreased the computational time.
- The varying values of VPs from 0.0015 to 0.015 can significantly affect the computational time and load-deflection curve behavior, a smaller value of the VP increases the computational time of the computer. The change in dilation angle, meshing, and types of steel and concrete elements portrayed the least impact on the load-deflection behavior of BCJ. Finally, it can be said that the proposed numerical model can accurately predict the behavior of GFRP-reinforced BCJ and can be employed for the practical applications.

Acknowledgment

The authors are thankful to the UET Taxila for the provision of the facility of CAD Lab for the finite element simulations. The authors acknowledge Dr. Afaq Ahmad for his kind help and support in performing finite element simulations. The careful review and constructive suggestions by the anonymous reviewers are gratefully acknowledged

References

[1] M, Mady, A. El-Ragaby, and E. El-Salakawy, "Seismic behavior of beam-column joints reinforced with GFRP bars and stirrups." *Journal of Composites for Construction*, 15(6): p. 875-886, 2011.

[2] C.E. Bakis, et al., "Fiber-reinforced polymer composites for construction—State-of-the-art review. " *Journal of composites for construction*, 6(2): p. 73-87, 2002.

[3] J. Correia, et al., "Durability of pultruded glass-fiber-reinforced polyester profiles for structural applications." *Mechanics of Composite Materials*, 42(4): p. 325-338, 2006.

[4] Y. Bai, et al., "Experimental investigations on temperature-dependent thermo-physical and mechanical properties of pultruded GFRP composites." *Thermochimica Acta*, 469(1-2): p. 28-35, 2008.

[5] A. El Refai, F. Abed, and A. Al-Rahmani, "Structural performance and serviceability of concrete beams reinforced with hybrid (GFRP and steel) bars." *Construction and Building Materials*, 96: p. 518-529, 2015.
[6] M. Robert, and B. Benmokrane, "Behavior of GFRP reinforcing bars subjected to extreme temperatures." *Journal of Composites for Construction*, 14(4): p. 353-360, 2009.
[7] M. Harajli, and M. Abouniaj, "Bond performance of GFRP bars in tension: Experimental evaluation and assessment of ACI 440 guidelines." *Journal of Composites for Construction*, 14(6): p. 659-668, 2010.
[8] B. Roy, and A.I. Laskar. "Cyclic performance of beam-column subassemblies with construction joint in column retrofitted with GFRP." in *Structures*. Elsevier, 2018.
[9] S.K. Ghomi, and E. El-Salakawy, "Effect of joint shear stress on seismic behaviour of interior GFRP-RC beam-column joints." *Engineering Structures*, 191: p. 583-597, 2019.
[10] H. Huang, et al., "Seismic behavior of a replaceable artificial controllable plastic hinge for precast concrete beam-column joint." *Engineering Structures*, 245: p. 112848, 2021.
[11] J.H. Kim, et al. "Experimental study on lateral behavior of post-tensioned precast beam-column joints." *in Structures.* Elsevier, 2021.
[12] K. Sakthimurugan, and K. Baskar, "Experimental investigation on rcc external beam-column joints retrofitted with basalt textile fabric under static loading." *Composite Structures*, 268: p. 114001, 2021.
[13] H. Wang, et al., "Cyclic behavior and hysteresis model of beam-column joint under salt spray corrosion environment." *Journal of Constructional Steel Research*, 183: p. 106737, 2021.
[14] J.G. Ruiz-Pinilla, et al., "RC columns strengthened by steel caging: Cyclic loading tests on beam-column joints with non-ductile details." *Construction and Building Materials*, 301: p. 124105, 2021.
[15] P. Sachdeva, A.D. Roy, and N. Kwatra. "Behaviour of steel fibers reinforced exterior beam-column joint using headed bars under reverse cyclic loading." in *Structures*. Elsevier, 2021.
[16] A.B. Ugale, and S.N. Khante. Hysteretic performance of reinforced concrete external beam-column joint subassemblies using non-conventional diagonal bars. in *Structures*. Elsevier, 2021.
[17] A.S. Borujerdi, D. Mostofinejad, and H.-J. Hwang, "Cyclic loading test for shear-deficient reinforced concrete exterior beam-column joints with high-strength bars." *Engineering Structures*, 237: p. 112140, 2021.
[18] S. Chen, K. Chen, and K.H. Tan, "Effect of profiled decking on composite beam-column joints with end-plate bolted connections under column-removal scenario." *Journal of Constructional Steel Research*, 182: p. 106668, 2021.
[19] Z. Chen, et al., "Seismic study on an innovative fully-bolted beam-column joint in prefabricated modular steel buildings." *Engineering Structures*, 234: p. 111875, 2021.
[20] R.Z. Al-Rousan, and A. Alkhawaldeh, "Behavior of Heated Damaged Reinforced Concrete Beam-Column Joints Strengthened with FRP." *Case Studies in Construction Materials,* p. e00584, 2021.
[21] X. Gao, and C. Lin, "Prediction model of the failure mode of beam-column joints using machine learning methods." *Engineering Failure Analysis*, 120: p. 105072, 2021.
[22] C.-K. Chiu, D.P. Lays, and W.A. Krasna, "Anchorage strength development of headed bars in HSRC external beam-column joints considering side-face blowout failure under monotonic loading." *Engineering Structures*, 239: p. 112218, 2021.
[23] S. Majumder, and S. Saha. "Quasi-static cyclic performance of RC exterior beam-column joint assemblages strengthened with geosynthetic materials." in *Structures*. Elsevier, 2021.
[24] L. Eddy, et al., "Analytical investigation of the role of reinforcement in perpendicular beams of beam-column knee joints by 3D meso-scale model." *Engineering Structures*, 210: p. 110347, 2020.
[25] J. Bian, et al. "Cyclic loading tests of thin-walled square steel tube beam-column joint with different joint details." in *Structures*. Elsevier, 2020.
[26] M.N. Hadi, H. Karim, and M.N. Sheikh, "Experimental investigations on circular concrete columns reinforced with GFRP bars and helices under different loading conditions." *Journal of Composites for Construction*, 20(4): p. 04016009, 2016.
[27] B. Benmokrane, O. Chaallal, and R. Masmoudi, "Glass fibre reinforced plastic (GFRP) rebars for concrete structures." *Construction and Building Materials*, 9(6): p. 353-364, 1995.
[28] A. Nour, et al., "Finite element modeling of concrete structures reinforced with internal and external fibre-reinforced polymers." *Canadian Journal of Civil Engineering*, 34(3): p. 340-354, 2007.
[29] T. Nguyen, T. Chan, and J. Mottram, "Influence of boundary conditions and geometric imperfections on lateral–torsional buckling resistance of a pultruded FRP I-beam by FEA." *Composite Structures*, 100: p. 233-242, 2013.
[30] J. Yang, T. Guo, and S. Chai. "Experimental and numerical investigation on seismic behaviours of beam-column joints of precast prestressed concrete frame under given corrosion levels." in *Structures*. Elsevier, 2020.
[31] A.M. Amiri, et al., "The effect of fly ash on flexural capacity concrete beams." *Advances in Science and Technology Research Journal*, 10(30), 2016.
[32] M. Najafgholipour, et al., "Finite element analysis of reinforced concrete beam-column connections with governing joint shear failure mode." *Latin American Journal of Solids and Structures*, 14(7): p. 1200-1225, 2017.
[33] M. Elflah, Theofanous, M., Dirar, S, Yuan, H., "Behaviour of stainless steel beam-to-column joints—Part 1: Experimental investigation." *Journal of Constructional Steel Research*, 152: p. 183-193, 2019.

[34] A. Niroomandi, M. Najafgholipour, and H.R. Ronagh, "Numerical investigation of the affecting parameters on the shear failure of Nonductile RC exterior joints." *Engineering Failure Analysis*, 46: p. 62-75, 2014.
[35] I.C. Muresan, and R. Balc. "Finite element analysis of an extended end-plate connection using the T-stub approach." in *AIP Conference Proceedings*. AIP Publishing, 2015.
[36. D.S. Simulia, Abaqus 6.12 documentation. Providence, Rhode Island, US, 2012. 261.
[37] M.Z. Afifi, Mohamed, H.M., Benmokrane, B., "Theoretical stress–strain model for circular concrete columns confined by GFRP spirals and hoops." *Engineering Structures*, 102: p. 202-213, 2015.
[38] A. Raza, Shah, SAR., Khan, AR., Aslam, MA., Khan, TA., Arshad, K., Hussan, S., Sultan, A., Shahzadi, G., Waseem, M., "Sustainable FRP-Confined Symmetric Concrete Structures: An Application Experimental and Numerical Validation Process for Reference Data." *Applied Sciences*, 10(1): p. 333, 2020.
[39] J. Wang, Chen, Y., ABAQUS application in civil engineering. 2006, Zhejiang University Press, China.
[40] Z. Huang, Liew, JYR., "Nonlinear finite element modelling and parametric study of curved steel-concrete-steel double skin composite panels infilled with ultra-lightweight cement composite." *Construction and Building Materials*, 95: p. 922-38, 2015.
[41] A. Raza, and Khan, QUZ, A. Ahmad, "Numerical Investigation of Load-Carrying Capacity of GFRP-Reinforced Rectangular Concrete Members Using CDP Model in ABAQUS." *Advances in Civil Engineering*, 2019, 2019.
[42] A.S. Genikomsou, and M.A. Polak, "Finite element analysis of punching shear of concrete slabs using damaged plasticity model in ABAQUS." *Engineering Structures*, 98: p. 38-48, 2015.
[43] J.Y. Wu, J. Li, and R. Faria, "An energy release rate-based plastic-damage model for concrete." *International journal of Solids and Structures*, 43(3-4): p. 583-612, 2006.
[44] G.Z. Voyiadjis, and Z.N. Taqieddin, "Elastic plastic and damage model for concrete materials: Part I-theoretical formulation." *The International Journal of Structural Changes in Solids*, 1(1): p. 31-59, 2009.
[45] R. Malm, "Predicting shear type crack initiation and growth in concrete with non-linear finite element method." KTH, 2009.
[46] D.S. Systèmes, Abaqus 6.10: Analysis user's manual. Providence, RI: Dassault Systèmes Simulia Corp, 2010.
[47] A. Raza, et al., "Structural performance of FRP-RC compression members wrapped with FRP composites." *Structures*, 27: p. 1693-1709, 2020.
[48] A. Raza, and Khan, QUZ, A. Ahmad, "Reliability analysis of proposed capacity equation for predicting the behavior of steel-tube concrete columns confined with CFRP sheets." *Computers and Concrete*, 25(5): p. 383-400, 2020.
[49] A. Raza, Shah, SAR., Alhazmi, H., Abrar, M., Razzaq, S. Strength Profile Pattern of FRP-Reinforced Concrete Structures: A Performance Analysis through Finite Element Analysis and Empirical Modeling Technique. *Polymers*, 13(8): 1265, 2021.
[50] A. Raza, et al., "Concentrically loaded recycled aggregate geopolymer concrete columns reinforced with GFRP bars and spirals." *Composite Structures*, 268: p. 113968, 2021.
[51] A. Raza, and U. Rafique, "Efficiency of GFRP bars and hoops in recycled aggregate concrete columns: Experimental and numerical study." *Composite Structures*. 255: p. 112986, 2020.
[52] A. Raza, et al., "Finite element modelling and theoretical predictions of FRP-reinforced concrete columns confined with various FRP-tubes." *Structures*,. 26: p. 626-638, 2020.
[53] L. Ali, et al., "Numerical Simulations of GFRP-Reinforced Columns Having Polypropylene and Polyvinyl Alcohol Fibers." *Complexity*, 2020, 2020.

3rd Conference on Sustainability in Civil Engineering (CSCE'21)
Department of Civil Engineering
Capital University of Science and Technology, Islamabad Pakistan

EXPERIMENTAL TESTING, FE MODELLING AND ANALYSIS OF GEOPOLYMER CONCRETE COLUMNS WITH STEEL REINFORCEMENT

[a]Adal Imtiaz*, [b]Faheem Butt, [c]Rana Muhammad Waqas

a, b, c: Department of Civil Engineering,
University of Engineering and Technology, Taxila,
a*: rajaadall@gmail.com
b: faheem.butt@uettaxila.edu.pk
c: rana.waqas@uettaxila.edu.pk

Abstract- This paper focuses on experimental testing and Finite Element (FE) modelling of steel reinforced Ordinary Portland Cement-OPC and Geopolymer Concrete-GPC columns. GPC was prepared by combining Fly Ash-FA, furnace slag-SG and adding steel fibres SF with volume fraction of 0.75%. Twelve 200x200mm columns having length of 1000mm with concrete cylinder compressive strength (fc') of 40 MPa were casted and tested for static loading on 5000KN Universal Testing Machine (UTM). Experimental results were validated through FE modelling on commercial software ABAQUS. Concrete Damaged Plasticity (CDP) model was used to define behaviour of concrete. It was found that axial load-deflection response closely matched with the laboratory results for columns loaded with zero eccentricity while load capacities for columns loaded with different eccentricity were over predicted in FE Model. It has been observed that load bearing capacity of GPC columns is lower than corresponding OPC columns but can be improved by addition of steel fibre. A constitutive model derived for high strength concrete has shown close agreement with experimental results [1] [2] [3].

Keywords- FE modelling, geopolymer concrete, quarry rock dust, steel fibres.

1 Introduction

Development of geopolymer concrete (GPC) has been increased due to growing demand of its being environmental friendly and alternative to OPC with better durability and curtails emission of carbon dioxide (CO2) during the production of cement used in OPC. GPC is a well-known cementitious material based on alumina-silicate and the main constituents are mainly industrial waste residuals such as fly ash (FA) and ground granulated blast-furnace slag (SG). Using by-products of industries as partially replacing cement is encouraged to enhance the physical, chemical and mechanical properties of concrete. Dense gel structure of geopolymer concrete makes it more durable than the OPC concrete [4]. Various Investigations have endorsed the use of slag (SG) to achieve encouraging outcomes at ambient curing conditions [5]. Fibres are generally included in concrete to control cracking due to plastic and drying shrinkages and decrease the permeability of concrete by decreasing bleeding water. Mechanical properties especially splitting tensile and flexural strength are also improved by addition of Steel fibre (SF) [6]. Adding SFs at 0.25, 0.5 and 0.75% of concrete (by volume) improves the ductility and load bearing capacity of GPC specimens [7]. Under different loading conditions, fibre reinforced GPC column specimen exhibit higher peak axial load and bending moment than those without steel fibres [8].

In order to validate experimental findings, behaviour of reinforced concrete columns was simulated through finite element analysis (FEA). It is commonly accepted that concrete damaged plasticity model has proved to be appropriate in modelling the reinforced concrete structures. Using Concrete damage plasticity (CDP) model in ABAQUS for FEA for prediction of the response of reinforced GPC and OPC concrete columns presented decent match between experimental curves and predicted load–displacement responses [9]. ABAQUS has been found to be an accurate tool for conducting FEA. This study focuses on experimental and numerical analysis to investigate steel reinforced OPC concrete and GPC columns prepared by low calcium fly ash and Slag (SG) with and without addition of 0.75% SF (by volume of composites). Total three types of reinforced concrete columns (Table 1) were prepared with different composition with four samples of each type tested for eccentricity 0, 15, 35 and 50 mm. Thus total of twelve samples of columns were prepared for experimental investigation through static load testing and FE modelling through ABAQUS for validation of experimental results.

2 Experimental Procedures

In order to cast steel reinforced columns made with OPC and Geopolymer concrete, the ingredients i.e. coarse aggregate, fine aggregates and binders (FA, SG) were mixed as per ratios given in Table 1.

Table 1- Mix proportion of OPC and GPC mixtures

Group ID	Specimen ID	Mix proportions (%)				Mix quantities (kg/m^3)								
		SF	**OPC**	**FA**	**SG**	**Sand**	**OPC**	**CA**	**SG**	**FA**	**Na_2SiO_3**	**NaOH**	**SP**	**Water**
OPC	CC-0F	0	100%	-	-	640	370	1201	-	-	107	53	4	170
GPC	GC-0F	0	-	50%	50%	643	-	1206	200	200	107	53	8	-
	GC-0.75F	0.75%	-	50%	50%	647	-	1214	200	200	107	53	12	-

Note: SF(Steel Fibres); OPC(Ordinary Portland Cement); FA (Fly ash); SG (Blast Furnace Slag); CA (Coarse Aggregates); SP (Superplasticizers); GPC (Geopolymer Concrete),

Mix design of all the mixes was prepared for 28-day compressive strength (fc') of 40 MPa. Four specimens of steel reinforced columns (200mm x 200mm x 1000mm) were casted for every type of mix. Ambient curing was carried out for columns and UTM of 5000 kN capacity was used for testing under static loading at eccentricity 0, 15, 35 and 50 mm. Load deflection behaviour was obtained for each type of column through experiment for validation by finite element modelling using ABAQUS.

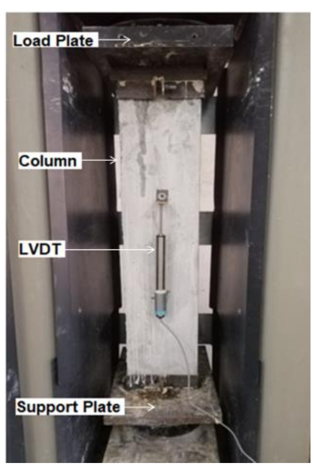

Figure 1: Experimental Setup

2.1 Materials.

To prepare specimen of conventional concrete, Type-II cement OPC conforming to ASTM C-150 [10] was used. GPC mixtures were prepared by using different proportions of binders i.e SG and FA. Fine aggregate's fineness modulus conformed to ASTM-C-136-06 [11] whereas water absorption and specific gravity was conforming to ASTM-C128-15 [12]. The Specific gravity of coarse aggregate (CA) was conforming to ASTM-C127-07 [13]. The commercially available hard-drawn, hooked end wire (steel) fibres (MasterFiber® S 65), conforming to the provisions of ASTM A820 [14], Type 1 were used. Grade 60 deformed steel bars conforming to ASTM A615 [15] were used as column reinforcement.

3 Finite Element Model

3.1 Methodology.

Commercially used software known as ABAQUS was used for numerical simulations of reinforced concrete columns. Concrete material and end steel plates (50mm thick) were modelled as a 3D solid homogeneous section while steel bar and rectangular ties were modelled as 3D deformable wire element with truss section having cross section area of 113.1 and 28.27 mm^2 respectively. In order to define concrete compressive behaviour, CDP model was used. Bottom of all columns was fixed and top end remained free for axial load application. Displacement controlled loading in form of displacement of 10 mm was applied at eccentricity 0, 15, 35 and 50mm for each type of column. Load deflection curves were obtained for each column and compared with the experimental results. No lateral loads have been studied.

3.2 Geometry of Model, Meshing and Boundary Conditions.

Reinforced concrete columns as per dimensions shown in Figure 2 were modelled in ABAQUS. Parts comprising of concrete column, steel plates and steel reinforcement were then assembled and connected through tied and embedded region constraints respectively. Steel plates were tied through master and slave surface concept i.e. bottom surfaces of top steel plate and column were taken as master surfaces whereas top surfaces of bottom steel plate and column were considered as slaves for equal distribution of applied load. Meshing of columns were carried out with reduced integration (C3D8R), 3D stress linear and quadratic hexahedral elements while steel bars were meshed using standard linear 3D truss elements (T3D2). Accuracy of results was calibrated for mesh size of 25mm. Point load in the form of displacement of 10 mm was applied axially to the column at eccentricity equal to 0, 15, 35 and 50 mm from centre of the column. Detail of geometry and meshed model along with application of constraints for steel-reinforced columns are shown in Figure 2.

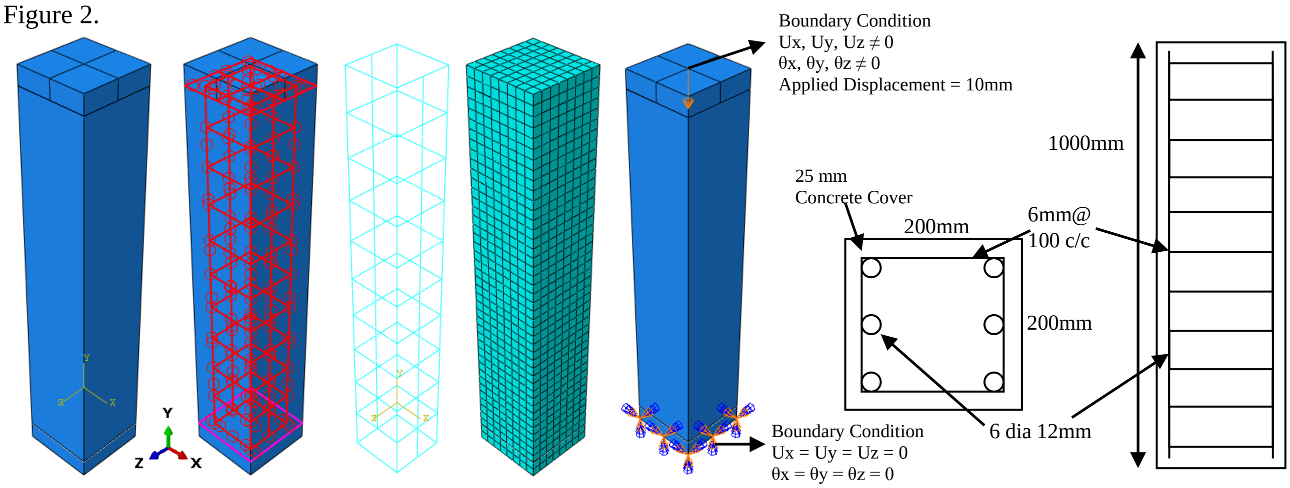

a) b) c) d) e) f) g)

Figure 2: FEA Model of Column, a. Geometry, b. Embedded region constraints, c. Steel mesh, d. Meshing, e. Boundary Conditions f. Column Cross Section and g. Longitudinal Section of Column

3.3 Material Properties.

In order to define the concrete behaviour, CDP model proposed by Liu and Chen [16], as shown in Figure 3 and 4, which describes the relationship between inelastic and plastic strain, and compression stress of concrete. Liu and Chen parameters [16] were used to determine values of damage parameter dc, inelastic strain ε_{in} and plastic strain ε_{pl}. Linear elastic behaviour was assumed in the reversible regime, whereas damage plasticity behaviour in irreversible regime for both GPC and OPC concrete. For modelling of linear elastic behaviour, properties of concretes and steel reinforcement are tabulated in Table 2.

Table 2-Different properties of concrete and steel

Material	Density, ρ (tonne/mm^3)	Poisson ratio, υ	Young's modulus, Ec (MPa)	Max Stress, MPa
OPC	$2.4\text{x}10^{-9}$	0.2	29725	fc'=40
GPC	$2.42\text{x}10^{-9}$	0.23	30150	fc'=40
GPC-SF	$2.42\text{x}10^{-9}$	0.23	34129.1	fcf'=40
Steel Bars	$7.85\text{x}10^{-9}$	0.3	200,000	fy=420
End Plates	$7.85\text{x}10^{-9}$	0.3	200,000	-

For concrete in irreversible regime, concrete damaged plasticity (CDP) model is used to define two failure mechanisms known as crushing due to compression and cracking due to tension. To model plastic behaviour of concrete, recommended values of the dilation angle (ψ)=36°, yield shape surface (Kc=2/3), and eccentricity (e=0.1) were used [17]. The value of stress ratio σ_{b0}/σ_{c0} is taken as 1.12, which is also quantified by Papanikolaou and Kappos [18] through proposed equation $\sigma_{b0}/\sigma_{c0} = 1.5\, f_c'^{-0.075}$ based on a large statistical data. Constitutive model derived for high strength concrete by Collin et al [3] was used to model compressive behaviour of both OPC and GPC concrete as per Table 3.

Table 3-Equations for material properties and constitutive model for GPC and OPC concrete

Material Property	GPC		OPC	
Elastic Modulus, Ec	$Ec_{GPC} = 4907.5\sqrt{fc'}$ [19]	(1)	$Ec_{OPC} = (3320\sqrt{fc'} + 6900)$ [21]	(2)
	For Steel Fibre Reinforced-SFR GPC			
	$Ecf_{GPC} = 21500 \text{ x } (\frac{fc'}{10})^{\frac{1}{3}}$ [20]	(3)		
Peak Strain, ε_{cp}	$\varepsilon_{cp} = 18.97 f_c' + 623.6$ [19]	(4)	$\varepsilon_{cp} = \frac{f_c'}{E_c}\frac{n}{n-1}$ [3]	(5)
	For SFR GPC [22]			
	$\varepsilon_{cpf} = \left[0.00050 + 0.00000072\left(\frac{v_f\, l_f}{d_f}\right)\right](f_{cof})^{0.35}$	(6)		
Tensile Strength	$f_t'=0.7\sqrt{fc'}$ [23]	(7)	$f_t'=0.33\sqrt{fc'}$ [24]	(8)
	$f_t'=0.6\,\eta\,(fc')^{\frac{2}{3}} V_f \frac{l_f}{d_f}$ [22] (For SFR GPC)	(9)		
Cracking Strain	$\varepsilon_{cr} = 0.000065 f_{ct}^{\ 0.54}$ [23]	(10)	$\varepsilon_{cr} = 0.000065 f_{ct}^{\ 0.54}$	(11)

Constitutive Model [1] [2] [3]

$$\sigma_c = f_c' \frac{n\,(\varepsilon_c/\varepsilon_{cp})}{n-1+(\varepsilon_c/\varepsilon_{cp})^{nk}} \quad \text{(MPa)} \tag{12}$$

Where,
fc'= Peak / Maximum stress
ε_{cp} = Strain at peak / maximum stress
$n = 0.8 + (f_c'/17)$
$k = 0.67 + (f_{cm}/62)$ when $\varepsilon_c/\varepsilon_{cp} > 1$
$= 1.0$ when $\varepsilon_c/\varepsilon_{cp} \leq 1$

For Steel Fibre Reinforced Concrete [25]

$$n=\beta= 1.093 + 7.4818\left(3V_f \frac{l_f}{d_f}\right)^{-1.387} \tag{12}$$

V_f=Steel fibre fraction in Volume
l_f , d_f = Length and diameter of fibre, respectively
η = Orientation factor of fibre which is taken as 0.5

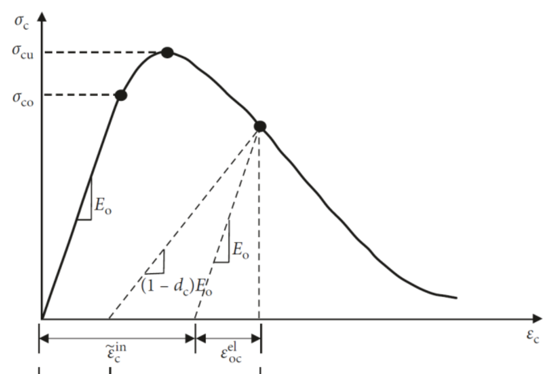

Figure 3: The plain concrete damaged plasticity model

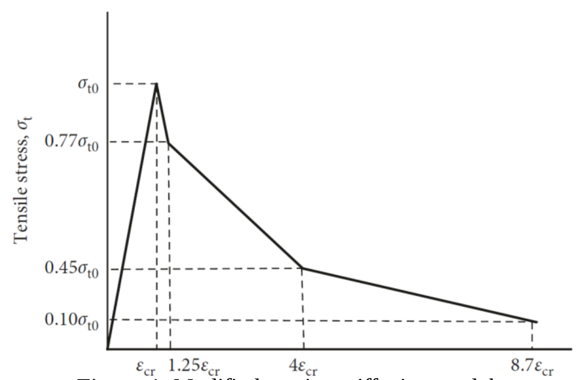

Figure 4: Modified tension stiffening model

4 Results and Discussions

Experimental results depicts that peak load capacity of GPC columns was reduced by 9.4%, 20.8%, 18.2%, 19.4% than corresponding OPC concrete columns for application of load on eccentricity 0, 15, 35 and 50mm, respectively. However, it was improved by 18%, 29.8%, 27.7% and 29.6% with addition of 0.75% of steel fibre fraction by volume in GPC columns. After comparison of results, obtained from experiments and FE modelling through ABAQUS, it has been observed that load deflection curve for concentrically loaded column were in good agreement with experimental curve.

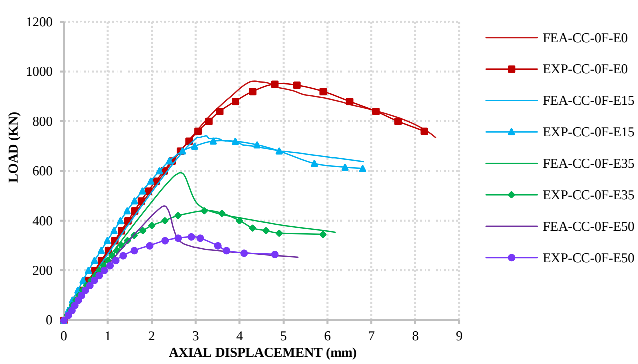

a)

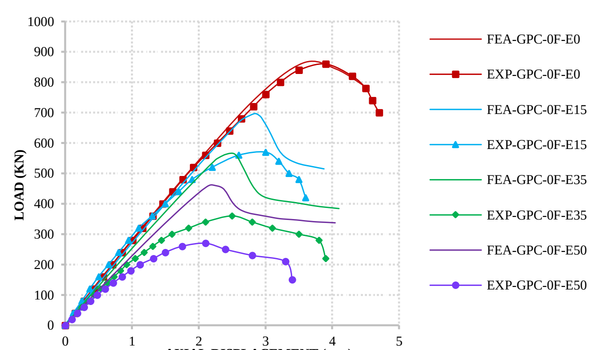

b)

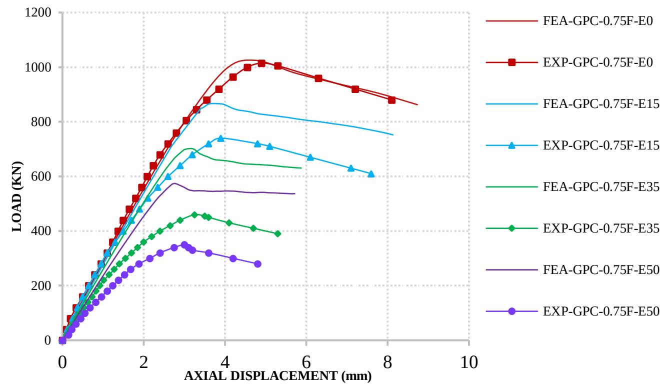

c)

Figure 5: Load vs Displacement Curve for a. OPC Column, b. GPC Column, and c. GPC Column with addition of 0.75% SF

Difference in peak load for the concentrically loaded column was 1.15%, 0.4% and 0.9% for OPC, GPC and GPC with Steel fibres, respectively. Notably, accuracy of 99% has been achieved by the model for accurately predicting concentrically loaded columns. However, load capacities for eccentrically loaded column were over predicted by the FE model and over prediction had a rising trend as the eccentricity of column is increased. Difference in axial deflection for peak load was 9.09%, 8.54% and 3.17% for concentrically loaded columns of OPC, GPC and GPC with 0.75% steel fibres respectively. Overestimation in results for eccentrically loaded columns was due to opening of laps of tie reinforcement resulting in discrepancies. Moreover, even small eccentricity resulting due to error in construction or imperfect geometry of material is of vital importance as it can significantly reduce ultimate axial capacity of columns.

5 Conclusion

Following conclusions can be made from the conducted study:

- FE Model has been found in good correlation with the practical results for concentrically loaded column with an accuracy of 99%. Difference in peak load and axial deformation for all three types of concentrically loaded columns is 1% and 3-9% respectively.
- The eccentrically loaded columns over predicted peak load carrying capacity of column due to opening of lap for rectangular ties used in experimental setup. Therefore, it is recommended to model ties in FE model accordingly for future studies.
- Load carrying capacity and ductility of GPC columns improves by addition of steel fibres in 0.75% volume fraction.
- The model can be used for further parametric studies and improvement for validation of experimental results for concentrically loaded columns.

References

[1] S. Popovics, "A numerical approach to the complete stress-strain curve of concrete," *Cement and Concrete Research,* vol. 3, no. 5, pp. 583-599, 1973.
[2] E. Thorenfeldt, "Mechanical properties of high-strength concrete and applications in design," *Material Science,* 1987.
[3] M. P. Collins, D. Mitchell and J. G. Macgregor, "Structural Design Considerations for High-Strength Concrete," *Concrete International,* vol. 15, no. 5, pp. 27-34, 1993.
[4] A. S. Genikomsou and M. A. Polak, "Finite element analysis of punching shear of concrete slabs using damaged plasticity model in ABAQUS," *Engineering Structures,* vol. 98, pp. 38-48, 2015.
[5] P. Nath and P. K. Sarker, "Effect of GGBFS on setting, workability and early strength properties of fly ash geopolymer concrete cured in ambient condition," *Construction and Building Materials,* vol. 66, pp. 163-171, 2014.
[6] A. Islam, U. J. Alengaram, M. Z. Jumaat, N. B. Ghazali, S. Yusoff and I. I. Bashar, "Influence of steel fibers on the mechanical properties and impact resistance of lightweight geopolymer concrete," *Construction and Building Materials,* vol. 152, pp. 964-977, 2017.
[7] P.SaranyA, P. Nagarajan and A.P.Shashikala, "Behaviour of GGBS-dolomite geopolymer concrete short column under axial

loading," *Journal of Building Engineering,* vol. 30, p. 101232, 2020.

[8] N. A.Farhan, M. N. Sheikh and M. N.S.Hadi, "Behaviour of Ambient Cured Steel Fibre Reinforced Geopolymer Concrete Columns Under Axial and Flexural Loads," *Structures,* vol. 15, pp. 184-195, 2018.

[9] M. Elchalakani, A. Karrech, M. Dong, M. S. M. Ali and B. Yang, "Experiments and Finite Element Analysis of GFRP Reinforced Geopolymer Concrete Rectangular Columns Subjected to Concentric and Eccentric Axial Loading," *Structures,* vol. 17, pp. 273-289, 2018.

[10] ASTM C150-07, "Standard Specification for Portland Cement," *ASTM International,* 2007.

[11] ASTM C136-06, "Standard Test Method for Sieve Analysis of Fine and Coarse Aggregates," *ASTM International,* 2006.

[12] ASTM C128-15, "Standard Test Method for Density, Relative Density (Specific Gravity), and Absorption of Fine Aggregate," *ASTM International,* 2015.

[13] ASTM C127-07, "Standard Test Method for Density, Relative Density (Specific Gravity), and Absorption of Coarse Aggregate," *ASTM International,* 2007.

[14] ASTM A820-11, "Standard Specification for Steel Fibers for Fiber-Reinforced Concrete," *ASTM International,* 2011.

[15] ASTM A615, "Standard Specification for Deformed and Plain Carbon-Steel Bars for Concrete Reinforcement," *ASTM International.*

[16] W. X. M. Liu and Z. Chen, "Parameters calibration and verification of concrete damage plasticity model of Abaqus," *Industrial Construction,* vol. 44, pp. 167-213, 2014.

[17] "Abaqus User Manual".

[18] V. K.Papanikolaou and A. J.Kappos, "Confinement-sensitive plasticity constitutive model for concrete in triaxial compression," *International Journal of Solids and Structures,* vol. 44, no. 21, pp. 7021-7048, 2007.

[19] S. Chitrala, G. J. Jadaprolu and S. Chundupalli, "Study and predicting the stress-strain characteristics of geopolymer concrete under compression," *Case Studies in Construction Materials,* vol. 8, pp. 172-192, 2018.

[20] Comite Euro-International Du Beton;, "CEB-FIP MODEL CODE 1990: DESIGN CODE," 1993.

[21] ACI 363 (1992), "State-of-the-Art Report on High-Strength Concrete (ACI 363R-92)," *ACI Journal Proceedings, 92(Reapproved).*

[22] N. A. Farhan, M. N. Sheikh and M. N. S. Hadi, "Axial Load-Bending Moment (P-M) Interactions of Geopolymer Concrete Columns Reinforced with and without Steel Fiber," *Structural Journal,* vol. 117, no. 1, pp. 133-144, 2020.

[23] D. Hardjito, S. Wallah, D. Sumajouw and B. Rangan, "The stress-strain behaviour of fly ash-based geopolymer concrete," *Development in Mechanics of Structures and Materials,* vol. 35, pp. 831-834, 2004.

[24] EN 1992-1-1 , "Design of concrete structures - Part 1-1 : General rules and rules for buildings," *Eurocode 2,* 2004.

[25] T. T.Tran, T. M.Pham and HongHao, "Experimental and analytical investigation on flexural behaviour of ambient cured geopolymer concrete beams reinforced with steel fibers," *Engineering Structures* , vol. 200, p. 109707, 2019.

3rd Conference on Sustainability in Civil Engineering (CSCE'21)
Department of Civil Engineering
Capital University of Science and Technology, Islamabad Pakistan

DESIGN OPTIMIZATION OF STEEL STRUCTURES THROUGH INTERNAL STRESS DIAGRAMS OF LOW-RISE BUILDINGS

[a] Engr. Asif Nazir*, [b] Engr. Faisal Amin, [c] Engr. Usama Khan

a: Department of Technology (Civil Division), The University of Lahore, Lahore, asifnazir835@gmail.com
b: Department of Civil Engineering, Lahore Leads University, faisal.amin@ucest.edu.pk
c: Department of Technology (Civil Division), The University of Lahore, Lahore, eusamakhan@gmail.com
* Corresponding author: Email ID: asifnazir835@gmail.com

Abstract- Steel has high strength to mass ratio. This is the reason to used steel in construction industries against heavy loading. Generally, Hot rolled section & cold formed sections are used in steel buildings. But, the loading effects through-out the member (Beam/Column) in not same, that is why these sections are not recommended and to attain optimum use of steel the tapered sections are to be used. In this study, a building with 24 m width, 126 m length and 9 m Eave height is selected for study. The loading is applied according to MBMA-2006 and Design is done as per AISI-ASD Design code. In addition to that, 2 different 3D Frames having 7m and 9m of Bay Spacing's are selected for steel building. At these two Bay spacing's, the building is analyzed by STAAD.pro, which is a well-known software for structural analysis. A comparative study is made for Base Reactions, Eave Moments, Horizontal defection, Vertical deflection and Weight of Steel required for the building. The results indicate that the building designed by following the internal stress diagrams gives Less values of Base Reactions, Horizontal deflection and Steel Weight of building as compared to building designed at maximum values of Shear and bending moments, which make it comparatively economical. In addition to that the results shows that while following the internal stress diagrams the segment length of 1.5m to 3.5m gives most economical results.

Keywords- Design Optimization, Steel Structure, Low-Rise Building

1 Introduction

Steel has high strength to mass ratio. This is the reason to used steel in construction industries which require large clear span. There covering material could be GI Sheets, PU panel, brick masonry or concrete walls etc. These walls are non-load bearing yet able to withstand lateral forces caused by seismic activity or wind. The design of steel buildings generally includes the design of structural elements including primary columns and rafters/trusses, secondary purlin, girts, sheeting, diagonal bracing etc. Hot rolled section, welded plate sections, cold formed sections, corrugated sheets, rods, cables are the materials generally used in steel buildings. Steel buildings are classified into conventional steel buildings (CSB) and Pre-engineered buildings (PEB) depending upon the design concept [1] [2].

The paper presented a comparison between pre-engineered building (PEB) and conventional steel building (CSB) design. In this study, 2 different 2D Frames were selected for each pre-engineered building and conventional steel building. By varying the tributary width and wind speed, the frames were analyzed by a software of structural analysis i.e., STAAD pro (V8i).

The design concept of PEB is to use only the required depth of member that is needed at that particular spot depending upon the bending moment. This results in the tapered sections throughout the span of the building. The tapered shape is obtained by the built-up members. Standard hot-rolled sections, cold-formed sections, corrugated sheets, etc. are also used along with the tapered sections, as described in different studies [2, 3]. The use of tapered sections results in reducing the cost of the building by cutting off unnecessary steel. Conventional steel buildings (CSB) consist of a truss system supported by steel columns. The selection of a truss type depends on the span and pitch of the roof. Generally, fink-truss is used for a large pitch, Pratt-truss is used for medium pitch and Howe-truss is used for smaller pitch. Lighting in steel buildings can be provided through skylights or wall lights and for more lighting, a north truss roof can be used [1].

The selection of the truss depends on the following, i.e., roof slope, transportation, fabrication, geometry of the building, climatic conditions. Trusses normally used standard hot rolled section connected together using gusset plates [1, 4].

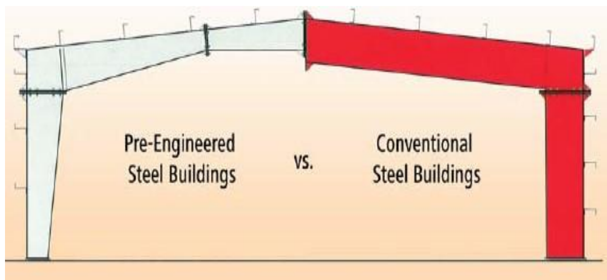

Figure 1: Pre-Engineering Building vs. Conventional Steel Building

The pre-engineered buildings (PEB) have been observed to be the most efficient economical and advantageous system particularly for the single-story system as compared to convention construction systems. Steel is the basic material that offers low cost, flexible in design, ductile and adaptable in different conditions and recyclable. Steel comes in variety of different shapes and colors, which makes it the most versatile and reliable construction material available. This means that we can achieve rapid installation of the structure with minimum energy, thus making a PEB sustainable. Infinitely recyclable, steel is a material that reflects the imperatives of the sustainable development. Steel is more common in the construction of single-story industrial structures rather than in tall buildings because of economy and serviceability problems.

The pre-engineered buildings (PEB) consist of main moment resisting frames connecting laterally secondary frames to the resist lateral forces. Secondary framing consist of purlins girts, eave struts, sag rods, flange braces and diagonal bracing. The purpose of secondary framing is to transfer the exterior loads to the main frame and eventually to the foundations. Bracing are important component of PEB buildings, because they provide lateral stability to the buildings by transferring longitudinal wind pressure to the column bases. The majority of structures that made in steel are generally low rise structured and normally used as cold storage in ware house, steel plant, automobile industries, garages and large thermal power stations. Ordinary steel structures typically require large clear span which are not economically achievable using other constructions techniques [5]. In construction industry, long span and column-free structures are very essential and pre-engineered building have fulfilled these requirements through its diverse design related to pre-fabrication and pre-casting [6]. There are many advantages in using PEBs such as, flexibility of expansion, reduced cost, less construction time, large clear spans, best quality control, less maintenance, energy efficient wall and roof systems, architectural diversity, [7], good strength, corrosive resistance, no residual oils, reduced energy loads etc. [6].

2 Materials & Methods

A building having dimension 25x100x10 m was selected and analyzed for both type of systems i.e. PEB & CSB. In this study, 16 different 2D Frames were selected for each pre-engineered building and conventional steel building. The software used was STAAD pro, which is universally accepted for such uses and purposes of the structural analysis program. Pinned supports were considered for both of the buildings. The Dead, Live, Wind-load were in according with MBMA-2006 (Metal Building Manufacturers Association-2006) and Seismic load were in accordance with UBC-1997 (Uniform

Building Code-1997). AISI-ASD (American Iron & Steel Institute-Allowable Stress Design) and MBMA-2006 (Metal Building Manufacturers Association-2006) protocols were adopted as design code and for load application respectively.

Following load combinations were taken: Dead + Live; Dead + Live + Wind/Seismic and Dead + Wind/Seismic.

Different parameters were selected depending upon the structural configuration of both types of frames. The parameters included were:

- Base reactions
- Moments at eave
- Horizontal displacement at eave
- Vertical displacement at ridge
- Steel take off.

3 Results & Discussions

3.1 Base Reactions

Both the structures are analyzed for different parameters as mentioned above. The first parameter selected is base reactions. For this purpose, pin supports are considered for both the frames. The base reactions after the analysis are plotted on a graph as shown below.

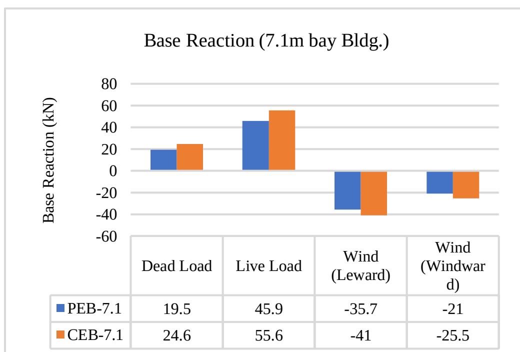

Figure 2: Comparison of Base Reactions at 7.1 Bay Spacing

The value of horizontal components of the reaction is negligible as compared to vertical component, so only the vertical components have been plotted in the graphs.

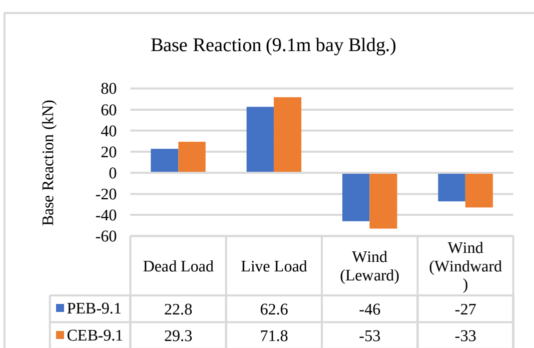

Figure 3: Comparison of Base Reactions at 9.1 Bay Spacing

The above analysis shows that the support reaction in PEB is on average 16 % lesser as compared to CSB system Lesser supports reaction means lighter foundations and hence reduction in the cost of footings.

3.2 Moments at Eave

The shear and bending moments of both the PEB and CSB are summarized in the graph as shown. It has been observed that that the shear and bending forces in PEB are less as compared to CSB that put impact on the weight of material required.

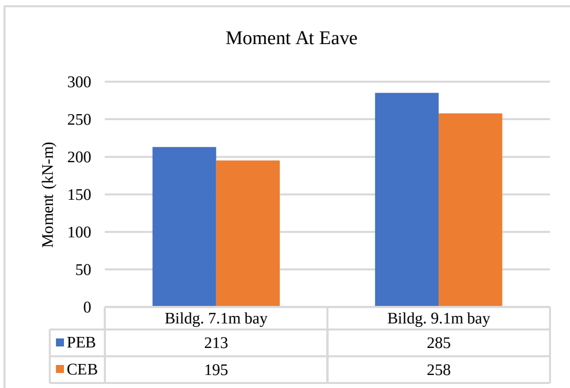

Figure 4: Comparison of Moment at Eave for CSB and PEB Frame

By comparing above graphs, the trend of difference in bending moment's values at eave is significant. On average the bending moments values in PEB are 24 % greater compared to CSB. The steel in PEB is provided in tapering based on the bending moments along the sections that make PEB economical.

3.3 Horizontal Displacement at Eave

The horizontal displacements at eave have also been studied and plotted in a graphical form as shown in the graph below.

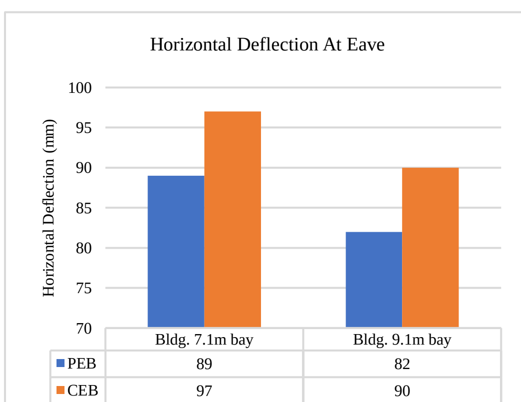

Figure 5: Comparison of Horizontal Deflection at Eave for CSB and PEB Frame

It has been observed that horizontal deflection at eave in PEB is less than by CSB by 20 %. Significant difference in horizontal deflection makes the PEB frame more serviceable and safer with respect to design point of view.

3.4 Vertical Displacement at Ridge

The vertical displacements at eave have also been studied and plotted in a graphical form as shown in the graph below. Vertical deflection is the important parameter to study. Below graphs shows that defection at ridge in PEB is more as compared to CSB frames. In CSB the truss member is closely connected that make it more stable against vertical deflection at ridge. Deflection at mid span in both frames is low in as compared to ridge.

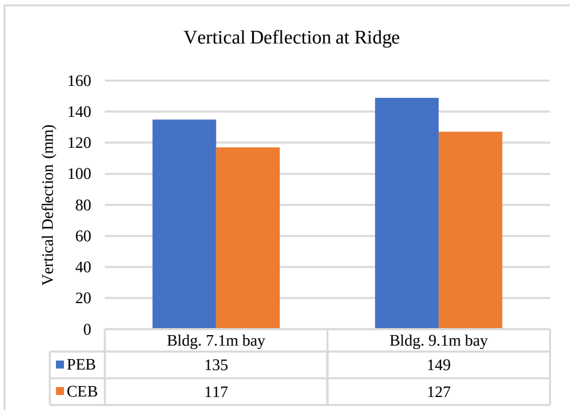

Figure 6: Comparison of Vertical Deflection for CSB and PEB Frame

Above graph shows that deflection trend is different at different loading. At wind speed 130 KPH the deflection in CSB 9 % less as compared to PEB. The deflection results show that PEB frame is lighter in weight as compared to CSB.

3.5 Steel Take off

The graph below shows the steel consumption of PEB frame and CSB frame. The amount of steel consumed by PEB is less as compared to CSB. This is because of the better design methodology of PEB in which the steel is provided depending upon the bending moments that are coming in the frame. This not only saves weight but also reduces the support reactions which in turn results in the lower foundation costs. However, in CSB this cannot be achieved as justified by the results below.

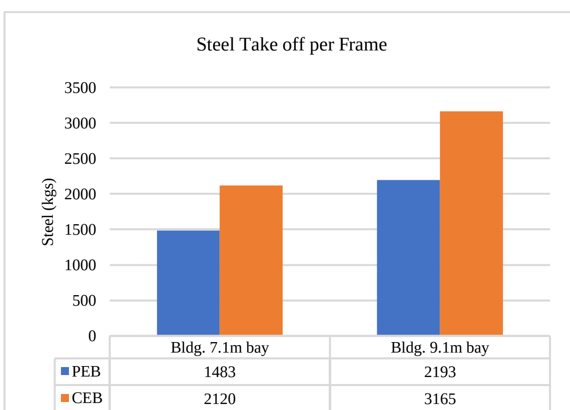

Figure 7: Comparison of Steel Take Off for CSB and PEB Frames

By changing load width, it is observed that the % age difference in weight reduction of PEB with respect to CSB almost remain same. At 7.1 m bay spacing the %age weight decrease is 30% and at 9.1 m bay spacing the PEB weight saving is almost 31 %. On average PEB saving is 30.5 % same as by varying wind speed.

3.6 Steel Take-off after making Segments

The graph below shows the steel consumption of PEB frame after making segments of a member. The graph shows that lesser the length of segment less will be the steel take-Off. The cost comparison is done by the assuming the fabricated steel rate at Rs. 200/kg.

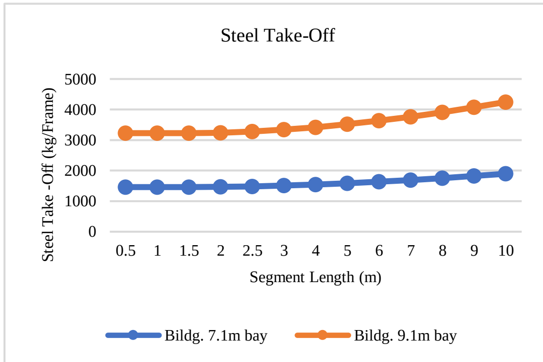

Figure 8: Steel Take-Off at different Segment Lengths

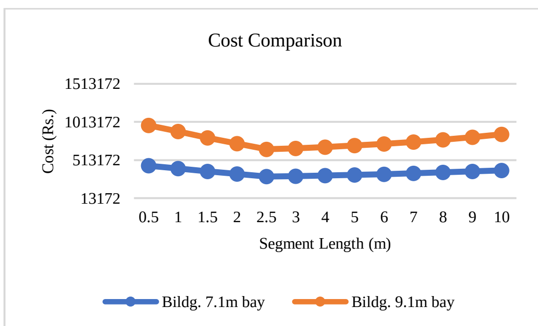

Figure 9: Cost Comparison at different Segment Lengths

The above Graphs shows that by decreasing the segment length the cost of structure decreases up to a certain limit. But after that cost increases rapidly. This is because of welding and erection charges.

4 Conclusions & Recommendations

On the basis of previous chapter, we can now easily conclude that Pre-Engineered buildings have numerous advantages over convention steel buildings.

In PEB system uses bending moments in order to calculate the depth of members this not only optimized the building but also reduced the base reactions. Decrease in base reactions results in reduction of footing sizes. This we cannot achieve in CSB. On an average base reaction of PEB are more than 16% lighter than CSB. The results have shown that the bending moments at Eave level in case of PEB is about 24% more than CSB. Because the connection at Eave is fully moment connection in case of PEB while in CSB the connection is pinned. Horizontal defection in PEB is lesser as compared to CSB. This means that PEB frame is more stable as compared to CSB frame. Thus, PEB is more serviceable. Vertical deflection in CSB is less simply because the members are braced together at regular interval while in PEB this is not the case. Future expansion in PEB is easier and faster as compared to CSB where it is more tedious and time taking. Earth quake resistance of PEB is better than CSB. This is because of its lighter weight. Erection of pre-engineered building is faster and efficient because it follows the same procedure in every project. In CSB the erection procedure is different for different projects thus making erection process tedious. ASD method is more economical as compared to LRFD method when Live load to Dead load ratios is significantly high in PEB. Steel take off for PEB is more than 30.5% lesser as compared to CSB. The percentage increases with the increase in loading. Furthermore, the cost of PEB is much lesser as compared to conventional steel buildings based on the above analysis.

References

[1] C. M. Meera, "Pre-Engineered Building Design of an industrial warehouse," IJESET, vol. 5, no. 2, pp. 75-83, June 2013.
[2] D. N. Subramanian, "Pre-engineered Buildings Selection of Framing System, Roofing and Wall Materials," The Master Builder, pp. 48-6, 2008.
[3] D. I. Assakkaf, Introduction to structural steel design, Department of Civil and Environmental engineering, University of Maryland, college park, 2002.
[4] L. M. Subashini and S. Valentina, "Comparative study of pre-engineered and conventional industrial building," Indian J. Sci. Technol, vol. 8, no. 32, pp. 14499-14502, 2015.
[5] D. P. Zoad, "Evaluation of Pre-Engineering Structure Design by IS-800 as against Pre-Engineering Structure Design by AISC," International Journal of Engineering Research & Technology (IJERT), vol. 1, no. 5, pp. 01-09, 2012.
[6] D. N. Subramanian, "Pre-engineered Buildings Selection of Framing System, Roofing and Wall Materials," The Master Builder, pp. 48-2, 2008.
[7] B. M. Lakshmi, M. k. M. v. Ratnam and M. k. S. S. Krishna Chaitanya, "Comparative Study of Pre-Engineered and Conventional Steel Building," IJIRT, vol. 2, no. 3, pp. 2349-6002, 2015.
[8] S. Firoz, S. C. Kumar and S. K. Rao, "Design concept of Pre-Engineered building," IJERA, vol. 2, no. 2, pp. 267-272, 2012.
[9] V. Srinivasan and T. Saravanan, "Reformation and market design of power sector," Middle - East Journal of Scientific Research, vol. 16, no. 12, pp. 1763-7, 2013.
[10] P. V. Raut and N. S. Agrawal, "Comparative Study of Pre-Engineering Building with Conventional Steel Building," IJRESTS, vol. 1, no. 8, pp. 302-309, 2015.
[11] S. A. Shah, and M. B. Kumthekar, "An over view of Pre-Engineering building system in India," in Proceedings of 27th IRF International Conference, Pune, India, 2015.
[12] A. A. Zende, A. V. Kulkarni and A. Hutagi, "Comparative Study of Analysis and Design of Pre-Engineered-Buildings and Conventional Frames," IOSR Journal of Mechanical and Civil Engineering, vol. 5, pp. 2278-1684, 2013.
[13] J. D. Thakar and P. P. Patel, "Comparative study of Pre-Engineered Steel Structure by varying width of Structure," International journal of advanced engineering technology, vol. 4, no. 3, 2013.
[14] G. S. Kiran, A. K. Rao and R. P. Kumar, "Comparison of Design Procedures for Pre-Engineering Buildings (PEB): A Case Study," International Journal of Civil, Architectural, Structural &Construction Engineering, vol. 8, no. 4, pp. 483-487, 2014.
[15] S. D. Charkha and L. S. Sanklecha, "Economizing Steel Building using Pre-engineered Steel Sections," International Journal of Research in Civil Engineering, Architecture & Design, vol. 2, no. 2, pp. 01-10, 2014.

3rd Conference on Sustainability in Civil Engineering (CSCE'21)
Department of Civil Engineering
Capital University of Science and Technology, Islamabad Pakistan

PREDICTING THE COMPRESSIVE STRENGTH OF FLY ASH BASED GEOPOLYMERS BY ANFIS MODELS

[a] Zainab Tariq, Khuram Rashid [b]*

a, b: Department of Architectural Engineering and Design, University of Engineering and Technology, Lahore, Pakistan
a: zainab.uet@gmail.com b: khuram_ae@uet.edu.pk

Abstract- Fly ash-based geopolymers are widely used material as precast and cast in situ round the world. But several factors influence its mechanical strength. Therefore, this work was designed to incorporate such factors in the prediction of mechanical strength through Artificial intelligence. In this work, four parameters were incorporated such as: (i) curing temperature (20, 60 and, 100 ºC), (ii) molarity of NAOH solution (8-16), (iii) alkali particle to precursor ratio (0.3–0.5) and (iv) Sodium silica to sodium hydroxide ratio (2–3). Adaptive neuro fuzzy inference system (ANFIS) was used for optimization in order to predict the corresponding compressive strength as output of geopolymer. A large database was used for purpose of training and after worth testing the model as required by ANFIS model. Analytical results by ANFIS were used to construct relationship between mechanical property as output e.g. compressive strength of geopolymers and different constituent parameters. It was observed that training and testing errors were in acceptable range (about 9%). Developed ANFIS model was used to prepare geopolymers which contains low calcium and it is FA based sustainable material, with compressive strength ranging from 25–35 MPa. Hence, validating the significance of the artificial-intelligence based modeling approach ANFIS to bring forth a novel application for design of low calcium, FA based-geopolymers.

Keywords- Hybrid Model, Adaptive Neuro Fuzzy Inference System (ANFIS), Influencing parameters, Fly Ash-based geopolymers, Optimization.

1 Introduction

Implementation of artificial intelligence (AI) based machine learning techniques have been demonstrated to be extremely useful for an ample scope of legitimate non-linear complications as shown from recently conducted relevant researches [1]. Various approaches based on Artificial intelligence have been implemented to check and integrate behavior of different parameters involved in non-linear pattern of mechanical properties. Different approaches are used for this purpose, for example artificial neural network based modelling which performs similar to the neurons of human brain, fuzzy systems, combination of neural network and fuzzy system named as neuro fuzzy system based modeling technique (NFS) and genetic fuzzy systems appeared to be vastly used in construction domain and management applications including simulation of constituent parameters attribute and modulation of nonlinear problems [2]. These modeling techniques have been used to simulate the non-linear and complicated behavior of sustainable materials e.g. to determining the Concrete mix proportions, estimation of compressive strength and other participating parameters for different sustainable construction materials [3]. In this paper AI based method e.g. Adaptive Neuro fuzzy inference system (ANFIS) is utilized to analyze the effect related to different elements involved in characterizes development for example part of alkali to precursor ratio (A/P), ratio of sodium silica to solution of sodium hydroxide (SS/SH), curing temperature for curing the sample under consideration represented as (T) and molarity (M) on compressive strength (Fc') as outtput. In order to counter problems related to non-linear functionality and complexity of various materials Jang presented model based on combination of neural network and fuzzified systems that is neuro fuzzy inference system [11]. Jang used this system for simulation of hugely nonlinear and comparatively complicated functions. An ANFIS is a hybrid model of ANN and Fuzzy system, this advanced fuzzy inference system (FIS) combines the knowledge reasoning and interpretation of FIS and ANN's ability of learning to direct information from inputs into an output [3]. The most salient aspect of ANFIS is its ability to educated itself, learn from previous knowledge or experimentation and extraction or depiction of knowledge from previously performed experiments or examples [4]. Which makes it most powerful tool to deal with inadequate data. NFS consists of combinations of models which bring together the self-learning aspect of ANN and knowledge presenting feature of fuzzy systems. NFS can be divided into two types e.g. type-1 NFS & type-2 NFS, depending upon fuzzy methods used. Mamdani and sugeno are two main categories in type-I and type- II which are based on fuzzy system whereas, type-II can further broke down into two sets as general based type-2 and interval type-2 based on fuzzy systems. In Mamdani type fuzzy system each of the two, the precedent and consequent of rules are composed of fuzzy sets [5]. Sugeno type systems however, uses the precedent sets as fuzzified values while the upcoming successive parameters are always work as functions of inputs parameters that can either be zero value or any other prime order depending upon the nature of upcoming parameter. Sugeno type fuzzy frameworks are more exact and computationally productive that is the reason generally NFS are carried out utilizing sugeno type fuzzy framework [1].

The absolute salient attribute of ANFIS is its capability to learn it self and to extract relative information from previously available database from various experiments, which makes it the most powerful tool to deal with insufficient or poor data. These features of ANFIS model make it easy to study and analyze procedure to estimate or predict relative output for some certain inputs. Depending upon the behavioral impact of vital parameters on the compressive strength as output consideration for geopolymers, the ANFIS model was utilized for its first, to predict the mechanical property e.g. Compressive strength along with validation by comparison with another model as well as by the experimental data.

2 Research Framework

2.1 Simulation by Adaptive Neuro Fuzzy Inference System

While using ANFIS tool in apps from MATLAB different parameters e.g. A/P, SS/SH, M and T are selected as input. All input data is further distributed in to two different parts. One part for training the system and other for testing outputs. Working methodology of ANFIS model is elaborated in Figure 1.

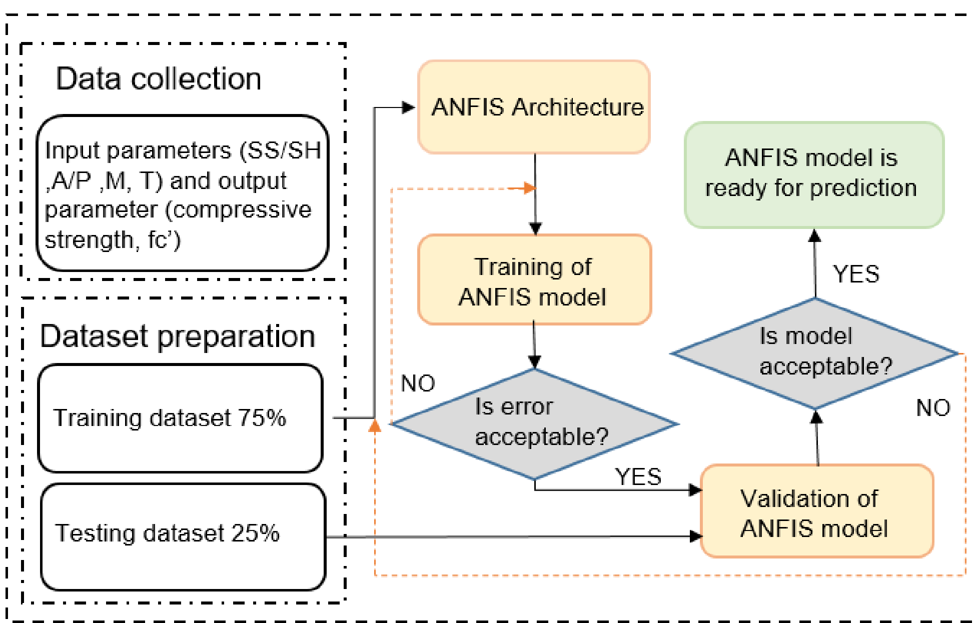

Figure 1 working methodology of ANFIS model

2.2 Mix design database

For the purpose of evaluating the compressive strength and to analyze the behavioral effect of various participating parameters, the database is selected from a study, where a machine learning modelling modeling method e.g. multivariate adaptive regression spline (MARS) model was utilized to access the design mix to prepare geopolymer from mixing different parts for desired compressive strength. For ANFIS model, about 75% part from whole dataset is selected for the training purpose and after completion of training the remaining 25% part is selected for testing the data against previous experiments and ANFIS model (Table 1 of Ref [6]).

2.3 Optimization by ANFIS

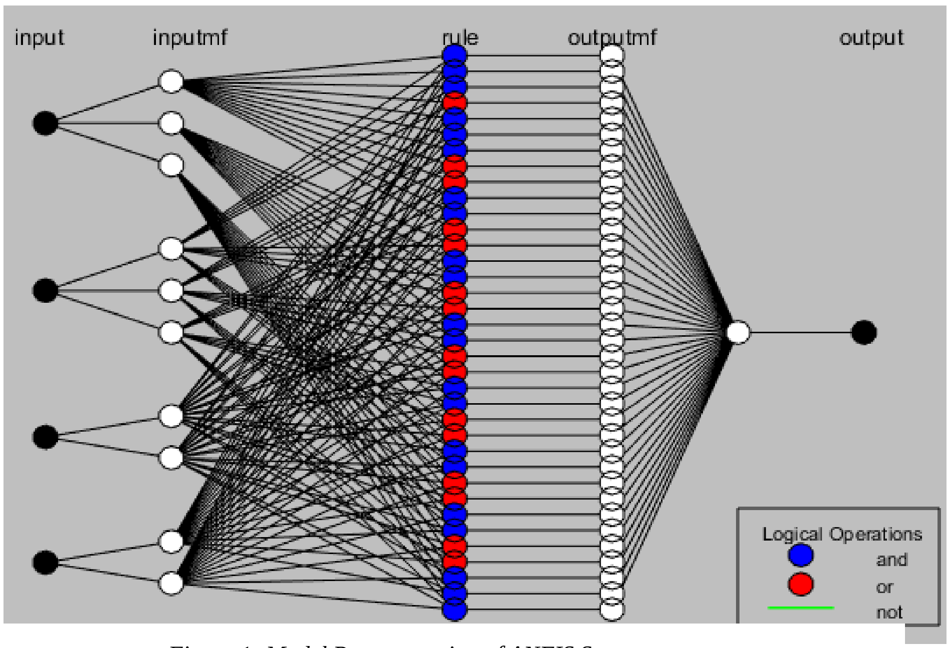

Figure 1: Model Representation of ANFIS Structure

There are five very important adjustments which are made in ANFIS for modeling which are number of input membership functions (MF), type of input and output membership function, method of optimization and number of iterations or total number of epochs. Triangularmf, trapezoidalmf, bell shapedmf, gaussianmf and sigmoidmf are types of MF for input parameters. For output MF we have either constant or linear MF. There are two types of optimization methods e.g. Hybrid and backpropagation[7][3][8]. After studing different researches for this purpose we have utilized triangular type of input MF with three MF for SS/SH & Alk/P and two MF for molarity and temperature each. Output MF was selected as constatnt. Hybrid optimization mehod give less testing and training error where as no. of echos were 500. Figure 2 shows model representation of ANFIS structure.

3 Results

For the purpose of evaluating the performance of developed predictive model, a verity of performance estimation parameters are used which includes coefficient of relation (R), root mean square error (RMSE) and mean absolute error (MAE). These methods are widely used to validate prediction problems in different machine learning models [9][10].

$$R = \frac{\sum_{i=1}^{n}(V_{ai}-\bar{V}_a)(V_{pi}-\bar{V}_p)}{\sqrt{\sum_{i=1}^{n}(V_{ai}-\bar{V}_a)^2}\sqrt{\sum_{i=1}^{n}(V_{pi}-\bar{V}_p)^2}} \quad (1)$$

$$RMSE = \sqrt{\frac{\sum_{i=1}^{n}(V_{ai}-V_{pi})^2}{n}} \quad (2)$$

$$MAE = \frac{\sum_{i=1}^{n}|V_{ai}-V_{pi}|}{n} \quad (3)$$

V_{ai} & V_{pi} are existent and estimated numeric values for compressive strengths, $\bar{V}_a$ & $\bar{V}_p$ are the absolute mean values of existent V_{ai} and estimated V_{pi} values whereas '*n*' is the total number of experiments previously conducted for purpose under consideration. Diminutive values for root mean error and mean absolute error indicates better correlation between compressive strength extracted from database and optimized compressive strength value. Predicted values for training exhibit better correlation with actual compressive strength obtained from experiments then values predicted from model testing. Values calculated for correlation coefficient, root mean square and Mean absolute error are provided in table 1. R^2 should be in range of 0.7 to 1 which shows better fitting of original and optimized compressive strength and yields better software for estimating compressive strength from existing database. Here we have satisfying relation for R^2 as depicted in table 1. Diminutive values for RMSE and MAE leading to little deviation of predicted values from actual values is a function of limited database which is extracted from existing literature.

Table 1 Error values for training and testing using ANFIS model

		Correlation co. (MPa)	Root mean Square (MPa)	Mean absolute error (MPa)
Training Process	ANFIS	0.74	2.806	0.348
Testing Process	ANFIS	0.90	5.533	1.106

A line graph consisting of scatter plot comprising existent and estimated values for compressive strength for training and testing data regimes are presented in Figure 3. Variation in existent and estimated compressive strength is also represented in Figure 4. Straight line shows when actual values are exactly same to predicted values.

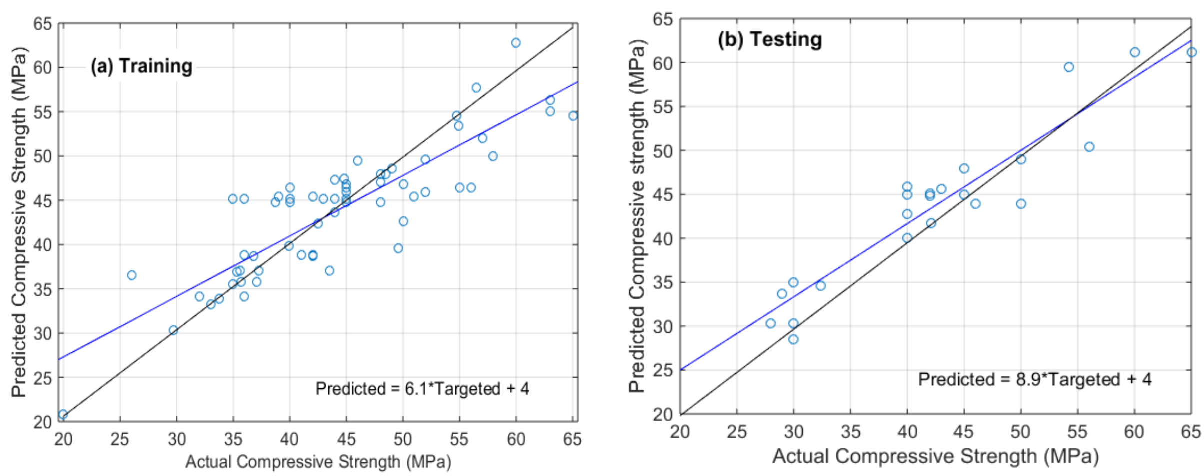

Figure 3 Scatter plot showing variance in predicted compressive strength w.r.t experimentally estimated compressive strength extracted from database for training and testing

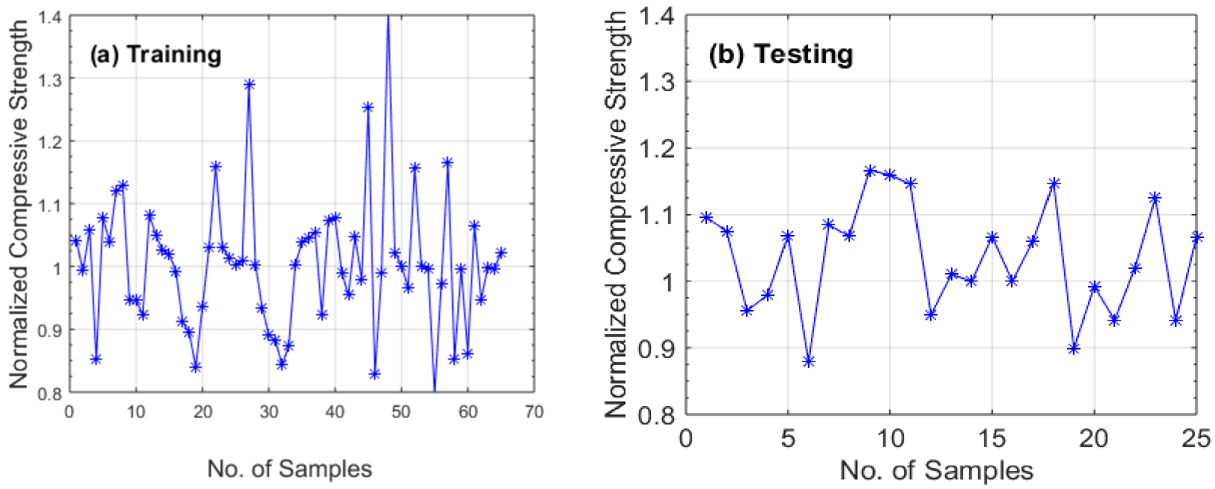

Figure 4 Compressive strength represented graphically as normalized for training and testing data set regimes

2.4 Combined influence of Parameters

Contour plots

Various contour plots extracted from trained and tested ANFIS model are shown in figures which elaborates relation of all four parameters with *fc'*. These plots can be used to find out designing parameters and there values for our required strength of geopolymers.

Effect of alkali/precursor ratio

Figure 5(b, e, & f) shows effect of alkali/ procures ratio and relationship of this ratio with SS/SH, molarity and temperature. Figure 5b shows that for a range of 0.2-1 with increasing ratio compressive strength of *fc'* also increases. Figure 5e show for lower Alk/P ratio combined with higher SS/SH ratio can result in increased compressive strength. Figure presents that for a certain fixed amount of molarity, if value for Alk/P ratio changes then different *fc'* can be obtained.

Effect of sodium silicate/ sodium hydroxide ratio

Figure 5(e) shows a strong relationship between SS/SH and Alk/P. For a range of 1-3 a higher range of compressive strength can be achieved for Alk/P ranging 0.6-0.7. SS/SH is also related to molarity which is shown in figures (h).

Effect of NAOH molarity

Figure 5d, f and g shows that for a specific value of molarity, a large number of various compressive strengths can be achieved by just changing values for Alk/p and SS/SH ratios. It can be seen from above figures that even for high value of compressive strength can be achieved by changing SS/SH and Alk/P even for reduced molarity. Whereas, overall trend (figure f) shows that by increasing molar value compressive strength decreases.

Effect of temperature

There exist a promising impact of temperature on compressive strength of geopolymers. For elevated temperatures initial setting time reduces but strength get increases as shown in figure c and g.

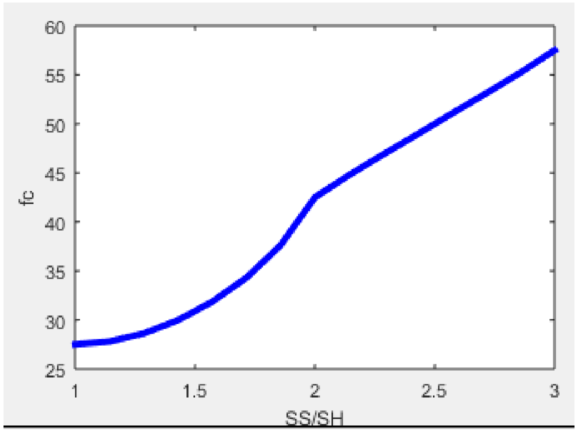
fc
60
55
50
45
40
35
30
25
1
1.5
2
2.5
3
SS/SH

(a)

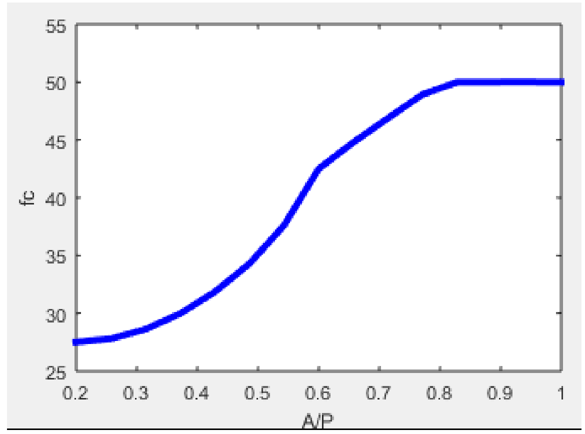
fc
55
50
45
40
35
30
25
0.2
0.3
0.4
0.5
0.6
0.7
0.8
0.9
1
A/P

(b)

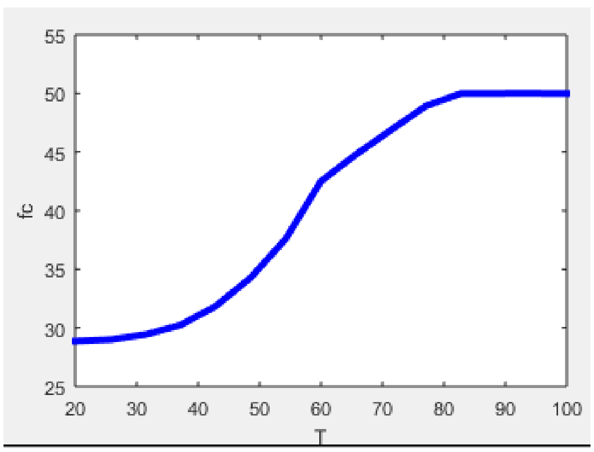
fc
55
50
45
40
35
30
25
20
30
40
50
60
70
80
90
100
T

(c)

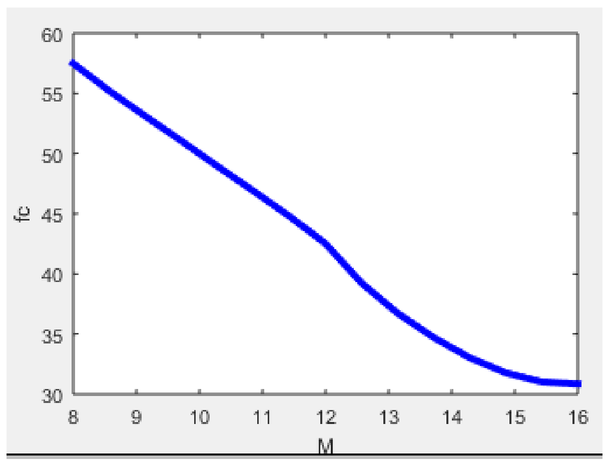
fc
60
55
50
45
40
35
30
8
9
10
11
12
13
14
15
16
M

(d)

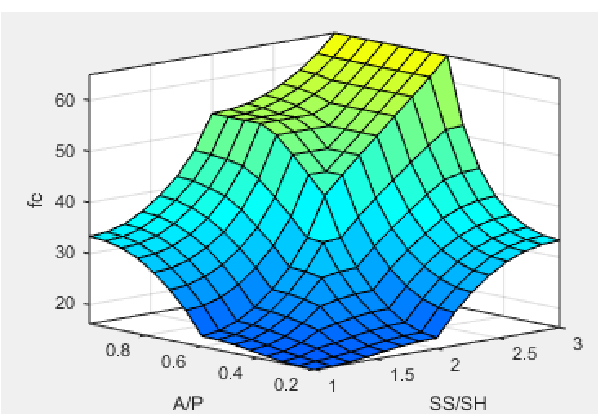
fc
60
50
40
30
20
0.8
0.6
0.4
0.2
A/P
1
1.5
2
2.5
3
SS/SH

(e)

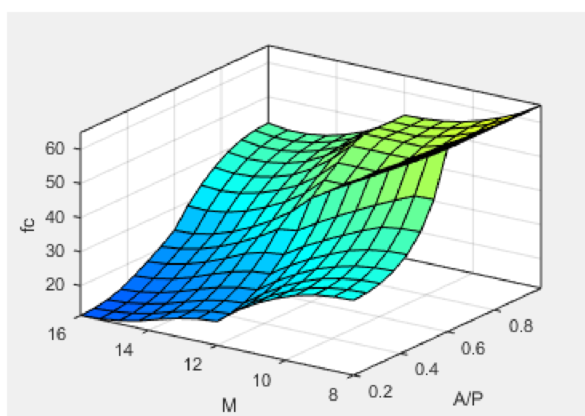
fc
60
50
40
30
20
16
14
12
10
8
M
0.2
0.4
0.6
0.8
A/P

(f)

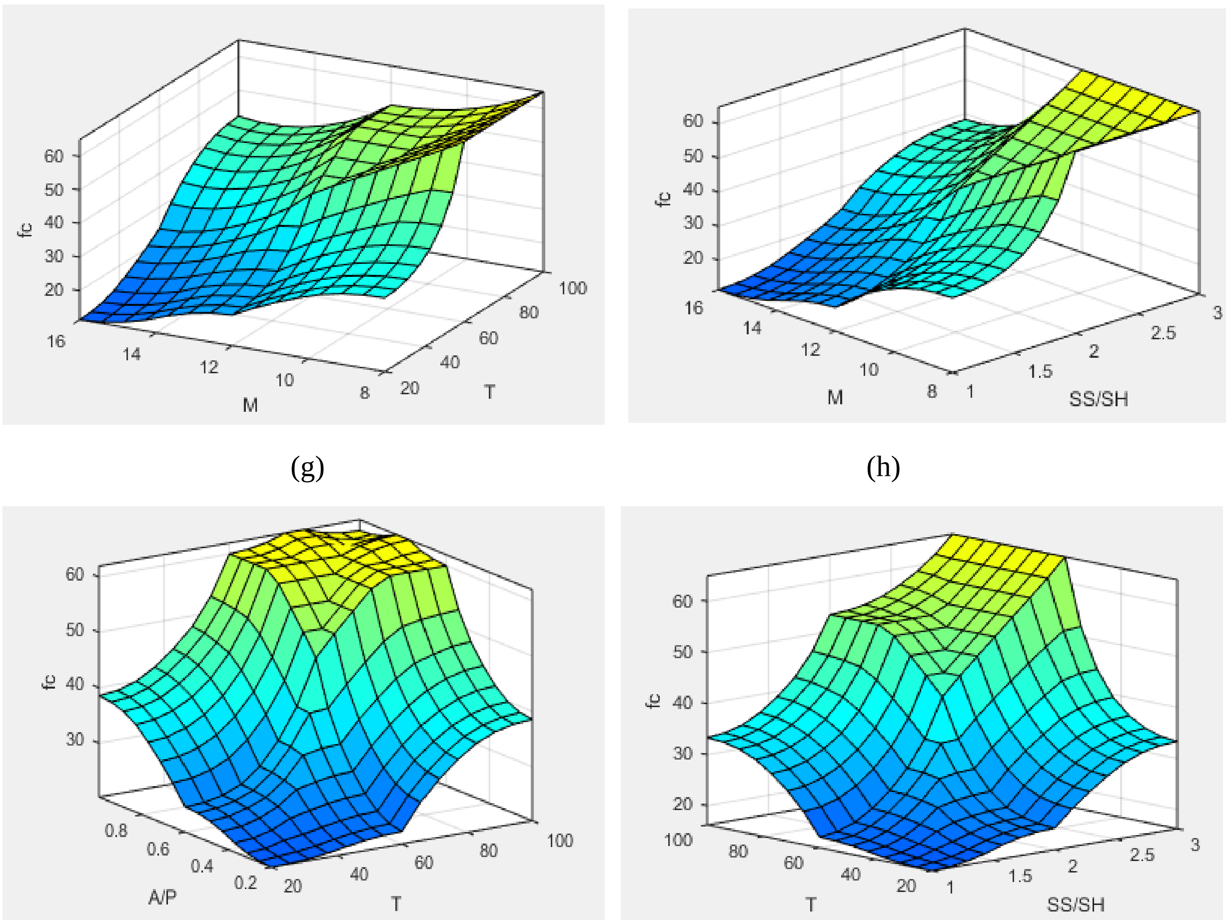

(g) (h)

(i) (j)

Figure 5 Relationship of different parameters w.r.t compressive strength (fc')

4 Conclusions

Artificial intelligent based modeling method e.g. ANFIS is used for optimization and design of geopolymer consisting low calcium part and which is Fly ash based with nominal compressive strength ranging from 25 to 35MPa.

After running the model the training error was found out around 8.45 which is considerbly less for the same database. Hence a better machine learning approach was utilized to design a geopolymers

ANFIS model was utilized to construct contour plots for presentation of correlation among four key input parameters with compressive strength (*fc'*). From these contour plots influence of each parameter in combination with other three parameters was assessed and mix design for different compressive strengths (20-35 MPa) were developed.

The experimental results showed compressive strength values in a range of 20 to 33 MPa for the geopolymers paste at ambient and heat curing with optimal compressive strength is attained for A/P = 0.4 and SS/SH =2.5.

The validation of model was done by computing the estimated compressive strength by keeping all the parameters same as for the experiment. The predicted compressive strength values are in good agreement with those calculated by the experiments. Hence ANFIS can be used for mix design of geopolymers pastes.

The experimental results, for checking by ANFIS with compressive strength above 35MPa represent strong agreement with the optimized compressive strength. Hence, constructed contour plots can be implemented for design of low calcium FA-based geopolymers.

Acknowledgement

Author would like to extend its gratitude to Dr. Tabassum Rashid for help regarding understanding Fuzzy logic and basic working of ANFIS modelling. The watchful reviews and constructive suggestions by the anonymous respectable reviewers are also gratefully acknowledged."

References

[1] G. G. Tiruneh, A. R. Fayek, and V. Sumati, "Neuro-fuzzy systems in construction engineering and management research," *Autom. Constr.*, vol. 119, no. June, p. 103348, 2020, doi: 10.1016/j.autcon.2020.103348.

[2] B. Vakhshouri and S. Nejadi, "Application of Adaptive Neuro-Fuzzy Inference System in High Strength Concrete," *Int. J. Comput. Appl.*, vol. 101, no. 5, pp. 39–48, 2014, doi: 10.5120/17687-8548.

[3] N. B. Siraj, A. R. Fayek, and A. A. Tsehayae, "Development and Optimization of Artificial Intelligence-Based Concrete Compressive Strength Predictive Models," *Int. J. Struct. Civ. Eng. Res.*, vol. 5, no. 3, pp. 156–167, 2016, doi: 10.18178/ijscer.5.3.156-167.

[4] A. Nazari and F. Pacheco Torgal, "Predicting compressive strength of different geopolymers by artificial neural networks," *Ceram. Int.*, vol. 39, no. 3, pp. 2247–2257, 2013, doi: 10.1016/j.ceramint.2012.08.070.

[5] K. V. Shihabudheen and G. N. Pillai, "Recent advances in neuro-fuzzy system: A survey," *Knowledge-Based Syst.*, vol. 152, pp. 136–162, 2018, doi: 10.1016/j.knosys.2018.04.014.

[6] W. Lokuge, A. Wilson, C. Gunasekara, D. W. Law, and S. Setunge, "Design of fly ash geopolymer concrete mix proportions using Multivariate Adaptive Regression Spline model," *Constr. Build. Mater.*, vol. 166, pp. 472–481, 2018, doi: 10.1016/j.conbuildmat.2018.01.175.

[7] T. J.ROSS, *Fuzzy Logic With Engineering Application*. 2010.

[8] M. C. Nataraja, M. A. Jayaram, and C. N. Ravikumar, "A Fuzzy-Neuro Model for Normal Concrete Mix Design.," *Eng. Lett.*, vol. 13, no. 2, pp. 98–107, 2006.

[9] E. M. Golafshani, A. Behnood, and M. Arashpour, "Predicting the compressive strength of normal and High-Performance Concretes using ANN and ANFIS hybridized with Grey Wolf Optimizer," *Constr. Build. Mater.*, vol. 232, p. 117266, 2020, doi: 10.1016/j.conbuildmat.2019.117266.

[10] D. Van Dao, S. H. Trinh, H. Ly, and B. T. Pham, "applied sciences Prediction of Compressive Strength of Geopolymer Concrete Using Entirely Steel Slag Aggregates : Novel Hybrid Artificial Intelligence Approaches," no. i, pp. 1–16, 2019, doi: 10.3390/app9061113.

[11] J.-S. Jang, "adaptive-network-based fuzzy inference system," *IEEE Transactions on Systems*, 1993.

CONSTRUCTION MANAGEMENT

3rd Conference on Sustainability in Civil Engineering (CSCE'21)
Department of Civil Engineering
Capital University of Science and Technology, Islamabad Pakistan

AN OVERVIEW ON FIREFIGHTING PROBLEMS IN REINFORCED CONCRETE BUILDINGS

[a] ***Muhammad Abrar***

a: Department of Civil Engineering, University of South Asia Lahore
* Corresponding author: Email ID: abrar19125@gmail.com

Abstract- Fire is the most common hazard which may cause damage of structures along with loss of lives of occupants. It causes reduction of reinforced concrete structure strength, weakness of steel and concrete bond and change in color of concrete. During a fire event, firefighting is the initial step to prevent huge damage that involves numerous difficulties and complications e.g. obstacles in timely response and firefighting resources. The purpose of the study is to analyze the firefighting problems faced by firefighters. This paper provides an overview on the challenges of firefighting in reinforced concrete buildings and their remedial measures. The damages due to fire, preparedness of firefighting and firefighting barriers are discussed by a brief study of state of the art. The outcomes provide fathom to firefighting and possible solutions.

Keywords- Firefighting problems, RC buildings firefighting, Fire damages.

1 Introduction

Fire is hazard and the most potential risk for structures. Specific guidelines are provided by international codes to counter this hazard for design of structures [1]. These guidelines provide a supervision to develop safety evacuation plans, establish fire safety drills and special training to staff for quick response. Reinforced concrete buildings are good in strength and structural accomplishment under a fire event caused by any sudden flame or ignition by any combustible material [2]. In written any such incident has not been noticed in which RC building completely collapse down. RC buildings experienced cracks on plaster and damage is countered by suitable repairing [3]. The type of repairing depends upon the situation of cracks and loss of strength measured by appropriate methods. The external and internal ignitions are the two main causes of fire. Internal fire can spread outside by means of windows and doors and can damage the exterior covering of building. The burned material placed outside of building generates cause of damages to the nearby parking vehicles and other small buildings if the fire affected building is bigger in height than the others.

Firefighting is an important initial element to keep the occupants safe and to reduce damage rate. Therefore, firefighting and emergency hazard response is a major issue in developing countries. Fire brigade play a vital role in fire extinguishing of buildings. RC high rise buildings have multiple stories, an extra effort is required to reach up to the fire affected area for fire extinguish purpose [4]. The response time increase with the increase of height of building and increase in distance that has to be travelled by firefighters. The fire department emergency response depends upon the availability. It means that to which extent resources are ready to respond. Capacity is the potential of resources to handle hazard and operational. Effectiveness: the capacity to coordinate assets sent to the dangers to which they are reacting. The protestation of life governs the importance of protecting property. Safety in terms of protection of property and efficiency are three main goals of firefighting. When safety is at stake, property can be sacrificed. Here Property to be considered is fire department property i.e. fire engine, fire house and tools. These asserts must be protected if there is no risk to safety [5].

The assessment of fire risk approach is used in buildings to assess the fire hazard safety level present in buildings. These approaches use probabilistic and statistical method by fault or event trees, ranking of fire risk method and multi criteria evaluation based stochastic computer simulation [6]. The fire can cause huge damage to property and lives of residents, if not deal with attention. The preparation for the firefighting is essential to extinguish fire before allowing to spreading and being out of control. Fire safety drills are important for trained specific staff to know how to respond if fire happens and spread suddenly. Firefighting includes problems related with response time. It is the time to reach the fire affected area. Type of access to active fire area matters a lot. The capacity of liquid/gas fire extinguishers and their usage techniques, petrochemical fire extinguish, presence of appropriate fire extinguish system and equipment i.e. smoke detectors, fire alarms, sprinkler system and alternate routes provided for safe evacuation [7]. The aim of the study is to analyze the problems/challenges faced by firefighters during firefighting in RC buildings. The appropriate provisions and preparation for fire firefighting are briefly dicusscud to provide possible solutions for the challenges of firefighting.

2 Damages Due to Fire in RC Structures

When exposed to fire, concrete can suffer huge damage but concrete is poor conductor of heat. Reinforced concrete structures when exposed to raised temperatures due to fire go through a significant change in material properties i.e. compressive strength, cracks in plaster and concrete cover, spalling of concrete loss of steel and concrete bond strengthening and its destruction may occur. [8].The cracks appeared on surface depends upon the intensity of damage of RC member. Due to this elevated temperature concrete structures may collapse down, although complete collapse of structure under fire has not been recorded yet. The damage of structure depends upon the type of fire, nature of combustible material present i.e. change in stress and strain ongoing stage and after fire. It also depends upon the fire resistivity of concrete structure because different types of concrete composites have different fire resistance [9]. The loss of human lives during fire living in RC buildings depends upon the occupancy rate, the average of people spend 90 % of their time in indoor [10].

The composites of cement show different behavior when exposed to fire, depends upon the type of material use in these composites [11].The RC structures which are taken as excellent performance structures may have impact of prevalent execution in fire and larger burn time [12]. As burn time increases the deformations of RC structure elements increases. The fire incidents in petrochemical areas have caused huge economical loss by damage of RC structures and causalities. During fire event in petrochemical areas, life of firefighters is at risk [13]. Fire damaged concrete assessment is done by visual inspection that involves spalling, cracking and color change. Guidance of temperature is provided by change in color. The color of spalling surface is different from original one. Quartz or chert aggregate particles cause cracking popouts, dehydration and spalling provides indications of temperature to which extent concrete was exposed as described in Fig 1. By heating at temperature of 300 °C or above this temperature, the normal concrete's color changed to pink (300-600 °C) after this converted to whitish gray (600-900 °C) and at peak temperature it lead to buff (900-1000 °C) [14].

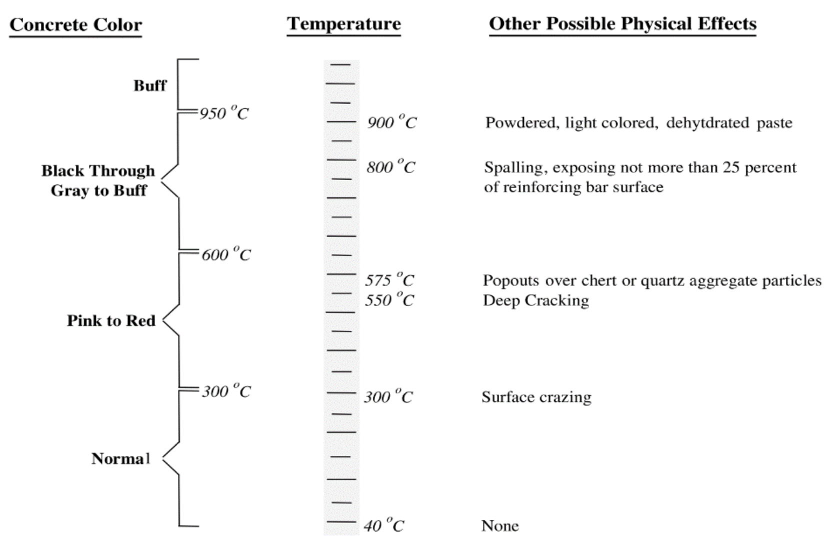

Figure 1: Change in colour of concrete by increase in temperature [14]

3 Preparedness of firefighting

A fire safety framework is an anticipation and concealment method received in the planning of a structure. Generally active and passive systems are adopted as fire protection systems. By utilizing equipment that work manually or automatically the active fire protection system is executed. It is applied by the persons present during fire event taking part in extinguishing operations. This method is used for taking early fire countermeasures, including, automatic sprinklers, emergency lighting, emergency communication equipment, upright pipe systems and hoses, fire lifts, fire alarms, smoke detectors, fire doors [15]. Water mist system is used if water in huge quantity is not available or accessible in confined space and found effective [16]. Efficiency of sprinkler system depends upon the extinguishment of fire and delivery of water to fire by designed amount. Classification of sprinkler system according to hazard type, density of water discharge, head generated by this discharge and area covered is explained is given in Table 1.

Along with building classification some subsidiary parameters are set which are based on height of building, people effected and area characteristics to describe the appropriate use of fire protection system. Based upon the rules and regulations, building having height of 21, 23 or 30m should have sprinkler system. The buildings built in 750, 1000, 1200 or 1500 m^2 area may require fire hydrants or building of any build area with height of 12m [17]. Fire extinguishers are placed in buildings for immediate response against fire. Firefighting staff use these fire extinguishers as an initial response to prevent spreading of fire to whole building or area in which fire is present. Smoke detectors provide detection of any kind of smoke as a result of burning of any material or even by a cigarette as different type of smoke detectors have specific smoke detection sensitivity. Emergency stairs provide means of egress to occupants and alternative route for accessing firefighting staff if main route stairs side under fire [18].

Table 1-Sprinkler hazard and requirements [19]

Occupancy	Hazard	Density of discharge	Sprinkler Heads	Coverage
Shops/mall	Ordinary Hazard III	5 mm/Min. m^2 over 216 m^2	15mm orifice head	12 m^2 of area
Cinema	Ordinary Hazard III	5 mm/Min. m^2 over 216 m^2	15mm orifice head	12 m^2 of area
Car park	Ordinary Hazard II	5 mm/Min. m^2 over 144 m^2	15mm orifice head	12 m^2 of area
Plant rooms	Ordinary Hazard I	5 mm/Min. m^2 over 72 m^2	15mm orifice head	12 m^2 of area
Office	Light Hazard	6 sprinkler heads operating at a flow of 48 l/min	10mm orifice head	21 m^2 of area
Ceiling Space	Light Hazard	6 sprinkler heads operating at a flow of 48 l/min	10mm orifice head	21 m^2 of area

4 Issues during firefighting and their remedial

The analysis of high rise RC structures reveal that many aspects exists which cause issues during firefighting. Insufficient fire resistance of structure cause early collapse of structure that can be overcome by taking into count the fire safety measures while designing RC structures to maintain technical characteristics for a specified time period . Large internal volumes without specific separation of fire barrios should be prevented. The division of high-rise building into fire compartments used horizontally fire walls and use vertically fire ceilings. The minimum fire compartment should be 1500 sq.-m. The access to active fire area in high-rise RC building is a major issue because elevators are often de energized due to fire, rescue elevators with special equipment having minimum capacity of 1000 kg should be provided in building for easy access of firefighting staff to their relevant place during fire [20]. Hence fire hazard is directly related to the lives of persons present in fire effected building.

Immediate response to fire may lead to reduce the damage, unqualified staff cannot respond as per the requirement. This issue can be solved by arranging fire safety drills to minimize response time. Safe evacuation of occupants is desire of firefighting staff. Evacuation exits lead to the outside of building, output to the stair well, exit to fire proof containers present on technical floors [21]. Firefighters face toxic gases during firefighting in RC buildings present in petrochemical areas, the problem can be resolved by use of toxic gas detectors and appropriate dress if toxic gas is detected [22]. Firefighters carryout firefighting operation in near flash out or flash out conditions. Low visibility and high temperature in a house building fire can create a difficult firefighting situation. Substantial radiation towards firefighters and ignition of smoke can be started. Gas cooling technique can be used to reduce fire flashing and ignition of fire gases. A fog nozzle produce small droplets of bursted water. While passing through hot gases the evaporation phenomenon occurs by keeping water volume to minimum and create a safer environment [23].

5 Conclusion

By conducting this study following conclusions can be drawn:

- Significant decrease in strength occurs along with crakes on members of RC structure and change in color while expenciencing high temperatures due to fire.
- Early countermeasure should be taken, automatic fire sprinklers and other fire safety equipment should be installed to extinguish active fire.
- Fire hazard should be taken into count while designing RC structures to provide a good fire resistance.
- Barriers to firefighting; access to active fire area, response time, fire safety drills should be minimized to reduce number of causalities and economical loss

The above outcome is favorable indicating the cracks, spalling and color changes due damages of fire in RC structures. Appropriate preparedness is essential for quick response to fire. Firefighting problems can be reduce by applying provided solutions.

Acknowledgment

The author would like to thank every person/department who helped and guide thorough out the research work, particularly Engr. Prof. Dr. Majid Ali and civil engineering department. The careful review and constructive suggestions by the anonymous reviewers are gratefully acknowledged.

References

[1] A. C. L. E. E. N. Antonio Bilotta, "Structural behaviour of FRP reinforced concrete slabs in fire," *Engineering Structures,* p. 16, 2020.

[2] T. G. Shuna Ni, "Predicting residual deformations in a reinforced concrete building structure," *Engineering Structures,* 2020.

[3] A. C. B. Shuna Ni, "Impact of physical seismic damage on the fire resistance of reinforced concrete walls," *Construction and Building Materials,* pp. 468-482, 2018.

[4] B. Behnam, "Effects of thermal spalling on the fire resistance of earthquacke-damaged reinforced concrete structures," *European Journal of Environmental and Civil Engineering,* 2019.

[5] I.-H. Y. D. L. H. C. K.-I. K. Minju Kim. Taehoon Kim, "Improvement of standards on fire safety performance of externally insulated high-rise buildings: focusing in the case in Korea," *Jounal of Building Engineering,* 2020.

[6] S. M. LO, "A fire safety assessment system for existing building," *Fire Technology,* vol. 35, 1999.

[7] J. N. S. L. H. W. J. Z. Zhikun Ding, "An approach integrating geographic information system and building information modelling to assess the building health of commercial buildings," *Journal of Cleaner Production,* 2020.

[8] M. C. A. A. S. S. P. Hemanth Kumar Chinthapalli, "Effectiveness of hybrid fibre-reinforced polymer retrofitting on behaviour of fire damaged RC columns under axial compression," *Engineering Structures,* 2020.

[9] P. C. W. S. Paolo Cioni, "Assessing fire damage to RC elements," *Fire safety journal,* pp. 181-199, 2001.

[10] Y.-M. T. C.-T. L. P.-L. K. J.-Y. H. Kuan-Li Wu, "The Roles of MicroRNA in Lung Cancer," *International Journal of Molecular Sciences,* 2019.

[11] M. F. J. F. K. H. J. H. Radek Štefan, "Thermal, spalling, and mechanical behaviour of various types of cementitious composites exposed to fire: Experimental and numerical analysis," *Construction and Building Materials,* 2020.

[12] A. C. B. Shuna Ni, "Post-fire seismic behavior of reinforced concrete structural walls," *Engineering Structures,* pp. 163-178, 2018.

[13] X. Z. H. S. H. S. Z. W. Yufeng Fan, "Design and Application of Toxic and Harmful Gas Monitoring System in Fire Fighting," *Sensors,* 2019.

[14] P. T. B. Georgali, "Microstructure of fire-damaged concrete. A case study," *Cement & Concrete Composites* , pp. 255-259, 2005.

[15] M. P. Hary Agus Rahardjo, "The most critical issues and challenges of fire safety for buildings sustainability in Jakarta," *Journal of Building Engineering,* 2020.

[16] C. W. Hengrui Liu, "Critical assessment on operating water droplet sizes for fire sprinkler and water mist systems," *Journal of Building Engineering,* 2020.
[17] J. P. R. L. C. d. S. F. Eduardo E.C. Rodrigue, "Comparative study of building fire safety regulations in different Brazilian states," *Journal of Building Engineering,* 2017.
[18] R. B. M. G. D. G. S. M. E. P. E. P. P. R. S. S. Samuel L. Manzello, "Summary of workshop large outdoor fires and the built environment," *Fire Safety Journal,* 2018.
[19] J. I. K. K. Khalid A.M. Moinuddin, "Reliability of sprinkler system in Australian shopping centres –A fault tree analysis," *Fire Safety Journal*, 2019.
[20] M. G. Tatiana Poliakova, "Fire safety issues in the design and construction of high-rise buildings," in *EDP Sciences*, 2018.
[21] I. E. T. Y. Eremin, "Fire danger of high-rise buildings: evacuation and protection of people from combustion products," *Fire Safety Journal,* pp. 141-146, 2014.
[22] X. Z. L. Y. X. T. Y. Z. B. C. Y. P. H. L. Y. N. Kai Ye, "A Multi-Scale Analysis of the Fire Problems in an Urban Utility Tunnel," *Energies,* 2019.
[23] S. Svensson, "Experimental Study of Gas Cooling During," *Fire Technology,* 2018.

3rd Conference on Sustainability in Civil Engineering (CSCE'21)
Department of Civil Engineering
Capital University of Science and Technology, Islamabad Pakistan

BARRIERS TO SUPPLY CHAIN MANAGEMENT IN THE CONSTRUCTION INDUSTRY OF PAKISTAN

[a] Sayyeda Shanzay Rahat*, [b] Muhammad Muneeb Malik, [c] Shaharyar Qaiser, [d] Abdullah Butt Shakeel

a: NUST Institute of Civil Engineering, National University of Sciences and Technology, srahat.bece17nice@student.nust.edu.pk
b: NUST Institute of Civil Engineering, National University of Sciences and Technology, mmuneeb.bece17nice@student.nust.edu.pk
c: NUST Institute of Civil Engineering, National University of Sciences and Technology, sqaiser.bece17nice@student.nust.edu.pk
d: NUST Institute of Civil Engineering, National University of Sciences and Technology, ashakeel.bece17nice@student.nust.edu.pk
* Corresponding author: Email ID: srahat.bece17nice@student.nust.edu.pk

***Abstract**:* Construction in Pakistan is mostly project-based, requiring productive and systematic use of available resources. In the modern world, the SCM approach has become a central component in developmental initiatives in the construction industry which helps in enhancing the productivity and efficacy of construction projects. Since, the implementation of SCM requires a systematic management technique along with effective technological aid, it may discourage the contractor especially in developing countries like Pakistan. Consequently, this paper highlights the identification of constraints to SCM in the construction industry of Pakistan. For acquisition of data, a questionnaire survey was conducted. After an in-depth literature review, extensive research led to the recognizance of nineteen crucial barriers to the successful commencement of the SCM approach. These obstructions were sorted into four more extensive classifications, specifically, Strategic Barriers, Technical Barriers, Individual Barriers, Organizational Barriers and Cultural Barriers. These recognized barriers were incorporated into the questionnaire in the form of Likert Scale items with a range of five possible responses to rank their perceived significance of each barrier. Due to the ongoing pandemic, quantitative technique of data collection was used which included the circulation of questionnaire among various construction organizations. The collected data was analyzed statistically and using Factor Analysis, the results helped identify seven major factors. This study helps identify the deep-rooted hindrances faced by construction industry of Pakistan for the initiation of Supply Chain Management system and will help us better understand the challenges that may pave the way for the establishment of Supply Chain Management in the construction industry of Pakistan and similar developing countries in the years to come.

Keywords- supply chain management, barrier analysis, factor analysis, construction supply chain, Principal Components Analysis

1 Introduction

Supply Chain Management (SCM) in the construction industry is a highly fragmented nexus of multiple levels of organizations from grass-root level to large scale enterprises comprising of stakeholders such as architects, suppliers, contractors, and indirect suppliers. SCM includes the movement of raw material, their storage, work in process inventory and consumed goods from starting point to consumption [1]. Construction industry plays a vital role in a country's economy, especially for developing countries like Pakistan. According to Pakistan Economic Survey, the country's construction industry accounts for 2.53% of Gross Domestic Product (GDP) and the sector employs 7.61% of the employed Pakistani labour force. The CPEC agreement between Pakistan and China has opened up a plethora of opportunities for the construction industry to thrive. The construction company in Pakistan is in developing stages and the competition within this industry has increased manifold in recent times. Therefore, the contractors have to work on strategies that increase the quality of their services while also decreasing the production unit costs, thus providing a competitive advantage to the construction firm. For this purpose, the successful implementation of Supply Chain Management focusing on the use of firm's suppliers, operations and technological capabilities is integral because the construction process includes a variety of parties which provide different services such as labour, materials, equipment and related information.

We conducted a quantitative content analysis of existing research, and it is certain from this extensive Literature Review that a successful supply chain management eliminates cost and time overruns while increasing the process efficiency which provides a competitive advantage to the construction firm [2]. Even though there may be a win-win approach for both the contractor and supplier but still there may be many barriers in the successful implementation of Supply Chain Management. A variety of researchers, such as, Akintoye [3] and Dianty [4], have classified these barriers. Major barriers identified by Akintoye [3] are: Insufficient understanding of Supply Chain Management concepts, Low commitment of senior management brass, Uncertainty of strategic benefits, Inadequate organizational hierarchy to support the system, Lack of commitment by partners and, Insufficient information technologies and related equipment.

The barriers identified by researches such as, [5], [6], [7], [8], [9], [10], [11], [12] and [13] are summarized and listed below:
Less availability of company information systems which enable sharing of information with the suppliers, insufficient consultants to guide the firms, negative impact on quality because of long-term working relation with the same supplier, supplier provided materials having inappropriate quality, inadequate informational technology infrastructure, contractor's inclination towards the clients' interests over the subcontractor and suppliers' needs, cost-oriented and short-term goals in the construction industry, suppliers lack interest in quality management, hindrance in implementation because of a a large variety of suppliers involved in a project, project-based work in construction sector instead of mass production, issues regarding management and storage of stock, increased transportation cost and supplier distance, lack of trust due to hostile relations among stakeholders, inadequate understanding of Supply Chain Management by top management, supplier's lack of interest in long-term association, low trust in supplier's commitment, unsupported organizational structure for a cooperation with the suppliers, top management's hesitancy for adaptation to new management styles.

The construction industry of Pakistan lacks any substantial research for the incorporation of SCM thus the identification of the barriers paves the way for future research for the integration, implementation and improvement of the supply chain process.

2 Research Methodology

2.1 Development of Research Framework

The selection of study population was first narrowed down based on extensive literature review and expert opinion to the following: Construction Firms, Design Consultancy Firms, Clients' Firms, Subcontractors' Firms, Suppliers' Firms, Others (Engineers, Architects, PhD Students).
These barriers were categorized into areas of concern, namely:

Table 1

S/no.	Areas of Concern
1	Strategic
2	Individual
3	Organizational
4	Cultural
5	Technological

2.2 Development of Measurement Tool

The measurement tool is in the form of an online questionnaire, keeping in mind the current pandemic. The barrier categories in Table 1 have been kept in mind for the development of the questionnaire. Likert Rating Scale has been used for the questionnaire.

Table 2

Barrier Categories	Supply-chain management barriers
Strategic barrier	Political instability
	Lack of creation of supply chain alliances
	Short-term decision-making perspectives
	Unchecked transportation costs
	Preference to project-based production over mass production
	Lack of top management commitment and support
Cultural barrier	Prioritization of client over supplier and subcontractor's needs.
	Mistrust among employees and supply-chain partners
	Excessive hiring of a single subcontractor and impacts on quality
	Subcontractors and suppliers are not allowed to participate in the early stages of the project
Technological barrier	Lack of information technology use by suppliers
	Poor ICT structure (information system and electronic trade systems) of companies to share information with suppliers
Individual barrier	Lack of education to employee and supplier employee
	Resistance to change of management system by suppliers
	Lack of motivation of suppliers to invest in quality management
	Lack of necessary tools, management skills and knowledge
Organizational barrier	Hindrances in stock storage and management for suppliers
	Low information quality, insufficient information exchange and, less transparency along with limited communication
	Serious problems with payments between customers, main contractors, sub-contractors and suppliers
	Lack the framework and measurement system

2.3 Data Collection

A total of 109 responses were obtained, out of which 2 were disregarded, leaving us with a sample size of 107.

Table 3

Contractor firms	37.6%
Client firms	21.1%
Supplier firms	3.7%
Subcontractor firms	2.8%
Note: Some respondents were part of multidimensional firms, thus involved in multiple categories.	

2.4 Data Analysis

2.4.1 Formation of Data Set

In this approach, we checked the Likert Type Items, extracted ordinal data for analysis, categorized factors using Mean of Likert Items (Strategic, Cultural, Individual, Technical, Organizational) and subsequently, inserted value labels (1: Strongly Disagree, 2:Disagree, 3:Undecided, 4:Agree, 5: Strongly Agree)

2.4.2 Normality Check

Since our sample size is 107 (>100), we consider Kolmogorov-Smirnov Normality Test. Significance for all variables is <0.05, thus being statistically significant and subsequently, Not Normally Distributed. For further confirmation, we took Log Base 10 of the variables, and data was still proven to be Not Normally Distributed.

Table 4

Tests of Normality

	Kolmogorov-Smirnova			Shapiro-Wilk		
	Statistic	df	Sig.	Statistic	df	Sig.
S	.127	107	.000	.959	107	.002
C	.094	107	.022	.978	107	.077
T	.185	107	.000	.868	107	.000
I	.108	107	.004	.957	107	.002
O	.107	107	.004	.968	107	.012

a Lilliefors Significance Correction

2.4.3 Factor Analysis

We conducted Principal Components Analysis. Eigen values greater than 1 were set to be retained in extraction. We then conducted Bartlett's Test of Sphericity: A significance p value of <0.01 is less than 0.05, it implied that data is statistically significant, thus variables are significantly correlated. Number of components retained by SPSS are 07 during Factor Reduction. These 7 components sufficiently explain the relation between initially selected 19 barriers. The cumulative percentage of Variance of 62.38% is the percentage of variance accounted for by these 7 components. (Which lies in the range of 40-60% in which most solutions typically exist.)

Table 5

	Initial Eigenvalues			**Extraction Sums of Squared Loadings**		
Component	**Total**	**% Of Variance**	**Cumulative %**	**Total**	**% of Variance**	**Cumulative %**
1	3.659	19.257	19.257	3.659	19.257	19.257
2	2.002	10.535	29.792	2.002	10.535	29.792
3	1.498	7.882	37.674	1.498	7.882	37.674
4	1.460	7.686	45.360	1.460	7.686	45.360
5	1.141	6.006	51.366	1.141	6.006	51.366
6	1.076	5.666	57.031	1.076	5.666	57.031
7	1.017	5.351	**62.382**	1.017	5.351	62.382
8	.957	5.036	67.418			
9	.907	4.773	72.191			
10	.783	4.119	76.310			
11	.756	3.980	80.290			
12	.692	3.642	83.933			
13	.675	3.553	87.485			
14	.571	3.007	90.492			
15	.463	2.435	92.927			
16	.418	2.200	95.127			
17	.367	1.933	97.060			
18	.321	1.690	98.750			
19	.238	1.250	100.00			

3 Results

In light of the results, the paper clearly exhibits the significant role of some of the factors that prevent the implementation of supply chain management. The responses from the concerned parties of the construction sector show how important and fruitful it will be for the construction industry of Pakistan to have a pervasive awareness of the barriers so that it would pave way for the better supply chain management. After a series of tests and analyses, the results showed that 7 factors identified were enough to sufficiently explain the relation between initially selected 19 barriers.

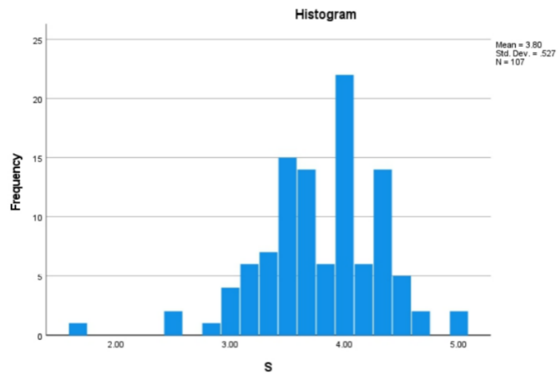

Figure 1: Statistical Deviation in Strategic Barriers

Research focuses mainly on the challenges to supply chain management adoption faced by stakeholders specializing in the construction industry of Pakistan. According to the results of the questionnaire survey, there are primarily seven factors that characterize the problem. The survey data revealed a commonality of viewpoints on important topics relevant to the five theme areas of concern. Although the percentage of replies may change between groups (and for some types of analysis, these variances must be considered).

This paper expands the scope of current literature review of the subject specifically for Pakistan by highlighting some of the most critical factors that needs to be addressed more often. The paper would also prove to be helpful for any future researchers who would like to explore the subject further.

Table 6

Prime Factors
Political instability and infrastructural hindrances
Project Based Production Tendencies over Mass Initiatives
Lack of Mutual Trust among Stakeholders
Lack of early involvement by grass root level stakeholders
Lack of understanding of the concept and unawareness of need
Lack of information system infrastructure and electronic trade systems
Less transparency with limited communication between suppliers and construction firms

4 Conclusion

It can be concluded from the paper that having a stable political environment, and developing an understanding of SCM will potentially help in the adoption of SCM. However, contractors who mainly focus on cutting costs and maximizing profit may hesitate to invest in consultancy. There it is recommended for the consultants to prioritize employer-contractor relationships in order to motivate the contractors. It can also be concluded that consultants and contractors are regularly inclined towards joint endeavors that will open them to professional management approaches and new advances while clients are less excited about executing such adjustments.
Recommendations:

- Establishment of an independent ombudsman organization to adjudicate and monitor procurement and administrative concerns, which might save significant time spent on conflict settlement.
- The adoption of an impartial contractor/consultant rating system will vastly enhance procurement procedures.

- The establishment of a specialized financial institution, which would serve towards the requests of the development business.
- Training is the most effective approach for resolving HR concerns inside the industry. To train the personnel, the company should utilize already established technical and vocational establishments.

Acknowledgment

The authors would like to express their sincere gratitude to Dr. Khurram Iqbal Ahmad Khan, HOD for the Department of Construction Engineering & Management, National University of Sciences and Technology, without whose kind guidance, encouragement and support, we could not have made it so far. The careful review and constructive suggestions by the anonymous reviewers are gratefully acknowledged.

References

[1] Lıu, X , Yang, J., Qu, S., Wang, L., Shishime, T. Bao, C.,2012, "Sustainable Production: Practices and Determinant Factors of Green Supply Chain Management of Chinese Companies", Business Strategy and the Environment, Volume 21, Issue 1, pp.1–16.

[2] Peter, N. J., Okagbue, H. I., Iroham, C. O., Opoko, P. A., & Akinola, A. (2020). Literature review of areas of application of supply chain management in construction industry. International Journal of Supply Chain Management, 9(3).

[3] Dainty, A. R. J., Briscoe, G., Millett, S., 2001. "Construction supply chain partnerships: skills, knowledge and attitudinal requirements", European Journal of Purchasing and Supply Management, vol. 7, no. 4, pp. 243–255,

[4] Xiaolong X, Yaowu W, Qiping S., Xiaoguo Y. ,. 2007. "Coordination mechanisms for construction supply chain management in the Internet environment", International Journal of Project Management, 25 (2007) 150–157.

[5] Akintoye, A., Mcintosh, G., Fitzgerald, F., 2000. "A Survey of Supply Chain Collaboration and Management In The UK Construction Industry", European Journal of Purchasing & Supply Management 6 (2000) 159-168.

[6] Vrijhoer; R., Koskela, L.J., Howell, G., 2001."Understanding construction supply chains: an alternative interpretation", 9th International Group for Lean Construction Conference, August 2001, National University of Singapore.

[7] Van, W. A:J:, 2005, Purchasing and Supply Chain Management: Analysis, Strategy, Planning and Practice, Thomson, London.

[8] Hatmoko, J.U.D., Scott, S., 2010, "Simulating the impact of supply chain management practice on the performance of medium-sized building projects", Construction Management and Economics, 28 (1),pp. 35-49.

[9] A. Segerstedt and T. Olofsson, "Supply chains in the construction industry", Supply Chain Management: An International Journal, vol. 15, no. 5, pp. 347-353, 2010.

[10] Chrisitien, B., 2011, Interpretive structural modeling of supply chain risks, International Journal of Physical Distribution & Logistics Management.

[11] G. A. Papadopoulos, N. Zamer, S. P. Gayialis and I. P. Tatsiopoulos, "Supply Chain Improvement in Construction Industry", Universal Journal of Management, vol. 4, no. 10, pp. 528-534, 2016.

[12] P. McDermotti and M. Khalfan, "Achieving Supply Chain Integration within Construction Industry", Construction Economics and Building, vol. 6, no. 2, pp. 44-54, 2012.

[13] Gosling, J., Towill, D.R., Naim, M.M., Dainty, A.R.J., 2015, "Principles for the design and operation of engineer-to-order supply chains in the construction sector", Industrial Marketing Management, Vol. 26, Issue 3,pp. 203-218.

3rd Conference on Sustainability in Civil Engineering (CSCE'21)
Department of Civil Engineering
Capital University of Science and Technology, Islamabad Pakistan

ANALYSIS OF MINERAL WOOL INSULATION ON RESIDENTIAL BUILDING

[a] Danish Adnan*, [a] Engr. Hafiz Aiman Jamshaid*, [c] Dr. Muhammad Babur*

a: Civil Engineering Department, University of Central Punjab, info@ucp.edu, pk
b: Civil Engineering Department, University of Central Punjab, aiman.jamshaid@ucp.edu.pk
c: Civil Engineering Department, University of Central Punjab, m.babur@ucp.edu.pk
*Email ID: danishadnan13@gmail.com

Abstract – Cooling and heating systems consume the major portion of total energy production to meet the thermal comfort needs of the masses. Providing resistance to the heat flow is one of the efficient and environmentally friendly methods to reduce the consumption of energy. For this purpose, thermal insulation is widely used. Material with high thermal resistivity is used to reduce heat loss and heat gain. This results in the reduction of energy consumption that is used for heating and cooling purposes hence cutting energy costs. This study is aimed to investigate the effects of insulation material on energy cost and energy performance on a house. A house is modelled using BIM technology. BIM can evaluate the building's energy performance and energy cost savings. Autodesk Revit 2021 is used for modeling the house. A comparison of the energy cost of the house is done before and after the installation of insulation material in the exterior walls and roof of the house. Mineral wool is used as an insulation material for the house. Mineral wool has two variants known as rock wool and glass wool. It contains 70% recycled material that makes it a greener material. It can be a costly product but it has less health risk during installation. It is easy to install. Mineral wool products are manufactured in different shapes and properties depending on the requirement. It covers a temperature range from -250 to 800+ degrees acting as a good physical barrier to heat transfer. It also performs well for soundproofing and fire protection.

Keywords- *Building Information Modelling (BIM), energy-efficient buildings, insulation material, mineral wool*

1 Introduction

The global energy demand will continue to increase as the world grows according to the IEA's annual projections. The global population was 7.7 billion in 2019 according to the IEA [1]. The IEA in its 2020 report predicts that the global population is expected to increase an additional 1.3 billion; from 7.7 billion in 2019, 9 billion population in 2040. Increased energy demand is predicted with developing economies and emerging markets. There is a forecast of a 19% increase in world energy demand. It means that the world would need twice as much energy as it produces today [1]. The energy demand is increasing day by day. It is expected to be more severe, especially in developing countries. The reason is the rapid growth of new buildings while the use of energy-efficient technologies is not having sufficient attention [2].

As a result of the rising energy demand, environmental issues are becoming more and more evident. The energy is converted from one form to another with the help of energy. It means energy is required to get energy. The gathering, processing, and delivery of fossil fuels are responsible for 8 percent of carbon emissions [3]. Approximately 40% of global CO_2 emissions are emitted from electricity generation through the combustion of fossil fuels to generate the heat needed to power steam turbines. Burning these fuels results in the production of carbon dioxide (CO_2)—the primary heat-trapping, "greenhouse gas" responsible for global warming [4]. Carbon dioxide (CO_2), an example of a pollutant, is widely known as a harmful substance to human health [5]. Greenhouse gases are gases in Earth's atmosphere that traps heat. Greenhouse gases allow the sunlight to pass through the atmosphere but they stop the heat that sunlight brings in to escape from the atmosphere. The cooling systems used in the summer season run on power generated by fossil fuels. Air conditioners emit air pollutants like chlorofluorocarbon that go into the environment and deplete the ozone layer. CO_2 and chlorofluorocarbon are an example of greenhouse gases. Carbon dioxide plays a strong contribution to the greenhouse gas effect. If no necessary steps are taken to reduce the emissions of CO_2 and other greenhouse gases, the Earth's average surface temperature is predicted to rise about 1.1– 6.4 °C by the end of 2100 [6].

Generally, when house construction takes place, walls are constructed using conventional materials i.e., solid bricks. The heat can be easily conducted through these walls in the summer season which makes it unbearable to live in that house. Then air conditioners are used to cool the house but that ends up causing huge electricity consumption. As explained above large consumption of electricity and air conditioners cause emissions of harmful pollutants i.e.CO_2 and other greenhouse gases. There is another way that can be used in the construction or renovation of the house. That is to insulate the exterior walls of the house with special materials that resist the transfer of heat to and from the house. Roof insulation can also be done. The most important advantage of insulation is the reduction in energy consumption of the house. Also, the use of air conditioners will be reduced to a huge extent. In this way, emission of harmful pollutants will be avoided and hence cost-saving due to less energy consumption.

Nowadays, energy efficiency in the building is the main objective in energy policy at regional, national, and international levels [7]. Based on the literature review using the famous database (ScienceDirect and researchgate.net) gave the idea of using the properties of insulation material and doing energy analysis using BIM technology. Building information modeling (BIM) is a technology that can help designers in predicting the energy efficiency of the structure, based on the model created by 3D visualization of data on the software.

In Pakistan, a large sum of resources is annually consumed within the building sector. Due to the large share of energy consumption in this sector, an analysis as accurate as possible of the heating and cooling loads of a building should be done. Energy performance analysis using BIM can save a lot of time and money. Building Information Modeling technology indicates optimization, design identification, comparison, and reduction of energy consumption in the initial phases of design as well as in retrofitting. This study includes a case study of a residential house. Its building information modeling is done in Autodesk Revit 2021. Energy performance analysis is done using Autodesk Insight.

2 Research methodology

2.1 Selection of software

AUTODESK Revit 2021 is selected to create a model for building information modeling. This software is used because of its wide range of tools for different designs and modeling available in it. Revit 2021 has all the required options to design a house from top to bottom. Another reason for the selection was the built-in plugin of Autodesk that allows performing energy simulation in this software. Autodesk insight is an energy-related tool used to get results for energy analysis. The results are obtained after running an energy simulation on a model in Autodesk Rivet 2021. It gives real-time feedback. It allows to visualize and interact with key performance factors and helps to make better and informative design decisions. It is a cloud-based service. It allows for simulation of building performance to optimize energy efficiency by using minimum hardware resources of the system and providing high-speed energy analysis.

2.2 Site selection

A five Marla house is modelled for the case study. The location for taking the weather into account is set as Sialkot, Punjab Province, Pakistan. It is a mild climate region. The area of the house is about 135.26 m^2. It is a single-story house of 4.2m (14 ft) height above ground level. The interior and exterior walls are made of 9-inch thickness. The front side of the house is south facing. Initially, there is no insulation material provided in the walls and roof of the house. The walls of the house are finished with cement plaster and paint. The roof is a 6-inch thick

RCC slab finished with ceramic tiles. The purpose of the study is to observe the thermal response with and without insulation material to make a comparison. The comparison of energy performance and energy cost.

2.3 Mineral wool – An insulation material

Mineral wool is an inorganic product manufactured from a mix of raw materials, which mainly consist of stone or silica. Stone or silica are heated to a high temperature until liquified by heat. The material prevents the process of conduction, convection, and radiation. Convection is prevented by trapping air in the open cell of the material, the wool matrix. Conduction is a process that requires pathways so it is reduced in mineral wool because there is very little solid material to provide pathways for the process. Heat transfer reduces because the material act as a physical barrier to radiations. With its good thermal properties, it also provides fire protection. Mineral wool has two main variants i.e., rock or stone wool and glass wool. Glass wool is made from spinning the strand of melted glass. It is usually made as rolls, slabs, and applied in-place or sprayed. Rock or stone wool is made from molten rock materials. Their final product of rock or stone wool is compressed into boards, mineral wool batts, or other forms. Mineral wool is used for insulation of cavity walls and exterior walls, flat roofs, thermal and acoustic insulation of partitioning walls and floors. Minera wool can withstand a temperature range of -250 to 800+ degrees. Its thickness is usually 30 to 120 mm (4-inch). Density is up to 120 kg/m^3. Its packaging is polyethylene bags. This material is used in the BIM of the house [8].

3 Results

The model is created (Fig 1) to examine the design in Autodesk Revit 2021. Then the type of materials, floors, and energy setting are defined for the model. Then the results were received after generating the energy model and sending it to the Autodesk cloud service.

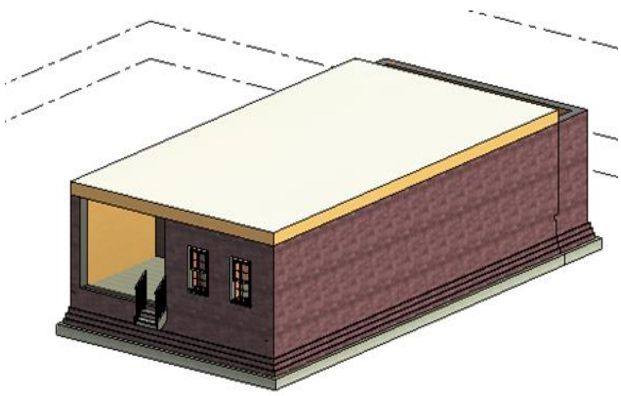

Figure 1: The 3D view of the Residential house simulation in Autodesk Revit 2021

The Autodesk insight gives mean energy cost and energy consumption using different parameters. The parameters are building orientation which is between 270 and 315 degrees, window to wall ratio i.e., 19% for southern walls, 15% for northern walls, 4% for western walls, and 0% for eastern walls, wall construction, and roof construction shown as BIM modelled, infiltration, lighting efficiency (no lighting efficiency in modelled house), no daylighting and occupancy control, no plug load efficiency, no HVAC, and no photovoltaic solar panels. The structure of the walls used in the model is high mass construction (construction with concrete) with no insulation, and the roof structure is dark with no insulation. Dark means the surface of the roof is dark-coloured or finished with dark-coloured material and absorbs the heat of the sun. This is a modelled scenario. The cost of energy consumption based on these parameters is 20.7 USD/m^2/y. Accordingly, the energy consumption is equal to 207 kWh/m^2/y.

In the energy performance settings in the edit type of the building element, there is a thermal resistance factor that is the important number R underneath analytical properties. The R-Value is known as imperial units of measurement ($ft^2 \cdot °F \cdot h/BTU$). High R-value means a slow rate of heat transfer through the insulation material. This number is determined based on the material's properties (in our case material is mineral wool). Going further into edit type the wall structure is enhanced by adding a layer of mineral wool as insulation/thermal resistant material. The same process goes for roofs. The software will add all of the layers added for thermal resistance and gives the final number called R. The 4-inch-thick layer of mineral wool as an insulation material is added inside for all the exterior walls (9 inches thick) and under roof slab (6 inches thick) of the house.

Initially, before installing insulation material the R-value of exterior walls and roof was zero. The 4-inch-thick layer of mineral wool with a plywood finish gives an R-value of 20.39 ($h.ft^2.F^o$)/BTU for exterior walls and 19.05 ($h.ft^2.F^o$)/BTU for the roof slab. So, the parameters i.e., roof and wall construction are adjusted by adding thermal resistance keeping all other parameters of Autodesk insight result the same. By adjusting the roof and wall construction parameter with an increase R number as mentioned above, the cost of energy consumption would be 18.4 USD/m2/y. Correspondingly, the energy use intensity would be equal to 166 kWh/m^2/y.

The consequences of this analysis show that the use of building information modeling technology for changing the parameters affecting energy consumption in the designed model is helpful. The changing of parameters can save up to 11.11% energy cost and 19.81% of energy use intensity. The adjusted parameters are roof and wall construction. The adjustment is the increased R-value.

Table 1 Comparison of results before and after optimizing parameters

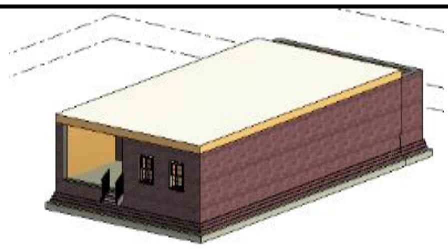

Building form		**Energy cost**	**Saving**	**Energy use intensity**	**Saving**
		USD/m^2/y	Percent	kWh/m^2/y	Percent
5 Marla House	BIM parameters Before optimization	20.7	0	207	0
	BIM parameters After optimization	18.4	11.11	166	19.81

Figure 2: Autodesk Insight results for wall and roof construction

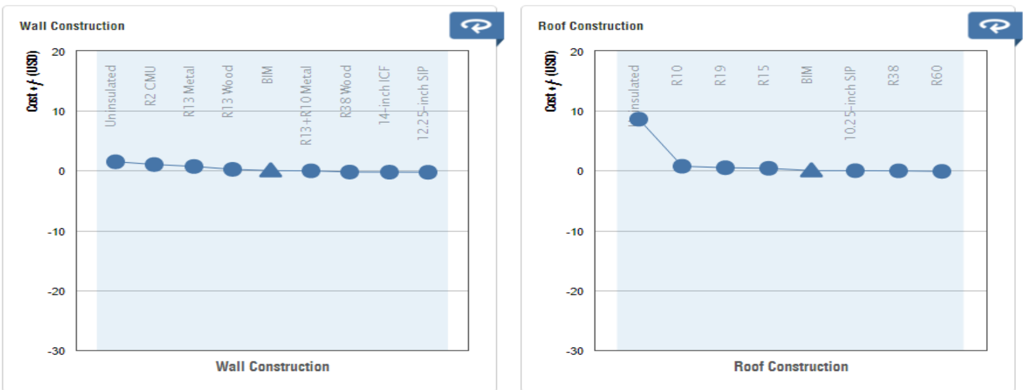

Figure 3: Zoom in results of Autodesk insight for wall and roof construction

The options are shown (Fig 2) as circles in the graph. The current setting (insulated one) is shown as a triangle from the model. It is named BIM. When the arrow is brought on any option, a small pop-up appears. The pop-up shows either the energy cost or energy consumption. It depends on whether we are showing the results in terms of energy cost or energy consumption. The BIM option means it is taken from the model in Revit. It is a baseline so it will be zero. The options other than BIM will have a positive or negative effect on energy consumption and energy cost. Each option represents a change. The change from the BIM option. The circular options with positive values show an increase of that amount in energy cost or energy consumption. The circular options with negative values show a decrease of that amount in energy cost or consumption. The saving difference compared with the BIM option can be observed with the negative values. Moving left from the current setting will cause an increase in energy cost and moving right will cause a decrease in energy settings. Almost all types of insulation materials would exist between this range. The R-value for the exterior wall is 20.39 (h.ft^2.F^o)/BTU and as can be seen in the wall construction graph it exists somewhere between R-13 wood and R-10 + R-13 metal.

Mean energy cost before insulation of wall and roof with mineral wool = 20.7 USD/m^2/y
Mean energy cost after insulation of wall and roof with mineral wool = 18.4 USD/m^2/y
Saving cost in 1 year = 2.27 USD/m^2/y
Mean energy consumption before insulation = 207 kWh/m^2/y
Mean energy consumption before insulation = 166 kWh/m^2/y

4 Conclusion

Following conclusions can be drawn from the conducted study:

- Using insulation material (Mineral wool) as a form of thermal resistance is effective. Effective in terms of reducing energy cost and energy consumption.
- The saving percent of energy cost due to mineral wool insulation is 11.11%.
- The saving percent in energy consumption is 19.81%.

Less energy consumption will lead to less emission of atmospheric damaging pollutants. It can be observed that mineral wool acted as a physical barrier in the transfer of heat. BIM helped in conducting energy analysis on the house. The Autodesk Insight's results and parameters helped in explaining the effects of insulation material on the house.

Acknowledgment

This study was supported by the Civil Engineering Department, the University of Central Punjab for a Final Year Project.

References

[1] CAPP, "CAPP." https://www.capp.ca/energy/world-energy-needs/.
[2] L. Aditya, T. M. I. Mahlia, B. Rismanchi, H. M. Ng, M. H. Hasan, and H. S. C. Metselaar, "A review on insulation materials for energy conservation in buildings," no. June, 2017, doi: 10.1016/j.rser.2017.02.034.
[3] "Climate Communication." https://www.climatecommunication.org/change/energy-use/.
[4] "Reducing Carbon Dioxide Emissions from Electricity Sector Using Smart Electric Grid Applications," doi: https://doi.org/10.1155/2013/845051.
[5] T. H. Oh and S. C. Chua, "Energy efficiency and carbon trading potential in Malaysia," *Renew. Sustain. Energy Rev.*, vol. 14, no. 7, pp. 2095–2103, 2010, doi: 10.1016/j.rser.2010.03.029.
[6] S. Guendahou, "ipcc." https://www.ipcc.ch/people/sabin-guendehou/.
[7] L. Pérez-Lombard, J. Ortiz, and C. Pout, "A review on buildings energy consumption information," *Energy Build.*, vol. 40, no. 3, pp. 394–398, 2008, doi: 10.1016/j.enbuild.2007.03.007.
[8] "ROCKWOOL," [Online]. Available: https://www.rockwool.com/north-america/products-and-applications/products/toprock-dd/?selectedCat=toprock downloads#Overview.

3rd Conference on Sustainability in Civil Engineering (CSCE'21)
Department of Civil Engineering
Capital University of Science and Technology, Islamabad Pakistan

ZERO ENERGY DESIGN: A CASE STUDY OF RESIDENTIAL BUILDINGS WITH SOLAR ENERGY AS ENERGY SOLUTION

[a] A. Moeez Usman, [b] Hafiz Aiman Jamshaid, [c] Dr. Muhammad Babur

a: Student, Department of Civil Engineering, University of Central Punjab, moeezchaudhry91@gmail.com.com
b: Lecturer, Department of Civil Engineering, University of Central Punjab, aiman.jamshaid@ucp.edu.pk
c: Asst. Prof., Department of Civil Engineering, University of Central Punjab, m.babur@ucp.edu.pk
* A. Moeez Usman: Email ID: moeezchaudhry91@gmail.com.com

Abstract- According to International Energy Agency, existing buildings are responsible for 40% of world's total primary energy consumption and 24% of global carbon emissions. In order to protect our environment from destruction the only effective solution is to cut down the emissions of CO_2 and reduce the consumption of non-renewable energy resources. This case study is about sustainable and energy efficient development of buildings at domestic level (residential buildings) in Punjab, Pakistan. As it is about sustainable development so our main focus is Triple Bottom Line (TBL). This can be achieved through zero energy design concept. It is a case study of two different existing residential buildings in Lahore. Each building is analyzed and the yearly primary energy consumption of each building is calculated individually. Calculations are made to determine the number of solar panels based on experimentally proved formulae. Area required to accommodate these panels is also calculated. At the end recommendations are given to make optimum use of solar energy. Energy saving passive solar techniques are proposed that can highly reduce the energy demand and carbon footprint.

Keywords- Adaptation to climate change, green buildings, residential buildings, zero energy design.

1 Introduction

With an increase in population, energy demand is also increasing at an alarming rate. It has a direct impact on global warming. If energy efficiency improvements are not made in the building sector, energy consumption can increase up to 50% by 2050 [7]. Nowadays, people are inclined towards maintenance and repair instead of new construction because it is cheap, less time consuming and comparatively ecofriendly [1]. Now, designers and contractors are required to initiate energy retrofits to upgrade the energy performance of existing buildings. There is an acute need for making sustainable building retrofits to overcome the problem of global warming in the construction sector. However, building retrofits remain slow due to lack of awareness, uncertain outcomes, and state policies [1].

The solution to achieve energy efficient buildings and reduced carbon footprint related to the operation of buildings is zero energy buildings. Zero-energy buildings improve energy efficiency and reduce the energy demand through various energy-saving measures. They use combination of insulation and renewable energy to reduce and meet the energy needs, thereby achieving the goal of not consuming nonrenewable energy. As a result, there is a reduction of carbon emissions into the atmosphere. Different energy conservation technologies have been employed to realize the concept of zero-energy buildings [7].

Developing countries like Pakistan are far behind the world in contributing to sustainable development and help against the increasing global warming. We really need to work to make optimum use of our renewable resources in order to protect our environment and energy resources for the future generation. In this case study two existing residential buildings are considered. The buildings are analyzed for their yearly primary energy consumption. After analyzing the climate and associated factors solar energy is proposed to be optimum renewable energy solution in our case. Then solar energy demand is calculated with reference to the primary energy consumption of each building. Finally, the number of panels are calculated for each of the residential buildings to fulfill the solar energy demand. Solar energy has a high potential in Pakistan. The main objective of this study is to highlight the techniques we can use to cut our non-renewable energy resources and shift to solar energy as a green and renewable energy resource.

2 Literature Review

The contribution from buildings towards energy consumption, has steadily increased reaching figures between 20% and 40% in developed countries [5]. On the other hand, 40% of total carbon dioxide emitted globally is produced by construction industry only [5]. Zero energy design concept is the optimum solution to this problem. The scope of zero energy design in buildings includes energy conservation, water conservation, environment protection, material conservation and health protection and comfort of occupants [4-6].

The renewable energy e.g. solar energy, wind energy, tidal energy and soil thermal energy should be adopted instead of fossil fuels whose consumption is a direct cause of global warming. Solar energy is the most abundant renewable energy resource available on earth and is also one of the cheapest. Both active and passive energy techniques are employed in zero energy design buildings. Active solar systems involve the use of electrical and mechanical devices that can capture and store heat energy from the sun and can also convert it into electricity. They require a backup system. These systems typically include photovoltaic panels, collectors, voltage controllers, blowers and pumps that work together to process the sun's usable heat. In contrast to active solar systems, passive solar systems do not make use of electrical and mechanical devices that can capture and store energy. Passive designs rely on greenhouse principles to trap solar radiation. A few examples are sunrooms, solar chimneys, trombe walls, solariums, greenhouses etc.

Active solar systems are of three types; Off-Grid, On-Grid and Hybrid systems. Off grid system is independent of the electricity supply by the state (Pakistan Water And Power Development Authority, WAPDA in our case). It requires a backup for energy storage. On grid system requires no backup for energy storage. It is based on net metering. The surplus energy produced by the solar panels is supplied to the grid and vice versa. As WAPDA turns out, the solar power also fails. Hybrid system has a backup for energy storage and has the net metering feature as well. If electrical energy is not available from WAPDA, the load will automatically switch to the solar power and vice versa.

Solar chimney is based on the principle of stack effect. The air inside the chimney gains heat and rises, thus making space for the air beneath. It is usually used for natural ventilation. Solar chimney should be made higher than the roof so that it is exposed to direct sunlight. According to Reyes et al., the wall-roof solar chimney enhances the night time ventilation three times than the roof solar chimney [2].

Solariums are the glass rooms which are used for passive solar heating. They also act as a buffer zone between the outer space and the dwelling. They permit abundant daylight. They are placed on the southern side of the building to gain maximum heat in winter season. The heat is accumulated in the solarium and is then transferred to the inner space of building through mechanical means via ducts [3].

Trombe walls are used for space heating in winter season. Its working principle is based on the principle of thermal siphon. It employs natural hot air for space heating. It is a thick concrete wall with a high heat absorbing material on its exterior surface. A glass cladding is placed at about 2 inches away from the concrete wall on the exterior side. This wall is placed on the south facing of the building. The concrete wall has vents at the floor level and at the roof level connected to the internal space of the building. During day-time the cool air from the internal space enters the trombe wall through the lower vent. Air between the concrete wall and the glass rises upon heating and escapes into the internal space through the upper vent [5].

Sunlight is used for lighting up the interior of the buildings, even those parts of the buildings which have no direct exposure to the sunlight. Now a days many countries are making use of proactive architectural lighting devices which sense and track the solar path and absorb 20%-36% more sunlight as compared to fixed solar devices [5]. Japanese sunflower fiber-optic light guide system is programmed such that it follows the solar path. Business Support Center in Duisburg, Germany is a practical example of this technology [5].

3 Methodology

Two residential buildings are considered for this study, both are in Lahore but at different locations. One is situated at Raiwind Road, Lahore and the other is located in the Bismillah Housing Scheme, Lahore. Number of occupants of the former building are 5 and the latter are 10 respectively.

Annual primary energy consumption for electricity use is calculated for each of the buildings using the data from the utility bills. Units consumed in the last 12 months have been summed up and converted into the primary energy in KWh.

There are different renewable energy resources like solar energy, thermal energy, wind energy, hydropower etc. Wind energy is not feasible in Lahore since the wind speed is usually less than 15 knots in this region. Thermal energy is an efficient renewable energy resource but it is not feasible for residential buildings as it requires a huge setup and is very expensive. For residential buildings, it is not feasible to have a thermal power plant. Same is the case for hydropower plant. Thus, the most suitable renewable energy source for the area under consideration is solar energy.

Data for solar radiations is analyzed for calculating the solar energy potential in Lahore. For this purpose a software, 'Climate Consultant' is used. This software provides ready-made graphical representation of solar radiations throughout the year based on last 30 years recorded data. The data for Lahore was not available on this software so the data of Amritsar has been used since coordinates of Amritsar (31.63˚N and 74.87˚E) are very close to that of Lahore. Also that Amritsar is approximately 50 kilometers from Lahore.

Following formula has been used for the calculation of the output of 1 solar panel.:

$$E = r \times PR \times A \times H$$

Where;

E = output of solar panel

r=efficiency of panels in percentage

PR=performance ratio

A=Total area of panel

H=annual average direct normal solar radiation on tilted panel (shadings not included)

The number of plates required to fulfil the energy demand of each of the residential building, following formula is used:

$$\text{No. of plates} = \frac{Electricity\ consumption(\frac{Kwh}{day})}{Output\ of\ 1\ plate(\frac{KWh}{day})}$$

4 Calculations and Results

Table 1 represents the covered area of each of the residential buildings in square feet and the primary energy consumption of each of the building in KWh/year. The electricity consumed by these buildings is produced by hydroelectric power plants. The hydroelectric power plants usually have efficiency of 90% [3]. So, the primary energy consumption for generating the electrical energy at hydro power plant is calculated by following conversion:

0.9 KWh of electricity consumption = 1 KWh primary energy consumption

Here electrical energy is converted to its source energy (primary energy) to make it relatable and comparable with other natural energy resources (solar energy in our case).

Table 1-Total yearly primary energy consumption

Residential Buildings	Total covered area (sq.ft)	Yearly electricity consumption (KWh/year)	Yearly primary energy consumption(KWh/year)
Raiwind Road (10 Marlas)	2846	5521	6134.3
Bismillah Housing Scheme (8 Marlas)	2949.96	12943.8	14382

Figure 1 is a graph plotted between months of the year on x-axis and solar radiations in Wh/m^2/hr on y-axis based on past 30 years data record. As indicated in the legend, yellow bar represents the direct normal radiations. Direct normal radiations are considered for the analytical calculations of solar panels. Green bar represents the global horizontal radiation and the orange bar represents total surface radiation.

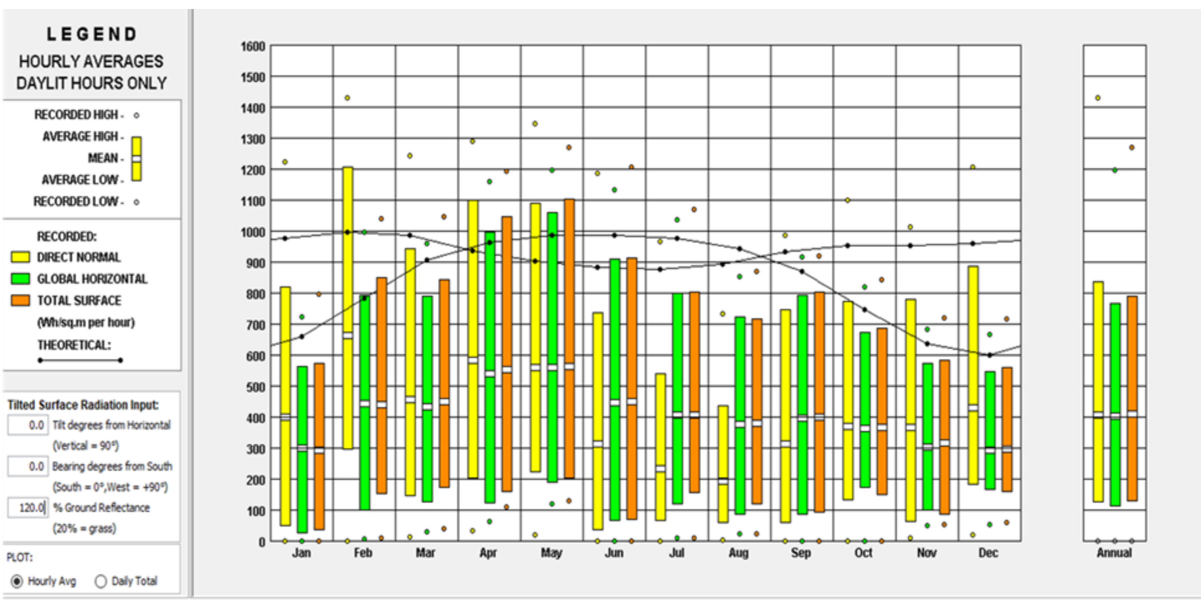

Figure 1: Graph of solar radiations vs time (Source: Climate Consultant Software)

Different types of solar panels are available in the market. Canadian Solar CS6U has been considered in this case. The same model is installed in our university campus. So we easily verified the specifications personally. It has following specifications: -

Table 2-Specifications of Canadian Solar CS6U

Peak efficiency	16.46%
Length of plate	6.43 ft
Width of plate	3.26 ft
Depth of plate	1.6 inches
Weight of plate	22.4 kg

Peak efficiency = 16.46%
Length of plate = 6.43 ft
Width of plate = 3.26 ft
Depth = 1.6 inches
Weight = 22.4 kg
Output of 1 plate denoted by 'E' is calculated as under:
E= r × PR × A × H
A = Area of 1 plate = 6.43*3.26 = 20.96 ft^2 = 1.95 m^2
r = 14% (conservatively)
PR=0.75
H= 200 Wh/m^2.h = 4.8 KWh/m^2.day(From figure 1)
E=1.95×0.14×4.8×0.75 = 0.9828 KWh/day.
For calculating the number of plates required to fulfil the energy demand:

$$\text{No. of plates} = \frac{Electricity\ consumption(\frac{Kwh}{day})}{Output\ of\ 1\ plate(\frac{KWh}{day})}$$

Table 3 gives the information of the number of plates required for each of the residential buildings to fulfil their energy demand.

Table 3-Number of solar panels

Residential Buildings	Yearly electricity consumption (KWh/year)	Daily electricity consumption (KWh/year)	Total number of plates required
Raiwind Road (10 Marlas)	5521	15.126	16
Bismillah Housing Scheme (8 Marlas)	12943.8	35.462	36

The area required for accommodation of these plates is also given in the tabular form in table 4.

Table 4-Area required for accommodation of solar panels

Residential Buildings	Number of plates required	Area required on rooftop for the accommodation of plates	Status of required space availability
Raiwind Road (10 Marlas)	16	335.36	Yes
Bismillah Housing Scheme (8 Marlas)	36	754.56	Yes

5 Recommendations

- The implementation of solar panels for our zero-energy design in the residential buildings not only reduce our nonrenewable energy resource dependency but it will also reduce the carbon footprint and will help in restoring our environment.
- Enough space should be available to accommodate the solar panels and care should be taken that there is no shading over the panels or hindrance to solar radiations.

- The angle of tilt of the solar plates should be determined by tracing the solar path to obtain the maximum efficiency of the plates.
- Hybrid solar system should be installed as we have acute problem of load shedding in our country.
- Passive solar techniques can also be employed for ventilation purposes. In Lahore there is a high cooling demand in summer. Solar chimneys integrated with earth-air heat exchangers can be used for ventilation in summer season.
- Different solar techniques can be implemented in addition to solar panels on industrial and commercial level. For example, proactive solar lighting devices can replace the electrical devices in office buildings and other workplaces.
- We can make use of earth-air heat exchangers integrated with solar chimneys in large closed spaces as in industries, schools, colleges and universities.
- Trombe walls can also be used for the ventilation purposes in winter season, where heat energy from sun is harvested and distributed to the required spaces through vents.
- Passive solar devices can be used to harvest heat energy at large scale in industries with a high demand of heat energy as for boilers in case of textiles industry.

References

[1] J. Lee, M. McCuskey Shepley and J. Choi, "Exploring the effects of a building retrofit to improve energy performance and sustainability: A case study of Korean public buildings", *Journal of Building Engineering*, vol. 25, p. 100822, 2019. Available: 10.1016/j.jobe.2019.

[2] J. Gao, A. Li, X. Xu, W. Gang and T. Yan, "Ground heat exchangers: Applications, technology integration and potentials for zero energy buildings", *Renewable Energy*, vol. 128, pp. 337-349, 2018. Available: 10.1016/j.renene.2018.

[3] J. Kristinnson, *Integrated Sustainable Design*, 1st ed. Delftdigitalpress, 2012, pp. 138-148.

[4] W. Feng et al., "A review of net zero energy buildings in hot and humid climates: Experience learned from 34 case study buildings", *Renewable and Sustainable Energy Reviews*, vol. 114, p. 109303, 2019. Available: 10.1016/j.rser.2019.

[5] Y. Yuan, X. Yu, X. Yang, Y. Xiao, B. Xiang and Y. Wang, "Bionic building energy efficiency and bionic green architecture: A review", *Renewable and Sustainable Energy Reviews*, vol. 74, pp. 771-787, 2017. Available: 10.1016/j.rser.2017.

[6] Y. Lu, X. Zhang, J. Li, Z. Huang, C. Wang and L. Luo, "Design of a reward-penalty cost for the promotion of net-zero energy buildings", *Energy*, vol. 180, pp. 36-49, 2019. Available: 10.1016/j.energy.2019.

[7] Z. Liu, W. Li, Y. Chen, Y. Luo and L. Zhang, "Review of energy conservation technologies for fresh air supply in zero energy buildings", *Applied Thermal Engineering*, vol. 148, pp. 544-556, 2019. Available: 10.1016/j.applthermaleng.2018.

3rd Conference on Sustainability in Civil Engineering (CSCE'21)
Department of Civil Engineering
Capital University of Science and Technology, Islamabad Pakistan

GENERAL OVERVIEW OF SAFETY PRACTICES IN THE CONSTRUCTION INDUSTRY OF PAKISTAN

[a] *Saad Tariq Malik*

a: Department of Civil Engineering, Altınbaş University, Istanbul, saadtariq54@gmail.com

Abstract- Construction Industry of Pakistan is growing rapidly. Whereas accidents and fatalities, rates are also increasing day by day. Because of the lack of seriousness and honesty from concerned regulatory bodies, the Situation is worsening on sites. There is no proper system in Pakistan to check the safety and risk management on Construction sites. Several researchers have proposed solutions to improve the quality of safety management but from the higher management to the lower, but no one is aware of the importance of safety rules. Since there is no safety training and workers are unskilled, the quality of construction is giving an alarming situation. It is a dire need of the hour to take necessary steps and implement the rules for the safety of workers and indeed improve the quality of construction. This research work highlights the current situation and provides a general overview of safety practices in the construction industry of Pakistan.

Keywords- Construction Industry, Pakistan, Safety management,

1 Introduction

The construction industry is vital to both the economy and society. However, it is often regarded as one of the most hazardous industries [1]. The performance of construction projects is significant when discussing safety regulations and requirements for construction projects. Because of its particular environment, uncertain site conditions, unpredictable human behavior, and hazardous activities, the construction industry has higher fatality and injury rates [2].To reduce the ratio of fatalities in Construction Industry globally, Developed countries have implemented several health and safety systems to manage on construction sites [3]. Because of such management consistent decrease in the accident ratio has been recorded for the last 20 years [4]. In developing countries like Pakistan, Mainly stakeholder's primary focus revolves around improving the quality of construction, minimizing cost, and reducing time. While safety factor lies on their least priority. Construction in underdeveloped countries of the world like Pakistan & India, is more labor-intensive than in developed countries, with 2.5-10 times as many workers per milestone [5].

The main dilemma is that all Safety regulatory bodies are almost ineffective and contractors are unable to provide proper recorded documentation of actual injuries and fatalities [6]; [7]. In the Construction industry of Pakistan, another main problem is cultural diversity which relates to differences in language, religion, and culture. This cultural diversity on one end has a bright side as the Construction Industry of Pakistan is providing job opportunities for all areas of the country. But it tends to inhibit safety on the worksite [8]. Various researchers have done research and efforts have been made globally to study safety performances in Construction Industry [9]; [10]; [11]; [12]; [13]; [14]; [15]; [16]; [17]. Therefore, safety systems have been implemented to prevent accidents and increase the performance of specific construction projects [18]; [19]. Right now the main focus is to achieve zero accidents and target ultimate safety performance [20]. For several sites, there are no programs, no briefing for new staff or employees, there is no identification of risks and no safety meetings take place. All the workers are responsible to learn from their own experience by doing mistakes. Not only that, there is a lack of medical facilities, shanty housing and low standard sanitation lead to a risky future of the construction site [8].

For contractors in developing countries like Pakistan, one of the most important steps in controlling costs of the construction project. The contractors are obligated to implement safety but as a business strategy which although has led to little improvement in global construction safety records. There is a significant difference between large and small contractors. Most of the firms have a safety policy of the site but it is limited to only paperwork and employees are unaware of safety rules and regulations. Unsafe conditions exist on many small and large sites and workers are faced with various kinds of risk [21].

Despite the recent growth of construction activities in recent years, Pakistan's construction industry is plagued by dangerous working conditions, owing to a lack of a clear regulatory structure [22]. Reactive and risky practices have become the standard in the construction industry as a result of a lack of safety infrastructure [7]. In any sector, the value of a strong regulatory system for enforcing safety legislation for worker safety cannot be overstated. Despite the industry's economic significance, the government is paying less consideration to worker protection, and as a result, institutional governance has little influence [22].

The main objective behind this research work is not only assessment of current safety practices in the construction industry of Pakistan, but it will also explain the causes of accidents and injuries, reasons behind violation of safety rules and regulations, and highlight the impact of safety management on construction sites.

2 Assessment of Safety practices in CI of Pakistan

The majority of the time, stakeholders demand better quality and speedy work at the minimum possible cost. But unfortunately, there is no specific budget for a safe and healthy work zone. Smaller construction companies do not have any policy for safety at construction sites thus exposing workers to the hazardous condition [26].

As per the annual assessment of the Pakistan Bureau of Statistics, from the total labor force (59.79Million), 7.4% (4.424 million) labor is associated with the construction industry. Table 1 shows a consistent increase in the rate of accidents and injuries i-e 14.55% in 2006 to 15.24% in 2012. Therefore, it lies in the 2nd place of the most injury lying industry just after agriculture sector [27].

Table 1: Occupational Accidents and Injuries; Division by different major industries of Pakistan (percentage-wise) [27]

Type of Industry	**Financial Year**						**Ranking**
	2006-2007	**2007-2008**	**2008-2009**	**2009-2010**	**2010-2011**	**2012-2013**	
Agriculture	40.94	46.84	50.43	50.2	49.8	49.1	1
Mining/Quarrying	0.29	0.09	0.33	0.1	0.2	0.2	
Manufacturing	15.21	12.72	13.96	12.8	15.8	13.3	3
Electricity, gas and water	0.87	0.51	0.71	0.4	0.2	0.5	
Construction	**14.55**	**14.93**	**14.54**	**14.3**	**13**	**15.2**	**2**
Retail Trade, Restaurants and Hotels	9.26	7.96	7.54	10.6	10.3	9.2	4
Transport/Communication	7.98	8.02	8.14	8	7.1	7.3	
Community/Social Services	10.56	8.39	4.33	3.5	3.3	5.1	
Other Industries	0.34	0.54	0.02	0.1	0.3	0.1	

2.1 Causes of Accidents and Injuries on construction site

The prevention of accidents is the key topic of construction safety. Several types of research were conducted to provide insights into the nature and causes of construction industry accidents. Some research listed the key causes of worker's death, while others established the main types of building accidents [28]. According to research work on 100 individual construction incidents. The study presented key accident factors in the form of employees' or team workforce (70% of accidents), workplace problems (49%), equipment deficiencies (including PPE) (56%), material adequacy and condition problems (27%), and risk management deficiencies (84 percent) [29].

In descending order, the main reasons for accidents on construction sites are the falling of workers from height, being killed from electrocution, being snatched in between machinery, and being struck by objects falling from height [30]. Another major reason for accidents on construction sites is a high number of unskilled workers because of higher illiteracy percentage [31]. According to the research report, causes of accidents in Malaysia are workers' negligence, failure to follow work protocols, working at height, operating equipment without safety measures, inadequate site management, rough work operations, workers' lack of experience and ability, failure to use personal protective equipment, and workers' poor attitude toward safety are the leading causes of construction accidents [32].

2.2 Level of safety awareness on construction sites

After doing an intensive amount of research an academic revealed that the primary focus of the majority of the contractors is revolving around increasing profit margin in a project. There are no rules and regulations for safety and the policies are not up to date. Another main point reveals that there are no training programs for existing and new workers on many sites. No safety drills are being practiced by any kind of workers and there are no safety engineers present on sites. So the workers are exposed to the dangerous work environment and the only way they can learn about safety procedures are by doing mistakes and this way they will get experience. By doing such 'mistakes' or 'errors', workers take a risk and some of the common incidents happen like workers falling from a height because of unreliable and unsafe placement of scaffolding or due to unavailability of safety belts. Also, there is no proper cleaning of the sites after the completion of any activity. Many things like pieces of steel, electric wires, or sharp objects are spread on the whole area which can create a risky mess for the workers. Another shocking point was discovered from the interviews conducted by different contractors and project managers are that accidents are not reported to concerned authorities as the contractors are afraid of their qualitative assessment by the client. In underdeveloped countries like Pakistan, Rules and regulations for safety management are not enforced properly [4].

It can be seen from figure 1, (a) 70% of the workers on construction sites are unaware of the safety rules and they think that labor does not need to take personal care and work in a comfort zone. (b) So, a higher percentage of workers tend to resist the training sessions and get easily annoyed if asked to follow basic safety precautions. (c) The majority of the workers and contractors believe that by following safety rules and taking precautions, the overall progress of the project will be affected. Very few of them think that taking safety measures has a positive effect on the quality of a project [8].

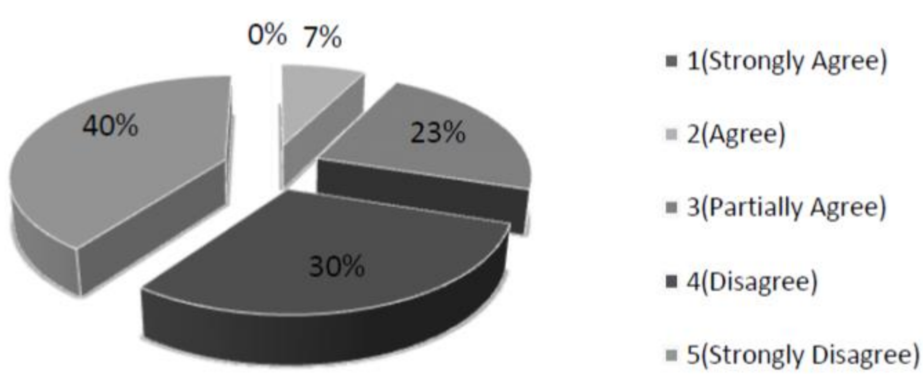

(a)

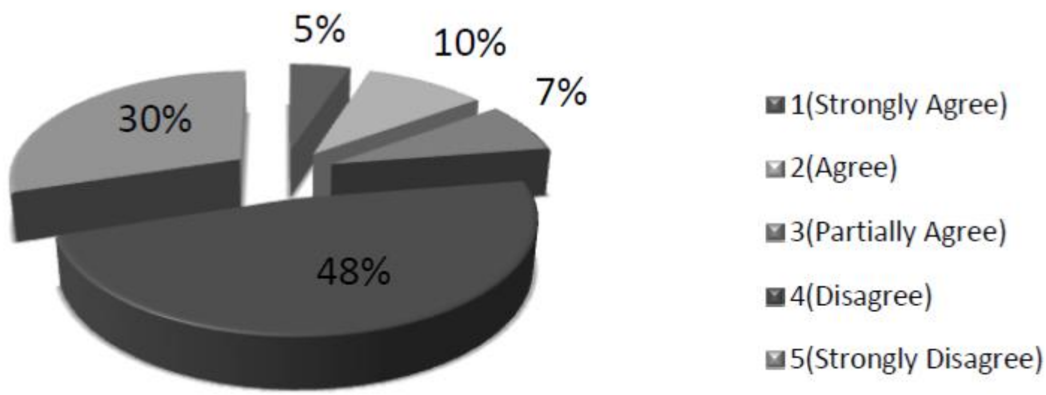

(b)

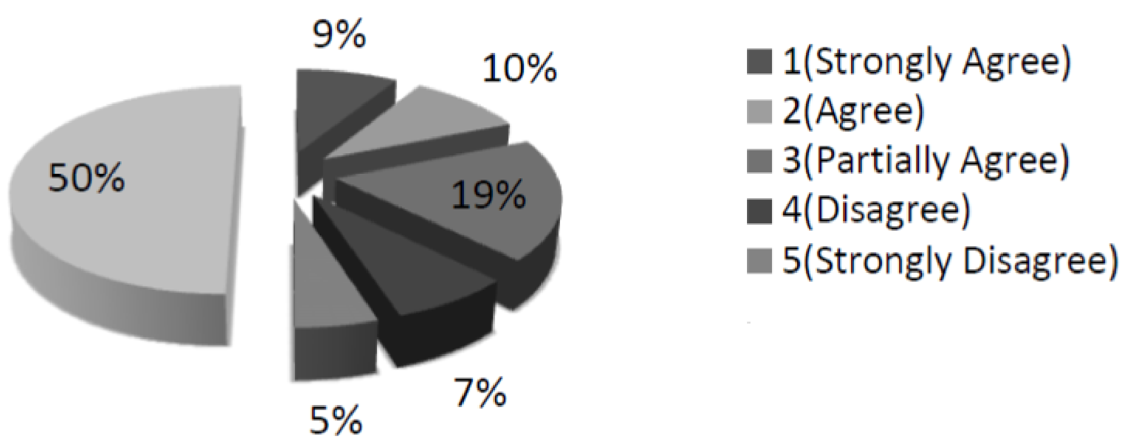

(c)

Figure 1: (a) level of awareness for safety, (b) Labor behavior toward safety measurements, (c) Impact of taking safety precautions

2.3 The reason behind violation of safety rules and regulations in Pakistan

With time majority of the construction firms do not upgrade their safety manuals [22]. Also, safety policies are prepared as a formality only for documentation purposes [31] [33]. Researchers evaluated the effect of awareness, physical and supportive environments on the culture of safety and highlighted neglected practices for safety such that; use of low-quality scaffolding without guards, faulty stepladders not correctly bound, working on a roof without the use of any protection, and hand-held deep excavation without using of any straps [34] [35]. The most commonly neglected activity on construction sites is safety training [36].

3 Impact of safety management on construction sites

Institutional procedures are not strong to formulate, implement and monitor safety rules and regulations. The deployment of safety management systems does not take place on construction sites. Data are not easily available on injury and death rates and scientific literature is not available on construction safety either. These must increase awareness of safety management in the country [4].

The Directorate of Workers Education (DWE), established in 1982 under the Ministry of Labor, is a training and educational body responsible for raising awareness and providing information on rights of labor and social issues by mounting various courses throughout the year for employees and union officials and management representatives (GOP, 2005). There are several strict rules and regulations on child labor and the facility of a minimum wage. Although there is a difference in wages of urban and rural areas. Government in central areas do revise periodically labor wages. But unfortunately, the implementation of safety regulations in Pakistan is not strictly followed. DWE works under the Ministry of Capital Administration & Development at the federal level. However, it has unsatisfactory performance. A secondary entity called `The Center for Improvement of Working Conditions & Environment (CIWCE) ` has been established in the Province of Punjab by the Labor & Human Resource department in Lahore which provides professional and authentic services in the OH&S sector [4].

Few of the private institutions also provide OH&S training for the industry, such as; OCSP, OCTI, and the Vivid Institute of Occupational Safety and Health, although also on a commercial basis (VIOSH). PEC also conducts workshops on safety awareness and mandatory short CPDs, however, such training sessions are for engineers and supervisors only, whilst for construction workers no training is arranged [37].

PEC has included OH&S clauses in their manuals; however, they are largely not implemented because any concerned regulatory body is not there [19].

a) Part I (General Contract Conditions) clause 19.1 of PEC's standard bid documents (PEC, 2007, p.90).

b) Precautions for safety: Part II (Particular contractual terms) clause 19.3 of the standard PEC bidding document. (PEC, 2007, p.152).

4 Results

This is an alarming situation in the Construction industry of Pakistan that in the 21st-century workers are not aware of their rights and they lack seriousness towards applying safety rules while working on site. Several types of research have been done in regards to creating awareness among the higher concerned regulatory bodies to start a proper campaign in the Construction Industry to minimize the ratio of injuries and accidents. Pakistan Engineering Council has included clauses from OH&S, But due to carelessness and the non-serious attitude shown by concerned regular authorities, there is no proper check and balance on constructions sites.

What the industry most likely lacks is a clear, detailed, and yet successful strategy. Workers often tend to decline the importance of using safety gear because of illiteracy. The majority of the Contractors on the other hand have only one main focus which is increasing profit margin. So, they ignore to formularize strategies for safety management on their sites. PEC is arranging seminars, webinars, and workshops, but those are limited to only engineers. Whereas there is no proper safety training given to workers before starting any activity.

5 Conclusion

The implementation of safety rules and regulations on projects is clearly neglected in Pakistan's construction industry. According to the Pakistan Bureau of Statistics' annual evaluation, the ratio of accidents and injuries plainly demonstrates the inadequacy of Pakistan's regulatory authorities. This research study gives an overview of safety practices being implemented in the Construction Industries of Pakistan and based on the findings following conclusions are made:

- H&S workshops help in creating awareness among the concerned professionals. Higher Education Commission can play a vital role here in the modification of the education system. The concerned department of HEC can make a policy for the Engineering department of the university to arrange health and safety training and workshops for students to participate and perform the drills practically on actual construction sites, before graduating. This will help the fresh engineers to realize the importance of safety and risk management.

- By introducing a Quality grading system for a construction company. If carefully incorporated in PEC safety rules and regulations documents, monthly reports for implementation of health and safety rules will be assessed and points will be granted on basis of performance. Not only it will help in creating healthy competition between companies, it will also help in creating more jobs for fresh and experienced engineers, thus lowering the ratio of unemployed Engineers.

- Pakistan's construction industry lacks serious commitment to implement safety rules and regulations on construction sites. As per the above discussion, the presence of a safety engineer is mandatory on every construction site to maintain the quality of work, irrespective of the category of company, given by PEC.

Just because of lack of safety and risk management Pakistan has gone through a severe catastrophe in the 2005 earthquake. Now the question arises that are all concerned departments including PEC are waiting for other disasters? Why the concerned higher authorities are not taking the necessary steps to overcome these major problems?

References

[1] Recarte Suazo, Guillermo Arturo and Jaselskis, Edward J, "Comparison of construction safety codes in United States and Honduras," *Journal of construction engineering and management,* vol. 119, no. American Society of Civil Engineers, pp. 560-572, 1993.

[2] Ho, Derrick Chong Pui and Ahmed, Syed M and Kwan, Jack Chu and Ming, Fox Young Wei, "Site safety management in Hong Kong," *Journal of Management in Engineering,* vol. 16, no. 6, pp. 34-42, 2000.

[3] Chan, Albert PC and Wong, Francis KW and Chan, Daniel WM and Yam, Michael CH and Kwok, Albert WK and Lam, Edmond WM and Cheung, Esther, "Work at height fatalities in the repair, maintenance, alteration, and addition works," *Journal of construction engineering and management,* vol. 7, pp. 527-535, 2008.

[4] Choudhry, Rafiq M and Fang, Dongping and Rowlinson, Steve, "Challenging and enforcing safety management in developing countries: A strategy," *International Journal of Construction Management,* vol. 8, pp. 87-101, 2008.

[5] Koehn, Enno "Ed" and Kothari, Rupesh K and Pan, Chih-Shing, "Safety in developing countries: professional and bureaucratic problems," *Journal of Construction Engineering and Management,* vol. 121, pp. 261-265, 1995.

[6] Farooqui, RU and Ahmed, SM and Panthi, K, "Developing safety culture in Pakistan construction industry--an assessment of perceptions and practices among construction contractors," in *Proceedings of the Fourth International Conference on Construction in the 21st Century: Accelerating Innovation in Engineering, Management and Technology (CITC IV 2007), Gold Coast, Australia,* 2007, pp. 420-437.

[7] Ali, Tauha Hussain, "Influence of national culture on construction safety climate in Pakistan," *Griffith University Nathan (Queensland),* 2006.

[8] Farooqui, RIZWAN U, "An exploratory study probing into the factors causing safety nonperformance in the Pakistani construction industry," in *45th Institute of Engineers Convention*, 2012, pp. 1-12.

[9] Jannadi, M Osama and Assaf, Sadi, "Safety assessment in the built environment of Saudi Arabia," *Safety Science,* vol. 29, no. 1, pp. 15-24, 1998.

[10] Sawacha, Edwin and Naoum, Shamil and Fong, Daniel, "Factors affecting safety performance on construction sites," *International journal of project management,* vol. 17, no. 5, pp. 309-315, 1999.

[11] Siu, Oi-ling and Phillips, David R and Leung, Tat-wing, "Safety climate and safety performance among construction workers in Hong Kong: The role of psychological strains as mediators," *Accident Analysis \& Prevention,* vol. 36, no. 3, pp. 359-366, 2004.

[12] Tam, CM and Zeng, SX and Deng, ZM, "Identifying elements of poor construction safety management in China," *Safety science,* vol. 42, no. 7, pp. 569-586, 2004.

[13] Choudhry, Rafiq M and Fang, Dongping and Mohamed, Sherif, "Developing a model of construction safety culture," *Journal of management in engineering,* vol. 23, no. 4, pp. 207-212, 2007.

[14] Alarc{\'o}n, Luis Fernando and Acu{\~n}a, Diego and Diethelm, Sven and Pellicer, Eugenio, "Strategies for improving safety performance in construction firms," *Accident Analysis \& Prevention,* vol. 94, pp. 107-118, 2016.

[15] Okoye, Peter Uchenna, "Improving the safety performance of Nigeria construction workers: a social ecological approach," *Universal Journal of Engineering Science,* vol. 4, no. 2, pp. 22-37, 2016.

[16] Misiurek, Katarzyna and Misiurek, Bartosz, "Methodology of improving occupational safety in the construction industry on the basis of the TWI program," *Safety science,* vol. 92, pp. 225-231, 2017.

[17] Dong, Shuang and Li, Heng and Yin, Qin, "Building information modeling in combination with real time location systems and sensors for safety performance enhancement," *Safety science,* vol. 102, pp. 226-237, 2018.

[18] Wilson, Joe M and Koehn, Enno "Ed", "Safety management: problems encountered and recommended solutions," *Journal of construction engineering and management,* vol. 126, no. 1, pp. 77-79, 2000.

[19] Awwad, Rita and El Souki, Omar and Jabbour, Melanie, "Construction safety practices and challenges in a Middle Eastern developing country," *Safety science,* vol. 83, pp. 1-11, 2016.

[20] Zwetsloot, Gerard IJM and Aaltonen, Markku and Wybo, Jean-Luc and Saari, Jorma and Kines, Pete and De Beeck, Rik Op, "The case for research into the zero accident vision," *Safety Science,* vol. 58, pp. 41-48, 2013.

[21] Farooqui, Rizwan U and Arif, Farrukh and Rafeeqi, SFA, "Safety performance in construction industry of Pakistan," in *First International Conference on Construction In Developing Countries, Karachi, Pakistan*, 2008, pp. 74-87.

[22] Raheem, A and Hinze, J, "Improving the existing regulatory infrastructure for worker safety in the construction industry of Pakistan," in *Proceedings of the International Conference on Safety, Construction Engineering and Project Management, Islamabad, August 19*, 2013.

[23] Makki, Anas A and Mosly, Ibrahim, "Determinants for safety climate evaluation of construction industry sites in Saudi Arabia," *International journal of environmental research and public health,* vol. 17, no. 21, p. 8225, 2015.

[24] Liu, Hao-Tien and Tsai, Yieh-lin, "A fuzzy risk assessment approach for occupational hazards in the construction industry," *Safety science,* vol. 50, no. 4, pp. 1067-1078, 2014.

[25] Patel, DA and Jha, KN, "Developing a process to evaluate construction project safety hazard index using the possibility approach in India," *Journal of Construction Engineering and Management,* vol. 143, 2017.

[26] Azhar, Nida and Farooqui, Rizwan U and Ahmed, Syed M, "Cost overrun factors in construction industry of Pakistan," in *First International Conference on Construction in Developing Countries (ICCIDC--I), Advancing and Integrating Construction Education, Research \& Practice*, 2008, pp. 499-508.

[27] "PBS (2012-2013). Pakistan Bureau of Statistics - Labour Force Statistics. Online at http://goo.gl/BGIoZu,," [Online].

[28] Sanni-Anibire, Muizz O and Mahmoud, Abubakar S and Hassanain, Mohammad A and Salami, Babatunde A, "A risk assessment approach for enhancing construction safety performance," *Safety science,* vol. 121, pp. 15-29, 2020.

[29] Haslam, Roger A and Hide, Sophie A and Gibb, Alistair GF and Gyi, Diane E and Pavitt, Trevor and Atkinson, Sarah and Duff, Alexander Roy, "Contributing factors in construction accidents," *Applied ergonomics,* vol. 36, no. 4, pp. 401-415, 2005.

[30] Nawaz, Tahir and Ishaq, Azam and Ikram, Amjad Ali, "Trends of safety performance in construction and civil engineering projects in Pakistan," *Civil and Environmental Research,* vol. 3, no. 5, pp. 23-40, 2013.

[31] Jafri, SF, "Safety and security polices, pre and planned construction phase," in *3rd International Conference on Construction in Developing Countries (ICCIDC--III) "Advancing Civil, Architectural and Construction Engineering and Management," July 4*, 2012, pp. 288-294.

[32] Hamid, Abdul Rahim Abdul and Majid, Muhd Zaimi Abd and Singh, Bachan, "Causes of accidents at construction sites," *Malaysian journal of civil engineering,* vol. 20, no. 2, pp. 242-259, 2008.

[33] Masood, Rehan and Farooqui, RU and Choudhry, Rafiq M and Riaz, Zainab and Munir, Yousuf, "Analyzing health and safety (H\&S) policy to evaluate top management commitment level," in *CIB W099 International Conference "Modeling and Building Health and Safety," September 10*, 2012, pp. 721-731.

[34] Mohamed, Sherif and Ali, TH and Quresh, AS, "Safety behavior in the construction industry in Pakistan," *Mehran University Research Journal Of Engineering And Technology,* vol. 25, no. 3, p. 207, 2006.

[35] Qazi, A and Ye, Lieping and Choudhry, R, "Demand and awareness of construction safety practices in Pakistan," in *CIB W099 International Conference on "Global Unity for Safety \& Health in Construction". 28-30 June 2006*, 2006, pp. 470-475.

[36] Zahoor, Hafiz and Choudhry82, Rafiq Muhammad, "The most neglected construction safety practices in Rawalpindi/Islamabad," *Modeling and Building Health and Safety,* pp. 312-322, 2012.

[37] Khan, Ahsan Ali, Sadia Ajmal, and Rizwan U. Farooqui, "Investigation of labor and management perception, commitment and attitude towards safety," *ICSCEPM'13,* 2013.

3rd Conference on Sustainability in Civil Engineering (CSCE'21)
Department of Civil Engineering
Capital University of Science and Technology, Islamabad Pakistan

BUILDING INFORMATION MODELING FOR HISTORIC STRUCTURES: A CASE STUDY OF HISTORIC SHRINES OF MULTAN

[a] Hafiz Noman Ahmad, [b] Syyed Adnan Raheel Shah, [c] Ahmed Faraz, [d]Sunera Imtiaz,

a: Department of Civil Engineering, Pakistan Institute of Engineering & Technology, Multan
b: Department of Civil Engineering, Pakistan Institute of Engineering & Technology, Multan.
c: Department of Architecture Design, NFC- Institute of Engineering & Technology, Multan.
d: Department of Building and Archi Engineering, Bahauddin Zakariya University, Multan.
* Corresponding author: Email ID: Adnanshah@piet.edu.pk

Abstract- Digital documentation is a new technology that works to secure quality information and helps in technical decision-making. This technology can also be used for infrastructure conservation and maintenance. In this study, one digital documentation technique as a securing and handling instrument of the essential information has been used. In this study, the methodology of the historical building information modeling (HBIM) system has been adopted to study the historic shrine building. In two stages, this technique was applied, the first one was portrayed by the exploratory exercises needed for the building, and the second one was to thoroughly define the calculation of a portion of the complicated, historical building information modeling (HBIM) system. The model development process also revealed few challenges, which were encountered during the information collection processing and analysis procedure. This study provides a pattern to apply the HBIM technique that will help to monitor and record the time to time conservation and rehabilitation process for historic buildings.

Keywords- Building, Historic Structures, Shrines, HBIM

1 Introduction

Digital information systems can be applied for architectural heritage management by digitizing and managing existing building stock data [1]. Public and private building history administration can follow digitalization by using modern IT methodologies and technologies, like some that software which is used in the building modeling, also the establishment of special processes [2]. The goal of this contribution is to demonstrate the preliminary findings of applying this technique to a building complex that began with its historical construction configuration. The social and social qualities of Italy which, with regulations that fail to encourage proper recovery, decontamination, and new development work, are considered traditionalists about existing history raise doubts about the conditions in which these are designed. Due to the lack of special Seismic-free and power legislation, there are approximately one-twenty lakhs civil or social and non-public structures at the Federal state, with higher than seventy percent of them erected before the 1980s [2, 3]. In this way, careful consideration of the possible benefits of an organized structure classification given huge completion and extreme latest day imitative task in the condition of security, capability, and condition is necessary. While the current city development and construction guidelines do not operate with precise intercessions, a genuine development in the planning and execution, both methodological and creative, is now required. As a result, the situations that have been solidifying regarding the interdisciplinary, electronic, also with contributed executives of the development cycle (starts from study to incorporated plan, starts from administration and decapitation of works to upkeep and deactivate of the structures), despite being delay in a few specific circumstances, can support another leaven in the development area. There are not uncommon for new administrative changes to urge, at individual levels, and the approval of building information modeling tactics and devices for public use, first by Europeans and then by Italians[4-6]. Administrative rules, along with the capabilities of the building information modeling system, made the coordination of these devices critical, not only in terms of structure development, and in terms of the improvement and development of the present cultural structure. In this vein, the acronym heritage building information modeling was created, which stands for both ancient-BIM and HBIM [7, 8]. To summarize, one needs to illustrate using the article guideline demonstrating for the software using instruments replication of present structures, both verifiable and not authentic [9]. The establishment of robust duplicate necessitates a thorough cycle of information gathering, which includes both literary exploration and structural investigations. Furthermore, mathematical data does not address every aspect of building information modeling (BIM) or historical building information modeling (HBIM): non-realistic information might be supplied as information base fields inside particular components. The measure of information that must be kept for an object, regardless of whether it is mathematical or helpful, is defined by a list in the reference principles. A threshold called Level of Reliability (LOR) that illustrates the ontological correlation of the single computerized component with its reporter in reality as a possible solution to this problem is also used [10]. Different studies have expresses the procedure that the reconciliation of data from total station and computerized photogrammetry may also be used to construct Building Information Modeling models [11].

This study has been designed for the application of Historic Building Information Modeling (HBIM), as public and private building history administration can follow digitalization by using modern IT methodologies and technologies, like the BIM technique using Revit software which is used in the building modeling. This study will serve as an example for the start of data digitalization of historic structures leading to conservation and rehabilitation.

2 Research Methodology

Examining and research are being done to define solid and legitimate techniques both for policy management and private substances, to improve the interface to develop and supervise Building Information Modeling models for the existing structure stock. This methodology is applied in the following steps as at different levels [2] are; (1) "Describe Model", Model indicates the attributes that Building Information Modeling objects should possess as the interaction progresses; (2) "Information securing", It incorporates completely gathering exercises of mathematical and non-mathematical data; (3) "Recreation Model", for example, formation of the advanced duplicate of the structure being referred to; (4) "Model verification", involving the essential investigation and Conflict Location tasks; (5) "Model remedy", It may need the merging of fresh reviews and acquisitions; (6) "Information the board", Where the model, together with the obtained data, is delivered into the executive's stage of information.

Each phase deals with a propane activity, but that it may be quite vital to do a recursive interaction concurrently so that the results are suitable for the unique office demands. In an anticipation of this interaction, this interaction results in a model that addresses not only an informatic structural model at a time to, a compartment of all information that is effective in the chronicles but can also be used as an explicit foundation but a true strong article that can be upgraded. The finished submissions thus far and associated with local innovations with enough two-dimensional representations to refurbish the three-dimensional example model [12]. The study of the impacts of prior reviews not only revealed problems with the unquestionable quality and accuracy of the information, but also the necessity of standardizing data to create an interesting data collection. The dedication in this respect reveals the initial findings obtained by the study of an authentic structural complex, which has undergone several long-term alterations. In particular, the study of the proven – precious configuration of the Bahauddin Zakariya Complex (as shown in Fig.1) located in Multan near to a clock tower, midway having a position with the heritage of Sufism, was our focus.

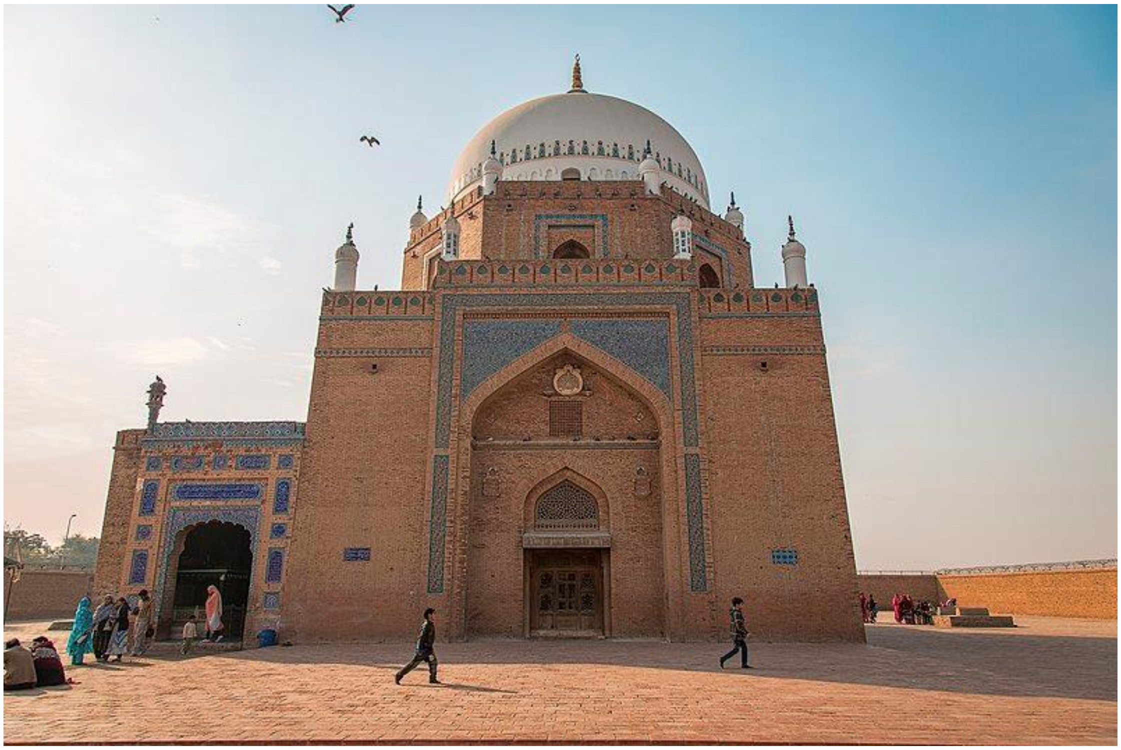

Figure 1. Case Study Area- Bahauddin Zakariya's Shrine

3 Data Analysis and Discussion

Bahauddin Zakariya's shrine is considered to be one of the most important temples in the southern part of Punjab. It was built in the early 18th century by the governor Durrani of Multan and Nawab Ali Muhammad Khan Khakwani and serves as the prototype of a particular architectural style in Multan. The sanctuary is located just to the north of the old walled city of Multan, is a large, square building, with a 51 - foot base. The walls make a great layout, which is on top of the square base. Surrounded by tapered cylindrical columns and at the very top of the tree is a white tomb. The temple is surrounded by a large courtyard of a few hundred square feet. Like most of the Muslim holy places, the grand structure creates the illusion in a vertical movement in the direction of the sky, which points to the harmony of the divine. Although the main building was built with polychrome earthenware tiles are the most well-known brands, blue tile around it. These tiles reflect a Central Asian, Persian, and Indian influence in the field of architecture. Glazed ceramic tiles are locally well-known as Kashi, and continue to be, a specialty of Multan. In the name of Kashi, suggesting a direct route to Kashgar, a city in the Province of Xinjiang in West China. In a tradition going back to the city of Kashan, in Central Iran, this also is known for its decorative tiles. However, over the centuries, Kashi Multan's work has a unique local style. The colors that are used with the tiles in the sanctuary are mainly cobalt blue, turquoise, and white and are located in the form of complex geometric patterns. These include scrolls, curves, pentagons, hexagons, and a command post. The floral patterns are inspired by local flowers, vines, and roses. Today Multan is known as the "City of Saints" because many other famous saints such as Shah Rukn-e-Alam, Sabzwari Multani, Muhammad Shah Yousaf Gardez, and Obmany Tabrez, are also buried in the same city [13, 14].

Figure 2. Google earths image of Bahauddin Zakariya

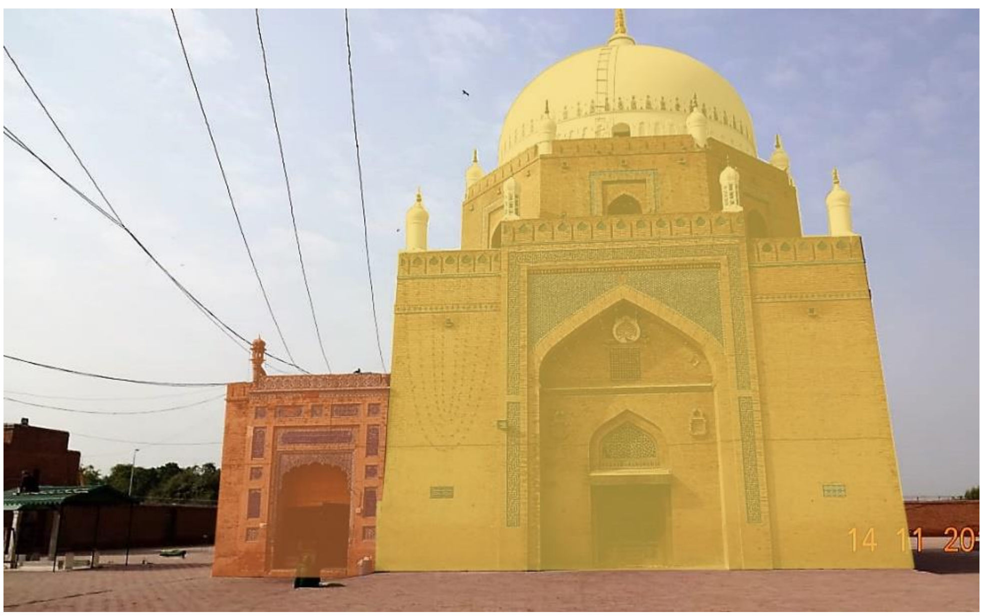

Figure 3. Scan Focus of Bahauddin Zakaria Complex Compound

The Study and observations about the complex Bahauddin Zakaria were thought carefully and thoughtfully, the project was taken over by a specialized professional as well the reliable information as shown in Fig.2. That is why it is important to understand the various tools to provide a consistent model of high quality. These operations have been divided into two distinctive phases; the first phase of the photogrammetric measurement and the second is the use of eligible equipment. For the structural study, a research review is conducted to open up an understanding about the components of the fields; and, in the course of this work, by the digital camera, the photos were taken, to make use of photographic activity, to obtain the first axis according to the set design, and the outer square as shown in Fig.3. Thus, the data developed to the point cloud can help to understand the importance of the structure inside it. Even as it is, is of no value for the next period, from the use of information modeling in the building model, the professional has revealed it to have a complete understanding of the features of the service, and will eliminate the need for a top-down review of archiving of all relevant parts of the building, the premises as shown in Fig.4.

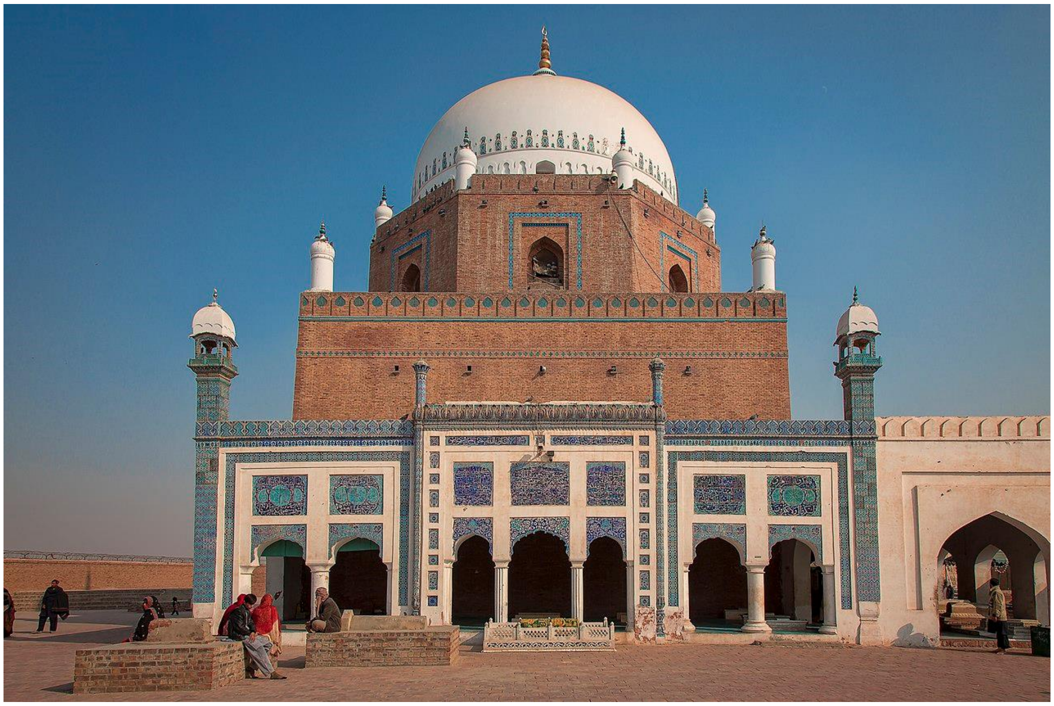

Figure 4. Snapshot of the Earth Photogrammetry Developed First Point Cloud.

The important hardware to the reproduction of complex's whole amount and the specific order re-engineering was accordingly classified i.e., total station, digital camera & measuring gadgets.

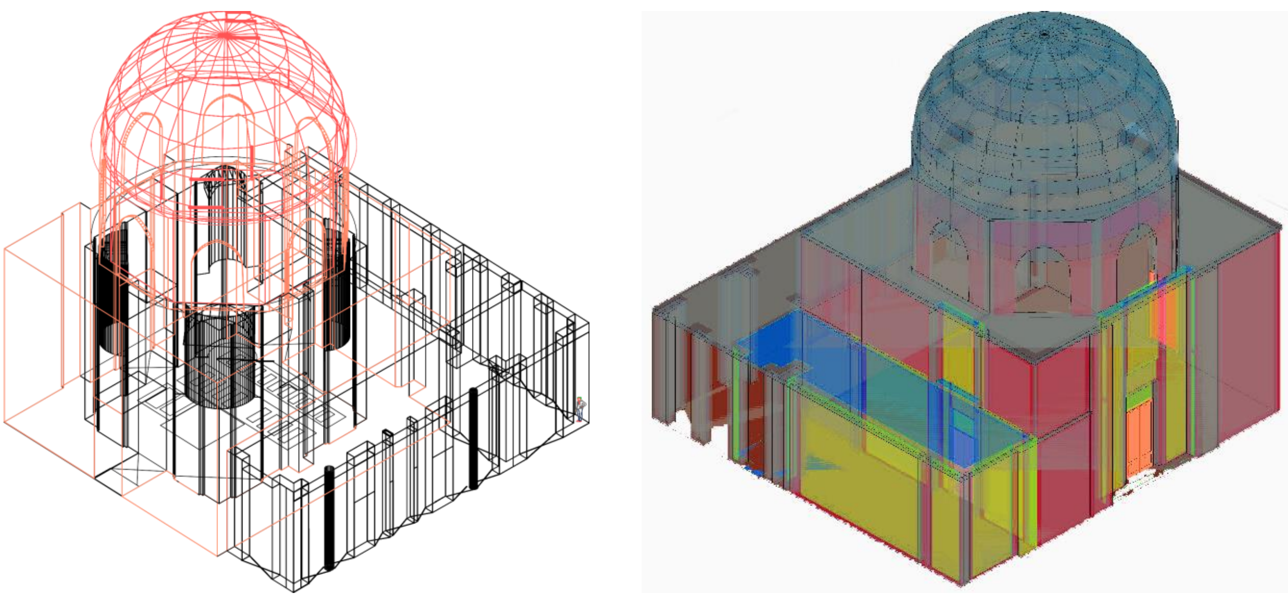

(a) (b)

Figure 5. (a). Structural information is shown with the help of Building Information Modelling (BIM) (b). An energy model is achieved with the help of Auto Desk Revit.

Period of information handling and results examination, the result was considered authentic. The result was considered authentic. Preparation for the photographic shootings, setting up dot cloud, took the photogrammetric cycle, which had merely affected the group region. Later by application of BIM, structural information is shown with the help of building information modeling (BIM) and the energy model is achieved with the help of auto desk Revit.

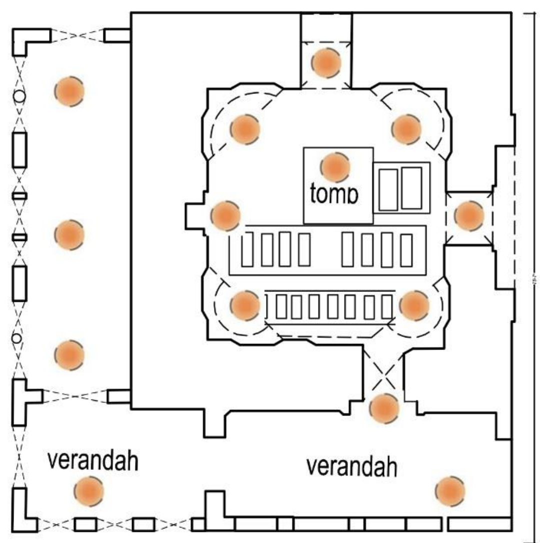

Figure 6. Study of the Building's Floor with Digital Gadgets.

The combined file including each output one had to deal with the yield files. had to deal with. In this respect, one needed to have a more "light" file that reacted to the requirements of the company at the same time. Results were regarded substantial to be accompanied by the Gadgets. Cloud was cleaned first, then the model was included in the Recap schedule. In addition, this software allowed the board to submit the file to the configuration controlled by the Building Information Modelling (BIM) stage, Revit, to carry out further manual cleaning and information.

The cloud and plants recently recuperated from the specialist office files were then taken to the building information modeling climate; the link between these two enables the integrity of the two-dimensional drawings to be confirmed as shown in Fig.6, at the next stage which exhaustively covered the 3-dimensional information. The information security measure was closed with an affirmation of the legitimacy of the information from the drawings and refurbishment of the model may be commenced here.

4 Conclusion

This study has been designed for the application of Historic Building Information Modeling (HBIM) using modern methodologies like the HBIM technique using Revit software which is used in the building modeling with the focus on the case study of Bahauddin Zakariya Shrine. This methodology helps to monitor and digitally document the shrine data and can also help in the time-to-time monitoring of structural health. Its utilization permits one to make extraordinary data sets, containing all the data, mathematical and something else, fundamental for the whole helpful existence of a structure. This information is vital if one can consider the conceivable outcomes identified with the administration and upkeep of structures. A comprehensive framework can help in the utilization of BIM technology for the digitization of records and data for complete analysis and conservation. Despite the interoperability concerns across different platform architectures, there are other difficulties, such as certain difficulties for government departments like the Archeology Department of Punjab, to alter their operational plan. These problems are combined with the difficulties mentioned with the requirement for reliable and scientifically regulated information that follows from top to bottom. Information such as mists can, for instance, be incorporated and utilized for subsequent purposes despite its rudimentary characteristics, to digitize the present structured stock and concurrently. In the first step, for example, the points mentioned can provide the article a thorough understanding of the issue that has been described. The social legacy of shrines gradually uses point mists that are included in an extended or computer-generated reality to provide higher structural pleasure. Therefore, it is possible to produce sketches for different reasons, using different instruments; depending on the cause, one may use arrangements that allow the administration to maintain further intricacies or rash to see and understand.

Acknowledgment

The authors would like to thank every person/department who helped throughout the research work, particularly XEN Mr. Ghulam Muhammad, Department of Archeology, and Mr. Carlo Giannattasio (University of Naples Federico II, Naples, Italy) for being an inspiration for this field of study.

References

[1] J. Nieto, J. Moyano, F. Rico, and D. Antón, "Management of built heritage via the HBIM Project: Acase study of flooring and wall tiling. Virtual Archaeology Review, 7, 14, 1–12," ed, 2016.

[2] C. Giannattasio, L. M. Papa, P. D'Agostino, and S. D'Auria, "The BIM Model for Existing Building Heritage: From the Geometric Data Acquisition to the Information Management," in *Congreso Internacional de Expresión Gráfica Arquitectónica*, 2020, pp. 311-322: Springer.

[3] C. dei Deputati, "Commissione parlamentare d'inchiesta sulle condizioni di sicurezza e sullo stato di degrado delle città e della loro periferia," *Relazione sui sequestri di persona a scopo di estorsione,* 2017.

[4] L. EU, "Directive 2014/24/EU of the European Parliament and of the Council of 26 February 2014 on public procurement and repealing Directive 2004/18/EC Text with EEA relevance," 2014, Available: http://data.europa.eu/eli/dir/2014/24/oj.

[5] DL, "Decreto Legislativo 18/04/2016, n. 50 - Codice dei contratti pubblici," 2016.

[6] DM, "Decreto Ministeriale 01/12/2017, n. 560," 2017.

[7] M. Murphy, E. McGovern, and S. Pavia, "Historic building information modelling (HBIM)," *Structural Survey,* 2009.

[8] R. Brumana, D. Oreni, A. Raimondi, A. Georgopoulos, and A. Bregianni, "From survey to HBIM for documentation, dissemination and management of built heritage: The case study of St. Maria in Scaria d'Intelvi," in *2013 Digital Heritage International Congress (DigitalHeritage)*, 2013, vol. 1, pp. 497-504: IEEE.

[9] S. Logothetis, A. Delinasiou, and E. Stylianidis, "Building Information Modelling for Cultural Heritage: A Review," *ISPRS Annals of Photogrammetry, Remote Sensing & Spatial Information Sciences,* vol. 2, 2015.

[10] C. Bianchini and S. Nicastro, "The definition of the Level of Reliability: a contribution to the transparency of Historical-BIM processes," *Dienne,* vol. 2, pp. 46-60, 2018.

[11] C. M. Bolognesi and S. Garagnani, "From a point cloud survey to a mass 3D modellng: Renaissance HBIM in Poggio a Caiano," 2018.

[12] C. Giannattasio, L. M. Papa, and P. D'Agostino, "El proceso BIM para la digitalización y la gestión del patrimonio universitario," in *Avances en expresión gráfica aplicada a la edificación*, 2019, pp. 421-432: Tirant lo Blanch.

[13] S. Imtiaz, S. A. R. Shah, M. K. Anwar, and M. M. Khan, "Damage Assessment of Historical Buildings: A Case Study of Historic Shrine of Multan, Proceeding of 2nd Conference on Sustainability in Civil Engineering, August , 2020.," 2020.

[14] S. Imtiaz and S. A. R. Shah, "Defects Analysis of Historic Buildings: A Case Study of The Multan Sharif (Madina-Tul-Awaliya)- City of Saints for Conservation and Restoration. ," *Proceedings of International Civil Engineering and Architecture Conference (ICEARC),17-20 April, Trabzon, Turkey.,* 2019.

WATER ENGINEERING

3rd Conference on Sustainability in Civil Engineering (CSCE'21)
Department of Civil Engineering
Capital University of Science and Technology, Islamabad Pakistan

AN OVERVIEW ON THE CAUSES AND IMPACTS OF FLOODS ON BUILDING CONSTRUCTION

Umair Abbas

Department of Civil Engineering, Lahore Leads University,umair.u4u@gmail.com

Abstract- This paper reviews the causes of Floods, Effects of floods on Buildings and Infrastructure, and socioeconomic disruption due to flood effects. Different researcher investigate different causes for floods, like Massive rainfall, Climate changes, urbanization, and deforestation, etc., and effects of floods on buildings are Buildings are partially destroyed or destroyed and due to flood effects on different areas social and economic losses like deaths, migration of residents from one place to another Infrastructure (Residential Buildings, Commercial Buildings, Road network's, etc.) are completely or partially destroyed. The Paper Concludes the causes of floods, effects of the flood on building construction, and socioeconomic disruption due to flood.

Keywords- Floods, Rainfall, Urbanization, Deforestation.

1 Introduction

Flooding is the most catastrophic event worldwide and one of the costliest. Depend upon the area, key flood-creating cycles can incorporate fluvial, precipitation, pluvial, seaside, bursting of dams, and snowmelt, which are examples. The cycles creating flooding for some random districts are meteorological systems (for example environmental streams, hurricanes, air flows) that can shift essentially starting with one area then onto the next [1]. Flooding is a situation where typically dry land gets lowered in the water. These phenomena can be caused normally by unnecessary precipitation and expanded surface water stream. It could likewise be human-made because of dam spillage, poor construction of drainage system and defective establishment of local area water conveyance pipes among others.

2 Causes of Floods

There is solid proof that the key systems creating flooding are as of now changing and will keep on changing with additional an Earth-wide temperature boost. Outrageous precipitation at various times (from sub-hourly through to many days)s is expanding and is projected to keep expanding in many areas all around the world with brief span precipitation bound to show more prominent increments, and also Climate change is one of the main reasons of compound floods [1]. Massive precipitation can have intense societal effects. These indirectly contribute to high streamflow and fluvial flooding and, all the more straightforwardly, pluvial flooding. Weighty precipitation can likewise trigger landslides. Flooding across Kenya is due to long rain periods in 2018 caused the dislodging of 0.3 million individuals instantly followed by the periods of ‘‘short rains'' from October to December season flooding of 2019.[2].Because of an earlier than-regular beginning of the South China Sea summer monsoon and an all the more toward the north. The drawn-out Meiyu framework with oddly heavy precipitation expands numerous streams caused Flash flooding, Urban flooding, and landslides, Causing devastation across huge spaces of China, especially in the River basin of Yangtze[3]. Heavy rainstorm precipitation desolated an enormous area of East Asia in summer 2020. Extreme flooding in the river of Yangtze dislodged a huge number of occupants amidst a notable general wellbeing emergency. This extreme stormy season was not expected from El Niño conditions[4]. The term El Niño alludes to a warming of the ocean surface (or better than anticipated sea surface temperatures) in the central and eastern tropical Pacific Ocean. El Niño occasions can upset ordinary climate designs in the United States and universally [5]. The study presents, the historical backdrop of floods is viewed as centering in antiquated Greece since the early Bronze Age. The progressing urbanization and deforestation during that time have prompted an expanding and unmanageable flood hazard. Greece experiences today flood varieties. Because of urbanization and deforestation, flood issues are more extreme these days than in the past. It is noted that the recurrence and event of outrageous flood occasions are expected to increment because of the progressions in the segments of the hydrological cycle that will be influenced by environmental change. Figure 2: shows the historical floods that affected the areas of Greece due to heavy rainfall [6].

Figure 2: Historical Flood is Greece [6]

From the hydrological viewpoint of flood characterization, flood types are dictated by the irregularity or sizes of hydrological drivers (e.g., precipitation, snowmelt, catchment wetness). Waterway flooding makes seriously harms human culture. Climate/Environmental change may additionally intensify flood risks. Past examinations distinguish the different patterns of flood extents and frequencies dependent on long-haul stream flow perceptions at a worldwide scale. Rainfall is the most predominant driver and one of the main reasons for floods [7]. Utilizing the information gathered from two rounds of public overviews (n = 903) across six Colorado people group overwhelmed in 2013, this investigation improves our comprehension of the variables that drive our belief about expected reasons for floods, focusing on environmental change. Thus, these convictions about environmental change are decidedly connected with the view of the dangers of future flooding. At last, belief about climate/environmental change was discovered to be an imperceptibly huge indicator of seen future flood hazard [8]. The characteristic reasons for yearly flood sources have been very much read and summed up the United States for different states; shockingly, evaluation of the normal reasons for outrageous (e.g., return time of at any rate 10 years) flood varieties is often restricted to the event and provincial scale examinations. For instance, investigations of this kind have analyzed the June 2008 flood varieties in Iowa, The basin of the river Ohio Southwestern USA sources of floods are return period of more than 10 years, specifically; focus on atmospheric cycles leading to substantial precipitation, which is a significant factor of the flood [9].

3 Effect of Floods on Buildings

Steady precipitation toward the end of 2002 due to this flood situation appeared in the catchment of Thames and caused flooding. The railroad lines were disturbed, 128 residential properties were affected, and the schools are destroyed due to flood, and making interruption in the everyday life of the town. Meetings recommend that for a gathering of town inhabitants. Flood in 2013 not just striking hydrological properties yet additionally in light of the institutional reaction to the crisis. Due to flood-restricted admittance to many parts of the town, immersing houses, and confining individual's admittance to fundamental assets, the neighborhood discernment was that flood specialists demonstrated unequipped for dealing with the actual crisis.[10]. The study intends to break down the impact of environmental changes on flood harm focusing on the Wonjucheon basin, which is a metropolitan stream flowing the city. In fast expansion in high causalities and property harm in metropolitan territories caused by urban flooding. In Korea, the Wonjucheon basin which was a metropolitan stream flowing through the downtown area was chosen as the objective basin. The Wonjucheon basin was a district where urban inundation happened much of the time because of the stream flooding in the past as shown in figure 3 which caused a lot of flood harm. The stream was flooded in 2006, 2010, 2011, and 2012 because of substantial rainfall. The affected /damaged area which includes Residential, Agriculture, and industrial (buildings and lands) show in figure 4, and flood damage/affected assets shown in table 1 [11].

Table 1- Flood Damage/affected Assets [11]

Asset Type	Assets
Residential	Residential properties, Home Supplies
Industrial	Facilities of Production
Agricultural	Agricultural land

(a). Heavy Rainfall in 2006 (b). Heavy Rainfall in 2010

(c). Heavy Rainfall in 2011 (d). Heavy Rainfall in 2012

Figure 3: Past stream flooding [11]

Figure 4: Flood Damage Area [11]

The examination applies the use of primary and secondary source of data collection for examination, the discoveries uncovered that the flooding happened because of heavy precipitation that kept going around four hours which made the inland water rise. The subsequent impact was that buildings and different properties were affected and mostly destroyed; individuals were displaced while a few groups lost their lives. All in all, huge damages to properties and loss of lives were recorded and emphasized on viable mitigation measures were made to decrease the impacts of the flood. As a result of a flood, buildings are partially and destroyed which are shown in Figures 5 a & b, below [12].

Figure 5 a: Partial Collapsed of Building [12]

Figure 5 b: Completely Destroyed Building [12]

Flooding overall can't be eliminated yet can be decreased. The examination in Suleja L.G.A.(Local Government area) uncovered that the area of structures near the stream not more than five meters while a few structures are found less than a meter from the waterway. A few structures built on the flood plain were destroyed alongside lives and properties[12]. The study centers around the assessment of direct harms brought about by 3 flood situations with various return periods of Trotuș River. The harm for three land use is residential properties, infrastructure, and Farmland. The outcomes showed that the major damages are registered for the private structure/residential. The flood events that occurred in the previous years fundamentally affect this territory, both on the people as well as on residential properties, destroyed infrastructure, and major impacts on the environment. The effect of flooding in this area is critical because of the presence of houses, about 1.200 structures being experienced in the 3 towns examined in this study, 95% of the structures which are residential properties. The flood events caused by the Trotus River and its tributaries since July 2005, huge damages to houses/residential and infrastructure was recorded. Table 2 shows the damages caused by two flood events (2005 and 2010)[13].

Table 2- 2005 and 2010 Flood Damages [13]

Affected Elements	**Year 2005 Amount Affected**	**Year 2010 Amount Affected**
Damaged Houses	116	86
Residential Property Destroyed	2	-
Provincial Roads	5.5 km	7.09 km
Roads of Village	-	1.17 km
Highways	-	0.9 km
Demolished Culverts	3	4
Agriculture Land	35 hectare	1 hectare

The study territory is situated on the shoreline of Tuscany in the region of Livorno of central Italy (Fig. 6 "b"). In September 2017, the precipitation event hit numerous little catchments nearby with the significant losses caused by the immersions of Rio Maggiore and Ardenza. The immersed region about 1.15 kilometers square, and the population affected is around 4 thousand, 4 people die and only one property in the Rio Maggiore catchment, and 4 deaths in the Ardenza catchment. Flood damages many buildings, foundations, retaining walls, interior flooring of buildings and plastering, etc. Authorities gathered 302 remuneration structures filled by the affected residents around there shown (Figure: 6, a, c), Floods damages to structures including buildings, foundations of the buildings, retaining walls at different places, interior flooring of buildings and plastering, etc.[14]

Figure 6: Rio Maggiore Area (a) region of Livorno (b) Damages (c) Affected buildings and residents [14]

The examination territory is situated along in south Quebec of, Canada. The Richelieu River takes source from the Lake Champlain at the US line and streams toward the north into the St. Lawrence River. The latest event happened between the 5th of June and 4th of August, 2011, bringing about more than US dollar of 88 Million damages to around 3,000 affected residential buildings. The majority of damages were noticed south of the Saint-Jean-sur-Richelieu. The examination territory considered in the investigations contains 8 hundred residential buildings. [15].Changes Environmental conditions raising the number of outrageous events, like extreme floods, have expanded the consideration of their impacts on the metropolitan system. Urban floods create significant hydrodynamic loads on the building. The investigation is done with experimental tests replicating masonry buildings with a scale of 1/10, while the impact of the flow hitting the building has been acquired by moving the structure/Building in the water. [16].

4 Socioeconomic Disruptions Due to Effects of Flood

Thailand has been experiencing repeating flood events and was most which are seriously influenced during the 2011 floods. Floods in 2011 during the long periods of October 2011 to December 2011, was one of the most ruinous floods as far as financial losses, social damages in ongoing many years. The 2011 floods were among the high-cost calamities in Thailand the financial losses were raised to over Trillions, 1.4 trillion in Thailand currency "Thai Baht" equal to forty-two Billion united states dollar and an extra recovery costs of over Forty-five Billion United States Dollar which are equal to 1.5 Trillion Thai Baht since the 2011 floods. A few territories including Ayutthaya and Pathumthani were seriously influenced because of the quality of the huge number of business endeavors that were immersed in over 2.5 meters of rising water. The Thai Small and medium enterprises accommodate 70% of the work and contribute forty-five percent "US $ 215 billion" towards the absolute of Thai National Gross Domestic Product (GDP) and international trade [17]. Due to the double influence of tropical storm Rumbia and Yagi, on August 18, 2018, Weifang city, Shandong Province, was hit by a progression of substantial rainfall, bringing about extraordinary precipitation and a potential flood hazard in the Mihe River basins. A few towns were flooded, and an enormous number of Residential Properties, agricultural land, and vegetable nurseries were destroyed. As indicated by insights, the catastrophe caused 26 people died, and one lack seventy thousand individuals were migrated, 14,130 residential buildings were collapsed, more than 2 lack nurseries were damaged and monetary/economics losses arrived at 22.292 billion Chinese yuan, including 14.658 billion Chinese yuan for horticultural damaged[18].In this paper, Flood damages in the Muzaffargarh region were analyzed. The investigation territory major flood influenced areas by floods before. Essential information was gained through surveys, The investigation shows that the flood was created by a heavy precipitation event in July 2010 in River Indus at the upper catchment spaces. This created the ever most elevated release in the River. The greater part of the land region was immersed. Additionally, the investigation showed that the immersion caused absolute assessed financial loss of about US $9.85 million Out of aggregate, the greatest harms of US Dollar 4.45 million were accounted for from farming area followed by infrastructure US Dollar 3.5 million[19].A comparative case study investigation was directed in 3 unique areas in the City of Hampton, The Hampton Roads space of Southeast Virginia is a level, flowing district with the most noteworthy estimated pace of the City of Hampton includes more than two hundred twenty-seven miles of shoreline along lakes, waterways, and the Chesapeake Bay, just as one hundred twenty-four miles of navigable waterfront making it exceptionally vulnerable to flowing flooding The city administration collected there were 938 losses in the repetition of floods inside the City of Hampton [20].In South China, 634 rivers flooded and almost 64000000 million individuals were influenced. The loss of life is almost 219 and more than 54 thousand properties were demolished as of 2020 August. During a dam-break flood, over 100 thousand individuals in Uzbekistan and Kazakhstan were cleared. About 81 thousand individuals were evacuated in Somali and Ethiopia and 78,000 in Congo during floods due to substantial precipitation. Numerous individuals influenced by the flood were inclosed during evacuation.A major flood in both Uzbekistan and Kazakhstan is due to the failure of the dam which is in Uzbekistan. Substantial rainfall and high breezes destroyed the dam wall, flooding enormous land territories in both adjoining nations. Many houses in both Countries were destroyed. In Uzbekistan, around 70 thousand individuals from 3 districts were cleared. 2 child deaths were recorded. In Kazakhstan, more than 31 thousand individuals from a district in the southern area, which is near the border of Uzbekistan, were cleared. Flooding in Yangtze river china demolished almost 400000 houses and damaged 5000000 hectares of agricultural land. it is assessed that immediate economic losses due to floods surpass 25 billion dollars [21]. Flooding essentially affects the socio-economic lives of occupants of the floodable regions in the chose networks and Adamawa State when all is said in done. Infrastructure and administrations like public and private structures or buildings, Road Networks, and Electricity supply offices are destroyed by flooding. In the aftermath of the 2019 floods in Adamawa State, an expected 381 houses were destroyed, 493 houses are partially destroyed, with more than 365 water and sanitation offices damaged influencing more than 12,000 people.The greater part of farmlands having crops was demolished and animals lost and an expected figure of around 12,000 people was evacuated from the selected communities[22].The investigation region is Draa Basin, and of Tafilalet basin of Morocco, Tafilalet basin on the November 5th, 1965, a flood Destruct the Ziz valley, due to this 25,000 individual's homeless. In Merzouga, the recent significant flood was recorded on May 26th, 2006 after extreme precipitation for three hours. The flood destroyed 140 residential houses and hotels, the disintegration of Taouz Merzouga Roads, Streets, destroyed the water distribution supply line of Merzouga and Taouz towns show in figure:7 A & B below [23]

Figure 7 A & B: Destroyed Houses, Roads and water Supply lines [23]

Draa basin the brutality of flood caused water disintegration which lessens the fertility of rural land. Photograph in Figure 8 A & B shows the floods in 2009 that disconnected a few towns of Beni Zouli from the public street N9, and afterward the stop of provisioning administrations/Services for15 days [24].

Figure 8 A & B: Draa Valley 2009 Flood [23]

This examination was led in four urban communities of Iran in 2017–2018. Ajabshir province and Azarshahr province are urban areas of Azerbaijan East territory situated on the west side of Iran. The two urban communities were badly affected by the magnificent huge flood in 2017. Specifically, Ajabshir province has 40 towns, of these, 3 towns were flooded, and due to flood-hit the towns, 20 people died because of the flood in the town of Chenar, yet no demise happened in the other 2 towns. The province of Azarsahhr was likewise affected due to the flood alongside the town of Chenar around there (Both are urban areas are near one another); in Azarshahr, around 22 individuals deaths were reported.[24].Floods are arranged into direct damages due to flood and indirect damages due to floods. Direct damages happen because of the actual contact of rising Flood with peoples, properties, or other components, and indirect damages are initiated by the immediate effects of the direct impact of the flood. These are additionally characterized into tangible damages and intangible damages depend upon regardless of whether these damages can be surveyed in money-related qualities [25].

5 Conclusions

The current study Present the causes of floods, Effects of flood on buildings, and socioeconomic disruptions due to flood effects.
The following conclusions are made:

- The major causes of floods are heavy rainfall in a particular area, many other causes will discuss in the above-reviewed paper-like climate change, urbanization, deforestation, return period, etc.
- Flood effects on buildings are also reviewed, due to floods buildings are partially or destroyed depends upon the nature of the flood, if the flood discharge is minimum it affect not catastrophic but partially affects the buildings if the flood discharge is maximum it will destroy the buildings.
- Residential Property Damages is in hundreds depends upon the amount of discharge enter residential areas.
- Flood disasters in a particular area create social and economic disruptions i.e. Deaths, Migration from that area, Infrastructure destruction, destroy agricultural lands, and Disturbed Transmission services, it will impact on country's economy.
- The deaths and affected people due to flood are in thousands, and the monetary losses are in million $ due to flood.

6 Acknowledgment

The author would like to thank Engr. Dr.Usman Farooqi, Assistant Professor, Department of civil engineering, Capital University of Science and Technology who helped throughout the work, with his constructive suggestions. I am very thankful to anonymous reviewers for their careful review and constructive suggestions.

References

[1] Westra S, Nathan R, Orr HG, Villarini G, Villalobos Herrera R,Fowler HJ Wasko C, "Incorporating climate change in flood estimation guidance.," *The Royal Society Publishing*, 2021.

[2] RUTGER DANKERS, RICHARD GRAHAM, KISWENDSIDA GUIGMA, LUKE JENKINS,MARTIN C. TODD, AUGUSTINE KIPTUM, MARY KILAVI, ANDREW NJOGU,AND EMMAH MWANGI DAVID A MACLEOD, "rivers and Subseasonal Predictability of Heavy Rainfall in Equatorial East Africa and Relationship with Flood Risk," *Journal of Hydrometeorology*, 2021.

[3] Xiaomeng LI, Guy J.-P. SCHUMANN, Lorenzo ALFIERI, Yun CHEN, Hui XU, Zhifang WU, Hong LU, Yamin HU, Qiang ZHU, Zhijun HUANG , Weitian CHEN, and Ying HU Huan WU, "From China's heavy precipitation in 2020 to a "glocal " hydrometeorological solution for flood risk prediction," *Advances in Atmospheric Sciences* , vol. volume 38, 2021.

[4] Shang-Ping Xie , and Renhe ZhangHistoric Zhen-Qiang Zhou, "Yangtze flooding of 2020 tied to extreme Indian Ocean conditions," *Proceedings of the National Academy of Sciences of the United States of America (PNAS)*, 2020.

[5] https://www.usgs.gov/faqs/what-el-ni-o-and-what-are-its-effects?qt news_science_products=0#qtnews_science_products.

[6] G. Antoniou · K. Voudouris · N. Kazakis · N. Dalezios5 · N. Dercas N. Angelakis, "History of foods in Greece: causes and measures for protection," *Natural Hazards*, 2020.

[7] Hanbo Yanga, Dawen Yang Wencong Yanga, "Classifying floods by quantifying driver contributions in the Eastern Monsoon Region of China," *Journal of Hydrology*, 2020.

[8] Elizab et hAAl brigh t & Deserai Crow, "Beliefs about climate change in the aftermath of extreme flooding," *Climatic Change*, 2019.

[9] Hamid Moradkhani & Upmanu Lall Katherine e. schlef, "Associated with extreme United States Floods Identifed via Machine Learning," *Scientific Reports*, 2019.

[10] Daniel H. de Vries Kseniia Puzyreva, "A low and watery place': A case study of flod history and sustainable community engagement in flod risk management in the County of Berkshire, England," *International Journal of Disaster Risk Reduction*, 2021.

[11] Dong-Ho Nam , Se-Jin Jeung and Byung-Sik Kim Dong-Ho Kang, "Impact Assessment of Flood Damage in Urban Areas Using RCP 8.5 Climate Change Scenarios and Building Inventory," *Water*, 2021.

[12] Kigun P.A., Alfred Y.B., Majidadi ST., Surajo L.A Birmah M.N., "Flood Assessment in Suleja Local Government Area, Niger State, Nigeria," *International Journal of Research Publication and Reviews*, 2021.

[13] José Luis Zêzereb , Iulia Crăciunc , Gabriel Lazăr , Iuliana Lazăr Roxana Țîncua, "Quantitative micro scale flood risk assessment in a section of the Trotuș River, Romania," *Land Use Policy*, 2020.

[14] Bernardo Mazzanti, Francesco Pistone, Fabio Castelli, Chiara Arrighi, "Empirical fash food vulnerability functions for residential building," *SN Applied Sciences*, 2020.

[15] Karem Chokmani, Miroslav Nastev, Rachid Lhissou and Anas Elalem]Khalid Oubennaceur, "Flood risk mapping for direct damage to residential buildings in Quebec,Canada," *International Journal of Disaster Risk Reduction*, 2019.

[16] Gianluca Zitti , Ersilia Giordano , Francesco Clementi , Giovanna Darvini , Stefano Lenci Matteo Postacchini, "Flood impact on masonry buildings: The effect of flow characteristics and incidence angle," *Journal of Fluids and Structures*, 2019.

[17] Shubham Pathak and Jorge Chica Olmo, "Analysing spatial interdependence among the 2011 Thailandflood-affected small and medium enterprises for reduction of disaster recovery time period," *Geoenvironmental Disasters*, 2021.

[18] Qi Zhou , Mingjie Li, Dianxing Song , Yanjun Wen Shuolin Geng, "Spatial–temporal diferences in disaster perception and response among new media users and the influence factors: a case study of the Shouguang Flood in Shandong province," *Natural Hazards*, 2021.

[19] S., Sajjad, A. & Rahman, Au. Mahmood, "Cause and damage analysis of 2010 flood disaster in district Muzaffar Garh, Pakistan. ," *Natural Hazards*, 2021.

[20] Aishwarya Borate,Shereen Hughes,Ross Weaver, David Imburgia, William A.Stiles Jr Anamaria Bukvic, "Exploring neighborhood-level resilience to floo ding: Why the context and scale matter," *Journal of Flood Risk Management*, 2021.

[21] Zbigniew W. Kundzewicz,Nigel Wright Slobodan P. Simonovic, "Floods and the COVID -19 pandemic A new double hazard problem," *WIREs Water*, 2020.

[22] B., Umar, H., Barde, M. M. and Adamu, S Abubakar,". Socio-economic Impact of Flooding on the Riverine Communities of River Benue in Adamawa State, Nigeria," *FUTY Journal of the Environment* , vol. 4, 2020.

[23] Ahmed Karmaoui & Balica Stefania, "A New Flood Vulnerability Index Adapted for the Pre-Saharan Region," *International Journal of River Basin Management*, 2019.

[24] Ali Ardalana, Abbas Ostadtaghizadeha, Yadolah Zarezadeh, Mohsen Souf Boubakran, Farzam Bidarpoorc, Abbas Rahimiforoushani Arezoo Yaria, "Underlying factors affcting death due to flood in Iran: A qualitative content analysis," *International Journal of Disaster Risk Reduction*, 2019.

[25] Luca Locatelli,María Guerrero, Beniamino Russo and Montse Martínez Eduardo Martínez-Gomariz, Socio-Economic Potential Impacts Due to Urban Pluvial Floods in Badalona in a Context of Climate Change," *Water*, 2019.

3rd Conference on Sustainability in Civil Engineering (CSCE'21)
Department of Civil Engineering
Capital University of Science and Technology, Islamabad Pakistan

APPLICABILITY AND EVALUATION OF IMERG PRECIPITATION PRODUCT: A SYSTEMATIC REVIEW

[a] Awais Ahmed Awan*, [b] Abdur Rehman Zahid, [c] Muhammad Irfan

a: Civil Engineering, The University of Lahore Islamabad Campus, 70063962@student.uol.edu.pk
b: Civil Engineering, The University of Lahore Islamabad Campus, 70063781@student.uol.edu.pk
c: Civil Engineering, The University of Lahore Islamabad Campus, irfan7235@yahoo.com
* Corresponding author: Email ID: awaisahmed3962@gmail.com

Abstract- The hydro-meteorological communities face major difficulty in accurately estimating precipitation over wider areas. One of the critical and influential factors in water resources management is the accuracy of integrated Multi-Satellite Retrieving for Globed Precipitation Measuring (IMERG) with their calibrated SPP denoted as IMERG Final and uncelebrated SPPs is known as IMERG Early and IMERG Late over different complex or simple topographical area. The purpose of this systematic review study is to conduct for accurate estimation of precipitation by using IMERG SPP. To achieve the aim we use the PRISMA Statement technique for deriving the related articles for detailed review those are published in recent years. From the years 2011 to 2021, the SCOPUS database was chosen to derive research publications written in English with keywords of "IMERG" AND "Precipitation" AND "IMERG Precipitation product". A total of 28 articles was extracted and after screening the titles and initial abstract thoroughly, only 8 articles were left for additional assessment. It was discovered that the IMERG-Final satellite precipitation product has the lowest likelihood of mistakes and the highest correlation with ground-based measurements and In addition, as compared to IMERG Early and IMERG Late satellite rainfall products, it demonstrated superior and capable accomplishment in estimating heavy precipitation occurrences over both highly complicated and less complicated topography regions. It is therefore recommended to apply the IMERG satellite rainfall product data before the commencement of design and construction of hydraulic structures.

Keywords- IMERG, Precipitation, SCOPUS, satellite precipitation product (SPP), hydraulic structures.

1 Introduction

Precipitation data from weather radar are subjected to major limitations such as errors that are dependent upon range, systemized, and random [1][2]. Data quality (obtained by weather radar) can be affected by surrounding obstruction, such as high-rise buildings, mountains, and other topographical features[1][3][4]. Radar network is expensive to purchase, install, manage and maintenance which severely limits their availability in many countries around the world. In the past, extreme precipitation measurements depend on the rain gauge network, but there are some limitations such that it cannot measure snowfall. Rain gauges have many types of errors such as water can evaporate from gauges due to high temperature. Weather radars have several flaws as well like Due to complicated atmospheric regimes, beam blockage, and variance in reflectivity-rainfall rate connections, the results are less exact.[1][2][5]. Satellite rainfall products are utilized as an alternate source to compensate for the lacking and limitations of ground-based precipitation measurement networks. [5]. Because rainfall varies widely in time and place, estimating it with ground data such as rain gauges and radars, as well as satellite observations, is difficult. [5].

The objective of this research is to assess the correctness of Integrated Multi-Satellite Retrieving for Globed rainfall measuring (IMERG). IMERG SPPs are at high terrain altitudes, to increase precipitation detection and reduce magnitude mistakes [6]. It has made the quantitative measurement of precipitation by satellite sensors is a significant source[1]. The result illustrated by IMERG SPP have high accuracy and are applicable in the most studied region and could be used in wide fields[4] regarding hydrological and hydro metrological applications of these Satellite products at an international scale.

Consequently, this study conducted a systematic review of published works in the circle of engineering utilizing the PRISMA statement[7] [8], evaluating the function of IMERG SPP in measuring and estimating precipitation, as it is one of the critical factors in the water resources management field to design the hydraulics structures and irrigation systems. After highlighting the positive and efficient results of this SPP. After this study, a future agenda was offered so that the researchers might address the concerns and issues in the future.

2 Significance of the work

The significance of this systematic review is useful for academia in which researchers, scientists get the platform of IMERG satellite precipitation product. This is the more advanced and latest application for measuring and estimating precipitation events. Since the novelty of this study in which the researchers will increase their researches regarding this SPP because the IMERG dataset has freely available on the NASA official website. This technique is more accurate and reliable to analyze and observe the rainfall data because the continuity and quality are more enhanced as compared to other opportunities. This study will also be helpful for the industrial people related to the hydrological department in which hydrologists and engineers use to implement the IMERG precipitation data for designing the hydraulic structures for a long duration and also the chance of disaster is sufficiently reduced.

3 Experimental Procedures

The methodology was divided into four stages. A research plan was devised in the first step to define the research database. The PRISMA statement was used to construct selection criteria in the second phase. The quality of the work was appraised in the third phase using an abstract and full-text examination. Data finalized was finished in the fourth phase in preparation for further analysis. The research and methodology flow chart is shown in Figure 1

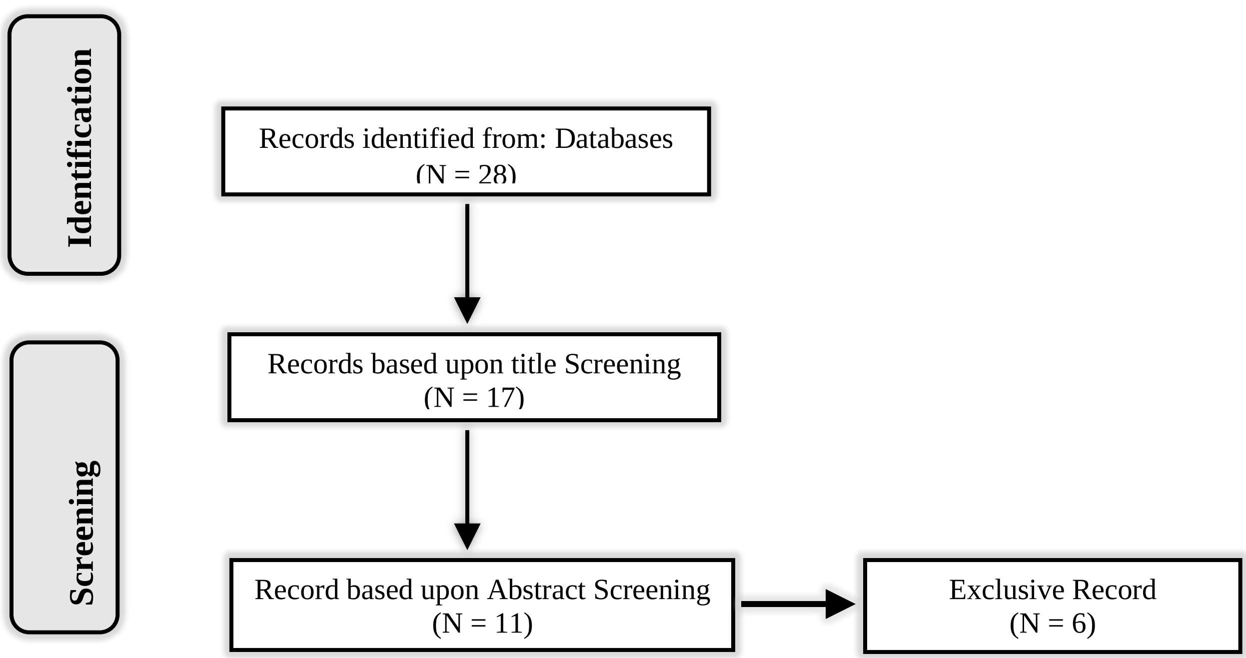

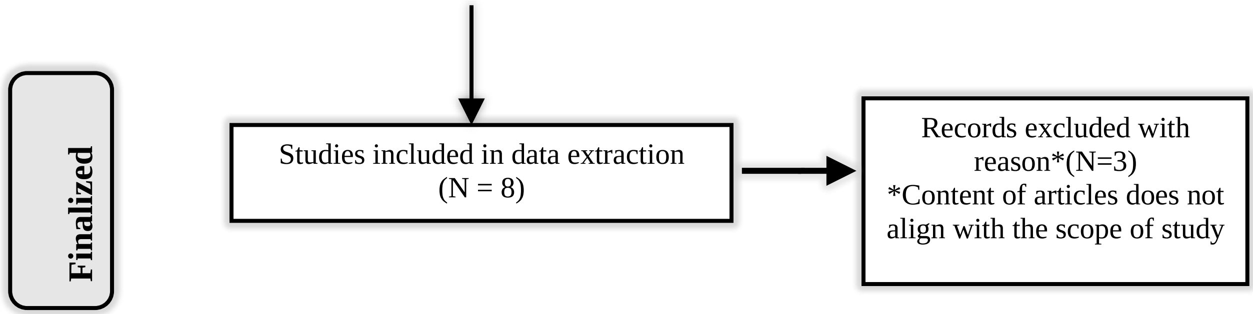

Figure 1: Research and Methodology Flow Chart

4 Research Methodology

4.1 Strategy for Researches.

Only the SCOPUS database was used for this systematic review, hence a strategy was designed to include related material accordingly with the study's scope. "IMERG" AND "Precipitation" AND "IMERG Precipitation product" were the search phrases in this database. The papers were limited by the years 2011 to 2021, with the additional restriction of only selecting research publications that have been published in the language of English.

4.2 Selected Criteria.

PRISMA statement was discovered by Liberati et al.[7]was for this systematic review, the selection criteria were employed. The concentration was totally on reviewing the keywords on "IMERG" AND "Precipitation" AND "IMERG Precipitation product" in the circle of water resources management. All articles published before 2011 were omitted from the study period, which ran from 2011 to 2021. These constraints resulted in the creation of 28 papers, which were then evaluated further at an afterward stage.

4.3 Quality Evaluation.

This study truly concentrated on researched-based articles and conferences. The acquired data were double-checked to maintain the reviewing process beneficial for the identified forms in which 6 papers were omitted based on title as our keywords used in gathered data were not matching or including in their titles. After that, all of the abstracts were rigorously read to ensure that the work's quality was sustained. It was found that there is repetition in some papers and the content is not fulfilling the requirements. Therefore, only 11 articles were retained for additional evaluation.

4.4 Extracted Data.

Following the assessment of quality, 8 articles with the following extracted characteristics were chosen:

- Original research publications were chosen, with no consideration given to publish analyzed reports or cased studies.
- The papers chosen were published in English Language and were on the topic of engineering circle.
- The articles that were included for systematic reviewing, published between the years 2011 to 2021.
- There were no country restrictions, and the articles came from all across the world.

5 Results

Explanation of the final included articles, as well as the debate based on those eight pieces of research, are offered in this part.

5.1 Discussion on Results.

The chosen 8 articles were truly concentrated on the measurement of precipitation by using IMERG satellite precipitation product is considered as one of the critical factors. It was revealed that the IMERG precipitation measurement varying with temporal scale, seasonal scale, and complexity of topography in a particular region[1] [4][6][9]. It is a precise measurement of precipitation that plays a vital part in a variety of climate metrological and water structure applications [2] such as predicting floods, hydrological process counterfeit, and managing water reproduction [10]. Using IMERG dataset used to design and maintenance of hydraulic structures to be safe from the natural disaster. IMERG data set comprises of three types which include IMERG Early, IMERG Late, and IMERG Final[1] [3] [9]. IMERG Early and IMERG Late SPPs were used to measure heavy rainfall and IMERG Final was used for the lightest rainfall[2][11]. IMERG Final has the lowest chances of estimation error and high correlation with ground observation[1] and showed better performance as compared to IMERG Early and IMERG Late. Hence IMERG dataset was more powerful and suitable data for application over the regions[4] where insufficient numbers of rain gauges, missing data information, or where gauge network stations were spars or inefficient[2].

5.2 Summarization of Included Articles.

Figure 2 depicts the overall overview of eight articles collected from every year. Between 2011 and 2021, their researches were a total of 8 published articles, and only 2017, 2020, and 2021 articles are concerned with our topic. In 2020 highest number of researched articles are published in the investigated field.

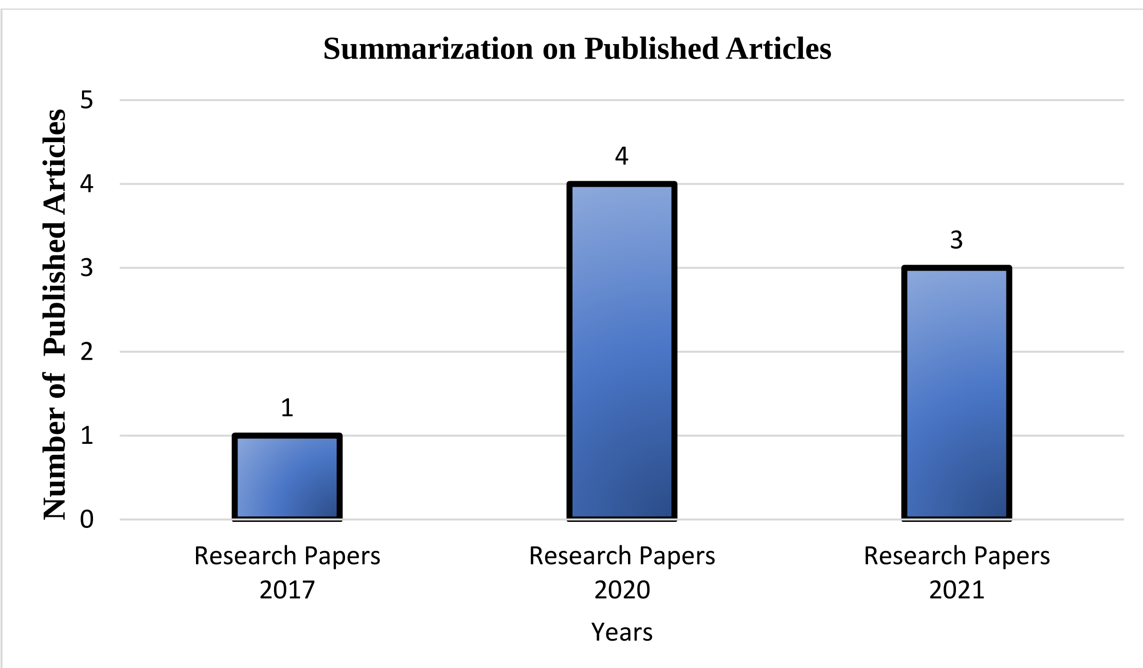

Figure 2: Summarization of Published Articles

5.3 Summarization of authors cited and journals.

The names of journals and authors, as well as their citations, have been discussed in this particular section. The following is a summary of Table 1. It is clear from Table 1 that the published articles received the most citations in 1) Remote Sensing in 2017, 2) Atmospheric Research in 2021 3) Remote Sensing in 2020 and 4) International Journal of Remote Sensing in 2020 and 5) Water (Switzerland) in 2020. Some journals, on the other hand, have few or no citations as mentioned in table 1.

Table 1- Summarization of authors, cited and journals

Sr. No	Journal Name	Author References	Year of publication	Citation received on the papers
1	Remote Sensing	Mahmoud M.T., Mohammed S.A., Hamouda M.A., Dal Maso M., Mohamed M.M. [1]	2021	0
2	Remote Sensing	Zhou C., Gao W., Hu J., Du L., Du L. [3]	2021	0
3	Atmospheric Research	Ma Q., Li Y., Feng H., Yu Q., Zou Y., Liu F., Pulatov B. [4]	2021	7
4	Atmospheric Research	Yang M., Liu G., Chen T., Chen Y., Xia C.[11]	2020	3
5	Water (Switzerland)	Saouabe T., El Khalki E.M., Saidi M.E.M., Najmi A., Hadri A., Rachidi S., Jadoud M., Tramblay Y. [10]	2020	2
6	International Journal of Remote Sensing	Gan F., Gao Y., Xiao L., Qin L., Huang Y., Zhang H. [9]	2020	3
7	Remote Sensing	Maghsood F.F., Hashemi H., Hosseini S.H., Berndtsson R. [2]	2020	6
8	Remote Sensing	Mayor Y.G., Tereshchenko I., Fonseca-Hernández M., Pantoja D.A., Montes J.M.[6]	2017	24
	Total Citation			**45**

6 Conclusion

Following conclusions can be drawn from the conducted study:

- All the three IMERG SPPs can measure the precipitation but the third product IMERG-Final SPP has the lowest chances of errors and it is reliable for all the globe. Therefore we recommend this precipitation product as the continuity and quality are enhanced as compared to any other satellite precipitation product.

- the IMERG data set is a great source of opportunity to understand the precipitation events occurring onto the different complex topographic regions and used to design and construct hydraulic structures to sustain in future as compared to ground-based data.

The aforementioned result is favorable, indicating that it should be investigated further. In the next step we will use the application of Web sciences, the science of direct, and also from google scholar to the detailed systematic review on IMERG satellite precipitation product for estimating the precipitation.

7 Future Agenda

IMERG is the best SPP to complement substitute ground precipitation measurement and is more accessible for mountainous and oceanic areas as well as plain areas. This research contributes to a deeper knowledge of IMERG products' global implementation and paves the way for future research into hydrological and hydro metrological applications. Therefore the precipitation data obtained from this satellite should be considered before the commencement of the construction and maintenance of any hydraulic structure to save from natural disasters.

Acknowledgment

The authors would like to thank every person/department who helped throughout the research work, particularly the Civil Engineering department, Muhammad Irfan. The careful systematic review and constructive suggestions by the anonymous reviewers are gratefully acknowledged.

References

[1] M. T. Mahmoud, S. A. Mohammed, M. A. Hamouda, M. D. Maso, and M. M. Mohamed, "Performance of the IMERG Precipitation Products over High-latitudes Region of Finland," *Remote Sens.*, vol. 13, no. 11, pp. 1–26, 2021.

[2] F. F. Maghsood, H. Hashemi, S. H. Hosseini, and R. Berndtsson, "Ground validation of GPM IMERG precipitation products over Iran," *Remote Sens.*, vol. 12, no. 1, pp. 1–23, 2020, doi: 10.3390/RS12010048.

[3] C. Zhou, W. Gao, J. Hu, L. Du, and L. Du, "Capability of imerg v6 early, late, and final precipitation products for monitoring extreme precipitation events," *Remote Sens.*, vol. 13, no. 4, pp. 1–22, 2021, doi: 10.3390/rs13040689.

[4] Q. Ma *et al.*, "Performance evaluation and correction of precipitation data using the 20-year IMERG and TMPA precipitation products in diverse subregions of China," *Atmos. Res.*, vol. 249, pp. 1–52, 2021, doi: 10.1016/j.atmosres.2020.105304.

[5] E. Muhammad, W. Muhammad, I. Ahmad, N. Muhammad Khan, and S. Chen, "Satellite precipitation product: Applicability and accuracy evaluation in diverse region," *Sci. China Technol. Sci.*, vol. 63, no. 5, pp. 1–10, 2020, doi: 10.1007/s11431-019-1457-3.

[6] Y. G. Mayor, I. Tereshchenko, M. Fonseca-Hernández, D. A. Pantoja, and J. M. Montes, "Evaluation of error in IMERG precipitation estimates under different topographic conditions and temporal scales over Mexico," *Remote Sens.*, vol. 9, no. 5, pp. 1–18, 2017, doi: 10.3390/rs9050503.

[7] A. Liberati *et al.*, *The PRISMA statement for reporting systematic reviews and meta-analyses of studies that evaluate health care interventions: explanation and elaboration*, vol. 62, no. 10. 2009.

[8] W. S. Alaloul, K. M. Alzubi, A. B. Malkawi, M. Al Salaheen, and M. A. Musarat, "Productivity monitoring in building construction projects: a systematic review," *Eng. Constr. Archit. Manag.*, pp. 1–26, 2021, doi: 10.1108/ECAM-03-2021-0211.

[9] F. Gan, Y. Gao, L. Xiao, L. Qin, Y. Huang, and H. Zhang, "An applicability evaluation of version 05 IMERG precipitation products over a coastal basin located in the tropics with hilly and karst combined," *Int. J. Remote Sens.*, vol. 41, no. 12, pp. 1–21, 2020, doi: 10.1080/01431161.2020.1723174.

[10] T. Saouabe *et al.*, "Evaluation of the GPM-IMERG precipitation product for flood modeling in a semi-arid mountainous basin in Morocco," *Water (Switzerland)*, vol. 12, no. 9, pp. 1–15, 2020, doi: 10.3390/w12092516.

[11] M. Yang, G. Liu, T. Chen, Y. Chen, and C. Xia, "Evaluation of GPM IMERG precipitation products with the point rain gauge records over Sichuan, China," *Atmos. Res.*, vol. 246, pp. 1–21, 2020, doi: 10.1016/j.atmosres.2020.105101.

3rd Conference on Sustainability in Civil Engineering (CSCE'21)
Department of Civil Engineering
Capital University of Science and Technology, Islamabad Pakistan

GIS-BASED IDENTIFICATION OF RIVER BANK EROSION AND FLOOD WATER MANAGEMENT

[a]Ghulam Abbas, [b]Ghufran Ahmed Pasha, [c] Usman Ali Naeem, [d]Usman Ghani

a, b, c, d, : Civil Engineering Department, University of Engineering and Technology Taxila,
ghulamabbas696@gmail.com, ghufran.ahmed@uettaxila.edu.pk, usman.naeem@uettaxila.edu.pk,
usman.ghani@uettaxila.edu.pk,

***Abstract*:** Indus River in Southern Punjab, Layyah started to erode the residential as well as agricultural land at the left bank (31°4'0.321"N, 70°49'41.066"E) in 2000. At that time the local Government constructed the spurs on the left bank to tackle the erosion problem of the flowing river. It proved to be a short-term solution because in 2010 despite the construction of spurs the river started to erode, eventually resulting in the construction of spurs at the left bank once again. The present research emphasizes, training the river in the peak flow duration and analyzing the river shifting behavior as well as applying the Geological information sources (GIS) and Remote Sensing (RS) methods for geomorphology analysis progress. To gather Remote Sensing information and topographical information for 20 years shifting of the river bank. Because the geomorphology of the Indus River is continuously changing, causes a decrease in the area of the Indus River day by day. GIS mapping of river erosion shows that from 2000 to 2010 the natural river cross-section is disturbed by 50km^2 to 48. 83km^2 and from 2010 to 2020 reduction of river area is from 48. 83km^2 to 31.02km^2. The Results Show that the change in the stream bank is because of different common and synthetic exercises like a flood, flow velocity, deposition of eroded materials, uprooting of the vegetation covers, and soil stability disturbances. Furthermore, around 200 interviews were also conducted with local community individuals discussing river erosion and floodwater management during the month of peak discharge. The statistics show that 59% of remarks were related to "inappropriate river training works" and 43% of remarks were about "poor floodwater management".

Keywords-: Land sat Images, Geographic Information System, erosion, Remote sensing.

1 Introduction:

The largest catchment and span-wise river is the Indus river of Pakistan. The Total agricultural land of Pakistan depends upon the Indus river irrigation system. The total length of the Indus River is 3481km from the North to the Arabian sea **[1]**Bank erosion is a natural geomorphic process or disturbance that occurs during or soon after floods. Riverbanks are temporary boundaries, between the aquatic and native ecosystems, and they regularly change under naturally dynamic hydrologic conditions. Although abundant research suggests that bank erosion is a basic ecological process[2]**.** Brahmaputra river which is situated in India pointed toward evaluating the genuine bank disintegration along the time of eighteen years (1990-2008). The study length of this river is a stream of Dibrugarh to town dhubri which is near about Bangladesh that's spanwise is 620km utilized for the geographic information system and remote sensing. Satellite images were used for study analysis from 1990 to 2008 [3]**.** The Bank of the river is very important like Ganga is one of the largest rivers in the world. It is the river of the Himalayas countries which devastated water every year by flooding. Mostly major river system changes the morphology every year. Like most major river systems, it changes course in space and time in the rugged plains. This study counted the variability in the parameters of the river by using historical and monthly discharge data [4]**.** In this research area GIS and Remote Sensing are used for river shifting measurement. Morphological changes occur due to discharge, LULC variations[5]**.** The morphometric boundaries, for example, the approximation of the zone to the level of the Cincinnati, Braided Ness Index, and the complete waterway of the island zone, were estimated from Landsat from 1955, 1977, 1990, 2001, 2003, and 2005. IRS satellite imagery investigations show that all the time these limits are brought together and all things are extended on a basic basis. The examination revealed that the bank's frustration was due to the obstruction of certain components such as riverine soil excavation, presence of hard rough zone, excessive piles of dirt and excavation, and obstruction of development of Farakka blast as a Common waterway[6]**.**

The principal objective of the paper with useful ideas for control the bank disintegration and moving of the Pravara River. An endeavor has been made here, to mechanism the GIS and RS strategies for stream change recognition utilizing customary to progress topographical information sources. The advances in Remote Sensing information and Topographical information are to actualize for acquiring 35 years' progressions brings about waterway stream. The angle or slant, water volume, water speed, and nature of the waterway are mindful edges for changing the stream's shape and size **[7].** River channel mapping is measured by using a Geographic information system also remote sensing. Local variations in riverbank and waterway centers existed regularly reviewed, and efforts were made to link these Inputs findings to appropriate natural and human interference affecting the river morphology[8]**.** In this study area, river banks identify by Remote sensing during the period of 103 years (1912-2015). River found highly shifting and meandering with sinuosity index[9]. The main reason for channel shifting in the southwest is the influence of natural river flow disturbance by human activities. There are some further dynamic changes like discharge capacity of the river, channel deposition load, the transport capacity of the river disturbed by human activities. The influence of river training is no relation between the engineering structure and the development of natural river flow streams[10].

The purpose of this literature study is to evaluate the shifting of Indus river erosion about 28.4 km along the part of Indus river in district Layyah Punjab Pakistan. In this study river is shifting toward the left bank in a 20-year time period this is called a temporal change in behavior of the natural channel. Furthermore, River channel mapping is measured by using a Geographic information system also remote sensing. Local variations present in riverbank and waterway centers were regularly reviewed, and efforts were made to link these Inputs findings to appropriate natural and human interference affecting the river morphology. This study aims to evaluate shifting river and total area of water streams by using the temporal change method with the help of a geographic information system and Remote sensing.

2 Methodology used for Analysis

2.1 Study area

Indus river is the largest river in Pakistan, which is an important river in the Asian region. Indus river length is 3,180km from source to mouth. A bulky part of the Indus River flows into the Karakoram and Himalayan mountain ranges. The main branches of the Indus River coordination are the Kabul, Jhelum, and Chenab rivers, which cause floods due to surplus water flow in the monsoon season. The study was conducted to highlight the erosion and flooding of the Indus River and its damages along Layyah in an area of about 65 km^2. The district covers a total area of 6,291 km^2 having a width of 88 km from east to west and a length of 72 km from north to south. Layyah district was hit by severe floods for many years, namely 1950, 1956, 1957, 1958, 1963, 1965, 1973, 1976, 1988, and 1992 and then till 2020. More than 31,658 houses, 154,000 families have been affected and washed away in the district Layyah, 500,000 all over Punjab Province in the major floods of 2010[11].

Figure 1: Study area of Indus river in district Layyah

2.2 Methodology Framework

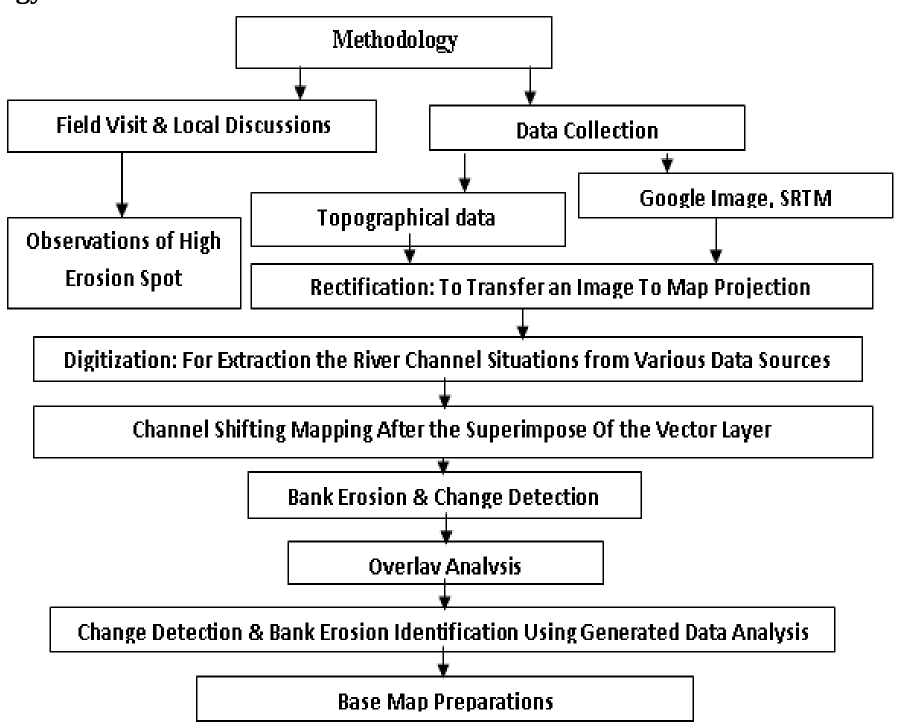

Figure 2: Flow chart

3 Geographical Information system analysis

ArcMap 10.4 GIS programming is used to investigate stream bank information. Satellite images were developed earlier in 2000, 2010, and 2020 to obtain the necessary information about the research zone. The additional segment captures the arrangement of satellite images to extract data. In this investigation, satellite images of Landsat Way 151, Line 039 were used for the years 2000, 2010, and 2020 and are ready to obtain the necessary data. The digital elevation model of 30 meters is used for this research study. The current research study includes both high and low flood season data. The table1 records the important limits of the information used in this research. The spatial analysis has been done by using DEM 30m. The Landsat images downloaded from USGS were chosen with accessibility.

Table 1: Data Source Used

Satellite	Date of acquisition	Season	Resolution	Path &Row	Source
Landsat 4,5	2000	High flow +Low flow	30m	151&39	USGS
Landsat 7	2010	High Flow +Low flow	30m	151 & 39	USGS
Landsat 8	2020	High Flow +Low flow	30m	151 & 39	USGS

The projection of Landsat images is WGS 1984 UTM Zone north 43 DATM Level -1B. Mathematical adjustment is a preparation phase, that is applied to avoid mathematical contradictions in the picture. It creates links between beautiful image arrangements and geographical directions. Therefore, to assure position information, I have included GPS from Google Earth and all images of the landscape connected**.** The NDWI technique is used to enhance the features and visibility of open, water, satellite imagery. Normalized difference water index (NDWI) enhance water properties when removing clouds error and other plant features from the surface. Water is extracted from selected satellite images using the following index. There is an equation for this.

$$NDWI = \frac{GREEN-SWIR}{GREEN+SWIR} \text{ .... } \quad \text{Equation 1}$$

ArcGIS has developed a model that focuses on green and shortwave infrared (SWIR) groups related to landscape information and NDWI image. The nominated variety is then improved by converting it to a polyhedron. This model was run on each of the 12 images of the high and low stream season. After that, a research study based on a questioner (https://docs.google.com/forms/d/e/1FAIpQLSe5XtlYO3ffoa6kQnIdbWrffR5ifwZZVUKl8wrJXRQ5r5m6A/viewform?usp=sf_link) consisting of about 200 interviews is being conducted which involves a discussion regarding river erosion and the main reason behind flooding.

4 Results

The stream disintegrated due to the deposition of silt in numerous places all through the local morphology of the Indus river. It tends to be seen from spatial information analysis of river erosion and area of water streams shifting that is maximum in left banks from 2000 to 2020. From Table 2, information uncovered that the zone of around 28.4 km has been dissolved from the Left bank from 2000 to 2020. GIS mapping of river erosion shows that from 2000 to 2010 the natural river cross-section is disturbed due to changing the area of water body 50km^2 to 48. 83Km^2 and from 2010 to 2020 again reduction of river area is from 48. 83 Km^2 to 31.02Km^2. Figure 3 shows the river shifting scenario along the Layyah district from 2000 to 2020.

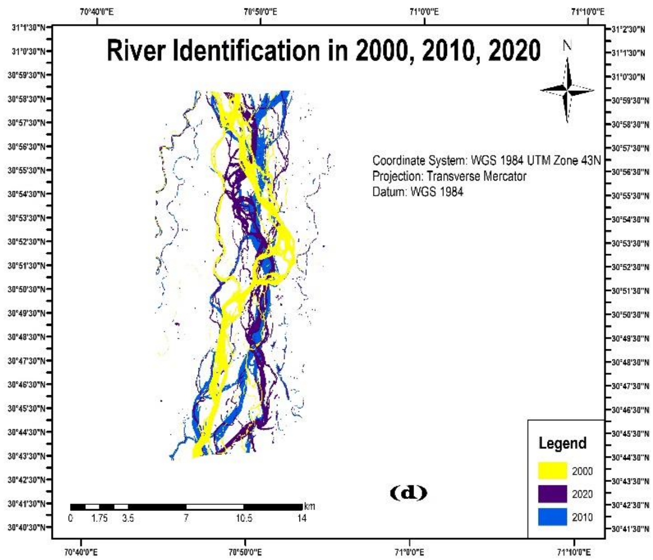

Figure 3: River shifting

Table 2:Indus river flow area

Satellite	Date of acquisition	Season	Area of watershed
Landsat 4,5	2000	High flow +Low flow	50km^2
Landsat 7	2010	High Flow +Low flow	48.83km^2
Landsat 8	2020	High Flow +Low flow	31.02km^2

The Results Show that the change in the stream banks is because of different common and synthetic exercises like flood, flow velocity, deposition of eroded materials, expulsion of the vegetation covers, and soil stability disturbances. Figure 4 shows that the hydrograph of 2000,2010, and 2020 present peak discharge in June, July, and august in this time duration Government Should have to train the natural river flow.

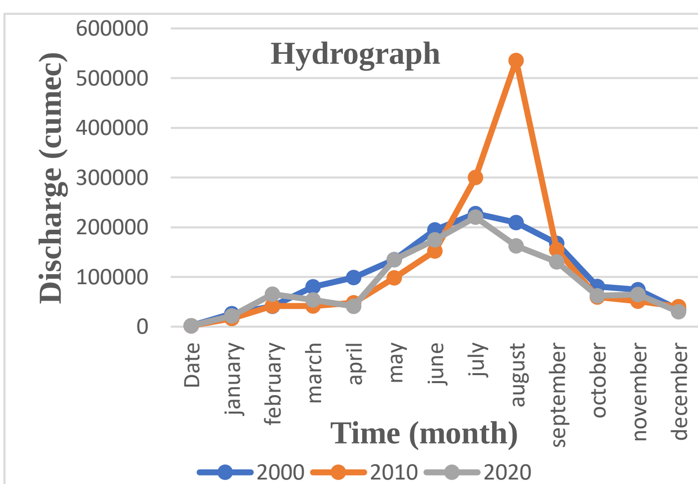

Figure :4 Hydrograph

The Authors have interviewed about 200 people from the local community of the study area to discuss river erosion and floodwater management during the monthly peak eruption. Statistics in figure 5,6 show that 59% of the comments were about "improper river training" and 43% were about "poor flood management".

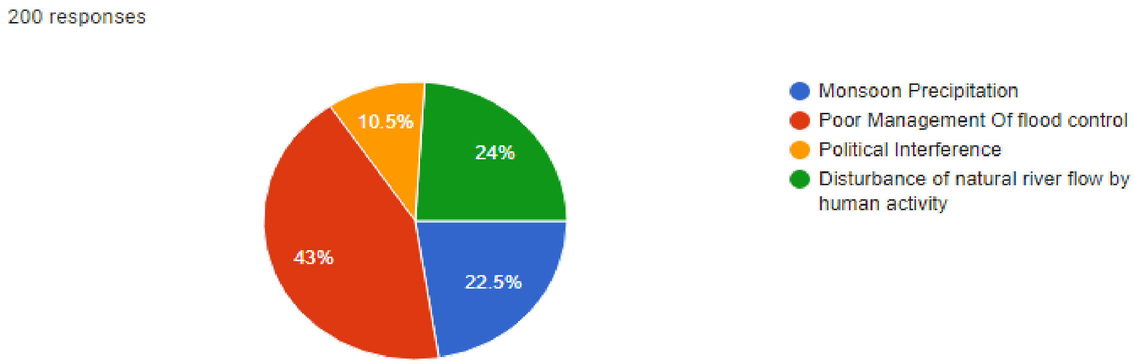

Figure 5: Survey Analysis of Layyah district community

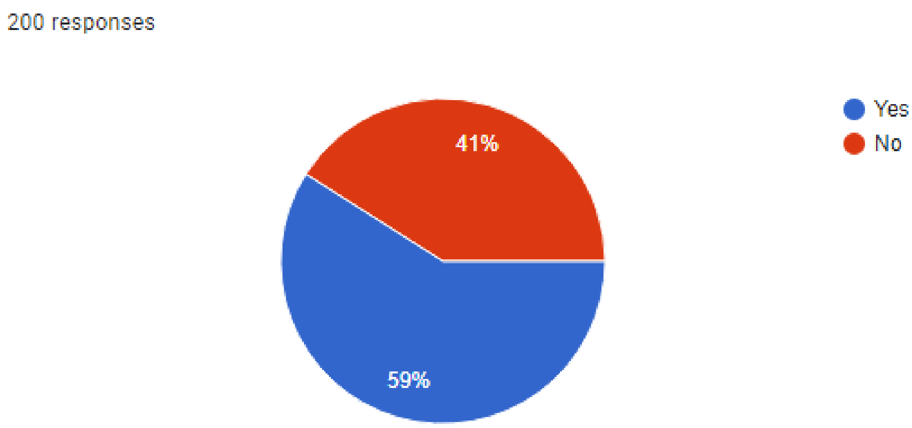

Figure 6: Survey Analysis of Layyah district community

It is about understanding and predicting more complex processes suggest practically through administrative results. Study area results will help in taking useful steps to keep safe agriculture land and lives near about Indus basin, not only in Pakistan but all over the world it saves the economy.

5 Conclusion and Discussion

Following conclusions and discussion can be drawn from the conducted study:

- Protection against Bank Erosion by constructing dikes is not a long-term solution as sometimes it becomes more effective for disturbing the river path flow by minimizing the natural river flow.
- GIS mapping of river erosion shows that from 2000 to 2010 the natural river cross-section is disturbed by changing watersheds of 50km^2 to 48. 83km^2 and from 2010 to 2020 reduction of river watershed is from 48. 83km^2 to 31.02km^2.
- The change in the stream bank is because of different common and synthetic exercises like a flood, flow velocity, deposition of eroded materials, uprooting of the vegetation covers, and soil stability disturbances.

- Around 200 interviews were also conducted with local community individuals discussing river erosion and floodwater management during the month of peak discharge. The statistics show that 59% of remarks were related to "inappropriate river training works" and 43% of remarks were about "poor floodwater management".

References

[1] H. U. A. Khan, S. F. A. Khalil, S. J. H. Kazmi, M. Umar, A. Shahzad, and S. B. Farhan, "Identification of River Bank erosion and inundation hazard zones using geospatial techniques—a case study of Indus River Near Layyah District, Punjab, Pakistan," *Geoplan J Geomat Plan,* vol. 4, pp. 121-130, 2017.

[2] J. L. Florsheim, J. F. Mount, and A. Chin, "Bank erosion as a desirable attribute of rivers," *BioScience,* vol. 58, no. 6, pp. 519-529, 2008.

[3] S. Archana, G. RD, and S. Nayan, "RS-GIS based assessment of river dynamics of Brahmaputra River in India," *Journal of Water Resource and Protection,* vol. 2012, 2012.

[4] J. K. Pati, J. Lal, K. Prakash, and R. Bhusan, "Spatio-temporal shift of western bank of the Ganga river, Allahabad city and its implications," *Journal of the Indian Society of Remote Sensing,* vol. 36, no. 3, pp. 289-297, 2008.

[5] A. K. Kar, R. Hembram, and H. Mohanty, "Study of Morphological Changes in Deltaic River of Odisha Using GIS," in *Water Management and Water Governance*: Springer, 2021, pp. 35-46.

[6] H. Momin, R. Biswas, and C. Tamang, "Morphological analysis and channel shifting of the Fulahar river in Malda district, West Bengal, India using remote sensing and GIS techniques," *GeoJournal,* pp. 1-17, 2020.

[7] P. K. Thakur, C. Laha, and S. P. Aggarwal, "River bank erosion hazard study of river Ganga, upstream of Farakka barrage using remote sensing and GIS," *Natural Hazards,* vol. 61, no. 3, pp. 967-987, 2012.

[8] N. Murtaza, N. Mohammed, S. Bhatti, S. Akhtar, S. Harrison, and S. Feretti, "Pakistan floods 2010: The DEC real-time evaluation report," *Think Ahead, Disaster Emergency Committee,* 2009.

[9] M. Bora and D. C. Goswami, "RS-GIS based assessment of the impact of Hatimura embankment on the channel planform of the Kolong River, Assam, India," *Geocarto International,* pp. 1-17, 2021.

[10] M. Witek-Kasprzak, Ł. Kasprzak, and J. Remisz, "The influence of river training on the location of erosion and accumulation zones (Kłodzko County, South West Poland)," *Open Geosciences,* vol. 12, no. 1, pp. 637-655, 2020.

[11] O. Shabir, "A summary case report on the health impacts and response to the Pakistan floods of 2010," *PLoS currents,* vol. 5, 2013.

3rd Conference on Sustainability in Civil Engineering (CSCE'21)
Department of Civil Engineering
Capital University of Science and Technology, Islamabad Pakistan

NUMERICAL INVESTIGATION OF FLOW BEHAVIOUR IN A ROUGH BANK OPEN CHANNEL WITH VEGETATION PATCHES

[1] Muhammad Bilal*, [2] Usman Ghani, [3] Muhammad Asif*

1: Civil Engineering Department, University of Engineering and Technology Taxila, hafizbilal39@gmail.com
2: Civil Engineering Department, University of Engineering and Technology Taxila, usman.ghani@uettaxila.edu.pk
3: Housing Urban Development and Public Health Engineering Department, masifshehzad667@gmail.com
* Corresponding author: Email ID: hafizbilal39@gmail.com

Abstract- In natural streams there exists a variation of roughness in stream-wise and transverse directions. In the present study, a numerical technique has been utilized to investigate the flow structure in an open channel comprising of various kinds of hydraulic roughness's. The channel roughness was consisted of roughness elements along the banks of the channel and circular vegetation patches along the center line of the channel. Bank roughness elements of two different lengths l_r were used {0.06 m,0.04 m} having pitch to height ratio *p/k* {9.67, 10.33}. Results captured by RSM model are presented in the form of depth-averaged velocities, contours of stream-wise velocity distribution and turbulent intensity. The results showed flow velocities in regions downstream of vegetation patches and roughness elements are small and supports the ecological habitat nourishment. Turbulence of minimum magnitude is observed and uniformly distributed in the free unobstructed regions. However, maximum of 5.8% turbulence has been observed in the flow zones of patches and bank roughness elements.

Keywords- Roughness Elements, Vegetation Patches, Computational Fluid Dynamic (CFD), Reynolds Stress Model (RSM), Open Channel Flow.

1 Introduction

Natural streams and rivers benefitted the human beings from the ancient times. To meet the necessities of communities' water from the water bodies are diverted for domestic and industrial use. The human activities over the rivers changed the natural geometry of the conveyance channels which disturbed the equilibrium between erosion and sediment deposition. To protect the water carrying structure a variety of river restoration techniques have been used. These restoration techniques include the protection shape of conveyance channel by a variety of methods i-e pitching, bioengineering, constructing embankments levees and spurs etc. The flow through rivers and fresh-water streams when encountered these different types of river protection structures imparts hydraulic resistance. These elements like vegetation, embayment's, gravel, cobbles etc. behave like a roughness element and encountered for hydraulic roughness and morpho dynamics in the field of hydraulic engineering. For the perspective of basic research, a river has been characterized as a channel which equipped with roughness elements [1]. Bed material of open channel, i.e., gravel bed comprises of small grains act as roughness elements and retard the flow. Variety of roughness elements are being used in the literature which includes rectangular, square, circular, octagonal, spherical, hemispherical in shape [2, 3, 4, 5, 6]. Literature studies suggested that three types of flows are generated by roughness elements depending on their pitch to height ratio *P/k*, *k*-type flow, un-reattached flow and *d*-type flow (*P* is the pitch between two consecutive elements, *k* and *d* are the two types where *k* is roughness height and *d* boundary layer thickness) [6].

In river streams commonly there exists a variation of roughness in lateral direction. It may be vegetation on one side or change in the size of gravel beds [7]. In open channels and wetland flows, vegetation also considered as the roughness which imparts resistance to the flow behaviour. Vegetation can be rigid or flexible, which grows naturally on the bed or along the banks of flowing channel. Vegetation in open channel flows changes the entire flow structure, induces turbulence, increases the hydraulic resistance along the wetted perimeter of channel and reduces the conveyance capacity of channel threshold [8, 9]. In open channel flows, vegetation colonializes themselves to behave as mono-specific patches which interacts the flow in very non-linear behaviour. These vegetation patches have a noteworthy effect on marine ecology, they are self-assembled by the clonal growth, resulting in the formation of a vegetation mixture. Few of the previous studies have investigated the flow field and geomorphological changes behind the isolated vegetation patch [10, 11]. Anjum [12] employed numerical CFD code FLUENT to study the mean flow characteristics through a configuration of circular vegetation patch. However, flow structure having more than one patch is considerably different from a single patch.

To the knowledge of the authors, the previous studies considered either vegetation patches or banks roughness elements independently. However, a study of flow characteristics in the presence of both vegetation patches and bank roughness elements has not been made in the past. The present study investigates mean flow behaviour and turbulence characteristics in a rectangular channel having both the vegetation patches and bank roughness elements of different pitch-to-height ratio *P/k*. Computational Fluid Dynamics technique was employed in this study. Reynolds Averaged Navier Stokes (RANS) equations were solved with the help of 3D numerical code FLUENT.

1.1 Numerical Model Validation.

The numerical model was validated against the experimental data of Li [13]. Flow domain comprises of 16 m length, 0.3 m width and 0.4 m height. Rigid circular bamboo cylinders of diameter (d = 4 mm) were used to model the circular vegetation patch (D = 0.06 m) at the center of flow domain. The stem density was described by n, the number of cylinders per bed area and the frontal area per volume a=nd. The bed slope was 0. 001.The vegetation patch occupied the entire water column i-e emergent in all the experimental series. The center of circular vegetation patch was considered as the origin having coordinates (0, 0, 0) in longitudinal, transverse, and vertical directions, respectively. The details of experimental setup could be found in Li [13]. Experiment no. 2 was selected and modelled for validation purpose. The discharge of 18.01 l/s was used and water depth taken was 0.13 m. The large mesh structure and computational time was reduced by selection of only 1 m length of the flow domain. Design-Modeler of ANSYS Workbench was used for creation of flow domain. To mesh the entire flow domain, unstructured mesh with tetrahedral elements was used. Three meshes of different sizes i.e., coarse, medium and fine were generated and consisted of 200 x 60 x 20, 400 x 120 x 40, 600 x 180 x 60 node numbers in stream-wise, lateral and vertical directions respectively. The difference of computational velocities between medium and fine mesh was less than 1%. Based on the mesh independence test, it was assumed that the results of our numerical model are mesh independent. As a result, medium sized mesh having node numbers 400 x 120 x 40 was selected for the simulation purposes.

After the successful generation of mesh, it was imported to the FLUENT for solving the fluid flow phenomena. Different boundary conditions were assigned on different surfaces of the flow domain. The inlet/outlet of the flow domain was mapped and provided with the periodic boundary condition. The component of velocity at the side walls, bed of channel and surfaces of vegetation cylinders is zero, therefore wall boundary condition was applied on these surfaces. The symmetry boundary condition was applied at the top free surface. The Reynolds stress turbulence closure model (RSM) was used for this numerical simulation. The SIMPLE algorithm was selected for the pressure-velocity coupling. For spatial discretization 2nd order upwind and standard wall function was used. All residual plots of numerical computation were set to be converged after attaining the value of 1 x 10^{-5}. In the lateral direction from origin, vertical lines located at y/D = 0, 0.58D, 1.17D and 1.75D (y is the distance in transverse direction from origin normalized with the vegetation patch diameter D) numerically computed velocities were investigated and compared to the experimentally measured velocities Li [13]. The Figure 1 shows that the normalized numerically computed velocities are in close agreement with the experimentally measured velocities. It indicates that our numerical model can simulate the flow in such situations.

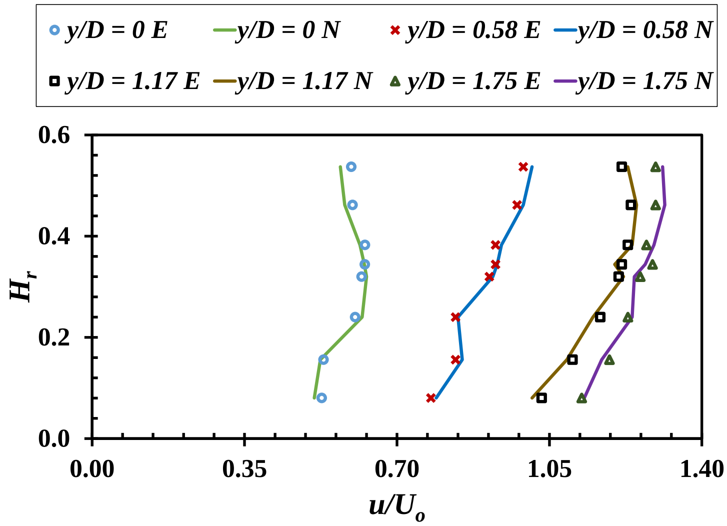

Figure 1: Validation of numerical model by comparing numerically computed results (N) with experimental data(E).

1.2 Numerical Simulation.

After successful validation process, two geometric configurations were considered for simulation purposes. These were comprised of circular vegetation patches along the center line along with bank roughness elements as shown in the Figure 2. The diameter of circular vegetation patch and individual cylinder was 0.06 m and 4 mm respectively. Bank roughness elements were modelled with rectangular elements attached to the side walls as shown in the Figure 2. The height k and width w_r of the roughness elements were kept same in both the cases. Therefor the relative submergence ratio $h/k < 10$ remained same in both the cases. However, roughness elements of two different lengths l_r were used {0.06,0.04} having pitch to height ratio p/k {9.67, 10.33}. The discharge of 18.01 l/s was used in both the cases. The schematic diagram of Case 1 is shown in figure 2.

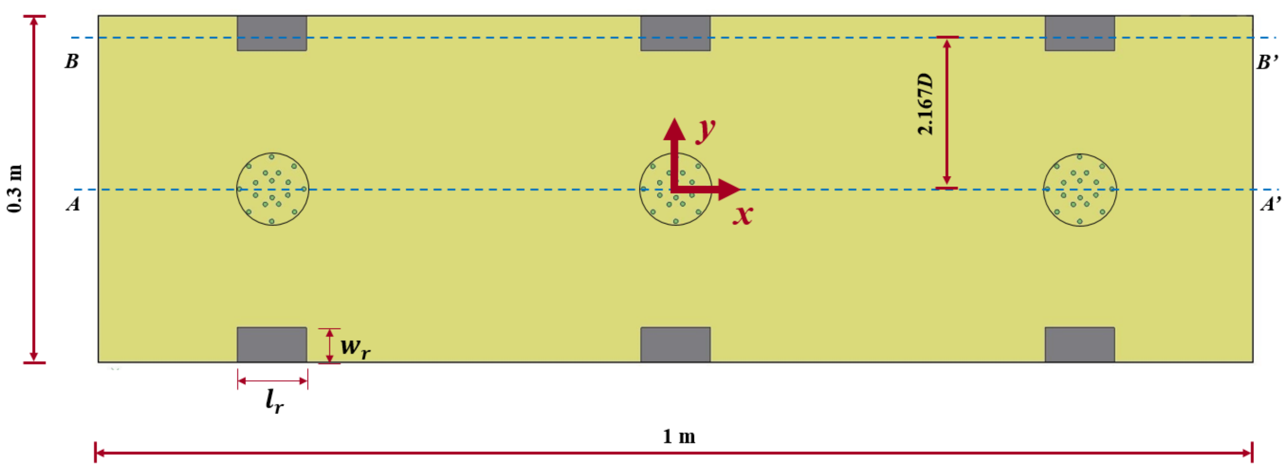

Figure 2: Schematic diagram of numerical model showing the geometrical details of the flow domain.

Table 2. Hydraulic Flow conditions of numerically simulated cases

Sr. No	*Q* (L/s)	*H* (cm)	Vegetation Patch *D* (m)	Vegetation cylinder *d* (mm)	Roughness		
					Height *k* (m)	width w_r (m)	Length l_r (m)
Case 1	18.01	13	0.06	4	0.03	0.03	0.06
Case 2	18.01	13	0.06	4	0.03	0.03	0.04

2 Results and Discussions

2.1 Depth-Averaged velocities

Numerically computed Depth-averaged velocities u_d were investigated at section *AA*' and *BB*' are shown in figure 3. The depth-averaged velocities were made dimensionless and normalized with the initial velocity *U* (*U* = *Q/A*). Section *AA*' passes through the origin i-e center of flow domain whereas section *BB*' is located at 2.167*D* in the transverse direction. From figure 3a distribution of depth-averaged velocities is highly non-uniform which illustrates that the flow in the vicinity of vegetated zone is highly non-uniform. The profile of u_d showed the rise in magnitude of velocities as the flow approached the vegetation patches and acquired a sawtooth distribution inside the vegetation patched regions. However, the decrease in magnitudes was observed in the flow zones just behind the vegetation patches. The reduction of velocities in the downstream of vegetated zones is due to the sheltering effects [14, 15]. At the upstream of vegetation patches, flow experiences a blockage and vegetation cylinders accelerated the flow. Due to the hindering effects of vegetation patch, an increase in depth-averaged velocities is rational. The alternate rise and fall in the distribution of u_d is due to the velocity difference between patched and wake zones. At section *BB*' magnitude of u_d is higher as compared to section *AA*'. However, a inflection instability in the velocity distribution was observed above the roughness elements. The reduction of the velocities above the roughness elements is due to acceleration of flow in lower zones. However, when the flow in low regions combines with the faster higher flow zones, a shear layer may develop which retards the flow slightly. The flow blockage in the case 1 is higher due to the small pitch to height ratio *P/K* at banks due to which the magnitude of u_d is slightly higher for case 1.

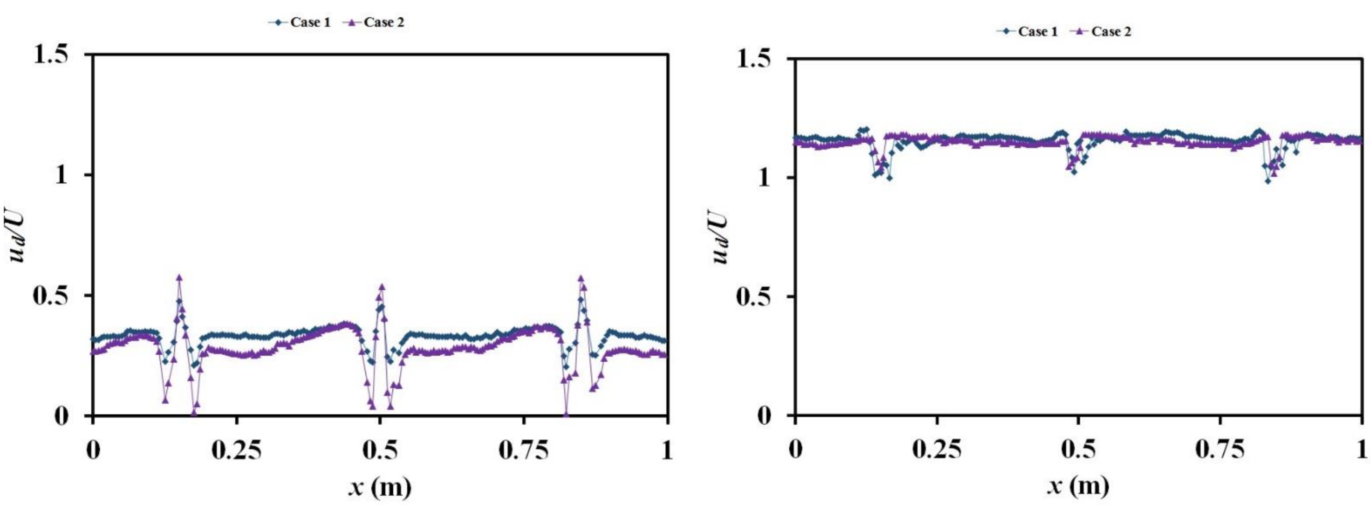

(a) (b)

Figure 3: Depth- averaged velocities at section (a). AA' (b) BB'

2.2 Contours of Stream-wise velocity

Figure 4 a-b shows the contours of stream-wise velocities along the horizontal plan at the z = 0.03 m. The longitudinal velocities are normalized with the average initial velocity U. The horizontal plan at z = 0.03 m passes through the top of Roughness elements. This surface was selected to study the flow resistance and wakes formed behind the vegetation patches and roughness elements. The flow zones located downstream of vegetation patches equipped with low velocity magnitudes. Meanwhile higher velocity regions can be observed adjacent to vegetation patches and roughness elements. When the flow approaches vegetation patches, it is diverted in the lateral direction away from the vegetated zones due to which a wake was formed downstream of circular patches having lower velocities. However, the increased hydraulic resistance accelerates the flow in regions adjacent to roughness elements and vegetation patches due to which noteworthy rise in magnitudes was observed. The interface of high velocity flow regions and low velocity zones are associated with the high shear stresses and scalar fluxes resulting in the lateral mass, oxygen defusal and concentration changes.

The flow zones downstream of vegetation patches supports the sediment depositions and ecological nourishments, which further enhanced the elongation and growth of vegetation mixture [14, 16]. A von Karman vortex street was also observed downstream of circular vegetation patches and is more elongated and prominent in case 1. The flow zones associated behind roughness elements are termed as the dead zones. The flow velocities were decelerated directly downstream of roughness elements. In the hydraulics engineering these dead zones have numerous advantages to promote the morphological diversity and enhanced ecological suitability for the nursery habitat and fish spawning [17, 18]. The overall magnitude of mean stream-wise velocity in case 1 is higher as compared to case 2. The increase in magnitude of velocities associated with both cases is 1.5 to 1.46 times that of the initial velocity.

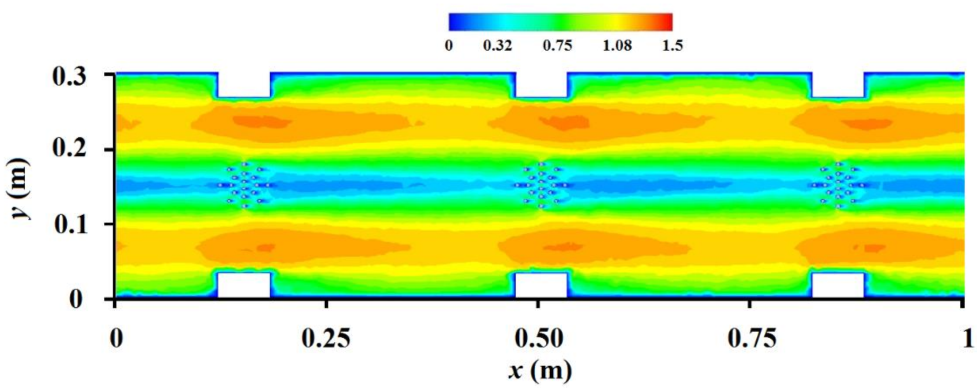

(a)

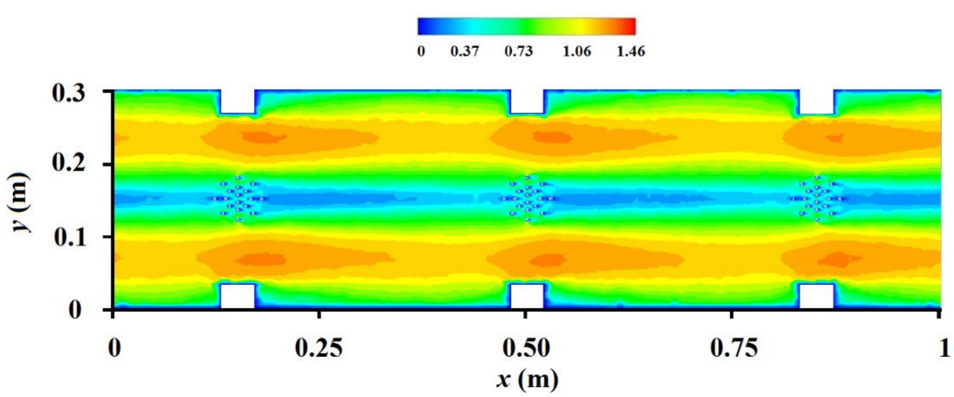

(b)

Figure 4: Contours of stream-wise velocity at z = 0.03 m (a). Case 1 (b) Case 2.

2.3 Turbulent Intensity

To quantify the turbulence in the flume turbulent intensity is investigated. Contour plots of turbulent intensity is investigated at the z = 0.03 m and shown in figure 5. A noteworthy difference was observed between the vegetated/roughness flow zones as compared to unobstructed free stream zones. Higher turbulences were observed in the vegetation patch zones and in the vicinity of roughness elements. The gradient of velocities in the dead zones and vegetated zones is higher due to which a larger turbulence was observed. Furthermore, the presence of wall in dead zones created a turbulence anisotropy which is also the responsible of higher percentage of turbulence at upstream and downstream of roughness elements. The distribution of turbulences in the vicinity of roughness elements flow zone is quite different as compared to flow zones associated at upstream and downstream of vegetation patches. The turbulence intensity is widely distributed and prolonged in the roughness elements flow zones, due to the turbulence anisotropy caused by the side walls. However, it is only confined in the vegetation patches and small magnitude is observed in the gaps located downstream of vegetation patches. The distribution of turbulent intensity in unobstructed free regions is uniform due to no effect of resistance. It can be seen in the figure that maximum 5.8, 5.6 % and minimum 0.59, 0.57 % of turbulent intensity has been observed for case 1 and 2 respectively. It can also be observed that size of roughness element has little contribution in the maximum turbulences in the dead zones.

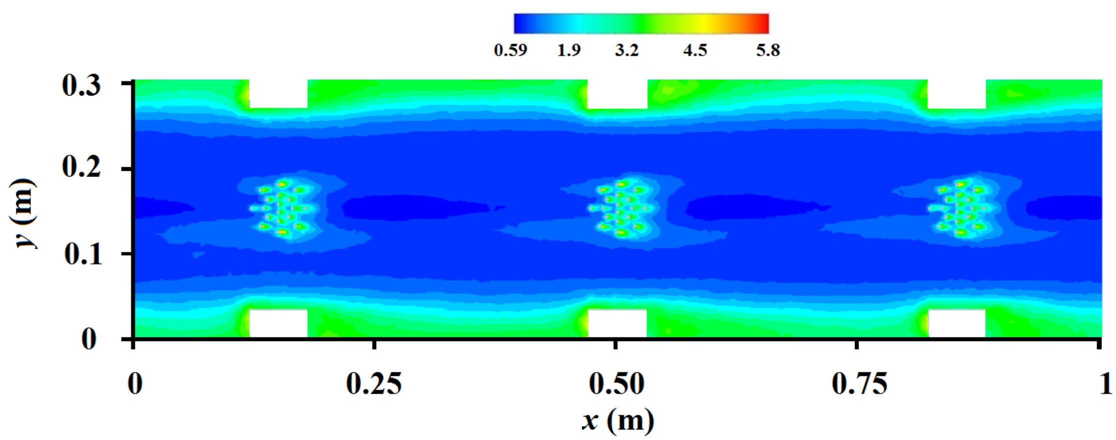

(a)

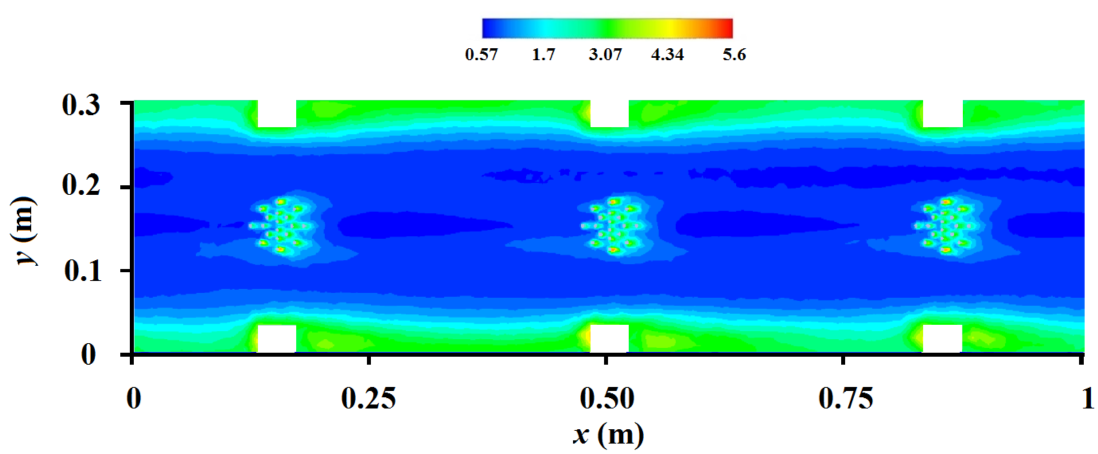

(b)

Figure 5: Contours of Turbulent Intensity at z = 0.03 m (a). Case 1 (b) Case 2.

3 Conclusion

In the present study, a CFD technique has been used to investigate the flow features associated with the combined effect of bank roughness of two sizes and central emerged vegetation patches. This study shows the noteworthy effects of flow phenomenon in the channel comprising of two types of hydraulic roughness's.

- The distribution of depth-averaged velocities are small and uniform in the d/s of vegetation patches which shifted to highly non-uniform in the vegetation patches and acquired saw tooth distribution. Increased magnitude with inflectional instability in the distribution of depth-averaged velocity was observed directly above the roughness elements. The flow regions located d/s of any type of roughness have minimum flow velocities and supports deposition of sediments and wildlife habitat.
- Maximum 5.8 % and minimum of 0.57 % turbulent intensity was observed and mainly associated with the hydraulic resistance to flow. The turbulent intensity is maximum in the zones equipped with roughness elements and vegetation as compared to the free unobstructed regions.

4 Acknowledgement

The careful review and constructive suggestions by the anonymous reviewers are gratefully acknowledged.

References

[1] T. Meile, J-L. Boillat and A. J. Schleiss, "Flow Resistance Caused by Large-Scale Bank Roughness in a Channel," Journal of Hydraulic Engineering, Vol 137, pp. 1588-1597, 2011.

[2] A. Abbaspour and S. H. Kia, "Numerical Investigation of Turbulent Open Channel Flow with Semi cylindrical Rough Beds," KSCE Journal of Civil Engineering, Vol 18, pp. 2252–2260, 2014.

[3] H. Romdhane, A. Soualmia, L. Cassan and L. Masbernat, "Velocity profiles over homogeneous bed roughness," Fluid Mechanics Research International Journal, Vol 2, PP. 148-154, 2018.

[4] P. Orlandi, S. Leonardi And R. A. Antonia, "Turbulent channel flow with either transverse or longitudinal roughness elements on one wall," Journal of Fluid Mechanics, Vol 561, PP. 279-305, 2006.

[5] S. G. Sajjadi, and J. N. Aldridge, "Prediction of turbulent flow over rough asymmetrical bed forms," Applied Mathematical Modelling, Vol 19, pp. 139-152, 1995.

[6] J. Cui, V. C. Patel, C-L. Lin, "Large-eddy simulation of turbulent flow in a channel with rib roughness," International Journal of Heat and Fluid Flow, Vol 24, pp 372-388, 2003.

[7] J. Li and S. S. Li, "Near-bed velocity and shear stress of open-channel flow over surface roughness," Environmental Fluid Mechanics, Vol 20, pp. 293-320, 2020.

[8] H. Nepf, "Drag, turbulence, and diffusion in flow through emergent vegetation," Water Resources Research, 35 pp. 479-489, 1999.

[9] H. Nepf and M. Ghisalberti "Flow and transport in channels with submerged vegetation," Acta Geophysical, Vol 56, pp. 753-777, 2008.

[10] S. Wunder, M. Trevisson, C. Heckele, L. Chagot, B. Murphy, S. McLelland, F. Moulin and O. Eiff, "Near wake of emergent vegetation patches in shallow flow," River Flow 2018 - Ninth International Conference on Fluvial Hydraulics, Vol. 40, 2018

[11] C. Liu, Z. Hu, J. Lei and H. Nepf, "Vortex Structure and Sediment Deposition in the Wake behind a Finite Patch of Model Submerged Vegetation" Journal of Hydraulic Engineering, Vol. 44, DOI: 10.1061/(ASCE)HY.1943-7900.0001408.

[12] N. Anjum, U. Ghani, G. A. Pasha, M. U. Rashid, A. Latif and M. Z. Y. Rana, "Reynolds stress modeling of flow characteristics in a vegetated rectangular open channel," Arabian Journal for Science and Engineering, pp. 43, pp. 5551–5558, 2018.

[13] W. Li, D. Wang, J-L. Jiao and K-J. Yang, "Effects of vegetation patch density on flow velocity characteristics in an open channel," Journal of Hydrodynamics, Vol 31, pp. 1052–1059, 2019.

[14] F. Zhao and W. Huai, "Hydrodynamics of discontinuous rigid submerged vegetation patches in open-channel flow," Journal of Hydro-environment Research, Vol 12, pp.148-160, 2016.

[15] N. Anjum, U. Ghani, G. A. Pasha, G.A., A. Latif, T. Sultan and S. Ali, "To investigate the flow structure of discontinuous vegetation patches of two vertically different layers in an open channel," water, Vol 10, 2019.

[16] A. M. Gurnell, K. Thompson, J. Goodson and H. Moggridge, "Propagule deposition along river margins: Liking hydrology and ecology," Journal of Ecology, Vol 96, pp. 553–565, 2008.
[17] K. Uno, N. Kazuuma, G. Tsujimoto and T. Kakinoki, "Trapping effect of fine sediment in wand" Journal of Japan Society of Civil Engineers, Ser. B3 (Ocean Engineering), Vol 69, pp. 922–927, 2013.
[18] I. Nezu and K. Onitsuka, "PIV Measurements of side-cavity open-channel flows-Wando model in rivers," Journal of visualization, Vol 5, pp. 77–84, 2002.

TRANSPORTATION ENGINEERING

3rd Conference on Sustainability in Civil Engineering (CSCE'21)
Department of Civil Engineering
Capital University of Science and Technology, Islamabad Pakistan

AN OVERVIEW OF COASTAL EROSION IMPACTS ON ROAD INFRASTRUCTURE

[a] ***Umair Ahmed* *, [b] *Nakhshab Ajaz***

a,b : GREN Construction (Pvt.) Ltd., umair.ahmed01@outlook.com , nakhshab.ajaz@outlook.com

Abstract- The most important areas for human and economic activities, as well as the environment, are coastal zones. To protect the natural beauty of the coasts, the vulnerability of coastal areas to natural impacts should be carefully studied. Coastal erosion is a concern at many coastal locations, and it is triggered by both natural and manmade factors. Coastal erosion places the lives of millions of people who live along the coast in jeopardy, and puts coastal infrastructure like roads and bridges at risk. Coastal erosion has a fast effect, making it a significant coastal threat. Coastal areas with road networks close to the shoreline are particularly vulnerable to the impact of climate change-related sea level rise. Coastal erosion has placed these areas road networks in jeopardy. Drastic reductions in water flow of Indus River into the delta, overexploitation of mangroves forests, dredging and channelization, various uses of coastal resources by different industries, and increase in sea level due to climate change and global warming are all anthropogenic factors leading to coastal erosion. Between 1984 and 2015, approximately 28,000 km^2 of the world's coastline is eroded, roughly twice as much as those created by accumulation processes. By 2100, the total "Cost of Coastal Environmental Degradation" (CoCED) in a group of 4 (four) countries affected by coastal flooding and erosion could exceed $3 billion. One of the main factors affecting road networks is sea level rise. When groundwater moves into the pavement base layers, sea level rise caused ground water to reach pavement layers. This groundwater results in reduction of pavement life by 50% and a up to 90% increase in rutting due to fatigue distress. Following the Hurricane Katrina, the Federal Highway Administration (FHWA) performed an inventory of coastal bridges and found that there are around 36, 000 bridges within 15 nautical miles that could be damaged by coastal storms.

Keywords- Coastal Erosion, Global Warming, Infrastructure, Pavements, Sea Level Rise

1 Introduction

The most important areas for human and economic activities, as well as the environment, are coastal zones. To protect the natural beauty of the coasts, the vulnerability of coastal areas to natural impacts should be carefully studied. The coastal zone is home to a large portion of the world's population, accounting for up to 37% of the total population [1]. The coasts have a lot of potential for economic development. Coastal waters, for example, serve as global trading highways. Ships carry approximately 90% of all global goods [2]. Coastal and maritime tourism was the largest tourism sub-sector in Europe in 2014, as well as the largest single maritime economic operation in terms of employment (3.2 million jobs) and value added (over 180 billion euros) [3]. Furthermore, the fishing industry is a significant contributor to the global economy. 90 percent of fishing boats are thought to operate in coastal waters. Mediterranean fisheries were determined to be worth $3.2 billion by the General Fisheries Commission for the Mediterranean (GFCM) [4]. Pakistan has a coastline that stretches for approximately 1001 kilometers and occupies an area of 240,000 square kilometers, bordering Iran to the west and India to the east [5]. Pakistan's fish and seafood industry is worth $1.5 billion, according to estimates [6]. This shows that coastal cities are an important part of any country's economy.

Coastal erosion is a phenomenon that affects almost all coastal states [7]. Coastal erosion is a phenomenon that affects almost all coastal states. Coastal erosion has been one of the most serious environmental problems in recent decades [8-11]. Between 1984 and 2015, approximately 28,000 km^2 of the world's coastline is eroded, about twice as many as were created by accumulation processes [12]. According to the Intergovernmental Panel on Climate Change (IPCC) Fifth Assessment Report [13], the potential scenario for coastal areas will deteriorate as a result of the steady rise in sea level and the likely increase in extreme events as a result of global warming linked to the use of fossil fuels and human pressure [14]. Only in Europe, the total coastal area lost each year due to coastal erosion (including houses and buildings) is estimated to be about 15 km^2. Mitigation initiatives are expected to cost about 3 billion euros per year, which is unacceptably high [15].

Coastal erosion puts millions of people living along the coast in danger, as well as coastal infrastructure. Coastal erosion has a lot of sudden effects, making it a significant coastal threat [16, 17]. The situation is even worse in low-lying deltaic regions of developing countries like Bangladesh, Pakistan and Philippines, which are inadequately equipped to deal with the dangers. One of the long term environmental processes like sea level rise (SLR) [18] and the increased frequency of short-term events like coastal flooding and storm surge [19], become the reason for coastal structural change and aggravate coastal erosion [20].

Infrastructure refers to the structures that allow a society to operate [21], and a community cannot survive long if all of these systems collapse completely (road networks, water supply, drainage, embankments, telecommunications etc.). These networks are often referred to as "lifelines" in disaster management and serve as the "vein" for disaster reduction strategies to propagate. The inadequacy of these infrastructure supports introduces the concept of "vulnerability due to infrastructure" and poses the issue of how well post-disaster activities can be managed. Roads are an integral part of coastal infrastructure. In case of any hazards turning into a disaster road network plays a very important role.

2 Literature Review

2.1 Coastal Erosion

Coastal erosion that contributes to the shaping of coastal landscape is mainly a natural phenomenon throughout history. Erosion, shipping, and deposition processes combine to create coastal ecosystems. Coastal erosion and accretion is the process of wave action, tidal waves, and wave currents wearing away land and removing beach or dune sediments [22]. Coastal erosion is caused by waves generated by hurricanes, wind, or fast-moving motor vessels. It may take the form of long-term loss of sediments and rocks, or simply the temporary re-distribution of coastal sediments. Erosion in one area can lead to accretion in another. Erosion is caused by a disparity of sand inputs and outputs [23]. When the inputs and outputs of sand are balanced, there is no transition, which is referred to as "steady state."Coastal erosion is impacting the coasts and road networks along the coast, as seen in figures 1 a and b.

a)  b) 

Figure 1 : Coastal Erosion, a. Estola Island, Pakistan, (IUCN) and b. A crumbling cliff edge at Tunstall, UK (Image: HullLive)

The main eroding causes of the coastline are rainfall and oceanic waves. Rain, wind, and high waves appear to pick up and drag the sand and earth from exposed beaches, washing it up and out into some other areas of coast. Although natural tides and waves follow similar patterns, their effect is minor in comparison to storms. Hurricanes, in particular, have enough water and power to erode coastlines, turning them into peculiar forms [16].

2.2 Factors Leading to Coastal Erosion

Anthropogenic factors leading to coastal erosion in Pakistan include a dramatic decrease in Indus River water flows into the delta, extinction of mangroves, dredging and channelization, various uses of coastal resources by different industries, and rising sea levels due to global warming [24]. Coastal developments including drainage infrastructure, building jetties, and land reclamation also lead to erosion. Coastal erosion is more common in river deltas or coastlines with somewhat soft sediments and a large number of beaches that are easily influenced by wave and tide movement [25]. Earthquakes, wind, tides, waves, rainfall, and cyclonic activity are all natural physical factors that contribute to coastal erosion [26].

The table below depicts "erosion hotspots," or areas that are impacted by coastal erosion due to natural or human-caused processes, which are found in Pakistan's coastal region, with medium to extreme erosion intensities.

Table 1 Coastal Location and Degree of Erosion for Pakistan's Coastline [27]

District	Location	Type of Coast	Erosion Intensity
Karachi	Phitti & Gizri Creeks	Mudflats/ Creek	Moderate
	Clifton	Beach	Low
	Hawksbay	Raised	Moderate
	DHA Phase-8	Creek and plain area	Moderate
	RasMurai	Raised	Low
Thatta	Kharo Chann	Estuarine mudflat	Severe
	Keti Bunder	Estuarine mudflat	Moderate
	Mirpursakao	Creek/mudflat	Moderate
	Ghorabari	Creek/mudflat	Moderate
	Ghoro Creek	Creek/mudflat	Severe
Sujjawal	Jati	Creek/mudflat	Severe
	Shah Bunder	Creek/mudflat	Severe
Badin	Badin	Creek/mudflat	Severe
	Shaheed Fazil Rahu	Creek/mudflat	Severe
Gwadar	Jiwani	Raised/flat	Very Severe
	Shadi Kor	Estuarine	Very Severe
	Pasni	Raised/flat	Severe
	Ras Shaheed	Raised	Severe
	Gwadar Bay	Raised/flat	Moderate
	Kalmat Khor	Lagoon	Moderate
	Ras Jaddi & Zarin	Raised	Moderate
	Ormara	Raised	Low
Lasbela	Damb	Sand dune	Very Severe
	Miani Hor	Lagoon	Moderate
	Sonmiani	Raised	Moderate
	Gaddani	Raised/flat	Moderate
	Hub	Estuarine	Moderate

2.3 Impacts of Coastal Erosion on Road Infrastructure

Coastal highways are one of the most important pieces of road infrastructure along the coast. Coastal highways are roads that are affected by their location in or near a coast's specific water level, wave, and sand transport system. The Great Lakes and all other non-riverine water bodies that can be impacted by coastal storm events are included in the coastal climate, which is usually associated with the oceans [28]. Highways in every coastal state are flooded and destroyed during coastal storms. Some of these roads run parallel to the coast and are used for entry and evacuation. Figure 2a shows some of these roads that run parallel to the coast, either directly along or inland from the sea. [29]. Figure 2b shows the damage caused by coastal erosion to the road infrastructure of Makran Coastal Highway. Some of these roads are major highways of critical importance that run across or along costal bays.

a)  b) 

Figure 2 Makran Coastal Highway, Pakistan (Image: Paki Holic)

The aggregated Cost of Coastal Environmental Degradation (CoCED) in the four countries caused by coastal flooding and erosion could exceed over US $ 3 billion by 2100, based on the worst-case scenario of regional relative sea-level rise, which corresponds to RCP 8.5. In addition, when population growth is factored in, the number of people affected in some countries could rise by 400 percent [30]. The eastern and western sides of the Indus River experienced erosion of an averaged 12.5 ± 0.55 m/year and 19.96 ± 0.65 m/year while Karachi coastline experienced erosion at a rate of 2.43 ± 0.45 m/year and accretion at a rate of 8.34 ± 0.45 m/year, respectively. Coastal erosion can be seen all over the coast. However, erosion rates vary across the study area, with the max. average erosion rate of 27.46 m/year in the Indus Delta region (IDR), which has a general pattern of erosion rising from west to east. The interdecadal transition from Karachi to the Indus River (IR) East zone showed an increasing linear pattern ($R^2 = 0.78$) from 1989 to 1999, 1999 to 2009, and 2009 to 2018. The west-to-east spatial pattern is positively associated with mean sea level rise (SLR). The mean sea level has risen from 1.1 to 1.9 mm/year, while the slope of coast line is decreasing in eastward direction and this rise is negatively corelated to the topography of the coastline [31]. Coastal road infrastructure is at risk of being damaged and destroyed as the sea level rises. Following Hurricane Katrina, the Federal Highway Administration (FHWA) performed an inventory of coastal bridges that could be damaged by coastal storms. The assessment estimated that there are over 36,000 bridges within 15 nautical miles of the coasts, based on very specific parameters [32]. About 1,000 of these bridges may be vulnerable to the same failure modes as those seen in recent coastal storms [33]. Coastal New England's sea level is forecast to rise 3.9–6.6 ft (1.2–2.0 m) by 2100. Many climate-change risk and adaptation studies have focused on surface-water flooding from sea-level rise (SLR) on coastal-road infrastructure, but few have focused on rising groundwater. The inland extent of SLR-induced groundwater rise will be three to four times that of surface-water rise. in New Hampshire's Seacoast District, potentially affecting 23 percent of the region's highways, according to groundwater modelling. As the unbound layers become saturated, the service life of the pavement is reduced. Where the ground water is expected to rise due to SLR , the pavements which are just 5 ft or 1.9 m above ground water level are at a very high risk of failure [34]. When groundwater moves into the pavement base layers, sea level rise caused ground water to reach pavement layers. This groundwater results in reduction of pavement life by 50% and a up to 90% increase in rutting due to fatigue distress [35]. This shows that not only direct affect is there on pavements by coastal erosion but also due to increased sea level the ground water is increased. The increased ground water level affects the base layers of roads and damages them causing billions of dollars of destruction.

3 Conclusion

Coastal erosion has many forms it could be in the form a Hurricane or a storm or it could be mainly due to rise in sea level. It was found that most coastal highways are at risk of getting damage by coastal erosion. These coastal roads play an important role of joining the coastal cities and are crucial part of economy. Following conclusion have been drawn from this study

- Due to global warming and climate change the coastal cities and coastal highways are at real risk of turning into disaster.
- The increased intensity of hurricane and storm affect the coastal roads and can cause major blockage of services during a catastrophic event.
- One of the main factors affecting road networks is sea level rise. When groundwater moves into the pavement base layers, sea level rise caused ground water to reach pavement layers. This groundwater results in reduction of pavement life by 50% and a up to 90% increase in rutting due to fatigue distress.
- Between 1984 and 2015, approximately 28,000 km^2 of the world's coastline is eroded, roughly twice as much as those created by accumulation processes.

Acknowledgment

The author would like to thank every person/department who helped throughout the research work, particularly Engr. Dr. Usman Farooqi. The careful review and constructive suggestions by the anonymous reviewers are gratefully acknowledged.

References

[1] UN, "Factsheet: People and Oceans," in *The Ocean Conference*, 2017: United Nations New York, NY, p. 7.
[2] H. W. Bange *et al.*, *World Ocean Review 2015: living with the oceans 5. Coasts-a vital habitat under pressure*. Maribus, 2017.
[3] D. Sartori *et al.*, "Guide to cost-benefit analysis of investment projects. Economic appraisal tool for cohesion policy 2014-2020," 2014.
[4] M. Randone *et al.*, "Reviving the economy of the Mediterranean Sea: actions for a sustainable future," *WWF Mediterranean Marine Initiative, Rome, Italy,* 2017.
[5] M. T. Qureshi, "Integrated Coastal Zone Management Plan for Pakistan," *IUCN-Pakistan. Qari, R., & Shaffat, M.(2015). Distribution and abundance of marine debris along the coast of Karachi (Arabian Sea), Pakistan. Pakistan Journal of Scientific and Industrial Research Series B Biological Sciences,* vol. 58, no. 2, pp. 98-103, 2011.
[6] P. Ministry of Planning Comission, "Pakistan Coastal Development through Integrated coastal zone management (ICZM)," Government of Paistan, Pakistan, 2020 2020.
[7] L. Van Rijn, "Coastal erosion and control," *Ocean & Coastal Management,* vol. 54, no. 12, pp. 867-887, 2011.
[8] N. Lenôtre, P. Thierry, D. Batkowski, and F. Vermeersch, "EUROSION Project. The Coastal Erosion Layer," *WP,* vol. 2, p. 45, 2004.
[9] A. Luijendijk, G. Hagenaars, R. Ranasinghe, F. Baart, G. Donchyts, and S. Aarninkhof, "The state of the world's beaches," *Scientific reports,* vol. 8, no. 1, pp. 1-11, 2018.
[10] M. Allen *et al.*, "Technical Summary: Global warming of 1.5° C. An IPCC Special Report on the impacts of global warming of 1.5° C above pre-industrial levels and related global greenhouse gas emission pathways, in the context of strengthening the global response to the threat of climate change, sustainable development, and efforts to eradicate poverty," 2019.
[11] E. C. Bird, "Coastline changes. A global review," 1985.
[12] L. Mentaschi, M. I. Vousdoukas, J.-F. Pekel, E. Voukouvalas, and L. Feyen, "Global long-term observations of coastal erosion and accretion," *Scientific reports,* vol. 8, no. 1, pp. 1-11, 2018.
[13] M. Tignor and S. Allen, "Fifth Assessment Report of the Intergovernmental Panel on Climate Change (IPCC)," *Cambridge, UK/New York, USA,* 2013.

[14] I. C. Change, "The Physical Science Basis; Stocker, TF, Qin, D., Plattner, G," *K., Tignor, M., Allen, SK, Boschung, J., Nauels, A., Xia, Y., Bex, V., Midgley, PM, Eds,* p. 1535, 2013.
[15] M. Kirkby *et al.*, "Pan-European Soil Erosion Risk Assessment for Europe: the PESERA map, version 1 October 2003. Explanation of Special Publication Ispra 2004 No. 73 (SPI 04.73)," Office for Official Publications of the European Communities, 2004.
[16] C. Martínez, M. Contreras-López, P. Winckler, H. Hidalgo, E. Godoy, and R. Agredano, "Coastal erosion in central Chile: A new hazard?," *Ocean & coastal management,* vol. 156, pp. 141-155, 2018.
[17] P. Narra, C. Coelho, and F. Sancho, "Multicriteria GIS-based estimation of coastal erosion risk: Implementation to Aveiro sandy coast, Portugal," *Ocean & Coastal Management,* vol. 178, p. 104845, 2019.
[18] A. Cazenave and G. L. Cozannet, "Sea level rise and its coastal impacts," *Earth's Future,* vol. 2, no. 2, pp. 15-34, 2014.
[19] S. Rahmstorf, "Rising hazard of storm-surge flooding," *Proceedings of the National Academy of Sciences,* vol. 114, no. 45, pp. 11806-11808, 2017, doi: 10.1073/pnas.1715895114.
[20] J. Pollard, T. Spencer, and S. Brooks, "The interactive relationship between coastal erosion and flood risk," *Progress in Physical Geography: Earth and Environment,* vol. 43, no. 4, pp. 574-585, 2019.
[21] B. Mallick, U. K. Das, S. S. Islam, S. K. Das, and M. N. Islam, "VULNERABILITY DUE TO LACK OF INFRASTRUCTURE OF COASTAL LIVELIHOOD DURING CYCLONE AILA 2009 IN BANGLADESH."
[22] M. F. Azemee, "The impact of sea level rise on coastal region of Selangor, Malaysia," Universiti Teknologi Mara Perlis, 2021.
[23] A. Williams, N. Rangel-Buitrago, E. Pranzini, and G. Anfuso, "The management of coastal erosion," *Ocean & coastal management,* vol. 156, pp. 4-20, 2018.
[24] T. Bein, C. Karagiannidis, and M. Quintel, "Climate change, global warming, and intensive care," *Intensive care medicine,* pp. 1-3, 2019.
[25] E. J. Anthony, N. Marriner, and C. Morhange, "Human influence and the changing geomorphology of Mediterranean deltas and coasts over the last 6000 years: From progradation to destruction phase?," *Earth-Science Reviews,* vol. 139, pp. 336-361, 2014.
[26] C. D. Storlazzi and G. B. Griggs, "Influence of El Niño–Southern Oscillation (ENSO) events on the evolution of central California's shoreline," *Geological Society of America Bulletin,* vol. 112, no. 2, pp. 236-249, 2000.
[27] M. Pakistan, "Coastal Erosion in Pakistan: A National Assessment Report," ed: by: WWF-Pakistan, MFF Pakistan and Government of Pakistan, 2014.
[28] M. Crichlow, "Professional development programme: Coastal infrastructure design," ed: St Augustine: Construction and Maintenance. Integrated Watershed Management …, 2001.
[29] S. L. Douglass, B. M. Webb, R. Kilgore, and C. Keenan, "Highways in the coastal environment: Assessing extreme events," United States. Federal Highway Administration, 2014.
[30] A. Bolle, L. das Neves, L. De Nocker, A. Dastgheib, and K. Couderé, "A methodological framework of quantifying the cost of environmental degradation driven by coastal flooding and erosion: A case study in West Africa," *International Journal of Disaster Risk Reduction,* vol. 54, p. 102022, 2021.
[31] S. Kanwal, X. Ding, M. Sajjad, and S. Abbas, "Three decades of coastal changes in Sindh, Pakistan (1989–2018): A geospatial assessment," *Remote Sensing,* vol. 12, no. 1, p. 8, 2020.
[32] Y. D. Murray, A. Y. Abu-Odeh, and R. P. Bligh, "Evaluation of LS-DYNA concrete material model 159," United States. Federal Highway Administration. Office of Research …, 2007.
[33] M. Volovski, J. Murillo-Hoyos, T. U. Saeed, and S. Labi, "Estimation of routine maintenance expenditures for highway pavement segments: accounting for heterogeneity using random-effects models," *Journal of Transportation Engineering, Part A: Systems,* vol. 143, no. 5, p. 04017006, 2017.
[34] J. F. Knott, J. S. Daniel, J. M. Jacobs, and P. Kirshen, "Adaptation planning to mitigate coastal-road pavement damage from groundwater rise caused by sea-level rise," *Transportation Research Record,* vol. 2672, no. 2, pp. 11-22, 2018.
[35] J. F. Knott, M. Elshaer, J. S. Daniel, J. M. Jacobs, and P. Kirshen, "Assessing the effects of rising groundwater from sea level rise on the service life of pavements in coastal road infrastructure," *Transportation Research Record*, vol. 2639, no. 1, pp. 1-10, 2017.

3rd Conference on Sustainability in Civil Engineering (CSCE'21)
Department of Civil Engineering
Capital University of Science and Technology, Islamabad Pakistan

A DIFFUSE DAMAGE MODEL FOR ASPHALT CONCRETE

[a] Awais Ahmed*, [b] Rawid Khan

a: Earthquake Engineering Center, University of Engineering & Technology Peshawar, awais.ahmed@uetpeshawar.edu.pk
b: Department of Civil Engineering, University of Engineering & Technology Peshawar, dr.rawid@uetpeshawar.edu.pk
* Corresponding author: Email ID: awais.ahmed@uetpeshawar.edu.pk

Abstract- Distress in a pavement is a serious problem which can reduce the service life of a pavement. For an efficient design and analysis of pavements, use of efficient yet accurate computational models play a key role. Several numerical models have been used in the past to understand the mechanics of cracking in asphalt concrete. Interface elements with cohesive zone model have been successfully employed by many researchers however, the method requires the crack path to be known a priori and the cracks can only grow along element boundaries. On the contrary, continuum damage/ plasticity models offer the ease of damage modeling, but these methods show mesh dependency. In this paper a phase field diffuse damage model integrated with cohesive zone concept is used to simulate damage in asphalt concrete. The proposed model can simulate multiple interacting cracks propagating arbitrarily through the finite element mesh without the need of any *ad hoc* criterion. The effectiveness of the model is demonstrated using a single edge notch beam. Numerical results are validated against experimental observations. The obtained load versus crack mouth opening displacement curve quantitatively and damage profile qualitatively show good agreement with the experimental observations. The proposed model successfully simulated sharp crack and does not suffer from mesh dependency problem. Additionally, the model is also able to overcome the issue of complaint material behavior before cracking due to the presence of dummy stiffness in the interface element formulations.

Keywords- Asphalt concrete, finite element method, phase field method, mode-I fracture.

1 Introduction

Distress in asphalt pavements can severely affect its performance. Cracking in pavements not only increases the maintenance cost but also can affect the durability and life span of the pavement. Therefore, it is pivotal to understand the damage mechanics of asphalt mixtures for an efficient design. Numerical analysis of materials and structures plays a key role in the design process and is useful to simulate damage under various boundary conditions.

A finite element method with interface elements is often used to simulate fracture in asphalt mixtures. Soares et al. [1] used interface elements with cohesive zone model to simulate fracture in an indirect tension test specimen. Song et al. [2] used interface elements with exponential cohesive constitutive law to simulate mode-I cracking in asphalt concrete beam. Dave et al. [3] used the cohesive zone model to simulate cracking in asphalt mixtures due to thermal loads. Due to the restriction of a crack to propagate along element boundaries in the interface element model, mesh independent crack growth methods like extended finite element method (XFEM) [4] is also explored by many researchers. Mahmoud et al. [5] and Islam et al. [6] used extended finite element method with cohesive zone model to simulate fracture in asphalt mixtures. Even though, XFEM is a good method to simulate mesh independent cracking, modelling complex crack typologies is still a challenge. Moreover, for the case of multiple interacting cracks the method becomes cumbersome from a computer implementation point of view. On the contrary, diffuse damage models were also used by some researchers. Park et al. [7] presented a viscoelastic damage model for the asphalt mixture. Chehab [8] proposed a viscoelastic-plastic approach for damage in asphalt mixtures. However, these methods suffer from mesh dependency problems. As the mesh is refined the dissipated energy approaches zero.

This paper presents a phase field model to simulate damage in asphalt mixtures. In the phase field method, a solid material is divided into damage and undamaged phases using a damage phase field variable. A free energy functional/crack potential is constructed based on the damage phase field variable and the whole system evolves towards the direction which minimizes this potential. The phase field model can efficiently simulate crack nucleation, propagation and complex crack typologies without the need of any crack tracking algorithm and with a simple computer implementation unlike interface element formulations. Moreover, the method does not suffer from the mesh dependency problem as observed in the continuum damage formulations. Bourdin et al. [9] used a variational approach to regularize the crack potential. The pioneering work of Bourdin et al. [9] on modelling brittle fracture in solids using phase field model has led to many advancements in this model. Miehe et al. [10] and Miehe et al. [11] presented a phase field model using thermodynamic considerations for damage modelling in brittle materials. Recently, Wu [12] extended the phase field model to simulate brittle and quasi-brittle fracture in solids by integrating a cohesive zone model with the phase field model.

In this paper the phase field model of Wu [12] is used to simulate quasi brittle fracture in asphalt concrete. To the best of authors knowledge, very little work has been done on simulating damage in asphalt mixtures using the phase field model. It is worth mentioning the work of Hou et al. [13] and Hou et al. [14] in simulating fracture in asphalt mixtures using phase field approach. However, their model can only simulate brittle fracture therefore it is not suitable for simulating quasi-brittle behaviour of asphalt mixtures.

The present contribution therefore aims at exploring the appropriateness of the phase field model for damage modelling in asphalt mixture. In particular, phase field model coupled with cohesive zone approach is used to simulate quasi brittle behaviour of asphalt mixture. Such a numerical tool will help in an efficient design, prediction and understanding of damage in asphalt pavements under various conditions. The bulk material is modelled as a homogeneous solid. Damage in asphalt concrete is represented with the damage phase field variable. The inelastic material behaviour around the crack tip is modelled using a bi-linear traction separation law. In order to solely investigate the performance of the phase field model to simulate damage in asphalt mixtures, numerical test at a uniform low temperature of -10ºC is performed. Therefore, strain rate/temperature effects are not considered in this contribution.

The remainder of the paper is organized as follows. Section 2 presents the governing equations of the phase field model and its finite element discretization. Section 3 discusses the analysed model problem and implementational aspects of the phase field model in a finite element computer program. A single edge notch beam is numerically simulated to investigate the performance of the phase field model. Numerical results are validated against the experimental observations of Song et al. [2]. Discussion on the analysis results is given in section 4. Section 5 presents main conclusions drawn from the analysis.

2 Diffuse damage model for asphalt concrete

Consider a body with domain Ω with its external boundary denoted by $\partial\Omega$. The body is subjected to prescribed displacements $\acute{u}$ on the surface $\partial\Omega_u$ and prescribed tractions $\acute{t}$ on the surface $\partial\Omega_t$, figure 1. The domain Ω is also subjected to a body force b and contains an internal sharp crack S. Within the context of phase field method, the crack surface is regularized over the localization band B, such that, the sharp crack surface A_s is approximated with a diffuse functional A_d.

$$A_s = \int_B \delta_s dV \approx A_d = \int_B \gamma(d, \nabla d) dV \qquad (1)$$

in which γ is the crack surface density function approximating the Dirac-delta function δ_s of a sharp crack. A damage phase field d is defined over the domain Ω such that d=1 representing the fully damaged material and $d = 0$ represents the undamaged material. The damage phase field, d varies between 0 and 1 within the localization band B.

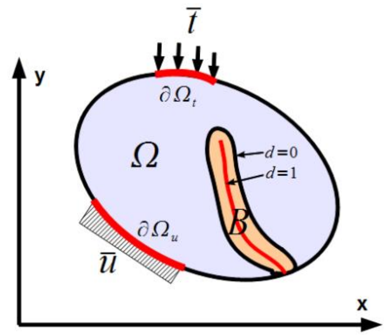

Figure 1: A solid body with a diffuse crack

2.1 *Governing equations*

The total potential Π of a system is defined as the sum of internal potential energy, fracture energy and external potential energy, mathematically given as

$$\Pi(u,d) = \int_\Omega \underbrace{\omega(d)\Psi_o}_{\text{strain energy density},\Psi} dV + \int_\Omega G_f \underbrace{\frac{1}{c_o}\left[\frac{1}{b}\alpha + b|\nabla d|^2\right]}_{crack\ surface\ density,\gamma} dV - \Pi^{ext} \quad (2)$$

G_f is the fracture energy, b is the length scaling parameter, α is the crack geometric function, Π^{ext} denotes the external potential energy, given as

$$\Pi^{ext} = \int_\Omega b \cdot u dV + \int_{\Gamma_t} \bar{t} \cdot u dA \quad (3)$$

$\omega(d)$ is the degradation function which describes the degradation of elastically stored energy Ψ_o and possess the following property $\omega(0) = 1, \omega(1) = 0, \omega'(1) = 0$. The governing equations in weak form can be obtained by the minimization of the total potential (2), which yield the following coupled system of equations

$$\int_\Omega \left(\frac{\partial\Psi}{\partial\epsilon} : \nabla^{sym}\delta u\right) dV + \int_\Omega b\delta u dV + \int_{\partial\Omega_t} \bar{t}\delta u dA = 0 \quad (4)$$

$$\int_B \left(\omega'(d)\frac{\partial\Psi}{\partial\omega}\delta d\right) dV + \frac{G_f}{c_o}\left(\frac{1}{b}\alpha'\delta d + 2b\nabla d \cdot \nabla\delta d\right) dV \le 0 \quad (5)$$

In accordance with the weighted residual method, the (u,d) and $(\delta u, \delta d)$ are identified as test and trial functions respectively. The problem is now stated as: Find $u \in U_u$ and $d \in U_d$ such that equations (4) and (5) are satisfied. The test and trial spaces, (U_u, U_d) and (V_u, V_d)respectively, are defined as

$$U_u := \{\boldsymbol{u} | \boldsymbol{u} = \bar{\boldsymbol{u}} \quad \forall x \in \partial\Omega_u\}, \qquad V_u := \{\delta\boldsymbol{u} | \boldsymbol{\delta u} = \boldsymbol{0} \quad \forall x \in \partial\Omega_u\} \quad (6)$$

$$U_d := \{d | \boldsymbol{d} \in [\boldsymbol{0}, \boldsymbol{1}], \quad \dot{d}(x) \ge 0 \forall x \in B\}, \qquad V_d := \{\delta d | \boldsymbol{\delta d} \ge \boldsymbol{0} \quad \forall x \in B\} \quad (7)$$

Equations (5) and (6) are supplemented with the constitutive relations. The relation between Cauchy stress σ and small strain ϵ is defined as $\sigma := \frac{\partial\Psi}{\partial\epsilon} = \omega\frac{\partial\Psi_o}{\partial\epsilon}$. For linear elastic material, the stress can be defined as $\sigma := \frac{\partial\Psi}{\partial\epsilon} = \omega(D:\epsilon) = \omega(D:\nabla^{sym}\delta u)$. Where D is the material elastic stiffness tensor. The damage driving force, Y, is defined as

$$Y := -\frac{\partial \Psi}{\partial d} = -\omega' \acute{Y} \tag{8}$$

With $\acute{Y} = \frac{\partial \Psi}{\partial \omega}$ is the effective damage driving force. Equations (4) and (5) can now be written as

$$\int_{\Omega} (\boldsymbol{\sigma}: \nabla^{sym} \delta \mathrm{u})\, dV \;+\; \int_{\Omega} b \delta \mathrm{u} \mathrm{dV} + \int_{\partial \Omega_t} \bar{\mathrm{t}} \delta \mathrm{u} \mathrm{dA} \;=\; 0 \tag{9}$$

$$\int_{\mathrm{B}} (\omega'(\mathrm{d}) \bar{Y}\, \delta \mathrm{d}) \mathrm{dV} + \frac{\mathrm{G_f}}{\mathrm{c_o}} \left(\frac{1}{\mathrm{b}} \alpha' \delta \mathrm{d} + 2\mathrm{b} \nabla d \cdot \nabla \delta \mathrm{d} \right) \mathrm{dV} \leq\; 0 \tag{10}$$

2.2 Discretization of weak form

Considering a two dimensional (2D) numerical problem, the domain Ω is divided into n_e number of finite elements. The displacement and damage phase field are approximated as

$$u^h(x) = \sum_I N_I(x)\, a_I^u \;, \qquad d^h(x) = \sum_I N_I(x)\, a_I^d \tag{11}$$

In which N_I is the standard finite element matrix of shape functions for the node I. a_I^u and a_I^d are the nodal unknown displacement and damage phase field degrees of freedom (dofs), respectively. Accordingly, the strain field and the gradient of damage phase field is given as

$$\epsilon^h(x) = \sum_I \mathbf{B}_I^u(x)\, a_I^u \;=\; \mathbf{B}^{\mathrm{u}} \mathbf{a}^{\mathrm{u}}, \qquad \nabla \mathrm{d}^{\mathrm{h}}(x) = \sum_I \mathbf{B}_I^d(x)\, a_I^d \;=\; \mathbf{B}^{\mathrm{d}} \mathbf{a}^{\mathrm{d}} \tag{12}$$

Incorporating the approximations into the weak form equations (9) and (10), the following two discretized equations are obtained

$$R^u = \int_{\Omega} (\mathbf{N}^{\boldsymbol{u}})^T b \, \mathrm{dV} + \int_{\partial \Omega_{\mathrm{t}}} (\mathbf{N}^{\boldsymbol{u}})^T \bar{\mathrm{t}} \, \mathrm{dA} - \int_{\Omega} (\mathbf{B}^u)^T \boldsymbol{\sigma} \, dV = 0 \tag{13}$$

$$R^d = -\int_{\Omega} (\mathbf{N}^d)^T \left(\omega' \bar{\mathrm{Y}} + \frac{\mathrm{G_f}}{\mathrm{c_o b}} \alpha' \right) \mathrm{dV} - \int_{\Omega} (\mathbf{B}^d)^T \left(\frac{2b}{\mathrm{c_o}} \mathrm{G_f} \nabla \mathrm{d} \right) \mathrm{dV} \leq \mathbf{0} \tag{14}$$

The above equations are solved in a nonlinear setting using Newton-Raphson iterative scheme.

2.3 Failure criterion

The equation $\bar{Y} = \frac{\partial \Psi}{\partial \omega}$ gives similar fracture response both in compression and tension. Therefore, a modified effective crack driving force $\bar{Y}$ is used to simulate fracture in brittle/quasi-brittle materials. In this work it is assumed that fracture occurs when the local principal tensile stress exceeds the tensile strength of the material. Consequently, the following form of effective crack driving force is used

$$\bar{Y} = max\left(\frac{f_t^2}{2E_o}, max\, \overline{Y_n} \right), \qquad \overline{Y_n} = \frac{1}{2E_o} (\sigma_1)^2 \tag{15}$$

in which f_t is the tensile strength of the material and E_o is the modulus of elasticity

2.4 Degradation function

Following Wu [12], the following form of degradation function is adopted

$$\omega(d) = \frac{(1-d)^p}{(1-d)^p + a_1 d + a_1 a_2 d^2} \qquad (16)$$

The parameters $p = 2, a_1 = 4l_{cz}/\pi b, a_2 = -0.5$ are used to simulate bilinear traction-separation law. l_{cz} is the Irwin's internal length.

3 Methodology

The phase field model is implemented in an object-oriented C++ language. An open source JIVE library is used for the implementation of the finite element code (JIVE is an open source numerical toolkit for the solution of partial differential equations). Table 1 presents the flow of computations in a finite element code with phase field model.

Table 1-Flow of computations in a finite element code with phase field model

- Initialization: The displacement $\mathrm{a}_{\mathrm{n}}^{\mathrm{u}}$, damage phase field $\mathbf{a}_{\mathbf{n}}^{\mathbf{u}}$ and $\bar{Y}_{\mathrm{n}}$ at time t_n are known
- For each loading step n to n+1
- Set $\left(a_n^{u(0)}, a_n^{d(0)}, \bar{Y}_n^{(0)}\right)$ equals to $\boldsymbol{\left(a_n^u, a_n^d, \bar{Y}_n\right)}$ $\boldsymbol{and\ j = 1}$
- For each iteration j
    - Calculate Cauchy stress: $\boldsymbol{\sigma}_{n+1}^{(j)}\left(a_{n+1}^{u(j)}, a_{n+1}^{d(j)}\right)$
    - Calculate history variable: $\mathrm{hist}_{\mathbf{n+1}}^{(\mathrm{j})} = \max\left(hist_n, \frac{\left(\sigma_{1(n+1)}^{(j)}\right)^2}{\boldsymbol{2E_o}}\right)$
    - Calculate $\bar{Y}_{\mathrm{n}}$: $\bar{Y}_{n+1}^{(j)} = \mathbf{max}\left(\frac{f_t^2}{2E_o}, hist_{n+1}^{(j)}\right)$
    - Calculate displacement and damage phase field $\left(a_{n+1}^{u(j)}, a_{n+1}^{d(j)}\right)$ using equations (13) and (14)
    - Check convergence
- If converged then update variables: $\boldsymbol{\left(a_n^u, a_n^d, \bar{Y}_n\right)}$ $equals\ to$ $\left(a_{n+1}^{u(j)}, a_{n+1}^{d(j)}, \bar{Y}_{n+1}^{(j)}\right)$
- Go to next step

3.1 *Single edge notch beam.*

A single edge notch beam of Song et al. [2] is numerically simulated in this work. Song et al. [2] performed test on a single edge notch beam. The geometry of the beam is shown in Figure 2a. The beam contains an initial notch of length 19mm. In the experiment crack mouth opening displacement (CMOD) is increased at a linear rate for a stable mode-I crack growth. The beam is made of asphalt mixture consisting of a 9.5 mm nominal maximum aggregate size (NMAS) and a performance grade (PG) 64-22 asphalt binder. The experiment was performed at low temperature (-10ºC) to characterize the fracture behaviour at low temperature.

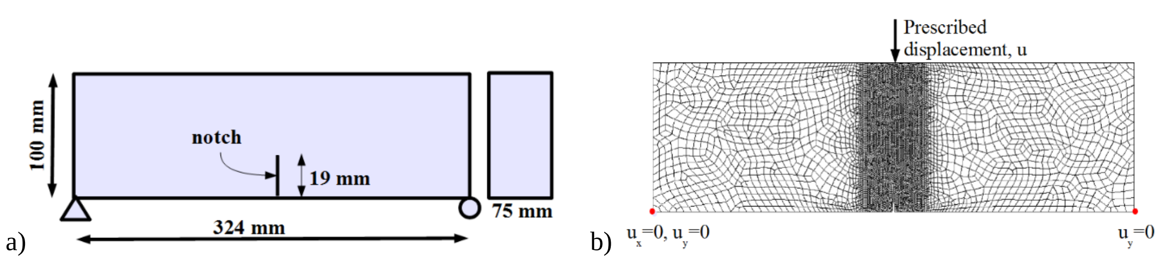

Figure 2: a. Geometry and boundary conditions of single edge notch beam and b. finite element mesh

Figure 2b shows the finite element mesh of the beam used in the numerical simulation. The beam is modelled with a two-dimensional, plane strain, 4-noded quadrilateral element. A minimum element size of 1 mm is used in the expected damage growth region whereas an element size of 5 mm is used in rest of the model. The notch width is taken as 2mm in the numerical model. Moreover, it is assumed that the bulk material essentially behaves elastically at low temperatures and therefore temperature effects are ignored. The bulk material is modelled as elastic, homogeneous material with modulus of elasticity E=14.2 GPa and Poisson's ratio ν = 0.3 [2]. The fracture properties used in the analysis are tensile strength f_t= 3.56MPa and fracture toughness G_f=0.344 J/m^2[2]. In the numerical simulation a downward displacement is applied in the middle of the top surface of the beam at a linear rate. The nonlinear finite element equations are solved using a Newton-Raphson iterative scheme with a tolerance of 1.0E-3.

4 Results and discussion

Figure 3a compares the load versus crack mouth opening displacement (P Vs CMOD) curve obtained from the present phase field model with that of experimental results. It is observed that the numerical result is in good agreement with that of experimental curve. Figure 3a also compares the P vs CMOD curve obtained by Song et al. [2] using a finite element analysis with interface elements. It is observed from the figure that the numerical result obtained by Song et al. [2] shows an initial complaint behaviour. This is due to the use of dummy stiffness in the interface formulation to simulate rigid interface before initiation of a failure. On the contrary, in the present phase field model the damage initiates once a failure criterion is met. Therefore, an initial high stiffness (portion of the curve before the peak load) is also well predicted by the present numerical model. Figure 3b shows the deformed shape of the beam representing mode-I fracture through an unstructured finite element mesh.

Figure 4 shows the damage growth in a single edge notch specimen at different levels of crack mouth opening displacements. It is observed from the figures that damage initiates at the notch tip before the peak load, figure 4a. After the formation of a macro crack (represented with a fully damaged zone $\omega = 1$) the load drops quickly which represents a fast crack growth. Moreover, the damaged zone ahead of the macro crack is large representing a large fracture process zone ahead of a crack tip compared to the damaged zone left and right sides of the macro crack. This represents a sharp crack as observed in the experiments of Song et al. [9]. As the load increases the damage region grow straight up to the top surface of the beam representing mode-I fracture. Additionally, it is observed that as the crack approaches the top surface of the beam the crack growth slows down this is also evident from the P Vs CMOD curve (figure 3a) where the load drop is more gradual in the later part of the curve.

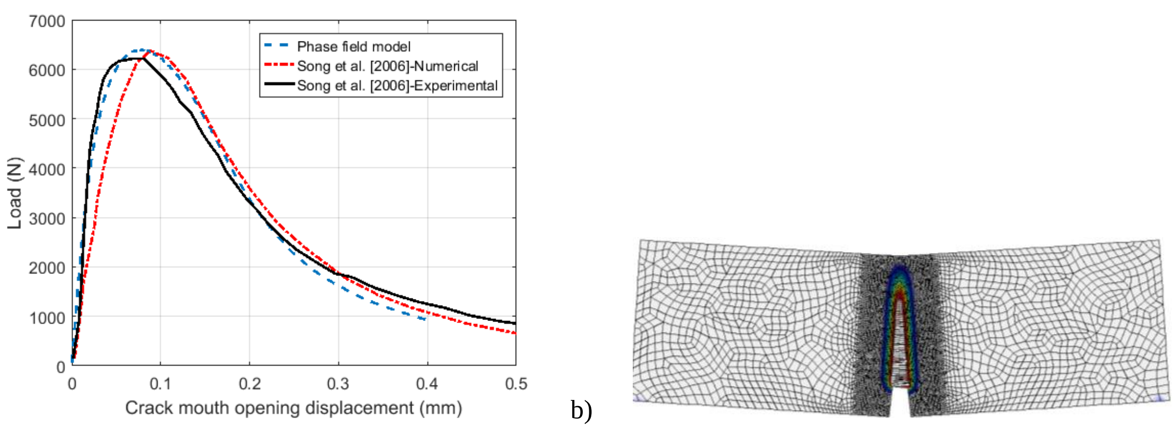

a) b)

Figure 3: a) Comparison of Load Vs Crack mouth opening displacement curve with the experimental results, b) deformed shape

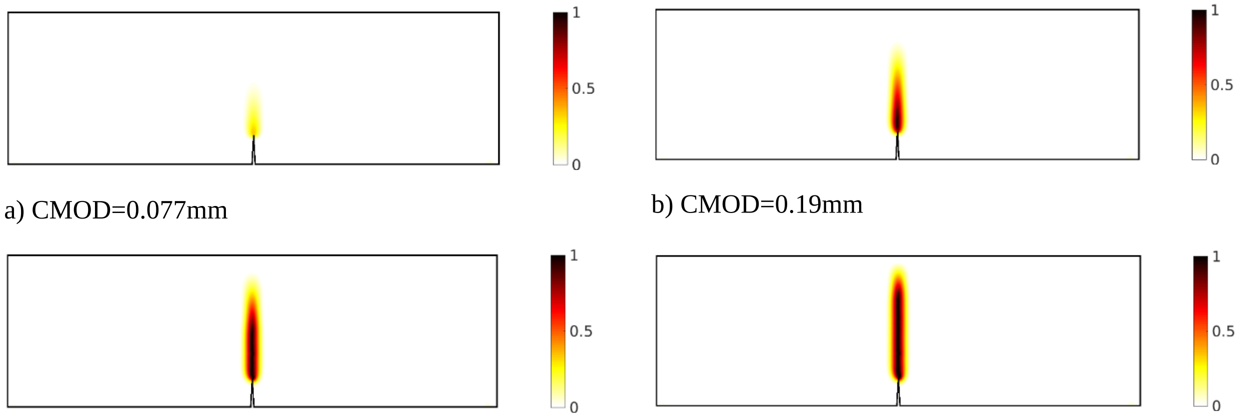

a) CMOD=0.077mm

b) CMOD=0.19mm

c) CMOD=0.31mm

d) CMOD=0.59mm

Figure 4: Damage growth at different instants of loading

5 Conclusion

In this contribution a phase field diffuse damage model is presented for the simulation of damage in asphalt concrete. A crack potential function regularized over a localization band is used to simulate sharp crack. A crack driving force integrated with the cohesive constitutive law is used to simulate nonlinear behaviour around the crack. A mode-I fracture in an asphalt concrete is numerically simulated and the results are compared with the experimental observations. It is observed that the presented model effectively and accurately simulated mode-I fracture in asphalt concrete at low temperature. The proposed model does not require the crack path to be known a priori as in the case of interface elements. Moreover, the model successfully simulated an initial stiff behaviour unlike interface element analysis which shows an initial complaint behaviour due to the use of dummy stiffness in its formulation. The phase field model does not require any special algorithm to track crack trajectories and can be easily implemented in a finite element code. At present the model is limited to simulate mode-I fracture without considering rate/temperature effects in asphalt concrete. Future work will focus on extending the model to the case of mixed mode cracking under various strain rates.

References

[1] J. B. Soares, F. A. C. Freitas and D. H. Allen, "Crack modeling of asphlatic mixtures considering heterogenity of the material", In *Transportation Research Record: Journal of Transportation Research Board*, vol 1832, pp. 113-120, 2003

[2] S. H. Song, G. H. Paulino and W. G. Buttlar, "Simulation of crack propagation in asphlat concrete using an intrinsic cohesive zone model", *ASCE Journal of Engineering Mechanics*, vol 132, pp. 1215-1223, 2006

[3] E. V. Dave and C. Hoplin, "Flexible pavement thermal cracking performance sensitivity to fracture energy variation of asphalt mixtures", *Road Materials and Pavement Design*, vol 16(sup1), pp. 1-19, 2015

[4] N. Moes, J. Dolbow and T. Belytschko, "A finite element method for crack growth without remeshing", *International Journal for Numerical methods in Engineering*, vol 46, pp. 131-150, 1999

[5] E. Mahmoud, S. Saadeh, H. Hakimelahi and J. Harvey, "Extended finite element modelling of asphalt mixtures fracture properties using semi-circular bending test", *Road Materials and Pavement Design*, vol 15, pp. 153-166, 2014

[6] M. R. Islam, M. J. Vallejo and R. A. Tarefder, "Crack propagation in hot mix asphalt overlay using extended fiinite element model", *ASCE Journal of Materials in Civil Engineering*, vol 29, pp. , 2017

[7] S. W. Park, Y. R. Kim and R. A. Scharpery, "A visco elastic continuum damage model and its application to uniaxial behavior of asphalt concrete", *Mechanics of Materials*, vol 24, pp. 241-255, 1996

[8] G. R. Chehab, "Characterization of asphalt concrete in tension using a viscoelastoplastic model", *Ph.D thesis. North Carolina State Uniersity, Raleigh, N.C.*, 2002

[9] B. Bourdin, G. A. Fracfort and J. J. marigo, "Numerical experiments in revisited brittle fracture", *Journal of the Mechanics and Physics of Solids*, vol 48, pp. 797-826, 2000

[10] C. Miehe, F. Welschinger and M. Hofacker, "Thermodynamically consistent phase-field model of fracture: variational principles and multi field FE implementations", *International Journal for Numerical Methods in Engineering*, vol 83, pp. 1273-1311, 2010

[11] C. Miehe, M. Hofacker and F. Welschinger, "A phase field model for rate-independent propagation: Robust algorithmic implementation based on operator splits", *Computer Methods in Applied Mechanics and Engineering*, vol 199, pp. 2765-2778, 2010

[12] J. Y. Wu, "A unified phase field theory for the mechanics of damage and quasi-brittle failure ", *Journal of the Mechanics and Physics of Solids*, vol 103, pp. 72-99, 2017

[13] Y. Hou, L. Wang, P. Yue and W. Sun, "Fracture failure interaction of asphalt by using a phase field approach ", *Material and Structures*, vol 48, pp. 2997-3008, 2015

[14] Y. Hou, W. Sun, Y. Huang, M. R. Ayatullahi, L. Wang, and J. Zhang , "Diffuse interface model to investigate the asphalt concrete cracking subjected to shear loading at low temperature ", *ASCE Journal of Cold Regions Engineering*, vol 31, pp. -, 2016

3rd Conference on Sustainability in Civil Engineering (CSCE'21)
Department of Civil Engineering
Capital University of Science and Technology, Islamabad Pakistan

UTILIZATION OF BAGASSE ASH FOR SERVICEABILITY ENHANCEMENT OF BITUMINOUS PAVEMENTS

[ac] Asad Zia*, [b] Ayaz Ahmad Khan, [a]Zhang Pu

a: School of civil engineering, Zhengzhou University, Zhengzhou city, China, asadzia005@gs.zzu.edu.cn
b: Department of civil engineering, Iqra National University, Peshawar, KPK, Pakistan, engrayaz50@gmail.com
c: Department of engineering and geology, G. D'Annunzio University of Chieti-Pescara, Italy. asad.zia@unich.it
* Corresponding author: Email ID: asadzia005@gs.zzu.edu.cn

Abstract- The serviceability of bituminous pavements can be enhanced by controlling the amount of deterioration. The filler of bituminous concrete has a vital role in reducing its deterioration. Stone dust is one of the materials that are commonly utilized as a filler in bituminous pavements. Numerous researches are carried out to replace the stone dust with suitable material. Sugarcane bagasse ash (SBA) can be used as a filler because of its low thermal conductivity compared to stone dust. Therefore, the overall aim of the research work is to select the best appropriate filler material for the serviceability improvement of bituminous pavements. The specific aim is to investigate sugarcane bagasse ash as a filler for reducing the degree of degradation in bituminous concrete. The rutting depth of the bituminous concrete incorporating SBA as a filler is evaluated. Various tests, i.e., softening point, grade penetration, flash and fire point, and wheel tracking test, are performed. AASHTO standards are followed to perform the tests. For the wheel tracking test, the percentage of coarse aggregates, SBA, and asphalt of grade 60/70 is 90.70%, 5%, and 4.30%, respectively. While two other samples with the same ratio instead that SBA is replaced with stone dust in the same amount are also prepared for comparison. It is concluded that replacing stone dust with SBA as a filler decreased the rutting depth of bituminous concrete. Based on the research results, the serviceability of bituminous pavements is expected to be enhanced by replacing the stone dust with sugarcane bagasse ash.

Keywords- Bituminous pavements, Serviceability, Deterioration, Sugarcane bagasse ash as a filler.

1 Introduction

The serviceability of the bituminous pavements is considerably related to the rate of deterioration. Therefore, the rise in the rate of deterioration is a serious issue, which needs special attention. One of the main factors that increase the deterioration is the increasing rate of rutting in bituminous pavements. Causes of the rutting include an upsurge in heat conductance of asphalt. Deteriorated bituminous pavements result in various damages like wear and tear of the tires and reduce the road's load-carrying ability. Furthermore, it might not be possible to drain out the rainwater from rutting deteriorated bituminous pavements [1,2].

The adhesion and cohesion of the bituminous mix were improved by adding the filler [3]. The filler upgrades the resistance of bitumen to water entrance due to its chemical affinity to asphalt mix [4,5]. The durability and serviceability of the bituminous mixtures are substantially related to filler type [6,7]. Sugarcane bagasse ash (SBA) is discarded out of factories and worthy terrains nearby that mills are used for dumping SBA, giving rise to several geo-environmental issues [8]. As sugarcane bagasse ash has pozzolanic and binder properties, it could enhance the engineering properties of soil and concrete [9,10]. Besides, the thermal conductance of the sugarcane bagasse ash (i.e., 0.046 W/mK) is much tiny as compared to that of stone dust (i.e., 1.7 W/mK) [11].

The rate of deterioration can be decreased by incorporating sugarcane bagasse ash (SBA) in bituminous pavements. The sugarcane bagasse ash is unique among the available types of fillers because of its cementitious properties and low-cost raw material. Therefore, the general aim is to evaluate the efficiencies of available fillers for serviceability upgrading of bituminous pavements. In this paper, the role of sugarcane bagasse ash as a filler for minimizing the deterioration of bituminous concrete is investigated in terms of the rate of rutting. Thus, the current study can help explore the effectiveness of the sugarcane bagasse ash as a filler.

2 Test procedures and specimens casting

2.1 Materials, mix design, and casting procedure

To obtain bitumen and bituminous concrete, the Durrani asphalt plant Nowshera, Khyber Pakhtunkhwa, Pakistan, is selected as a source. Gadoon Amazai Industrial Estate, located in district Swabi, Khyber Pakhtunkhwa, Pakistan, is chosen as an examination area with an average annual air temperature between 7 ºC to 24 ºC. The sugar mills are the best option for collecting sugarcane bagasse ash (SBA), where a considerable amount of sugarcane bagasse is used to run the boiler [12]. Therefore, SBA from the Khazana sugar mill (KSM) Peshawar, Khyber Pakhtunkhwa, Pakistan, is used in the current study. From the sugar mill, about 15 Kg SBA is collected in bags, and then to remove the dust and other impurities, it is passed through sieve No 200. To avoid moisture interference, SBA is stored in a dry place. Bitumen of grade 60/70 is used. For the wheel tracking test, four samples are cast. BC1 and BC2 are prepared by mixing the bitumen, aggregates, and sugarcane bagasse ash (SBA) in percentages of 4.30%, 90.70%, and 5%, respectively. While samples of BC3 and BC4 having the same ratio with 5% of stone dust at the place of SBA are also prepared. The samples are prepared according to AASHTO R-30 [13]. The aggregates are mixed with bitumen at 120 ºC.

2.2 Testing procedure and specimens.

All tests are made following AASHTO standards. The grade penetration test is performed according to AASHTO M-208 [14]. The entire procedure for the grade penetration test is according to AASHTO M-208, except the depth of bitumen is kept 10 mm more than the expected depth of bitumen. As per the requirements of the AASHTO M-208, the test is repeated for three samples. The consistency of bitumen is determined by using softening point of bitumen. The softening point of bitumen is carried out according to AASHTO M-81, and M-82 and tests are repeated for two specimens [15].

Figure 1. (a) Sample for wheel tracking test before placing (b) after placing in the wheel tracking test apparatus

AASHTO M-20 is used to conduct flash and fire point tests for finding the temperature at which a flash will appear at the bitumen surface, and then it takes fire [16]. The rutting depth of bituminous concrete is determined by using the wheel tracking test. The maximum reduction in-depth (depression) caused by repeated passes of a loaded wheel at any location on specimen along wheel track is taken as the rutting depth [17]. Four samples (two of SBA and two stone dust) are cast for a wheel tracking test. The separate sample and pair of samples after placing in the wheel tracking test apparatus are shown in Figure 1.

3 Experimental Results and Analysis.

3.1 Grade penetration test

This test is utilized to determine the penetration grade of asphalt, which is helpful to select bitumen of appropriate grade keeping in mind the climate condition of the project area. According to AASHTO M-208, the temperature-wise distribution of bitumen penetration grade is recorded in Table 1.

Table 1. Temperature-wise distribution of bitumen penetration grade

Serial No. (1)	**Average Annual Temperature of air** (2)	**Penetration grade of bitumen** (3)
1	Equal to or less than 7 °C, cold	80/100 grade
2	7 to 24 °C, Medium	60/70 grade
3	More than 24 °C, hot	40/50 grade

Since the test area is Gadoon industrial estate with an average annual air temperature between 7 °C to 24 °C, bitumen of grade 60/70 is right to use in the above site area.

The outcomes of the grade penetration test are given in Table 2. The penetrations for the tested samples of bitumen in the 10th of mm are 67, 65, and 70. Therefore, the average penetration depth for the tested three samples is 67.33. This complies with the range (i.e., 60 to 70) for grade 60-70 bitumen. Therefore, as per the test results, the grade of the selected bitumen is 60/70.

Table 2. Results of the grade penetration test

Details	**Actual**	**AASHTO M-208**	
Bitumen pouring temp (°C)	90	90	90
Cooling room temp (°C)	26	0.06	0.06
Water temp (°C)	24.9	24 - 26	24 - 26
Loads in gm	100	100	100
Time duration in seconds	5	5	5
Penetration	Sample 1	Sample 2	Sample 3
(10th of mm)	67	65	70
Average Penetration (mm/10)	67.33		
Bitumen Grade	60 - 70		

3.2 The softening point of bitumen

The softening point of sample 1 and sample 2 is carried out. The average softening point for the tested bitumen is noted at 48.5 °C. This complies with the specifications of AASHTO for bitumen of grade 60/70, i.e., 47 °C to 54 °C. This proves that the selected bitumen is suitable to be used in pavements.

3.3 Flash and fire point test

The results of flash and fire point tests are shown in Table 4. The flash and fire points for the tested bitumen are 232 °C and 415 °C, respectively. The flash and fire points specified by AASHTO M-20 for grades 60-70 are 232.22 °C and 416 °C, respectively. The deviations of flash and fire points of tested bitumen from that specified by AASHTO M-20 are within the allowable ranges. This shows the suitability of the selected bitumen for pavements.

Table 3. Results of flash and fire point test

Details	Actual	AASHTO M-20
Flash point (ºC)	232	232
Fire point (ºC)	415	416

3.4 Wheel tracking test

The wheel tracking test is performed to check the suitability of replacing of filler of the stone dust with sugarcane bagasse ash (SBA). So, the samples of both SBA and stone dust are prepared and tested for rutting. The rutting depths of the tested samples for the wheel passes of 15000 and 20000 are outlined in Table 4. The rutting depths of 12 mm and 15 mm are noticed for BC1 and BC2, respectively. Whereas for BC3 and BC4, the rutting depths of 16 mm and 20 mm are noted.

Table 4. Rutting depth

Samples	No. of Passes (Nos)	Rutting Depth (mm)
With Bagasse ash	------	------
BC1	15000	12
BC2	20000	15
With Stone dust	------	-------
BC3	15000	16
BC4	20000	20

The highest rutting depth of 20 mm is noticed for the stone dust specimen BC4 for 20000 passes. This is 5 mm greater than that of the BC2 sample of bituminous concrete with SBA as a filler for the same number of passes. For each number of passes, the rutting depth of each bituminous concrete sample having SBA as a filler is less than the samples possess stone dust as a filler. The average rutting depth of the samples with SBA as a filler is 13.5 mm, whereas that of the specimens incorporating stone dust as a filler is 18 mm. The mean rutting depth for the SBA samples as a filler is 4.5 mm lower than bituminous concrete samples incorporating stone dust. This could be because of the bagasse ash's cementitious nature, which decreases the conductance of the heat by a strong packing effect among the particles.

Figure 2 displays the percentage comparison of the rutting depth of both types of examined samples. On the contrary to the rutting depth of samples containing stone dust, the rutting depths of sugarcane bagasse ash samples are 25% less for the similar wheel passes of 15000 and 20000, respectively. In each case, the rutting gets decreased for the SBA sample than the stone dust samples in the significant amount.

The bituminous concrete specimens which possess SBA as a filler outperformed their companions with stone dust to reduce the rutting depth. The cementitious composition of materials helped improve the bond strength among the neighbouring materials in the same mix. So, the decreased rutting depth of SBA samples might be attributable to the cementitious nature of sugarcane bagasse ash by enhancing the bond strength. SBA increased resistance to the passage of heat transfer from one part to another of the bituminous concrete sample by its binding effect, and thus the rutting did go to more depth. This ensured that sugarcane bagasse ash could be utilized usefully as a filler for bituminous pavements compared to the stone dust for serviceability enhancement by controlling the rate of deterioration.

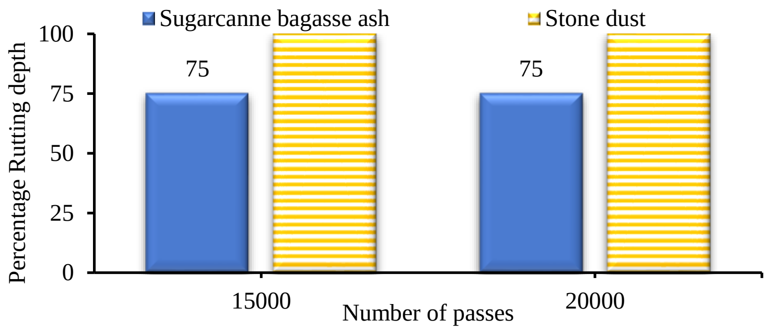

Figure 2. Comparison of rutting depth of sugarcane bagasse ash

4 Discussions

The serviceability of bituminous pavements intensely relies on filler materials' characteristics, reliability, and chemical bond [5]. Various types of filler materials are accessible nowadays. As a filler, stone dust is the most commonly used material in bituminous pavements. Similar to fine aggregates (sand), stone dust possesses small cementitious properties [18]. Because of this tendency, the chemical bonding of stone dust with surrounding aggregates in the bituminous concrete needs to be enhanced. This will help to make bituminous concrete more compelling in opposing abrasion triggered by the movement of various types of traffic. Hence, it is needed to utilize such filler to make a solid bond with the aggregates. Therefore, it is crucial to explore the efficiency of filler materials for the serviceability improvement of bituminous pavements. Sugarcane bagasse ash with cementitious properties [19, 20] might be useful in this regard.

Thus, initial research is aimed to examine the rutting depth of bituminous concrete incorporating sugarcane bagasse ash as a filler for the enhanced serviceability of bituminous pavements. It is deduced that bituminous concrete specimens that possess sugarcane bagasse ash as a filler outdone the samples of bituminous concrete comprising stone dust to decrease rutting depth. Accordingly, the deterioration of the bituminous pavements can be less in sugarcane bagasse ash samples; convincingly, it is highly expectable to upsurge the serviceability of bituminous pavements.

5 Conclusions and Recommendations

Sugarcane bagasse ash and stone dust are investigated as a filler for the possible use in improving the serviceability of bituminous pavements by reducing the amount of deterioration. Following conclusions are made from this research work:

- The average rutting depth of 13.5 mm and 18 mm is noted for the bituminous concrete samples of sugarcane bagasse ash and stone dust, respectively.
- By comparing the rutting depths of stone dust samples and sugarcane bagasse ash samples, the rutting depth for the stone dust is 25% lesser for the similar number of wheel passes of 15000 and 20000, respectively.

Based on the experimental outcomes, sugarcane bagasse ash as a filler is likely to be more advantageous in improving the serviceability of bituminous pavements by reducing the deterioration in terms of reduced rutting depth. Therefore, it is recommended to evaluate other types of filler materials for the serviceability enhancement of bituminous pavements.

Acknowledgment

The authors would like to thank those who help out during the investigation.

References

[1] C. Yavuzturk, K. Ksaibati, and A. D. Chiasson, "Assessment of Temperature Fluctuations in Asphalt Pavements Due to Thermal Environmental Conditions Using a Two-Dimensional, Transient Finite-Difference Approach", *Journal of materials in Civil Engineering*, vol. 17, 2005.

[2] Ikechukwu, A. F., & Hassan, M. M, "Assessing the Extent of Pavement Deterioration Caused by Subgrade Volumetric Movement Through Moisture Infiltration", *International Journal of Pavement Research and Technology*, 1-17, 2021.
[3] Mahan, Hanaa Mohammed. "Influence of mineral filler-asphalt ratio on asphalt mixture performance." *Journal of Babylon University/Engineering Sciences*, vol. 4, 2013.
[4] Miro R., Martinez A.," Effect of Filler on the Aging Potential of Asphalt Mixtures", Technical University of Catalonia, 2004.
[5] Chaturabong, P., & Bahia, H. U. (2018). Effect of moisture on the cohesion of asphalt mastics and bonding with surface of aggregates. *Road Materials and Pavement Design*, 19(3), 741-753.
[6] Craus, J., I. Ishai, and A. Sides,." Some physico-chemical aspects of the effect and role of the filler in bituminous paving mixtures", *Journal of Association of Asphalt Paving Technologists*, vol. 47, pp. 558-587, 1978.
[7] Zulkati, A., Diew, W. Y. and Delai, D.S. "Effects of Fillers on properties of Asphalt-Concrete Mixture", *Journal of Transportation Engineering*, ASCE, vol. 138, No. 7, pp 902-910, 2012
[8] Cokca, E., Yazici, V., and Ozaydin, V., "Stabilization of expansive clays using granulated blast furnace slag (GBFS) and GBFS-cement," *Geotechnical and Geological Engineering*, vol. 27(4), pp 489- 499, 2009.
[9] Janjaturaphan, S., and Wansom, S., "Pozzolanic activity of industrial sugar cane bagasse ash," *Suranaree Journal of Science and Technology*, vol. 17 (4), pp 349-357, 2010.
[10] Khan, M. A., Zia, A., Sadiq, M. M., & Pu, Z., "Suitability of partial replacement of cement with sugarcane bagasse ash and sand with stone dust for concrete", *NED University Journal of Research*, 15(1), pp 51-61, 2018.
[11] Mangesh V Madurwar Sachin, Mandavgan, Rahul V Ralegaonkar, Development and feasibility analysis of Bagasse ash bricks, *Journal of Energy Engineering*, vol. 141, 2015.
[12] Ali, Khurshid, N. U. Amin, and M. Tahir Shah. "Physicochemical study of bagasse and bagasse ash from the sugar industries of NWFP, Pakistan and its recycling in cement manufacturing", *Journal of the chemical society of Pakistan*, vol. 31(3), pp 375-378, 2009.
[13] AASHTO M-208, Standard Specification for Cationic Emulsified Asphalt. 2018.
[14] AASHTO M-81, Standard Specification for Cutback Asphalt (Rapid-Curing Type). 92nd Edition, 2004.
[15] AASHTO M-20, Standard Specification for Penetration-Graded Asphalt Cement. 2004.
[16] AASHTO T-324, Standard Method of Test for Hamburg Wheel-Track Testing of Compacted Hot Mix Asphalt (HMA). 2019.
[17] AASHTO R-30, Standard Practice for Mixture Conditioning of Hot-Mix Asphalt (HMA). 2019.
[18] Manchiryal R.K., Dewangan A. & Gupta D.P. "Implementation and analysis of strength characteristics of concrete using crusted stone dust as fine aggregate", *International Journal of Research in Engineering & Applied Sciences*, vol. 4(10), pp. 21-28, 2014.
[19] Zia, A., Khan, M. A., and Pu, Z., "Incorporation of bagasse ash and stone dust in cement concrete", in Conf. *1st Conference on Sustainability in Civil Engineering*, Capital University of Science and Technology, Islamabad, Pakistan, 2019, paper ID 102.
[20] Zia, A., Khan A, A, "Effectiveness of Bagasse Ash for Performance Improvement of Asphalt Concrete Pavements", *SN Applied Sciences*, vol. 3, P#502, 2021.

3rd Conference on Sustainability in Civil Engineering (CSCE'21)
Department of Civil Engineering
Capital University of Science and Technology, Islamabad Pakistan

COMPARISON OF ACTUAL TRUCK TRAFFIC WITH LIVE LOAD MODELS USED FOR DESIGN OF BRIDGES IN PAKISTAN

[a]Asif Jalal*, [b]Muhammad Farjad Sami, [c] Zeeshan Mehmood, [d]Ahsan Abbas

a: Civil and Environmental Engineering, North Dakota State University, USA, asif.jalal@ndsu.edu *
b: Civil Engineering Department, Muslim Youth University, Islamabad, farjad.sami@myu.edu.pk c, xishi07@yahoo.com
d: ahsanali2556@gmail.com

Abstract- Live load models representing truck traffic, primarily governs design of bridges in Pakistan. Bridge design is done using Pakistan Code of Practice for Highway Bridges 1967 (CPHB) and AASHTO LRFD Bridge Design Specifications (AASHTO Specifications). Legal limits are imposed by National Highway Authority (NHA) to prevent overstressing of bridges. . In order to meet heavy load carrying demands from various industries, the service-level truck traffic has changed significantly in axle configuration, axle weights, traffic volume and gross vehicle weights. In this study, characteristics of live loads (axle weights and Gross Vehicle Weight (GVW)) of actual truck traffic are compared with live load models NHA legal load specifications to elaborate the significance in change in code of practice. The samples truck traffic data recorded at Ayub Bridge Peshawar (411 trucks) have been used for Analysis. From the analysis it was found that all types of vehicles surpass the limitation by significant value. Approximately, 60% vehicle violates the GVW limit prescribed by NHA with nearly equal contribution by both light and heavy vehicles. Similarly, 84% vehicle violates the axle load limit that includes almost all 6-axles and 5-axles trucks. The live load models of NHA Specification projects much less load effects as compared to the effects caused by actual truck traffic and hence the bridges are stressed much greater than considered during design. Hence, existing live load model are not the true representations of actual truck traffic, and requires development of a new live load model in addition with strict enforcement of load limitations.

Keywords- Bridge design load, Axle load, Gross Vehicle Load, NHA legal limits.

1 Introduction

The Highway Bridges needs to be designed so that these can safely carry the anticipated loads that it will experience in its service or design life. Live load (Trucks) are the primary governing factor in bridge design and their lifelong structural performance depends significantly on the live loads to which bridges will be exposed during their lifetime [1]. Bridges may get damaged and deteriorated due to overloading [2] as well as due to aging and environmental effects.

There are number of design vehicle load used in different systems. It was highlighted during First World War (1914-1918) that some standard loading for bridge design should be there to cater heavy equipment, and other needs of Military. In 1922 Standard Loading Train was introduced for the first time in Britain [3]. Industrial progress along with technological advancement compelled Indian Road Congress (IRC) to develop some sort of standard loading for Highway Bridge Design which were adopted by PHB Code, 1967 later on. AASHTO in 1935 introduced the idea of a train of trucks. In 1944 idea of hypothetical trucks was introduced by AASHTO [4]. These trucks are called H (with two axles) and HS (with three axles) classes of trucks. These were used only for the purpose of design and have no resemblance with any truck on road.

A truck train loading and 70-ton military tank is used for highway loading, according to PHB, 1967. HL-93, commonly represents AASHTO LRFD Live Loading [5]. It is hypothetical Live Load Model used to analyze bridges having a design period of 75 years at max [6]. This Live Load Model has a set of loads which produce extreme load effects approximately equal to that caused by exclusion vehicles.

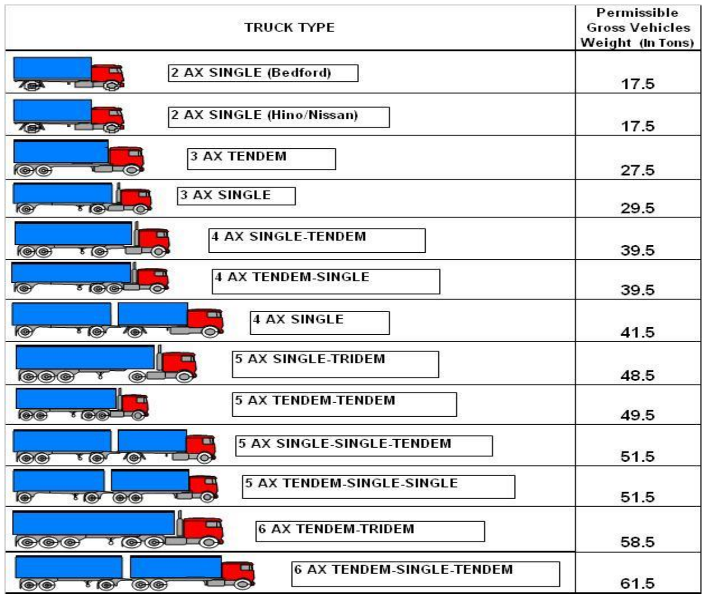

Figure 1 NHA legal loading limitations for each type of Truck [7]

In Pakistan, bridges design is done using Pakistan Code of Practice for Highway Bridges 1967 (CPHB) and AASHTO LRFD Bridge Design Specifications [8] based on America traffic statistics. By installing weight stations on National highways, National Highway Authority (NHA) enforce limits on gross weights and axle weights. However, rising fuel prices, competition between transporters and development of powerful truck engines lead to illegal overweight. Thus, there is a need to characterize actual truck traffic and its load effects on the bridges and compare it with current live load models and NHA Legal Load Limits (Figure-1). Similarly, there is need to also consider the axle weight limitation [9]. The NHA axle Load limitations for these trucks are such that the weight of front, rear, tandems and tridems axles must not exceed 5.5, 12, 22 and 32 tons respectively.

Service-level truck traffic has a significant deviation with respect to axle weights, axle configuration, gross vehicle weights and traffic volume in Pakistan as compared to United States and Canada [10]. No such literature or analysis were found that emphasis to update the current code of practice according to Pakistan traffic. Thus, PBH Code live load model based on 1961 AASHTO Specifications and current NHA Legal Load Limits may not truly represent service-level truck traffic of Pakistan. Therefore, current study aim is to determine live load characteristics (axle configuration, axle weights, and gross vehicle weights) and comparison of actual truck traffic load characteristics with NHA legal loads [1].

2 Research Methodology

Data is collected by using WIM technology that gives an excel sheet comprising axle weights, axles spacing, gross weight, velocity of approaching vehicle etc. Bugs and errors are removed from collected data by filtration. Ayub bridge in Peshawar is selected to analysis the traffic load trend in Pakistan. The Ayub bridge is comparatively highly exposed to heavy trucks.

2.1 Weight-in-Motion (WIM) Technology

WIM system acquires vehicle weights, axle loads, axle spacing, speed, and other vehicle information as vehicles drive over sensors. This data is used in the evaluation of bridges to repair or replace them. On the basis of the speed of the moving vehicle they are divided into two groups. Low speed vehicle is categized if its speed is less than 15 km/h while above are called as high speed. The most important component of WIM is Mass sensor and is positioned on or within the road system. They may be permanent, semi-permanent or temporary. Most WIM systems can classify and/or identify the vehicle to which the weighed axle belongs [11].

2.1.1 Load Cell

Typically load cell WIM system has a load cell. The load cell has two in-line scales, one axle sensor and at least one inductive loop. Likewise bending plate, load cell is positioned in travel lane at right angle to the direction of traffic movement. WIM load cell systems have a single load cell having two scales. These scales detect and weigh both sides, right and left, of axle simultaneously. A load cell has durable material such as steel with a strain gauge attached. The strain gauge has a wire for transmitting the electric current. When load is applied on cell, wire beneath strain gauge gets compressed and altered slightly. This change causes a change in resistance and hence follow of current changes. Weight is calculated with the help of this change. After summation of values from each scale axle weight is obtained.

2.1.2 WIM Data Acquisition Process

WIM electronics capture the digital signal outputs from sensor and the data from it are converted from binary strings to ASCII files and then further convert it to Excel files through a software i.e. Trafman 6.0 as shown in Figure 2. The Excel files contain data of lane codes, recording time, vehicle speeds, axle numbers, vehicle lengths, axles spacing, GVWs, and axle weights. The data is then further filtered out before an analysis to be carried out.

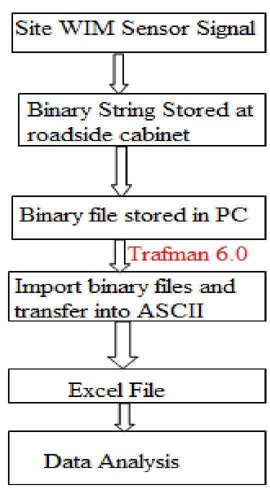

Figure 2 WIM Data Acquisition Process at Site

3 Results

Axle configuration and axle weights have been changed significantly over time but for design of bridges still CPHB 1967 and AASHTO specifications are used [7]. In order to check the adequacy of bridges, we did a case studies of simply supported RC-girder bridges i.e., at Ayub site, Peshawar.

3.1 Characterization of truck traffic

Axle weight, axles spacing and gross vehicle weight record from 411 trucks from Ayub Bridge gathered over a time span of 10 days was used to estimate loading trends of various truck types crossing bridge. The span of Ayub bridge is taken as 25 m. The random data was collected without classification as separate axle vehicles. To capable the data to compare with NHA provisions and limit, there is need to classify the data.

Table 1 Classification according to their number of axles

Number of axles	Number of vehicles	Percentage of total traffic (%)
2 axles vehicle	154	37.47
3 axles vehicle	66	16.06
4 axles vehicle	33	8.03
5 axles vehicle	3	0.73
6 axles vehicle	155	37.71
Total vehicles	411	

Table 1 shows the classification of traffic data according to their number of axles. Current studies concern about the heavy trucks with large number axles to deal with worst case. The data illustrates the significance of the site as quantity of six axle vehicle is comparable to small cars. The number 2 axles and 6 axles vehicles dominate the data by sharing approximately 37% each of total traffic. The 5-axle vehicles were found in least amount of only 3 (less than 1%).

Table 2 Vehicle weights description

Description	Weight (tons)
Minimum gross vehicle weight	6.88
Maximum gross vehicle weight	88.12
Mean gross vehicle weight	37.35
Minimum axle weight	2.72
Maximum axle weight	11.34
Mean axle weight	6.95

Table 2 describes the characteristics of gross and axle weights to make comparison with NHA weight limits. The weight varies between 6.88 ton to 88.12 ton with 37.35 ton as a mean, while axle weight changes between 2.72 ton to 11.34 ton with mean of 6.95 ton. Figure 3 illustrates the comparison of mean and maximum gross vehicle weights with the NHA limitations.

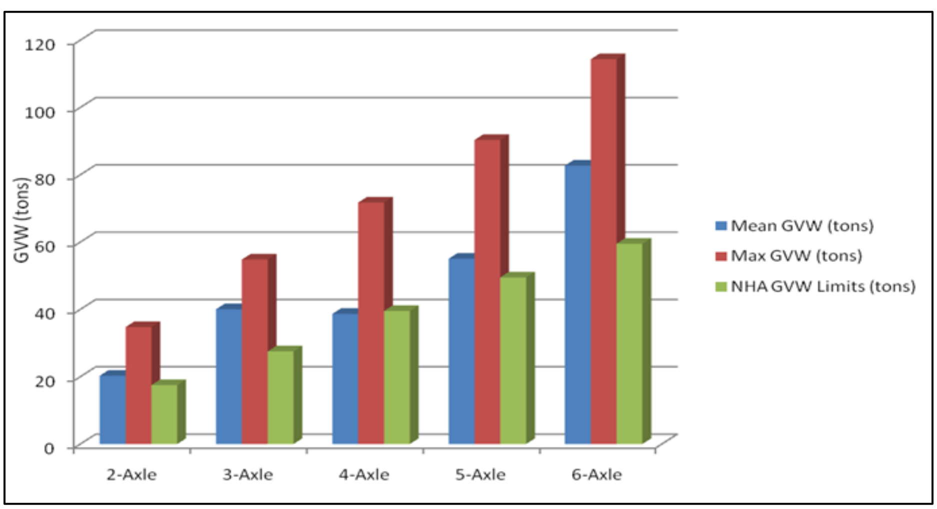

Figure 3 Comparison of mean, maximum and NHA gross vehicle weight limits

3.2 Comparison

Bridges are meant to bear the load of heavy traffic especially the trucks. In case if actually trucks load exceed the provision advised by authority might be very detrimental to lives and properties. Therefore, there is need to identify the violation and propose the appropriate action. Figure 4 explains the number of trucks in each axle category that violate the NHA prescribed limitations. The data clarity verify that all types of vehicles violate the limitations by significant amount. Smaller vehicles like 2-axles and 3-axles vehicles dramatically surpass the limit by 59% and 85% respectively. Similarly, heavy load traffic like 6-axles trucks considerably exceed the thresholds by 57%. Likewise, 21% of medium sized vehicle passes the NHA requirements. The number of 5-axle vehicle were insignificant therefore can't be consider but still 1 violates out of 3. Around 60% of total traffic violates the prescribed thresholds.

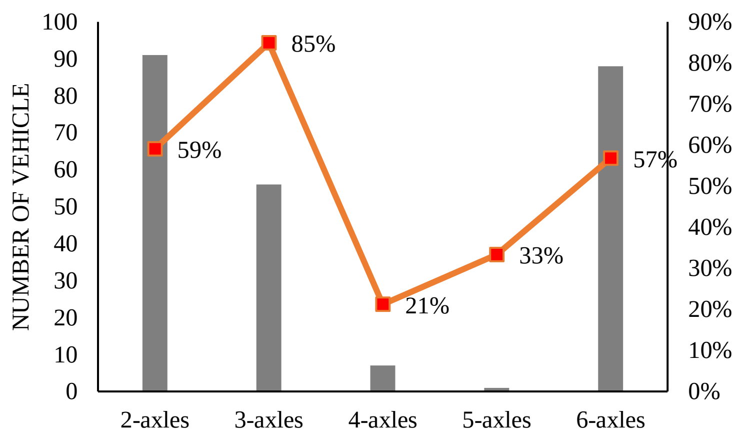

Figure 4 Vehicles that violates the NHA gross weight limitations

Similarly, Figure 5 illustrates the quantity of automotive that outstrip the axle load limits to point out the danger of point load on bridge. If any of axle surpass the required value is classify as a violated vehicle. Figures of axle load violation is more alarming than gross weight violation. All category of trucks passes the value by considerable amount. More than 73% and 95% of 2-axle and 3-axle exceed the obligation. Almost all heavy trucks violate the permissible limit while only 3% of 6-axle vehicle are traveling within allowable limit. In addition, 4-axles vehicles show comparatively moderate rise of 42%. Overall, 87% of trucks crosses the NHA limitation that is serious threat to existing bridges designed for lower design load.

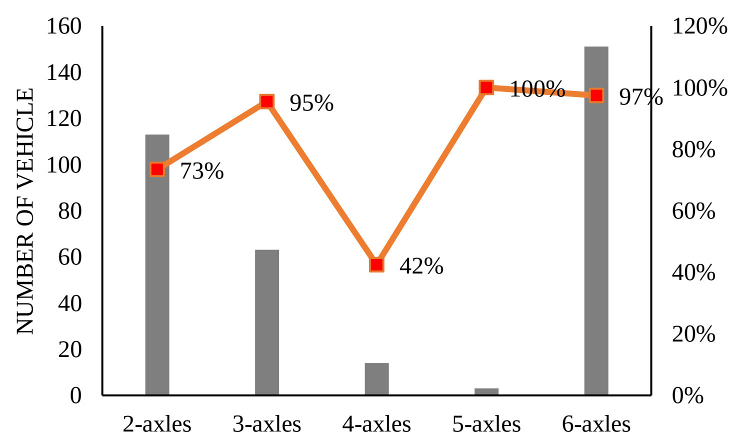

Figure 5 Vehicles that violates the NHA axle weight limitations

There is need to enhance the current research on other bridges also and formulate new code of practice that in actual illustrates the current traffic situation of Pakistan. Current research proposes the methodology and analysis parameters to lay a predefined path for other engineers and researcher.

4 Conclusion

Results of the case study indicate that bridges in Pakistan are potentially subjected to more extreme effects than they were actually design for, owing to prevailing traffic trends. From the study it is concluded that actual truck traffic of Pakistan is significantly different in axle weights and gross vehicle weights than the values specified NHA Legal Load limits. The load effects because of real truck traffic is much higher as compared to the indication by live load models of AASHTO Specification, PHB Code, and legal load limits of NHA. Thus, bridges may be considerably overstressed than that being assumed in bridge design. Hence, existing live load model of NHA legal limits are not the true representations of actual truck traffic of Pakistan, thus, there is requirement of developing a new live load model and also to ensure strict enforcement of load limitations.

Acknowledgment

The authors are thankful to every person/department who helped in any part and any form in research work. Our profound gratitude especially goes to our FYP supervisor Dr. Shahid and Dr. Muhammad Ali from UET Peshawar who provided us WIM Data of Ayub Bridge Peshawar.

References

[1] I. Shahid, S. Farooq, A. Noman, and A. Arshad, "Comparison of live load effects for the design of bridges," *J. Environ. Treat. Tech.*, vol. 5, no. 2, pp. 85–96, 2017.
[2] E. Dehghan-Niri, D. D. Cortes, S. Zamen, F. Alvidrez, and D. Jauregui, "Simplified Comparison of Oversize and Overweight Vehicles Permit Fee Structure in the US Western States," *Transp. Res. Rec.*, vol. 2674, no. 10, pp. 963–988, 2020.
[3] M. M. Chrimes, "THE DEVELOPMENT OF CONCRETE BRIDGES IN THE BRITISH ISLES PRIOR TO 1940.," *Proc. Inst. Civ. Eng. Build.*, vol. 116, no. 3, pp. 404–431, 1996.
[4] R. M. Barker and J. A. Puckett, *Design of highway bridges: An LRFD approach*. John wiley & sons, 2021.
[5] M. Kozikowski, "WIM based live load model for bridge reliability," *Civ. Eng. Diss. Student Res.*, p. 2, 2009.
[6] I. Shahid, A. K. Noman, S. H. Farooq, and A. Arshad, "Extrapolation of Live Load Effects to 75 Years Return Period for Highway Bridges," *J. Environ. Treat. Tech.*, vol. 5, no. 4, pp. 132–140, 2017.
[7] S. Shahid, I. Ahmad, and M. A. Arshad, "AN ASSESSMENT OF VEHICULAR LIVE LOADS FOR BRIDGE DESIGN IN PAKISTAN," *Int. J. Bridg. Eng.*, vol. 6, no. 1, pp. 9–22, 2018.
[8] L. Aashto, "Bridge design specifications." American Association of State Highway and Transportation Officials …, 1998.
[9] H. Pollaris, K. Braekers, A. Caris, G. K. Janssens, and S. Limbourg, "Iterated local search for the capacitated vehicle routing problem with sequence-based pallet loading and axle weight constraints," *Networks*, vol. 69, no. 3, pp. 304–316, 2017.
[10] S. Ali, M. Javed, and B. Alam, "A comparative study of live loads for the design of highway bridges in Pakistan," *IOSR J. Eng.*, vol. 2, p. 96, 2012.
[11] B. Jacob, "Weigh-in-motion of Axles and Vehicles for Europe," *Final Rep. Proj. WAVE, LCPC, Paris*, 2002.

3rd Conference on Sustainability in Civil Engineering (CSCE'21)
Department of Civil Engineering
Capital University of Science and Technology, Islamabad Pakistan

THE EFFECT OF USING JUTE FIBER ON DEFORMATION RESISTANCE OF ASPHALT CONCRETE

[a] Muhammad Fawad Rashid, [b] Muhammad Farhan Hassan, [c] Aamar Danish, [d] Ahtsham Ahmed*

a: Department of Civil Engineering, University of Engineering and Technology Taxila, fawad.rashid@students.uettaxila.edu.pk
b: Department of Civil Engineering, University of Engineering and Technology Taxila, farhanhassan.uet@gmail.com
c: Civil Engineering Department, Faculty of Engineering Sciences, National University of Modern Languages Rawalpindi, aamardanish@gmail.com
d: School of Energy, Geoscience, Infrastructure and Society, Heriot-Watt University Edinburgh, Scotland, aa2073@hw.ac.uk
* Corresponding author: Muhammad Fawad Rashid, Email ID: fawad.rashid@students.uettaxila.edu.pk

Abstract- Pavement distresses are a major problem not only in Pakistan but throughout the world which leads to premature pavement failures. As the pavement construction is expected to increase with passing time, studies and research have been done for the improvement of asphalt pavements performances from both sustainability and functional perspectives. Reinforcing the bituminous mixture with fibers could provide an improvement in Asphalt Concrete (AC). Asphalt concrete modified with fibers is termed as Fiber Reinforced Asphalt Concrete (FRAC). In this study jute fiber is used as a reinforcing material to investigate the FRAC materials specifically its effect on deformation resistance. The effects of jute fiber modification on mixing procedure and performance of modified AC were observed later by several laboratory tests. Results showed that the optimum binder content increases 4-5% and the stability of jute fiber modified asphalt concrete increases up to 29% however, the flow value decreases up to 7% at 0.5% jute-fiber concentration. Addition of jute fiber significantly improved the deformation resistance of asphalt concrete. Whereas from the sustainability perspective, it leads to concept of the new market to utilize waste fibers thereby lessening the environmental consequences.

Keywords- Asphalt Concrete, Fiber-reinforced asphalt concrete (FRAC), Jute Fiber.

1 Introduction

Transportation system of any nation is of great significance for its advancement and economy [1, 2]. An economy appears to be on track if an efficient infrastructure exists. It is too difficult to put the economy on the high quick way without an efficient transport framework. The huge increment in traffic volume in recent couple of decades has causes premature pavement failures of the entire road structure in Pakistan. A resultant penetration of water is caused by temperature cracking, fatigue or alligator cracking and rutting distresses leading to partial or complete pavement-failure, making it necessary to improve the properties of pavement. In hot weather extremes problem is aggravated due to bitumen's lower stiffness [3]. In this situation it is an ideal opportunity to explore this issue and propose suitable solution and methodology.

These limitations call for research and innovation in materials and techniques and innovations in pavement engineering to advance the pavements in terms of durability and resistance to distresses and thereby requiring lesser maintenance [4]. The research to achieve these goals has culminated into development of the techniques that are collectively known as 'modification of asphalt' [5]. They employ various types of fibers and polymers that are applied to the asphalt. Fiber application is very advantageous for increased durability as it improves fatigue and rutting resistance, increases service life, and reduces thermal cracking [4]. Fiber-reinforced asphalt concrete materials (FRAC) are utilized for overlays and maintenance of pavements and bridge-deck membranes in traditional mixes. They're also employed in multi-course flexible pavements and composite pavements. Performed studies show that fiber increases dynamic modulus [6], rutting resistance

[7], freeze-thaw resistance, the tensile strength at low temperature and the fatigue cracking resistance [8]. Jute fiber is compatible with hot mix asphalts (HMA) and jute fiber modified asphalt mixtures have appropriate mechanical properties (modulus, rut resistance and tensile strength) [9]. Jute fiber absorbs light components of bitumen increasing bitumen viscosity resulting in higher fracture resistance in tension mode for HMA mixtures [10]. From different tests like Marshall test and Drain down test, it is concluded that stone mix asphalt with using jute fiber gives very good result and can be used in flexible pavement [11]. The increase in length of jute fiber causes reduction in flow values [12]. This study uses different percentages of jute fiber incorporating fiber size of 20 mm to explore the impact on dry mixing process. Marshal Stability test was performed for flow and stability values to investigate jute fiber's impact on Optimum Binder Content (OBC) and to find resistances against distresses in asphalt concrete.

1.1 Jute Fiber.

Jute is a long, lustrous, soft vegetable fiber that may be spun into strong, coarse threads. Jute is one of the most cost-effective natural fibers, second only to cotton in terms of production and number of applications. Jute fiber is composed of lignin (12-14%), pentosan (14-16%), cellulose (50-64%), and other materials like moisture, ash, proteins and fats [13]. Jute is the most affordable natural fabric, and it is completely biodegradable and recyclable, making it environmentally friendly [14].

Asphalt modification with addition of jute fiber gives higher which restricts road cracking and the crack propagation along with having the additional benefit of jute encased with asphalt, offering higher resistance to biodegradation [15]. Additionally, benefits like drain down prevention and improved fatigue performance by enhancing crack resistance of asphalt material are also achieved. For asphalt overlay applications, the abundantly available and low-cost jute materials make it a stronger competitor than the high-cost synthetic materials derived from scarce resources.

2 Research Methodology

Initially, aggregate to be used for the project was selected and brought from Margalla stone quarry. Then the bitumen grade of 60/70 was selected. Based on material properties, a fine gradation of NHA class B was preferred over the NHA class A gradation. The dosages of 0.5% and 1.0% were selected by weight to determine Optimum Binder Content through Marshal Mix Design. In the end, a comparison was drawn for different results obtained from unmodified, 0.5% jute modified and 1% jute modified asphalt concrete. A conclusion was drawn through experimental results.

The primary goal of this study was to determine the impact of fiber addition in the dry technique on the performance of hot mix asphalt. This research is a part of the research study that used various types of fibers with an explicit focus on their effects on the permanent deformation behavior and was done only to facilitate the future researches with the fact that despite any significant effect of the permanent deformation behavior, there are other horizons that can and should be explored as far as the Jute Fiber Modification of Asphalt Concrete is concerned.

3 Experimental Details

Various type of tests performed on the aggregate, bitumen and asphalt concrete mixtures have been discussed. For this study, Class B aggregate of NHA Specification was used because it is easy to make a comparison of the test results in case of fine classifications. The physical properties of the aggregate and the bitumen used in this study are listed in Table 1. In dry method, fibers are added to the pre-heated aggregate in accordance with ASTM-D1559 standard. After this, bitumen is added to the aggregate & fiber mixture gradually and Marshall Mix design test is performed on unmodified and polypropylene modified asphalt concrete samples to select suitable type of aggregate and corresponding economical asphalt binder content. This recommended mixture is known as job-mix formula (JMF).

3.1 Sample Preparation

Minimum requirement of NHA is of 3.5 percent of asphalt content by weight of the total mixture for Class A and Class B. Normally, bitumen in 3 to 6 percent by total weight of mixture is added for the OBC determination. Mixture for jute fiber-modified and unmodified mixtures was prepared for 3.5, 4.0, 4.5, 5.0, and 5.5% asphalt. Three samples, two compacted and one loose one with a total weight of each sample 1200g are prepared. 0.5% (6g) and 1.0% (12g) fiber by weight of the total sample were added. Compacted samples were prepared at first by the dry method and after being placed in testing mould, 75 blows on each side were subjected using hammer of 4.5 kg. Resultant sample was cylinder with 4-inches inner diameter and 2.5 inches height. Mixture was then prepared for the loose sample with no compaction effort (Blows). Calculation of values different parameters was the performed using the formulae listed in Table 2.

Table 1 - Physical properties of the aggregates and bitumen

Aggregates			**Bitumen**		
Source		Margalla	Source	ARL 60/70	
Type		100 % crushed	Penetration Test (25°C)	64	ASTM D5
Los-Angeles Abrasion Value		23.18 %	Flash point	264°C	ASTM D92
Soundness	Coarse aggregate	3.20 %	Softening point	48°C	ASTM D36
	Fine aggregate	4.80 %	Ductility (5cm / min)	> 100 cm	ASTM D113
Elongation Index		2.30 %	Specific gravity	1.034	ASTM D70
Flakiness Index		6.10 %			
Sand Equivalent		76 %			

Table 2 – Different parameters for Marshal Stability Test

Bulk specific gravity of aggregates, $\boldsymbol{G_{sb}}$	$G_{sb} = \dfrac{P_1 + P_2 + \cdots\cdots\cdots + P_N}{\frac{P_1}{G_1} + \frac{P_2}{G_2} + \cdots\cdots\cdots + \frac{P_N}{G_N}}$	Voids in Mineral Aggregates, VMA	$VMA = 100 - \dfrac{G_{mb} \times P_s}{G_{sb}}$
Effective specific gravity of aggregate, $\boldsymbol{G_{se}}$	$G_{se} = \dfrac{P_{mm} - P_b}{\frac{P_{mm}}{G_{mm}} - \frac{P_b}{G_b}}$	Air voids, $\boldsymbol{V_a}$	$V_a = 100 \times \dfrac{G_{mm} - G_{mb}}{G_{mm}}$
Effective Asphalt Content, $\boldsymbol{P_{be}}$	$P_{be} = P_b - \dfrac{P_{ba}}{100} \times P_s$	Voids filled with asphalt, VFA	$VFA = 100 \times \dfrac{VMA - V_a}{VMA}$

3.2 Determination of Stability using Marshall Stability and Flow Test.

Stability maybe defined as the maximum load resistance of the sample and flow is defined as the deformation corresponding to maximum load (Stability) at standard temperature of 60°C. For determining stability, compacted Marshall samples are kept in the water bath at 60°C ±1°C temperature for 30 to 40 minutes and then tested in Marshall Stability tester. Loading is applied on the specimen at the constant rate of 51 millimeters per minute, until sample fails. Total number of Newton (lbs.) or kgs force at which sample fails is recorded as Marshall Stability value. Deformation corresponding to this force is recorded as flow and expressed in units' of 1/100 inches.

a) b) c)

Figure 1: a. Jute fibers before addition. b. Jute-fiber modified sample being prepared. c. Compacted and loose samples ready for Marshall stability test

3.3 Calculation of Optimum Binder Content

After calculations six graphs are plotted between asphalt content on x-axis and unit weight, VMA, VFA, V_a, flow, and stability on y-axis. Of the various methods used worldwide to find out Optimum Binder Content are used worldwide; one is to use following three graphs against mentioned criteria for the calculation of optimum asphalt content (a) Bitumen content against maximum stability (b) Bitumen content against maximum unit-weight (c) Bitumen content against 4% air voids. Average of all three asphalt contents obtained from above three graphs is reported as optimum asphalt content (OAC) or optimum bitumen content (OBC).

4 Results

The results of various tests performed on the asphalt concrete mixtures and their analysis, have been discussed. Results of three kind of asphalt concrete mixtures were tabulated. Graphs between unit weight, VMA, VFA, V_a, stability and flow against asphalt content have been plotted. For modified mixture, results showed in Table 3 reveal that the optimum binder content's value increases by adding jute fiber.

Table 3 - Optimum binder content of unmodified and Jute modified mixtures

Criteria	Unmodified		Jute Modified			
			Fiber percent		OBC	
		OBC	0.5	1.0	0.5	1.0
Bitumen content against maximum stability	4.5		4.2	4.45		
Bitumen content against maximum unit-weight	4.7	4.57	5.5	5.5	4.73	4.78
Bitumen content against 4% air voids	4.5		4.5	4.4		

Figure 2 to Figure 4 show graphical plot between asphalt content and various parameters of Marshall test for unmodified and jute fiber modified asphalt mixtures. Stability of the jute fibers samples is more when compared to the unmodified samples with 0.5% Jute-fiber modification being more stable than 1.0% Jute-fiber modified asphalt mixture, meaning that low jute fiber content can achieve greater stability as compared to higher one. Flow values of jute modified samples are less than those of unmodified samples at 0.5% and slightly increases at higher fiber concentration which means modified samples are more stable against the traffic loads.

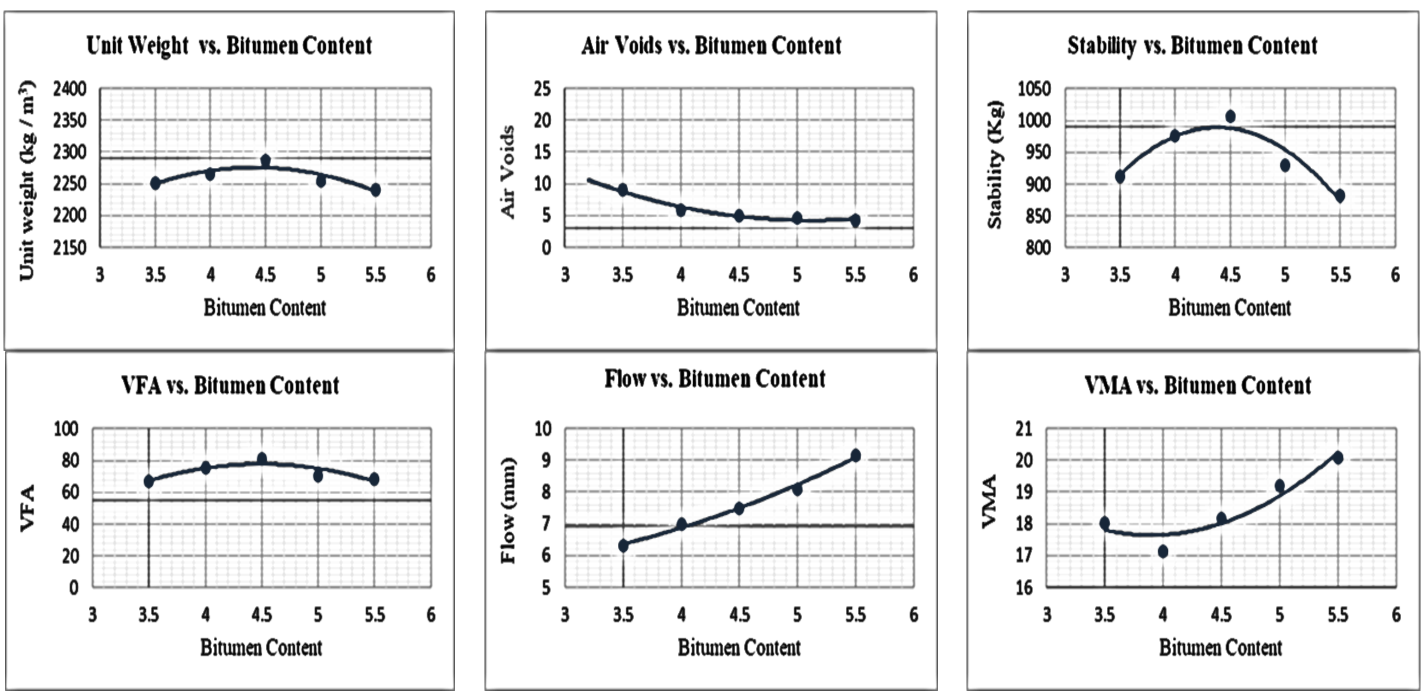

Figure 2: Graphs for unmodified specimen

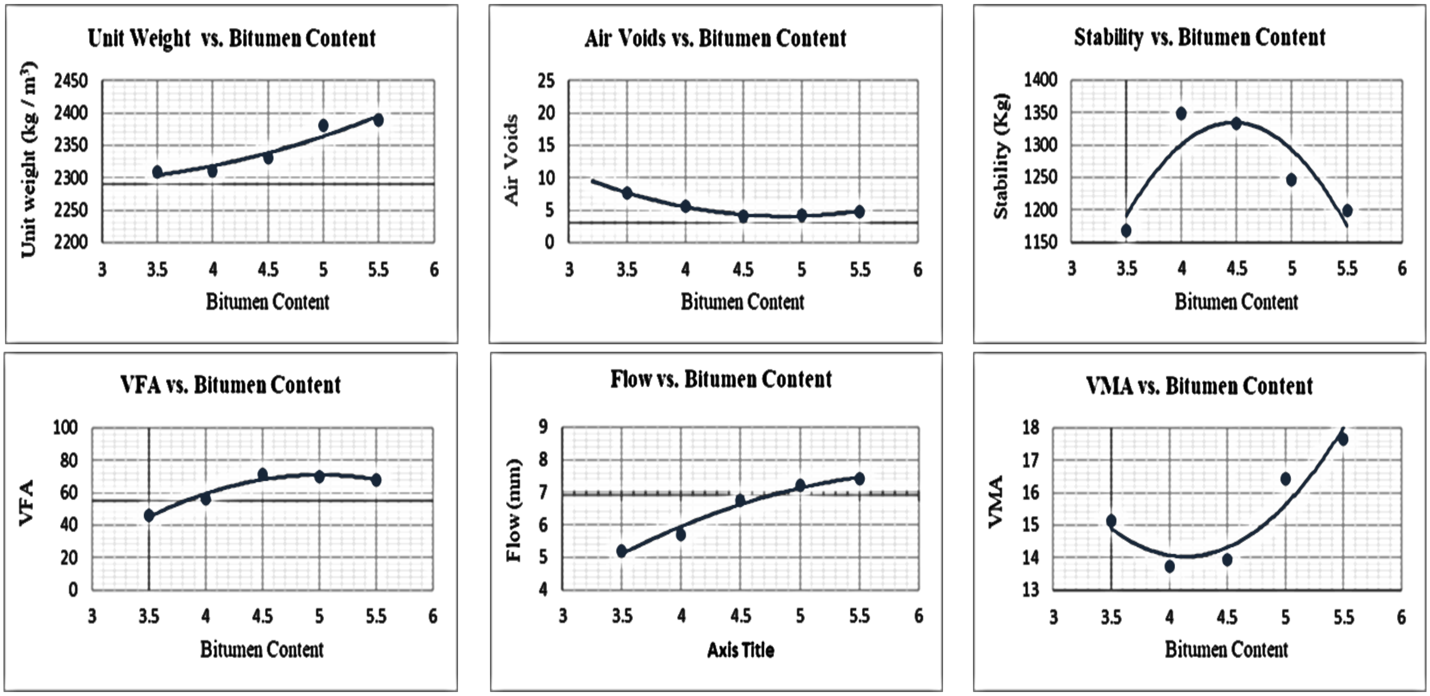

Figure 3: Graphs for 0.5% jute modified mixture

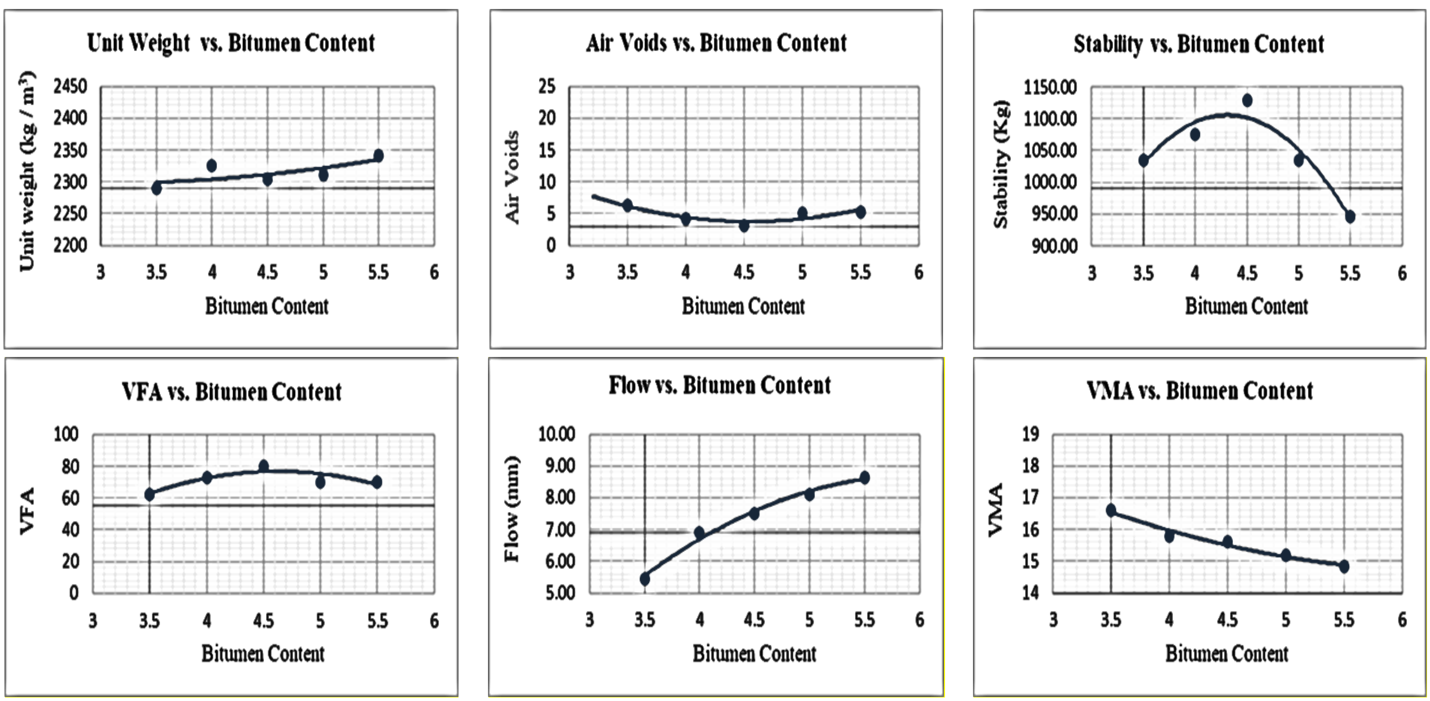

Figure 4: Graphs for 1.0% jute modified mixture

Figure 5a reveals the stability of 0.5% jute fiber modified sample is highest among all other samples at OBC while Figure 5b shows minimum flow at optimum asphalt content in case of 0.5% jute modified samples as compared to other samples. Also, mix-design criteria at optimum binder content is also verified for unmodified and jute modified samples.

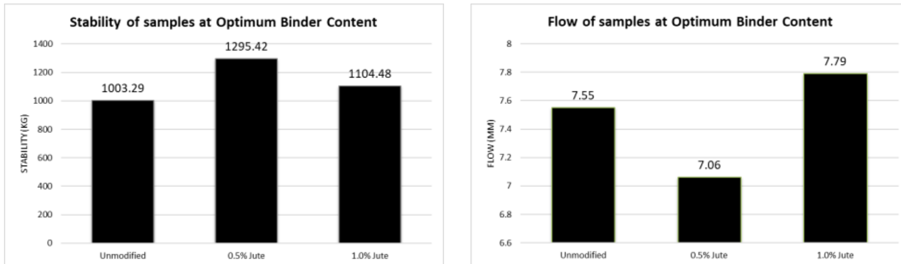

Figure 5: a. Stability of the control & modified samples at OBC. b. Flow of the control & modified samples at OBC

5 Conclusion

In this study, jute fibers were used as modification in asphalt concrete. The primary goal of this study was to determine the impact of fiber addition in the dry technique on the performance of hot mix asphalt. For the experiment, jute fiber was added to the asphalt mixture at 0.5 percent and 1.0 percent by weight. Based on the findings, it can be inferred that modifying jute fibers improved the HMA's various qualities. Jute addition, for example, increased the stability of asphalt mixtures by up to 29% and 10% at 0.5 percent and 1.0 percent Jute-fiber content, respectively, and increased the Optimum Binder Content by up to 4-5 percent. In comparison to the unmodified asphalt mixture, VFA, overall unit weight, air voids, and flow all decreased with the inclusion of jute fiber. At 0.5 percent jute fiber, the modified mixture performed best.

References

[1] M. F. Rashid, N. Ahmad, and A. Ahmed, "THE EFFECT OF USING POLYPROPYLENE FIBER ON DEFORMATION RESISTANCE OF ASPHALT CONCRETE," in *2nd Conference on Sustainability in Civil Engineering (CSCE'20).* , CUST, Islamabad Pakistan, 2020.

[2] M. F. Rashid, N. Ahmad, and A. Ahmed, "THE EFFECT OF USING STEEL FIBER ON DEFORMATION RESISTANCE OF ASPHALT CONCRETE," presented at the 2nd Conference on Sustainability in Civil Engineering (CSCE'20). CUST, Islamabad Pakistan, 2020.

[3] A. Arshadi, "Importance of asphalt binder properties on rut resistance of asphalt mixture," 2013.

[4] A. Qadir, "Rutting performance of polypropylene modified asphalt concrete," *International Journal of Civil Engineering,* vol. 12, no. 3, pp. 304-312, 2014.

[5] S. Tapkın, Ü. Uşar, A. Tuncan, and M. Tuncan, "Repeated creep behavior of polypropylene fiber-reinforced bituminous mixtures," *Journal of Transportation Engineering,* vol. 135, no. 4, pp. 240-249, 2009.

[6] S. Wu, Q. Ye, N. Li, and H. Yue, "Effects of fibers on the dynamic properties of asphalt mixtures," *Journal of Wuhan University of Technology-Mater. Sci. Ed.,* vol. 22, no. 4, pp. 733-736, 2007.

[7] H.-x. Chen, N.-l. Li, C.-s. Hu, and Z. Zhang, "Mechanical performance of fibers-reinforced asphalt mixture," *J Chan Univ (Nat Sci Ed),* vol. 24, no. 2, pp. 1-5, 2004.

[8] Q. Xu, H. Chen, and J. A. Prozzi, "Performance of fiber reinforced asphalt concrete under environmental temperature and water effects," *Construction and Building materials,* vol. 24, no. 10, pp. 2003-2010, 2010.

[9] P. K. Banerjee and M. Ghosh, "Studies on jute–asphalt composites," *Journal of applied polymer science,* vol. 109, no. 5, pp. 3165-3172, 2008.

[10] H. Chen and Q. Xu, "Experimental study of fibers in stabilizing and reinforcing asphalt binder," *Fuel,* vol. 89, no. 7, pp. 1616-1622, 2010.

[11] E. R. C. Mir Mudasir Nazir, Dr. TK Lohani, "USE OF JUTE FIBRE IN BITUMINOUS MIXES " *International Journal For Technological Research In Engineerin,* vol. 6, no. 7, pp. 2347 - 4718 2019.

[12] D. R. G. UMAR MAJID RESHI, "EFFECT ON BITUMINIOUS MIXES BY ADDING COAL ASH AND JUTE FIBRE IN FLEXIBLE PAVEMENTS," *Journal of Emerging Technologies and Innovative Research,* vol. 5, no. 7, pp. 517-522, 2018.

[13] M. A. Khan, S. Shehrzade, M. Sarwar, U. Chowdhury, and M. Rahman, "Effect of pretreatment with UV radiation on physical and mechanical properties of photocured jute yarn with 1, 6-hexanediol diacrylate (HDDA)," *Journal of Polymers and the Environment,* vol. 9, no. 3, pp. 115-124, 2001.

[14] O. Abiola, W. Kupolati, E. Sadiku, and J. Ndambuki, "Utilisation of natural fibre as modifier in bituminous mixes: A review," *Construction and Building Materials,* vol. 54, pp. 305-312, 2014.

[15] B. Das and P. Banerjee, "Interface bond and compatibility of jute with asphalt," *Composites Part B: Engineering,* vol. 53, pp. 69-75, 2013.

3[rd] Conference on Sustainability in Civil Engineering (CSCE'21)
Department of Civil Engineering
Capital University of Science and Technology, Islamabad Pakistan

DEVELOPMENT OF USER- FRIENDLY TOOL FOR SPECIFICATION OF HIGHWAY WORKS

Furqan Qamar [a], Suzannah Heard [b] and Shunde Qin[c]

a: Corresponding Author. Associate WSP UK.Email: furqan.qamar@wsp.co.uk
b: Graduate Engineer, WSP UK c: Principal Engineer, Jacobs UK

Abstract- In the construction industry, worldwide, there are certain standards or specifications for the design, construction and maintenance of infrastructure. In the United Kingdom, Standards for Highways are used for the preparation of the construction contracts. Depending on the type of works, different guidance documents are available. These guidance documents are very lengthy and consist of various appendices. It is commonly acknowledged that these are not user friendly and require improvement in preparation and implementation. Review of literature has shown that no such tools are readily available for highway contracts. The aim of this paper is to develop a tool for the preparation of specification for highway works, to reduce the preparation time, to develop the consistent document and improve quality. Volume 1 and 2 of The Manual of Contract Documents for Highway Works (MCHW) was considered in the development of this tool. After the addition of technical data, using the MCHW, past specifications were examined to determine a consistent format. Macros were used to program the tool on a Microsoft Word document. First, the variable words, within the template, were identified and tagged so they could be coded. The user interfaces were then created and reviewed to ensure that they were user friendly. The specification was then tested on a project where works were to be completed. After testing, it was concluded that, with the step by step guide, the tool was user friendly and easy to use. This helped save time, when completing the specification, by more than 50% and reduced the overall cost of project.

Keywords- Manual of contract document for highway works (MCHW), Highways England (HE), Specifications, appendices, tool.

1 Introduction

In the United Kingdom, for all highway construction works procurement processes, with or on behalf of Highways England (HE), the Standards for Highways are used for the preparation of the construction contracts. They provide the essential documents for the design, construction and maintenance of highways [1]. Depending on the type of works to be completed, there are different manuals providing guidance notes. The Manual of Contract Documents for Highway Works (MCHW) provides the documents required for the preparation of contracts for trunk road works. Trunk roads are motorways and all-purpose roads for which the overseeing organisations are responsible. MCHW was first published in 1992 and consists of six volumes and an introduction incorporating the mandatory requirements of EU legislation [1]. Table 1 details the type of volumes included in MCHW.

The Specification for Highway Works is Volume 1 of the MCHW. It contains the requirements and approval procedures during construction, improvement or maintenance work, goods or materials on trunk road networks. The specification can be used to ensure that the works meet the required standard whilst helping contractors to price the projects. Volume 2 of the MCHW gives advice and guidance on how to implement the information given in Volume 1 and provides examples of Appendices for contracts. Technical data and project specific information is included within the contracts. The remaining volumes are not considered in the scope of this paper.

Table 1: MCHW volumes

Volume	Name
0	Manual Contract Document for Major Works and Implementation Requirements
1	Specification for Highway Works
2	Notes for Guidance on the Specification for Highway Works
3	Highway Construction Details
4	Bills of Quantities for Highway Works
5	Contract Documents for Specialist Activities

To assist in the designing and constructing of highways, tools are commonly used to handle sets of data [2,3]. Fox et.al have researched 'Practical Tools for Low-Carbon Road Design and Construction'. They found that tools can add value during the design, construction and reporting by simplifying the process, ensuring clarity and improving the quality. Furthermore, comparison studies have been completed in the past on the MCHW. For example, Eadie et al. investigated, through surveys, the most popular methods of measurement for civil engineering work. They concluded that the MCHW was not user friendly [4,5]. A literacy research has shown that no such tools are readily available for highway contracts. This paper, therefore, illustrates the development of the tool for the Specification for Highway Works.

WSP regularly work with HE, requiring the Specification for Highway Works to be used to develop contracts. Currently, this is extremely time consuming as the content of the contracts are bespoke for each project. This paper describes a tool which significantly reduces the time to fill in the contract, helping to save money on future projects. It ensures no aspects of the contract are missed which could result in the contract being rejected. Further to this, the tool allows for the contracts to be user friendly and the quality of the contracts is maintained [6,7].

2 Methodology

Figure 1 shows a flow diagram of the methodology for developing the specification template tool.

2.1 Background Information

For the specification, the up to date information and consequent formatting needed compiling into a single report to enable it to be used as a template for the tool. To complete this, Volume 2 of the MCHW, which contains guidance notes for the Specification for Highways Works, was used to ensure that the Appendices were included. Volume 1 was also used as it included technical data. Originally, only the general and bearings sections were included in the template, however, now the tool is operational, the remaining sections have been incorporated. After adding the technical data, using the MCHW, past specifications were examined to determine a consistent format and to confirm what other information was needed. An example of this was background information regarding the project and works to be completed. This also helped to incorporate the cover pages and other information included within the specification. Using previous projects, parts of their specifications were identified that could be useful for the tool.

2.2 Creating the tool

Once the formatting and the template was completed, Macros were used to program the tool on a Microsoft Word document. First, the variable words, within the template, were identified and tagged so they could be coded. An example of the variable words included the name of the project, the project number and the date. To tag the variable words, the words were highlighted and then, within Developer, Design Mode were selected, and the properties changed to include a tag. Afterwards, the user interfaces were created, and peer reviewed to ensure they were user friendly. The first user interface included the variable information that would be consistent throughout the report, such as the project name. The next user interface was to specify which Appendices and sections needed to be within the specification. These were split into tabs so that the user could easily see which Appendices were relevant for the works they wanted to complete. For example, there was a "general" tab and a bearings tab which led to the relevant Appendices and sections. The final user interface included the variable information that needed to be filled in, based upon which sections and Appendices were included within the specification. Once the information was incorporated in the user interfaces, it was formatted.

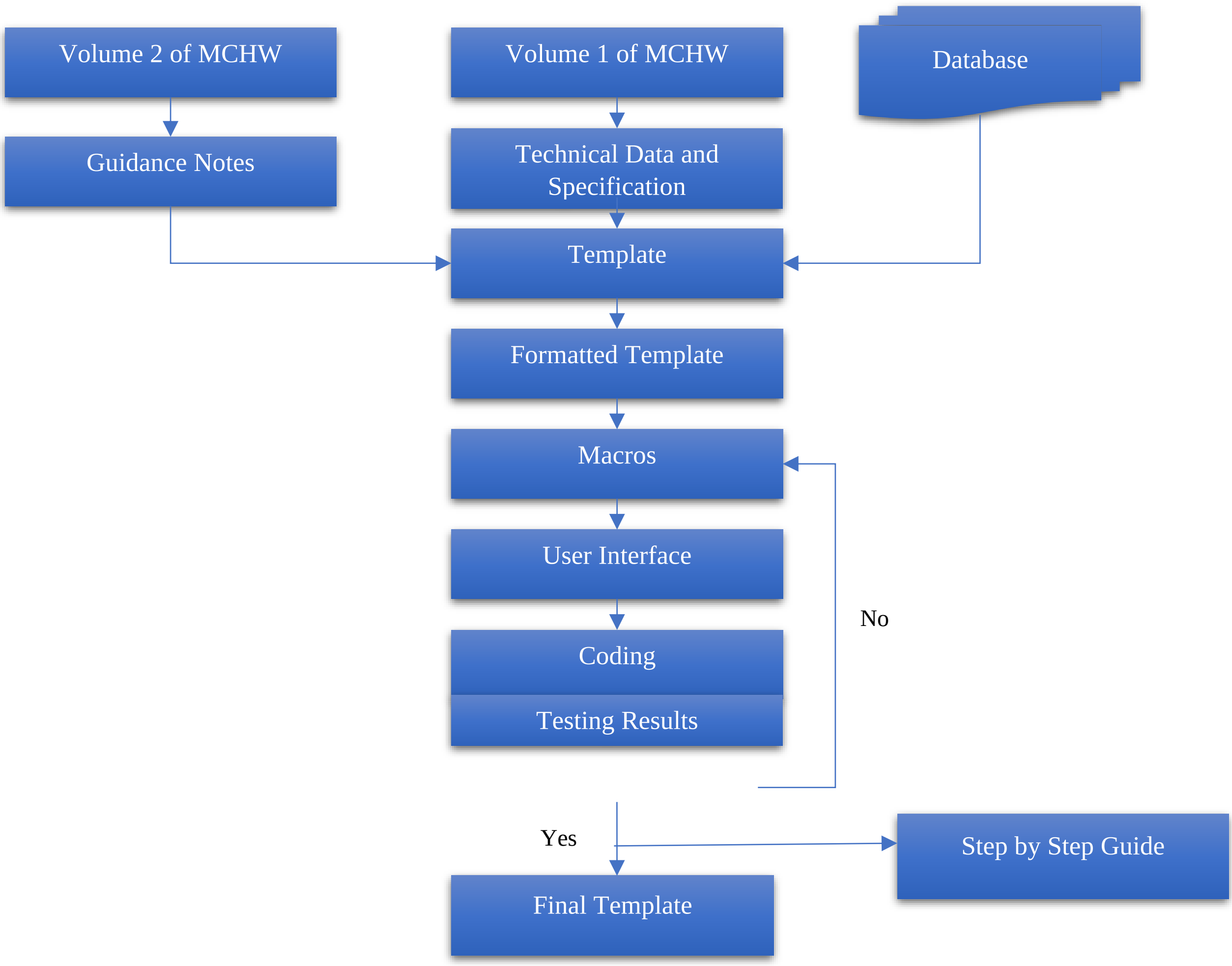

Figure 1: Flow diagram of methodology steps for the specification template

The final part of the tool to be completed was the coding. This was accomplished by using the Macros and ensuring that, when the user interfaces were filled in, the information was then inputted into the correct places. An example of the coding used for the variable words can be seen in Figure 2.

The Appendices were also added to the specification, in the correct order and with the correct formatting. The specification was then tested on a project where works were to be completed, to ensure accuracy. After testing the coding, any errors were corrected. The document was finally modified into a template so that original cannot be modified. A step by step guide was created for anyone wishing to use the tool. The specification was then tested by other users, within the Company, who confirmed that the guide and tool were easy to use and accurate.

```
'Updating the Project Title in the document.
    Project_Title = Me.TextBox1.Value
    For Each CC In ActiveDocument.ContentControls
        If CC.Title = "TX_Title" Then
            CC.Range.Text = Project_Title
        End If
    Next CC
    For i = 1 To ActiveDocument.Sections.Count
        For Each CC In doc.Sections(i).Headers(wdHeaderFooterPrimary).Range.ContentControls
            If CC.Title = "TX_Title" Then
                CC.Range.Text = Project_Title
            End If
        Next CC
        For Each CC In doc.Sections(i).Footers(wdHeaderFooterPrimary).Range.ContentControls
            If CC.Title = "TX_Title" Then
                CC.Range.Text = Project_Title
            End If
        Next CC
    Next i
```

Figure 2: Coding used to set up the tool with the variable words

3 Results and Discussion

Figure 3 shows the results of the tool and demonstrates the process for using the tool.

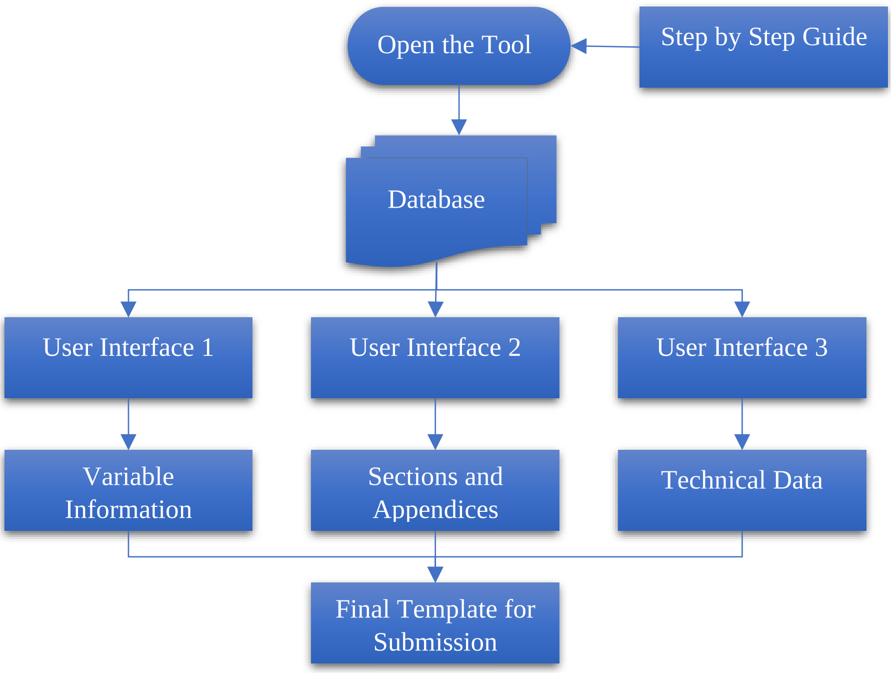

Figure3: Flow diagram demonstrating how the tool is used

Figure 4 shows the first user interface where variable information, including the area and project title, would need to be inputted.

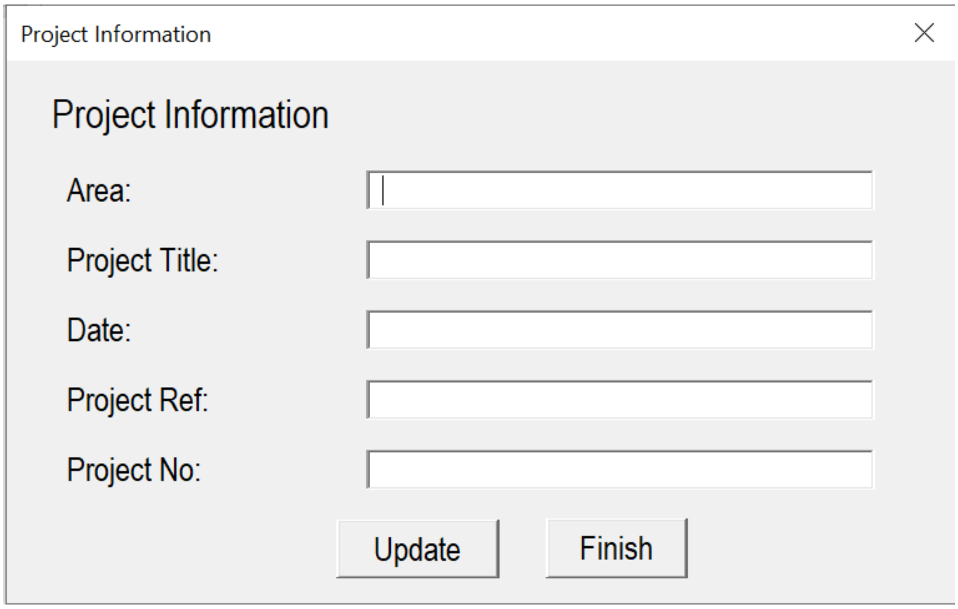

Figure 4: User interface 1 of the tool for the Specification of Highways Works

The tool allows only the data to be input into the interface and then, because the specification is formatted, the information is kept constant, helping to improve the overall quality of the specifications. The data only needs to be entered once; the tool then inputs the variable information into the correct places within the specification.

User interface 2 is shown in Figure 5 and allows users to tick which Appendices are appropriate for the works to be completed.

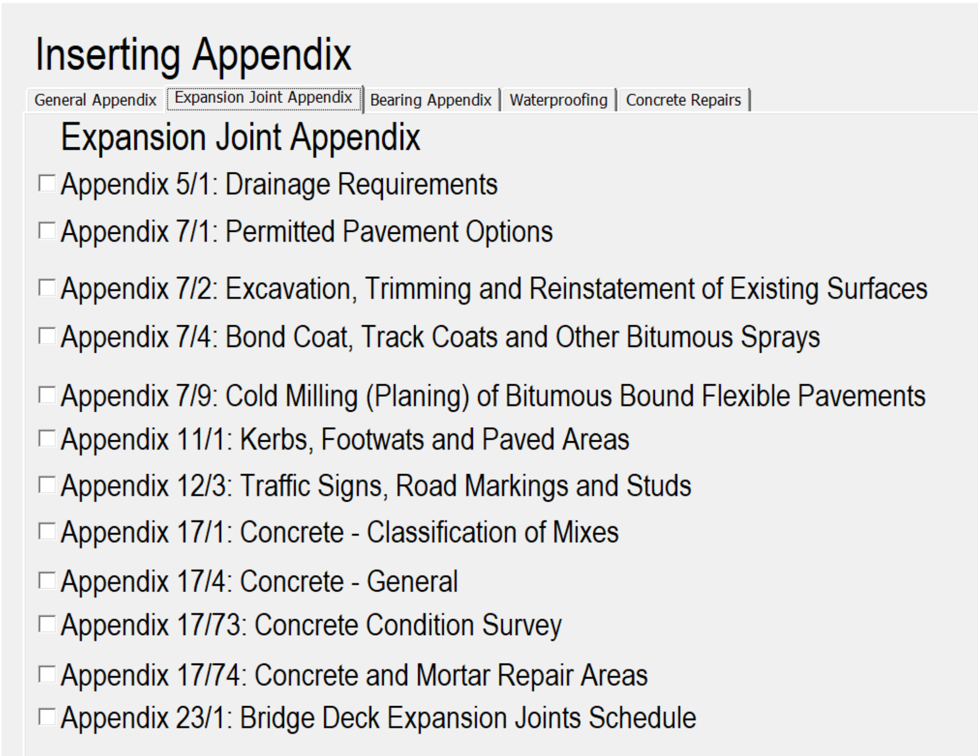

Figure 5: User interface 2 of the tool for the Specification of Highways Works

Figure 5 demonstrates the different tabs that contain the specific Appendices relating to the works. This is beneficial as it ensures that all the technical and non-technical information is considered and readily available to input at the same location. This helps to ensure that no parts of the specification could be missed, which could result in rejection of the whole specification by the Client.

Figure 6 shows user interface 3 where the technical data for the Appendices and sections are inputted.

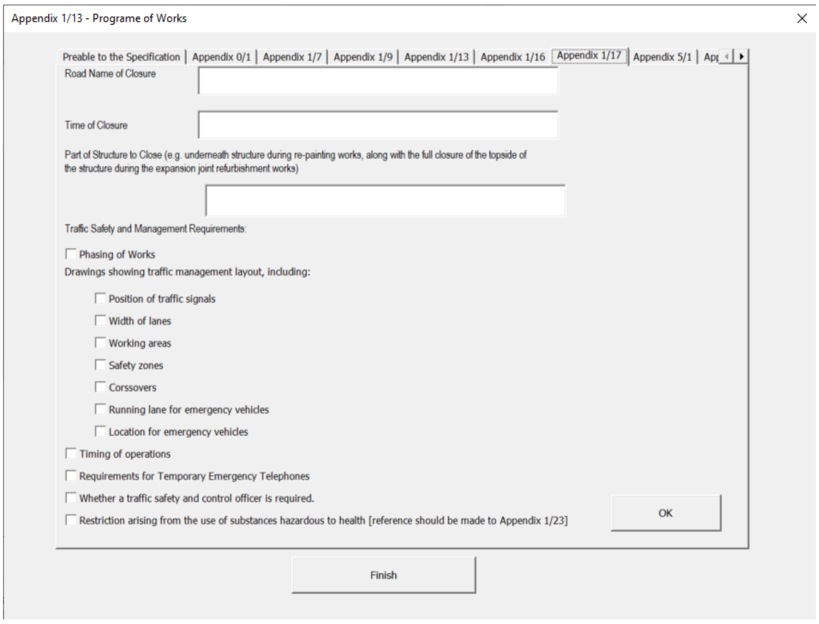

Figure 6: User interface 3 of the tool for the Specification of Highways Works

Similar to the other interfaces, all the variable information for the specification can be input in the same area and the tool will ensure it is positioned into the correct place. This helps to significantly reduce the time, by up to 50%; it usually takes a week to complete a specification without the tool, therefore, the tool aids efficiency on time and consequently helps to save money on projects.

Finally, after testing the tool on an additional project, it was concluded that, with the step-by-step guide, the tool is user friendly and easy to use. This again helped to save time when completing the specification and resulted in the preparation of a good quality document.

Currently, the tool is limited to a few clauses from the specification which are, the concrete repair, joint replacement and resurfacing. However, it is possible to add further clauses to the specification, when needed, as the template has now been prepared.

4 Conclusion and Recommendations

The development of a user-friendly tool for the Specification for Highways Works has been represented in this paper. The following conclusions have been drawn:

- The development of the tool helps to significantly save time when completing specifications as all the information is input into the same place once only. This can help projects to save money as it saves time.
- The quality of the documents are improved as the tool ensures there is consistent formatting throughout.
- As the information needed to be input into the document is located in the tool, it helps to ensure that none is missing from the specification, which could lead to it being rejected.
- Finally, it has been demonstrated that using the tool and the step-by-step guide helps to make the MCHW user friendly and simple to use.

Based on the developed and tested tool, the following recommendations are made:

- A similar tool needs to be implemented for other construction elements and new designs in a future study.
- The tool needs to be developed in a future study to work out the actual time and cost savings in a project.

Acknowledgment

The authors would like to thank WSP UK Ltd as an organisation who have given the opportunity to carry out this study. The careful review and constructive suggestions by the anonymous reviewers are gratefully acknowledged.

References

[1] DfT (Department for Transport), Manual of Contract Documents for Highway Works, 2009. https://www.standardsforhighways.co.uk/ha/standards/mchw/vol0/sect0.

[2] J.Fox, D.Bell and G.Edmond, "A practical tool for low-carbon road design and construction", *Proceedings of the Institution of Civil Engineers -Transport,* Vol 164, Issue 3, pp 165-179, 2011.

[3] R.Eadie, P. Millar and N.Harte, "A comparison between CESMM3 and MCHW as methods of measurement for civil engineering work," *International Journal of Procurement Management*, Vol 6, Issue 5, 2013.

[4] G.Aouad, S.Wu, A.Lee , "nD modelling, present and future" ,*Virtual Futures for Design, Construction and Procurement,. Oxon:Blackwell Publishing* , 158-170, Chapter 12, 2009.

[5] E.Best,"The development of a BIM based building measurement learning tool". *Proceedings of Australian Universities Building Education Association Annual Conference (AUBEA)*, Auckland, New Zealand, 21-24, (2008).

[6] R.Eadie, C.McKeown, K.Anderson, "The impact of recession on construction procurement routes". International Journal of Procurement Management. 6, 1, 24-38, (2013).

[7] O.Kwon, J.Son, S.Lee,"Study on the application of 3D-based BIM for school facilities to increase cost management efficiency". *Journal of the Korea Institute of Building Construction*. 10, 6, 49-60, 2010.

3rd Conference on Sustainability in Civil Engineering (CSCE'21)
Department of Civil Engineering
Capital University of Science and Technology, Islamabad Pakistan

FRACTURE RESISTANCE OF WARM MIX ASPHALT MODIFIED WITH RECLAIMED ASPHALT PAVEMENT

[a] Saad Tayyab*, [b]Arshad Hussain, [c] Fazal Haq, [d] Afaq Khattak,

a: School of Civil and Environmental Engineering (SCEE), National University of Sciences and Technology (NUST) Islamabad,
b: School of Civil and Environmental Engineering (SCEE), National University of Sciences and Technology (NUST) Islamabad, drarshad@nit.nust.edu.pk
c: National Institute of Transportation (NIT), Military College of Engineering NUST Risalpur, fhaq.tn15@nit.nust.edu.pk
d: Department of Civil Engineering, International Islamic University Islamabad (IIUI), afaq.khattak@iiui.edu.pk
* Corresponding author: Email ID: saadtayyab@nit.nust.edu.pk

Abstract- The two-key requirement of asphalt pavement are sustainability and durability. Sustainability of pavement includes replacing percentages of virgin aggregate with Reclaimed Asphalt Pavement (RAP) with the help of Warm Mix Asphalt (WMA) additives, however durability involves performance parameters like fracture resistance of asphalt. The addition of RAP content increases the production temperature of asphalt and may degrade its performance. Therefore, researchers recommend different percentages of WMA additives to lower mixing and compacting temperature of asphaltic pavement. The current research work has been carried out to optimize the percentages of RAP and Sasobit that have best fracture resistance as compared to Hot Mix Asphalt (HMA) and thus allow us to minimize the construction cost of pavement structure. Varying percentages of RAP (0%, 20%, 40% and 60%) and Sasobit (0%, 2%, 4% and 6%) as WMA additive were used. Fracture resistance of asphalt was evaluated by Semi Circular Bending (SCB) test in the laboratory. The resistance of WMA to fracture was improved with the increase in percentages of RAP and Sasobit up to certain limit, whereas the addition of RAP to HMA showed a decrease in fracture resistance due to the stiffer nature of aged binder in RAP.

Keywords- Fracture Resistance, Sasobit, Warm Mix Asphalt (WMA) and Reclaimed Asphalt Pavement (RAP),

1 Introduction

The emerging trend on conserving natural materials over the last decades and reducing the consumption of fuel in road construction gaining popularity throughout the world. Utilizing WMA additives and RAP in combination may have significant contribution to achieve durable, sustainable and green pavement structures [1]. WMA additives reduce the compacting and mixing temperature of asphalt mix by 20-55ºC than the traditional HMA. The compaction and mixing of traditional HMA are 145-150ºC and 150-155ºC respectively. Owing to the reduction in mixing and compacting temperature with the help of WMA additives will result in numerous benefits including longer service life, fuel saving, decreases in greenhouse gases and ease in mixing and compaction [2]. Another recent research by World Bank on temperature reduction concluded that every 10ºC of temperature during asphalt preparation results in decrease of greenhouse gases emission by 1 kg and fuel by 1 liter per ton of asphalt mix [3].

WMA additives are new technology in pavement and initiated in Europe over the last decade and still achieving high interest in the world. WMA additives are broadly classified as; chemical additives, organic additives and foaming based additives. Workability of asphalt mix increases with the addition of these additives and/or decreases the viscosity of asphalt binder using nominal heat. WMA technologies permits the mixing, transporting, and paving practice at considerably reduced temperature. By using these latest technologies, we can produce asphalt mix as much as 100ºF lower than ordinary

HMA. Sasobit is an organic WMA additive and used in this study for WMA preparation. It is an artefact of Sasol Wax in South Africa, which is a long-chain hydrocarbon, fine crystalline and formed from gasification of natural gas or coal feed stocks by the process of Fischer-Tropsch (FT) which produce a mix of hydrocarbons with molecular chain lengths of more than C5 to C100 carbon atoms. The chemical formula of Sasobit is C_nH_{2n+2} and registered as number 8002-74-2 by Chemical Abstract Service [4, 5]. For production of WMA, Sasol endorses to add Sasobit at a rate of 0.8% to 3% by mass of bitumen, but not to exceed 4% but numerous researchers have been concluded that addition of Sasobit up to 8% of the binder can improve mechanical properties of asphalt mix.

RAP material is obtained from asphalt pavement structure which may consider incapable of carrying further traffic load, having distresses beyond a certain level or has passed its service lifetime. The partial replacement of RAP in fresh asphalt mixes helps in cost reduction of material, preserving fresh binder and natural aggregate and RAP disposal problem [6]. The virgin asphalt pavement recycling dates back to 1915 [7] but momentous use of RAP in HMA indeed initiated in the mid of 1970s due to excessive prices of asphalt binder as a result of the oil impediment. Many latest researches have been carried out to better use RAP in both WMA and HMA [8-10]. Moreover, historical data as mentioned by West [11] stated that mixes having RAP will have the same or even better performance as compared to virgin HMA, but it will need to be carefully designed and constructed. In typical asphaltic mix design with the addition of RAP rarely crosses the limit of 20% to 25% in addition to hot-in-place recycling (HIPR) or cold-in-place recycling (CIPR), which can make use of 80-100% of RAP. The limited usage of RAP in asphalt pavement is due to the miss management and not correctly separation of different stockpiles of RAP sources. Due to economic crises together with environmental related issues, Departments of Transportation (DOT) in US are being enforced for raising the RAP contents up to 50% in Flexible pavements. The increased percentage of RAP usage has the potential to impact structural performance and durability of the pavements. Researches have concluded that higher RAP contents effect the rutting, fatigue and fracture characteristics of HMA as well as WMA [12].

Singh, Ashish et al. [6] evaluate the WMA mix containing different percentages (0%, 10%, 20%, 30%, and 40%) of RAP and different WMA technologies (2% Sasobit and 0.5% Evotherm) for tensile strength ratio and SCB tests. The virgin bitumen used in this research work was viscosity graded (VG-30) or 60/70 penetration grade. It was concluded from the SCB test results that Sasobit based WMA mix performed better in fracture than Evotherm based WMA. Pirmohammad, Khanpour et al. [13] conducted a comparative study of virgin WMA and crumb rubber modified WMA for fracture strength. In both cases WMA was prepared by using 3% of Sasobit by weight of 60/70 penetration grade binder. The result of fracture test showed that crumb rubber greatly enhances the fracture strength of WMA. Lee, Park et al. [14] and Yeon, Kim et al. [15] compared the resistance to fracture of HMA and WMA. Three different types of WMA additives (Pewo, Evotherm and Sasobit) were utilized in this research works. They concluded from their research works that WMA was better in fracture resistance than HMA irrespective of WMA technologies. As a result, WMA is less susceptible to brittle fracture than HMA. Pirmohammad and Ayatollahi [16] find out that fracture resistance of WMA is similar to HMA and some WMA additives make the mixture stronger than HMA even without any RAP. Yoo, Jeong et al. [17] compared the HMA and WMA mixture for fracture resistance by using 60/80 penetration grade bitumen. Both the mixtures were further modified by different polymers. The results showed that the fracture resistance of unmodified (without any polymers) WMA mixture was higher than the unmodified HMA. While the addition of polymers to HMA adversely affect the fracture resistance.

Mogawer, Austerman et al. [18] conducted a research on WMA with high percentage of RAP to evaluate the fatigue cracking, fracture resistance, reflective cracking, stiffness, moisture damage and rutting. Sonne Warmix was chosen as WMA additive and 1% by weight of base binder (PG58-28) was added to produce WMA mix. Different mixtures of HMA and WMA with 0%, 25% and 40% RAP were prepared for comparison. The results indicated that asphalt mixture's resistance to fracture decreases with the addition of high percentage of RAP and the same trend was observed for the addition of Sonne Warmix. The SCB test results indicated that HMA with 0% RAP performed better in fracture resistance than HMA with 25% and 40% RAP. On the other side, WMA with 25% and 40% RAP performed better in fracture resistance than WMA with 0% RAP. Kim, Mohammad et al. [19] characterized the fracture properties of HMA and WMA on 5 laboratory mixtures and more than 20 field projects by SCB and indirect tension test. Three different percentages of

RAP (15%, 20% and 30%) were used. They concluded from the test results that addition of WMA additives does not adversely affected the fracture properties of asphalt mix as compared to HMA mixture at intermediate temperature.

Furthermore, it was observed that the addition of RAP up to 30% improve the fracture resistance of WMA mixture. Thus, the best possible percentages of RAP and Sasobit are 40% and 6% respectively keeping in view the fracture resistance of Asphalt Mix. Thus, WMA technology provide the opportunity of using higher percentages of RAP thus the production temperature of Asphalt will reduce along with better performance and additional environmental benefits.

2 Objective and Scope

To promote the pavement recycling approach and lower temperature by WMA technology in Pakistan. This research has been planned to explore the fracture resistance of asphalt mixes with varying percentages of RAP and Sasobit as WMA additive and to categorize any special attentions that must be met to consume higher RAP content at lower temperature. Test matrix for performance test is shown in Table 1.

Table 2: Test Matrix for Performance Testing

S.no	Gradation	Binder	Percentage of RAP replaced	Sasobit content (% of bitumen)	Fracture Resistance of HMA by SCB test
1	NHA Class B Gradation	ARL 60/70	0	0	3
				2	3
				4	3
				6	3
2			20	0	3
				2	3
				4	3
				6	3
3			40	0	3
				2	3
				4	3
				6	3
4			60	0	3
				2	3
				4	3
				6	3
Total					**48**

3 Research Methodology

3.1 Asphalt Binder.

In the current research study bitumen having penetration grade of 60/70 were utilized as a base binder supplied by Attock Refinery Limited (ARL) Rawalpindi. Selecting 60/70 penetration grade of bitumen is that it is appropriate for colder to moderate range of temperature and typically used in Pakistan. The fundamental properties of the binder after laboratory evaluation are given in Table 2.

3.2 WMA Additive.

Sasobit is used as WMA technology in this research study in the form of prills and was imported from the chemical manufacturing South African company Sasol as shown in Figure 1. The recommended dosage of Sasobit by the manufacturer is 0.8 % to 3% by weight of binder but in this research 0%, 2%, 4% and 6% of Sasobit has been added by weight of OBC. The reason of selecting the percentage of Sasobit beyond the recommended dosage limit is due to their better performance according to past literature. Sasobit can be added either pre-blended to the binder or can be introduced directly to the mix bowl. The technical specifications of Sasobit as per manufacturer data sheet are shown in Table 3.

Table 1-Laboratory Tests Performed on Virgin Bitumen

S No	Test Description	Standard	Results
1	Penetration Test	AASHTO T 94-03	62
2	Flash Point (°C)	AASHTO T 48-89	261
3	Fire Point (°C)	AASHTO T 48-89	282
4	Specific gravity	AASHTO T 228	1.03
5	Softening Point (°C)	AASHTO T 53	48
6	Viscosity Test (Pa.sec)	AASHTO T 316	0.271
7	Ductility Test (cm)	AASHTO T 51	>100

Table 2-Basic Properties of Sasobit

Properties	Test Method	Units	Specification	Typical Values
Congealing Point	ASTM D 938	^{0}C	100 - 110	101
Penetration at 25 ^{0}C	ASTM D 1321	0.1 mm	0 - 2	<1
Penetration at 65 ^{0}C	ASTM D 1321	0.1 mm	0 - 13	11
Brookfield Viscosity at 135 ^{0}C	Sasol 1010	cP	10 - 15	12
Visual Color Compliance	Visual	-	Pass / Fail	Pass

3.3 RAP Material.

To accomplish the objective of this research work, milled RAP material was collected from Islamabad-Lahore Motorway (M-2) and brought to Transportation Laboratory (SCEE, NUST) for replacing natural aggregates and preparation of samples for Marshall Mix Design and fracture resistance. Aged binder content of RAP was determined by ignition method and found to be 3% of the total RAP.

Figure 1: Sasobit Prills

3.4 Virgin Aggregates.

Virgin aggregates were collected from Margalla crush plants in Margalla Hills Taxila Pakistan. These natural aggregates were tested in the laboratory as per standard procedures to check the suitability of aggregates in road construction. The properties of aggregate are presented in Table 4. NHA Class B gradation was used, which was specified by National Highways Authority (NHA) Pakistan in 1998 and widely used for flexible pavement in all over the country. The virgin aggregates were blended with 20%, 40% and 60% RAP, the gradation falls within the upper and lower limits of NHA Class B gradation as presented in Figure 2.

Table 3: Physical Properties of RAP and Virgin Aggregates

Test	Standard		Result	Limits
Flakiness Index	ASTM D 4791		10.20%	≤ 15 %
Elongation Index			3.80%	≤ 15 %
Aggregate Absorption	Fine	ASTM C 128	2.50%	≤ 3 %
	Coarse	ASTM C 127	0.69%	≤ 3 %
Impact Value	BS 812		15%	≤ 30 %
Los Angles Abrasion	ASTM C131		20.60%	≤ 45 %
Specific Gravity	Fine Agg	ASTM C 128	2.62	-
	Coarse Agg	ASTM C127	2.64	-

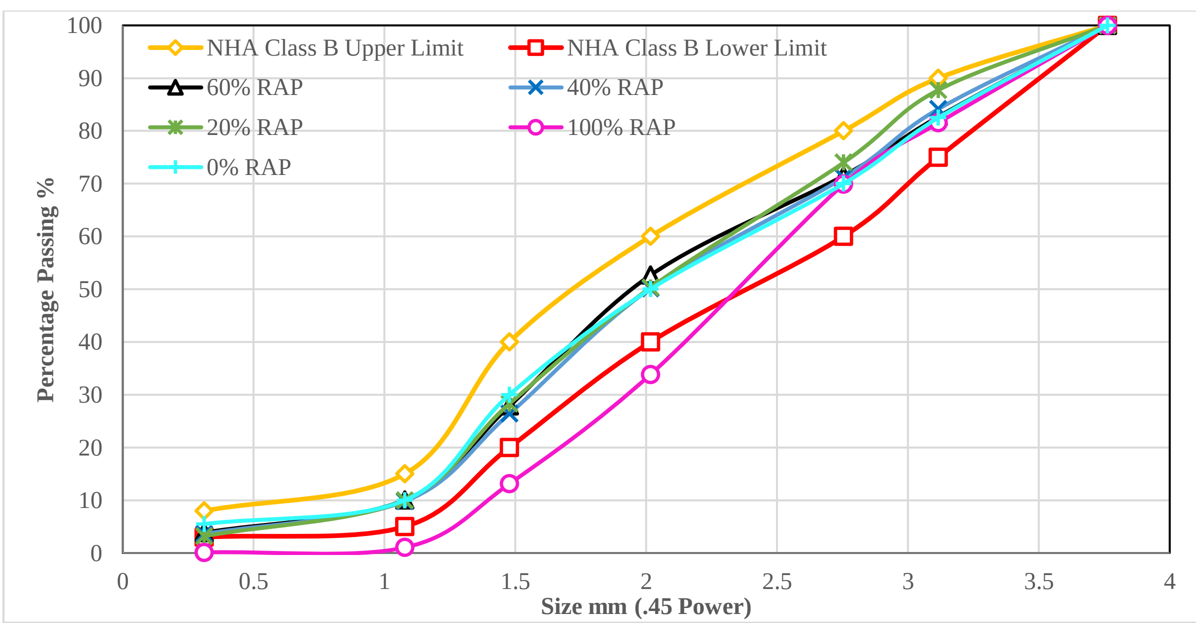

Figure 2: Gradation Curves

4 Laboratory Investigation

4.1 Marshall Mix Design

Marshall Mix Design was carried out for HMA with different percentages of RAP (0%, 20%, 40% and 60%) to determine Optimum Binder Content (OBC) as per ASTM D6927. Total 1200 grams of samples with standard dimensions were prepared by mixing at 160ºC and compacted at 135ºC temperature subjected to 75 number of blows on each side. Three replicates were prepared for each percentage of binder at the increment of 0.5%, ranging from 3.5% - 5.5%. The OBC at 4% air voids was determined to be 4.34%.

4.2 *Semi Circular Bending Test*

For SCB tests and checking fracture resistance via UTM, specimens were prepared through Superpave mix design procedure. The materials were heated after sieving at 105°C - 110°C until a constant weight achieved. The HMA was mixed and compacted at a temperature of 160±5ºC and 135ºC respectively. However, the WMA was mixed and compacted at a temperature of 125±5ºC and 100ºC respectively. Samples of 150 mm diameter for SCB test were prepared through Superpave Gyratory Compactor by providing 125 gyrations to each sample. Three replicates' samples were prepared for each percentage of change in RAP and Sasobit. Water-cooled masonry sawing machine was used for cutting the sample into our desired dimensions of 150 mm diameter and 57 mm thick circular discs. These circular discs were halved by the said machine. In the end, an artificial crack called notch in the center of the specimen of lengths (25 mm, 32 mm and 38 mm) with a thickness of 3 mm was generated to provide a predefined path for the crack. Figure 3 shows the overall procedure from gyratory sample to a cracked SCB test sample.

Figure 3: Preparation of Semi Circular Shaped SCB Test Samples from Gyratory Samples

SCB test for fracture resistance of asphalt was conducted in Transportation laboratory (SCEE, NUST) through a 25KN capacity (25KN of static loading at various frequencies) of Universal Testing Machine (UTM-25KN). This equipment had an environmental chamber for maintaining the desired test temperature (-16ºC to 60ºC), a hydraulic chamber for pressure application and a central system for data acquisition.

Subsequently, the samples were kept in the environmental chamber of UTM-25KN and permitted to a minimum of two hours to achieve a constant test temperature before testing. Afterward, a sample was kept on three-point bending fixture for testing. The fixture was composed of two roller supports and the span length between the support was 120 mm and lubricating oil was applied on the supports before test to lessen the effect of friction during testing. Then a monotonic load was applied vertically on the top center of semi-circular sample at the rate of 0.5 mm/min and the load continue to increase with deformation and decline gradually with the initiation of crack. The load Vs displacement were recorded from start to the end of test. The test was stopped after the load reaches to 25-50% of peak load.

A widely used parameter for the interpretation of fracture resistance of asphalt mix is critical strain energy release rate which is also known as J-integration. Greater the value of J-integration for a given mix more will be its resistance to fracture. It can be obtained by using "(1)":

$$J\text{-integral} = -\frac{1}{b}\left(\frac{dU}{da}\right) \quad (1)$$

Where:

- J-integral = release rate of critical strain energy (kJ/m2)
- b = sample thickness (m)
- U = Strain energy to failure (KJ)
- a = depth of notch in (m)
- dU/da = variation of strain energy with the depth of notch (kJ/m).

5 Results and Discussion

While evaluating the resistance of asphalt mix to fracture comparison between control specimens and specimens modified with different percentages of RAP and Sasobit according to ASTM D 8044-16 were considered. Total of 48 samples were prepared at OBC. The samples were tested at 25^{o}C ((HT+LT)/2+4^{o}C) by adjusting the temperature of environmental.

The load (KN) and displacement (m) data after each test was plotted on a graph as shown in Figure 4. The information obtained from the graph are: (i) strain energy to failure (U) as per the provided (ii) peak Load and (iii) displacement at peak load. The strain energy to failure was calculated by finding the area under the curve up to peak load. The strain energy to failure was plotted against each notch depth and a best fit line joining these three points was drawn as shown in Figure 5. The slope of which is known as change of strain energy with notch depth $\left(\frac{dU}{da}\right)$. The change of strain energy with notch depth was divided by the average thickness of the specimen to determine critical strain energy release rate (J-integration) as explained in "(1)".

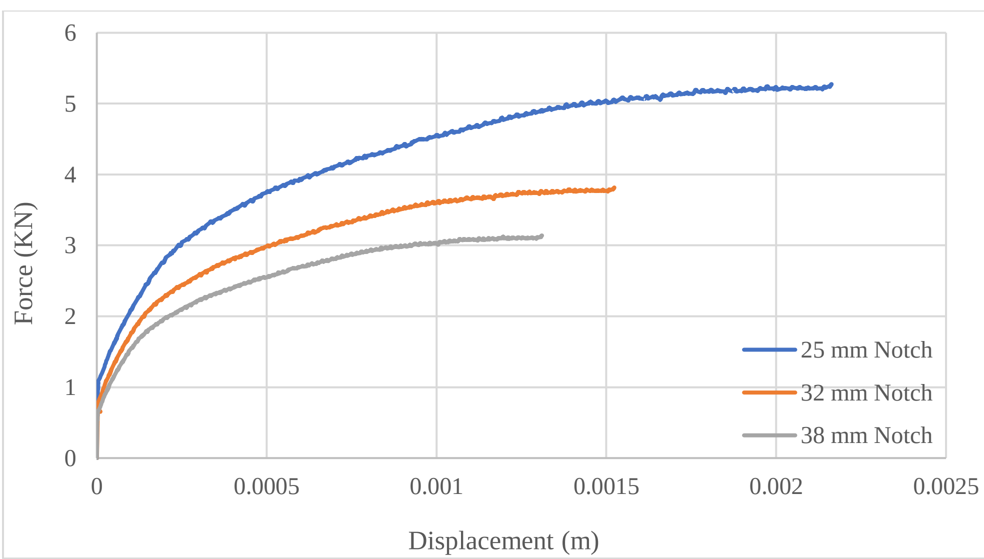

Figure 4: Force vs Displacement Curve

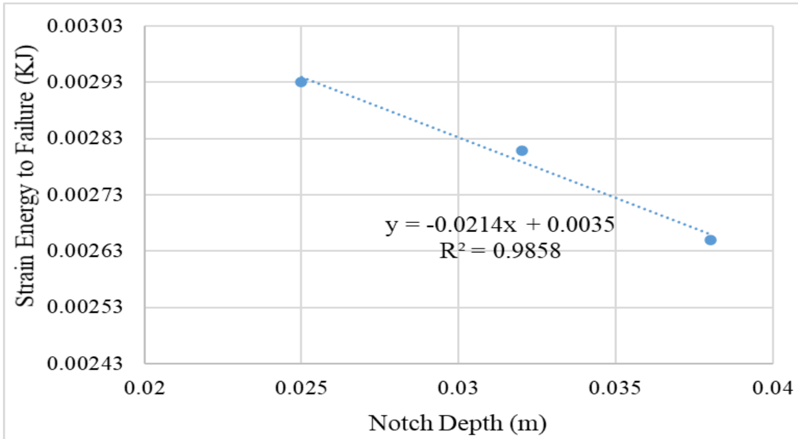

Figure 5: Strain Energy to Failure Vs Notch Depth

5.1 Effect of Mix Properties on Fracture Resistance

Fracture resistance of asphalt mix vary greatly by increasing or decreasing the percentages of RAP and Sasobit. J-integral vs each percentage change of RAP and Sasobit is presented in Figure 6.

It can be extracted from the results that fracture resistance of asphalt mix increases as the Sasobit percentage increases as it acts as asphalt flow improver and results in more flexible matrix. However, the resistance of WMA to fracture increases by adding RAP in the mix up to 20 percent but fracture resistance tends to decrease by increasing the percentage of RAP beyond 20 percent of the mix. However, fracture resistance decreases with the addition of RAP to HMA which is because of stiffness of aged binder in RAP.

Furthermore, fracture resistance of WMA is negatively affected as compared to control samples when the percentage of RAP increases beyond 40% because of higher percentage of aged binder coming from RAP. COV for each percentage of RAP, Sasobit and notch depth are presented in Figure 7. The COV value of every mix falls within the range of acceptable limit, which is 20%.

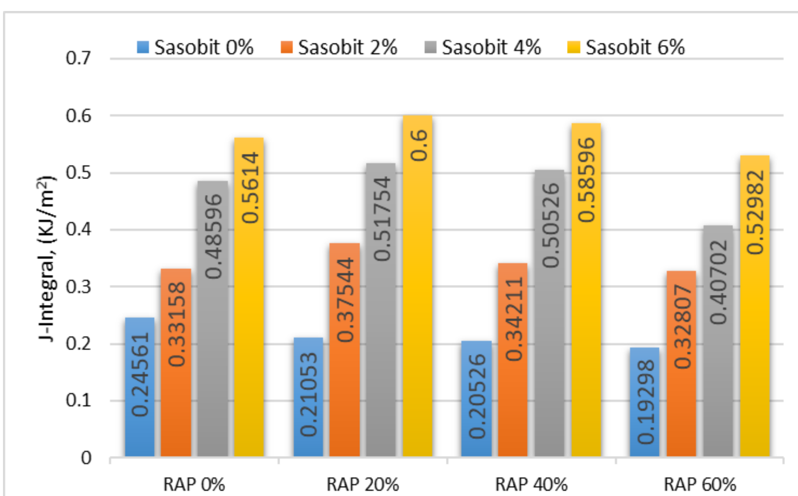

Figure 6: J-Integral for Each Mix

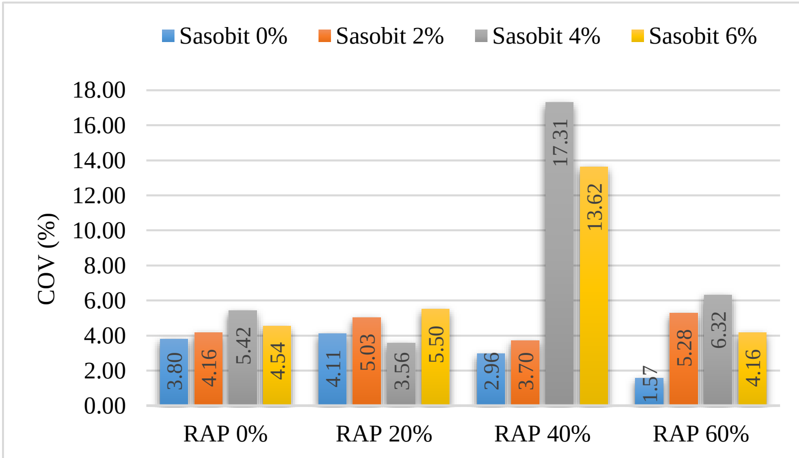

Figure 7: Coefficient of variance

Keeping in view the enhanced properties in term of fracture resistance of Sasobit addition and RAP to the HMA, it should be encouraged in field as the construction cost will reduced to higher extent by addition of recommended percentage of RAP equal 40%. Furthermore, it will provide additional benefits like longer haul distances because of reduced production temperatures and will be helpful in pavement construction in cold areas. It will also reduce the emission of greenhouse gases because of lower mixing temperature at asphalt plant.

6 Conclusion

Based on the Performance tests, the following conclusions can be summarized.:

- Addition of RAP alone to HMA results in decrease of fracture resistance due to the increase in stiffness characteristics with the RAP addition and then increases by the addition of Sasobit as WMA additive.
- The effect of RAP might be compromised in fracture resistance by introducing RAP more than 40%.

Based on the results, it is recommended with confidence that WMA containing RAP content can be designed to meets the required volumetric and desired criteria that can perform equal to or better than virgin HMA.

Acknowledgment

We owe enormous gratitude to Sasol chemicals, a division of Sasol South Africa (Pty) Ltd for providing Sasobit for our research work whenever requested.

References

[1] S. Caro, D. P. Beltrán, A. E. Alvarez, C. J. C. Estakhri, and B. Materials, "Analysis of moisture damage susceptibility of warm mix asphalt (WMA) mixtures based on Dynamic Mechanical Analyzer (DMA) testing and a fracture mechanics model," vol. 35, pp. 460-467, 2012.

[2] J. Zhu, K. Zhang, K. Liu, X. J. C. Shi, and B. Materials, "Performance of hot and warm mix asphalt mixtures enhanced by nano-sized graphene oxide," vol. 217, pp. 273-282, 2019.

[3] M. M. Taher, M. J. J. o. F. Aman, and A. Sciences, "Effects of advera® warm mix additive on the rheological properties of unaged and short term aged asphalt binders," vol. 9, no. 7S, pp. 650-666, 2017.

[4] K.-W. Damm, "Asphalt flow improvers-a new technology for reducing mixing temperature of asphalt concrete mixes with high resistance against permanent deformation," in *PERFORMANCE TESTING AND EVALUATION OF BITUMINOUS MATERIALS PTEBM'03. PROCEEDINGS OF THE 6TH INTERNATIONAL RILEM SYMPOSIUM HELD ZURICH, SWITZERLAND, 14-16 APRIL 2003*, 2003.

[5] A. Syroezhko, M. Baranov, S. Ivanov, N. J. C. Maidanova, and Chemistry, "Influence of natural additives and those synthesized by the Fischer-Tropsch method on the properties of petroleum bitumen and quality of floated asphalt," vol. 54, no. 1, pp. 26-31, 2011.

[6] D. Singh, P. K. Ashish, S. F. J. C. Chitragar, and B. Materials, "Laboratory performance of recycled asphalt mixes containing wax and chemical based warm mix additives using semi circular bending and tensile strength ratio tests," vol. 158, pp. 1003-1014, 2018.
[7] S. Zhao, B. Huang, X. Shu, M. J. C. Woods, and B. Materials, "Comparative evaluation of warm mix asphalt containing high percentages of reclaimed asphalt pavement," vol. 44, pp. 92-100, 2013.
[8] I. Maha, B. S. Subagio, F. Effendhi, and H. J. J. o. t. E. A. S. f. T. S. Rahman, "Performance of Warm Mix Asphalt Concrete Binder Course (AC-BC) With Reclaimed Asphalt Pavement," vol. 11, pp. 1745-1753, 2015.
[9] T. B. Moghaddam, H. J. C. Baaj, and B. Materials, "The use of rejuvenating agents in production of recycled hot mix asphalt: A systematic review," vol. 114, pp. 805-816, 2016.
[10] A. A. Tayebali, P. N. P. Khosla, H. Malladi, and A. Kusam, "Impact of WMA Technologies on the Use of RAP Mixtures in North Carolina," 2015.
[11] R. West, "Performance studies of asphalt pavements with greater than 25% RAP," in *RAP ETG meeting in December*, 2009, pp. 12-09.
[12] I. L. Al-Qadi, Q. Aurangzeb, S. H. Carpenter, W. J. Pine, and J. Trepanier, "Impact of high RAP contents on structural and performance properties of asphalt mixtures," 0197-9191, 2012.
[13] S. Pirmohammad, M. J. R. M. Khanpour, and P. Design, "Fracture strength of warm mix asphalt concretes modified with crumb rubber subjected to variable temperatures," vol. 21, no. sup1, pp. S57-S75, 2020.
[14] S.-J. Lee, J. Park, J.-P. Hong, and K. W. Kim, "Fracture Resistance of Warm-Mix Asphalt Concretes at Low Temperatures," 2013.
[15] K.-S. Yeon, S. Kim, H.-J. Lee, K. W. J. J. o. T. Kim, and Evaluation, "Low temperature tensile characteristics of warm-mix asphalt mixtures," vol. 42, no. 4, pp. 903-911, 2014.
[16] S. Pirmohammad and M. R. Ayatollahi, *Fracture Behavior of Asphalt Materials*. Springer Nature, 2020.
[17] M.-Y. Yoo, S.-H. Jeong, J.-Y. Park, N.-H. Kim, and K.-W. J. T. r. r. Kim, "Low-temperature fracture characteristics of selected warm-mix asphalt concretes," vol. 2208, no. 1, pp. 40-47, 2011.
[18] W. Mogawer, A. Austerman, L. Mohammad, M. E. J. R. M. Kutay, and P. Design, "Evaluation of high RAP-WMA asphalt rubber mixtures," vol. 14, no. sup2, pp. 129-147, 2013.
[19] M. Kim, L. N. Mohammad, and M. A. J. T. r. r. Elseifi, "Characterization of fracture properties of asphalt mixtures as measured by semicircular bend test and indirect tension test," vol. 2296, no. 1, pp. 115-124, 2012.

GEOTECHNICAL ENGINEERING

3rd Conference on Sustainability in Civil Engineering (CSCE'21)
Department of Civil Engineering
Capital University of Science and Technology, Islamabad Pakistan

ASSESSMENT OF GROUND TO AIR HEAT TRANSFER SYSTEM FOR LOCAL SOIL CONDITIONS

[a]Muhammad Tayyab Naqash, [b]Qazi Umar Farooq, [c]Ouahid Harireche*

Department of Civil Engineering, Islamic University of Madinah, Saudi Arabia,
[a] engr.tayyabnaqash@gmail.com; [b]qaziumar@gmail.com; [c] ouahidharireche@gmail.com
[*]Corresponding author: umar@iu.edu.sa; qaziumar@gmail.com;

Abstract- Northern Pakistan has an extremely cold climate that requires a heating system during the winter season. On the contrary, extreme heat with high humidity and electric power cutoff cause inhabitant discomfort in summer. In this paper, an assessment of shallow geothermal feasibility is proposed to provide heating during winter and cooling during summer. The capital is considered the study area; nevertheless, it can be extended to other regions of the country, such as Northern areas that are extremely cold during winter and southern areas that are very hot during the summer. Furthermore, for the location under consideration, it is found that the soil strata in different regions are not the same. Therefore, the current paper also focuses on assessing shallow geothermal energy for different soil types in the selected region. Isotherms and precipitation contours have been developed that are based on 36 years of data. Islamabad receives the highest precipitation throughout the year; therefore, wet, and dry soil conditions are considered. The numerical model is validated with the analytical expression with the soil of Madinah Saudi Arabia. The result showed that different soil conditions affect the ground temperature for the same region having a similar climatic condition.

Keywords- Geothermal, Renewable energy, Climatic condition, Ground temperature.

1. Introduction

Pakistan imports fossil fuel in the form of petroleum and hardly accomplishes the domestic energy demand. Geographically it lies between (24^0–37^0) North latitudes and (62^0–75^0) East longitudes and has a wide range of thermal variation from place to place. Mountains dominate the north areas with humid to arid climatic conditions; higher altitudes receive winter precipitation as snow. The middle Indus River basin is tropical and continental, whereas an arid climate characterizes the lower Indus River basin. Baluchistan is characterized by an arid climate that receives the lowest rainfall and is prone to desertification [1] [2]. It has been found that while the considerable potential for geothermal energy is available, no appreciable practical steps have been undertaken in this regard. Zaigham et al. [5] show that the hydro-geothermal option is one of the most viable renewable sources considering Pakistan's tectonic system. Soil temperature varies from month to month due to incident solar radiation, rainfall, seasonal cycle in overlying air temperature, local vegetation, soil type, and depth. Aftab et al. [3] studied the exploration prospects of geothermal energy in Pakistan. Kazmi and Sheikh [4] studied a Hybrid geothermal–PV–wind system for a village in Pakistan. They found that enough geothermal energy is available from hot springs to cater to the perennial base load requirement of the small community. Zeb et al. measured the thermal transport properties of porous igneous basalt rocks using the Transient Plane Source (TPS) technique under ambient air conditions saturant in pore spaces[5].

Luckily, Pakistan receives plenty of sunshine; therefore, shallow geothermal energy resources are available in all the regions from various depths and can be used for cooling & heating of buildings and supply of hot water during the winter season [6].

2. Selected region

This study investigates the effects of both dry and wet soil; therefore, the capital Islamabad has been considered as the study case. The city has variation in soil profiles and receives higher precipitation than other parts of the country. The climatic data used in the paper is based on 36 years mean values obtained from RET screen [7]. The earth temperature for different years is considered, and the cosine function is used to derive the amplitude for the Islamabad climate (See **Figure 1**). Whilst **Figure 2** shows the isotherms of earth temperature for the whole Pakistan.

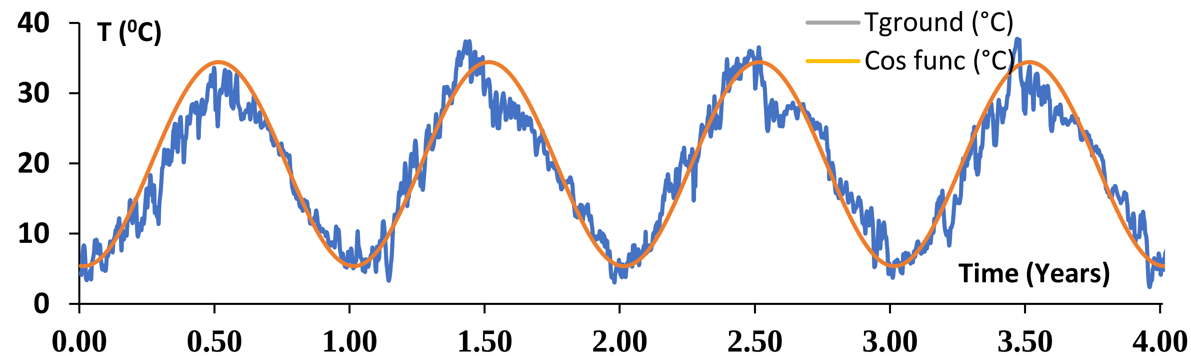

Figure 1: Earth temperature for Islamabad city based on RET screen database [7]

The station used for the climatic data is located at Latitude equal 33.7^0 N and Longitude 73.1^0 E. The 36 years Air temperature - average (°C) is 20.6, Air temperature - minimum (°C) is -0.06, Air temperature - maximum (°C) is 42.6, Earth temperature (°C) is 19.9 (°C) with Amplitude 14.6 and Phase shift 0.1.

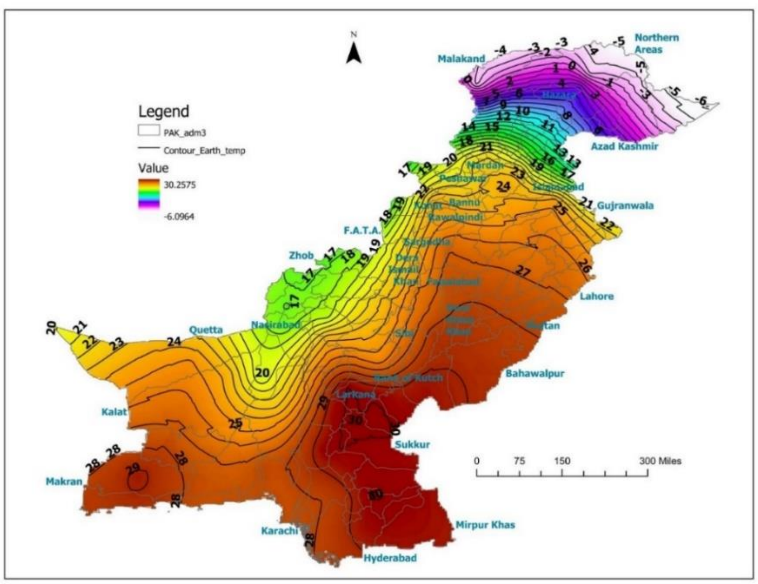

Figure 2: Mean annual Isotherms of Earth temperature based on 36 years of data.

Six cases of different soil characteristics have been considered in this study; the details of the study cases are shown in Table 1.

Table 1: Considered soil types.

Type of soil	Cases	Description of soil
	Case 1	Soft cohesive soil
Type 1-Fine (CL/ML)	Case 2	Stiff Cohesive soil
	Case 3	Hard Cohesive Soil
	Case 4	loose sandy soil
Type-2 Granular (SP/SW)	Case 5	Medium sandy soil
	Case 6	Dense Sandy Soil

In this study, the top soft/loose superficial soil has been ignored. Soil profiles consistent with the workable depth of 3m - 15m have been adopted [8]. The most intercepted soil types of the region and their respective thermal and geotechnical properties are considered. The thermal conductivity values are calculated as per [9]. They are based on respective soil types and degree of saturation. In contrast, the volumetric heat capacity has been selected based on [10] [11].

3. Soil Temperature and Numerical simulations

The heat balance scenario on the ground surface due to fluxes (conductive, convective, and thermal radiation) is shown in **Figure 3**. It is beneficial to estimate the maximum soil temperature at a certain lying depth. The air temperature is assumed to fluctuate sinusoidally throughout the year. The soil damped the temperature depending on its thermal diffusivity.

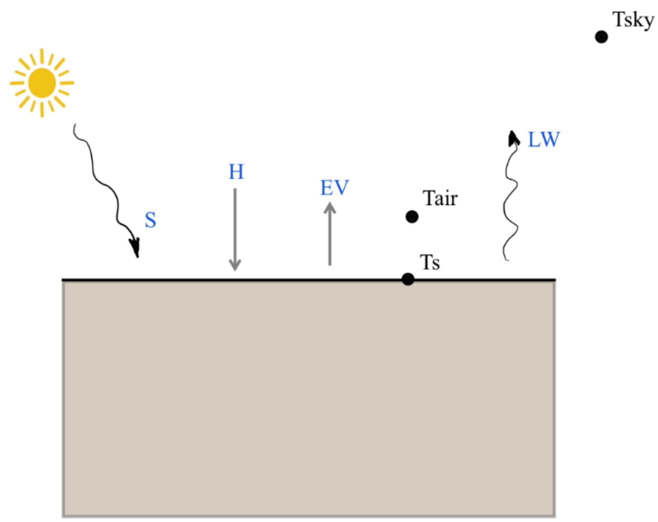

Figure 3: Heat fluxes on the ground surface

The cosine function given by Eq. (1) is used to model fluctuations in temperature data throughout the year.

$$T_s(t) = T_{sm} - A_s cos(\omega t - \phi_s) \quad \textbf{(1)}$$

The soil temperature is the ambient soil temperature at a particular depth. It is based on a mathematical model describing the soil's standard temperature curve shown by Eq (2) [12]. Analytically, ground temperature varies with location and time and is based on the assumption that the ground's surface temperature varies periodically. The soil is a homogeneous heat-conducting semi-infinite medium with constant thermal diffusivity. The average ground temperature "T" is a function of depth z and time t and has the analytical expression given by Eq (2) [12].

$$T(z,t) = T_{sm} - A_s exp\left(-\frac{z}{L}\right) cos\left(\omega t - \phi_s - \frac{z}{L}\right) \quad \textbf{(2)}$$

COMSOL Multiphysics numerical code [13] has been implemented to model the soil profile that was initially validated using climatic data of Islamabad and soil conditions for Madinah Saudi Arabia. The details of soil and climatic and conditions for Al-Madinah area can be found at [14]. The required parameters for Madinah climate that has been used in the model validation were: T_{sm} = 29.6 ^oC, L = 2.8345 m, α = 8.12 x 10^{-7} m^2/s, A_s = 11.16 ^{0}C, ϕ_s = 0.39. The validation is based on the values obtained from COMSOL for the 4^{th} year due to transient. The numerical model is validated using the analytical Eq (2).

4. Results and discussions

Depend on the groundwater measurement point's location, considerable differences can be seen in the temperatures at increasing depth. A deeper ground loop installation usually decreases the annual operating cost to run the heat pumps. During a GHP system's service life, these accumulated savings may compensate for the higher initial cost of burying the ground loop at a higher depth. To determine the optimal depth, it is essential to investigate the seasonal change in soil temperature with depth using the soil's thermal properties. The variations of temperature throughout the 4^{th} year at 2 m, 4 m, 6 m, and 8 m depths have been shown (See **Figure 4**) for 6 considered cases. These depths show the fluctuation of the temperature during the year. From there, it can be observed that the temperature of the ground becomes constant at about 8 m depth. Furthermore, it can be seen that installing the geothermal system at a depth of 2 m onward is feasible as the temperature difference is reasonable for heating and cooling systems.

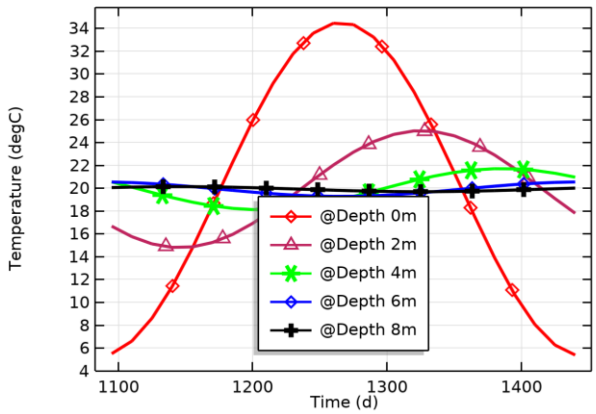

a) Case 1 Soft cohesive Soil

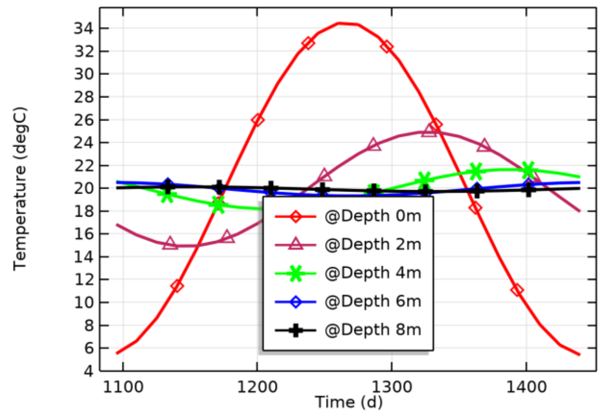

b) Case 2 Stiff Cohesive soil

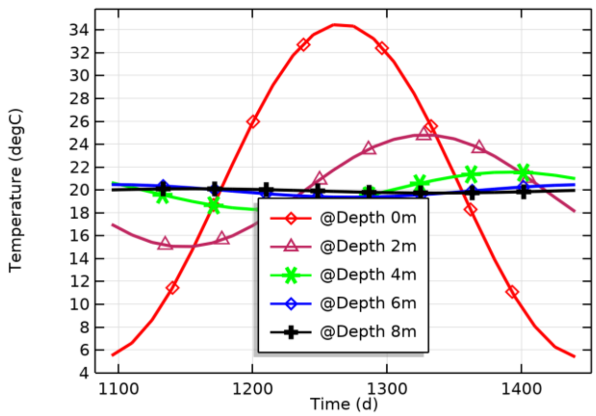

c) Case 3 Hard Cohesive Soil

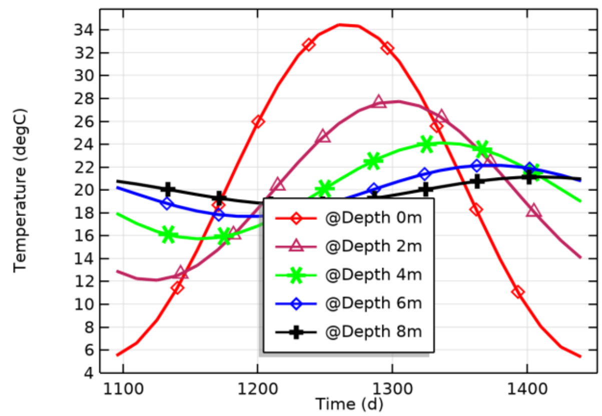

d) Case 4 loose sandy soil

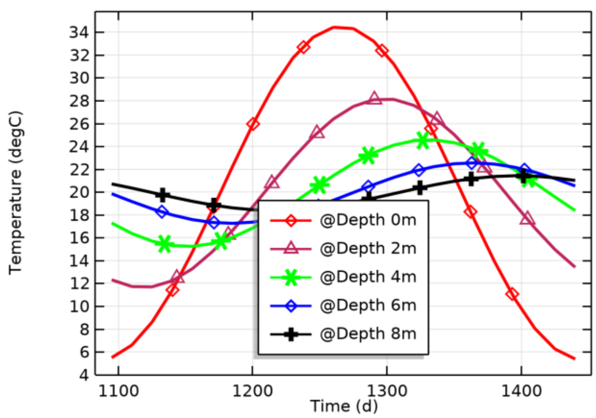

e) Case 5 Medium sandy soil

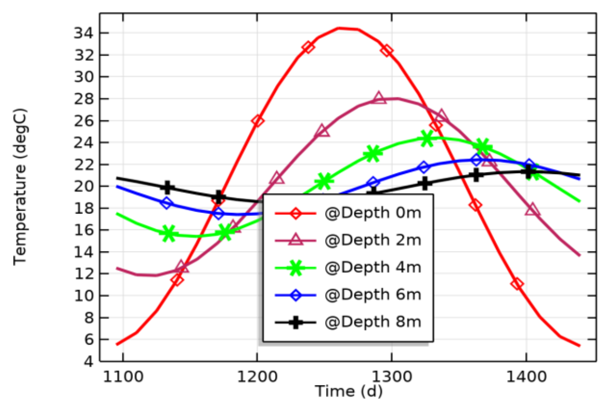

f) Case 6 Dense Sandy Soil

Figure 4: Daily temperature variations against Different Depth for Cohesive soils (a-c) and Granular Soils (d-f).

The variation of temperature and depth has been shown in **Figure 5** for the studied fine and granular soil cases.

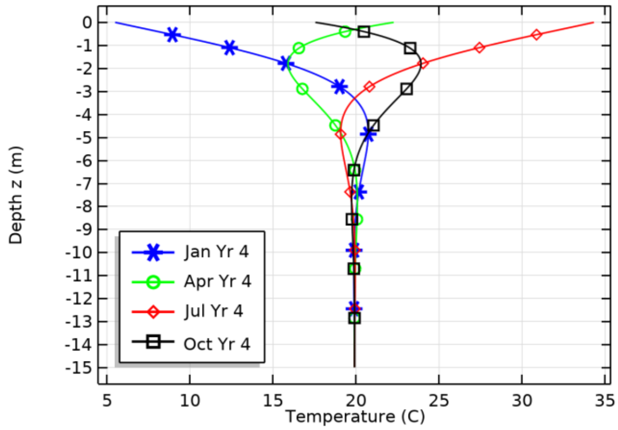

a) Case 1 Soft cohesive Soil

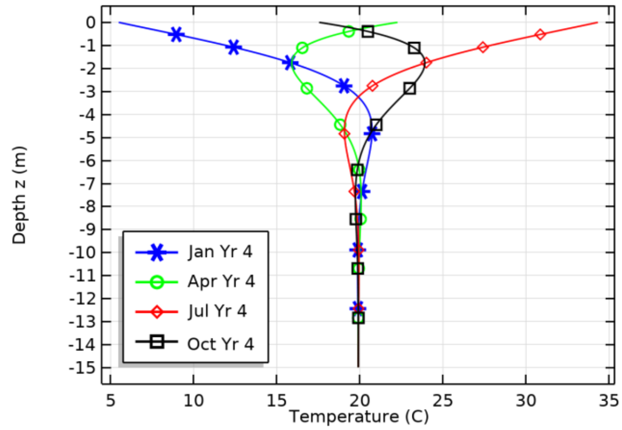

b) Case 2 Stiff Cohesive soil

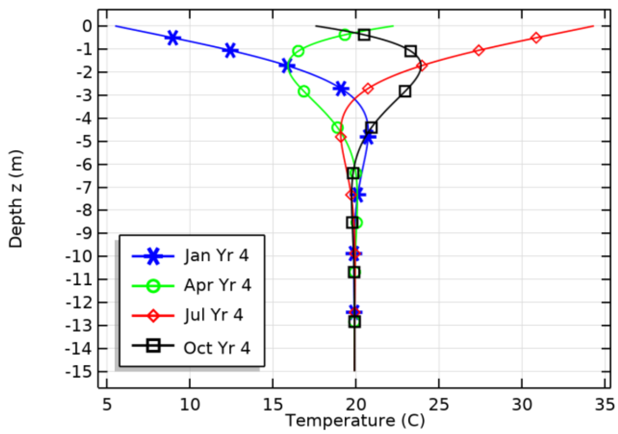

c) Case 3 Hard Cohesive Soil

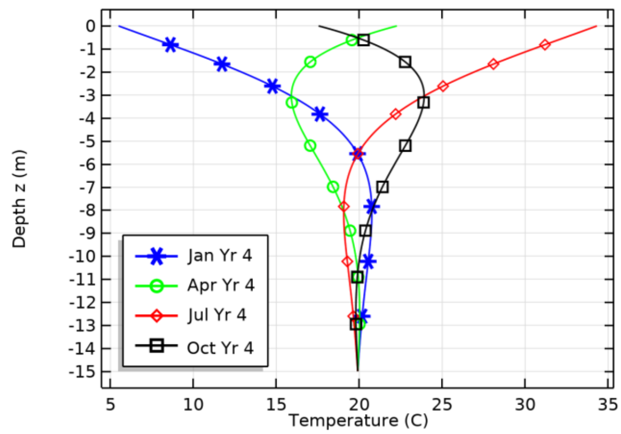

d) Case 4 loose Sandy Soil

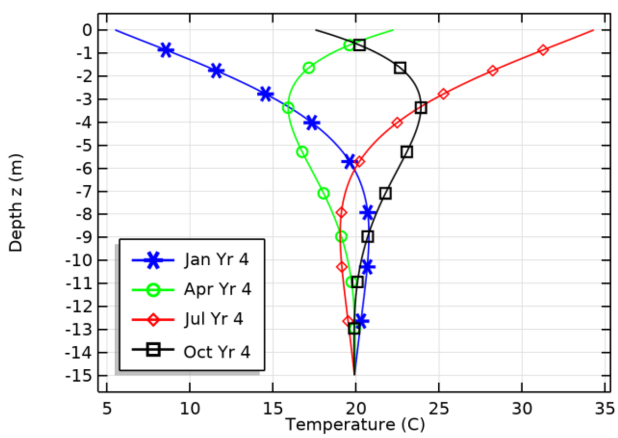

e) Case 5 Medium Sandy Soil

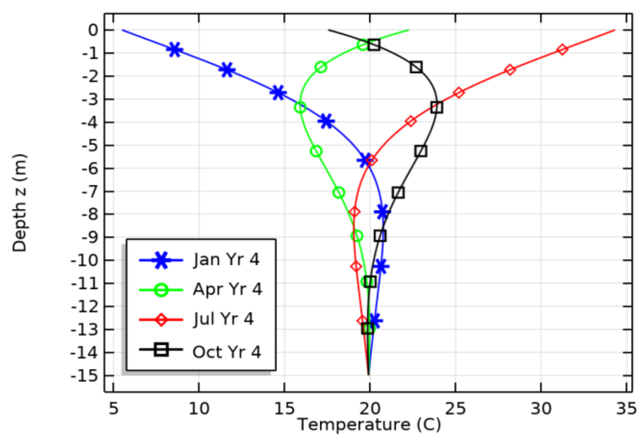

f) Case 6 Dense Sandy Soil

Figure 5: Subsurface Seasonal Temperature gradient for Islamabad region Cohesive soils (a-c) and Granular Soils (d-f)

The above results reflect more heat-trapping and low conductivity of cohesive soils as compared to the sandy soils. The primary reason for such difference is the smaller grain and respective pore size. The air, a natural insulator present in the pores, is extensively distributed along the smallest thread like clay particles and a heat transfer barrier. In coarse grain soil, the granular particles have larger interparticle voids and larger grain to grain contact, which permits conduction. The mineralogical comparison of both soil types can be helpful for further elaborating heat transfer in regional soils.

5. Conclusions

The paper has dealt initially with the climatic data and subsurface thermal conditions. Different local soils of Islamabad are assessed for the potential usage of shallow geothermal applications. Some interesting conclusions can be drawn. It has been observed that the cohesive soils of the studied region are less conductive and have low thermal disparity concerning the seasonal variations. At the same time, sandy soils are easily affected by climatic conditions. In cohesive soils, the stable subsurface temperature gradient is intercepted at a depth of 7 m.

Nevertheless, in granular soils, effects of seasonal and climatic variations reached up to 15 m depth. The Installation of geothermal HVAC systems can be more efficient and cost-effective in clayey and fine soils than the granular soils. The comprehensive experimental and field investigations of heat transfer mechanism in local soils under various geotechnical conditions such as soil type, porosity, density, and mineral composition are potential future research topics. These can be used in the feasibility design of geothermal systems.

6. Appendix

$T(z,t)$	=	Temperature	[K]
T_{sm}	=	Annual average temperature at the ground surface	°C
A_s	=	Maximum annual temperature variation from average	°C
a	=	Thermal diffusivity of soil	m^2/sec
ω	=	Angular frequency of temperature fluctuations	1/day
α	=	Thermal diffusivity	[m^2/s]
K	=	Thermal conductivity	[W/(m.K)]
ϕ_s	=	Phase angle	[rad]
S	=	Solar radiation	
H	=	Convective heat flux	
Ev	=	Evaporative heat flux	
GHP	=	Geothermal Heat Pump	
GSHP	=	Ground Source Heat Pump	
ρ	=	Density	g/cm^3
k	=	Thermal Conductivity	(W m^{-1} K^{-1})
Cv	=	Heat Capacity	MJ/m^3

References

[1] R. Anjum, X. He, J. I. Tanoli, and S. T. Raza, "Contemporary temperature fluctuation in urban areas of pakistan," *Atmosphere*, 2017, doi: 10.3390/atmos8010012.

[2] K. Muzaffar Khan, T. Sultan, Q. Umar Farooq, K. Khan, and F. Ali, "Development of superpave performance grading map for Pakistan," *Life Science Journal*, 2013.

[3] S. M. Aftab, M. A. Farooqui, and T. Maqsood, "EXPLORATION PROSPECTS OF GEOTHERMAL ENERGY IN PAKISTAN," 2019, doi: 10.1130/abs/2019am-338378.

[4] S. W. S. Kazmi and M. I. Sheikh, "Hybrid geothermal–PV–wind system for a village in Pakistan," *SN Applied Sciences*, 2019, doi: 10.1007/s42452-019-0643-9.

[5] A. Zeb, M. Abid, M. A. Zeb, M. O. Qureshi, U. Younas, and I. Batool, "Measurement and prediction of thermal conductivity of volcanic basalt rocks from Warsak area," *Advances in Materials Science and Engineering*, 2020, doi: 10.1155/2020/4756806.

[6] I. A. Gondal, S. A. Masood, and M. Amjad, "Review of geothermal energy development efforts in Pakistan and way forward," *Renewable and Sustainable Energy Reviews*. 2017, doi: 10.1016/j.rser.2016.12.097.

[7] Natural Resources Canada, "RETScreen ® International," *RETScreen Clean Energy Project Analysis Software*, 2013.

[8] I. M. Sheikh, M. K. Pasha, V. S. Williams, S. Q. Raza, and K. S. A. Khan, "Environmental Geology of the Islamabad-Rawalpindi Area, Northern Pakistan Regional Studies of the Potwar Plateau Area, Northern Pakistan," in *Regional Studies of the Potwar Plateau Area, Northern Pakistan*, 2007.

[9] Y. Dong, J. S. McCartney, and N. Lu, "Critical Review of Thermal Conductivity Models for Unsaturated Soils," *Geotechnical and Geological Engineering*, 2015, doi: 10.1007/s10706-015-9843-2.

[10] N. H. Abu-Hamdeh, "Thermal properties of soils as affected by density and water content," *Biosystems Engineering*, 2003, doi: 10.1016/S1537-5110(03)00112-0.

[11] O. T. Farouki, "THERMAL PROPERTIES OF SOILS.," *CRREL Monograph (US Army Cold Regions Research and*

Engineering Laboratory), 1981, doi: 10.1119/1.1424590.
[12] H. S. Carslow, J. C. Jaeger, and J. E. Morral, "Conduction of Heat in Solids, Second Edition," *Journal of Engineering Materials and Technology*, 1986, doi: 10.1115/1.3225900.
[13] COMSOL, "COMSOL Multiphysics® Modeling Software," *Comsol*, 2016. .
[14] Q. U. Farooq and M. T. Naqash, "Performance of Shallow Building Foundations under Infrequent Rainfall Patterns at Al-Madinah, Saudi Arabia," *The Open Civil Engineering Journal*, vol. 15, no. 1, pp. 91–103, Apr. 2021, doi: 10.2174/1874149502115010091.

3rd Conference on Sustainability in Civil Engineering (CSCE'21)
Department of Civil Engineering
Capital University of Science and Technology, Islamabad Pakistan

APPRAISAL OF AN ENVIRONMENT-FRIENDLY GEOPOLYMER FOR CIVIL ENGINEERING APPLICATIONS

[a]Tahah Ali Taga[*],[b]Muhammad Usman Arshid

[a,b] Department of Civil Engineering, University of Engineering and Technology Taxila
*Corresponding author: Email ID: tahataga@gmail.com

Abstract- The phenomenon of growing urbanization compels planners to think about those regions where soils are problematic. The deficient engineering properties imply the use of conventional stabilizers such as Portland cement (PC) and lime but these cause huge CO2 emissions which impart detrimental effects on the environment. Further, the recycling of waste to produce value-added products is the need of time. Ground granulated blast furnace slag (GGBS) is generated during iron manufacturing as an industrial waste byproduct. The eggshell is food waste. Geopolymer formation utilizing these base precursors in the presence of alkaline activators comprising sodium hydroxide (NaOH) and water glass (Na2SiO3) can prove alternate construction material. Four precursor composites (ESP: GGBS) – 70:30, 50:50, 30:70, and 0:100 were selected to evaluate the influence of growing slag content on the mechanical strengths of composites. Optimum activator content (OAC) and Maximum dry density (MDD) were determined by modified proctor test whereas mechanical properties were examined via unconfined compressive and split tensile strength test. The primary aim of this study is to examine the mechanical strengths of GGBS and eggshell-powder-based geopolymers. All composites have shown significantly greater strength values than achieved via cement stabilized soils required for subgrade and subbase construction. This new geopolymer product offered a cost-effective and eco-friendly solution to the issue of waste disposal and vulnerable soil improvement at the same time.

Keywords: Eggshell powder, GGBS, Geopolymer, Alkali Activation, Cheap geopolymer

1. Introduction

The concept of recycling waste for sustainable development has gained much attention in recent times. The issues related to waste disposal and scarcity of available land for this purpose have motivated experts to think of unconventional yet useable techniques. In countries like Pakistan, municipal waste and industrial waste disposal is a major concern. Poultry waste lies in the category of municipal waste. It may be produced from restaurants, bakeries, fast food centers, hatcheries, and poultry farms [1]. Environmental problems are produced when these wastes are deposited into the landfill. To address this issue, the application of such wastes in the construction industry should be encouraged.

Ground granulated blast furnace slag (GGBS) and eggshells are produced in abundance annually. Their mineralogical composition renders them suitable to utilize as a construction material. Grinding of eggshell waste into suitable particle size eggshell powder (ESP) is not much labor and energy intensive. Since the chemical composition of ESP is quite like cement which makes it apposite to use in construction materials for partial replacement [2] [3].

Ground granulated blast furnace slag (GGBS) is a glazed, granular material that consists of SiO_2, CaO, $Al_2O_3$and MgO. In iron making, the molten blast furnace slag is generated as a byproduct. It is then rapidly cooled by immersing it in water, and then crushed into a fine powder to improve its reactivity. It is often used in concrete for binding purposes due to the high mass percentage of SiO_2, Al_2O_3, and CaO [4].

1.1. Background

Joseph Davidovits introduced the geopolymer technology about 30 years ago [5]. Subsequently, a lot of work has been done in this area. The utilization of geopolymer in mortar and concrete has emerged in the recent past, and currently, considerable work has been carried out on geopolymer concrete and mortar [6] [7]. The concept of geopolymer– soil is relatively novel and still limited work has been done on it [8] [9].

A review study was conducted to appraise the strength enhancement of soft soil by the introduction of industrial by-product-based geopolymers [10] . Different combinations of fly ash (FA) and slag (S) were added to the soil to check the influence on its chemical and engineering properties. UCS of slag-based geopolymer soil was much higher than the fly ash-based geopolymer stabilized soil [11]. Another work was done to check the varying properties of FA-GGBS geopolymer under different combinations of sodium hydroxide (NH) and sodium silicate (NS) solutions [12] . It was detected that NH or NS solution alone resulted in low strength development when used with FA and FA+ GGBS pastes. Better strength was achieved with the NHNS solution. Kumar et al. explored the impact of GGBS on the microstructure, reaction, and mechanical properties of fly ash-based geopolymer. The highest compressive strength was achieved at 80% replacement of slag [13].

Significant literature is available where GGBS is added in other industrial waste materials' geopolymers to enhance mechanical strengths and reduce the curing age. However, no work has been reported in which combination of ESP and GGBS has been utilized for geopolymer synthesis. Hence, the concept of inserting slag in ESP is innovative.

1.2. Purpose of the study

The current research aimed to evaluate the mechanical strengths of eggshell powder-and GGBS based geopolymers. The effect of curing time and precursor ratio on strength development was also examined. A strength comparison was done between this geopolymer product and conventional cement stabilized soil.

2. Materials and Experimental Methodology

2.1. Materials

Ground granulated blast furnace slag (GGBS) of grade 80 standard ASTM C989 was locally sourced from Dewan cement limited Karachi. Eggshells were collected from a hatchery. The inner organic layer of eggshells was removed by washing and cleaning properly and air-dried for 24 hours. The eggshells after air drying were crushed, and a fine powder of the required particle size was achieved via grinding. Sodium silicate (Na_2SiO_3) and sodium hydroxide (NaOH) were procured from the local market. NaOH with 99% purity in flakes form was selected. The activator ratio of (Na_2SiO_3/NaOH) 2 was adopted as the optimum ratio from the previous literature [14]. NaOH flakes were dissolved in water to form a solution and stirred for at least 10 min to ensure complete dissolution of flakes. The solution is then mixed with Na_2SiO_3 in prescribed proportions after cooling to prepare alkaline activators.

The base precursors GGBS and ESP have a specific gravity of 2.81 and 2.14, respectively. The chemical composition of ESP is quite similar to grade 43 OPC which consists of 61% CaO, 20% SiO_2,6%Al_2O_3,4%Fe_2O_3, and 2% MgO. Four precursors' ratios were adopted as- 70ESP:30GGBS, 50ESP:50GGBS, 30ESP:70GGBS and 0ESP:100GGBS to investigate their impact in geopolymerization.

2.2 Experimental Procedure

Eggshell powder and GGBS were mixed in a dry state to form a homogenous mixture. Liquid alkaline activator solution was inserted in this mixture and mixed thoroughly for 3-5 minutes. Modified proctor test was performed on all composite following ASTM D1557 [15]. For all precursor combinations, the activator content was added between 12-40% to identify the optimum activator content (OAC) and maximum dry density (MDD). Samples of diameter 38mm and 76.2mm height were formed via cylindrical split mold for unconfined compressive strengths and split tensile strengths test. Three samples for each curing age were prepared and tested to minimize the margin of error. The samples were kept at room temperature and tested per ASTM D2166 [16]for unconfined compressive strengths. The samples were positioned laterally in the same apparatus to measure split tensile strengths under ASTM C 496 [17].

Table 1: Experimental setup of ESP: GGBS geopolymer

Methodology	Standard followed	ESP: GGBS	Activator percentage (%)	Curing period (Days)
Modified Proctor test	ASTM D1557	(70:30), (50:50), (30:70), (0:100)	12-40	-
Unconfined compressive strength	ASTM D2166	(70:30), (50:50), (30:70), (0:100)	OAC	1,3,7,28
Split tensile strength	ASTM C 496-96	(70:30), (50:50), (30:70), (0:100)	OAC	1,3,7,28

3. Results and discussion

3.1 Modified proctor test (MPT) results of geopolymer mixes

The effect of activator content and precursor ratio on compaction of geopolymer mix was examined. The activator content varied between 12%-40% with an increment of 4% to identify the optimum activator content (OAC) where the maximum dry density (MDD) is attained.

For different combinations of precursors, the compaction curves are plotted in figure 1. The curves revealed that as the MDD of a precursor combination is increased, its OAC is decreased. This behavior is in line with some previous studies [18] [8]. The minimum MDD of 1.684 g/cm3 was achieved for GGBS: ESP=100:0 combination with maximum optimum activator content of 28.6%. It is observed that a decrease in ESP content decreases MDD while increases the OAC. For example, the MDD for 70ESP:30GGBS is 1.867 g/cm3 which decreased to 1.825 g/cm3 for ratio 30ESP:70GGBS. The optimum activator content enhances slightly from 19.2% to 21% for decrement of ESP 70% to 30% but it jumps abruptly for 0ESP.

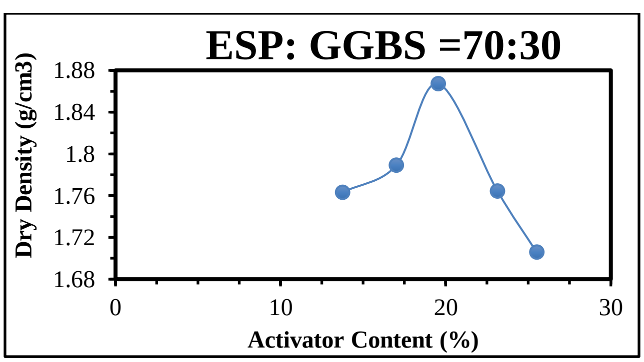

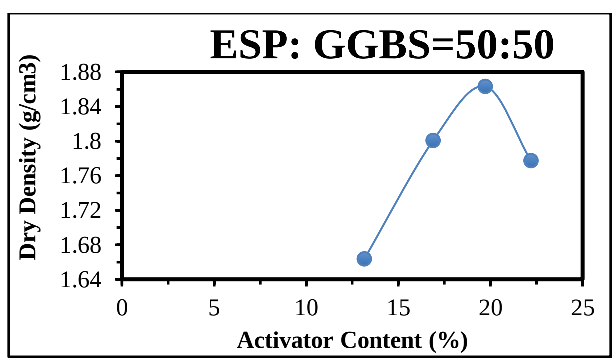

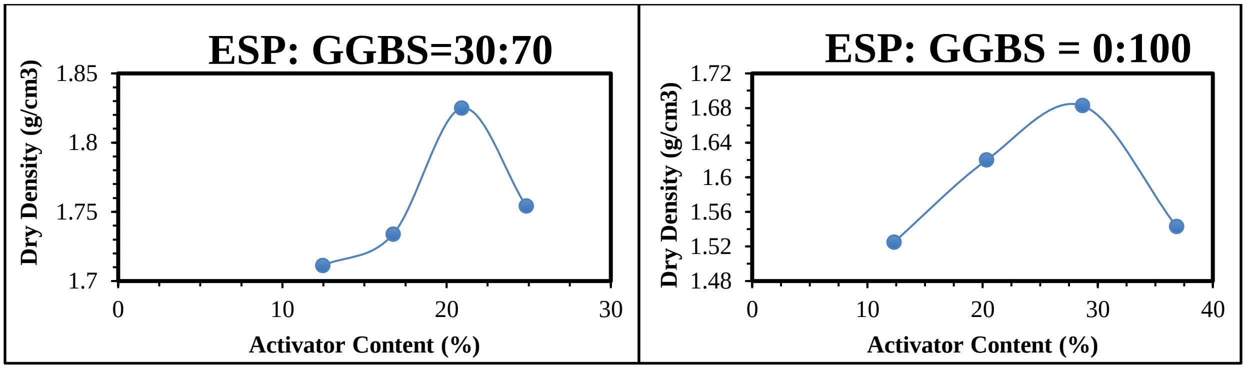

Figure 1. Compaction Curves for different geopolymer composites

3.2 Unconfined Compressive Strength of geopolymer mixes

The influence of the precursor ratio on the unconfined compressive strength of geopolymer mixes has been evaluated. Figure 2 displays the axial stress-strain behavior of GGBS, and ESP-based geopolymer samples after 1 day,3 days,7 days, and 28 days of air curing. The graphs represented a general trend that the increment of GGBS content enhances the compressive strength linearly. One of the reasons behind this phenomenon is the presence of additional silica in the solution which helps in formulating the C-S-H geopolymer gel. The fineness of GGBS over ESP may be the other controlling factor. The finer particles of GGBS possess a larger surface area than ESP particles resulting in their higher reactivity [14]. Lowering of ESP from 70% to 0% improved the compressive strength. It is also observed that the highest peaks are attained at 28 days curing period.

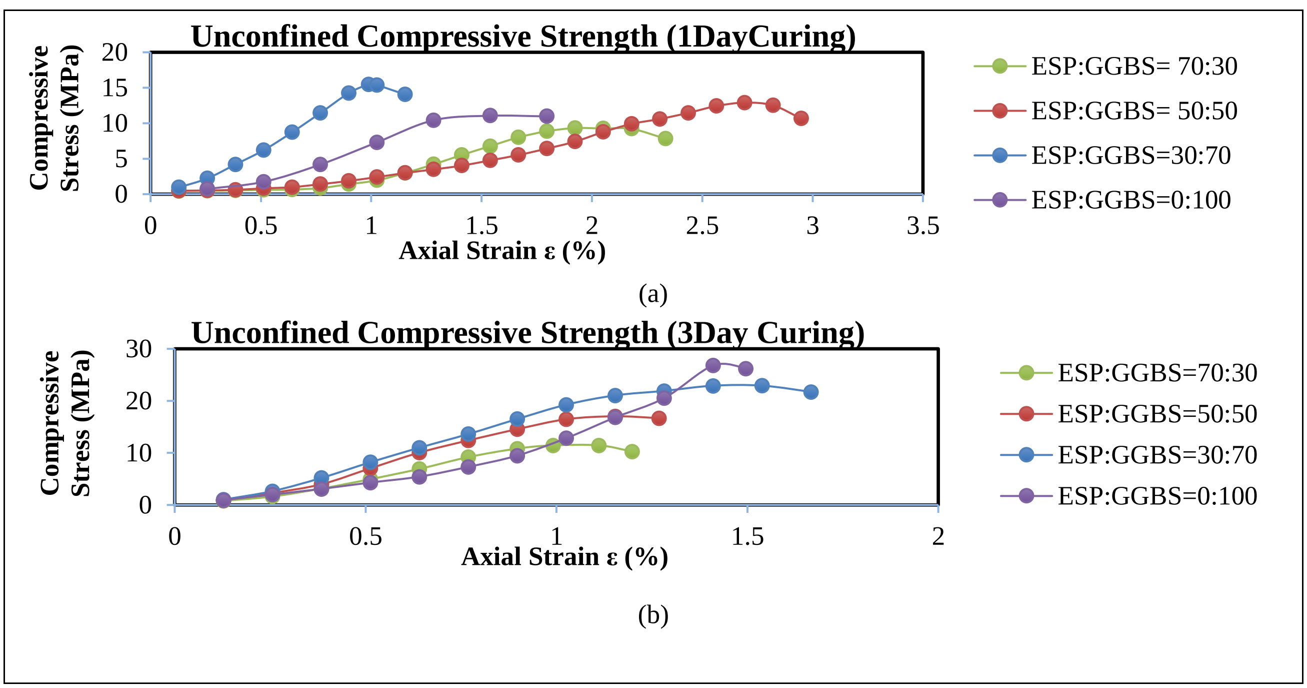

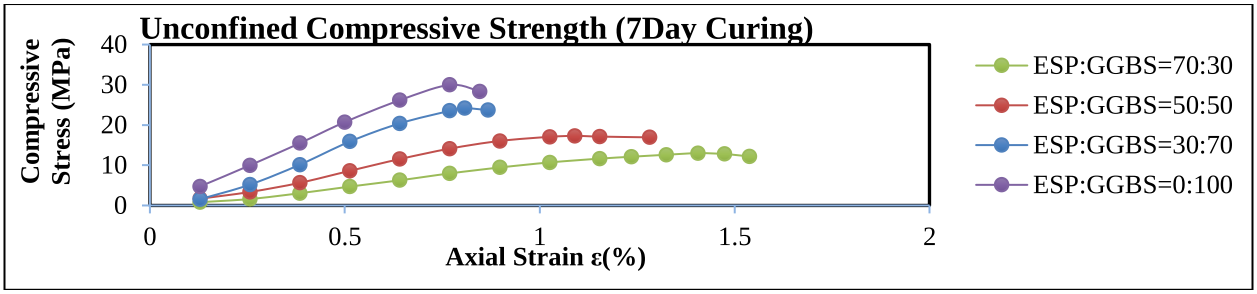

(c)

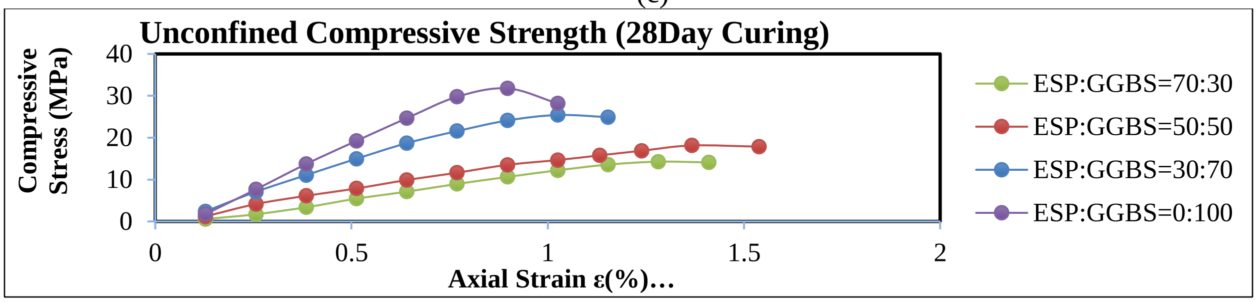

(d)

Figure 2: Axial Stress-Strain behaviour of four precursor combinations at various curing ages (a) 1-day Curing (b) 3 days curing (c) 7 days curing (d) 28 days curing.

Figure.3 compares the unconfined compressive strengths of ESP: GGBS geopolymer. The strength development of geopolymer mix with curing duration is quite similar to Portland cement. For instance, the compressive strength for 30ESP:70GGBS was 15.45MPa at 1-day curing which increased to 25.42MPa after 28 days. It is also deduced from the chart that all composites indicate early strength development. For example, the strength improvement for the 50ESP:50 GGBS composite from 1day to 3 days was 32.04% which diminishes to 4.9% from 7days to 28 days. Due to the high dissolution potential of GGBS and available Ca for geopolymerization, this quick strength gain is more evident [10] [11].

Figure 4 describes the comparison of unconfined compressive strength with the standard given in "General Specifications" of the national highway authority published by the ministry of communications (1998) [19]. According to these specifications, for subgrade construction, the minimum compressive strength at seven days should be 2.94 MPa for cement stabilized soils. Whereas for sub-base the minimum threshold value of laboratory compressive strength is 4.9 MPa. All precursor combinations satisfy this minimum criterion marginally.

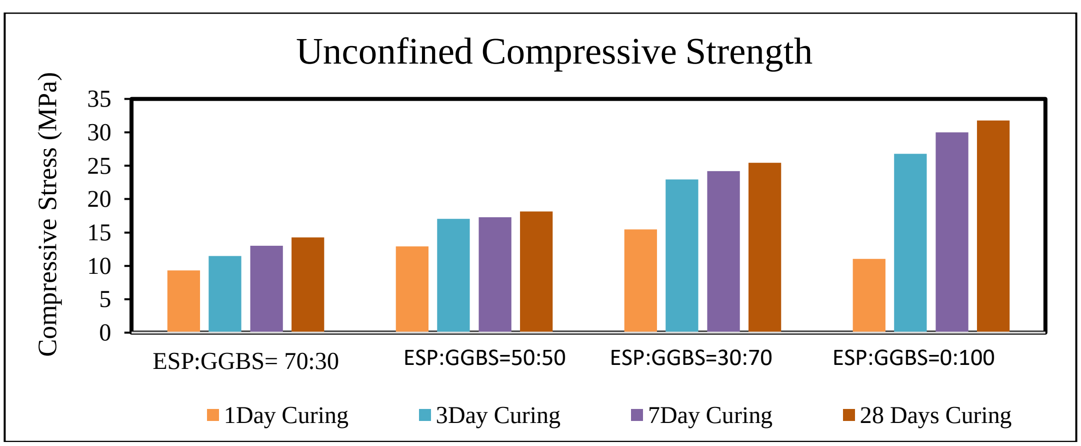

Figure 3: The strength development pattern of different precursor composite at varying curing periods

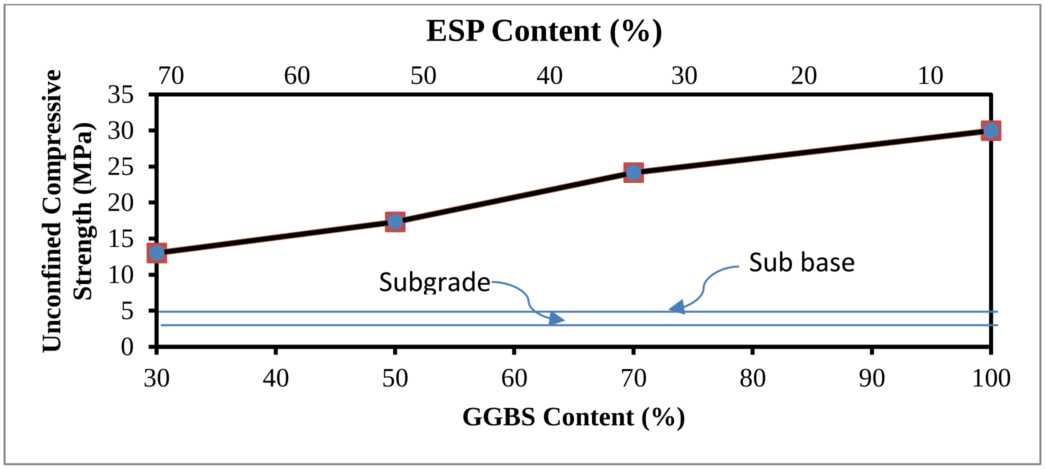

Figure 4: Comparison of UCS values with cement stabilized subgrade and subbase courses

3.3 Split Tensile Strength (STS) of geopolymer mixes

Figure 5 represents the split tensile strengths of four precursor ratios at 1,3,7 and 28 days of air curing at ambient temperature. Generally, higher ESP content lowers the STS whereas higher GGBS content improves the tensile strength. For precursor combination 70ESP:30GGBS, STS values are 1026.37 KPa, 1070 KPa, 1158.33 KPa while for geopolymer mix 30ESP:70GGBS, STS achieved as 1235.97KPa, 1277.36 KPa and1509.55 KPa for 3,7 and 28 days of curing, respectively. This increasing fashion of tensile strengths with growing slag percentage is due to the same reason as discussed previously in compressive strengths results. Significant SiO2 available in slag augments the reaction kinetics. The development of tension cracks at higher strains not only split the samples into two halves but also indicate their brittle nature as can be observed by a sudden loss of tensile strength after peak attained (Figure 6).

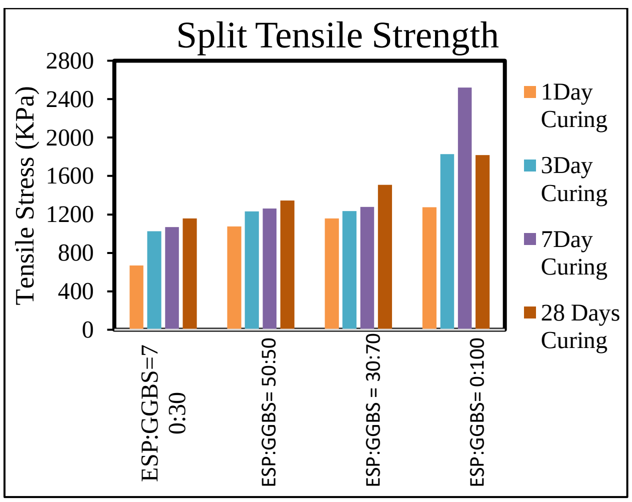

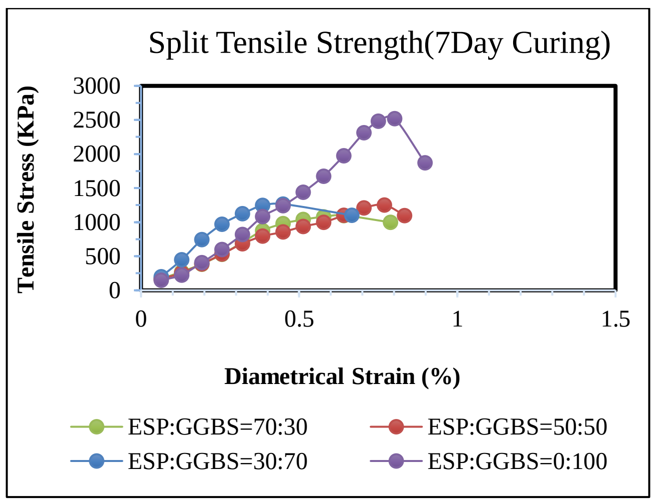

Figure 5: Effect of curing duration on Split tensile strengths (STS) *Figure 6: Tensile stress vs diametrical strain (%) behaviour*

The pavement construction through problematic regions where weak soils are encountered and need to be stabilized for subgrade and subbase formation, the geopolymer formed can be a suitable alternative to place as subbase and subgrade layers. The strength requirements are fulfilled as established in the previous section. The optimum combination of geopolymer proves to be a cost-effective alternative to the soil stabilized with any conventional stabilizer.

4. Conclusion

The current study is an assessment to examine the suitability of the new geopolymer mix in engineering applications. The mechanical strength of GGBS and ESP-based geopolymer was appraised to check the appropriateness of geopolymer composites to replace the usage of traditional stabilizers for problematic soils. Following are the principal conclusions of this work:

- The findings of this study reveal that the geopolymer mixture formed by reusing waste shown reasonably good strength as compared to the soils improved via conventional stabilizers.
- Increasing slag content in the combination increases the overall composite strength.
- It is deduced from the results that all precursor combinations fulfill the minimum criterion threshold for subbase and subgrade compressive strengths. However, the 50ESP: 50GGBS composite can be identified as optimum because the eggshell powder is much cheaper than GGBS.
- This geopolymer product suggested an eco-friendly way out of the problem of discarding these wastes and divert their utility in construction.

References

[1] P. Pliya and D. Cree, "Limestone derived eggshell powder as a replacement in Portland cement mortar," Construction and Building Materials, no. 95, pp. 1-9, 2015.

[2] W. G. A. J. M. L. S. Kamaruddin, "Chemical and fresh state properties of foamed concrete incorporating palm oil fuel ash and eggshell ash as cement replacement," Int. J. Eng. Technol, pp. 350-354, 2018.

[3] A. A. G. W. I. M. K. H. S. S. &. B. I. A. Jhatial, " Green and sustainable concrete–the potential utilization of rice husk ash and egg shells," Civil Engineering Journal, pp. 74-81, 2019.

[4] B. B. Serdar Aydın, "Effect of activator type and content on properties of alkali-activated slag mortars," Composites Part B: Engineering, vol. 57, pp. 166-172, 2014.

[5] J. Davidovits, "Geopolymers: inorganic polymeric new materials," Journal of Thermal Analysis and calorimetry, pp. 1633-1656, 1991.

[6] G. D. L. J. D. E. &. R. N. Habert, "An environmental evaluation of geopolymer based concrete production: reviewing current research trends," Journal of cleaner production, pp. 1229-1238, 2011.

[7] D. W. S. E. S. D. M. &. R. B. V. Hardjito, "Fly ash-based geopolymer concrete," Australian Journal of Structural Engineering,, pp. 77-86, 2005.

[8] S. H. C. S. A. C. A. A. M. M. D. Chayakrit Phetchuay, "Calcium carbide residue: Alkaline activator for clay–fly ash geopolymer," Construction and Building Materials, vol. 69, pp. 285-294, 2014.

[9] N. G. S. F. L. &. P. A. T. Cristelo, "Effect of calcium content on soil stabilisation with alkaline activation," Construction and Building Materials, pp. 167-174, 2012.

[10] M. j. Yaghoubi, A. Arulrajah and M. M. Disfani, "Effects of industrial by-product based geopolymers on the strength development of a soft soil," Soils and Foundations, no. 58, pp. 716-728, 2018.

[11] B. Singhi, A. I. Laskar and M. A. Ahmed, "Investigation on Soil–Geopolymer with Slag, Fly Ash and their blending," Arabian Journal for Science and Engineering, vol. 41, pp. 393-400, 2016.

[12] T. Phoo-ngernkham, A. Maegawa and N. Mishima, "Effects of sodium hydroxide and sodium silicate solutions on compressive and shear bond strengths of FA–GBFS geopolymer," Construction and Building Materials, no. 91, pp. 1-8, 2015.

[13] S. Kumar, R. Kumar and S. P. Mehrotra, "Influence of granulated blast furnace slag on the reaction, structure and properties of fly ash based geopolymer," Journal of Materials Science, vol. 45, pp. 607-615, 2010.

[14] P. Shekhawat, G. Sharma and R. M. Singh, "Strength behavior of alkaline activated eggshell powder and flyash geopolymer cured at ambient temperature," Construction and Building Materials, no. 223, pp. 1112-1122, 2019.

[15] "ASTM D1557-12e1, Standard Test Methods for Laboratory Compaction Characteristics of Soil Using Modified Effort (56,000 ft-lbf/ft3 (2,700 kN-m/m3))," ASTM International, West Conshohocken, PA, 2012.

[16] "ASTM D2166 / D2166M-16, Standard Test Method for Unconfined Compressive Strength of Cohesive Soil," ASTM International, West Conshohocken, PA, 2016.

[17] "ASTM C496 / C496M-17, Standard Test Method for Splitting Tensile Strength of Cylindrical Concrete Specimens," ASTM International, West Conshohocken, PA, 2017.

[18] S. H. S.-L. S. Patimapon Sukmak, "Strength development in clay–fly ash geopolymer," Construction and Building Materials, vol. 40, pp. 566-574, 2013.

[19] N. H. Authority, "General Specifications," Ministry of communications Government of Pakistan, 1998.

[20] A. &. Y. A. P. K. Parkash, "A review study of egg shell powder as a cement replacing material in concrete," international journal of latest research in engineering and computing (IJLREC), 2017.

[21] J. Davidovits.Washington, DC:U.S Patent 4,349,386, 1982.

[22] C. H. S. S. C. C. A. A. A. &. D. M. M. Phetchuay, "Calcium carbide residue: Alkaline activator for clay–fly ash geopolymer," Construction and Building Materials, pp. 285-294, 2014.

3rd Conference on Sustainability in Civil Engineering (CSCE'21)
Department of Civil Engineering
Capital University of Science and Technology, Islamabad Pakistan

EXPERIMENTAL INVESTIGATION OF SHEAR STRENGTH OF SAND MIXED WITH TIRE SHRED

[a]Farhan Ahmad, [b]Muhammad Anwar, [c]Arshad Jamal*, [b,d]Mudassir Iqbal

a: Department of Civil Engineering, University of Engineering and Technology, Taxila, Pakistan. Email: engrfarhan51@gmail.com
b: Department of Civil Engineering, University of Engineering and Technology, Peshawar, Pakistan. Emails: 15pwciv4287@uetpeshawar.edu.pk; mudassiriqbal@uetpeshawar.edu.pk
c: Department of Civil and Environmental Engineering, King Fahd University of Petroleum and Minerals, KFUPM, PO BOX 5055, Dhahran 31261, Saudi Arabia.
d: Shanghai Key Laboratory for Digital Maintenance of Buildings and Infrastructure, School of Naval Architecture, Ocean and Civil Engineering, Shangai Jiao Tong University, Shanghai, China.
* Corresponding author: Email ID: arshad.jamal@kfupm.edu.sa

Abstract- The rapid increase in industrialization, urbanization, and modernization has significantly increased the scrap tire production rate. The innovations, advancements, and continuous up-gradation of the technological products also enhance its production rate, making it one of the emerging waste streams in the world. About 13.5 million tons of scrap tires are generated every year around the globe. Scrape tires significantly damage the environment because of their complex degradation process. In this research work, the shredded scrap tires of different sizes (i.e., 50mm, 75mm, and 100mm) are introduced to the sand for investigating its shear strength characteristics, which is utilized in earth embankment, mechanically stabilized walls (MSE) and landfill. In this study, an attempt is carried out to examine the shear strength properties of the sand mixed with various sizes of tire shred by using large-scale direct shear test apparatus in order to investigate the optimum values of tire shred size as well as the mix ratio of sand tire mix at which maximum shear strength is obtained.

Keywords-tire shred, mixing ratio, shear strength**,** large scale direct shear test

1 Introduction

Waste materials like scrap tires, rubbers, plastics, glass, etc., are usually produced in every society. These wastes are usually disposed to the landfill, which is a menace to the global environment and causing serious problems. Every year over 13.5 million tons of scrap tires are produced globally. The accumulation of these tires in huge amounts can damage the environment because of its difficult degradation process relative to other waste streams. The adverse effect of waste scrape tires includes environmental degradation, fire, effect the agricultural growth of plants, and ill effects on human health. In order to tackle this problem and to utilize these scrap tires, one of the effective ways is to utilize these scrap tires as an aggregate in the construction industry. The utilization of shredded scrap tires as an aggregate has the most significant advantages, such as 1) lightweight having density ranges from 500 to 1040 kg/m^3 .2) Good drainage. 3) Low earth pressure. 4) Improve the shear strength of sand when incorporated owing to the mechanical properties of rubber[1-5]. As a result of these advantages, tire shreds are widely utilized in many applications like slope stability structures, landfill covers, road embankment, retaining wall backfill etc. In the current study, the shredded tires are utilized to enhance the shear strength characteristics of sand. The two parameters on which shear strength primarily depends are cohesion and friction angle. The binding effect of soil grain results from cohesion, whereas friction angle is owing to friction between soil particles. The mathematical relation representing the shear strength of soil is given by $s = c + \sigma \tan \theta$. Where "s" and "σ" indicate total shear stress and normal stress, whereas "c" indicates cohesion and "θ" indicates internal friction angle. It is found that for pure, clear sand, cohesion is zero so shear strength also is zero at zero confining pressure, whereas shear strength values range from 0.5 to 2 kPa for unclear sand. Also, shear strength is about 200 kPa for highly plastic clay, while for medium plastic clay, it is between 10 to 100 kPa. So, by utilizing sand in a certain project where shear strength is also the major concern, one should improve the shear strength characteristics because of the reasonable lower shear strength of sand. It has been examined that by incorporating elastic materials such as small pieces of scrap tires in sand reasonably improves its shear strength[5-7]. Ghazavi et al.[8] utilized scrap tire in filling areas. The study found that the utilization of the scrap tire buried form/ filling area is more beneficial because of its combustible nature and low lateral pressure due to its light nature. Yoon et al. [9]found that the tires being lightweight aggregates, can be utilized to construct embankment due to their lower backfill pressure and high strength. Bernal et al.[10] found that the incorporation of scrap tires in sand produces reinforcement and enhances its shear strength compared to sand alone. The study reported that at 30%, tire shred by volume resulted in the friction angle of 65.8 degrees, whereas the friction angle of pure sand 34.8 degrees. Humphrey et al. [11, 12] investigated that sand tire mixture can undergo significant compression at low normal pressure. The study reported that when tire shred experiences load, their compressibility decreases because the compression in tire shreds is mainly plastic. Thereby, to reduce plastic compression, preloading can be done when it has been filled. Edil et al. [13] investigated that when 10% of scrap tire shreds by volume are introduced in the sand, it significantly enhances its shear strength. Bali et al. [14] investigated the effect of tire chips in different percentages on the shear strength characteristics of sand. Locally available tire chips of size 20x10 mm were utilized and found that significant improvement in sand shear strength was observed when tire chips up to 40% by weight were incorporated in the sand. It was reported that shear strength properties were improved up to 30% as compared to pure sand. Rkaby et al. [15] examined the influence of varying percentages of granulated rubber on the shear strength properties of sand. The percentage by weight of granulated rubber mixed with sand ranged between 0 and 50%. The shear strength of sand was reported to increase by increasing the granulated rubber contents up to 20% compared with pure sand, followed by a gradual decrease in the shear strength of sand for granulated rubber percentages between 30-50%. From the brief assessment of the current literature review, it is concluded that utilization of shredded scrap tires aggregates in the construction industry is a viable solution to effectively utilizing these waste tires effectively thereby reducing the hazardous material from the environment. Also, from the literature review it is concluded that the influence of shear strength on the sand tire mixture depends upon the shape, size and texture of tire shreds, tire shreds content, mixing ratio, confining pressure and normal stress. The current study aims to investigates the shear strength characteristics of sand when various sizes of tire shreds (i.e 50mm, 75mm and 100mm) are incorporated at different percentages. The study also aims to investigate the optimum tire shred size and mixing ratio at which maximum shear strength is obtained.

2 Materials and Methods

2.1 Materials

Materials mainly used in this research work include sand and tire shreds. For sand, Sieve analysis was carried using standard stated procedures (shown in Figure 1(a)). Locally available sand was utilized, passing through a 4.75mm sieve and retaining on 0.075mm sieve. The sand was classified as well-graded sand according to the Unified Soil Classification System (USCS), ASTM-D2487[16]. The specific gravity of sand used in the analysis was 2.67. For mixing tire shreds with sand, the scrap tires were cut into pieces of various sizes of length (50mm, 75mm, and 100mm), whereas the width of tire shreds was kept constant at 5mm for all samples. These tires were mixed with sand in various ratios, as shown in Table 1. Figure 1(b) indicates the sand tire mixture.

Table 1- *Sand-tire shred mixing ratios*

S/No	Tire Size (50 mm)	Tire Size (75 mm)	Tire Size (100 mm)
1	20/80	20/80	20/80
2	30/70	30/70	30/70

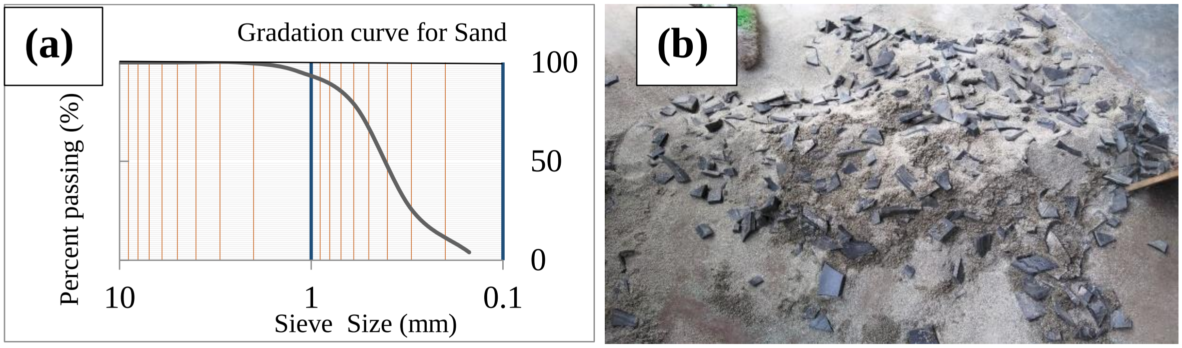

Figure 1: *(a) Gradation curve of sand. and (b) Sand-tire mix.*

2.2 Experimental Setup and Sample Preparation

The apparatus used for the large-scale direct shear test is shown in Figure 2(a). The apparatus consists of two shear boxes upper and lower shear boxes whereas the dimension of the upper shear box is 2ft x 2ft x 1ft (600mm x 600mm x 300mm), and that of the lower one is 2ft x 2.5ft x 1ft(600mm x 750mm x 300mm). The upper shear-box is fixed while the lower shear box is movable and can shear over the upper shear box. To avoid friction among the two boxes, lubricant is used. Normal and shear forces are applied with hydraulic jacks. Horizontal shear force is applied on lower boxes, and normal vertical load is applied on the upper shear box shown in Figures 2 (b) and (c), respectively. The base plate was used for the uniform distribution of normal load. A horizontal load cell is connected to the lower boxes, which can measure horizontal shear displacement, where is vertical load cell is connected at the top of the upper box, which measures vertical displacement. The experimental setup for the shear test is presented in Figure 2(a).

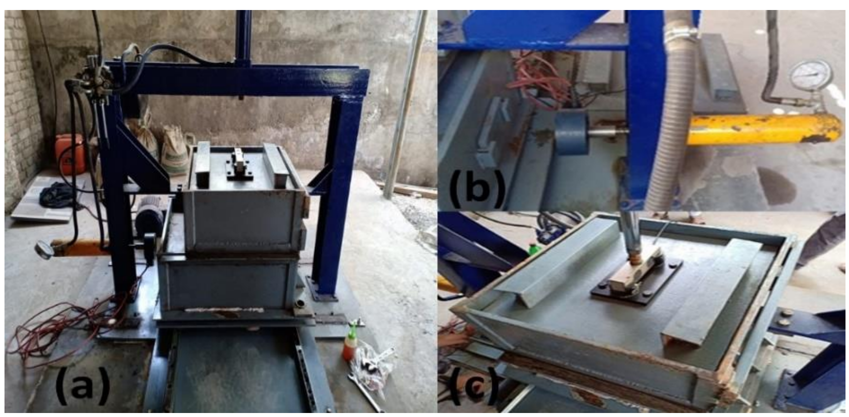

Figure 2: *(a) Experimental setup for large-scale direct shear test. (b) Hydraulic Jack (Horizontal loading). (c) Hydraulic jack (Vertical Loading)*

2.3 Experimental program

To find shear strength properties of the sand-tire mix, large-scale direct shear tests were performed. For this purpose, a number of tests are performed on the sand-tire mix and on sand alone is shown in Table 2. First three tests were performed only on pure sand, and the rest were performed on the sand-tire mix. Tires of different sizes, i.e., 50mm, 75mm, and 100mm, were used in combination with sand. Before performing the test, a modified proctor has been performed on the sand-tire mix in order to determine the compaction test ratio of maximum dry density, which was used as a reference for the shear test.

2.3.1 Direct Shear Tests for Pure Sand Mixes

During the first phase, tests were performed on pure sand in order to study the shear strength characteristics of pure sand before performing on the sand-tire mix. Upper and lower boxes are filled with sand and then compacted sand in each shear box. First of all, a normal-vertical load is applied on the base plate of the upper box, and after the application of the normal-vertical load, the horizontal load is applied on the lower box. To determine shear displacement horizontal transducer is attached to the lower box. Horizontal load is applied on the lower box, and the resulting displacement is measured by a load cell, as indicated in Figure 2(b). Similarly, the normal vertical load is exerted on upper boxes, and the corresponding displacement is measured by the vertical load cell, as shown in Figure 2(c). Three tests were performed on pure sand in normal load. The first test was conducted at 20kN, the second at 30kN, and finally, the third set of tests were performed at a load of 40kN. And in each case, data is collected by the data logger. After plotting the data, we get the shear strength properties of pure sand under different normal loads.

2.3.2 Direct Shear Tests for Sand-Tire Shred Mixes

After performing tests on pure sand, tests were conducted on sand–tire mix. First of all, sand is mixed with 50mm tire shred size, and tests were performed under different normal loading, i.e., 20kN, 30kN, and 40kN, respectively. After that, 50mm and 75mm tire shred sizes were mixed with sand in various ratios, and tests were performed, respectively. Table 2 shows the details of the tests which were performed.

Table 2- *Details of Large-scale Direct Shear Tests*

S/No	Tire Size (mm)	Mixing Ratio (Tire/Sand)	Normal Load (KN)
1	-	Only Sand	20,30,40
2	50, 75, 100	Sample with Maximum Dry Density	20,30,40

3 Results and discussion

As the shear strength of soil depends on shear strength parameters that are a,) Friction angle b) Cohesion. Increasing these two parameters will enhance the soil shear strength. The Graphs are shown in Figure 3(a-g), which indicates the effect of normal stress on shear stress of pure sand as well as sand mixed with tire shred in different proportions. From the results shown in Figure 3 and Table 3, it may be noted that increasing the ratio of tire shred is accompanied by corresponding friction angle increases, increasing the shear strength of sand tire mix. However, a decrease in shear strength at higher tire chip/shreds ratios and size occurs because of the segregation phenomena which happens in the sand tire mix during its compaction; the sand and tire shreds particles separate from one another as a result instead of compaction bulging occurs which cause a decrease in shear strength. Also, using tire shred in suitable proportion will increase the friction between the sand and tire, which also accounts for an increase in shear strength of the sand-tire mix. Figure 4 indicates the variation of angle of internal friction with both percentages of tire shreds and their sizes. It may be noted from Figure 4 that angle of internal friction increases with increase in size and percentages of tire shreds with attaining a maximum value for 100mm tired size with a mix ratio of 20%. Any increase in the percentage of tire shred would lead to a reduction in value of the angle of internal friction. From the test results, the friction angle for pure sand is measured as 32 and the corresponding shear strength is 75 kPa. Whereas for sand tire mix, the friction angle obtained is 46˚, and the corresponding shear strength is 106 kPa, as shown in Table 3. So it means that using tire shred in suitable proportion with sand significantly enhances the shear strength of the soil. Also, from Table 3, it can be noted that friction angle and shear strength reach maximum values, i.e. (106 kPa and 46˚) and then start to decrease with further increase in percentage and size so it can be concluded that sand tire mix attains maximum shear strength using optimum values of tire shred size and percentage.

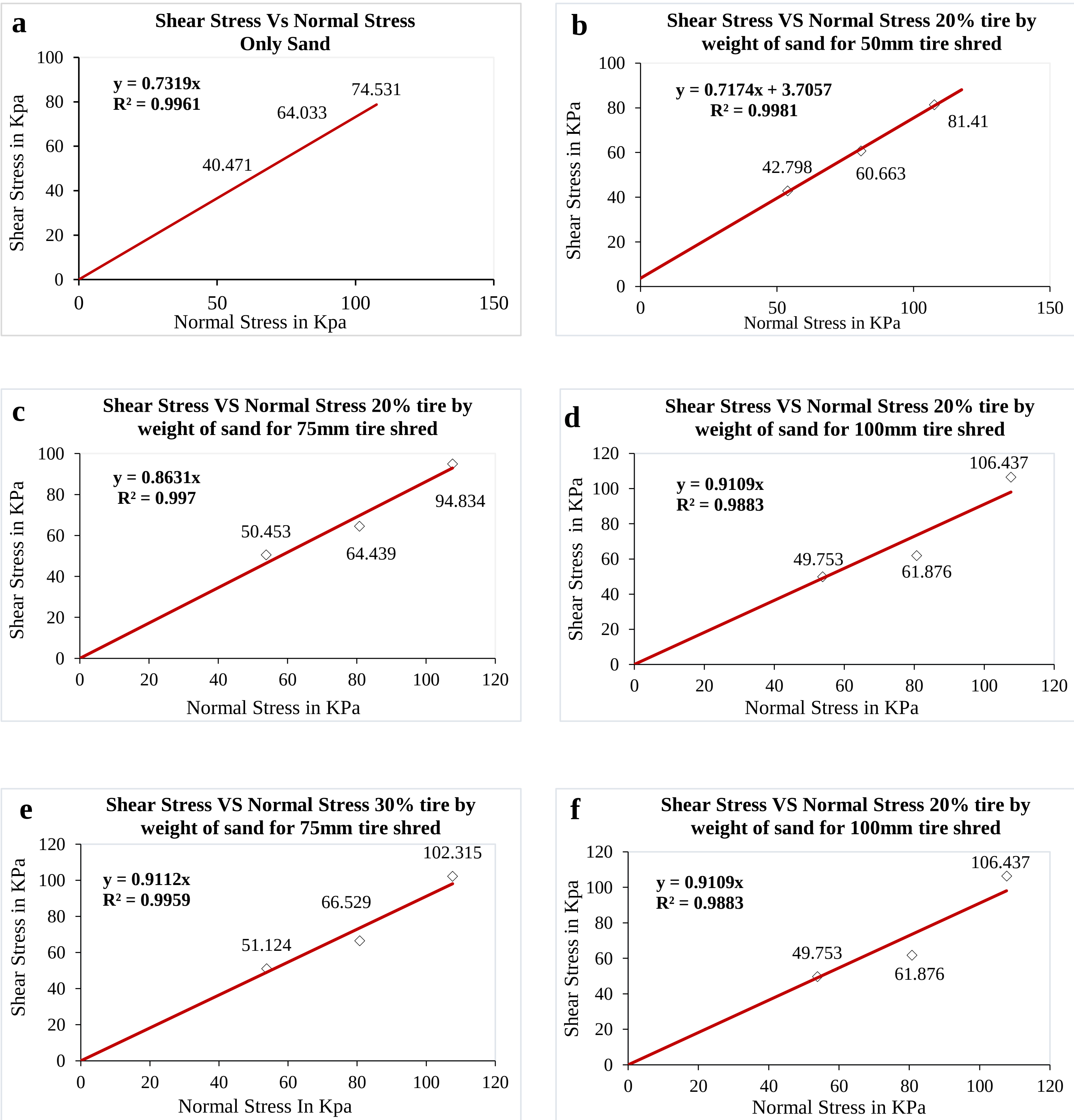
a
Shear Stress Vs Normal Stress
Only Sand
y = 0.7319x
R² = 0.9961
74.531
64.033
40.471
Shear Stress in Kpa
Normal Stress in Kpa
b
Shear Stress VS Normal Stress 20% tire by weight of sand for 50mm tire shred
y = 0.7174x + 3.7057
R² = 0.9981
42.798
60.663
81.41
Shear Stress in KPa
Normal Stress in KPa
c
Shear Stress VS Normal Stress 20% tire by weight of sand for 75mm tire shred
y = 0.8631x
R² = 0.997
50.453
64.439
94.834
Shear Stress in KPa
Normal Stress in KPa
d
Shear Stress VS Normal Stress 20% tire by weight of sand for 100mm tire shred
y = 0.9109x
R² = 0.9883
49.753
61.876
106.437
Shear Stress in KPa
Normal Stress in KPa
e
Shear Stress VS Normal Stress 30% tire by weight of sand for 75mm tire shred
y = 0.9112x
R² = 0.9959
51.124
66.529
102.315
Shear Stress in KPa
Normal Stress In Kpa
f
Shear Stress VS Normal Stress 20% tire by weight of sand for 100mm tire shred
y = 0.9109x
R² = 0.9883
49.753
61.876
106.437
Shear Stress in Kpa
Normal Stress in KPa

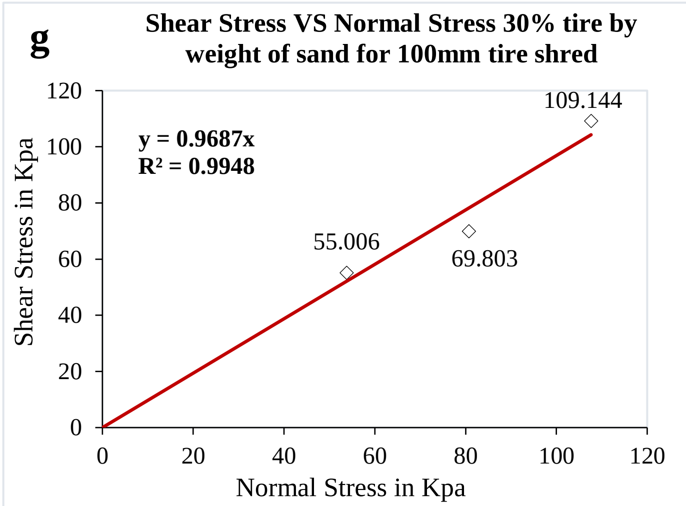

Figure 3: *Shear stress vs normal stress graphs for 50, 75 and 100mm tire sizes at 20% and 30% tire by weight of sand.*

Table 3*-Tests results*

Size of TDA (mm)	Percentage of TDA (%)	Normal load (kN)	Shear Stress (kPa)	Friction Angle
Sand	0	20	40.47	
		30	64.03	32
		40	74.53	
50	20	20	42.8	
		30	60.66	36
		40	81.41	
50	30	20	46.09	
		30	57.78	39
		40	89.63	
75	20	20	50.45	
		30	64.44	40
		40	94.83	
75	30	20	51.12	
		30	66.53	43
		40	102.32	
100	20	20	49.75	
		30	61.88	46
		40	106.44	
100	30	20	55.01	
		30	69.8	44
		40	109.14	

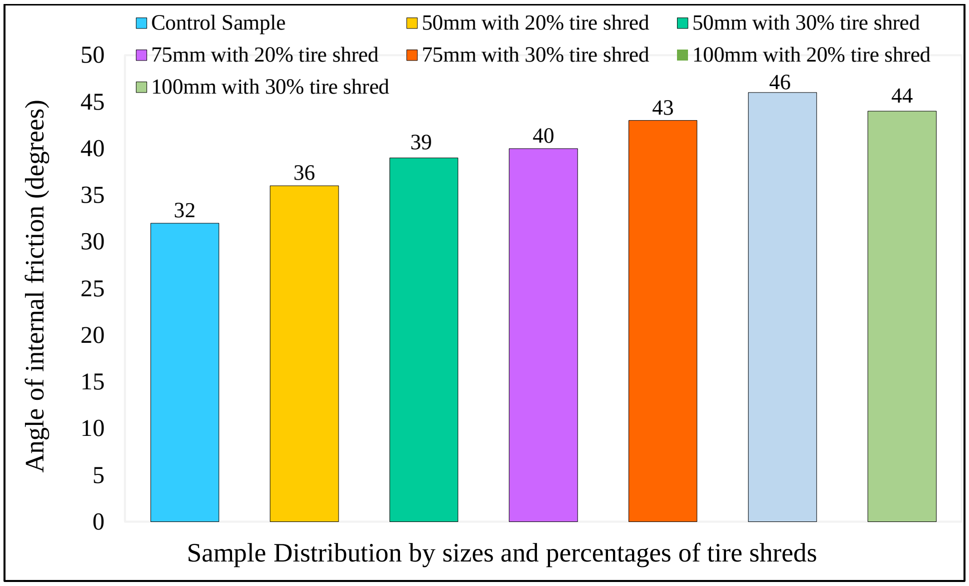

Figure 4:Variation of angle of internal friction with coresponding percentages and sizes of tire shreds."

4 Conclusion

This study was aimed to investigate the shear strength properties of sand mixed with varying proportions of tire shreds. The shear strength properties of sand tire mix containing various sizes of tire-shreds (i.e., 50mm, 75mm, and 100mm) were evaluated. The following points summarize the main conclusions of the study.

- It was concluded that the shear strength of sand mixed with tire shred of different sizes increases with an increase in the size of tire shred up to a certain limit beyond which it starts to decrease. It was found that the maximum shear strength is attained at 100mm tire shred size with a mixing ratio of 20% tire-shred and 80% sand as compared to pure sand alone. At that mixing ratio, maximum shear strength of 106kPa with friction angle of 46˚ was obtained as compared to pure sand without tire shred containing shear strength 75kPa with a friction angle of 32˚.
- The optimum values of mixing ratio containing 20% tire shred and 80% sand were obtained at 100mm size of tire shred
- A substitution of scrap tire shreds as an aggregate up to 20% can be utilized with a maximum size of 100mm with reasonable shear strength.

Acknowledgement

"The careful review and constructive suggestions by the anonymous reviewers are gratefully acknowledged."

References

1. Attom, M.F., *The use of shredded waste tires to improve the geotechnical engineering properties of sands.* Environmental Geology, 2006. **49**(4): p. 497-503.
2. Edinçliler, A. and V. Ayhan, *Influence of tire fiber inclusions on shear strength of sand.* Geosynthetics International, 2010. **17**(4): p. 183-192.
3. Neaz Sheikh, M., et al., *Shear and compressibility behavior of sand–tire crumb mixtures.* Journal of Materials in Civil Engineering, 2013. **25**(10): p. 1366-1374.
4. Anbazhagan, P. and D. Manohar, *Energy absorption capacity and shear strength characteristics of waste tire crumbs and sand mixtures.* International Journal of Geotechnical Earthquake Engineering (IJGEE), 2015. **6**(1): p. 28-49.

5. Anbazhagan, P., D. Manohar, and D. Rohit, *Influence of size of granulated rubber and tyre chips on the shear strength characteristics of sand–rubber mix.* Geomechanics and Geoengineering, 2017. **12**(4): p. 266-278.
6. Mohamad, E.T., et al., *Effects of relative density on shear strength characteristics of sand-tire chips mixture.* Electronic Journal of Geotechnical Engineering, 2013. **18**(4): p. 623-632.
7. Anwar, M. and F. Ahmad, *Optimum Values for Mixing Ratio and Tire Shred Size of Sand Tire Mix*. 2020.
8. Ghazavi, M., *Shear strength characteristics of sand-mixed with granular rubber.* Geotechnical & Geological Engineering, 2004. **22**(3): p. 401-416.
9. Yoon, Y., S. Cho, and K. Kim, *Engineering properties of tire treads for soil reinforcement.* Journal of the Korean Geoenvironmental Society, 2007. **8**(1): p. 49-55.
10. Bernal, A., et al., *Interaction between tire shreds, rubber-sand and geosynthetics.* Geosynthetics International, 1997. **4**(6): p. 623-643.
11. Humphrey, D.N. and W.P. Manion. *Properties of tire chips for lightweight fill*. in *Grouting, soil improvement and geosynthetics*. 1992. ASCE.
12. Ahmed, I., *Laboratory study on properties of rubber-soils.* 1993.
13. Edil, T.B. and P.J. Bosscher, *Development of engineering criteria for shredded waste tires in highway applications*. 1992: Wisconsin Department of Transportation, Division of Highways, Bureau of ….
14. Bali Reddy, S., D. Pradeep Kumar, and A. Murali Krishna, *Evaluation of the optimum mixing ratio of a sand-tire chips mixture for geoengineering applications.* Journal of Materials in Civil Engineering, 2016. **28**(2): p. 06015007.
15. Al-Rkaby, A.H., *Strength and Deformation of Sand-Tire Rubber Mixtures (STRM): An Experimental Study.* Studia Geotechnica et Mechanica, 2019. **41**(2).
16. Soil, A.C.D.-o. and Rock, *Standard Practice for Classification of Soils for Engineering Purposes (Unified Soil Classification System) 1*. 2017: ASTM International.

3rd Conference on Sustainability in Civil Engineering (CSCE'21)
Department of Civil Engineering
Capital University of Science and Technology, Islamabad Pakistan

DEVELOPMENT OF EMPIRICAL CORRELATIONS BETWEEN INDEX AND STRENGTH PROPERTIES FOR INDIGENOUS SUBGRADE SOILS

[a] Zakirullah, [b] Kashif Riaz, [c] Muhammad Bilal, [d] Naveed Ahmad*

[a, b,c,d](Department of Civil Engineering ,University of Engineering and Technology, Taxila)
* Corresponding author: Email ID: zakir6897@gmail.com

Abstract-The California Bearing Ratio (CBR) is an important design parameter for the subgrade layer in a flexible pavement structure. Determination of CBR value is a very common laboratory test to estimate the stiffness modulus and shear strength of sub-grade soil for the pavement design. CBR test is technically an extensive and time-consuming process and may lead to delay in execution of construction projects and thus cause an increase in construction costs. Therefore, it is extremely important for the geotechnical engineer to develop a predictive model for quick assessment of geo-material behavior which is used in civil infrastructures. In this study, an attempt has been made to develop regression models both Single and Multiple linear Regression Analysis (SLRA & MLRA) to determine the soaked CBR value from soil basic properties like Liquid limit, Plastic limit, Plasticity index, optimum moisture content, and Maximum Dry Density of some subgrade sample gathered from twenty-one different locations of Rawalpindi Division, Pakistan. From both SLRA and MLRA models coefficient of correlation, the R^2 value is found in between (0.80 –0.98) indicating a very good correlation between soaked CBR and soil basic properties. Predicted CBR values were also compared with actually calculated values and a very good agreement was found between the two.

Keywords- SLRA, MLRA, Predictive, LL, PL, PI, OMC, MDD, Soaked CBR.

1 Introduction

The transportation systems usually act as a backbone of a country. The Road network covers a large portion of the transportation system, as most of the freight is transported through roads. One of the primary elements in the road networks is the pavement. The performance of the road pavement depends upon the strength of the subgrade material. Subgrade serves as a suitable foundation of the pavement structure, which is a compacted layer of natural local soil deposit from the borrow pits. Load from the moving vehicles on the road surface is ultimately transferred to the subgrade that may be a natural soil deposit of compacted fill material. [1] The suitability of subgrade soil is typically evaluated before the beginning of construction activity starts. Geographical variations in soil properties from one location to another make it to carry out investigation for its suitability for the intended purpose. [2] Statistical empirical correlations play a vital role in civil engineering analysis and designs.

The correlation model development is advantageous and acts as a foundation for the judgment of the validity of the CBR values. In past, many researchers have developed the correlation model for the prediction of CBR value through some of the basic soil properties obtained from Atterberg's limits test and compaction tests like LL, PL, PI, MDD, and OMC. Some prediction models for the determination of the CBR value from literature are presented in Table 1.

Table 1- Correlations of CBR with Soil Index properties

Ref No	Proposed correlations	No. of Materials used	Coefficient of Determinations (R^2)	Remarks
3	CBR= -0.01(LL)-0.425(PI)+1 CBR=O.79(Cu) + 8.5 CBR=0.7Cu +0.045MDD +3.4	59	0.9 0.8 0.8	Fine and coarse grain soil
4	CBR= -4.8353–1.56856(OMC) +4.6351(MDD)	20	0.82	Fine Grained Soils
5	CBR = 0.0262 (L.L) + 0.0283 (O.M.C) 0.142+ (%fines) +1.043(M.D.D)17.029	11	0.84	Well graded sand containing silt
6	CBR = – 0.728(PL) - 0.221(SL) – 0.341(MDD+ 1.126(OMC) +43.012 CBR=1.492(PL)-0.58(SL)–0.05(MDD) +0.398(OMC)+39.06	5	0.86 to 0.99	NA
7	CBR = - 0.172 (PI)+0.404 (MDD) - 0.089 (OMC) +3.51 CBR = 0.151 (FF)+0.045(PI) + 14.58	NA	NA	Fine Grained Soils
8	CBR = 1.04 (PL)+13.56 CBR = 0.22 (LL)+28.87 CBR = 50.28 (MMD)-70.22 CBR = 9.42 (SG)+10.91 CBR =10.43 (SG)+56.19	8	NA	lateritic soil(A-2-4)
9	CBR= [Fs+264PI^2-56PI-5](1.44-4.23PI) CBR =(8.44-16.1PI) [Fi+488PI^2-314PI+45]	24	NA	Fine Grained Soils (Silty Clay)
10	Log10(CBR) = 0.29(GM) - 0.024(PI) +1.23	NA	NA	Base coarse material
11	CBR = 11.805 - 0.126 (LL) + 0.234 (PL) -0.246(SL)	12	% Error=-25	Alluvial soil
12	CBR=-(0.014LL)- (0.015PI) +(0.011OMC) +(2.100MDD) -0.258	8	0.97	Fine Grained soils
13	CBR=2.19+0.062(FF) +0.0888(LL) CBR=17.029+0.142(FF)+0.0262(LL)+0.0283(OMC) +1.043(MDD	11	0.082 0.836	Well graded sand containing silt
14	CBR_{10}= -0.728(PL) -0.221(SL) 0.341(MDD)+1.126(OMC)+43.012 CBR_{30}= - 1.492(PL) -0.58(SL) -0.05(MDD) - 0.398(OMC)+39.0 CBR_{56}= -2.682(PL)+0.467(SL)+1.073(MDD)-0.233(OMC) -58.406	5	0.82 to 0.9	Fine grained soils
15	CBR=35.23e$^{-0.5(LL)}$	10	0.967	Fine and coarse grain soil

Where: CBR(%) = California Bearing Ratio , CBR(10,30,56)=CBR for 10,30 and 56 blows, Cu =Coefficient of Uniformity (Cu), LL(%)= Liquid Limit, PL(%)=Plastic Limit, PI(%)=Plasticity Index, OMC(%)= Optimum moisture content, MDD(%)=Maximum Dry Density, SG = Specific gravity; FF=% Fines; SL = shrinkage limit, F=Fines, %; S=Sand, %; G=Gravel, %Fi=initial state factor; Fs=soaking state factor.

2 Materials And Methodology

2.1 Sample Collection

Cumulatively twenty-one disturbed soil samples out of which 6 were collected from Rawalpindi (RWP), 5 from Attock (ATG), 5 from Chakwal (CHK), and 5 samples were collected from Jhelum (JMR) of the Rawalpindi Division, Pakistan having latitude 32.5˚N to 34.0˚N and longitude 72˚E to 74˚E at a depth of about 1m from the ground surface.

Figure 1: Study districts included in the Rawalpindi Division.

2.2 Methodology

Twenty-one different types of soil samples were collected from the district of Rawalpindi, Attock, Chakwal, and Jhelum. Soil samples were taken with the help of different sampling equipment's and almost 50 kg of soil sample was collected from each district site and then stored in plastic bags to avoid the loss of moisture content of the soil. Different means of transport were adapted for the transportation of samples depending upon site distance from the laboratory. All the Soil samples have been tested in the laboratory as per the specification of AASHTO to determine soil index and strength properties. Atterberg's limits test was conducted to obtain the value of liquid limit, plastic limit, and plasticity index of the soil. Grain size analysis was conducted by sieving the different types of soil samples through a set of sieves to obtain the values of % fines, % gravels, and % sands other particle size distribution characteristics of the soil. Modified proctor tests were used to determine the maximum dry density and optimum moisture content. Soaked CBR value obtains on the base of modified proctor test, soil sample compacted in the CBR mold according to MDD and OMC. Table.2 shows the laboratory testing program for this research study. Both single linear regression analysis and multiple linear regression analysis techniques are used for empirical relation and investigating the correlation between two or more variables.

Table 2: Laboratory Testing Program

S.NO	Test Names	Standard (AASHTO)
1	Grain Size Analysis	AASHTO T-88
2	Atterberg Limits	AASHTO T,89 T 90
3	AASHTO Soil Classification System	AASHTO M-145
4	Modified Proctor Test	AASHTO T-180
5	Soaked CBR Test	ASHTO T-193

3 Results and Discussion

All 21 soil samples were tested for the development of empirical correlations between soil index properties and CBR according to AASHTO standards. A summary of the experimental results of the tested soil sample is given in Table 3. The grain size distribution of different soils showed that soil samples can be classified into fine-grained soil and coarse-grained soil. The gravel percentage ranges from 0-47, sand=1-78% and Fines (silt & clay) =21-98%. From Atterberg limit test results it was observed that the soil liquid limit lies in a range of 21-33%, plastic limit =17-21% and shrinkage limit 5-12%. Modified proctor test results of soil samples showed that OMC was ranging from 8-13% and maximum dry density 119-134 Ib/ft3. Soaked CBR test results indicated that overall CBR values were ranging from 5-11%. Soil samples were classified as A-4, A-3, A-6, and A-2-4 according to the AASHTO soil classification system.

Table 3-Results of Laboratory Test for Soil Samples

Soil Type	Sample ID	LL	PL	PI	GRIAN SIZE DISTRIBUTION			Compaction Characteristics		Soaked CBR value
AASHTO		%	%	%	Gravel (%)	Sand (%)	Fines, (%)	OMC (%)	γd_{max} (lb./ft^3)	%
A-4	RWP-1	30	19	10	1	3	96	13	121	6
A-4	RWP-2	28	20	8	6	5	88	13	125	7
A-4	RWP-3	29	20	9	6	8	86	12.5	120	6
A-4	CHK-1	24	17	7	1	34	65	9.5	129	10
A-4	CHK-2	27	19	8	3	7	90	12	129	8
A-4	RWP-4	23	17	6	0	42	58	9	128	8
A-4	ATG-1	28	19	5	0	4	96	11	126	8
A-4	ATG-2	30	21	9	0	2	98	12	119	6
A-4	RWP-5	25	18	6	3	6	91	10	130	9
A-4	ATG-3	26	17	9	2	5	93	10	128	8
A-4	RWP-6	29	20	9	1	2	97	12	122	7
A-4	CHK-3	28	19	8	0	3	97	12	125	7
A-6	ATG-4	33	22	12	0	2	98	15	119	5
A-4	CHK-4	30	21	10	0	8	92	13	120	6
A-6	CHK-5	31	20	11	0	28	72	14	122	6
A-2-4	JMR-1	25	18	7	15	46	39	11	132	10
A-2-4	JMR-2	28	17	8	48	30	23	13	133	9
A-3	JMR-3	23	NP	NP	17	64	19	9	135	10
A-2-4	JMR-4	21	NP	NP	0	78	22	9	134	10
A-2-4	ATG-5	26	NP	NP	2	72	26	11	127	8
A-2-4	JMR-5	28	NP	NP	0	78	22	13	120	7

4 Linear Regression Analysis (LRA)

The Linear Regression Analysis technique is used to formulate the correlation between CBR and other soil basic properties. The single linear regression analysis (SLRA) has one X-axis and one Y-axis variable. So CBR is taken as the dependent variable and plotted on Y-axis while soil basic properties like Liquid Limit, Plastic Limit, Plasticity Index, Optimum Moisture Content, and Maximum Dry Density are taken as independent variables and plotted on X-axis and then simple scatter graph is plotted on Microsoft Excel and the then suitable trend line is chosen based on the coefficient of determination of higher value. The multiple linear regression Analysis has one Y-axis and two or more X-axis variables. So for MLR by using statistical software SPSS version 2013 in which soaked CBR taken is a Dependent variable and other soil index properties like LL, PL, PI, OMC, and MDD are the Independent variables.

4.1 Single Linear Regression Analysis Models for CBR

In the SLRA model were chosen suitable scatter trend line and drawn scatter graph between soaked CBR and soil basic properties (LL, PL, and MDD) is presented fromFig.2 to Fig.4, and their correlations as shown in Table 5.The strength of these correlations were checked on basis of the coefficient of correlation R^2 according to criteria proposed by pellinen in Table 4.

From Fig.2 there is linear relationship exists between soaked CBR and Liquid Limit and it notice from this Fig with an increase in the liquid limit of soil soaked CBR value tends to decrease. The empirical correlation between soaked CBR and Liquid limit is presented in Table .5. It has regression coefficient, R2 = 0.8509. Fig.2 and (1) from Table.5 indicating very little scatter and good correlations according to criteria proposed by Pellinen in Table 4.

From Fig.3 there is are linear relationship exists between soaked CBR and Plastic Limit and.it notices from this Fig with an increase in the Plastic limit of soil soaked CBR value tends to decrease. The empirical correlation between soaked CBR and PL is presented in Table 4. It has a coefficient of correlation (R2) = 0.8085. Similarly, Fig.3 and (2) from Table 5, indicating very little scatter and good correlations according to criteria proposed by Pellinen in Table 4.

It is observed from Fig.4 that there are linear relationship exists between soaked CBR and MDD. It notices from this Fig as maximum dry density increases also CBR values increases. The correlation between soaked CBR and MDD is presented in Table 5. It has coefficient correlation, R2 = 0.9134. Fig.4 and (3) from Table 5 indicating very little scatter and good correlations according to criteria proposed by Pellinen in Table 4.

Table 4- Criteria for goodness of fit statistical parameters [16]

S.NO	**Criteria**	**coefficient of correlation R^2**
i.	Excellent	>0.9
ii.	Good	0.7-0.89
iii.	Fair	0.4-0.69
iv.	Poor	0.2-0.39
v.	Very Poor	<0.2

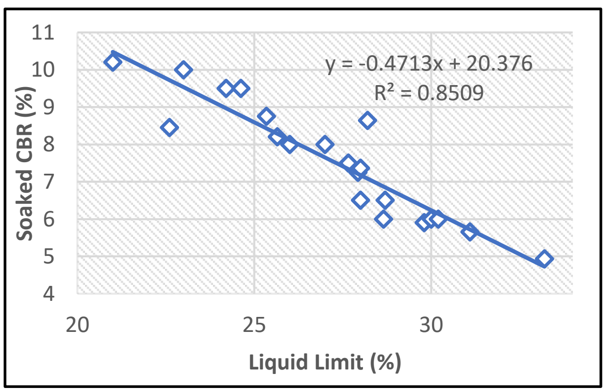

Fig. 2: Correlation between LL and Soaked CBR

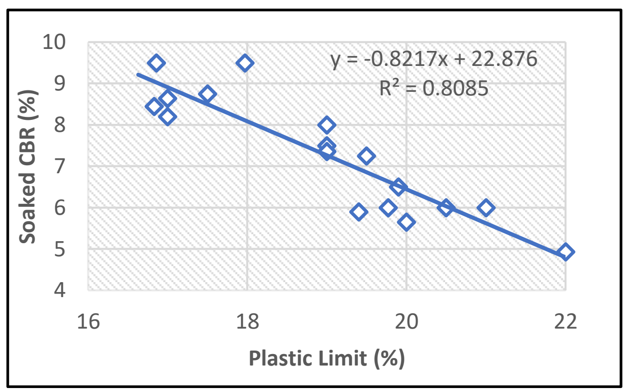

Figure 3: Correlation between PL and Soaked CBR

4.2 Multiple Linear Regression Analysis Models for CBR

In the MLRA by using IBM SPSS statistics software as a solver tool and soaked CBR taken as dependent variables and remaining soil properties as independent variables. With help of SPSS software were calculated acceptable empirical relation which as shown in Table 6.

Soaked CBR = (LL, PL, PI, OMC, and MDD)

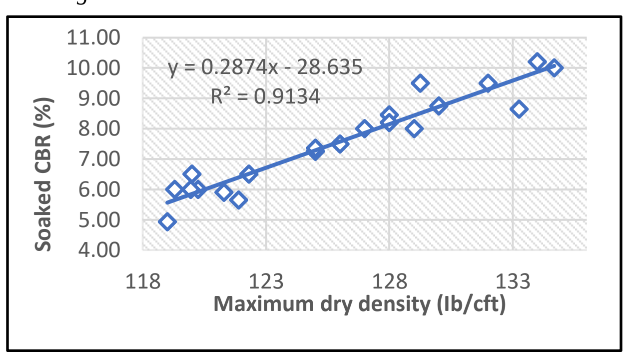

Figure 4: Correlation between MDD and soaked CBR

Table 5-Single Linear Regression

Equation No	Correlation	R^2
1	CBR= -0.4713(LL) + 20.37	0.8509
2	CBR= -0.8217(PL) + 22.876	0.8085
3	CBR= 0.2874(MDD)- 28.635	0.9134

Table 6-Multiple Linear Regression

Equation No	Correlation	R^2
4	CBR= -0.151(LL) + 0.019(PL) -0.048(PI) +0.180(MDD) -9.706	0.975
5	CBR= -0.159(LL)-0.127(OMC) +0.179(MDD)-9.191	0.977
6	CBR= -0.026(PL)-0.761(OMC) +16.720	0.760
7	CBR= -0.235(LL) + 0.172(MDD) - 7.724	0.975
8	CBR= -0.337(OMC) +0.207(MDD)-14.574	0.971

5 Validity of Regression Analysis Models

To check the validity of Regression Analysis Models by comparison between experimental soaked CBR and predicted Soaked CBR values. Predicted soaked CBR values were obtained on the basis of MLRA correlation from Table 6.
Eq.5 presents the correlation between Soaked CBR values and LL, OMC, and MDD. Based on (5) were calculated predicted Soaked CBR values. It is observed from Fig.5 that the predicted CBR values are very close to Experimental soaked CBR values and the coefficient of regression from (5) is (R^2)=0.977.

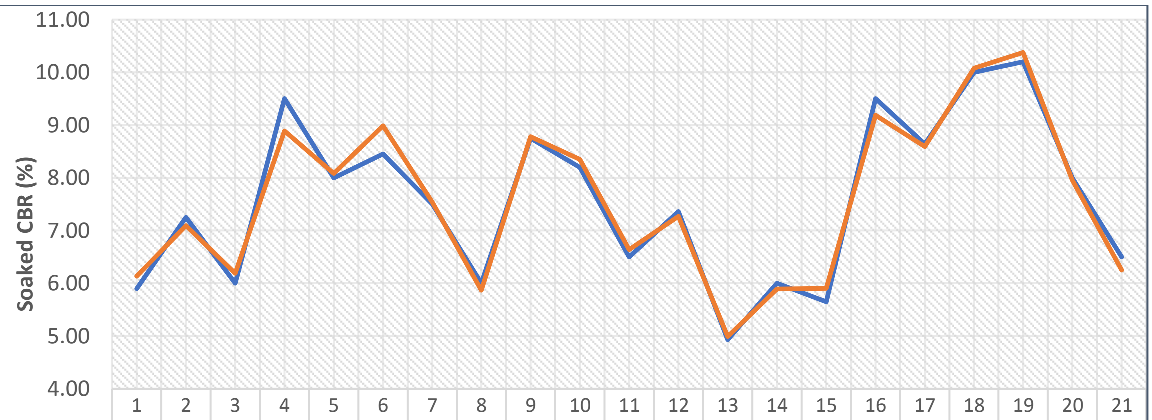

	1	2	3	4	5	6	7	8	9	10	11	12	13	14	15	16	17	18	19	20	21
Expermental CBR	5.90	7.25	6.00	9.50	8.00	8.45	7.50	6.00	8.75	8.20	6.50	7.36	4.93	6.00	5.65	9.50	8.64	10.00	10.20	8.00	6.5
Predictive CBR	6.13	7.09	6.19	8.89	8.08	8.98	7.54	5.87	8.78	8.35	6.64	7.27	4.99	5.89	5.90	9.19	8.59	10.08	10.38	7.95	6.25
%Error	3.79	-2.23	3.08	-6.86	1.03	5.95	0.48	-2.22	0.34	1.76	2.09	-1.22	1.20	-1.89	4.31	-3.39	-0.59	0.78	1.70	-0.58	-4.01

Fig.5: comparison b/w Experimental CBR and Predictive CBR for LL, OMC, and MDD

Eq.5 indicating a very good correlation according to criteria proposed by Pellinen in Table 4 and percentage error is less than 4%.Which can be successfully used for preliminary prediction of CBR value for locally available soils in Rawalpindi Division., Pakistan for sub-grade soils.

6 Conclusion

Following conclusions can be drawn from the conducted study:

- The present study's empirical relations can be used for the successful prediction of soaked CBR value for locally available soils in Rawalpindi Division., Pakistan.
- From Fig.2 through Fig.4 shows the effects of plasticity and compactions parameter on the soaked CBR value when Soaked CBR value tends to increases with the increase in the Maximum Dry Density. But soaked CBR values decrease with the increase in the Liquid limit, Plastic limit, Optimum moisture content, and Plasticity index.
- It is observed from the multiple linear regression models that is very small differences between the experimental soaked CBR values and predicted soaked CBR values and the coefficient of correlation R^2 is found above 0.80. This indicates is a very good relationship exists between soaked CBR value and soil basic properties according to criteria proposed by Pellinen in Table 4.

For the comprehensive model to make for Pakistani soils to predict CBR value from soil index properties by collecting more number of soil samples and types of soil from different locations of Pakistan.

References

[1] Charman, J H.: Laterite in road pavements. Construction Industry Research and Information Association, London; CIRIA, 1974, http://worldcat.org/isbn/0860172759.

[2] Jay Ameratunga, Nagaratnam Sivakugan and Braja M. Das: Correlations of Soil and Rock Properties in Geotechnical Engineering, A Text Book January 2016, DOI 10.1007/978-81- 322-2629-1, ISSN 2364-5156, Springer Publisher (2015).

[3] Z. U. Rehman and U. Khalid "Prediction of CBR Value from Index Properties of different Soils" Technical Journal, University of Engineering and Technology (UET) Taxila, Pakistan, Vol. 22 No. II-2017

[4] Naveen B Shirur "Establishing Relationship between CBR Value and Physical Properties of Soil" IOSR Journal of Mechanical and Civil Engineering (IOSR-JMCE), Volume 11, Issue 5 Ver. I (Sep- Oct. 2014), PP 26-30

[5] Z. S. Janjua "CORRELATION OF CBR WITH INDEX PROPERTIES OF SOIL" International Journal of Civil Engineering and Technology (IJCIET), Volume 7, Issue 5, September-October 2016

[6] K. Roksana, T. Islam "Relationship between CBR and Soil Index Properties of Bangladesh Soil Samples Journal of Modern Science and Technology, Vol. 6. No. 2. June 2018 Issue. Pp.1-9

[7] C Lavanya and N.D Kumar "SLRA and MLRA Based Correlations of Geotechnical Parameters of Fine Grained Soils" IOP Conf. Series: Materials Science and Engineering, 1126 (2021) 012084.

[8] BELLO. "Regression analysis between properties of subgrade lateritic soil". Leonardo Journal of Science, Issue 21, pp. 99-108, 2012.

[9] M. Zumrawi. "Prediction of CBR value from index properties of cohesive soils". In Proceedings of the Annual Conference of Postgraduate Studies and Scientific Research 17-20, Friendship Hall, Khartoum, Vol. 1, pp. 111-117. 2012.

[10] S. A. Kleyn. "Possible development in pavement foundation design". The South African Institution of Civil Engineers, 5(12), pp. 286- 292, 1955.

[11] Patel, Rashmi S., and M. D. Desai. "CBR predicted by index properties for alluvial soils of South Gujarat." In Proceedings of the Indian geotechnical conference, Mumbai, pp. 79-82. 2010.

[12] M. Korde and P. R. K. Yadav, "A Study of Correlation between CBR Value and Physical Properties of Some Soils," Int. J. Emerg. Technol. Adv. Eng., vol. 5, no. 7, pp. 237–239, 2015.

[13] Z. S. Janjua, P. G. Student, and J. Chand, "CORRELATION OF CBR WITH INDEX PROPERTIES," vol. 7, no. 5, pp. 57–62, 2016.

[14] K. Roksana and A. Muqtadir, "Relationship between CBR and soil index properties of Bangladesh soil samples" Journal of Modern Science and Technology, .August,2018,doi:10.13140/RG.2.2.32196.94084.

[15] Ravichandra A. H, Shivakumar. K "Prediction of CBR Value by Using Index Properties of soil" International Research Journal of Engineering and Technology (IRJET) , Vol: 06 no: 07, 2019

[16] Zulfiqar Ali and S Bala Bhaskar "Basic statistical tools in research and data analysis" Indian J Anaesth. 2016 Sep; 60(9): 662–669,doi: 10.4103/0019-5049.190623

ENVIRONMENTAL ENGINEERING

3rd Conference on Sustainability in Civil Engineering (CSCE'21)
Department of Civil Engineering
Capital University of Science and Technology, Islamabad Pakistan

IDENTIFYING AND RANKING OF CRITERIA FOR THE SUSTAINABLE LOCATION OF WASTE TRANSFER STATION: A WAY OUT FOR WASTE TO ENERGY AND THREE R'S APPROACH.

[a] Rasool Bux[1]*, [b] Dr. Muhammad Saad Memon, [c] Dr. Sonia Irshad Mari, [d]Masroor Ali

a: Industrial engineering and management, Mehran University of engineering and technology Jamshoro, bux.45@outlook.com
b: Industrial engineering and management, Mehran University of engineering and technology Jamshoro, saad.memon@faculty.muet.edu.pk
c: Industrial engineering and management, Mehran University of engineering and technology Jamshoro sonia.irshad@faculty.muet.edu.pk
d: Industrial engineering and management, Mehran University of engineering and technology Jamshoro, m.emasroorali@hotmail.com
* Corresponding author: Email ID: saad.memon@faculty.muet.edu.pk

Abstract- Solid waste becomes a civic concern in this contemporary world. The public is more conscious about its possible hazards to the environment, health, and societal standard. To get rid of this, the countrywide concept is to reduce and recycle solid waste and build up large and distant landfills. In this circumstance, the waste transfer station is an attractive substitute to lessen solid waste by extracting recyclable and energy potential material and creates an incorporating nexus that lead to cost-effective deliveries from household to remote landfill facilities. Siting the waste transfer station in populated urban centers required the key functional role from a technical and financial perspective that assures environmental threats, people's health, and safety. Locating a waste transfer station is a complex assignment that comprises the evaluation of various factors: economic, social, and environmental. The purpose of this study is to identify and rank criteria for the sustainable location of the waste transfer station. For this, existing literature was studied and different factors were identified and ranked according to its frequency in literature. The study found that environmental concern is on priority following social and economic factors for locating waste transfer stations. Moreover, river, population density, and proximity to road constraint were ranked first in environmental, social, and economic factors respectively.

Keywords- Solid waste management. The waste transfer station, waste to energy, three R's Approach

1 Introduction

Household waste and waste from commercial and institutional locations, for instance, businesses, schools, and hospitals are known as Municipal solid waste (MSW) as stated by Environment Protection Agency (EPA)[1]. This waste must be amassed regularly and transported effectively. Moreover, it must be disposed of to assure healthy and sanitary life standards [2]. Municipal Solid waste generation is proportional to population growth. This is problematic for many developing countries. Solid waste management has been facing numerous challenges because of rapid urbanization, inadequacy in a financial and technical capacity, an ineffective policy that has made the herculean task for municipal management to deliver quality service to the citizen. The decision of location waste transfer station is long term planning that which has long term impact on environment society and from economic perspective. [3]Solid waste is a social catastrophe that requires a definition of credible government policies, suitable location of the waste transfer station, landfill site, and required technical support. Clear City, has an outcome of effective solid waste management services. The unpolluted city is a successful city for residents to become healthful. It improves social morality, moreover, it also attracts tourists. It has thus been suggested that the cleanliness of a city can be used as a proxy indicator for the social values of its residents, which is a major objective of social development programmers [1].

The criteria on which decision would be taken for the location of waste transfer station has played a vital role in waste management[4] Solid waste also damages the environmental condition in society. According to the Global Waste Management Outlook report, 2015 issued by the UNEP agency stated that an improved version of solid waste management would minimize 15 to 20 percent of greenhouse gas emissions. Therefore by locating a suitable site, solid waste would be handled effectively [1].

further, a study showed that forty percent of solid waste is not collected from the street which is disposed of in open-air [5]. That has become the major reason for many problems including health problems, environmental pollution, an untidy city, damaging sewerage, and mass transit network in the city. Furthermore, a study showed that these open disposed of solid waste in the street is an inhabitant place for bacteria that spread viral and bacterial diseases. That results in a decline in health standards and an increase in medical expenditure.

Multi-criteria identifying and ranking are techniques commonly that require decision-makers to assign weightings of importance to the decision criteria based on the criteria are ranked.[4] This study has focused to identify and rank the criteria for the sustainable location of waste transfer stations from existing literature. This will help the policymaker, engineers, and government to consider the criteria and their importance while deciding for locating waste transfer stations, especially in urban centers.

2 Role of Waste Transfer Station in Solid Waste Management

The waste generated by households must be amused regularly and transport effectively. A waste transfer station in solid waste management provides a consolidating nexus between the collection program of municipal solid waste management and landfill site. In the waste transfer station, solid waste is collected to the waste transfer station where a recyclable material and material with energy value would be extracted from the whole waste. The remains are transported to the landfill site. Waste transfer stations save collection time and costs associated with transportation. Moreover, by extracting recyclable and energy value material a substantial amount of solid waste is reduced for the landfill site.

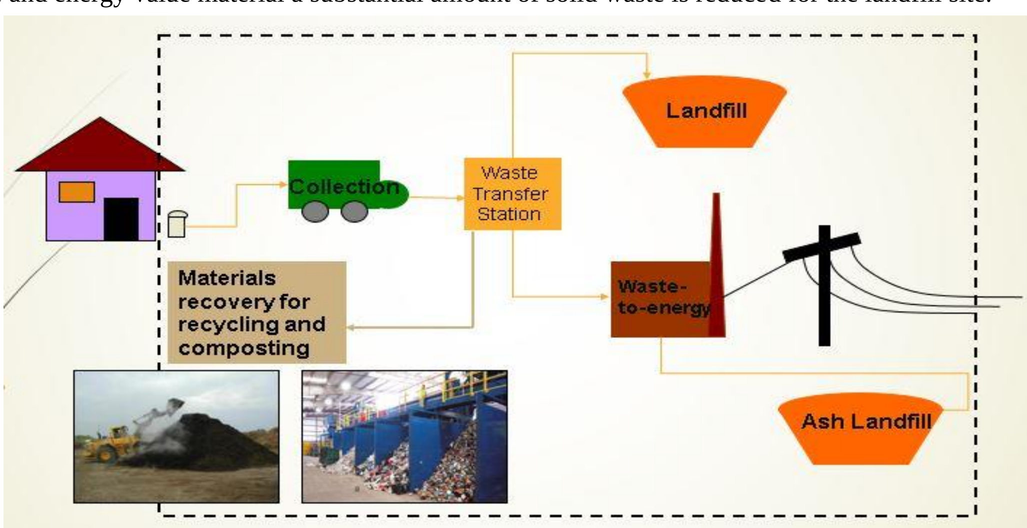

Figure 1: Role of a waste transfer station in solid waste management

3 Sustainable Location of Waste Transfer Station

Locating a waste transfer station is a complex assignment that comprises the evaluation of various factors: economic, social, and environmental. By examining the criteria of deferent factor, a sustainable location of waste transfer station would be located. For any sustainable city, the sustainable mechanism for getting rid of waste has paramount importance this Waste Transfer Station provides a sustainable solution for our growing urbanization. Hence its sustainable location must weigh the importance of social, economic, and environmental constraints.

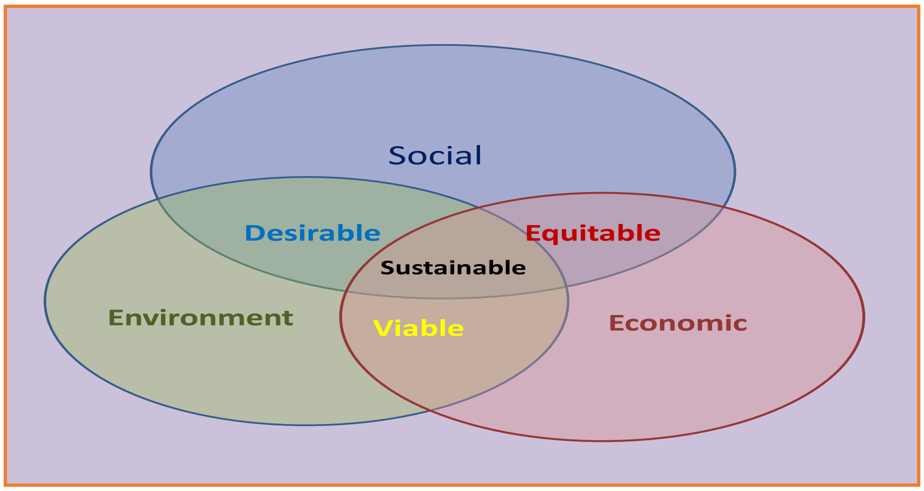

Figure 2: locating sustainable waste transfer station

4 Results and Discussion

Determination and ranking of relevant criteria for a potential location for a waste transfer station in an urban Centre required consideration of different factors: economic, social, and environmental. In the literature review, different authors (s) have considered different criteria. Here according to weightage different criteria were ranked. Weightage would be given to those criteria in which deferent authors have worked.

4.1 Environmental Criteria.

In the literature review author(s) have work on different criteria for an environmental factor, according to the frequency of their work here in chart 1 these criteria were weightage and ranked. As result shows that rivers have the highest weightage and are ranked as one and follows slope, geology soil, and drainage respectively.

Table 1- Criteria for environment factor

Environmental Factor	Author(s)	Weightage	Rank
Rivers	[6] [7][8][9] [10] [11][12][13]	8	1
Geology	[6][7] [10][14][15]	4	3
Drainage	[9] [14]	2	5
Slop	[6] [9][10][14][11] [16][13]	7	2
Soil	[10] [14][11][15]	3	4
Vegetation criteria	[7] [10]	2	5

4.2 Social Criteria

The location of the waste transfer station matters most from a social perspective as it is directly linked to people's health and living conditions. Moreover, if the waste is a nearby populous or major place, as Mosque, shopping mall, schools, and hospital, it creates a problem for the public and increases the chance of health issues especially viral disease. Here in social factors, four criteria were kept in consideration. The population density secures the highest rank in social factor whereas land cover, major place: Mosque, shopping mall, schools and hospital, and distance from railway secure second third and fourth rank respectively.

Table 2. Criteria for Social factor

Social Factor	Author(s)	Weightage	Rank
Population density (Person per hector)	[6] [8] [9] [10] [14][11] [16][13]	8	1
land use/cover	[6][10][8] [14] [11][16][15]	6	2
Major place	[7] [9] [12]	3	3
Distance From Railway	[10]	1	4

4.3 Economic Criteria

Economic consideration in the location of the waste transfer station has priority because in solid waste management most of the cost is associated with transportation activity. By locating an optimal location transportation activity would be minimized. Keep in view this scenario, the criteria were set to minimize the total transportation cost. Moreover, land value is also considered as in urban center land value is more than their outskirt. In the literature review location of the waste transfer station with respect to road and landfill site is considered. However in deferent research paper proximity to road secure highest rank fallowing land value and proximity to a landfill site.

Table 3. Criteria for Economic factor

Economic Factors	Author(s)	Weightage	Rank
Proximity to Roads	[6] [8] [9] [10] [14][11] [16][13]	8	1
Land Value	[6][10][8] [14] [11][16][15]	6	2
Proximity to Landfill	[10]	1	4

5 Scope of research

The sustainable location of waste transfer stations especially in the urban center is a challenging task. Because there are multiple factors are linked with this. Which include environmental. The economic and social factors. However, this study will help engineers, policymakers, and the government to consider these factors while taking decisions regarding the location of a waste transfer station. These factors have been identified from existing literature and ranked according to their frequency in the existing literature.

6 Conclusion

Identifying the criteria for optimal location of waste transfer stations has improved the efficacy of solid waste management. In this study, criteria were categorized into three factors that are environmental, social, and economic. First, Rivers, the slope of surface and geology of surface has tope three criteria in environmental factor respectively. Second, Population density, land cover, and land use have ranked as the top three criteria in social factors respectively. Third, in economic consideration proximity to the road, land value and proximity to landfills are prioritize in different study respectively. For the optimal location, these three factors must be assured for the best location which is eco-friendly cost-effective, and wouldn't disturb the social ethos of society.

Acknowledgment

The authors acknowledged Dr. Muhammad Saad Memon and Masroor Ali for their valuable suggestions and expert guidance. I would also like to acknowledge Aamir Ali for their support. Especially, the careful review and constructive suggestions by the anonymous reviewers are gratefully acknowledged.

References

[1] Global Waste Management Outlook. 2016.

[2] M. Drahansky et al., "We are IntechOpen , the world ' s leading publisher of Open Access books Built by scientists , for scientists TOP 1 %," Intech, vol. i, no. tourism, p. 13, 2020.

[3] M. M. Sk, S. A. Ali, and A. Ahmad, "Optimal Sanitary Landfill Site Selection for Solid Waste Disposal in Durgapur City Using Geographic Information System and Multi-criteria Evaluation Technique," KN - J. Cartogr. Geogr. Inf., vol. 70, no. 4, pp. 163–180, 2020.

[4] A. E. Torkayesh, B. Malmir, and M. Rajabi Asadabadi, "Sustainable waste disposal technology selection: The stratified best-worst multi-criteria decision-making method," Waste Manag., vol. 122, pp. 100–112, 2021.

[5] W. Sabir, S. N. Waheed, A. Afzal, S. M. Umer, and S. Rehman, "A Study of Solid Waste Management in Karachi City," J. Educ. Soc. Sci., vol. 4, no. 2, pp. 144–156, 2016.

[6] R. Jaybhaye, N. Mundhe, and B. Dorik, "Site Suitability for Urban Solid Waste Disposal Using Geoinformatics: A Case Study of Pune Municipal Corporation, Maharashtra, India," Cloud Publ. Int. J. Adv. Remote Sens. GIS Int. J. Adv. Remote Sens. GIS, vol. 3, no. 1, pp. 769–783, 2019.

[7] B. Kebbi, I. U. Kaoje, I. M. Dankani, and I. Ishiaku, "Site Suitability Analysis for Municipal Solid Waste Disposal in," vol. 21, no. 7, pp. 1–10, 2016.

[8] S. Bera, M. Ahmad, and A. Kumar, "Suitable Site Selection for Urban Solid Waste Management using GIS Technique- a Case Study of Dhanbad Block," Int. Res. J. Eng. Technol., vol. 3, no. 7, pp. 1600–1605, 2016.

[9] K. Township, B. State, T. M. Ngumom, and H. W. Terseer, "Site Suitability Analysis for Solid Waste Disposal using Geospatial Technology : A Case Study of," vol. 6, no. 3, pp. 980–985, 2017.

[10] B. SURAJIT, A. MOBIN, and L. PREET, "Site Suitability Analysis for Solid Waste Dumping in Ranchi City, Jharkhand Using Remote Sensing and Gis Techniques," i-manager's J. Civ. Eng., vol. 8, no. 2, p. 26, 2018.

[11] G. I. S. Methods, "Selection of Suitable Site for Municipal Solid Waste Disposal Sites for the Available online www.jsaer.com Journal of Scientific and Engineering Research , 2017 , 4 (11): 36-45 Selection of Suitable Site for Municipal Solid Waste Disposal Sites for the ," no. November 2017, 2020.

[12] S. A. Shah, "Analyzing site suitability for solid waste disposal through GIS multi-criteria decision making hierarchy process," 3C Tecnol. innovación Apl. a la pyme, vol. 7, no. 4, pp. 65–80, 2019.

[13] F. D. Emmanuel, A. A. Musa, and Z. Nanpon, "Site suitability analysis and route optimization for solid waste disposal in Yola Town, Adamawa State Nigeria," South African J. Geomatics, vol. 6, no. 1, p. 130, 2017.

[14] E. Sustainability, Integrated Waste Management in India, no. March. 2020.

[15] P. K. Dara and T. B. Reddy, "Municipal Solid Waste Landfill Sites Selection for Visakhapatnam City under Vision 2020 Using GIS and AHP," Int. J. Contemp. Res. Rev., vol. 9, no. 06, pp. 20181–20194, 2018.

[16] D. K. Kibetu and D. Muchiri, "Using GIS to Select Ideal Sites for Municipal Wastes Transfer Station : Case Study of Embu Municipality," vol. 4, no. January 2016, pp. 1–7, 2020.

3rd Conference on Sustainability in Civil Engineering (CSCE'21)
Department of Civil Engineering
Capital University of Science and Technology, Islamabad Pakistan

EFFECT OF HEAVY CONSTRUCTION ON THE AMBIENT ENVIRONMENT OF AL-MASJID-E-NABAWI (ﷺ) AND HAREM AL-MADINAH

[a] Qazi Umar Farooq *, [a] Wadea K. Sindi , and [a] Ayed E. Alluqmani

a: Department of Civil Engineering, Islamic University of Madinah,41411 Saudi Arabia
a: umar@iu.edu.sa; b: wadeas@iu.edu.sa; c: dr.ayed@iu.edu.sa
* Corresponding author: Email ID: umar@iu.edu.sa; qaziumar@gmail.com

Abstract- Al Masjid-e-Nabwi sharif is one of the holiest places in Islam. Everyday thousands of pilgrims from each part of the world, visit the masjid to offer regular and optional prayers. To accommodate the rapidly increasing number of pilgrims, throughout history, the complex of Harem Al-Madinah undergoes various expansions. The most recent expansion was announced in 2012 and construction was in full swing during the 2014-15 fiscal year. The expansion project not only involves heavy construction but also requires demolishing of pre-existing buildings in the surroundings. The key objective of this investigation is to monitor the effect of nearby heavy construction activities on the critical environmental indicators of the prophet's masjid and surrounding areas. In this study, the vital ambient air quality parameters and noise levels were measured at different locations of Masjid during peak hours. The results are then compared with international health and safety standards. It has been observed that overall indoor air quality (IAQ) was within tolerable limits. However, there were noise impacts at some locations. The health and safety measure adopted by the authorities comply with international standards and similar procedures can be applied to the other parts of the world where heavy construction is required in the built-up urban areas.

Keywords- Harem Al Madinah, Air quality, Dust concentration, Carbon oxides, Noise Level.

1 Introduction

The historic city of Al Madinah Al Munawara is a northwestern city in the kingdom of Saudi Arabia. The most important landmark of the city is the prophet Muhammad ﷺ's Masjid. It is the 2nd masjid built in Islam during the lifetime of the Prophetﷺ. The first built masjid "Quba" is also located in the city towards the south of the masjid-e-Nabawi. Millions of Muslims from all over the globe visit the masjid every year. For example in 2019 alone about 2.5 million pilgrims performed the hajj including (1.9 million foreign pilgrims) and almost all of them visited Masjid-e-Nabawi[1]. The national and local authorities of the kingdom endeavors to provide a safe and healthy environment to the visitors. The number of pilgrims to the prophet's masjid is in constant increase through history and the masjid undergoes various expansions. The prophetﷺ build the masjid in 622 CE with an area of 1050 m^2. The masjid undergoes first expansion during the lifetime of the prophetﷺ after the battle of Khyber in 628CE and the area was increased to 2475m^2. The area of the masjid increased up to 500 % in 1994 during the era of the late King Fahad of Saudi Arabia [2][3]. The current expansion was inaugurated in 2012 by the late King Abdullah of Saudi Arabia and will increase the capacity of the worshippers up to 800,000 in the first phase[4][5].

The recent images of the masjid taken on bright sunny afternoon (after Asar prayer) of 19th March 2021 are shown in *Figure 1*. *Figure 1(a)* shows the panoramic view of the masjid-e-Nabawi from the south i.e., qibla direction. Whereas the ongoing eastern expansion site is shown in *Figure 1(b).*


a) Panoramic view of Masjid


b) Recent expansion Site

Figure 1: a) Panoramic View of Masjid from South and b) Image of an ongoing Expansion as of March 2021.

Most of the current and prospective construction for the expansion project requires heavy earthwork and RC construction. The construction industry is one of the largest material consumer and pollution contributor [6]. Heavy construction activities cause the release of various environmental distresses including but not limited to noise, dust, and vibrations. Studies regarding monitoring and implementation of environmental policies reveal that these distresses can be controlled by proper implementation of policies [7]. Most of the environmental and health policies are developed based on international guidelines such as world health organization (WHO) guidelines for air quality [8], American Society of Heating, Refrigerating and Air-Conditioning Engineers (ASHRAE) standards for indoor air quality [9], The National Institute for Occupational Safety and Health (NIOSH) standards and US environmental protection agency (EPA) guidelines. Despite the above guidelines and efforts, the economic real-time environmental monitoring system is required to be developed for the construction industry[10]. Apart from air quality, noise generation is additional environmental distress generated by the construction industry. It is associated with the health hazard, and required to be monitored and addressed[11].

Since Masjid e Nabawi is a unique project which is daily visited by thousands of pilgrims as well as there is a heavy construction site in the vicinity, both occupational and indoor standards are required to be implemented simultaneously. The study is innovative in terms of scrutinizing the environmental distresses, generated by the combination of heavy construction activities and high crowd intensity. In this study, various environmental parameters are compared with the most relevant standard applied at the specific location.

2 Methodology

In this study, the key ambient environmental parameters were measured at the most important locations of Al-Masjid-e-Nabawi ﷺ and the results are then compared with the respective ideal and threshold values provided by relevant indoor and outdoor quality standards. The measurement locations were selected based on the intensity of visitors. For example, all the visitors to the masjid like to offer salaam to the prophet Muhammad ﷺ, and want to offer salah at Riyadh-ul-Jannah. These two locations are always crowded and marked as locations A and B in this study. An effort has been made to cover at least one location of different crowd intensity and the nomenclature of the location has been decided on the likelihood of people intensity in descending order.

All the measurement locations are marked on the google maps satellite image acquired in March 2021[12] and presented in *Figure 2.* The two expansion sites are also indicated in the figure. The western expansion has already been completed and marked as resent expansion. Whilst the eastern expansion is still under construction and has been divided into two zones marked as Zone A and Zone B. The other vital locations include an internal courtyard, the previous northern expansion, two exterior courtyards, and the most crowded basement car parking.

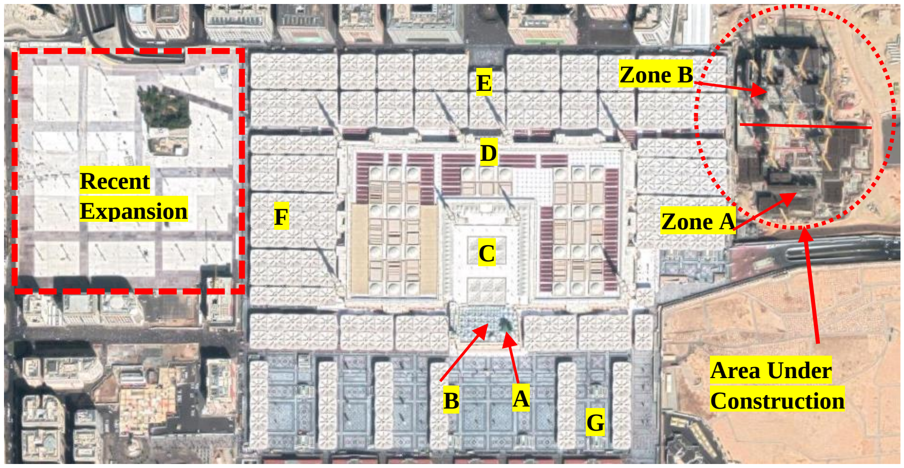

Figure 2 The Satellite Image of Masjid-e Nabawi Complex March 2021 with measurement Locations

A detailed description of all the measurement locations is presented in *Table 1*. The locations A to G are the harem areas where the likelihood of the people is always there, except for the current unusual circumstances applying COVID-19 protocols. The expansion sites are not yet open to the public and hence not included in the table.

Table 1 Description of Measurement Locations at Al-Harem

Sr. No	Location Description	Location Symbol	Remarks
1	Site for offering Salam to Prophet ﷺ	A	Critical and most crowded location
2	Riyadh-ul-Jannah الروضة الشريفة	B	Critical and most crowded location
3	2nd Internal Courtyard	C	Crowded in Peak Season
4	Northern King Fahad Extension	D	Crowded only during Obligatory Prayers in Peak Season.
5	Northern Exterior Courtyard	E	Passageway /crowded in Peak Season
6	Western Exterior Courtyard	F	Passageway /crowded in Peak Season **Close to recent expansion**.
7	Basement Car Parking 1-A (The Upper Deck)	G	Always Crowded during obligatory Prayers

The data for the air quality parameters have been obtained from the comprehensive routine reports prepared by the *"Technical Committee for the expansion of the Prophet's Mosque"*, and *"Madinah Al Munawara Development Authority."* In this study, four indoor air quality parameters, i.e., Relative humidity, Noise levels, carbon dioxide, and carbon monoxide were compared with the designated international standards. The time for the measurement was chosen is late August 2014 which corresponds to late Shawal and early Dul-Qidah 1435AH. The time marks the Hajj season when most of the international pilgrims start arriving in Madinah. The construction activities were in full swing at the time and many demolishing projects were also going on around the Harem area. Since Masjid is most crowded at Isha prayer due to the arrival of local residents. The data of environmental parameters just after Isha prayer has been used in the comparison. The four air quality parameters and their designated international guidelines are summarized in *Table 2*. The only outdoor air quality parameter is used in the study for the under-construction sites namely zone A and Zone B is inhale able Particulate Matter PM_{10}. The construction site (Zone A and B) is not yet open to the public.

Table 2: List of detrimental parameters with international Health and Safety Standards

Sr. No	Parameter	Symbol (units)	Guideline /Criteria
1	Relative Humidity	RH (%)	ASHRAE
2	Noise Level	-(dB)	WHO & NIOSH
3	Carbon dioxide	CO_2 (ppm)	NIOSH/EPA
4	Carbon monoxide	CO (ppm)	WHO
5	Particulate Matter (only for construction Zones A and B)	PM_{10} (mg/m^3)	WHO

3 Results and Discussions

Madinah al Munawara is mostly a dry region with a desert climate and very limited precipitation [13]. The annual average relative humidity in the city is about 24%. As per ASHRAE standards, the comfortable relative humidity values range between 30 to 60%. Figure 3 represents the variation of relative humidity at studied locations of the harem. The upper and lower limits of the ASHRAE standards are marked as maximum and minimum and indicated by bold lines. The indoor relative humidity (location A to D) is within a comfortable zone, reflecting the performance of Haram Al Madinah's HVAC system. The Masjid is supported by one of the world's largest air-conditioning systems. The courtyards and the parking lot have low humidity values implying the outdoor conditions. The northern courtyard has a relatively better humidity reading due to continuous mist spray. The indoor relative humidity values drop to the lower limit on Thursday 21st of August 2014, whilst the readings improve on Saturday 23rd August. The reason behind this is the variation in crowd intensity. The Masjid is usually very crowded on Thursday night as many people visit the masjid at the beginning of the weekend. On the other hand, it is generally less crowded on Saturday night as Sunday is the first working day of the week in the kingdom.

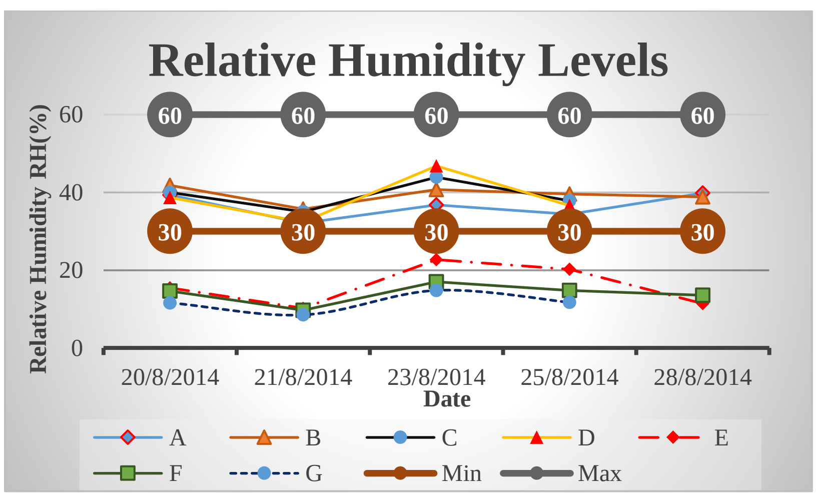

Figure 3: Relative humidity at Selected locations of Harem After Isha Prayer

The noise levels at various locations of the harem are shown in Figure 4. The lower limit of 55 dB shown by a bold grey line represents the world health organization (WHO) standard value for an educational facility. While the upper limit of 80dB is the maximum tolerable limit for the workplace established by Occupational safety and health (NIOSH). The noise level readings for all locations are above WHO standard due to high crowd intensity and as such no significant noise was observed due to construction activity. This can be seen by comparing the noise history of location F (the closest to the construction area) and C (far from the construction zones). The car parking has the overall highest noise levels due to vehicle engines and horns. On Thursday 21st August, the parking location G has a drop in noise levels as visitors like to stay longer on weekends. All the noise readings are below the threshold value of 80dB.

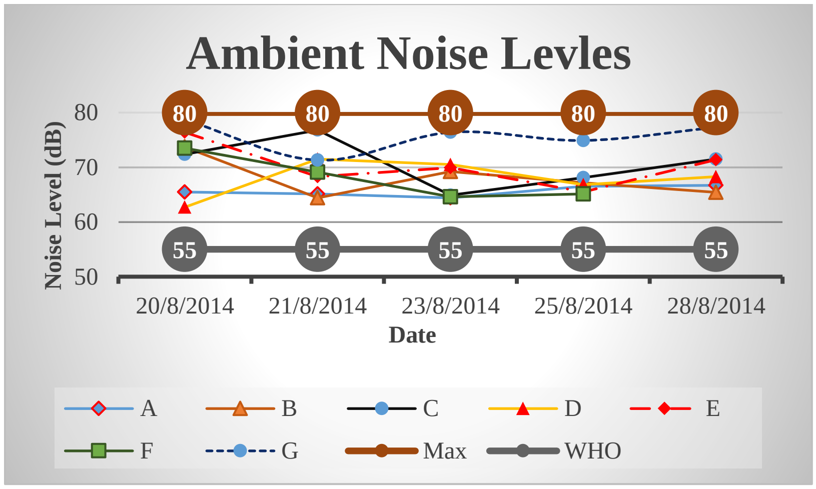

Figure 4 Ambient Noise Levels at Selected locations

The carbon dioxide levels in the masjid and surroundings are less than the threshold value of 1000 ppm established by NIOSH and US EPA, except for location B i.e. Riyadh-ul-Jannah. The location is extremely crowded at night, particularly on Thursdays and Fridays see Figure 5. The situation can lead to suffocation and people with respiratory disorders are recommended to avoid the peak hours' time. The ventilation at the location can be further improved by modifying the HVAC system. The CO_2 levels at other studied locations reflect that the CO_2 concentration at location B is not affected by the heavy construction.

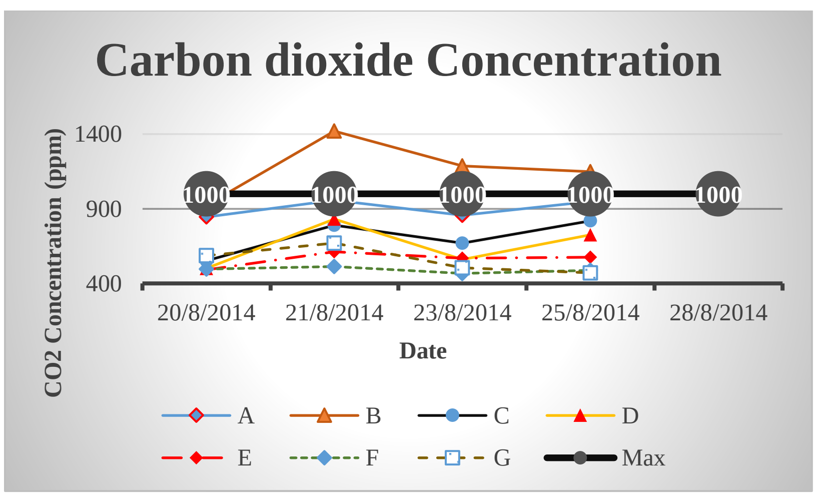

Figure 5 Carbon dioxide Concentration at various locations of Harem

The carbon monoxide concentration at all reference points is far below the benchmark value of 10 ppm set by the World health organization. The car parking has slightly higher readings of CO on Thursday due to idling vehicles which should be discouraged. The CO concentration history for the last week of August 2014 for various locations of the masjid and the benchmark value is shown in Figure 6.

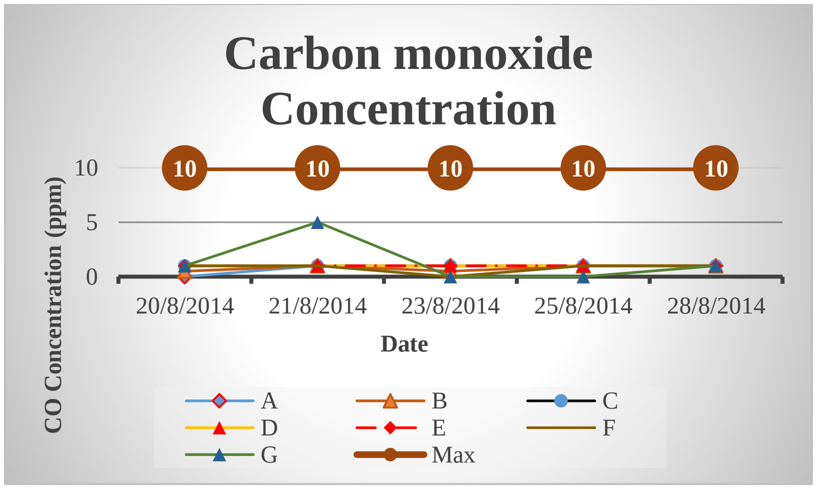

Figure 6 Carbon monoxide Concentration at studied locations

Due to limitations, the dust concentration data is only measured at construction zones A and B. It is measured in terms of inhalable particles having size <= 10 µm i.e., PM_{10}. The readings are taken for the whole month during peak working hours. The PM_{10} concentration in ppm for both the construction zones is shown in Figure 7. The PM_{10} concentration is very high as compared to the annual and daily outdoor air quality guideline reference values of WHO. This is particularly due to the marble cutting and other construction activities and the staff is provided with the best available safety equipment. The physical observation of dust concentration has not been reported in the prayer zones.

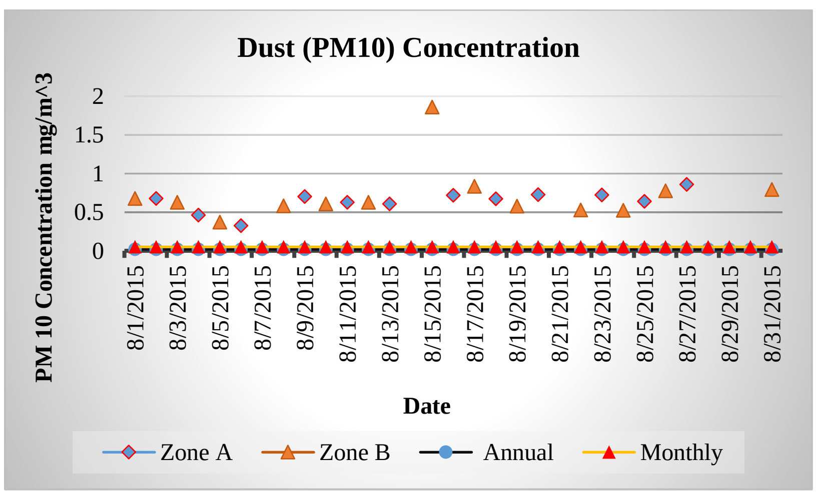

Figure 7: Dust Concentration at Zone A and Zone B

4 Conclusions

The ambient air quality of Masjid-e-Nabwi (ﷺ) complex including courtyards is not significantly affected by the nearby heavy construction of expansion projects. However, measurements of various air quality parameters revealed some interesting information which is summarized as follows:

- The HVAC system of the masjid is functioning quite nicely and maintaining comfortable indoor humidity levels despite the dry weather of the city.
- The overall environment of the masjid becomes noisy after prayers and pilgrims are required to be educated and guided to keep the decorum of the holy place even after completing the salah.

- The parking lots have sometimes higher carbon monoxide concentrations due to congestion and idling of vehicles and visitors must be reminded by signboards etc. to stop the engines while waiting for passengers in the parking areas.
- The dust concentration in terms of inhaling PM_{10} is very high in the construction zones A and B of the expansion project. Although the construction activities are currently standstill, in case of resumption the public access to the areas near these zones should be restricted.
- Riyadh-ul-Jannah becomes overcrowded on weekends and has a high CO_2 concentration due to crowd intensity. Better crowd management techniques such as the current practice of issuing permits for praying in the noble Rawdah due to COVID 19 Protocols can be permanently adopted.

5 Recommendations

The IoT-based smart devices can be installed in large construction projects to continuously measure various air quality parameters, this enables the authorities to take real-time actions and accordingly guide the works and other stakeholders. Mandatory dust masks for workers and availability of respiratory support equipment must be ensured by the HSE engineers on sites where heavy marble installation is necessary. Buildings with high crowd intensity, such as public offices with long queues, etc., must be equipped with properly designed ventilation systems. The systems should be capable of accommodating higher CO_2 levels.

Acknowledgment

The authors would like to thank, *"Technical Committee for the expansion of the Prophet's Mosque"*, and *"Madinah Al Munawara Development Authority"* for the technical data and general support. The cooperation of the above authorities is highly acknowledged.

Repentance

The authors seek the mercy of Allah (SWT) and ask his forgiveness if any information or phrase has been inadvertently misinterpreted or has been presented out of context.

References

[1] Hajj Statistics Report, "Hajj Statistics 1435H-2014G," vol. 2014, p. 42 (in Arabic), 2014, [Online]. Available: http://www.cdsi.gov.sa/english/index.php?option=com_content&view=article&id=42&Itemid=138.

[2] A. Alshehri, M. Arif, and E. Felamban, "Simulation of Crowd in the Corridor of Ziara in Masjid-e-Nabwi, Madinah," in *Traffic and Granular Flow '15*, Cham: Springer International Publishing, 2016, pp. 353–360.

[3] "The Prophet's Mosque Architecture and Expansions," *The Agency of the General Presidency for the Affairs of the Prophet's Mosque*. https://wmn.gov.sa/public/?page=page_927618.

[4] "Saudi Arabia: The largest expansion of the Prophet's Mosque," *almadenahnews*. https://www.almadenahnews.com/article/175105-السعودية-أكبر-توسعة-للمسجد-النبوي.

[5] Usama A. Nassar, "Expansion of the Prophet Mosque as a Catalyst for Sustainable Urban Development in Al-Madinah Almunawarah in Saudi Arabia," *Journal of Urban Planning, Landscape & Environmental Design*, vol. 2, no. 1: GREEN, pp. 99–115, 2017, doi: https://doi.org/10.6092/2531-9906/5142.

[6] A. Horvath, "CONSTRUCTION MATERIALS AND THE ENVIRONMENT," *Annual Review of Environment and Resources*, vol. 29, no. 1, pp. 181–204, Nov. 2004, doi: 10.1146/annurev.energy.29.062403.102215.

[7] J. Hong *et al.*, "An empirical analysis of environmental pollutants on building construction sites for determining the real-time monitoring indices," *Building and Environment*, 2020, doi: 10.1016/j.buildenv.2019.106636.

[8] E. Dekker *et al.*, "WHO Air quality guidelines 2005," *International Journal of Life Cycle Assessment*, 2018.

[9] ASHRAE, "Standard 62-1989: Ventilation for acceptable indoor air quality, American Society of Heating, Refrigerating and Air-conditioning Engineers," *American Society of Heating, Refrigerating and Air-Conditioning Engineers*, 1989.

[10] D. Cheriyan and J. Choi, "A review of research on particulate matter pollution in the construction industry," *Journal of Cleaner Production*, vol. 254, p. 120077, May 2020, doi: 10.1016/j.jclepro.2020.120077.

[11] J. F. Mahdi, N. Akhter, A. W. Khan, and S. Irfan, "Health Hazards Associated with Noise Due to Civil Construction Activity," *Journal of Southwest Jiaotong University*, vol. 55, no. 2, 2020, doi: 10.35741/issn.0258-2724.55.2.39.

[12] "Google Maps," *March 2021*. https://www.google.com/maps/@24.4687669,39.6112954,1053m/data=!3m1!1e3!5m1!1e7.

[13] Q. U. Farooq and M. T. Naqash, "Performance of Shallow Building Foundations under Infrequent Rainfall Patterns at Al-

Madinah, Saudi Arabia," *The Open Civil Engineering Journal*, vol. 15, no. 1, pp. 91–103, Apr. 2021, doi: 10.2174/1874149502115010091.